Harnessing the Nitrile Functionality to Heterocycles via Thermal and Photochemical Strategies

A dissertation submitted in partial fulfillment for the degree of

Doctor of Philosophy

Submitted By

Hirendra Nath Dhara

Roll No. 196122015

Department of Chemistry

Indian Institute of Technology Guwahati

Guwahati-781039, Assam, India

August, 2024

Harnessing the Nitrile Functionality to Heterocycles via Thermal and Photochemical Strategies

A dissertation submitted in partial fulfillment for the degree of

Doctor of Philosophy

Submitted By

Hirendra Nath Dhara

Roll No. 196122015

Under the supervision of

Prof. Bhisma Kumar Patel

Department of Chemistry

Indian Institute of Technology Guwahati

Guwahati-781039, Assam, India

August, 2024

DEDICATED WITH LOVE

To My Parents, Sister & Family

For Their Unwavering Support &

Endless Encouragement

भारतीय प्रौद्योगिकी संस्थान गुवाहाटी
Indian Institute of Technology Guwahati

INDIAN INSTITUTE OF TECHNOLOGY GUWAHATI
Department of Chemistry

STATEMENT

I do hereby declare that the matter embodied in this thesis is the result of investigations carried out by me in the Department of Chemistry, Indian Institute of Technology Guwahati, Assam, India, under the guidance of Prof. Bhisma K. Patel. This thesis has been submitted by me to the Department of Chemistry, Indian Institute of Technology Guwahati for the award of the degree of Doctor of Philosophy.

In keeping with the general practice of reporting scientific observations, due acknowledgements have been made wherever the work described is based on the findings of other investigators. I further declare that this work has not been submitted anywhere else for any degree, diploma, associateship or membership, etc. of any Institute or University to the best of my knowledge.

Hirendra Nath Dhara

November, 2024 **Hirendra Nath Dhara**

IIT Guwahati

INDIAN INSTITUTE OF TECHNOLOGY GUWAHATI
Department of Chemistry

CERTIFICATE

This is to certify that Hirendra Nath Dhara has been working under my supervision since July 2019 as a regular registered Ph.D. student. His thesis entitled **"Harnessing the Nitrile Functionality to Heterocycles via Thermal and Photochemical Strategies"** is an authentic record of the results obtained from the research work in the Department of Chemistry, Indian Institute of Technology Guwahati, Assam, India. I am forwarding his thesis to submit for the Ph.D. (Science) degree from this institute. I certify that he has fulfilled all the requirements according to the rules of this institute regarding the investigations embodied in his thesis and this work has not been submitted elsewhere for a degree.

November, 2024
IIT Guwahati

Prof. Bhisma K. Patel
(Thesis Supervisor)
Department of Chemistry
IIT Guwahati

भारतीय प्रौद्योगिकी संस्थान गुवाहाटी
Indian Institute of Technology Guwahati

ACKNOWLEDGEMENT

I would like to express my sincere gratitude to all the people around me who have helped, supported, and encouraged me throughout my Ph.D. journey.

First and foremost, I want to express my deepest respect and profound gratitude to my supervisor, Prof. Bhisma K. Patel, for providing me the opportunity to work under his guidance. His continuous support and inspiration through creative and unique scientific ideas helped me to explore the domain of my work presented in this thesis. I feel blessed to have him as my mentor, who gave me moral support and freedom throughout my entire journey.

I would also like to extend my sincere gratitude to the doctoral committee members, Prof. Achalkumar Ammathnadu Sudhakar, Prof. Chandan Das, Prof. Dipankar Srimani, and Prof. Bhubaneswar Mandal, for their timely evaluation of my Ph.D. work, encouragement, and valuable suggestions. Their insightful advice and guidance helped me to improve my work significantly.

My honest regards to all the faculty and staff members of the Department of Chemistry, IIT Guwahati for their cooperative nature. I would like to thank Babulal da and Kula Kamal Senapati sir for single-crystal XRD, Imdadul da for NMR, Aniruddha da, Diganta da, Shyamal da, Basab da, Tapu da, Michael bhaiya, John bhaiya, Lipika mam and Abhilasha mam for various official work and support in the Department of Chemistry.

I wish to express my sincere gratitude to MHRD for the financial support and to IIT Guwahati for providing all the necessary facilities for my research work. I am grateful to the Central Instruments Facility (CIF) for the 600 MHz NMR and single-crystal XRD facilities, MHRD for the 400 MHz NMR facility under the COE-FAST program, DST for the 500 MHz NMR facility under the DST-FIST program, NECBH, IIT Guwahati, and DBT, Govt. of India for the 400 MHz NMR and single-crystal XRD facilities. I would also like to thank the Central Instruments Facility (CIF), IIT Guwahati, especially for allowing me to become an operator for the 600 MHz NMR instrument. I would like to express my gratitude and a big thanks to all the instrument operators both inside and outside IIT Guwahati for successfully carrying out all the instrumental experiments required during my research work.

The entire Patel lab, both past and present, deserves tremendous credit for making my journey beautiful. I have been fortunate to have come across wonderful lab seniors, including Suresh bhaiya, Bilal bhaiya, Amitava da, Anjali didi, Subhendu da, Tipu bhaiya, Ashish bhaiya, and Nikita didi, whose help, precious suggestions, encouragement, insightful feedback, and constant inspiration have been invaluable. I would also like to thank the postdoctoral lab

seniors, Pakiza didi, Binoy bhaiya, Kamal bhaiya, Bhaskar bhaiya, and Gongutri didi, for their love and support.

I would like to express my heartiest thanks to my co-lab members and friends, Tamanna Bubul, and Parbin for their healthy discussions and encouragement. I want to heartily appreciate all my very talented and hardworking juniors Pritishree, Raju, Dinabandhu, Shalini, Deepjyoti, Supriya, Manjunath, and Sadiur for their diligence and for maintaining a friendly environment in the lab. I am incredibly grateful for the countless moments of fun and inspiration we have shared. Your unwavering companionship has made this journey truly unforgettable. Truly, I have lived the happiest and most memorable moments of my journey with these outstanding juniors. I would like to thank all the M.Sc trainees and summer interns Prashant, Priyabrata, Pankaj, Avishek, Angshuman, Akshar, Amisha, Koustuv, Pratip, Gyanesh, Berlina, Sourasish, Gourab, Amrit, Shreya, Usashi, Shalini, Debolina, Hrithik, Dabasish, Snehasih and Anushka for their encouragements.

I would also like to extend my deepest gratitude to my senior Amitava da who has guided and supported me throughout my Ph.D. journey. His invaluable advice, expertise, and encouragement have been instrumental in shaping my research and personal growth. I would like to thank my junior Ph.D. student, Supriya, M.Sc. project student Koustuv, and summer intern Sourasish and Amrit for their assistance, support, and for allowing me to guide them during their projects and sharing the basic ideas, techniques, and knowledge of Chemistry.

I would also like to thank my Ph.D. friends, seniors, and juniors here at IITG, Archana didi, Arup da, Subhamoy da, Avijit da, Retwik da, Sudip da, Bipin Bhaiya, Samir da, Chandrakant bhaiya, Debojit da, Sujan didi, Sandip da, Sayanta da, Araghni da, Sandip Bhaiya, Rahul, Nandan, Surjya, Biman, Himani, Rabu, Bijoy, Subhajit, Tripti, Hirak, Rupkumar, Sukesh, Subhrajyoti, Santanu, Mongoli, Mithu, Arup, Pranam, Amlan, Gopi da, Subhadip Poria, Aniket, Bikram, and Sourav for making the journey a lot better, easier and entertaining.

I would like to extend my sincere gratitude to Arup Da, Subhamoy Da, Ashish bhaiya, and Mongoli for their invaluable guidance in teaching me essential experimental techniques. Their patience and expertise were instrumental in helping me master these skills, and their support significantly contributed to my research progress. I deeply appreciate their willingness to share their knowledge and invest time in my learning process.

I would like to express my heartfelt gratitude to all my teachers, official staff, and lab attendants from school through college. Their dedication, encouragement, and unwavering support have played a significant role in shaping my academic journey and personal growth.

Each of them has imparted valuable knowledge and life lessons that have been instrumental in my development. A special thanks to my all tuition teachers Manik Kaku, Milan Sir, Arnab Kaku, Kanchan Sir, Biren Sir, Gayen Sir, Tapas Sir (English), Pratibha Mam, Rana Sir, Sanjib (SG) Sir, Sibhnath (SS) Sir, Tapas Sir (Chemistry practical), Sobha Mam, and Avijit Sir. Additionally, I would like to express my gratitude to Ramakrishna Mission Residential College, Narendrapur, including all the monks, professors, staff, lab attendants, and everyone else at the institute. I am deeply appreciative of their influence and encouragement throughout my educational journey.

I would like to thank all my friends from school through college. Their support, encouragement, and companionship have been a constant source of strength and joy throughout my educational journey. Each of them has played a significant role in making my experiences memorable and meaningful. I am deeply thankful for their friendship and the positive impact they have had on my life.

I would like to express a big thanks to all my village friends, seniors, and juniors specially Bapan Kaka, Hari Kaka, Jahar da, Madhu Kaka, Giri Kaka, Amit, Raja, Jyoti, Suvendu, Soumen, and all others giving various kinds of entertainment during my educational journey.

Finally, my Ph. D. endeavor could not have been completed without the endless love, unending support, tolerance, and blessings from my parents, and family. I would like to express my deepest gratitude to my Ma, Baba, sister (Mou), Didi, Boro dada, Chhoto dada, Dida (grandmother), Dada babu, all uncles, aunts, and other family members. Their unwavering support, love, and encouragement have been the foundation of my achievements. They have provided me with the strength and motivation to pursue my goals and have stood by me through every challenge. I am profoundly grateful for their sacrifices, understanding, and constant belief in me.

Last but not the least, I am thankful to Almighty for continuous blessing during my research career to accomplish this remarkable journey.

Hirendra Nath Dhara

भारतीय प्रौद्योगिकी संस्थान गुवाहाटी
Indian Institute of Technology Guwahati

SYNOPSIS

The contents embodied in this thesis are divided into five chapters based on experimental results obtained during the research period including an introductory chapter.

The introductory chapter summarizes the thermal and photochemical approach to access *N*-heterocycles using nitrile (C≡N) functionality. This chapter includes a brief discussion about transition-metal-catalyzed addition or addition/cyclization, insertion of an alkyne into the nitrile (C≡N), photochemical cascade addition/cyclization to access *N*-heterocycle leading to the formation of C–C, C–O, and C–N bonds.

Chapter II describes a visible-light-mediated solvent-switched photosensitizer-free synthesis of polyfunctionalized quinolines and pyridines.

Chapter III demonstrates a Pd(II)-catalyzed three-component synthesis of furo[2,3-*d*]pyrimidines from β-ketodinitriles, boronic acids, and aldehydes.

Chapter IV defines a cascade synthesis of furo-pyrrolo-pyridines via Pd(II)-catalyzed dual N−H/C annulative-cyclization.

Chapter V illustrates a visible-light-driven electron-donor-acceptor (EDA) complex-initiated synthesis of thio-functionalized pyridines.

CHAPTER I. An Overview to Access *N*-Heterocycles under Thermal and Photochemical Approaches Using Nitrile (C≡N) Functionality

The *N*-heterocycles constitute one of the largest areas of research in organic chemistry. Among the different heterocyclic compounds, *N*-heterocycles have maintained the interest of researchers and their unique structures have led to several applications in various areas of research. Because of the extensive interest in *N*-heterocycles, the synthesis of these compounds has always been an important area in organic synthesis. In particular, the highly substituted π-conjugated fused polycyclic *N*-heterocycles or fused *N*,*O*-heterocycles are versatile building blocks of many natural products and found to be useful in functional materials such as luminescent, organic semiconductors, liquid crystal displays (LCDs), organic light-emitting diodes (OLEDs), and numerous others multifaceted applications. Owing to their importance, a

large number of synthetic approaches have been developed to access of *N*-heterocyclic compound. Among these methods, the transition metal-catalyzed addition and cyclization to a nitrile functionality serves as one of the elegant methodologies. The nitrile (–CN) group having a polar unsaturated C≡N triple bond, is one of the most flexible and effective functional groups in organic synthesis. Despite sufficient stability and being intrinsically inert, the nitrile group can be transformed into various other functional groups such as amine, amide, aldehyde, ketone, and carboxylic acid which can undergo further intramolecular cyclization. In this regard, the photochemical and thermal addition of nucleophiles/radicals to the nitrile followed by cyclization, or intermolecular [4 + 2], [3 + 2], [2 + 2 + 1], and [2 + 2 + 2] cycloadditions are well explored (Figure I.1).

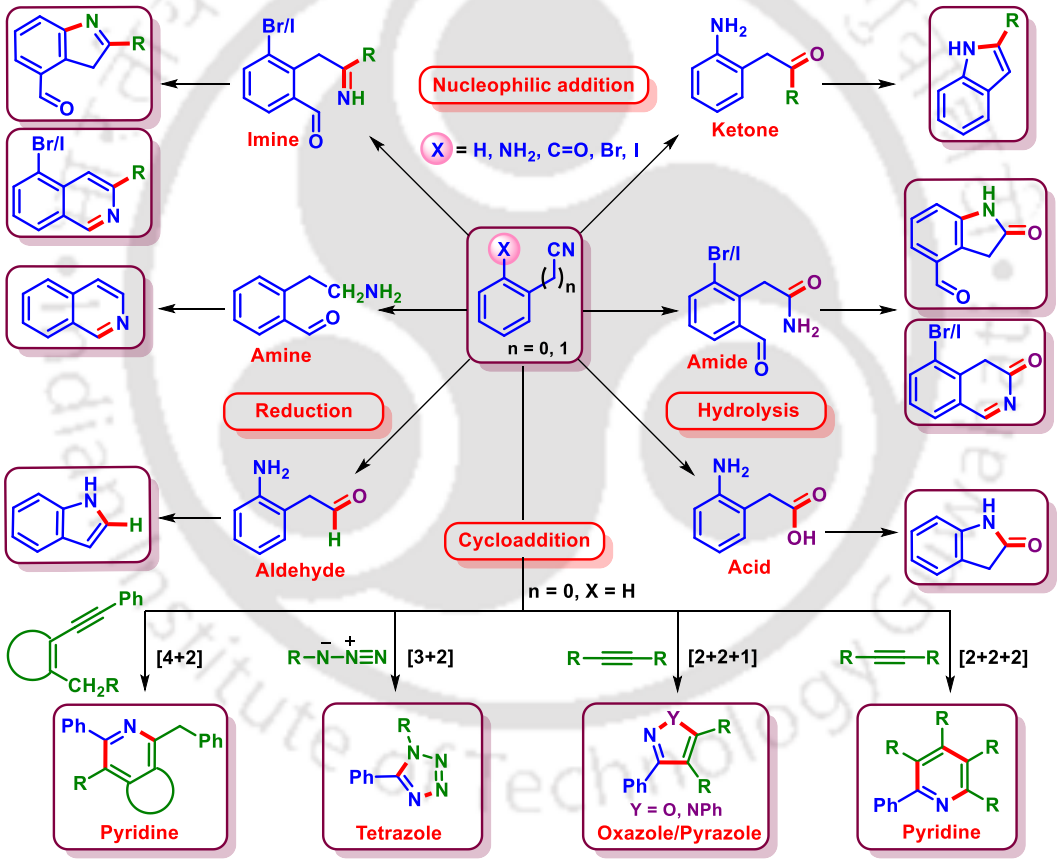

Figure I.1. *Conversion of nitrile to other functional groups and N-heterocycles.*

One of the most cost-effective and straightforward methods to introduce nitrile functionality is through the use of malononitrile, which serves as a precursor to design compounds like (E)-2-(1,3-diphenylallylidene)malononitrile (dicyanodiene) and 2-(2-oxo-2-phenylethyl)malononitrile (β-ketodinitrile) (Figure I.2). These precursors feature an olefinic

double bond and a keto group in proximity to the nitrile functionality. Consequently, these synthetic intermediates are highly valuable for the synthesis of *N*-heterocycle. However, these synthetic precursors remain less explored in literature either thermally or photochemically.

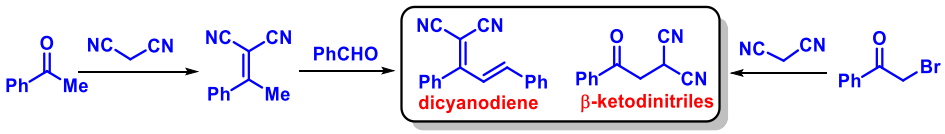

Figure I.2. *Synthesis of nitrile precursors.*

This introduction chapter describes newer methodologies of visible-light mediated and thermal synthesis of *N*-heterocycles from dicyanodiene and β-ketodinitrile via the construction of C–C and C–N bonds concerning the following:

I.1. Transition-metal-catalyzed synthesis of *N*-heterocycles via cascade addition/cyclization to nitrile.

I.2. Access to carbo and nitrogen-heterocycle via alkyne insertion into the nitriles.

I.3. Access to *N*-heterocycles via photochemical cascade addition/cyclization.

I.1. Transition-Metal-Catalyzed Synthesis of *N*-heterocycles via Cascade Addition/Cyclization to Nitrile:

I.1.1. Transition Metal-Catalyzed Cascade Addition/Cyclizations of Nitrile:

Cascade cyclization is a class of chemical reactions where sequential reactions are performed in the same pot and the product of the first reaction is the substrate for the subsequent steps and so on. In this rapidly growing field of catalysis, the transition metal-catalyzed cascade addition/cyclizations of nitriles (CN) have provided a suitable path to produce a diverse range of *N*-heterocycles through the formation of C–C and C–N bonds. The reactions can proceed either via nucleophilic/electrophilic or free radical mechanisms. Most of the commonly reported addition reactions of nitrile can be classified into three general categories. In these reactions, the transformation of the nitrile group to an iminyl group (C=N) occurs through the addition reaction: (a) utilizing the σ-coordination of nitrogen to the metal, acting as a Lewis acid, (b) via transition metal-catalyzed 1,2-insertion, or (c) through *in situ* generation of a radical in the presence of transition metals, followed by subsequent cyclization (Scheme I.1.1.1).

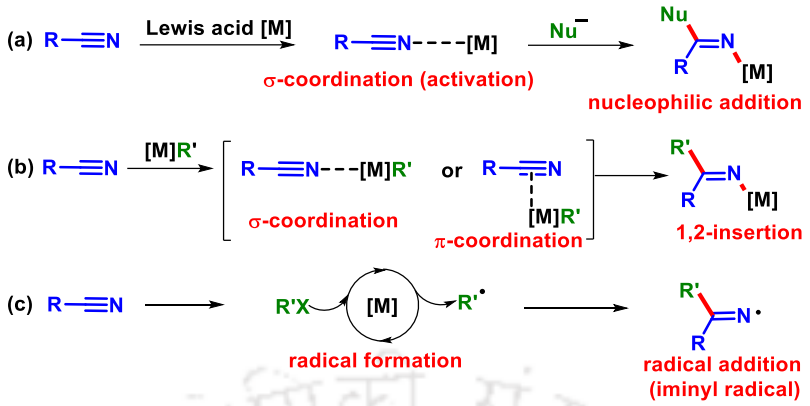

Scheme I.1.1.1. *Transition-metal-catalyzed addition to nitrile.*

I.1.1.1. Transition-Metal-Catalyzed Nucleophilic/Electrophilic Cascades Cyclization:

In this transition-metal-catalyzed cascades reaction, the nitrile precursors react with different coupling partners such as amine, Grignard reagent, arylboronic acids, aryl iodides, indoles, arylhydrazines, aryl carboxylic acid to afford various *N*-heterocycles.

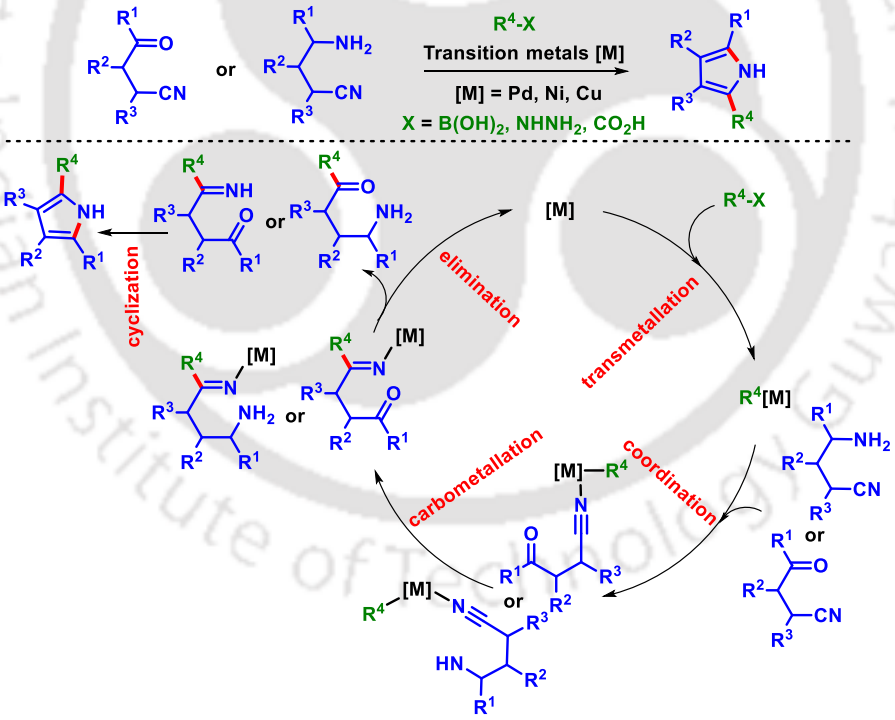

Scheme I.1.1.1.1. *Carbometalation of nitriles to synthesize N-heterocycles.*

I.1.1.2. Transition-Metal-Catalyzed Radical Cyclization:

In recent years, the transition-metal-catalyzed radical cascade reaction involving the nitrile functionality also provides diverse opportunities for constructing various important heterocycles and carbocycles. A general mechanism of nitrile group as a radical acceptor in cascade reaction is shown in Scheme I.1.1.2.1.

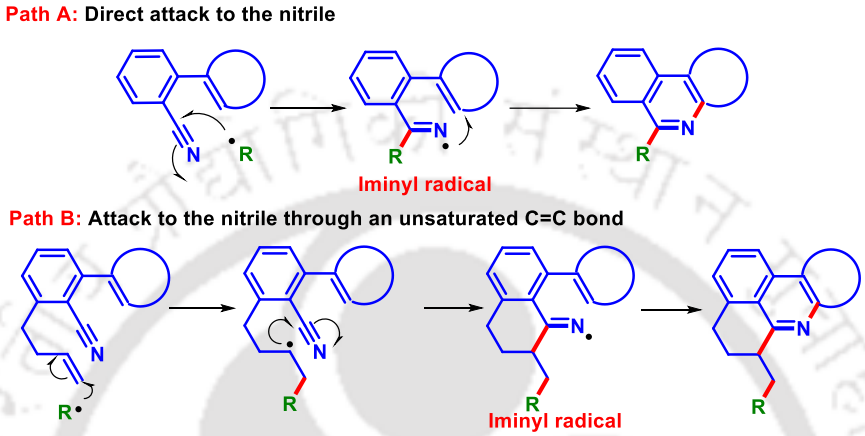

Scheme I.1.1.2.1. *Nitrile as a radical acceptor for synthesis of N-heterocycle.*

I.2. Access to Carbo and Nitrogen-Heterocycle via Alkyne Insertion into the Nitriles:

Effective transformation of nitriles is a fascinating area, which has attracted extensive attention in organic chemistry. In this endeavor, the insertion of alkyne into nitriles extends a variety of reactions toward the formation of diverse carbo and nitrogen-heterocycles via constructing C–O and C–N bonds.

I.2.1. Insertion of Alkyne via Carbometalation of Nitrile:

The alkyne insertion to nitrile is developed as a convenient route to synthesize different carbocycles involving carbometalation followed by intramolecular cyclization. In the field of oxidative alkyne annulation, Larock's group developed an intramolecular carbopalladation of the cyano group for the synthesis of 2,3-diarylindenones from 2-iodobenzonitrile (Scheme I.2.1.1).

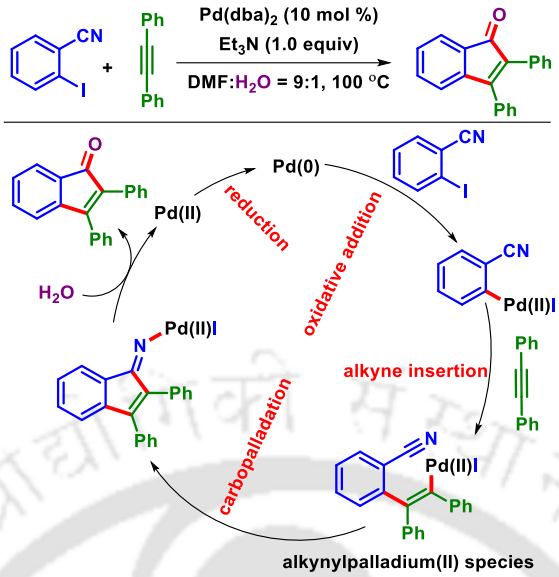

Scheme I.2.1.1. *Alkyne insertion into the nitrile via carbometalation.*

I.2.2. Alkyne Insertion via Cycloaddition of Nitrile:

Transition-metal catalyzed cycloaddition has also revolutionized the field of organic synthesis by facilitating the construction of complex organic molecules in a highly efficient manner. In this regard, the transition-metal-catalyzed cycloadditions *viz.* [2 + 2 + 1], [2 + 2 + 2], [3 + 2], [4 + 2] between alkyne and nitrile has been a convenient approach for the synthesis of various *N*-heterocycles. A general mechanistic pathway for this cycloaddition between alkynes and nitrile is shown in Scheme I.2.2.1.

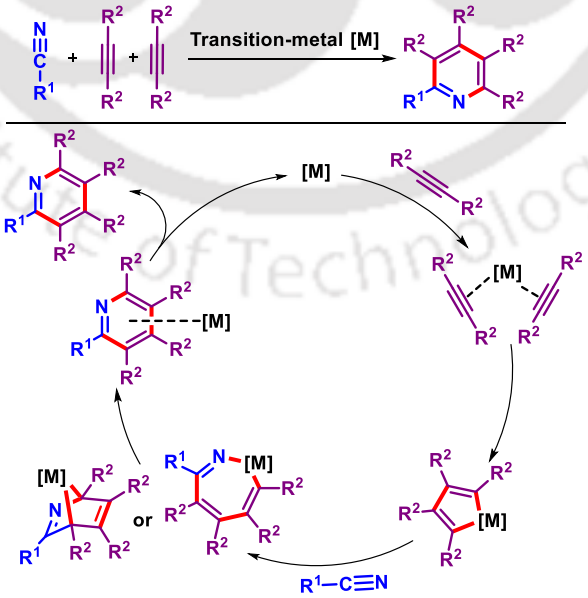

Scheme I.2.2.1. *Alkyne insertion via [2 + 2 + 2] cycloaddition of nitriles.*

I.2.3. Intramolecular Alkyne Insertion into the Nitrile:

The nitrile-triggered access to synthesize *N*-heterocycles proceeds when both the nitrile and alkyne are an integral part of the same molecules such as *o*-alkynylarylnitriles (Figure I.2.3.1). Here, the alkyne moiety is fixed at the ortho position with respect to the nitrile group, facilitating nucleophilic addition followed by intramolecular cyclizations, leading to *N*-heteroarenes (attack through nitrile). Another possible approach to accessing nitrogenous heterocycles involves the nucleophilic attack of an *N*-nucleophile on the nitrile, followed by annulation with the alkyne (attack through *N*-nucleophile).

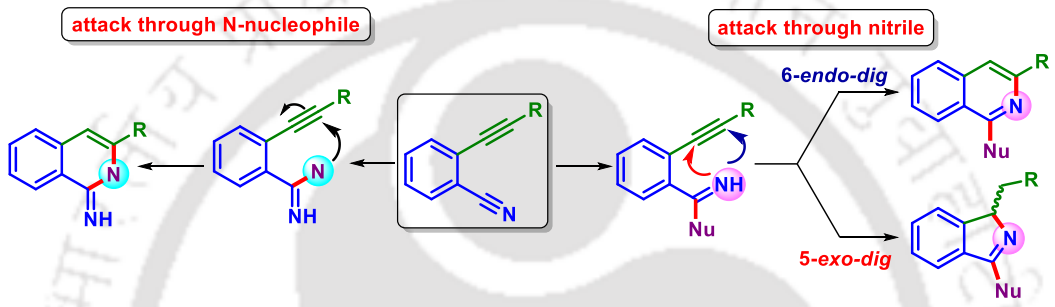

Scheme I.2.3.1. *Different approaches to access N-heterocycles from o-alkynylarylnitriles.*

I.3. Access to *N*-heterocycles via Photochemical Cascade Addition/Cyclization:

I.3.1. Access to *N*-heterocycles in the Presence of Photocatalyst via SET Process:

The construction of C–C and C–N bonds using photoredox catalysis has grabbed significant attention giving prominence to the nitrile functionality. In contrast, a radical is generated in the presence of photocatalysts (PC) in its excited state (PC*) via single electron transfer (SET) by the influence of visible light (Scheme I.3.1.1). The generated radical reacts to the cyano group to obtain an iminyl radical which subsequently underwent intramolecular cyclization to access *N*-heterocycles through a radical or a cationic species. The photocatalyst is further regenerated to its ground state either via oxidative quenching or reductive quenching cycle (Scheme I.3.1.1).

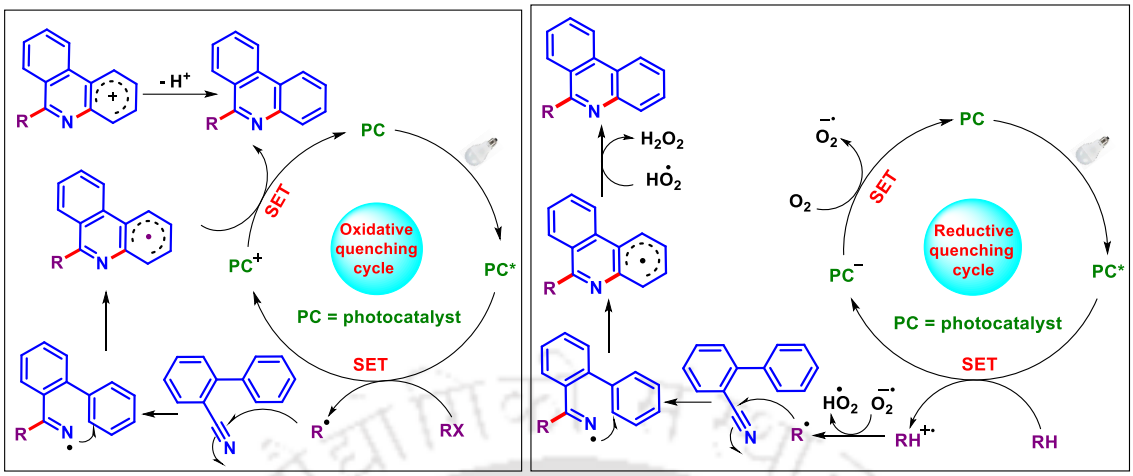

Scheme I.3.1.1. *Visible-light mediated radical addition to nitrile.*

I.3.2. Synthesis of *N*-heterocycles via Formation of Electron-Donor-Acceptor (EDA) Complex:

The formation of an electronically excited state upon the absorption of photons is a key feature of all photochemical processes. Despite the emerging exploration of photo redox catalysts in organic transformations, the potential of electron-donor-acceptor (EDA) complexes, which do not require an exogenous photosensitizer, has been progressively recognized recently. The interaction of an electron-rich substrate (D) with an electron-accepting molecule (A) leads to the formation of an electron-donor-acceptor (EDA) complex in the ground state which can absorb the visible light and eliminate the necessity for an external photocatalyst. However, the two components independently may not absorb visible light, but the resulting EDA complex does. This ground-state EDA complex by absorbing light can undergo a single electron transfer (SET) process from an electron donor to an electron acceptor producing a charge-separated state (Figure I.3.2.1). If the electron transfer has a sufficiently long lifetime, the charge-separated species can react in various ways through the *in-situ* generation of reactive radical species.

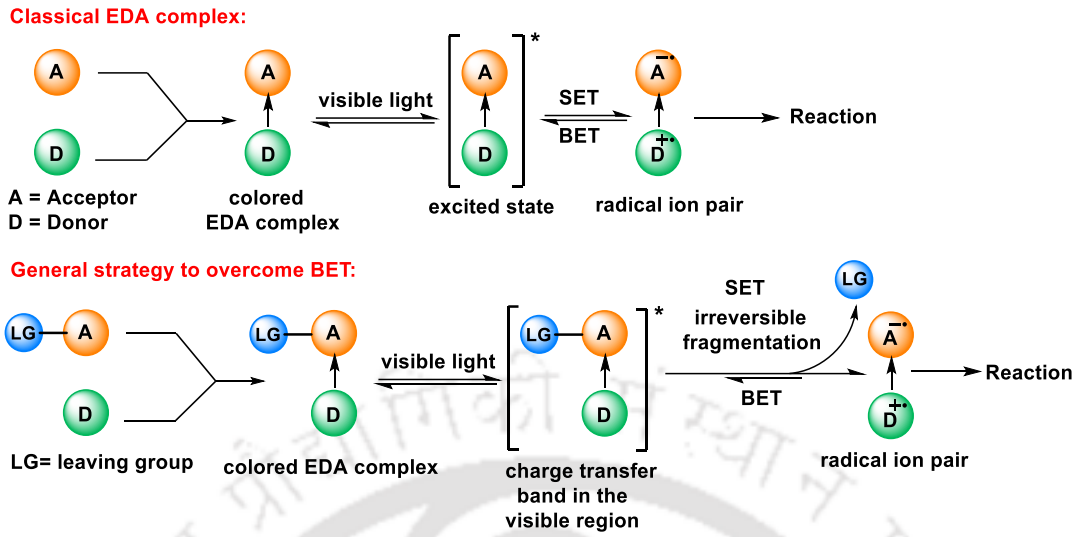

Figure I.3.2.1. *Schematical representation for the formation of the EDA complex.*

CHAPTER II. Visible-Light-Mediated Solvent-Switched Photosensitizer-Free Synthesis of Polyfunctionalized Quinolines and Pyridines

OL | Organic Letters

Org. Lett. **2023**, *25*, 471−476

pubs.acs.org/OrgLett Letter

This chapter describes a solvent-switched regio-divergent Pd(II)-catalyzed site-selective cascade addition/cyclization of (E)-2-(1,3-diarylallylidene)malononitrile and arylboronic acid to access 2,4,6-triarylnicotinonitrile and (Z)-2-aryl-4-styrylquinoline-3-carbonitrile under visible-light irradiation. This process is in two different solvents (2,2,2-trifluoroethanol (TFE) vs ethyl alcohol (EtOH)) switched synthesis of quinolines and pyridines is illustrated from (E)-2-(1,3-diphenylallylidene)malononitriles via a Pd(II)-catalyzed photochemical process. The active catalyst [L_2Pd(0)] generated serves as an exogenous photosensitizer. The process offers predominantly Z-alkenylated quinolines and pyridines in TFE and EtOH, respectively.

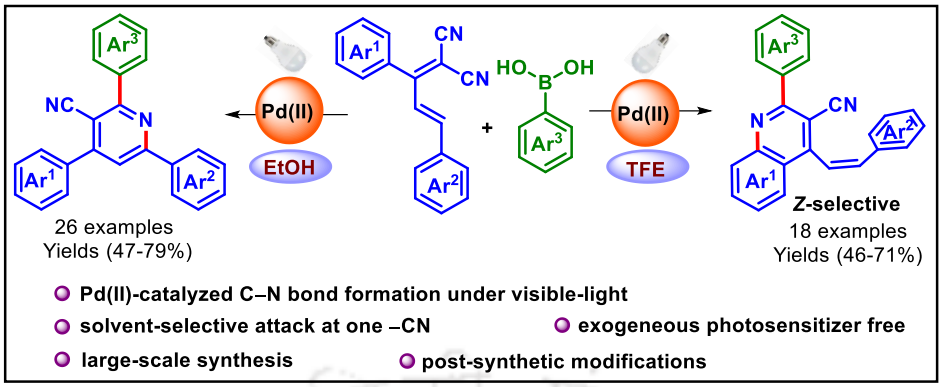

Scheme II.1. *Synthesis of quinoline and pyridine using nitrile.*

Next, this methodology was explored with various other dicyanodienes and boronic acids under the optimized reaction conditions. To understand the mechanistic path, several control experiments including, radical trapping, and a parallel and competitive KIE experiment were carried out.

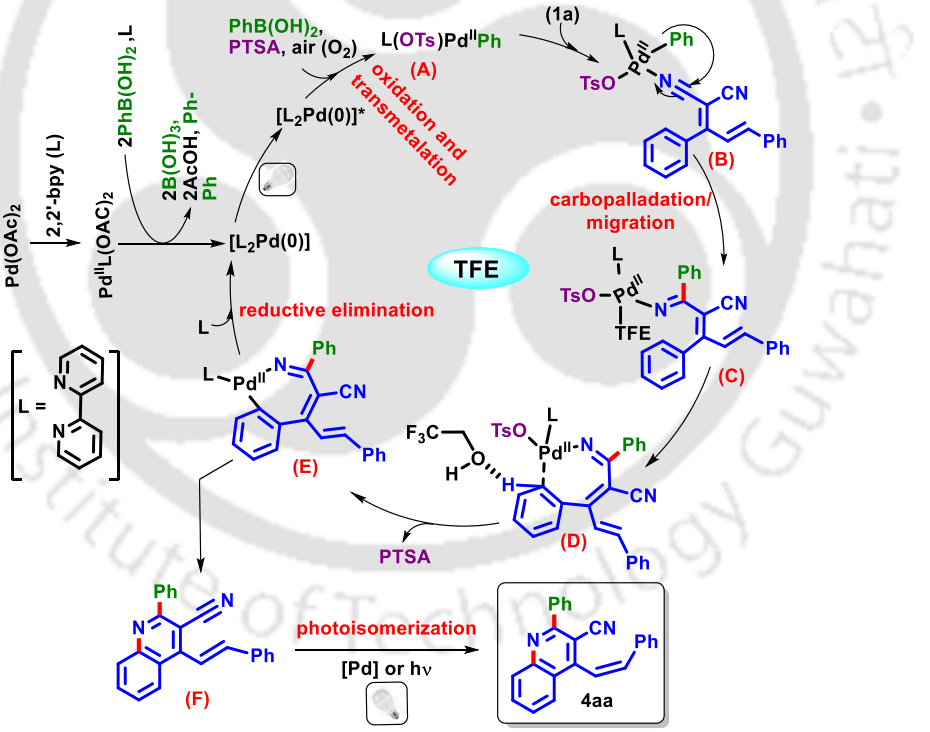

Scheme II.2. *Proposed reaction path in TFE.*

Based on the control experiments and previous literature reports a plausible mechanism is depicted (Scheme II.2 and Scheme II.3). Initially, $Pd(OAc)_2$ combines with ligand 2,2′-bpy (L) to form a $Pd(II)(bpy)(OAc)_2$ complex. Next, the reduction of this Pd(II)-complex in the

presence of phenylboronic acid and 2,2′-bpy generates [L_2Pd(0)] species (detected from HRMS) which via photoexcitation (a MLCT process confirmed by UV-experiments) form a [L_2Pd(0)]* species under visible-light irradiation. Furthermore, in the presence of air (O_2), [L_2Pd(0)]* undergoes oxidation followed by transmetalation with phenylboronic acid producing an aryl-Pd(II) intermediate (A) which is facilitated through M→Z σ-interaction between the Pd and the boron center. (confirmed by quenching experiments). The Pd(II) center of intermediate **A** coordinates with the nitrile group proximate to the phenyl ring of **1a** to give intermediate **B**. Next, the aryl ring migrates to the nitrile via an intramolecular carbopalladation to form a Pd-ketimine complex (**C**). Furthermore, the more electronegative TFE can accelerate the C–H metalation step via H-bonding and facilitate the metalation in polar acidic or fluorinated solvents (HFIP and TFE). Thus, the interaction of TFE enhances the electrophilicity of the *ortho* C–H bond through H-bonding thereby facilitating the cyclopalladation via the formation of a 7-membered metallacycle (**D**). This is then transformed to intermediate **E** with concurrent elimination of PTSA. Next, the reductive elimination of intermediate **E** delivers the *E*-alkenylated quinoline (**F**) and regenerates Pd(0). This *E*-alkenylated quinoline (**F**) undergoes photoisomerization in the presence of a Pd catalyst or induced by photoexcitation to afford the *Z*-alkenylated quinolone (**4aa**). Thus, the predominant formation of *Z*-isomer may be due to the low rotational energy barrier of the C=C double bond in the excited state (Scheme II.2).

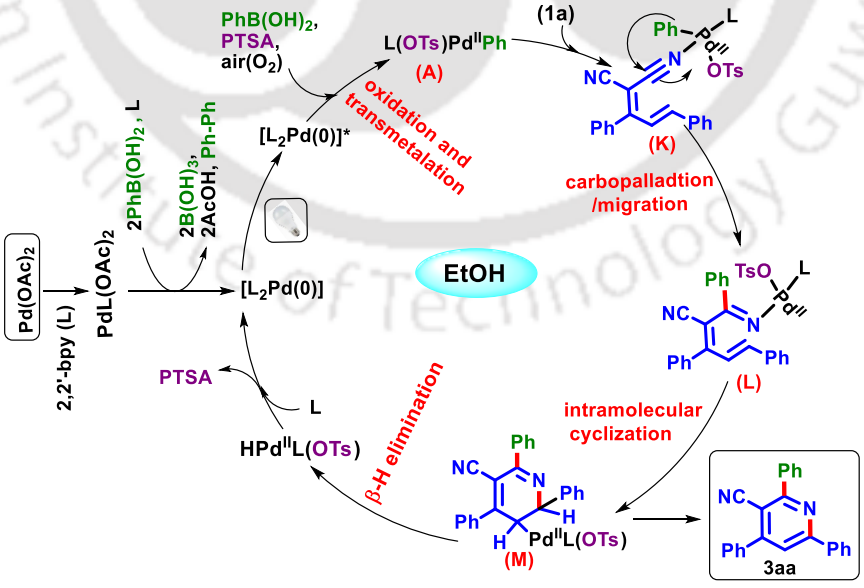

Scheme II.3. *Plausible reaction path in EtOH.*

Similarly, for the formation of pyridine in EtOH, the aryl palladium (**A**) coordinates with the nitrile group toward the olefinic *E*-double bond of **1a** to give intermediate **K**. Next, migration of the phenyl ring via carbopalladation gives intermediate **L**, which is followed by an intramolecular cyclization giving a six-membered Pd-complex (**M**). Finally, β-H elimination of intermediate (**M**) delivers pyridine (**4aa**) with the generation of HPd(II)L(OTs), which is easily transformed to Pd(0) with the elimination of PTSA (Scheme III.3).

CHAPTER III. Pd(II)-Catalyzed Three-Component Synthesis of Furo[2,3-*d*]pyrimidines from *β*-Ketodinitriles, Boronic Acids, and Aldehydes

OL | Organic Letters

Org. Lett. **2023**, *25*, 9070−9075

pubs.acs.org/OrgLett Letter

This chapter illustrates a Pd(II)-catalyzed three-component synthesis of 2,4,6-triarylfuro[2,3-d]pyrimidines from β-ketodinitriles, boronic acids, and aldehydes has been developed. The participation of both nitrile (–CN) groups led to the concurrent construction of furo-pyrimidine via the formation of C–C, C=C, C–O, C–N, and C=N bonds. The compounds show excellent photoluminescence properties with absorption maxima ranging from 348 to 387 nm and emission from 468 to 533 nm. The synthetic utility of the protocol was further demonstrated through a few postsynthetic manipulations.

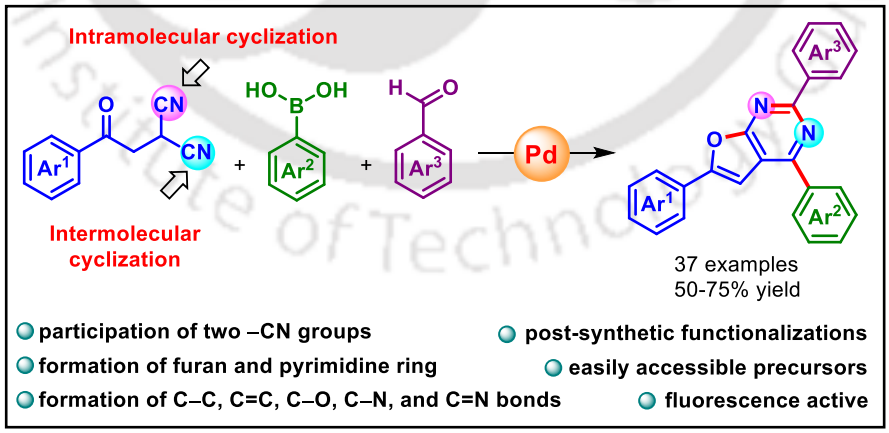

Scheme III.1. *Synthesis of furo[2,3-d]pyrimidines via the addition of boronic acid to nitrile.*

Having established the best-optimized conditions, the effect of substituents on β-ketomalononitriles, boronic acids, and aldehydes was studied. Based on the experimental findings and the literature reports, a plausible reaction pathway is depicted in Scheme III.2. Initially, the β-ketodinitrile (**1**) undergoes an acid-catalyzed enolization in the presence of PTSA·H_2O to afford intermediate **I**. Intermediate **I** then undergoes further acid-catalyzed intramolecular cyclization to afford a five-membered cyclic intermediate **1′** that reacts with benzaldehyde **a′** to form imine intermediate **1a′**. The nitrile group of imine **1a′** then coordinates with aryl-Pd(II) complex (**B**) (which is formed via transmetalation of Pdcatalyst **A** and phenylboronic acid **a**) to form an intermediate **C**. Carbopalladation of intermediate **C**, followed by migration of the phenyl group to the nitrile generates Pd-ketimine complex **D**, which underwent an intramolecular cyclization giving cyclic intermediate **E**. Finally, aromatization via β-H elimination of intermediate **E** afforded furo-pyrimidine **1aa′** and regenerates the Pd catalyst for the next catalytic cycle.

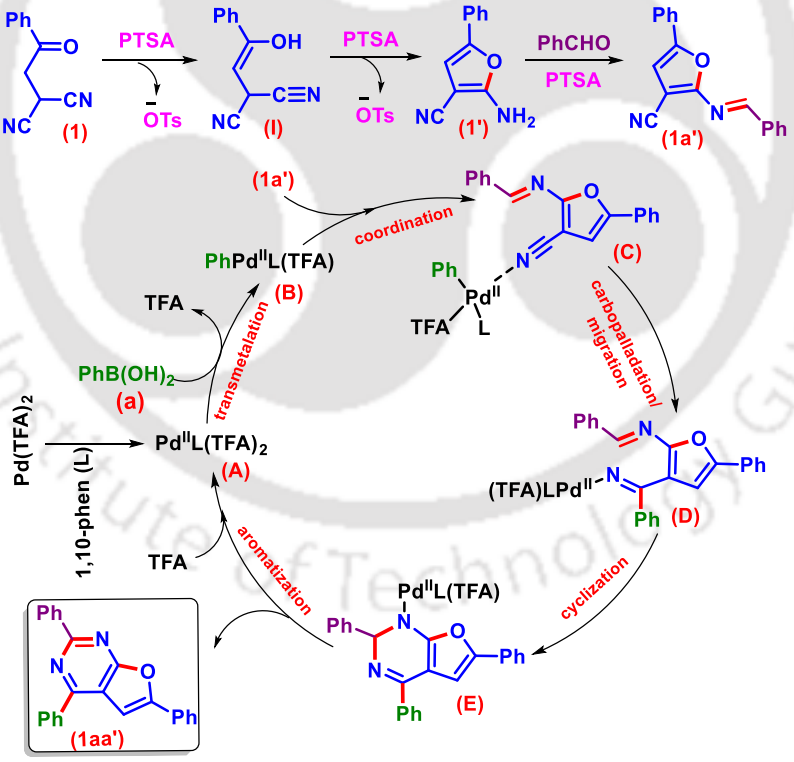

Scheme III.2. *Proposed reaction pathway.*

CHAPTER IV. A Cascade Synthesis of Furo-Pyrrolo-Pyridines via Pd(II)-Catalyzed Dual N−H/C Annulative-Cyclization

Chemistry A European Journal
Chemistry Europe
European Chemical Societies Publishing

Chem. -Eur. J. **2024,** e202403470

This chapter focuses on a Pd(II)-catalyzed non-template synthesis of furo[2,3-b]pyrrolo[2,3-d]pyridines from β-ketodinitriles and buta-1,3-diynes has been accomplished via dual annulative cyclization. The participation of both the nitrile (–CN) groups led to the concurrent construction of three heterocycles viz. furan, pyrrole, and pyridine forming C–C, C=C, C–O, C–N, and C=N bonds in one pot. The synthetic utility of the protocol was further demonstrated through a few post-synthetic manipulations.

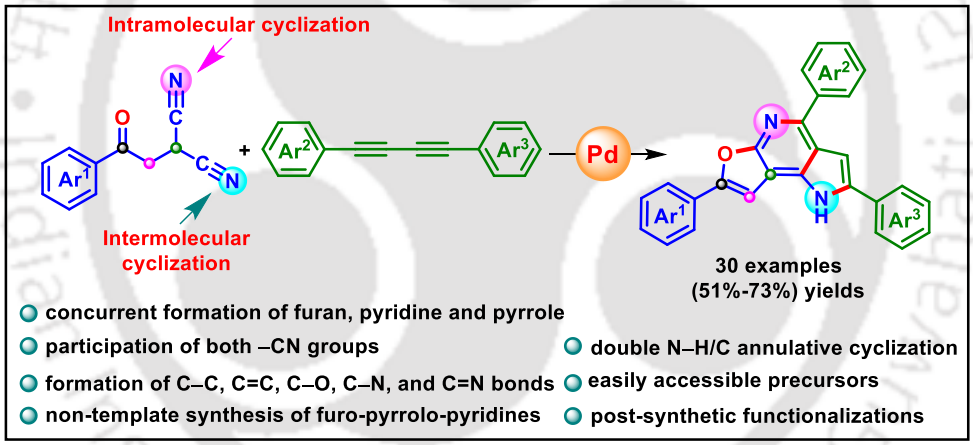

Scheme IV.1. *Synthesis of furo-pyrrolo-pyridines via insertion of alkyne to nitrile.*

With the best-optimized conditions, the effect of substituents on β-ketodinitriles and diynes was tested. Next, several control experiments were carried out to elucidate a plausible reaction mechanism for this Pd(II)-catalyzed cascade cyclization. Based on the experimental findings and from the literature reports, a plausible mechanistic pathway has been depicted in Scheme IV.2. In the presence of $TsOH{\cdot}H_2O$, β-ketodinitrile (**1**) undergoes an acid-catalyzed enolization to afford an enol-intermediate (**I**) which on intramolecular cyclization (5-*exo*-dig) afforded a five-membered cyclic furan intermediate (**1′**). Next, the amino group of intermediate (**1′**) participates in a deprotonative coordination with the *in situ* generated Pd(II) complex (**A**)

[which is formed via coordination of $Pd(OAc)_2$ with ligand 1,10-phenanthroline (L)] to form intermediate (**B**) with elimination of AcOH. Next, one of the alkyne sides of the diyne (**a**) is inserted into the N atom, giving an alkynyl Pd(II) intermediate (**C**). Subsequently, the intermediate (**C**) undergoes an intramolecular insertion (6-*exo-dig*) to the nitrile through a carbopalladation, giving an imine Pd complex to construct a pyridine ring (**D**). Next, the imine Pd-complex (**D**) endures an intramolecular 5-*endo-dig* cyclization via aminopalladation with another alkyne side to give a Pd-bound furo-pyrrolo-pyridine intermediate (**E**). Finally, protonolysis followed by aromatization of intermediate **E** afforded the furo-pyrrolo-pyridine (**1a**) and regenerates the Pd-catalyst (**F**) for the next catalytic cycle.

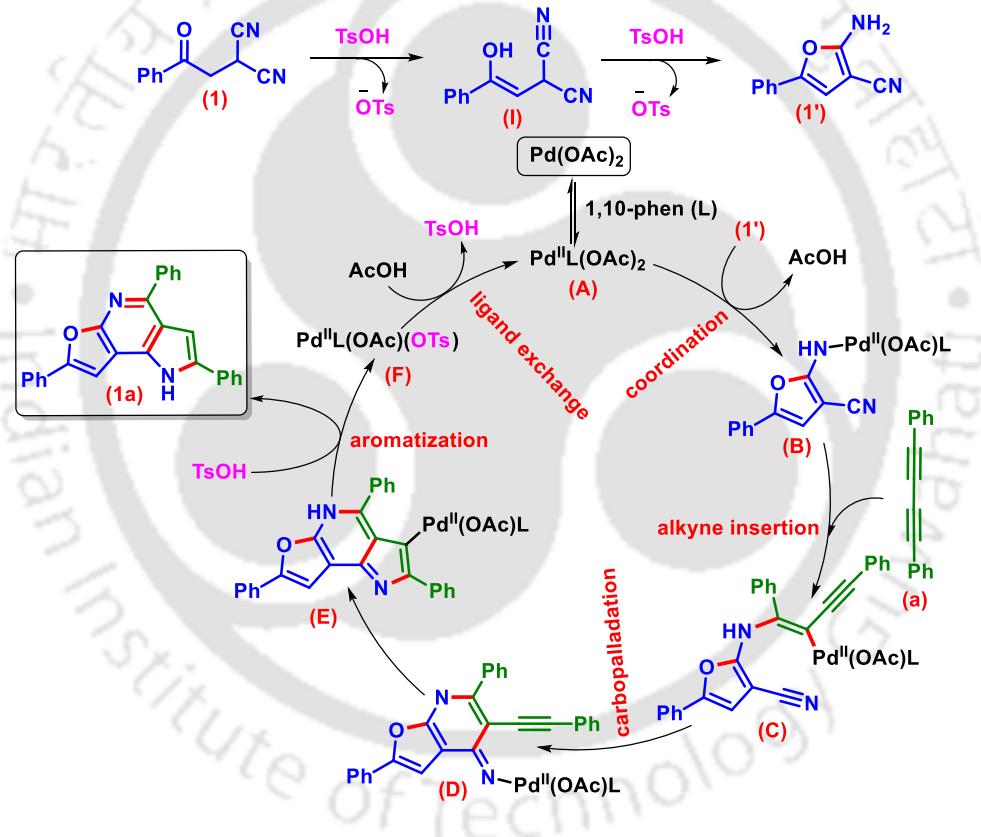

Scheme IV.2. *Proposed reaction pathway.*

CHAPTER V. Visible-Light Driven Electron-Donor-Acceptor (EDA) Complex Initiated Synthesis of Thio-functionalized Pyridines

ChemComm *Chem. Commun.* **2023**, *59*, 7990–7993

ROYAL SOCIETY OF CHEMISTRY

COMMUNICATION View Article Online View Journal | View Issue

This chapter demonstrates a visible/solar-light-induced electron-donor-acceptor (EDA) aggregated/mediated radical cyclization between (E)-2-(1,3-diarylallylidene)malononitriles and thiophenols lead to poly-functionalized pyridines. The two reacting partners form an EDA complex that absorbs light and triggers the single-electron transfer (SET) to generate thiol radical which undergoes addition/cyclization with dicyanodiene through the formation of C–S and C–N bonds.

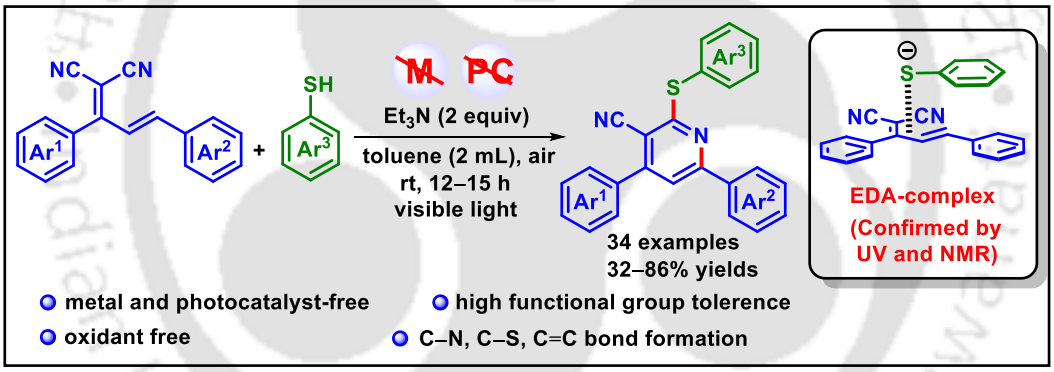

Scheme V.I. *Synthesis of thio-functionalized pyridine via EDA complex.*

A few experiments including radical trapping, and reaction in the N_2 atmosphere, were conducted to depict a plausible mechanistic pathway. The formation of EDA complex between (**1**), thiophenol (**a**), and Et_3N in toluene has been confirmed by the appearance of a light-yellow color upon mixing and a progressive red shift in the visible region. To find further evidence for the EDA complex formation, ^{19}F nuclear magnetic resonance (^{19}F NMR) measurements were carried out between (*E*)-2-(1-(4-fluorophenyl)-3-phenylallylidene)malononitrile (**4**) and thiophenol (**a**). The chemical shift of the –F group of (**4**) distinctly moved downfield with increasing ratios of (**a**) and Et_3N.

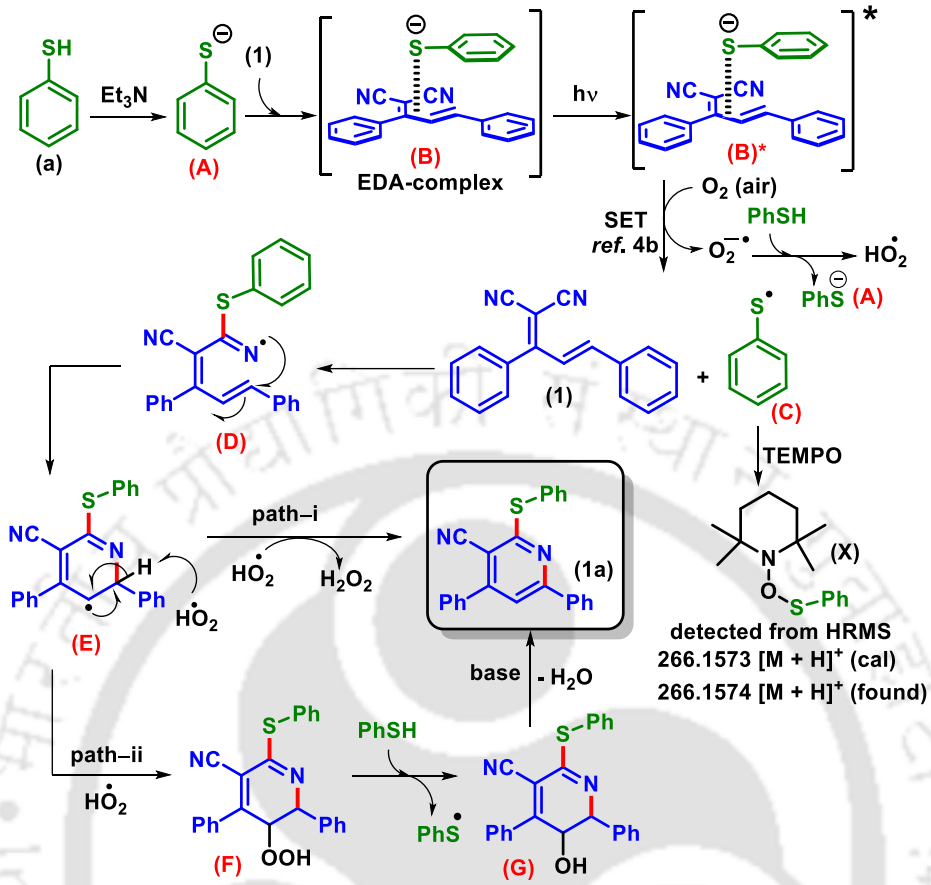

Scheme V.2. *Plausible reaction mechanism.*

Based on the experimental results and previous literature reports a plausible mechanism is outlined in Scheme V.2. Initially, the thiolate ion (**A**) is formed in the presence of Et_3N, which interacts with the dicyanodienes (**1**) to generate an EDA complex (**B**), which exhibits strong absorption in the visible-light region (λ_{max} = 414 nm). Under visible-light irradiation, the EDA complex (**B**) is excited to complex (**B***) which transfers an electron to O_2 and generates a superoxide radical anion $O_2^{\bullet-}$ and a thiol radical (**C**) (detected from HRMS of its TEMPO-adduct). This radical anion $O_2^{\bullet-}$ reacts further with another molecule of thiophenol (**a**) to generate a thiolate anion (**A**) and $HO_2^{\bullet}$ radical. Next, the thiol radical (**C**) attacks one of the nitrile groups of **1** to produce an iminyl radical (**D**), which on intramolecular (6-*endo*-trig) cyclization generates a carbon-centered radical intermediate (**E**). The final product **1a** can be obtained by any of the two possible pathways. In path-i, aromatization of intermediate (**E**) through a proton abstraction by $HO_2^{\bullet}$ affords the thiopyridine **1a** (H_2O_2 detected by Mohr's salt).

In path-ii, the intermediate (**E**) reacts with the *in situ* generated $HO_2^{\bullet}$ radical to provide a hydroperoxide intermediate (**F**). This is then followed by cleavage of the peroxide bond and abstraction of a proton from thiophenol (**a**) to provide an intermediate (**G**). Finally, loss of water from intermediate **G** in the presence of the base leads to (**1a**).

CONTENTS

CHAPTER I

An Overview of Accessing N-Heterocycles via Thermal and Photochemical Approaches Using Nitrile (C≡N) Functionality

भारतीय प्रौद्योगिकी संस्थान गुवाहाटी
Indian Institute of Technology Guwahati

CHAPTER I

An Overview of Accessing *N*-Heterocycles via Thermal and Photochemical Approaches Using Nitrile (C≡N) Functionality

I.1. Introduction:

Nitrogen heterocycles are a significant class of organic compounds possessing at least one nitrogen atom incorporated within a ring structure. These nitrogen-containing heterocycles are prevalent in natural products, pharmaceuticals, and materials science due to their diverse chemical and biological properties. They play crucial roles in drug discovery, serving as key components in drugs targeting various diseases. *N*-heterocycles exhibit a wide range of physical properties, making them valuable in materials science for applications such as dyes, polymers, and electronic materials. Developing efficacious synthetic procedures to access various nitrogen heterocycles is one of the most important research areas in synthetic chemistry. *N*-heterocycles such as pyrroles,[1] pyrimidines,[2] pyridines,[3] quinolines,[4] indoles,[5] imidazoles,[6] isoquinolines/isoquinolones,[7] furopyrimidines,[8] imidazopyridines,[9] furopyridines,[10] triazoles,[11] quinazolines/quinazolinones,[12] and other fused *N*-heterocycles[13] (Figure I.1.1) unquestionably are the molecular frameworks of an extensive range of natural products and having high biological potential. Furthermore, *N*-heterocyclic compounds have also been found to be significant intermediates in organic synthesis and pharmaceutical industries, particularly as antibacterial, antifungal, antiviral, anticancer, and anti-inflammatory agents.[14] Additionally, the versatility, stability, and unique electronic properties of *N*-heterocycles make them indispensable in material chemistry.[15] They have essential applications in light-emitting diodes (OLEDs), organic semiconductors, organic photovoltaic cells, luminescent materials, liquid crystal displays (LCDs), sensors and imaging, and numerous other multifaceted applications.[15]

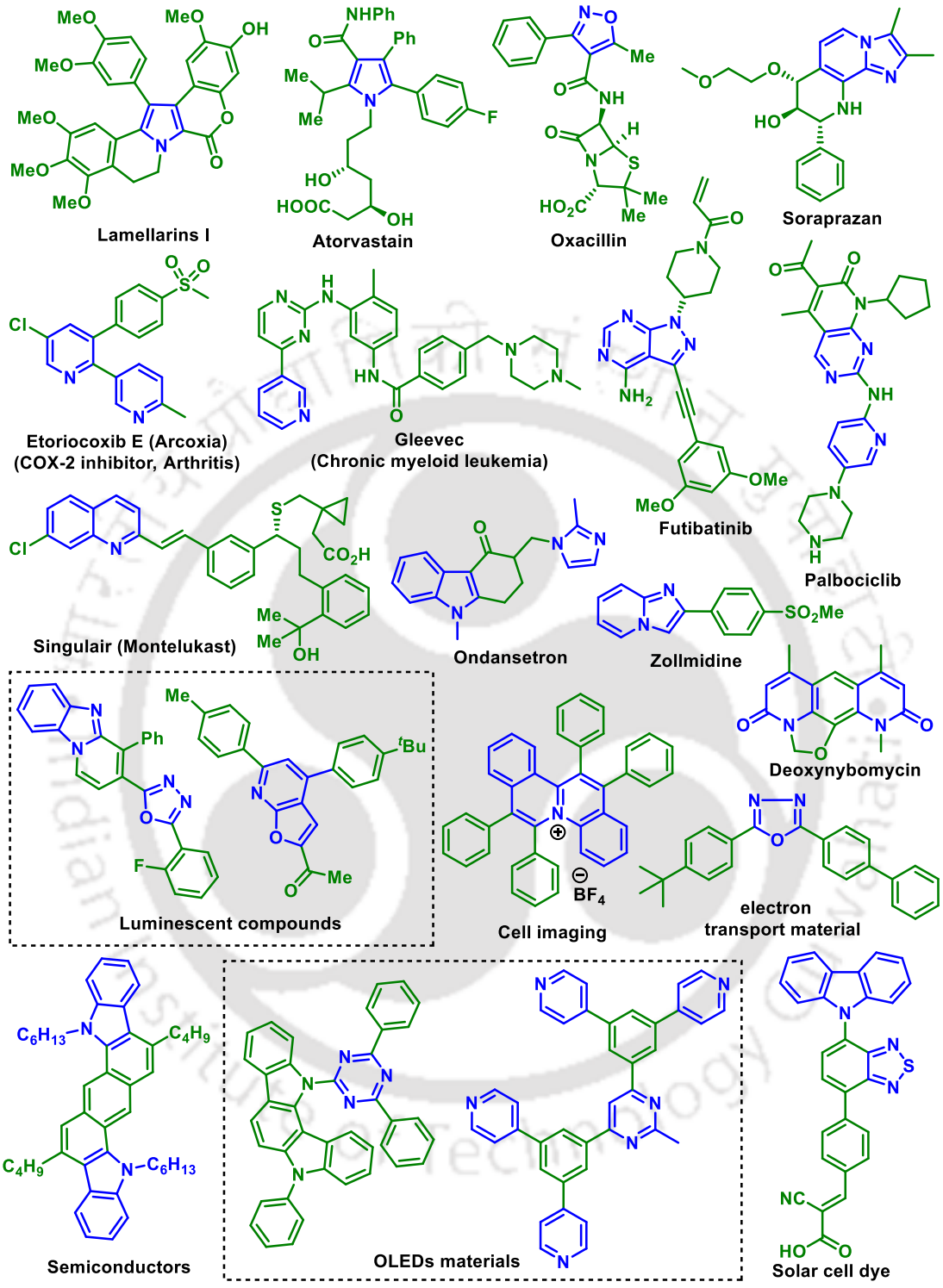

Figure I.1.1. *Some bio-active and functional materials containing N-heterocycles.*

Among the various established methods, synthesizing nitrogen-heterocycles using nitrile functionality is of great interest and represents an exciting aspect of thermal and photochemical processes. The cyano (–C≡N) group generally serves as the most important precursor for various functional groups and intermediates such as imines, ketones, amides, acids, amines, and aldehydes. Additionally, it functions as a directing group in C–H functionalizations and serves as a radical acceptor in radical cascade reactions.[16] The transformation of nitriles into other functional groups mostly occurs via hydrolysis, reduction, and nucleophilic addition, under metal and metal-free conditions.[16] These transformations exploit the electrophilic reactivity of the carbon center in the cyano group, the nucleophilic nature of the nitrogen atom due to its lone electron pairs, and the π-coordination site of the C≡N triple bond. Due to the polar unsaturated C≡N triple bond, nitriles easily transform to carbonyl, amine, imine, amide, and acid functionalities. Furthermore, cyclization with appropriate functional groups, particularly with keto or amine groups, or via intramolecular amination using –Br or –I group, or amination of the C–H bond, leads to the formation of diverse *N*-heterocycles (Figure I.1.2). In contrast, intermolecular [2 + 2 + 2], [2 +2 + 1], [3 + 2], and [4 + 2] cycloadditions of nitriles with alkynes or azides yield pyridines, oxazoles, pyrazoles or tetrazoles without shifting functional groups, integrating the nitrogen atom of the nitrile into these heterocycles (Figure I.1.3). Therefore, the presence of nitrile group presents a captivating and evolving opportunity for constructing *N*-heterocyclic moieties after being appropriately functionalized or activated within an organic compound.

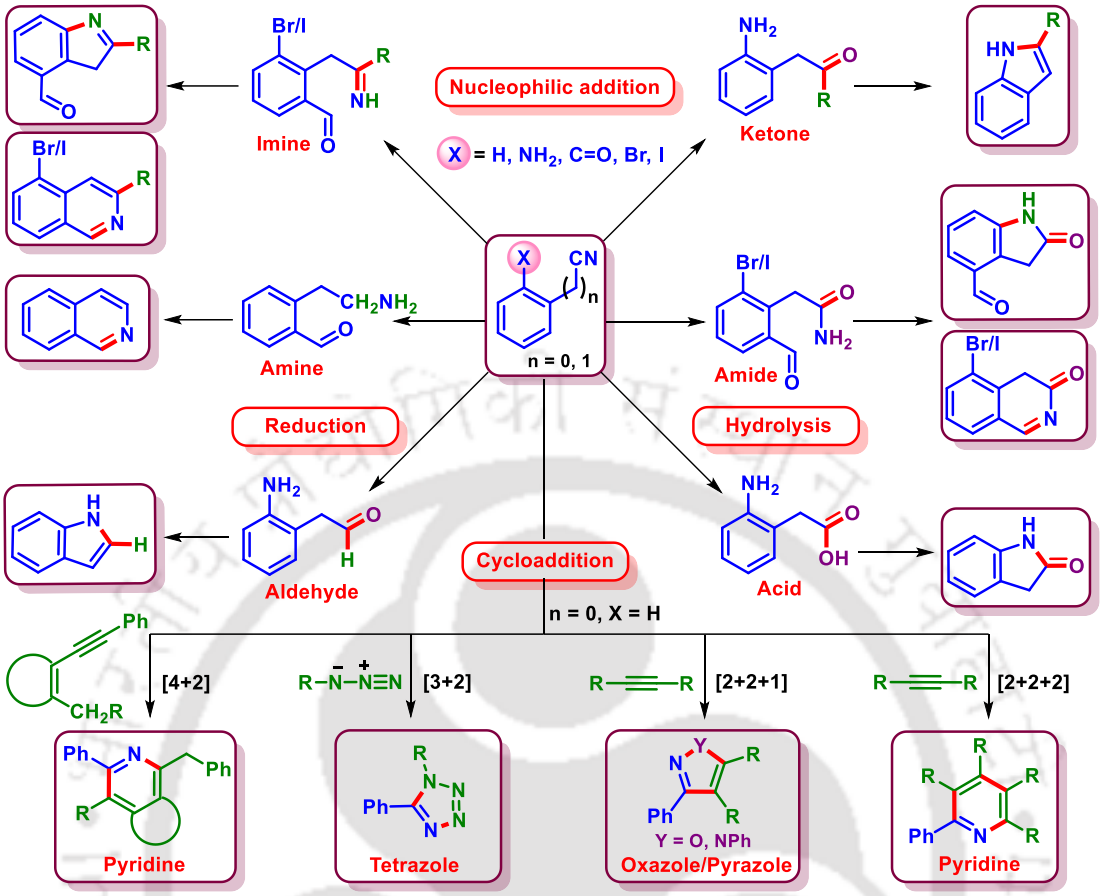

Figure I.1.2. *Transformation of nitrile to other functionalities and N-heterocycles.*

One of the most cost-effective and straightforward methods to introduce nitrile functionality is through the use of malononitrile, which serves as a precursor to design compounds like (*E*)-2-(1,3-diphenylallylidene)malononitrile (dicyanodiene) and 2-(2-oxo-2-phenylethyl)malononitrile (β-ketodinitrile) (Figure I.1.3). These precursors feature an olefinic bond and a keto group in proximity to the nitrile functionality. Consequently, these synthetic intermediates are highly valuable for the synthesis of *N*-heterocycle.

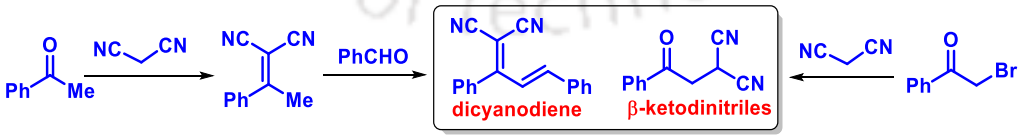

Figure I.1.3. *Synthesis of dicyanodiene and β-ketodinitrile.*

The exploration of these compounds in thermal and photochemical approaches remains relatively limited in the literature. Here, we provide a few reports that utilize both dicyanodiene and β-ketodinitriles for the construction of nitrogen heterocycles, oxygen heterocycles, and

carbocycles.[17] For example, in 2013, Dong's group developed a straightforward and effective method to synthesize substituted 2-aminopyridines through a formal [5 + 1] annulation strategy of 2,4-pentadienenitriles with aqueous NH_2OH (Scheme I.1.1).[17a] The protocol involves a successive aza-nucleophilic addition of hydroxylamine to the olefinic bond, followed by an intramolecular aza-cyclization and dehydration leading to the formation of functionalized pyridines. This reaction combines both the formation and modification of the 2-aminopyridine moiety, thereby enhancing the diversity of pyridines using readily accessible starting materials.

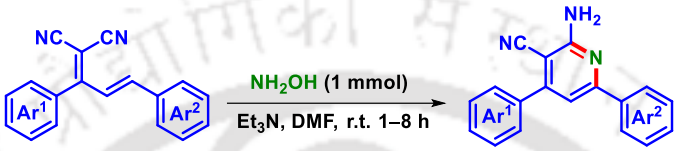

Scheme I.1.1. *Synthesis of functionalized pyridines from dicyanodienes.*

In 2013, Huang's group developed a sequential [2 + 3] and [3 + 2] annulation reaction of allene and γ-substituted allenoates to access bicyclic [3,3,0]octenes in the presence of phosphine-catalyst (Scheme I.1.2).[17b] The reaction involves the activation of three active sites of the γ-substituted allenoate, followed by sequential [2 + 3] and [3 + 2] annulations facilitated by a phosphine catalyst.

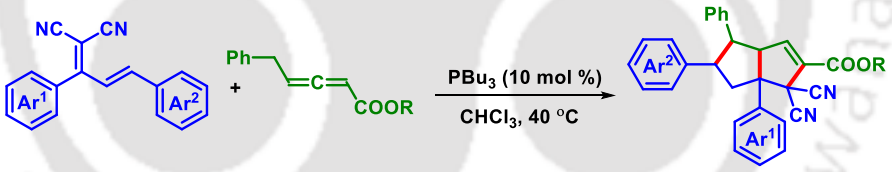

Scheme I.1.2. *Phosphine-catalyzed [2 + 3] and [3 + 2] annulations.*

In the same year, He *et al.* established a phosphine-catalyzed [4 + 1] annulation involving 1,1-dicyano-2,4-diaryl-1,3-dienes with allylic derivatives, specifically ethoxycarbonyl-activated allylic acetate (Scheme I.1.3).[17c] This method efficiently constructs polysubstituted cyclopentenes, yielding moderate to excellent yields of the products. The strategy can also be achieved through regioselective [3 + 2] annulations, utilizing dienes as C2 units by selecting differently substituted substrates.

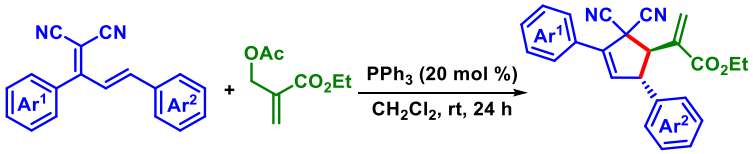

Scheme I.1.3. *Phosphine-catalyzed [4 + 1] annulation.*

In the same year, Chen's group disclosed a chemo-, stereo-, and γ,δ-regioselective exo-Diels-Alder cycloaddition strategy by using electronically deficient β-substituted 2,4-dienes and 2,4-dienals through activation of trienamine (Scheme I.1.4).[17d]

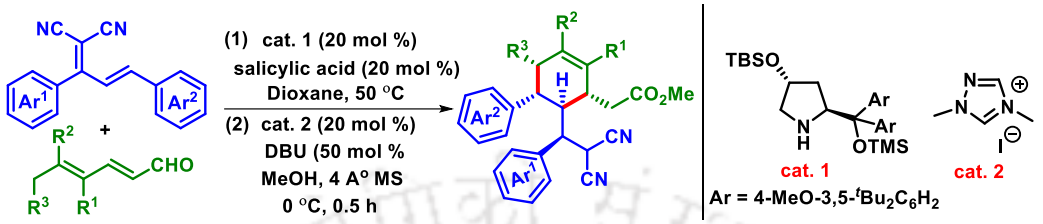

Scheme I.1.4. *Exo-Diels-Alder cycloaddition by using dicyanodiene.*

In 2016, a [1 + 4] annulation reaction of α-dicarbonyl compounds with 1,1-dicyano-1,3-dienes was established by Zhou and coworkers (Scheme I.1.5).[17e] In this strategy, the reaction involves cyclopropanation, base-catalyzed cyclopropane rearrangement followed by [1 + 4] annulation involving Kukhtin–Ramirez adducts enabling to construction of cyclopentenimines and cyclopentenones.

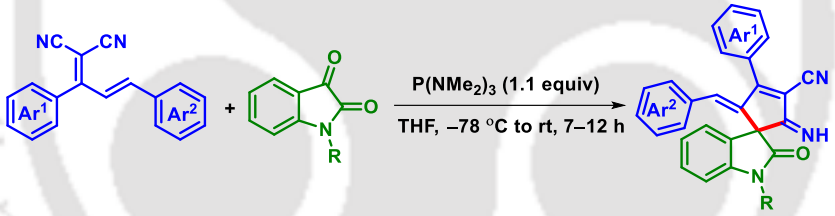

Scheme I.1.5. *Synthesis of cyclopentenimines via [1 + 4] annulation using dicyanodiene.*

In 2017, Zhang *et al.* established a phosphine-catalyzed [4 + 2] cycloaddition of an electronic deficient diene, alkyl vinyl ketone, and dicyanodiene to synthesize functionalized cyclohexenes (Scheme I.1.6).[17f] This protocol yielded an extensive range of cyclohexenes in moderate to good yields.

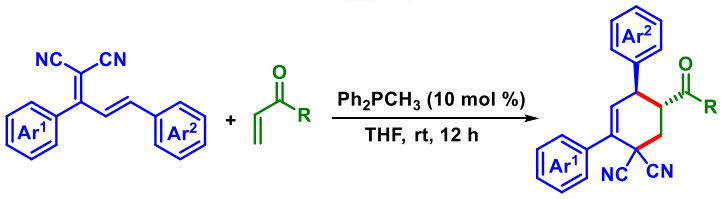

Scheme I.1.6. *Phosphine-catalyzed [4 + 2] cycloaddition to synthesize functionalized cyclohexenes.*

In 2018, Han and co-workers established a reaction to synthesize functionalized cyclopentenes via cycloaddition of β-ketodinitriles with electronic deficient nitro-olefins (Scheme I.1.7).[18a] In this protocol, TBAF (tetrabutylammonium fluoride) assists the reaction as an organocatalyst, facilitating the synthesis of diastereoselective cyclopentenes having a quaternary allylic carbon center that carries both carboxamide and nitrile groups.

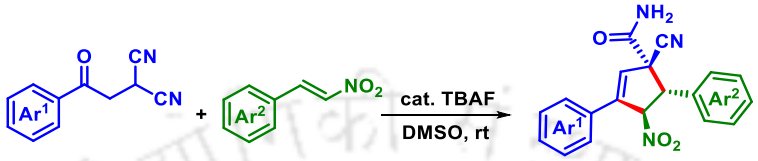

Scheme I.1.7. *Access to functionalized cyclopentenes using β-ketodinitriles.*

In 2019, Ban and Song's group reported a diastereoselective approach for synthesizing cyclopentenes containing a chiral quaternary center (Scheme I.1.8).[18b] Herein, the protocol is initiated via a thiosquaramide-catalyzed Michael–Henry reaction of nitroolefins and β-ketodinitriles, forming products with good yields and excellent diastereoselectivity.

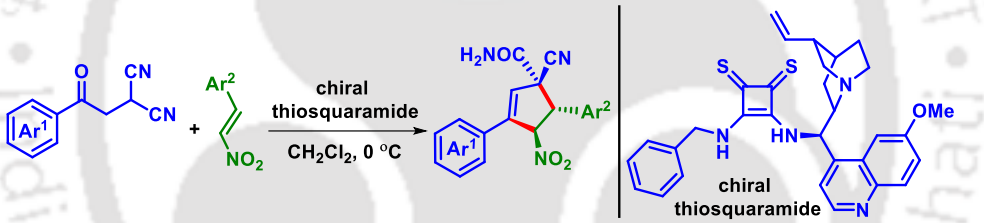

Scheme I.1.8. *Access to substituted cyclopentenes using β-ketodinitriles.*

In 2020, a similar Pd(II)-catalyzed reaction was described by Yu and co-workers for the formation of functionalized 1*H*-pyrrole-3-carbonitriles via an addition/ cyclization reaction of arylboronic acids to β-ketodinitriles through the construction of C–N bond (Scheme I.1.9).[18c]

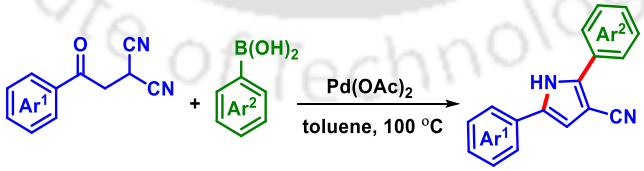

Scheme I.1.9. *Pd(II)-catalyzed synthesis of functionalized pyrroles using β-ketodinitriles.*

In 2022, Li and coworkers developed a diastereoselective annulation strategy to access functionalized fused cyclopentenes containing a cyano-substituted all-carbon quaternary center using phenacylmalononitriles and maleimides (Scheme I.1.10).[18d] The mechanistic investigation

reveals that the reaction involves tandem Michael addition/aldol/rearrangement of maleimides and phenacylmalononitriles leading to the fused cyclopentenes.

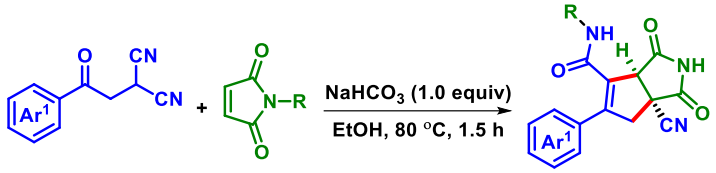

Scheme I.1.10. *Access to bicyclic cyclopentenes using β-ketodinitriles.*

In the same year, Xiong's group also established a visible-light-mediated eosin Y-catalyzed cascade phosphinoylation/cyclization to access 5-phosphoryl-functionalized pyrroles using phenacylmalononitriles and secondary *H*-phosphine oxides (Scheme I.1.11).[18e] Herein, the protocol discloses a photo-induced selective addition of phosphorous radical to one of the –CN groups of β-ketodinitrile, followed by a nucleophilic addition and aromatization, leading to the construction of C(sp^2)–P bonds.

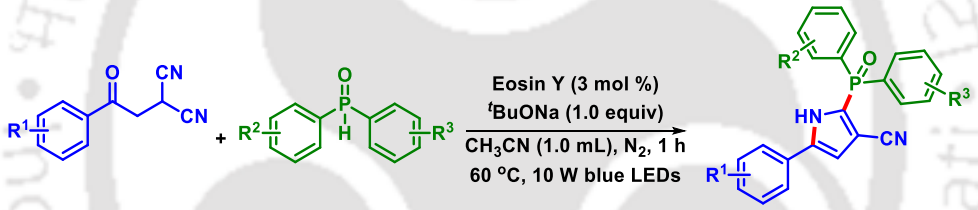

Scheme I.1.11. *Metal-free synthesis of phosphoryl-functionalized pyrroles using β-ketodinitriles.*

This thesis report comprises different methodologies representing the construction of *N*-heterocycles from dicyanodiene and β-ketodinitrile under thermal and photochemical conditions. These methodologies focus on the formation of C–C, C=C, and C–N bonds and cover the following aspects:

I.2. Transition-metal-catalyzed synthesis of *N*-heterocycles via cascade addition/cyclization to nitrile.

I.3. Access to carbo and nitrogen-heterocycle via alkyne insertion into the nitriles.

I.4. Access to *N*-heterocycles via photochemical cascade addition/cyclization.

I.2. Transition-Metal-Catalyzed Synthesis of *N*-heterocycles via Cascade Addition/Cyclization to Nitrile:

Cascade cyclization is a class of chemical reactions where sequential reactions are performed in the same pot and the product of the first reaction is the substrate for the subsequent steps and so on. A cascade method, also recognized as a domino or tandem reaction, involves the synthesis of organic molecules through the stepwise construction of individual bonds in the target molecule. However, forming several bonds in a single sequence is made much more efficient without isolating the intermediates, varying reaction conditions, or adding reagents.[19]

Cascade strategies contribute significantly to both the science and art of total synthesis, offering improved practical efficiency and enhancing the aesthetic appeal of synthetic planning. Cascade reactions have not only succeeded in the realm of total synthesis[20] but have also garnered attention in organic methodologies. In recent years, cascade addition/cyclization has emerged as a highly attractive approach for constructing a wide range of *N*-heterocycles.[21] In this regard, transition metal-catalyzed thermal or photochemical cascade addition/cyclizations using nitriles (–CN), have been recognized to be effective for constructing a diverse range of *N*-heterocycles via the construction of C–C and C–N bonds. Among the various cascade methods, we will explore several approaches for synthesizing diverse *N*-heterocyclic compounds using different nitrile compounds, categorized as follows:

I.2.1. Transition-metal-catalyzed nucleophilic/electrophilic cascade addition/cyclization

I.2.2. Transition-metal-catalyzed radical cascade addition/cyclization

I.2.1. Transition Metal-Catalysed Cascade Addition/Cyclizations:

Cascade addition/cyclizations in the presence of metal catalysts using nitrile (–CN) functionality represent a significant strategy in organic synthesis for producing a diverse range of *N*-heteroarenes. These reactions enable the efficient formation of multifaceted molecular frameworks by sequentially forming multiple bonds in a single operation. By harnessing the versatile reactivity of nitrile groups, these catalytic processes facilitate the construction of different *N*-heterocycles and other structurally complex molecules. Several transition metals such as Pd, Cu, Mn, Ni etc. have been frequently used in nitrile-triggered reactions. The transformations can proceed either via nucleophilic/electrophilic or free radical mechanisms. Most of the commonly reported addition reactions of nitriles can be classified into three general

categories. In these reactions, the transformation of the nitrile group to an iminyl group (C=N) occurs via the addition reaction: (a) utilizing the σ-coordination of nitrogen to the metal, acting as a Lewis acid, (b) via transition metal-catalyzed 1,2-insertion, or (c) through *in situ* generation of a radical in the presence of transition metals, followed by subsequent cyclization (Figure I.2.1.1).

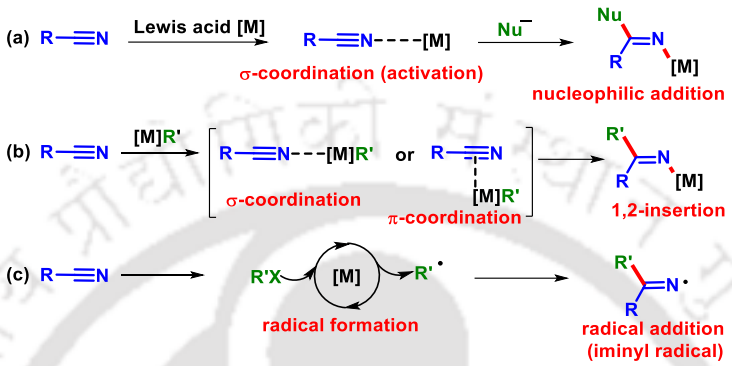

Figure I.2.1.1. *Transition-metal-catalyzed addition to nitrile.*

The carbometallation strategy using nitrile functionality is shown in Figure I.2.1.2. Initially, an aryl-metal species is formed via the transmetallation of other coupling partners with the transition metal. In the next step, coordination followed by the addition of the aryl group via carbometallation of nitrile delivers an imine or ketone, and the metal catalyst is regenerated. Finally, ketone or imine is involved in cyclization with the proximal amine or keto group of the starting nitrile compounds providing heterocycles.

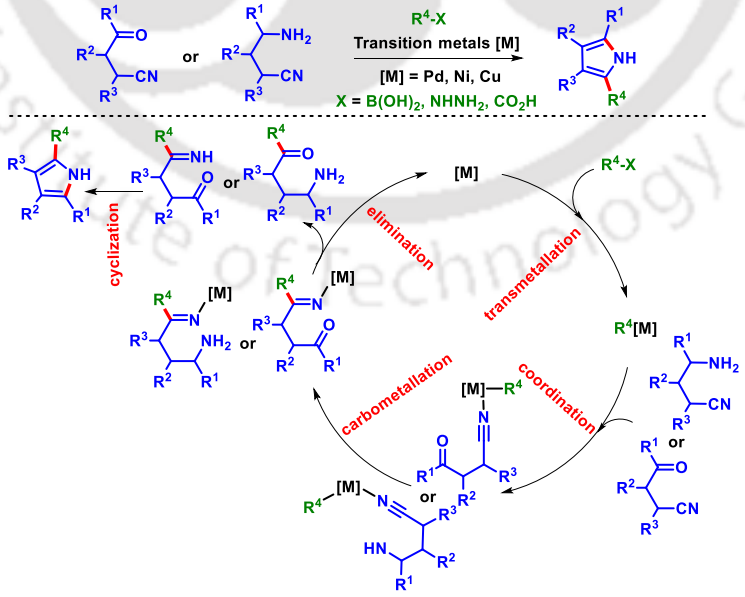

Figure I.2.1.2. *General mechanism to access N-heterocycles via carbometallation of nitriles.*

I.2.1.1. Transition-Metal-Catalyzed Nucleophilic/Electrophilic Cascades:

In nucleophilic and electrophilic cascade reactions, several coupling partners such as Grignard reagent, amine, arylboronic acids, aryl iodides, indoles, aryl carboxylic acid, and arylhydrazines have been explored to synthesize *N*-heteroarenes. In this process, the nitrile group acts as an electrophilic partner and undergoes addition with aryl nucleophiles generated from the coupling partners.

Li and coworkers revealed a method to access 3,4-dihydroquinazolines and quinazolines through a Cu(II)-catalyzed cascade addition/cyclization of aromatic nitriles with 2-aminobenzylamines followed by oxidation in the presence of molecular oxygen (Scheme I.2.1.1.1).[22] Herein, the dual catalytic function of a copper catalyst involves both cascade coupling and aerobic oxidation, with oxygen used as the terminal oxidant.

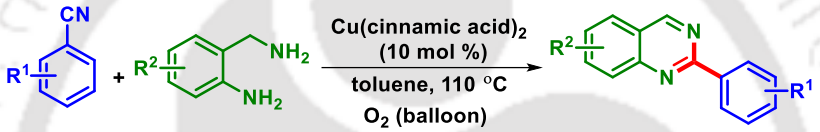

Scheme I.2.1.1.1. *Access to quinozalines from nitriles in presence of Cu(II)-catalyst.*

Recently, Dutta's group developed a Pd-catalyzed dual annulation strategy for accessing *N*-6-functionalized norcryptotackieines, involving amphipathic amines, 2-iodobenzyl cyanide, and variously functionalized 2-bromobenzaldehydes (Scheme I.2.1.1.2).[23] The reaction sequence includes an intermolecular followed by an intramolecular amination, efficiently producing the products.

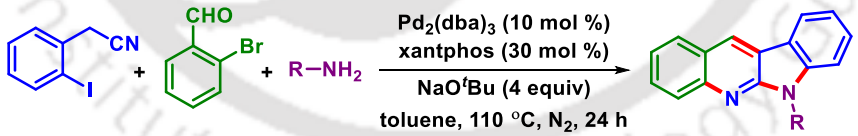

Scheme I.2.1.1.2. *Pd-catalyzed one-pot annulation strategy using nitriles.*

In 2014, Hsieh and coworkers reported a Cu(I)-mediated synthesis of substituted phenanthridines *via* an addition reaction of Grignard reagent to the cyano group followed by an intramolecular cyclization (Scheme I.2.1.1.3).[24] The mechanistic studies supported that the reaction progressed *via* a Cu(I)/Cu(III) catalytic cycle.

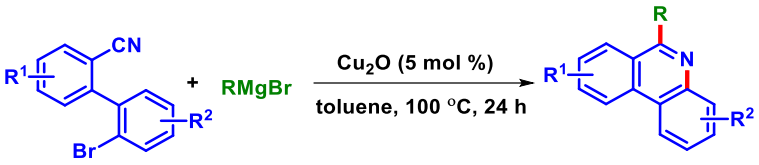

Scheme I.2.1.1.3. *Access to phenanthridines via addition/cyclization of Grignard reagent to nitrile.*

Similarly, Togo and co-workers developed a three-step synthesis of phenanthridines via the addition reaction of *o*-cyanobiaryls (Scheme I.2.1.1.4).[25] The process involves the addition of MeLi, EtMgBr, BuLi, PhLi, and *p*-methylphenyllithium to 2-cyanobiaryls, followed by reactions with H_2O and molecular iodine at 60 °C, providing 6-methyl-, 6-ethyl-, 6-butyl-, 6-phenyl, and 6-(*p*-methylphenyl)phenanthridines.

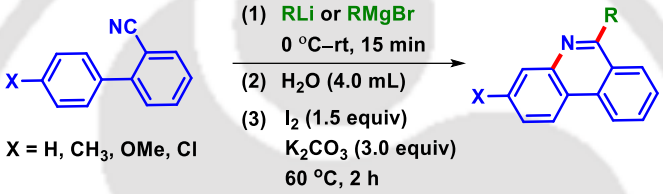

Scheme I.2.1.1.4. *Synthesis of phenanthridines using nitriles.*

In 2017, a Pd(II)-catalyzed addition/cyclization using arylboronic acids and *N*-(2-(cyanomethyl)phenyl)acetamide to access 2-substituted indoles was reported by Wu and Chen's group (Scheme I.2.1.1.5).[26] The reaction demonstrates excellent substrate tolerance and remarkable chemoselectivity.

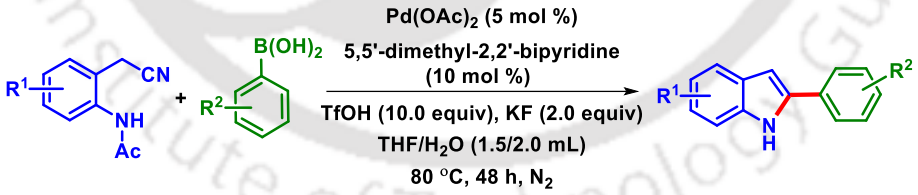

Scheme I.2.1.1.5. *Access to indoles from nitriles using $Pd(OAc)_2$.*

Yang and co-workers established a reaction to synthesize poly-substituted imidazoles through the addition/cyclization of arylboronic acids to aminoacetonitriles in the presence of $Pd(TFA)_2$ via the construction of C–C and C–N bonds (Scheme I.2.1.1.6).[27]

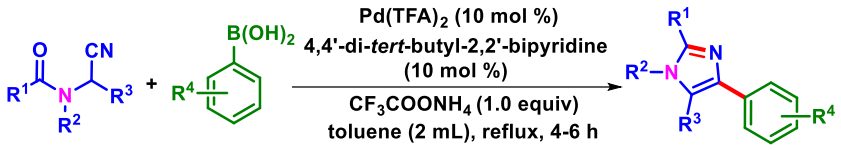

Scheme I.2.1.1.6. *Construction of functionalized imidazoles using nitriles.*

Chen's group disclosed a Pd(II)-catalyzed synthesis of 2-(4-arylquinazoline-2-yl)anilines containing a free $-NH_2$ group via a nucleophilic addition followed by an intramolecular cyclization of 2-(quinazoline-3(4*H*)-yl)benzonitriles and arylboronic acids (Scheme I.2.1.1.7).[28] The free $-NH_2$ group in the product is advantageous for further synthetic expansions, enhancing its diversity in both synthetic chemistry and medicinal chemistry.

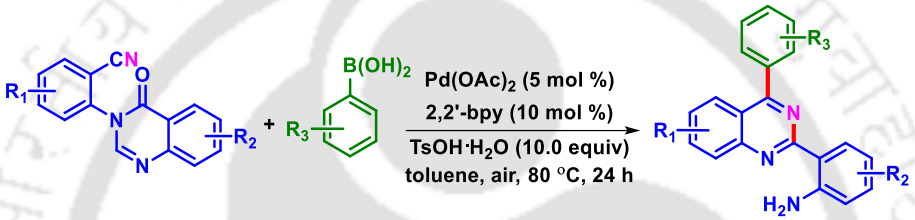

Scheme I.2.1.1.7. *Pd(II)-catalyzed cyclization of quinazolinone-based nitriles.*

Similarly, a Pd(II)-catalyzed cascade reaction to access benzofuro[2,3-*c*]pyridines via the coupling of 2-(cyanomethoxy)chalcones with arylboronic acids was described by Li's group (Scheme I.2.1.1.8).[29] The mechanism suggests that the reaction involves sequential carbopalladation of the nitrile, followed by intramolecular Michael addition, cyclization, and subsequent aromatization, leading to the formation of the product.

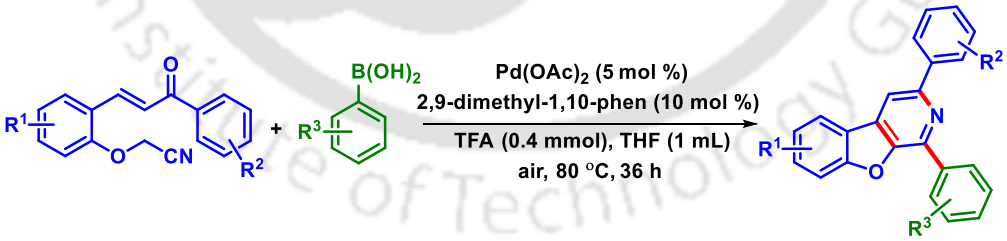

Scheme I.2.1.1.8. *Synthesis of benzofuro[2,3-c]pyridines via Pd(II)-catalyzed cascade cyclization.*

Neuville's group described a Cu(II)-mediated three-component assembly of cyanamides, 2-cyanoarylboronic acids, and amines for the synthesis of benzimidazo[1,2-*c*]quinazolines (Scheme I.2.1.1.9).[30] Initially, a Cu-catalyzed nucleophilic addition of amine and arylcyanamide

forms a guanidine unit, which then reacts with 2-cyanoarylboronic acid via Chan-Evans-Lam type coupling. This is followed by an intramolecular cyclization with the 2-cyano group to yield quinazolin-4(*H*)-imines. Finally, an intramolecular C–H amination of quinazolin-4(*H*)-imines produces benzimidazo[1,2-*c*]quinazolines.

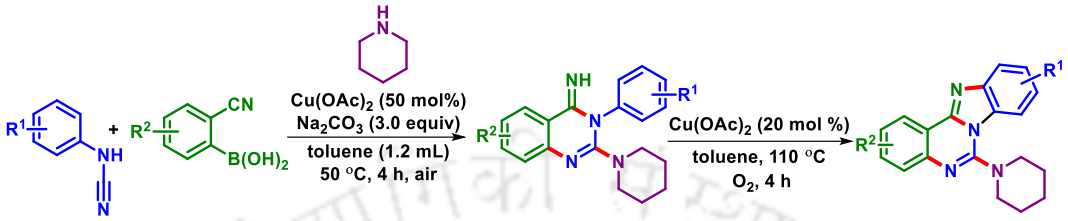

Scheme I.2.1.1.9. *Cu(II)-promoted two-step synthesis of benzimidazo[1,2-c]quinazolines.*

Our group also developed a photochemical strategy to access 3-cyanopyrroles and 3-cyanopyridines via a cascade addition/cyclization using β,γ-ketodinitriles with aryl boronic in the presence of $Pd(OAc)_2$ (Scheme I.2.1.1.10).[31] The reaction proceeds through visible-light irradiated forming an active Pd(0) catalyst from $Pd(OAc)_2$ and 2,2′-bipyridine in DCE, leading to photoexcitation via metal-to-ligand charge transfer (MLCT).

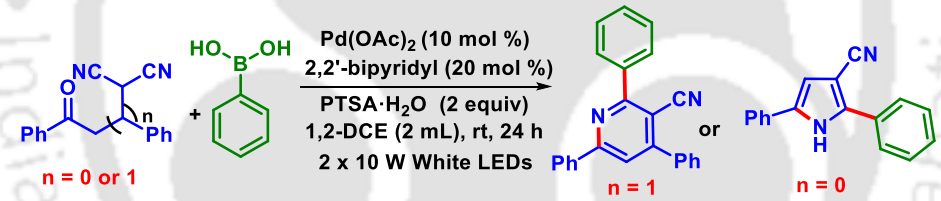

Scheme I.2.1.1.10. *Photochemical synthesis of functionalized pyridines and pyrroles.*

Earlier, a Pd(II)-catalyzed synthesis of oxazolin-containing polycyclic heterocycles was developed by Liao's group via the addition/cyclization of arylboronic acids to (hetero)arene tethered *O*-acyl cyanohydrin units (Scheme I.2.1.1.11).[32]

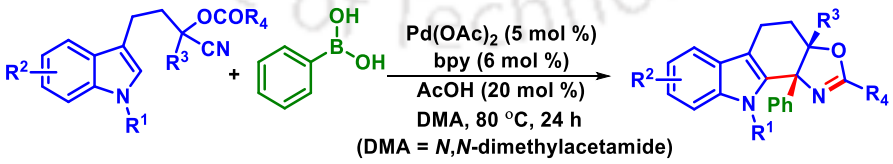

Scheme I.2.1.1.11. *Synthesis of polycyclic oxazolines in presence of $Pd(OAc)_2$.*

In 2018, Bao and co-workers described a method to synthesize quinazolinones via a Cu(II)-catalyzed reaction of 2-halobenzamides and nitriles (Scheme I.2.1.1.12).[33] The reaction involves a nucleophilic addition of 2-halobenzamides to the nitriles, followed by an intramolecular S_NAr reaction in the presence of ^tBuOK, yielding the desired products.

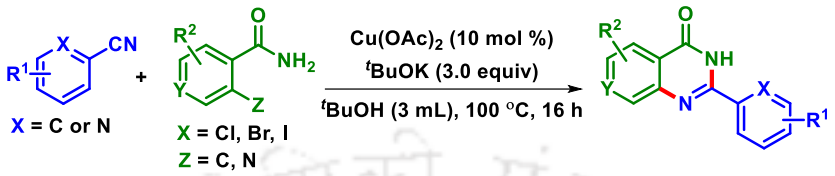

Scheme I.2.1.1.12. *Access to quinozalinones using nitriles.*

Kumar's group explored a regioselective cyclization reaction to access polysubstituted phenanthridines via Pd(II)-coupling of aryl iodides and alkyl/aryl nitriles (Scheme I.2.1.1.13).[34] The reaction is initiated via a Pd(II)-catalyzed nucleophilic addition of aryl iodides to nitriles, followed by imine-directed C–H activation, resulting in the formation of product having new C–C and C–N bonds.

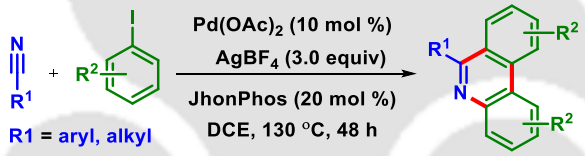

Scheme I.2.1.1.13. *Pd(II)-catalyzed addition/cyclization of aryl iodides to nitriles.*

Chen's group introduced a Pd(II)-catalyzed addition reaction of *N*-substituted indoles to 2-(cyanomethoxy)chalcones, leading to access indolyl-substituted benzofuro[2,3-*c*]pyridines. This protocol, involving direct C–H addition followed by sequential intramolecular addition, cyclization, and aromatization, delivers products (Scheme I.2.1.1.14).[35] This method is also extended to thiophene, furan, and pyrrole, providing access to various substituted benzofuro[2,3-*c*]pyridines.

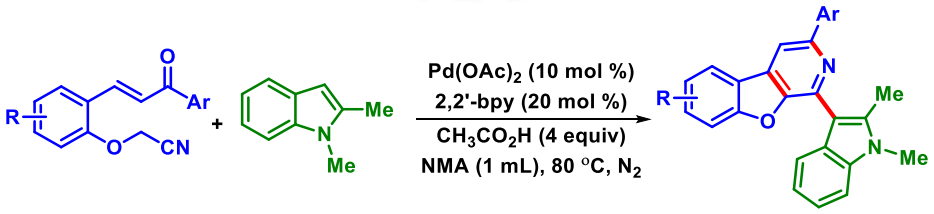

Scheme I.2.1.1.14. *Pd(II)-catalyzed addition/cyclization of indoles to nitriles.*

Similarly, Chen *et al.* explored a decarboxylative addition/cyclization method to access oxazoles and imidazoles between aromatic carboxylic acids and aliphatic nitriles in the presence of Pd(II)-catalyst (Scheme I.2.1.1.15).[36]

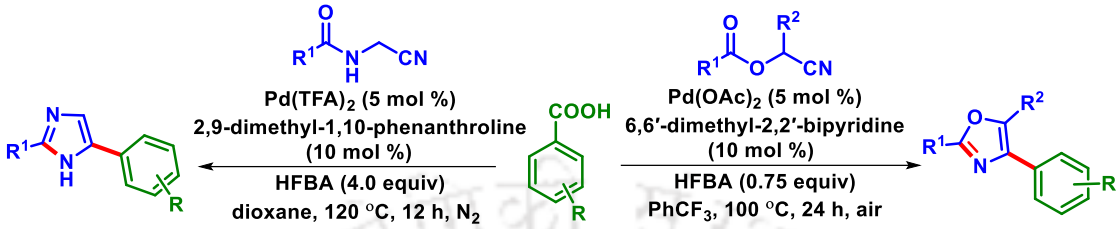

Scheme I.2.1.1.15. *Pd(II)-catalyzed addition of carboxylic acids to nitriles.*

In 2022, a Ni(II)-catalyzed reaction to access pyrazole and pyridazin-3(2*H*)-one derivatives was disclosed by Lv and co-workers via addition, condensation, followed by an annulation of dinitriles and boronic acids with hydrazine hydrochlorides (Scheme I.2.1.1.16).[37]

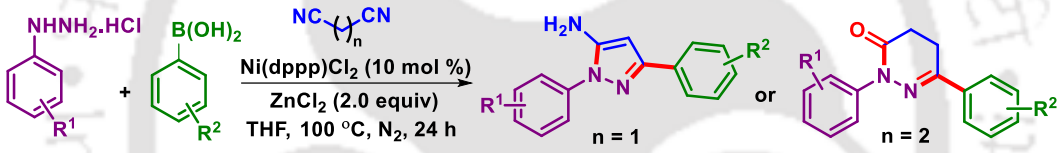

Scheme I.2.1.1.16. *Ni(II)-catalyzed annulation reactions with phenylhydrazine.*

I.2.1.2. Transition-Metal-Catalyzed Radical Cascades Addition/Cyclization:

Radical cascade addition/cyclization is a powerful approach for the efficient synthesis of *N*-heterocycles, utilizing transition metal catalysts to generate radical intermediates that can undergo sequential bond formation in a single step. The process involving nitrile functionality provides a suitable approach for constructing various *N*-heteroarenes. A general mechanism of a radical cyclization using the nitrile group is shown in Figure I.2.1.2.1. An iminyl radical forms when an *in situ* generated radical attacks the cyano group of a precursor (Path A). Alternatively, an iminyl radical can also form via an intramolecular cyclization of an alkenyl radical, forming before an *in-situ* generated radical attacks to the C=C bonds or other unsaturated groups like isocyanides (N≡C), appropriately positioned relative to the nitrile functionality (Path B). Finally, the insertion of nitrile onto the aryl ring through the iminyl radical yields the *N*-heterocycle. This

sequence highlights the versatile role of the nitrile group in facilitating the construction of different *N*-heterocycles via radical cascade reactions.

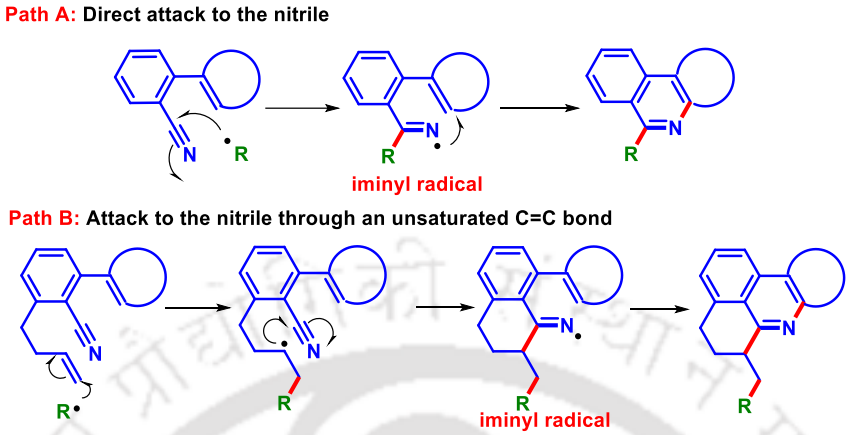

Figure I.2.1.2.1. *General radical addition/cyclization mechanism using the nitrile.*

In 2016, Cui *et al.* described a silver(I)-mediated synthesis of phosphorylated quinazolinones from *N*-cyanamide alkenes via a radical cascade phosphorylation/cyclization (Scheme I.2.1.2.1).[38] The reaction involves the in situ generation of a phosphorus radical, followed by its addition to N-cyanamide alkenes and subsequent intramolecular cyclization, leading to the products.

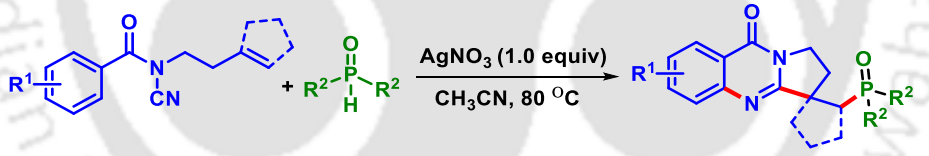

Scheme I.2.1.2.1. *Ag(I)-catalyzed phosphorylation/cyclization of N-cyanamide.*

In the same year, Cui and co-workers also established a Cu(I)-catalyzed trifluoromethylation/cyclization of unactivated alkenes to access 4-quinazolinone derivatives (Scheme I.2.1.2.2).[39] The reaction involves Cu-catalyzed trifluoromethylation of both unactivated terminal and internal alkenes using Togni's reagent. The process consists of the formation of the C(sp^3)–CF_3 bond and an α-alkyl radical through the attack of an *in situ*-generated CF_3 radical. Finally, the formation of an iminyl radical followed by cyclization leads to the final product.

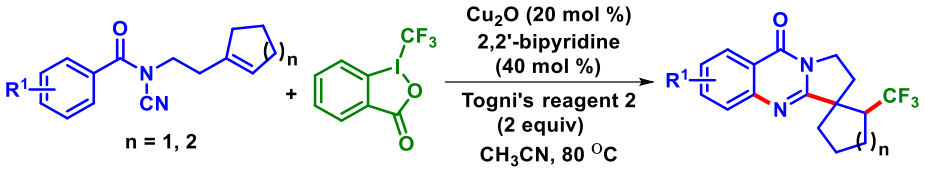

Scheme I.2.1.2.2. *Cu(I)-catalyzed radical cascade cyclization to synthesize 4-quinazolinones.*

In 2018, Li and coworkers disclosed a Cu(II)-catalyzed oxidative radical cascade cyclization to access nitrile-substituted pyrido[4,3,2-*gh*]phenanthridines by using 2-cyano-3-arylaniline-derived acrylamides with acetonitrile in the presence of *tert*-butyl peroxy benzoate (TBPB) (Scheme I.2.1.2.3).[40] Herein, the direct C–H bond functionalization of acetonitrile, followed by an intramolecular addition/cyclization of carbon and iminyl radicals, delivers the product.

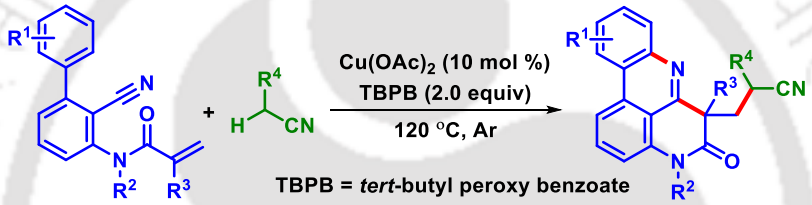

Scheme I.2.1.2.3. *Synthesis of cyano-substituted pyrido-phenanthridines.*

Li *et al.* also explored an Ag(I)-mediated synthesis of pyrido-phenanthridines using α-keto acids and 2-cyano-3-arylaniline acrylamides (Scheme I.2.1.2.4).[41] This methodology proceed through a decarboxylative cyclization of an *in situ* generated acyl radical, forming C–C and C–N bonds along with a quaternary carbon center.

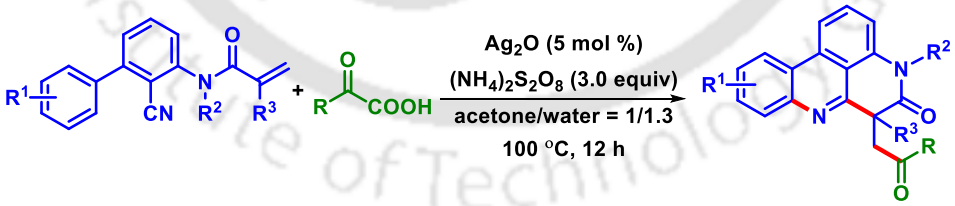

Scheme I.2.1.2.4. *Ag(I)-mediated radical cyclization reaction of nitriles.*

Liao and coworkers established a Cu(I)-catalyzed synthesis of difluorinated bicyclic amidines containing imine moieties via the difluoroalkylation of an alkene/nitrile of *N*-cyanamide alkene, followed by insertion/cyclization with good functional group compatibility (Scheme I.2.1.2.5).[42]

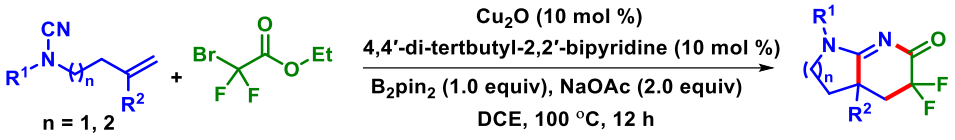

Scheme I.2.1.2.5. *Cu(I)-catalyzed difluoroalkylation of alkene/nitriles.*

Sun's group described a Fe(III)-catalyzed strategy for the formation of deuterium-labeled phenanthridines using 2-cyano-3-arylaniline-derived acrylamides and $NaBD_4$ (Scheme I.2.1.2.6).[43] The reaction proceeds via the addition of an *in-situ* generated deuterium radical followed by nitrile insertion/cyclization, leading to the formation of deuterated phenanthridine. In this process, the iron salt $Fe(NO_3)_3{\cdot}9H_2O$ was employed to promote the generation of the deuterium radical.

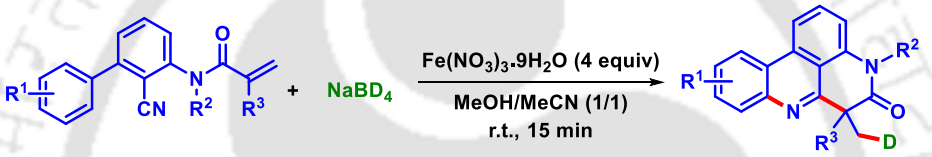

Scheme I.2.1.2.6. *Fe(III)-catalyzed synthesis of deuterated phenanthridines.*

In 2019, Kang and coworkers reported an addition reaction of benzyl radical to the nitriles followed by an intramolecular cyclization to synthesize *NH*-indoles in the presence of Cu(II)-catalyst (Scheme I.2.1.2.7).[44]

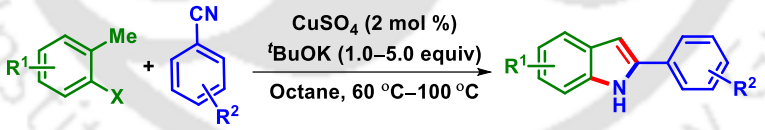

Scheme I.2.1.2.7. *Cu(II)-catalyzed synthesis of NH-indoles using nitriles.*

Ji and Wang's group demonstrated a Mn(III)-catalyzed regioselective synthesis of pyrrolopyridine derivatives by reacting multifunctionalized 3-isocyano-[1,1′-biphenyl]-2-carbonitriles with arylboronic acids (Scheme I.2.1.2.8).[45] The reaction initiates with the formation of an aryl radical from arylboronic acid, which subsequently attacks the isocyanide, followed by addition and sequential intramolecular cyclization, resulting in the formation of products.

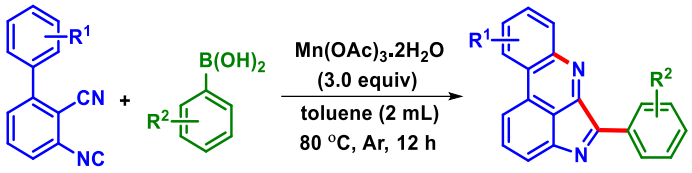

Scheme I.2.1.2.8. *Mn(III)-catalyzed radical cascade cyclization using nitriles.*

In the recent past (2021), a manganese(III)-mediated radical cyclization of multi-substituted 2-isocyano-6-alkenyl(alkynyl) benzonitriles with arylboronic acids was developed by Ji and co-workers (Scheme I.2.1.2.9).[46] This one-step method provides a way to synthesize pyrroloisoquinoline derivatives by forming two C–C bonds and one C–N bond via radical cascade cyclization.

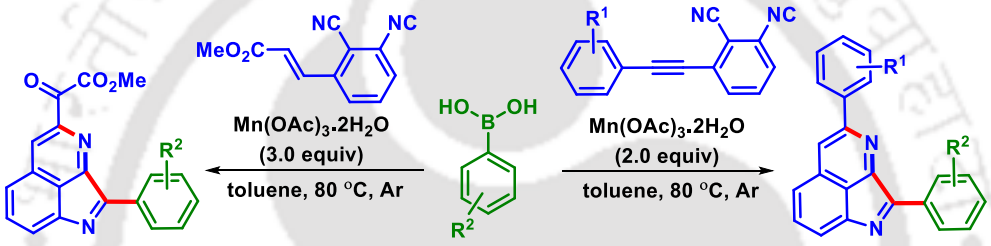

Scheme I.2.1.2.9. *Mn(III)-catalyzed radical cyclization of nitriles.*

I.3. Access to Carbo and Nitrogen-Heterocycle via Alkyne Insertion into the Nitriles:

Transition-metal-catalyzed insertion of alkynes into nitriles represents a versatile and efficient strategy for constructing both carbo- and nitrogen-heterocycles via the formation of C–C and C–N bonds efficiently and economically. This approach influences the inherent reactivity of alkynes and nitriles to form complex cyclic structures through sequential bond-forming processes. In these reactions, the alkyne serves as a key building block that inserts into the nitrile group, facilitating the formation of diverse heterocyclic frameworks. Transition metal catalysts, such as palladium, and rhodium often play a crucial role in these transformations, enabling the activation and insertion of alkynes into nitriles under mild conditions. Despite their flexibility to transform into several other functional groups, nitrile functionalities have long been considered inactive in organometallic reagents, even though they serve as ligands in certain metal catalysts like $PdCl_2(CH_3CN)_2$ and $PdCl_2(C_6H_5CN)_2$.[47] Therefore, the intrinsic inertness of

the nitrile (–CN) group towards organometallic reagents makes transition-metal-catalyzed alkyne annulation approaches involving nitrile functionalities an inspiring and exciting prospect in organic chemistry.

I.3.1. Access to Carbocycles via Alkyne Insertion into Nitriles:

The alkyne insertion method has emerged as an appropriate direction for various carbocycles involving intramolecular cyclization with nitrile. In 2002, Larock and co-workers developed a method to access 2,3-diarylindenones using 2-iodobenzonitriles and internal alkynes through an intramolecular carbopalladation of nitrile (Scheme I.3.1.1).[48] A probable mechanism for this annulation is shown in Scheme I.3.1.1. The process initiates with the oxidative addition of Pd(0) into the C–I bond, forming an aryl-Pd(II) complex. Subsequently, alkyne insertion occurs with the *in situ* generated aryl-Pd, leading to the formation of an alkenylpalladium(II) intermediate This intermediate then undergoes nucleophilic addition to the adjacent nitrile group. Finally, hydrolysis of the resulting complex yields a diverse array of 2,3-diarylindenones.

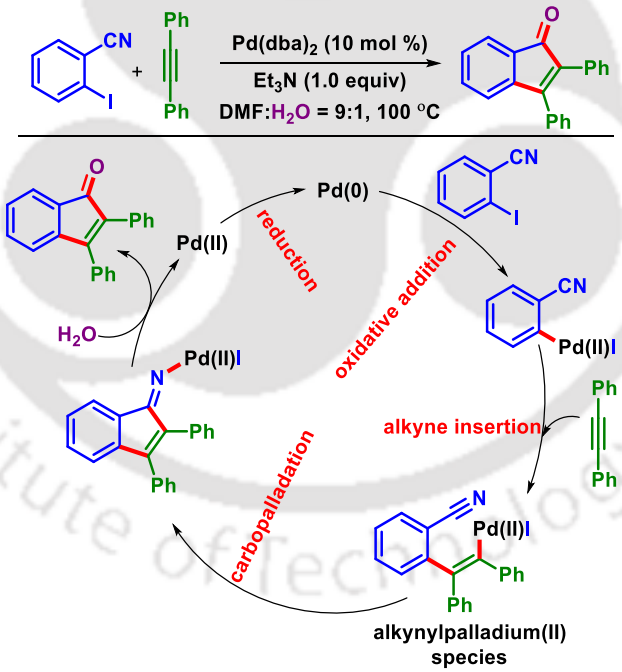

Scheme I.3.1.1. *Access to indenones in the presence of Pd(0)-catalyst.*

Following this approach, they also established a Pd(II)-catalyzed method to synthesize 3,4-disubstituted 2-aminonaphthalenes using 2-iodophenylacetonitriles and internal alkynes (Scheme I.3.1.2).[49] This protocol is started via the *in situ* generation of Pd(0) and oxidative

addition with the C–I bond. This is followed by alkyne insertion with the aryl–Pd, followed by nucleophilic addition of alkenylpalladium(II) to the nitrile, and finally aromatization gives the product.

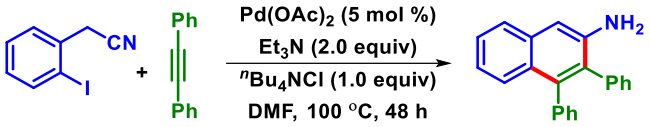

Scheme I.3.1.2. *Synthesis of 2-aminonaphthalenes in the presence of Pd(II)-catalyst.*

In 2005, Murakami's group disclosed a Rh(I)-catalyzed [3 + 2] annulation approach for synthesizing 2,3-indenones using 2-cyanophenylboronic acids and internal alkynes (Scheme I.3.1.3).[50] The reaction proceeds through an intramolecular nucleophilic addition of an *in situ* generated organo-rhodium(I) complex, followed by cyclization and subsequent hydrolysis to yield the product.

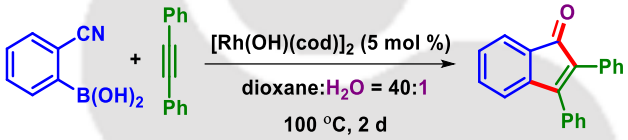

Scheme I.3.1.3. *Rh(I)-catalyzed alkyne insertion to the nitrile.*

In 2016, Tsukamoto and co-workers developed an annulation strategy to synthesize 3,4-disubstituted 2-naphthalenamines using internal alkynes and *o*-(cyanomethyl)phenylboronates leading (Scheme I.3.1.4).[51]

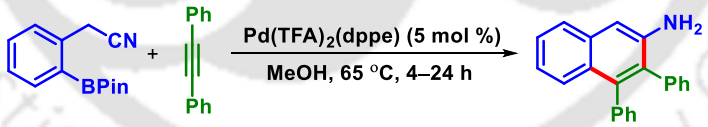

Scheme I.3.1.4. *Access to 2-aminonaphthalenes via alkyne insertion to nitrile.*

I.3.2. Synthesis of *N*-heterocycles via Alkyne Insertion into Nitriles:

The [2 + 2 + 2] cycloaddition of nitrile and alkyne catalyzed by transition metals is a versatile method for constructing *N*-heterocycles. This reaction typically involves the assembly of one molecule of nitrile and two molecules of alkyne to form a six-membered ring containing nitrogen atoms. Transition metals such as cobalt, nickel, ruthenium, and rhodium are commonly employed as catalysts due to their ability to activate and coordinate both nitriles and alkynes effectively.

A general mechanism for the metal-catalyzed cycloaddition of alkynes with nitriles for the formation of pyridine is shown below (Scheme I.3.2.1). Initially, coordination of the metal catalyst [M] with two alkynes leads to the formation of a metallacyclopentadiene intermediate via oxidative coupling. Subsequently, the nitrile coupling partner coordinates and follows one of two possible ways: (i) intramolecular [4 + 2] cycloaddition to form a bicyclic complex or (ii) insertion into the [M]–C bond to generate a cycloheptametallacycle. Finally, isomerization or reductive elimination of the bicyclic complex or cycloheptametallacycle, respectively yields the pyridine, and the metal is regenerated.

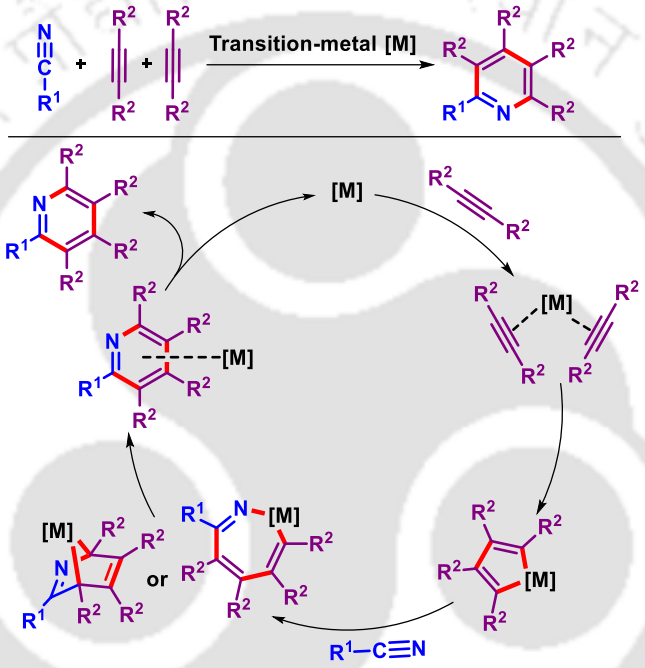

Scheme I.3.2.1. *General mechanism of [2 + 2 + 2] cycloaddition using nitriles.*

I.3.2.1. Alkyne Insertion via [2 + 2 + 2] Cycloaddition Reaction Using Nitrile:

The [2 + 2 + 2] cycloaddition reaction of nitrile with alkyne-nitrile or alkyne-alkyne with an alkyne provided functionalized pyridine. In 2005, Louie *et al.* reported an efficient protocol to synthesize cyclopentane-fused pyridines. They utilized a combination of a Ni(0) catalyst and an imidazolylidene ligand, involving the [2 + 2 + 2] cycloaddition of methyl-terminated tethered alkynes with benzonitriles, leading to the formation of cyclopentane-fused pyridines (Scheme I.3.2.1.1).[52] This protocol is also subjected to synthesizing multi-substituted pyridine using an untethered alkyne, 3-hexyne.

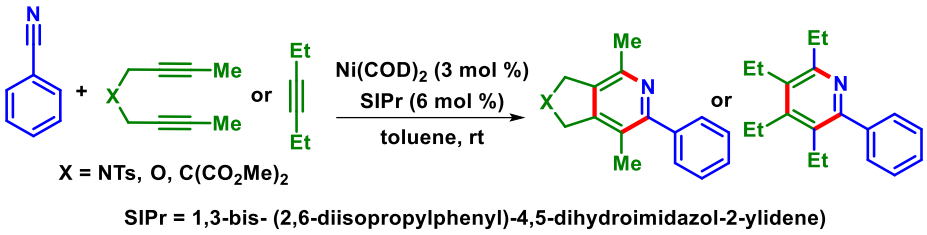

Scheme I.3.2.1.1. *Ni(0)-catalyzed [2 + 2 + 2] cycloaddition of alkyne and benzonitrile.*

In 2012, a similar Ir(I)-catalyzed cycloaddition methodology for α,ω-diynes accommodating an extensive range of nitriles was established by Takeuchi's group, in the presence of DPPF or BINAP (Scheme I.3.2.1.2).[53] This method enables both aliphatic and aromatic nitriles to efficiently react with α,ω-diynes, resulting in the formation of pyridines. Notably, high regioselectivity was achieved using unsymmetrical diynes containing two different internal alkyne moieties.

Scheme I.3.2.1.2. *Access to pyridines from nitriles via [2 + 2+ 2] cycloaddition.*

In 2021, a Co(II)-catalyzed intermolecular [2 + 2 + 2] cycloaddition was reported by Yoshikai and coworkers, utilizing internal alkynes and unactivated nitriles to synthesize multi-substituted pyridines (Scheme I.3.2.1.3).[54] This reaction initiates via oxidative coupling of two alkynes, followed by the insertion of the nitrile into a cobaltacyclopentadiene intermediate, and concludes with a C−N reductive elimination.

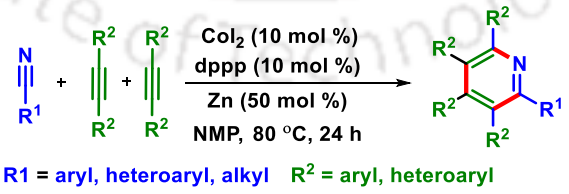

Scheme I.3.2.1.3. *Co(II)-catalyzed intermolecular [2 + 2 + 2] cycloaddition to access pyridines.*

I.3.2.2 Alkyne Insertion via [2 + 2 + 1] Cycloaddition Reaction Using Nitrile:

In addition to the methodologies mentioned, [2 + 2 + 1] cycloaddition reactions involving nitriles and diphenylacetylene have also been explored to synthesize *N*-heterocycles.

For example, in 2012, Jiang *et al*. established a regioselective [2 + 2 + 1] cycloaddition of internal alkynes and nitriles to access functionalized 1,3-oxazoles using a Cu(II) catalyst (Scheme I.3.2.2.1).[55] Mechanistic studies revealed that the transformation proceeds through an enamide intermediate, which forms via the nucleophilic attack of water.

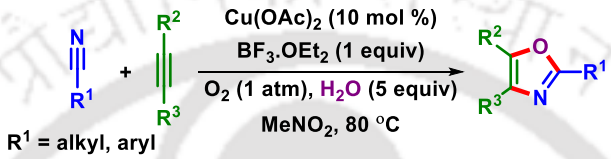

Scheme I.3.2.2.1. *Cu(II)-catalyzed [2 +2 + 1] cycloaddition to access functionalized 1,3-oxazoles.*

In 2020, Tonks and coworkers demonstrated a [2 + 2 + 1] cycloaddition reaction to synthesize pyrazoles using nitriles and internal alkynes using Ti-imido complexes (Scheme I.3.2.2.2).[56] This reaction mechanism proceeds through the interaction of the nitrile and alkyne to produce a six-membered Ti-metallacycle intermediate, followed by reductive elimination to yield the pyrazole with N–N bond formation.

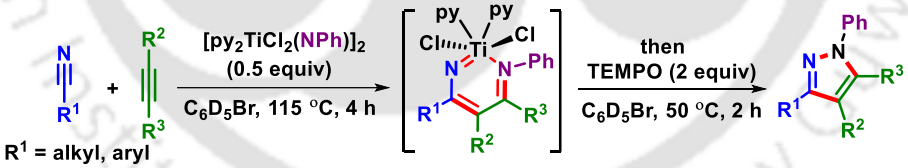

Scheme I.3.2.2.2. *Synthesis of pyrazoles via [2 + 2 + 1] cycloaddition of nitriles and alkynes.*

I.3.2.3. Synthesis of *N*-Heterocycles via Intramolecular Alkyne Insertion into the Nitriles:

The synthesis of *N*-heterocycles via nitrile-triggered reactions can also proceed when both the nitrile and alkyne are integral parts of the same molecule, such as *o*-alkynylarylnitriles (Figure I.3.2.3.1).[57-60] Here, the alkyne moiety is fixed at the *ortho* position with respect to the nitrile group, facilitating nucleophilic addition followed by intramolecular cyclizations, leading to *N*-heteroarenes (attack through nitrile). Another possible approach to accessing *N*-heterocycles

involves the nucleophilic attack of an *N*-nucleophile on the nitrile, followed by cyclization with the alkyne (attack through *N*-nucleophile).

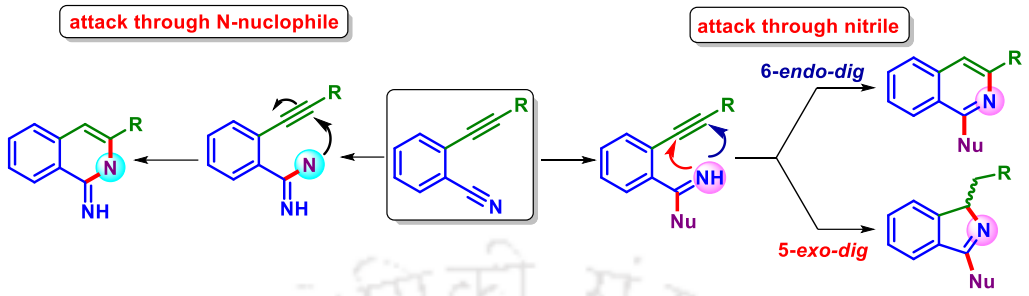

Figure I.3.2.3.1. *Different approaches to access N-heterocycles from o-alkynylarylnitriles.*

In 2016, Anand and co-workers reported a solvent-free metal-catalyzed regioselective approach to access 1-aminoisoquinolines and/or 1-aminoisindolines (Scheme I.3.2.3.1).[58] This method involved aminative cyclization of *o*-alkynylbenzonitriles with secondary amines. The choice of metal catalyst significantly influenced the regioselectivity of the reaction: Cu-based catalysts preferred 6-*endo-dig* cyclization, leading to 1-aminoisoquinolines, whereas triflates of metals such as Zn, Ag, Bi, Sc, and Yb favored 5-*exo-dig* cyclization, resulting in the formation of 1-aminoisindolines.

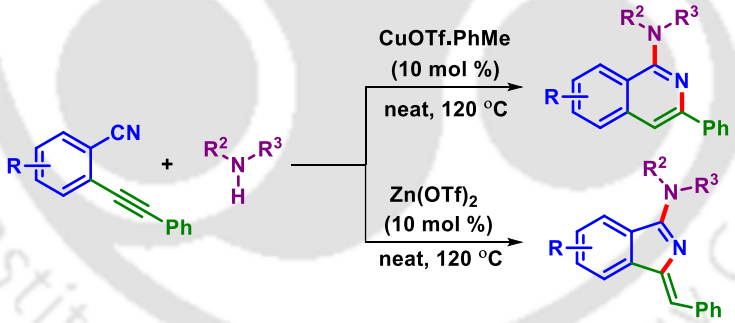

Scheme I.3.2.3.1. *Regioselective aminative cyclization of 2-alkynylbenzonitriles.*

In 2017, Kumar *et. al.* disclosed a Pd(II)-catalyzed one-pot strategy of 2-chloroqunoline-3-carbonitriles allowed to synthesize of sulfur-substituted benzo[*b*][1,6]-naphthyridines using a sodium sulfide nucleophile (Scheme I.3.2.3.2).[59] The reaction was also extended to synthesize nitrogen-substituted benzo[*b*][1,6]-naphthyridines using secondary amines as nucleophiles.

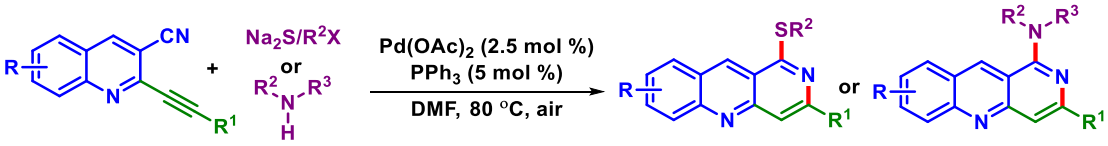

Scheme I.3.2.3.2. *Pd(II)-catalyzed formation of benzo-naphthyridine using o-alkynylbenzonitriles.*

In 2018, the Liang's group described a Cu(II)-catalyzed hetero-annulation strategy for synthesizing benzo[4,5]imidazo[2,1-*a*]isoquinoline derivatives using 2-iodoanilines and 2-alkynylbenzonitriles (Scheme I.3.2.3.3).[60] Herein, the heterocycle is formed via an attack by the *N*-nucleophile, with the sequential formation of three C–N bonds through the cleavage of one C–I bond and two N–H bonds.

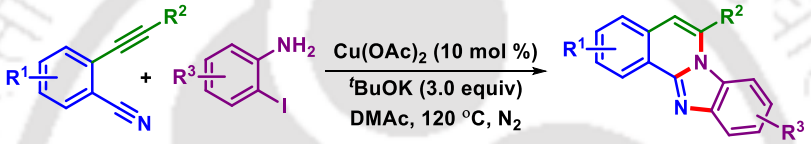

Scheme I.3.2.3.3. *Cu(II)-catalyzed cyclization of 2-iodoaniline and o-alkynylbenzonitriles.*

I.4. Access to *N*-heterocycles via Photochemical Cascade Addition/Cyclization:

The synthesis of nitrogen-containing heterocycles via photochemical cascade addition and cyclization is a fascinating and versatile method in organic chemistry. This approach often involves the generation of reactive intermediates under light irradiation, which then undergo a series of addition and cyclization reactions to form complex *N*-heterocyclic structures.

I.4.1. Access to *N*-heterocycles in the Presence of Photocatalyst:

Owing to their importance, simplicity, efficiency, and unique activation, visible-light-irradiated radical cascade addition/cyclizations have been magnificently employed for the construction of *N*-heterocycles.[61] This approach harnesses visible light as a mild and effective trigger for radical generation and subsequent cyclization reactions, thereby facilitating the synthesis of diverse *N*-heterocyclic compounds. In this background, construction of the C–C and C–N bonds using photoredox catalysts has garnered significant attention, highlighting the importance of nitrile functionality. In the presence of visible light, a radical is generated through

the excitation of photocatalyst (PC) to their excited state (PC*) via a single electron transfer (SET) process (Figure I.4.1.1). The generated radical undergoes a reaction with the nitrile to form an iminyl radical, which then undergoes an intramolecular cyclization to afford *N*-heterocycles either through radical or cationic intermediates. The photocatalyst is further regenerated to its ground state either via reductive or oxidative quenching cycles (Figure I.4.1.1).

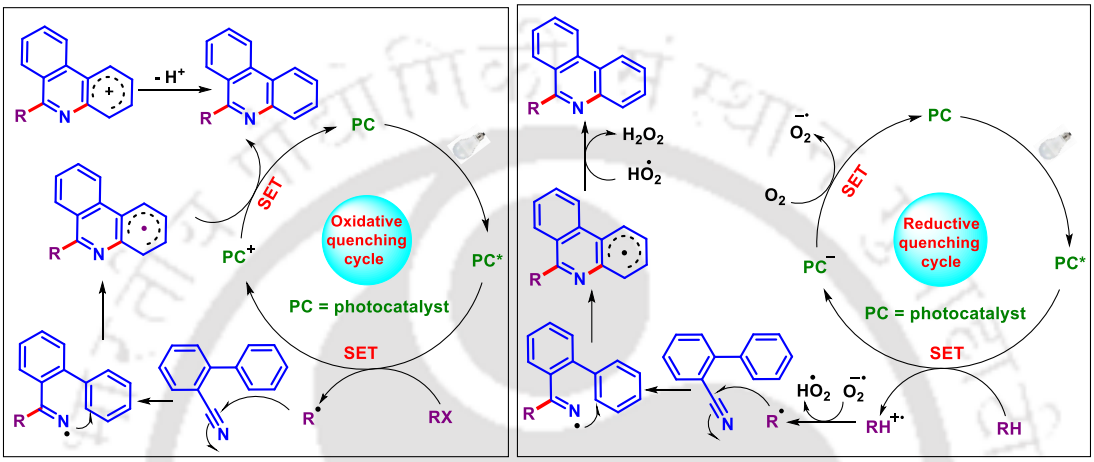

Figure I.4.1.1. *Photochemical radical addition to nitrile.*

In 2016, Yu *et al.* developed an Ir(III)-catalyzed intramolecular radical addition/cyclization to synthesize quinazolinones in the presence of white LEDs (Scheme I.4.1.1).[62]

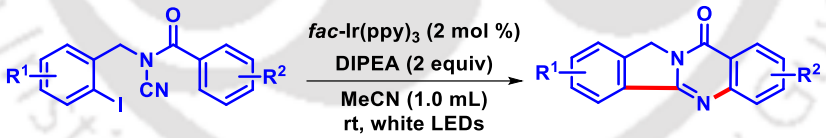

Scheme I.4.1.1. *Ir(III)-catalyzed synthesis of quinazolinone derivatives using nitrile.*

In 2017, a visible-light-induced metal-free cascade cyclization for the synthesis of pyrido[4,3,2-*gh*]phenanthridin-6-yl)acetate derivatives was established by Sun and co-workers (Scheme I.4.1.2).[63] The method was initiated via an intermolecular ester radical-radical addition to a C=C double bond of *N*-arylacryl amide followed by cyclization through the nitrile group.

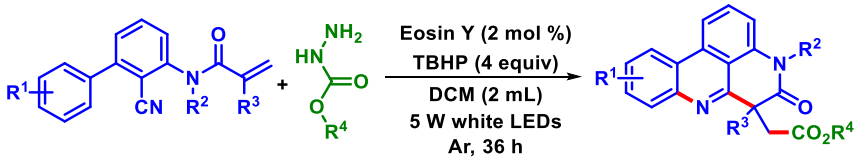

Scheme I.4.1.2. *Access to pyrido-phenanthridine derivatives using eosin Y catalyst.*

In 2018, Sun's group also developed a visible-light-induced decarboxylative alkylation strategy for aliphatic carboxylic acids using eosin Y as an organic photocatalyst (Scheme I.4.1.3).[64] The reaction involves decarboxylation to produce an alkyl radical from the aliphatic carboxylic acid, which then reacts to the C=C bond of *N*-arylacrylamide, followed by insertion and cyclization with a nitrile, resulting in alkylated phenanthridines.

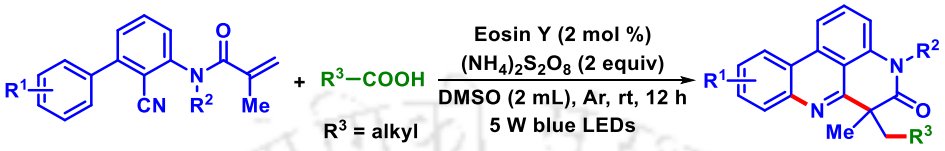

Scheme I.4.1.3. *Eosin Y catalyzed decarboxylative alkylation of N-arylacrylamide.*

In 2019, Fu *et al.* disclosed a visible-light-induced Ir(III)-catalyzed trifluoromethylthiolation of *N*-(*o*-cyanobiaryl)acrylamides using *N*-trifluoromethylthiosaccharin as a source of the SCF_3 radical (Scheme I.4.1.4).[65] The reaction proceeded via trifluoromethylthiolation of the C=C bond by the SCF_3 radical, followed by nitrile insertion and cyclization, affording SCF_3-containing phenanthridines in modest to good yields.

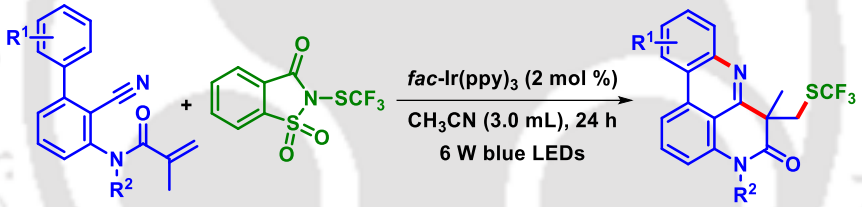

Scheme I.4.1.4. *Ir(III)-catalyzed synthesis of SCF_3-containing phenanthridines.*

Natarajan's group also reported a method for constructing 2-substituted benzothiazoles from alkyl/aryl nitriles and thiophenols using eosin Y as a photocatalyst (Scheme I.4.1.5).[66] The protocol involves an oxidative radical addition of thiophenols to nitriles, followed by an intramolecular cyclization, sequentially forming C–S, and C–N bonds and yielding the desired product.

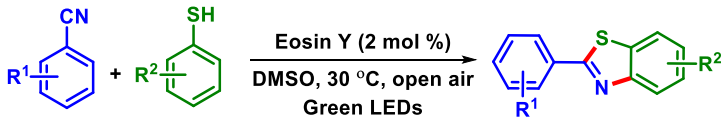

Scheme I.4.1.5. *Eosin Y catalyzed synthesis of benzothiazoles.*

In 2023, our group also developed a metal-free approach to access thio-functionalized pyrroles and pyridines using β,γ-ketodinitriles, thiophenols, and eosin Y as a photocatalyst under green light irradiation (Scheme I.4.1.6).[67] Herein, the reaction proceeds by the involvement of selective participation of one of the nitrile (–CN) groups by an *in situ* generated thiyl radical (Scheme I.4.1.6).

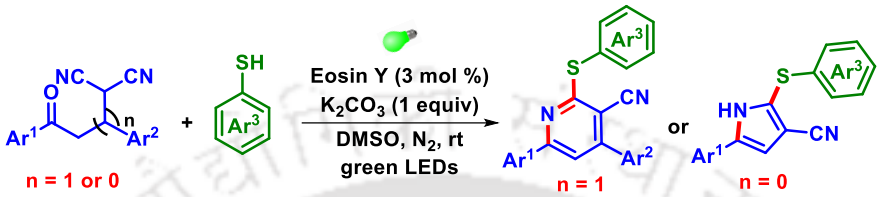

Scheme I.4.1.6. *Synthesis of thio-functionalized pyrroles and pyridines from β,γ-ketodinitriles.*

I.4.2. Access to *N*-heterocycles via Formation of Electron-Donor-Acceptor (EDA) Complex:

The formation of an electronically excited state upon the absorption of photons is a key feature of all photochemical processes. Despite the emerging exploration of photo redox catalysts in organic transformations, the potential of electron-donor-acceptor (EDA) complexes, which do not require an exogenous photosensitizer, has been progressively recognized recently. Between 1950 and 1952, the electron transfer hypothesis was proposed by Mulliken, which precisely explained electron transfer phenomena based on the colored electron-donor–acceptor (EDA) complex.[68] The interaction of an electron-rich compound (D) with an electron-acceptor molecule (A) leads to the formation of an electron-donor-acceptor (EDA) complex in the ground state, which can absorb visible light and eliminate the requirement of an external photocatalyst. However, the two components independently may not absorb visible light, but the resulting EDA complex does. This ground-state EDA complex by absorbing light can undergo a single electron transfer (SET) process from an electron donor to an electron acceptor producing a charge-separated state (Figure I.4.2.1).[69] If the electron transfer has an adequately long lifetime, various reactions can be carried out by the charge-separated species through the *in situ* generation of reactive radical intermediates.[70]

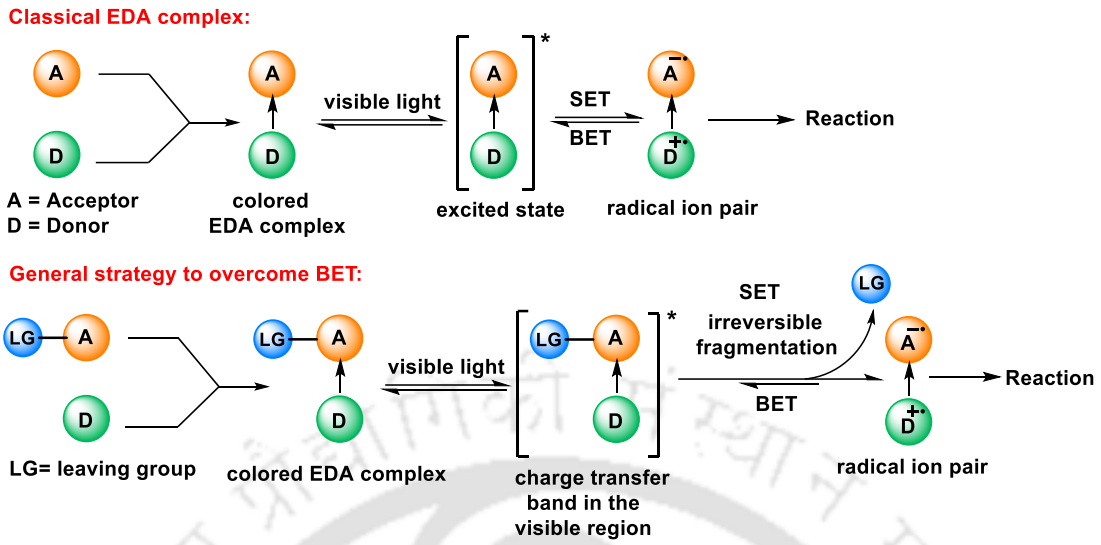

Figure I.4.2.1. *Schematical representation for the formation of the EDA complex.*

Classification of Formation of EDA Complex:

Electron Donor-Acceptor (EDA) complexes are non-covalent assemblies formed between electron-rich (donor) and electron-deficient (acceptor) molecules. These complexes are characterized by charge-transfer interactions where electrons are partially transferred from the donor to the acceptor. The classification of EDA complexes[69c] can be broadly divided based on their components and the nature of the interaction between the donor and acceptor:

1. σ-type interactions
2. Anion-π interactions
3. Hydrogen bonding
4. Halogen bonding

The unique reactivity of EDA complexes enables novel and efficient pathways for constructing *N*-heterocyclic structures. Several groups have developed the synthesis of N-heterocycles via EDA complex formation using various starting precursors. Here are a few notable examples of such syntheses using different varieties of starting precursors. For example, In 2018, Miao's group developed a photochemical strategy to synthesize highly stereo and regioselective (*E*)- and (*Z*)-C6-(vinyl sulfone)phenanthridines via reactions of isocyanides, alkynes, and sulfinic acids (Scheme I.4.2.1).[71] Herein, this protocol is initiated via the formation of an EDA complex through the reaction of arylsulfinic acid and biaryl isocyanide in the presence of pyridine and water.

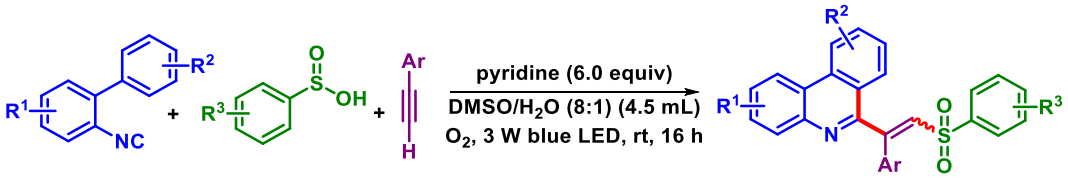

Scheme I.4.2.1. *Three-component synthesis of phenanthridine derivatives via EDA complex formation.*

In 2020, Miao and coworkers also established a visible-light-induced synthesis of phenanthridine heterocycles via a decarboxylative cyclization/hydrogenation of α-oxocarboxylic acids and 2-isocyanobiaryls (Scheme I.4.2.2).[72] Herein, the reaction proceeds via EDA complex-initiated decarboxylation, radical addition/cyclization, followed by *in situ* photochemical reduction of ketones to alcohols leading to the products.

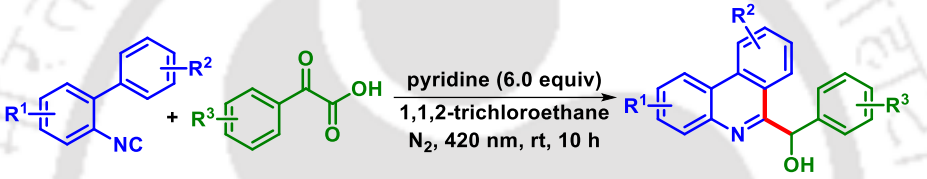

Scheme I.4.2.2. *Synthesis of phenanthridine derivatives via decarboxylation strategy.*

I.5. Conclusion:

In conclusion, we have detailed various efficient and straightforward methodologies for constructing diverse *N*-heterocycles via transition-metal-catalyzed cascade addition/cyclization, alkyne insertion, and photochemical cascade addition/cyclization. The use of nitrile (C≡N) or cyano precursors in these approaches has significantly advanced the synthesis of various essential *N*-heterocycles from specifically designed reactants. All these methods provide an efficient route and showcase the versatility of nitriles in reactions, highlighting their significance in forming *N*-heterocycles. In photochemical cascades, harnessing light energy to generate radicals, either in the presence of photocatalysts or through the electron-donor-acceptor (EDA) complex, has been effectively demonstrated to trigger cyclization and facilitate the formation of *N*-heterocycles. Furthermore, several thermal and photochemical methods utilizing nitrile-containing synthetic precursors, such as dicyanodienes and β-ketodinitriles, have been described, offering broad opportunities for accessing various molecular frameworks in synthetic organic chemistry. However, these precursors remain underexplored either thermally or photochemically. Featuring an olefinic bond and a keto group close to the nitrile functionality, they possess

significant potential for the synthesis of *N*-heterocycles. Therefore, in the following chapters of this thesis, we present newer methodologies for the straightforward and efficient synthesis of various *N*-heterocycles, including functionalized pyridines, quinolines, furo-pyrimidines, and furo-pyrrolo-pyridines, utilizing functionalized or activated nitrile precursors such as dicyanodienes and β-ketodinitriles.

I.6. References:

[1] (a) Trofimov, B. A.; Sobenina, L. N.; Demenev, A. P.; Mikhaleva, A. I. *Chem. Rev*. **2004**, *104*, 2481–2506. (b) Furstner, A. *Angew. Chem., Int. Ed*. **2003**, 42, 3582–3603. (c) Fan, H.; Peng, J.; Hamann, M. T.; Hu, J.-F. *Chem. Rev*. **2008**, *108*, 264–287. (d) Lee, H.; Lee, J.; Lee, S.; Shin, Y.; Jung, W.; Kim, J.-H.; Park, K.; Kim, K.; Cho, H. S.; Ro, S. *Bioorg. Med. Chem. Lett*. **2001**, *11*, 3069–3072. (e) Wurz, R. P.; Charette, A. B. *Org. Lett*. **2005**, *7*, 2313–2316. (f) Walsh, C. T.; Garneau-Tsodikova, S.; Howard-Jones, A. R. *Nat. Prod. Rep*. **2006**, 23, 517–531. (g) Thirumalairajan, S.; Pearce, B. M.; Thompson, A. *Chem. Commun*. **2010**, *46*, 1797–1812. (h) Bhardwaj, V.; Gumber, D.; Abbot, V.; Dhiman, S.; Sharma, P. *RSC Advanced*. **2015**, *5*, 15233–15266.

[2] (a) Movassaghi, M.; Hill, M. D. *J. Am. Chem. Soc.* **2006**,*128*, 14254–14255. (b) Hill, M. D.; Movassaghi, M. *Chem. Eur. J.* **2008**, *14*, 6836–6844. (c) Ahmed, K.; Choudhary, M. I.; Saleem, R. S. Z. *Eur. J. Med. Chem.* **2023**, *259*, 115701.

[3] (a) Yuan, C.; Chang, C.-T.; Axelrod, A.; Siegel, D.; *J. Am. Chem. Soc.* **2010**, *132*, 5924–5925. (b) Fischer, D. F.; Sarpong, R. *J. Am. Chem. Soc*. **2010**, *132*, 5926–5927. (c) Wang, P.; Verma, P.; Xia, G.; Shi, J.; Qiao, J. X.; Tao, S.; Cheng, P. T. W.; Poss, M. A.; Farmer, M. E.; Yeung, K.-S.; Yu, J. Q. *Nature*. **2017**, *551*, 489–494. (d) Semple, G.; Ashworth, D. M.; Baker, G. R.; Batt, A. R.; Baxter, A. J.; Benzies, D. W. M.; Elliot, L. H.; Evans, D. M.; Franklin, R. J.; Hudson, P.; Jenkins, P. D.; Pitt, G. R.; Rooker, D. P.; Sheppard, A.; Szelke, M.; Yamamoto, S.; Isomura, Y. *Bioorg. Med. Chem. Lett.* **1997**, *7*, 1337–1342. (e) Kusakabe, K.; Tada, Y.; Iso, Y.; Sakagami, M.; Morioka, Y.; Chomei, N.; Shinonome, S.; Kawamoto, K.; Takenaka, H.; Yasui, K.; Hamana, H.; Hanasaki, K. *Bioorg. Med. Chem.* **2013**, *21*, 2045–2055. (f) Kumarihamy, M.; Fronczek, F. R.; Ferreira,

D.; Jacob, M.; Khan, S. I.; Nanayakkara, N. P. D. *J. Nat. Prod*. **2010**, *73*, 1250−1253. (g) Jessen, H. J.; Gademann, K. *Nat. Prod. Rep.* **2010**, *27*, 1168−1185.

[4] (a) Mandal, A.; Khan, A. T. *Org. Biomol. Chem.* **2024**, *22*, 2339−2358. (b) Barluenga, J.; Rodríguez, F.; Fañanás, F. J. *Chem. Asian J.* **2009**, *4*, 1036−1048. (c) Sharma, V.; Mehta, D. K.; Das, R. *Mini. Rev. Med. Chem.* **2017**, *17*, 1557−1572. (d) Prajapati, S. M.; Patel, K. D.; Vekariya, R. H.; Panchal, S. N.; Patel, H. D. *RSC Adv.* **2014**, *4*, 24463−24476. (e) Weyesa, A.; Mulugeta, E. *RSC Adv.* **2020**, *10*, 20784−20793. (f) Ramann, G. A.; Cowen, B. J. *Molecules* **2016**, *21*, 986.

[5] (a) Kochanowska-Karamyan, A. J.; Hamann, M. T. *Chem. Rev*. **2010**, *110*, 4489−4497. (b) Saxton, J. E. *Nat. Prod. Rep*. **1996**, *13*, 327−363. (c) Smart, B. P.; Oslund, R. C.; Walsh, L. A.; Gelb, M. H. *J. Med. Chem.* **2006**, *49*, 2858−2860. (d) Eicher, T.; Hauptmann, S. *The Chemistry of Heterocycles; Wiley-VCH: Weinheim*, **2003**. (e) Petit, S.; Duroc, Y.; Larue, V.; Giglione, C.; Léon, C.; Soulama, C.; Denis, A.; Dardel, F.; Meinnel, T.; Artaud, I. *ChemMedChem*. **2009**, *4*, 261−275. (f) Thanikachalam, P. V.; Maurya, R. K.; Garg, V.; Monga V. *Eur. J. Med. Chem*. **2019**, *180*, 562−612.

[6] (a) Lin, Y.-D.; Tsai, W.-W.; Lu, C.-W. *Chem. Eur. J.* **2023**, *29*, e202203040. (b) Sharma, P.; LaRosa, C.; Antwi, J.; Govindarajan, R.; Werbovetz, K. A. *Molecules* **2021**, *26*, 4213.

[7] (a) Zhou, S.-Q.; Tong, R.-B. *Chem. Eur. J*. **2016**, *22*, 7084−7089. (b) Kashiwada, Y.; Aoshima, A.; Ikeshiro, Y.; Chen, Y. P.; Furukawa, H.; Itoigawa, M.; Fujioka, T.; Mihashi, K.; Cosentino, L. M.; Morris-Natschke, S. L.; Lee, K. H. *Bioorg. Med. Chem*. **2005**, *13*, 443−448. (c) Li, K.; Ou, J.; Gao, S. *Angew. Chem., Int. Ed*. **2016**, *55*, 14778−14783. (d) Bentley, K.W. *Nat. Prod. Rep*. **2006**, *23*, 444−463. (e) Bhadra, K.; Kumar, G. S. *Mini-Rev. Med. Chem*. **2010**, *10*, 1235−1247. (f) Giri, P.; Kumar, G. S. *Mini-Rev. Med. Chem*. **2010**, *10*, 568−577. (g) Gutteridge, C. E.; Hoffman, M. M.; Bhattacharjee, A. K.; Milhous, W. K.; Gerena, L. *Bioorg. Med. Chem. Lett.* **2011**, *21*, 786−789. (h) Liu, Y.; Li, W.; Morris-Natschke, S. L.; Qian, K.; Yang, L.; Zhu, G.; Wu, X.; Chen, A.; Zhang, S.; Nan, X.; Lee, K. *Med. Res. Rev*. **2015**, *35*, 753−789.

[8] (a) Zhao, A.; Gao, X.; Wang, Y.; Ai, J.; Wang, Y.; Chen, Y.; Geng, M.; Zhang, A.; *Bioorg. Med. Chem.* **2009**, *17*, 7324–7336. (b) Li, C.; Zhang, F. *Tet. Lett.* **2017**, *58*, 1572-1575. (c) Gangjee, A.; Li, W.; Lin, L.; Zeng, Y.; Ihnat, M.; Warnke, L. A.; Green, D. W.; Cody, V.; Pace, J.; Queener, S. F. *Bioorg. Med. Chem.* **2009**, *17*, 7324-7336. (d) Robins, M. J.; Nowak, I.; Rajwanshi, V. K.; Miranda, K.; Cannon, J. F.; Peterson, M. A.; Andrei, G.; Snoeck, R.; Clercq, E. D.; Balzarini, J. *J. Med. Chem.* **2007**, *50*, 3897-3905. (e) Amblard, F.; Aucagne, V.; Guenot, P.; Schinazic, R. F. Agrofoglio, L. A. *Bioorg. Med. Chem.* **2005**, *13*,1239–1248. (f) Sniady, A.; Durham, A.; Morreale, M. S.; Marcinek, A.; Szafert, S.; Lis, T.; Brzezinska, K. R.; Iwasaki, T.; Ohshima, T.; Mashima, K.; Dembinski, R. *J. Org. Chem.* **2008**, *73*, 5881-5889. (g) Pyo, J. I.; Hwang, E. J.; Cheong, C. S.; Lee, S.-H.; Lee, S. W.; Kim, I. T.; Lee, S. H. *Synth. Met.* **2005**, *155*, 461–463.

[9] (a) Bagdi, A. K.; Santra, S.; Monir, K.; Hajra, A. *Chem. Commun.* **2015**, *51*, 1555–1575. (b) Rupert, K. C.; Henry, J. R.; Dodd, J. H.; Wadsworth, S. A.; Cavender, D. E.; Olini, G. C.; Fahmy, B.; Siekierka, J. *Bioorg. Med. Chem. Lett*. **2003**, *13*, 347–350. (c) Enguehard-Gueiffier, C.; Gueiffier, A. *Mini-Rev. Med. Chem*. **2007**, *7*, 888–899. (d) Shukla, N. M.; Salunke, D. B.; Yoo, E.; Mutz, C. A.; Balakrishna, R.; David, S. A. *Bioorg. Med. Chem*. **2012**, *20*, 5850–5863. (e) Du, B.; Shan, A.; Zhang, Y.; Zhong, X.; Chen, D.; Cai, K. *Am. J. Med. Sci*. **2014**, *347*, 178–182. (f) Sana, S.; Dannarm, S. R.; Tokala, R.; Dastari, S.; Sathish, M.; Kumar, R.; Sonti, R.; Shankaraiah, N. *Org. Chem. Front.* **2023**, *10*, 4800–4808.

[10] (a) Wu, Z.; Robinson, R. G.; Fu, S.; Barnett, S. F.; Defeo-Jones, D.; Jones, R. E.; Kral, A. M.; Huber, H. E.; Kohl, N. E.; Hartman, G. D.; Bilodeau, M. T. *Bioorg. Med. Chem. Lett*. **2008**, *18*, 2211–2214. (b) Martin, M. W.; Newcomb, J.; Nunes, J. J.; Bemis, J. E.; McGowan, D. C.; White, R. D.; Buchanan, J. L.; DiMauro, E. F.; Boucher, C.; Faust, T.; Hsieh, F.; Huang, X.; Lee, J. H.; Schneider, S.; Turci, S. M.; Zhu, X. *Bioorg. Med. Chem. Lett*. **2007**, *17*, 2299–2304. (c) Rodriguez, A. L.; Williams, R.; Zhou, Y.; Lindsley, S. R.; Le, U.; Grier, M. D.; Weaver, C. D.; Conn, P. J.; Lindsley, C. W. *Bioorg. Med. Chem. Lett.* **2009**, *19*, 3209–3213. (d) Debenham, J. S.; Madsen-Duggan, C. B.; Toupence, R. B.; Walsh, T. F.; Wang, J.; Tong, X.; Kumar, S.; Lao, J.; Fong, T. M.; Xiao, J. C.; Huang, C. R. R. C.; Shen, C.-P.; Feng, Y.; Marsh, D. J.; Stribling, D. S.; Shearman, L. P.; Strack, A.

M.; Goulet, M. T. *Bioorg. Med. Chem. Lett*. **2010**, *20*, 1448–1452. (e) Parcella, K.; Eastman, K.; Yeung, K.-S.; Grant-Young, K. A.; Zhu, J.; Wang, T.; Zhang, Z.; Yin, Z.; Parker, D.; Mosure, K.; Fang, H.; Wang, Y.-K.; Lemm, J.; Zhuo, X.; Hanumegowda, U.; Liu, M.; Rigat, K.; Donoso, M.; Tuttle, M.; Zvyaga, T.; Haarhoff, Z.; Meanwell, N. A.; Soars, M. G.; Roberts, S. B.; Kadow, J. F. *ACS Med. Chem. Lett*. **2017**, *8*, 771–774.

[11] (a) Naito, Y.; Akahoshi, F.; Takeda, S.; Okada, T.; Kajii, M.; Nishimura, H.; Sugiura, M.; Fukaya, C.; Kagitani, Y. *J. Med. Chem.* **1996**, *39*, 3019–3029. (b) Patil, P. S.; Kasare, S. L.; Haval, N. B.; Khedkar, V. M.; Dixit, P. P.; Rekha, E. M.; Sriram, D.; Haval, K. P. *Bio. Med. Chem. Lett.* **2020**, *30*, 127434. (c) Menendez, C.; Gau, S.; Lherbet, C.; Rodriguez, F.; Inard, C.; Pasca, M. R.; Baltas, M. *Eur. J. Med. Chem.* **2011**, *46*, 5524–5531.

[13] (a) Chen, Z.; Hu, G.; Li, D.; Chen, J.; Li, Y.; Zhou, H.; Xie, Y. *Bioorg. Med. Chem.* **2009**, *17*, 2351–2359. (b) Michael, J. P. *Nat. Prod. Rep.* **1995**, *12*, 465–475. (c) Kuarm, B. S.; Reddy, Y. T.; Madhav, J. V.; Crooks, P. A.; Rajitha, B. *Bioorg. Med. Chem. Lett.* **2011**, *21*, 524–527. (d) Vlahakis, J. Z.; Lazar, C.; Crandall, I. E.; Szarek, W. A. *Bioorg. Med. Chem.* **2010**, *18*, 6184–6196. (e) Gu, X.; Ren, Z.; Tang, X.; Peng, H.; Zhao, Q.; Lai, Y.; Peng, S.; Zhang, Y. *Eur. J. Med. Chem.* **2012**, *51*, 137−144. (f) Bright, S. A.; Brinkø, A.; Larsen, M. T.; Sinning, S.; Williams, D. C.; Jensen, H. H. *Bioorg. Med. Chem. Lett.* **2013**, *23*, 1220−1224. (g) Khan, I.; Ibrar, A.; Abbas, N.; Saeed, A. *Eur. J. Med. Chem.* **2014**, *76*, 193–244. (h) Zhang, L.; Peng, X. M.; Damu, G. L. V.; Geng, R.-X.; Zhou, C.-H. *Med. Res. Rev.* **2014**, *34*, 340–437. (i) Albrecht, B. K.; Gehling, V. S.; Hewitt, M. C.; Vaswani, R. G.; Cote, A.; Leblanc, Y.; Nasveschuk, C. G.; Bellon, S.; Bergeron, L.; Campbell, R.; Cantone, N.; Cooper, M. R.; Cummings, R. T.; Jayaram, H.; Joshi, S.; Mertz, J. A.; Neiss, A.; Normant, E.; O'Meara, M.; Pardo, E.; Poy, F.; Sandy, P.; Supko, J.; Sims, R. J.; Harmange, J.-C.; Taylor, A. M.; Audia, J. E. *J. Med. Chem.* **2016**, *59*, 1330−1339. (j) Becerra, A.; Quintero, C.; Morales, V.; Valderrama, M.; Aguirre, A.; Faúndez, M. A.; Rojas, R. S. *Bioorg. Med. Chem.* **2017**, *25*, 2681–2688. (k) Tariq, S.; Somakala, K.; Amir, M. *Eur .J. Med. Chem.* **2018**. *143*, 542–557. (l) Khandelia, T.; Ghosh, S.; Panigrahi, P.; Shome, R.; Ghosh, S. S. Patel, B. K. *J. Org. Chem*. **2021**, *86*, 16948–16964. (m) Kim, J.;

Park, M.; Choi, J.; Singh, D. K.; Kwon, H. J.; Kim, S. H.; Kim, I. *Bioorg. Med. Chem. Lett.* **2019**, *29*, 1350–1356.

[14] (a) Novak, P.; Muller, K.; Santhanam, K. S. V.; Haas, O. *Chem. Rev*. **1997**, *97*, 207–282. (b) Curran, D.; Grimshaw, J.; Perera, S. D. *Chem. Soc. Rev*. **1991**, *20*, 391–404. (c) Higgins, S. J. *Chem. Soc. Rev*. **1997**, *26*, 247–257. (d) Tsuboyama, A.; Iwawaki, H.; Furugori, M.; Mukaide, T.; Kamatani, J.; Igawa, S.; Moriyama, T.; Miura, S.; Takiguchi, T.; Okada, S.; Hoshino, M.; Ueno, K. *J. Am. Chem. Soc*. **2003**, *125*, 12971–12979. (e) Wang, Y. Z.; Epstein, A. J. *Acc. Chem. Res*. **1999**, *32*, 217–224. (f) Ulrich, G.; Ziessel, R.; Harriman, A. *Angew. Chem., Int. Ed*. **2007**, *47*, 1184–1201. (g) Pu, S. Z.; Liu, G.; Shen, L.; Xu, J. K. *Org. Lett*. **2007**, *9*, 2139–2142. (h) Maeda, H.; Mihashi, Y.; Haketa, Y. *Org. Lett.* **2008**, *10*, 3179 –3182. (i) Li, C.-S.; Tsai, Y.-H.; Lee, W.-C.; Kuo, W.-J. *J. Org. Chem.* **2010**, *75*, 4004–4013. (j) Moni, L.; Gers-Panther, C. F.; Anselmo, M.; Müller, T. J. J.; Riva, R. *Chem. Eur. J*. **2016**, *22*, 2020–2031. (k) Ibrahim, M. M.; Al-Refai, M.; Al-Fawwaz, A.; Ali, B. F.; Geyer, A.; Harms, K.; Marsch, M.; Kruger, M.; Osman, H.; Azmi, M. N. *J. Fluoresc*. **2018**, *28*, 655–662. (l) Ghosh, S.; Pal, S.; Rajamanickam, S.; Shome, R.; Mohanta, P. R.; Ghosh, S. S.; Patel, B. K. *ACS Omega.* **2019**, *4*, 5565–5577. (m) Majee, S.; Shilpa, Sarav, M.; Banik, B. K.; Ray, D. *Pharmaceuticals* **2023**, *16*, 873.

[15] (a) Friend, R. H.; Gymer, R. W.; Holmes, A. B.; Burroughes, J. H.; Marks, R. N.; Taliani, C.; Bradley, D. D. C.; Dos. Santos, D. A.; Bredas, J. L.; Logdlund, M.; Salaneck, W. R. *Nature* **1999**, *397*, 121–128. (b) Mitschke, U.; Bauerle, P. *J. Mater. Chem*. **2000**, *10*, 1471–1507. (c) Gondek, E.; Kityk, I. V.; Danel, A.; Wisla, A.; Sanetra, J. *Synth. Met*. **2006**, *156*, 1348–1354 (d) Abet, V.; Nuñez, A.; Mendicuti, F.; Burgos, C.; Alvarez-Builla, J. *J. Org. Chem*. **2008**, *73*, 8800–8807. (e) Ahmed, E.; Briseno, A. L.; Xia, Y.; Jenekhe, S. A. *J. Am. Chem. Soc*. **2008**, *130*, 1118–1119. (f) Mutai, T.; Tomoda, H.; Ohkawa, T.; Yabe, Y.; Araki, K. *Angew. Chem., Int. Ed*. **2008**, *47*, 9522–9524, *Angew. Chem.* **2008**, *120*, 9664–9666. (g) Manna, S. K.; Mandal, A.; Mondal, S. K.; Adak, A. K. Jana, A.; Das, S.; Chattopadhyay, S.; Roy, S.; Ghorai, S. K.; Samanta, S.; Hossain, M.; Baidya, M. *Org. Biomol. Chem*. **2015**, *13*, 8037–8047. (h) Paramasivam, M.; Chitumalla, R. K.; Singh, S. P.; Islam, A.; Han, L.; Rao, V. J.; Bhanuprakash, K. *J. Phys. Chem. C* **2015**, *119*,

17053–17064. (i) Qian, X.; Zhu, Y.-Z.; Chang, W.-Y.; Song, J.; Pan, B.; Lu, L.; Gao, H.-H.; Zheng, J.-Y. *ACS Appl. Mater. Interfaces.* **2015**, *7*, 9015–9022. (j) Lin, G.; Peng, H.; Chen, L.; Nie, H.; Luo, W.; Li, Y.; Chen, S.; Hu, R.; Qin, A.; Zhao, Z.; Tang, B. Z. *ACS Appl. Mater. Interfaces.* **2016**, *8*, 16799–16808. (k) Chen, C. H.; Wang, Y.; Michinobu, T.; Chang, S.-W.; Chiu, Y. C.; Ke, C.-Y.; Liou, G.-S. *ACS Appl. Mater. Interfaces*. **2020**, *12*, 6144–6150.

[16] (a) Kukushkin, V. Y.; Pombeiro, A. J. L. *Chem. Rev.* **2002**, *102*, 1771–1802. (d) Zhou, C.; Larock, R. C. *J. Am. Chem. Soc*. **2004**, *126*, 2302–2303. (e) Shimizu, H.; Murakami, M. *Chem. Commun*. **2007**, 2855–2857. (f) Rach, S. F.; Kühn, F. E. *Chem. Rev*. **2009**, *109*, 2061–2080. (g) Xin, X.; Xiang, D.; Yang, J.; Zhang, Q.; Zhou, F.; Dong, D. *J. Org. Chem*. **2013**, *78*, 11956–11961. (h) Ping, Y.; Wang, L.; Ding, Q.; Peng, Y. *Adv. Synth. Catal*. **2017**, *359*, 3274–3291. (i) Cheng, K.; Wang, G.; Meng, M.; Qi, C. *Org. Chem. Front.* **2017**, *4*, 398–403. (j) Rakshit, A.; Dhara, H. N.; Sahoo, A. K.; Patel, B. K. The Renaissance of Organo Nitriles in Organic Synthesis. *Chem. - Asian J.* **2022**, *17*, e202200792 (k) Kanda, T.; Naraoka, A.; Naka, H. *J. Am. Chem. Soc*. **2019**, *141*, 825–830. (l) Paul, B.; Maji, M.; Kundu, S. *ACS Catal.* **2019**, *9*, 10469–10476. (m) Sun, K.; Lv, Q.-Y.; Lin, Y.-W.; Yu, B.; He, W.-M. *Org. Chem. Front*. **2021**, *8*, 445–465.

[17] (a) Xin, X.; Huang, P.; Xiang, D.; Zhang, R.; Zhao, F.; Zhang, N.; Dong, D. *Org. Biomol. Chem.* **2013**, *11*, 1001–1006. (b) Li, E.; Huang, Y. *Chem. Commun.* **2014**, *50*, 948–950. (c) Tian, J.; Sun, H.; Zhou, R.; He, Z. *Chin. J. Chem.* **2013**, *31*, 1348–1351. (d) Ma, C.; Jia, Z.-J.; Liu, J.-X.; Zhou, Q.-Q.; Dong, L.; Chen, Y.-C. *Angew. Chem., Int. Ed.* **2013**, *52*, 948–951. (e) Zhou, R.; Zhang, K.; Han, L.; Chen, Y.; Li, R.; He, Z. *Chem. Eur. J.* **2016**, *22*, 5883–5887. (f) Chen, P.; Zhang, J.; Zhang, J. *Adv. Synth. Catal.* **2018**, *360*, 682–685.

[18] (a) Alishetty, S.; Shih, H.-P.; Han, C.-C. *Org. Lett*. **2018**, *20*, 2513–2516. (b) Chen, C.; Wei, R.; Yi, X.; Gao, L.; Zhang, M.; Liu, H.; Li, Q.; Song, H.; Ban, S. *J. Org. Chem*. **2019**, *84*, 15655–15661. (c) Wang, Z.; Chen, W.; Luo, H.; He, C.; Zhang, G.; Yu, Y. *Synthesis*. **2020**, *52*, 1659–1665. (d) Gao, L.; Li, G.; Li, X.; Zhang, G.; Zhang, M.; Li, Q.;

Ban, S. *Org. Chem. Front.* **2022**, *9*, 2390–2395. (e) Xiong, B.; Shi, C.; Xu, W.; Liu, Y.; Zhu, L.; Tang, K.-W.; Yin, S.-F.; Wong, W.-Y. *Adv. Synth. Catal.* **2022**, *364*, 4392–4401.

[19] (a) Tietze, L. F. *Chem. Rev*. **1996**, *96*, 115–136. (b) Tietze, L. F.; Beifuss, U. *Angew. Chem., Int. Ed*. **1993**, *32*, 131–163. (c) Padwa, A.; Bur, S. K. *Tetrahedron*. **2007**, *63*, 5341–5378. (d) Li, Y.-M.; Wang, S.-S.; Yu, F.-C.; Shen, Y.-H.; Chang, K.-J. *Org. Biomol. Chem*. **2015**, *13*, 5376–5380. (e) Zhang, X.; Xie, X.; Liu, Y. *Chem. Sci*. **2016**, *7*, 5815–5820.

[20] (a) Nicolaou, K. C.; Edmonds, D. J.; Bulger, P. G. *Angew. Chem., Int. Ed*. **2006**, *45*, 7134–7186. (b) Grondal, C.; Jeanty, M.; Enders, D. *Nature Chem*. **2010**, *2*, 167–178.

[21] (a) Watanabe, T.; Ueda, S.; Inuki, S.; Oishi, S.; Fujii, N.; Ohno, H. *Chem. Commun*. **2007**, 4516–4518. (b) Yao, P.-Y.; Zhang, Y.; Hsung, R. P.; Zhao, K. *Org. Lett.* **2008**, *10*, 4275–4278. (c) Zhu, J.; Xie, H.; Chen, Z.; Li, S.; Wu, Y. *Chem. Commun*. **2009**, 2338–2340. (d) Verma, A. K.; Kesharwani, T.; Singh, J.; Tandon, V.; Larock, R. C. *Angew. Chem., Int. Ed*. **2009**, *48*, 1138–1143. (e) Lv, X.; Bao, W. *J. Org. Chem*. **2009**, *74*, 5618–5621. (f) Wang, F.; Cai, S.; Liao, Q.; Xi, C. *J. Org. Chem*. **2011**, *76*, 3174–3180. (g) Zhang, L.-L.; Chen, S.; Gao, Y.-Z.; Zhang, P.-B.; Wu, Y.-L.; Tang, G.; Zhao, Y.-F. *Org. Lett*. **2016**, *18*, 1286–1289. (h) Zhang, P.-B.; Zhang, L.-L.; Gao, Y.-Z.; Tang, G.; Zhao, Y.-F. *RSC Adv*. **2016**, *6*, 60922–60925. (i) Wang, S.-S. Fu, H.; Wang, G.; Sunb, M.; Li, Y.-M. *RSC Adv*. **2016**, *6*, 52391–52394. (j) Chen, W.; Zhang, Y.; Li, P.; Wang, L. *Org. Chem. Front*. **2018**, *5*, 855–859.

[22] Li, C.; An, S.; Zhu, Y.; Zhang, J.; Kang, Y.; Liu, P.; Wang, Y.; Li, J. *RSC Adv*. **2014**, *4*, 49888–49891.

[23] Majhi, B.; Parwez, A.; Palit, S.; Dutta, S. *J. Org. Chem.* ***2022***, *87*, 14695−14705.

[24] Chen, Y.-F.; Hsieh, J.-C. *Org. Lett*. **2014**, *16*, 4642–4645.

[25] Kishi, A.; Moriyama, K.; Togo, H. *J. Org. Chem.* **2018**, *83*, 11080−11088.

[26] Yu, S.; Qi, L.; Hu, K.; Gong, J.; Cheng, T.; Wang, Q.; Chen, J.; Wu, H. *J. Org. Chem*. **2017**, *82*, 3631–3638.

[27] Yu, H.; Xiao, L.; Yang, X.; Shao, L. *Chem. Commun*. **2017**, *53*, 9745–9748.

[28] Zhang, Y.; Shao, Y.; Gong, J.; Hu, K.; Cheng, T.; Chen, J. *Adv. Synth. Catal*. **2018**, *360*, 3260–3265.

[29] Xiong, W.; Hu, K.; Lei, Y.; Zhen, Q.; Zhao, Z.; Shao, Y.; Li, R.; Zhang, Y.; Chen, J. *Org. Lett*. **2020**, *22*, 1239–1243.

[30] Rodrigues, R.; Tran, L. Q.; Darses, B.; Dauban, P.; Neuville, L. *Adv. Synth. Catal*. **2019**, *361*, 4454–4460.

[31] Rakshit, A.; Kumar, P.; Alam, T.; Dhara, H.; Patel, B. K. *J. Org. Chem.* **2020**, *85*, 12482–12504.

[32] Cui, S.-Q.; Cheng, N.; Ma, Q.-Q.; Wei, Z.-L.; Liao, W.-W.; *Org. Chem. Front.* **2022**, *9*, 123–128.

[33] Yu, X.; Gao, L.; Jia, L.; Yamamoto, Y.; Bao, M. *J. Org. Chem*. **2018**, *83*, 10352–10358.

[34] Jaiswal, Y.; Kumar, Y.; Pal, J.; Subramanian, R.; Kumar, A. *Chem. Commun*. **2018**, *54*, 7207–7210.

[35] Xiong, W.; Chen, Z.; Shao, Y.; Li, R.; Hu, K.; Chen, J. *Org. Chem. Front.* **2020**, *7*, 756–762.

[36] Dai, L.; Yu, S.; Lv, N.; Ye, X.; Shao, Y.; Chen, Z.; Chen, J. *Org. Lett*. **2021**, *23*, 5664–5668.

[37] Chen, L.; Lv, N.; Zhen, Q.; Chen, Z.; Ge, J.; Chen, J. *Org. Chem. Front.* **2022**, *9*, 1955–1959.

[38] Zheng, J.; Zhang, Y.; Wang, D.; Cui, S. *Org. Lett*. **2016**, *18*, 1768–1771.

[39] Zheng, J.; Deng, Z.; Zhang, Y.; Cui, S. *Adv. Synth. Catal*. **2016**, *358*, 746–751.

[40] Shang, J.-Q.; Wang, S.-S.; Fu, H.; Li, Y.; Yang, T.; Li, Y.-M. *Org. Chem. Front*. **2018**, *5*, 1945–1949.

[41] Shang, J.-Q.; Wang, X.-X.; Xin, Y.; Li, Y.; Zhou, B.; Li, Y.-M. *Org. Biomol. Chem*. **2019**, *17*, 9447–9455.

[42] Li, Z.; Wu, Y.-H.; Xi, J.-M.; Wei, Z.-L.; Liao, W.-W. *Org. Lett.* **2021**, *23*, 9591–9596.

[43] Ji, L.; Gu, W.; Liu, P.; Sun, P. *Org. Biomol. Chem.* **2020**, *18*, 6126–6133.

[44] Shan, X.-H.; Zheng, H.-X.; Yang, B.; Tie, L.; Fu, J.-L.; Qu, J.-P.; Kang, Y.-B. *Nat Commun.* **2019**, *10*, 908–916.

[45] Xu, P.; Zhu, Y.-M.; Wang, F.; Wang, S.-Y.; Ji, S.-J. *Org. Lett*. **2019**, *21*, 683–686.

[46] Xu, P.; Zhu, Y.-M.; Liu, X.-Y.; Zhou, X.-Z.; Wang, S.-Y.; Ji, S.-J. *Chin. Chem. Lett*. **2021**, *32*, 413–416.

[47] (a) Fleming, F. F.; Wang, Q. *Chem. Rev*. **2003**, *103*, 2035–2077. (b) Rach, S. F.; Kühn, F. E. *Chem. Rev*. **2009**, *109*, 2061–2080.

[48] Pletnev, A. A.; Tian, Q.; Larock, R. C. *J. Org. Chem*. **2002**, *67*, 9276–9287.

[49] Tian, Q.; Pletnev, A. A.; Larock, R. C. *J. Org. Chem*. **2003**, *68*, 339–347.

[50] Miura, T.; Murakami, M. *Org. Lett.* **2005**, *7*, 3339–3341.

[51] Tsukamoto, H.; Ikeda, T.; Doi, T. *J. Org. Chem*. **2016**, *81*, 1733–1745.

[52] McCormick, M. M.; Duong, H. A.; Zuo, G.; Louie, J. *J. Am. Chem. Soc*. **2005**, *127*, 5030–5031.

[53] Onodera, G.; Shimizu, Y.; Kimura, J.; Kobayashi, J.; Ebihara, Y.; Kondo, K.; Sakata, K.; Takeuchi, R. *J. Am. Chem. Soc*. **2012**, *134*, 10515–10531.

[54] Wang, C.-S.; Sun, Q.; García, F.; Wang, C.; Yoshikai, N. *Angew. Chem., Int. Ed*. **2021**, *60*, 9627–9634.

[55] Li, X.; Huang, L.; Chen, H.; Wu, W.; Huang, H.; Jiang, H. *Chem. Sci.* **2012**, *3*, 3463–3467.

[56] Pearce, A. J.; Harkins, R. P.; Reiner, B. R.; Wotal, A. C.; Dunscomb, R. J.; Tonks, I. A. *J. Am. Chem. Soc*. **2020**, *142*, 4390–4399.

[57] (a) Mishra, P. K.; Chatterjee, S.; Verma, A. K. *ACS Omega*. **2020**, *5*, 32133–32139. (b) Li, J.; Chen, L.; Chin, E.; Lui, A. S.; Zecic, H. *Tetrahedron Lett*. **2010**, *51*, 6422–6425. (c) Shen, H.; Xie, Z. *J. Am. Chem. Soc*. **2010**, *132*, 11473–11480.

[58] Reddy, V.; Jadhav, A. S.; Anand, R. V. *Eur. J. Org. Chem*. **2016**, *2016*, 453–458.

[59] Kumar, R.; Asthana, M.; Singh, R. M. *J. Org. Chem*. **2017**, *82*, 11531–11542.

[60] Liu, X.; Deng, G.; Liang, Y. *Tetrahedron Lett*. **2018**, *59*, 2844–2847.

[61] (a) Bergonzini, G.; Cassani, C.; Wallentin, C.-J. *Angew. Chem., Int. Ed*. **2015**, *54*, 14066–14069. (b) Fu, W.; Xu, F.; Fu, Y.; Zhu, M.; Yu, J.; Xu, C.; Zou, D. *J. Org. Chem*. **2013**, *78*, 12202–12206. (c) Ji, W.; Tan, H.; Wang, M.; Li, P.; Wang, L. *Chem. Commun*. **2016**, *52*, 1462–1465. (d) Tang, S.; Deng, Y.-L.; Li, J.; Wang, W.-X.; Ding, G.-L.; Wang, M.-W.; Xiao, Z.-P.; Wang, Y.-C.; Sheng, R.-L. *J. Org. Chem*. **2015**, *80*, 12599–12605. (e) Zhou, L.; Lokman Hossain, M.; Xiao, T. *Chem. Rec*. **2016**, *16*, 319–334. (f) Xia, D.; Li,

Y.; Miao, T.; Li, P.; Wang, L. *Green Chem.* **2017**, *19*, 1732–1739. (g) Deng, Q.; Xu, Y.; Liu, P.; Tan, L.; Sun, P. *Org. Chem. Front.* **2018**, *5*, 19–23.

[62] Han, Y.-Y.; Jiang, H.; Wang, R.; Yu, S. *J. Org. Chem.* **2016**, *81*, 7276–7281.

[63] Li, X.; Fang, X.; Zhuang, S.; Liu, P.; Sun, P. *Org. Lett.* **2017**, *19*, 3580–3583.

[64] Yu, Y.; Yuan, W.; Huang, H.; Cai, Z.; Liu, P.; Sun, P. *J. Org. Chem.* **2018**, *83*, 1654–1660.

[65] Zhu, M.; Fu, W.; Guo, W.; Tian, Y.; Wang, Z.; Ji, B. *Org. Biomol. Chem.* **2019**, *17*, 3374–3380.

[66] Natarajan, P.; Muskan, M.; Brar, N. K.; Kaur, J. J. *Org. Chem. Front.* **2018**, *5*, 1527–1531.

[67] (a) Sahoo, A. K.; Rakshit, A.; Dahiya, A.; Pan, A.; Patel, B. K. *Org. Lett.* **2022**, *24*, 1918–1923. (b) Sahoo, A. K.; Rakshit, A.; Pan, A.; Dhara, H. N.; Patel, B. K. *Org. Biomol. Chem.* **2023**, *21*, 1680–1691.

[68] (a) Mulliken, R. S. *J. Am. Chem. Soc.* **1950**, *72*, 600–608. (b) Mulliken, R. S. *J. Am. Chem. Soc.* **1952**, *74*, 811–824. (c) Mulliken, R. S. *J. Phys. Chem.* **1952**, *56*, 801–822.

[69] (a) Crisenza, G. E. M.; Mazzarella, D.; Melchiorre, P. *J. Am. Chem. Soc.* **2020**, *142*, 5461–5476. (b) Li, T.; Liang, K.; Tang, J.; Ding, Y.; Tong, X.; Xia, C. *Chem. Sci.* **2021**, *12*, 15655–15661. (c) Chen, Z.; Xue, F.; Liu, T.; Wang, B.; Zhang, Y.; Jin, W.; Xia, Y.; Liu, C. *Green Chem.* **2022**, *24*, 3250–3256. (d) Shen, J.; Li, J.; Chen, M.; Chen, Y. *Org. Chem. Front.* **2023**, *10*, 1166–1172. (e) Chen, Z.; Xue, F.; Zhang, Y.; Jin, W.; Wang, B.; Xia, Y.; Xie, M.; Abdukader, A.; Liu, C. *Org. Lett.* **2022**, *24*, 3149–3154. (f) Saux, E. L.; Zanini, M.; Melchiorre, P. *J. Am. Chem. Soc.* **2022**, *144*, 1113–1118. (g) Chen, Z.; Jin, W.; Xia, Y.; Zhang, Y.; Xie, M.; Ma, S.; Liu, C. *Org. Lett.* **2020**, *22*, 8261–8266. (h) Bahamonde, A.; Melchiorre, P. *J. Am. Chem. Soc.* **2016**, *138*, 8019–8030. (i) Ho, H. E.; Pagano, A.; Rossi-Ashton, J. A.; Donald, J. R.; Epton, R. G.; Churchill, J. C.; James, M. J.; O'Brien, P.; Taylor, R. J. K.; Unsworth, W. P. *Chem. Sci.* **2020**, *11*, 1353–1360. (j) Beato, E. P.; Spinnato, D.; Zhou, W.; Melchiorre, P. *J. Am. Chem. Soc.* **2021**, *143*, 12304–12314.

[70] (a) Lima, C. G. S.; de M. Lima, T.; Duarte, M.; Jurberg, I. D.; Paixão, M. W. *ACS Catal.* **2016**, *6*, 1389–1407. (b) Yang, Z.; Liu, Y.; Cao, K.; Zhang, X.; Jiang, H.; Li, J. *Beilstein J. Org. Chem.* **2021**, *17*, 771–799. (c) Tavakolian, M.; Hosseini-Sarvari, M. *ACS Sustainable Chem. Eng.* **2021**, *9*, 4296–4323. (d) Saxena, B.; Patel, R. I.; Sharma, A. *Adv. Synth. Catal.* **2023**, *365*, 1538–1564.

[71] Li, Y.; Miao, T.; Li, P.; Wang, L. *Org. Lett.* **2018**, *20*, 1735–1739.

[72] Shi, W.; Ma, F.; Li, P.; Wang, L.; Miao, T. *J. Org. Chem.* **2020**, *85*, 13808–13817.

भारतीय प्रौद्योगिकी संस्थान गुवाहाटी
Indian Institute of Technology Guwahati

CHAPTER II

Visible-Light Mediated Solvent-Switched Photosensitizer-Free Synthesis of Poly-functionalized Quinolines and Pyridines

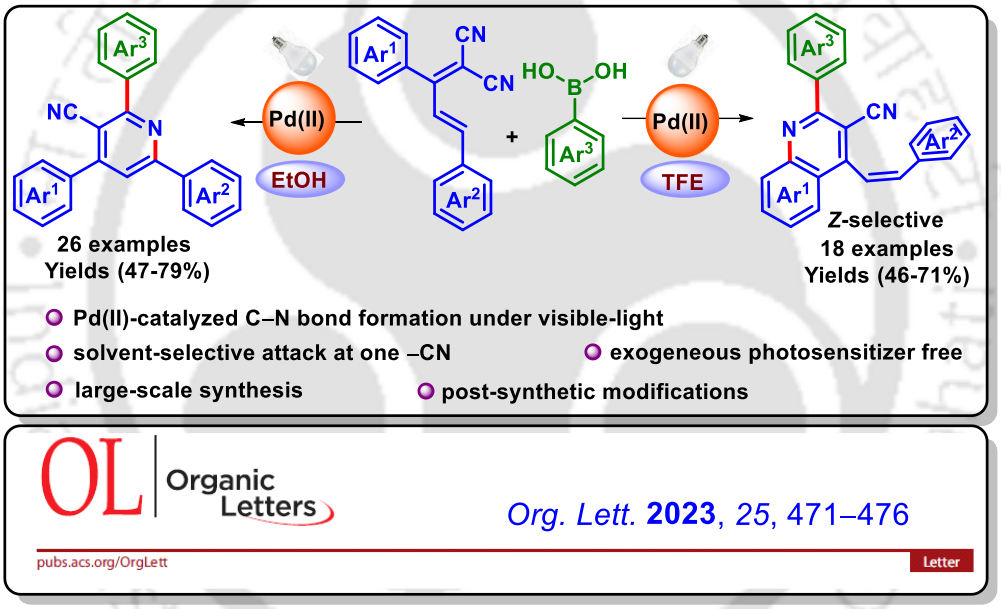

ABSTRACT: A solvent (TFE vs. EtOH) switched synthesis of quinolines and pyridines is illustrated from (*E*)-2-(1,3-diphenylallylidene)malononitriles via a Pd(II)-catalyzed photochemical process. The active catalyst [$L_2Pd(0)$] generated serves as an exogenous photosensitizer. The process offers predominantly *Z*-alkenylated quinolines and pyridines in TFE and EtOH respectively. Further, large-scale synthesis and a few interesting post-synthetic modifications have been demonstrated.

CHAPTER II

Visible-Light Mediated Solvent-Switched Photosensitizer-Free Synthesis of Poly-functionalized Quinolines and Pyridines

II.1. Introduction:

Among nitrogenous heterocycles, quinolines and pyridines have grabbed significant attention due to their prevalence in natural products and biologically active compounds (Figure II.1.1.).[1] Quinolines and pyridines are found to display a range of biological activities and have various applications.[2] Quinoline analogues such as chloroquine and hydroxychloroquine have been used against infectious diseases.[2d,2e] There are some well-established traditional methods for synthesizing quinolines and pyridines,[3] but the newer methodology is always interesting.[4] In this context, the photochemical approach has gained tremendous importance for the synthesis of *N*-heterocycles.[5] In photochemical transformations the combination of photocatalyst and visible light enables the molecule to cross the energy barrier at room temperature.[6] However, without any exogenous photocatalysts, several elegant approaches have also been established under visible light.[7] In recent years, the visible-light-induced photoexcited chemistry of Pd has become an emerging arena of investigation.[7]

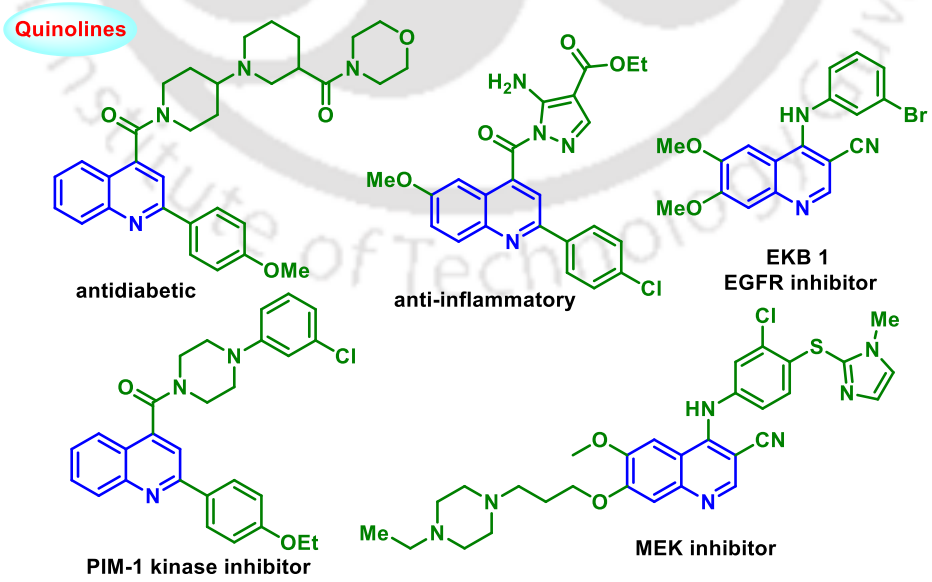

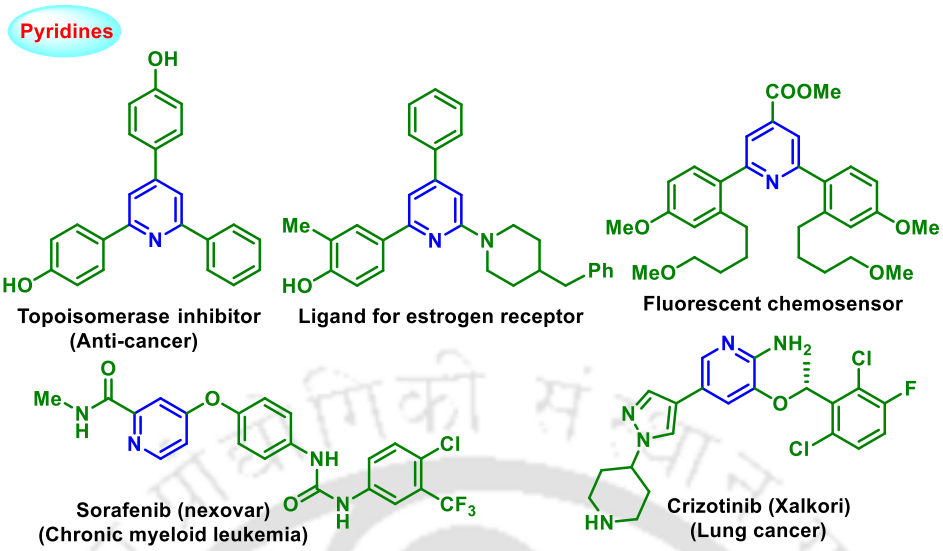

Figure II.1.1. *Representative biologically active Quinolines and Pyridines.*

Lately, the nitrile-triggered reactions have gained immense importance in serving as acceptors which in combination with a suitable nucleophilic partner, leads to carbocycles and heterocycles.[8] Furthermore, nitrile-triggered C–H functionalization is an emerging area due to its flexibility and sustainability in organic transformation. In this method, a metal (M) is inserted into the C–H bond by coordinating with the nitrile through chelation with the metal center thereby forming a C–M species, which takes part in many coupling reactions.[8] Some of these transformations provide access to functionalize quinolines and pyridines via the formation of C–C and C–N bonds. In 2019, Chen and Shao's group reported a Pd(II)-catalyzed addition of arylboronic acids with 2-aminostyryl nitriles to access 2-arylquinolines [Scheme II.1.1 (i)].[9] In 2021, Chen *et al*. demonstrated a Pd(II)-catalyzed three-component reaction of nitriles for the synthesis of 2-arylquinoline-4-carboxylates involving addition, ring expansion followed by esterification [Scheme II.1.1 (ii)].[10] In 2017, a Cu(I)-catalyzed [2 + 2 + 2] synthesis of multisubstituted pyridines was developed by Chen's group which is initiated via alkenylation of nitriles with vinyliodonium salts [Scheme II.1.1 (iii)].[11] A similar [2 + 2 + 2] cycloaddition of α,ω-diynes with nitriles using Ir(I)-catalyzed is reported by the Takeuchi group to access pyridines [Scheme II.1.1 (iv)].[12] Taking cues from the literature, we envisaged that the cascade addition/cyclization of nitrile functionality under metal or metal-free conditions would lead to the formation of *N*-heterocycles.[8,13]

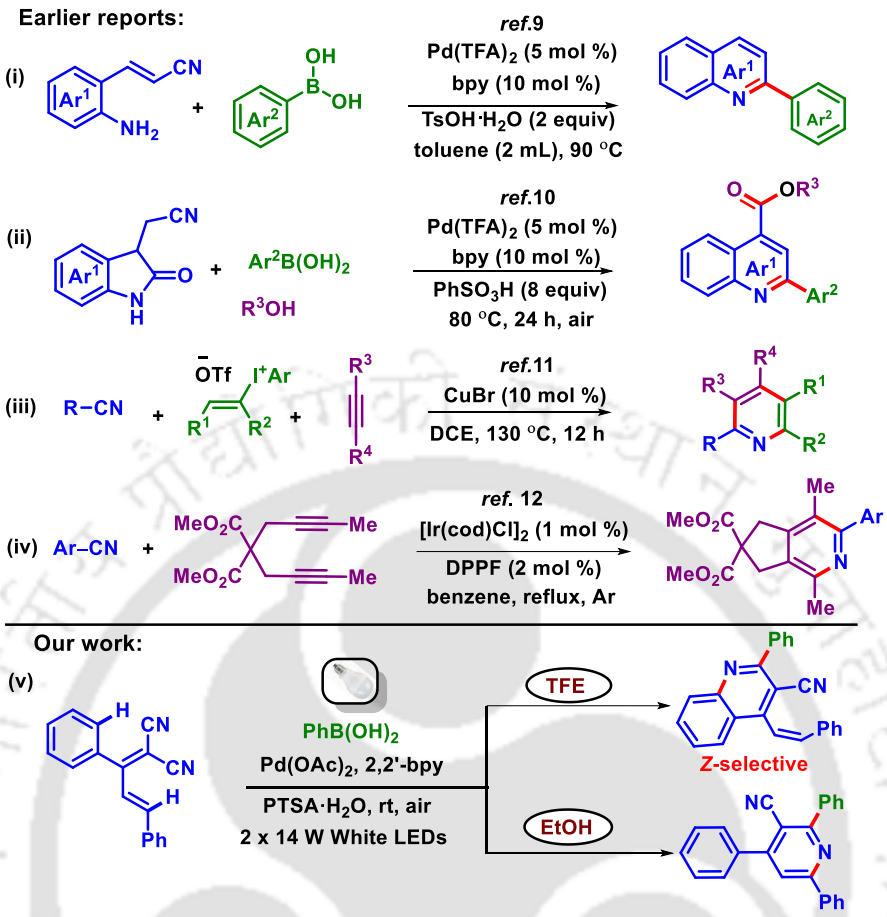

Scheme II.1.1. *Strategies for the Synthesis of Quinolines and Pyridines Using Nitriles.*

Inspired by these nitrile-triggered reactions, it was hypothesized that the dicyanodiene, (*E*)-2-(1,3-diphenylallylidene)malononitrile (**1a**) can undergo cascade addition/cyclization with arylboronic acid under the irradiation of visible-light. To realize this, a reaction was carried out between dicyanodiene (**1a**, 0.25 mmol) and phenylboronic acid (**2a**, 1.0 mmol) in 1,2-dichloroethane (DCE, 2 mL) under irradiation of white light (2 x 14 W) (flux = 46 mW/cm^2) in the presence of $Pd(OAc)_2$ (10 mol %), 2,2′-bipyridyl (20 mol %) and PTSA.H_2O (4 equiv). Gratifyingly, two new products, one a major *viz.* (*Z*)-2-phenyl-4-styrylquinoline-3-carbonitrile (**4aa**, 31%) and the other a minor, 2,4,6-triphenylnicotinonitrile (**3aa**, 20%) were isolated. A closer observation of the structures of **3aa** and **4aa** reveals that both are quite dissimilar and must be originating from two different competitive paths, which are frequently associated due to the solvent effect. The influence of fluorinated solvent on metal-catalyzed regiospecific C–H activation via H-bonding interaction leading to a specific product is well-documented.[14] Due to the strong H-bonding

ability, fluorinated solvents such as hexafluoroisopropanol (HFIP) and 2,2,2-trifluoroethanol (TFE) alter the selectivity in many reactions.[14] To determine whether the present selectivity is controlled by similar H-bonding interaction, the reaction was performed in TFE instead of DCE. Surprisingly, the selectivity improved in favor of (**4aa**) in 63% and the other product (**3aa**) in 15% yields. Unexpectedly, the *Z*-configuration was found to be the major product irrespective of the solvents used. Thus, herein, we unveiled a solvent-switched regio-divergent Pd(II)-catalyzed site-selective cascade addition/cyclization of dicyanodiene (**1a**) and arylboronic acid to access 2,4,6-triarylnicotinonitrile (**3aa**) and predominant (*Z*)-2-aryl-4-styrylquinoline-3-carbonitrile (**4aa**) under visible-light irradiation [Scheme II.1.1 (v)]. After a series of optimization, the optimal condition for the synthesis of 2,4,6-triarylnicotinonitrile (**3aa**) was found to be the use of phenylboronic acid (**2a**, 1.0 mmol), $Pd(OAc)_2$ (10 mol %), 2,2′-bipyridyl (20 mol %), *p*-toluenesulfonic acid ($PTSA{\cdot}H_2O$) (1.0 mmol) in ethanol. For (*Z*)-2-aryl-4-styrylquinoline-3-carbonitriles (**4aa**) the best condition was the use of boronic acid (**2a**, 0.75 mmol), $Pd(OAc)_2$ (10 mol %), 2,2′-bipyridyl (20 mol %), $PTSA{\cdot}H_2O$ (0.75 mmol) in TFE (see Table II.1.1).

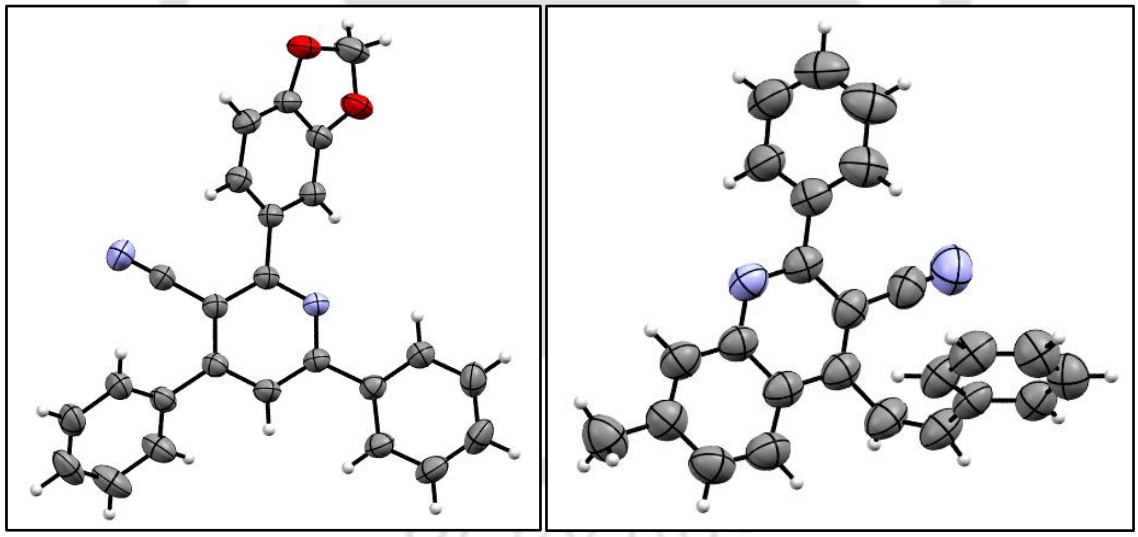

Figure II.1.2. *ORTEP diagram of pyridine derivative (**3aj**, CCDC 2184661) and quinoline derivative (**4ba**, CCDC 2184664) with 50% ellipsoid probability.*

II.2. Strategies for the Synthesis of Pyridines:

Owing to the versatile utility of pyridine in biological and synthetic fields, several methods have been employed for their synthesis via metal-free or transition-metal-catalyzed reactions.[15] A few of these strategies are enlisted below. One of the most widespread methods for the synthesis of

pyridines is the two-step Hantzsch approach, which involves the oxidation of 1,4-dihydropyridines (DHPs), which is formed via a one-pot pseudo-four-component reaction of 2 equiv of a 1,3-dicarbonyl derivative, an aldehyde, and a source of ammonia (Scheme II.2.1).[15a] Few others are the [5 + 1] condensation of 1,5-diketones with ammonia,[15c] and the Kröhnke synthesis.[15d]

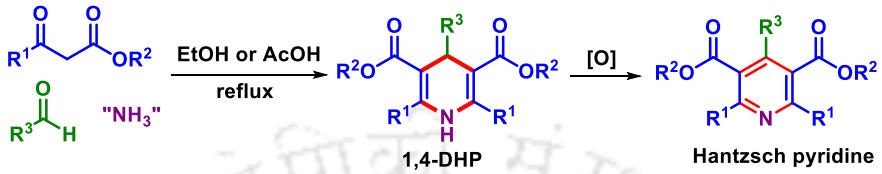

Scheme II.2.1. *General Hantzsch pyridine synthesis.*

Later on, several transition metal-mediated annulation protocols were explored. For example, Larock and coworkers developed a [4+2], two-step, palladium-catalyzed coupling of vinylic imines with terminal alkynes, followed by a subsequent copper-catalyzed cyclization route to 2,4-di- and 2,4,5-trisubstituted pyridines (Scheme II.2.2).[16]

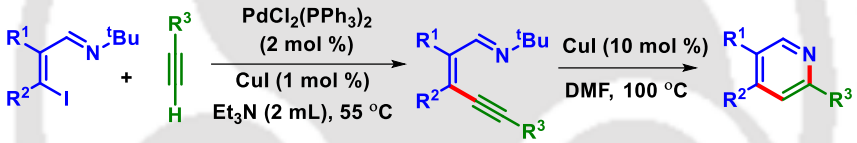

Scheme II.2.2. *[4+2] palladium-/copper-catalyzed route to pyridines.*

The past couple of decades have witnessed a surge in thermal and transition metal-assisted [4 + 2] hetero Diels-Alder reactions involving 1-azadienes and alkynes (Scheme II.2.3),[17] although inverse electron demand Diels-Alder strategies have also been explored.

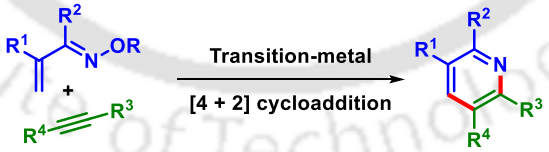

Scheme II.2.3. *Synthesis of pyridines via [4 + 2] cycloaddition.*

Earlier, researchers utilized the transition metals to catalyze the [2 + 2 + 2] cycloadditions of alkynes with nitriles to synthesize pyridines (Scheme II.2.4),[18a–e] and some other groups achieved the synthesis of substituted pyridines via a metal-free [2 + 2 + 2] cycloaddition approach.[18f-g]

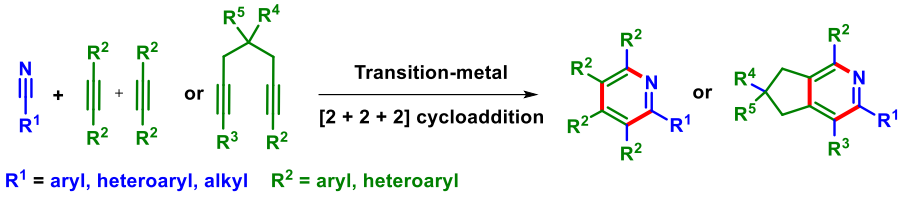

Scheme II.2.4. *Synthesis of pyridines via [2 + 2 + 2] cycloaddition.*

In the recent past, a Pd(II)-catalyzed cascade reaction of nitrile precursors with arylboronic acids has shown tremendous progress in affording pyridine scaffolds. In this regard, the Chen, Hu, and Li groups demonstrated the construction of 2,6-disubstituted pyridines via a Pd(II)-catalyzed C–C, C–N cascade coupling using δ-ketonitriles and arylboronic acids (Scheme II.2.5).[19]

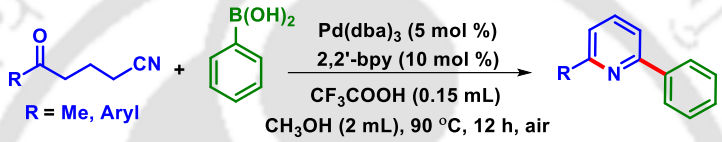

Scheme II.2.5. *Pd(II)-catalyzed cascade synthesis of pyridines.*

Chen and co-workers also developed a method to synthesize 2,6-diarylpyridines *via* a Ni(II)-catalyzed C–C and N–C coupling of ketonitriles with arylboronic acids (Scheme II.2.6).[20]

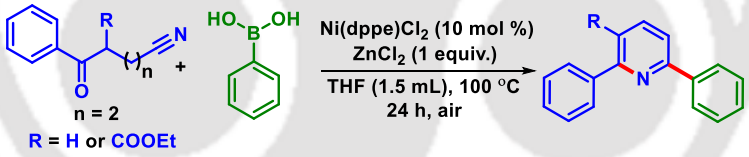

Scheme II.2.6. *Ni (II)-catalyzed synthesis of substituted pyridines.*

II.3. Strategies for the Synthesis of Quinolines:

Quinoline is one of the most important *N*-heterocyclic compounds known to have an extensive range of applications in medicinal, bioorganic, industrial chemistry, and synthetic organic chemistry.[21–27] Since the late 1800s, several methods have been known for the synthesis of quinoline and its derivatives. Some conventional techniques such as Skraup, Doebner-von Miller, Friedlander, Pfitzinger, Conrad-Limpach, and Combes synthesis are well-established for synthesizing quinolines (Scheme II.3.1).[21] Some of the strategies are described below.

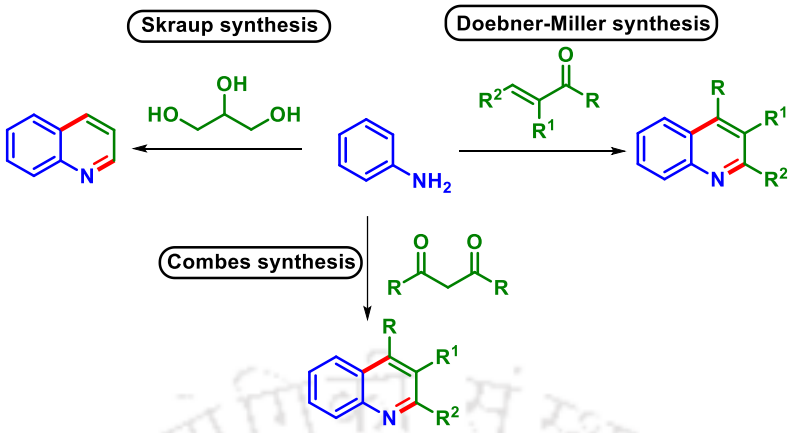

Scheme II.3.1. *General method for the synthesis of substituted quinolines.*

In 2015, Rangappa's group developed a synthesis of 2-phenylquinolines from 2-aminobenzyl alcohol and acetophenone using a catalytic amount of sodium hydroxide and a stoichiometric amount of T3P-DMSO as an oxidant (Scheme II.3.2).[22]

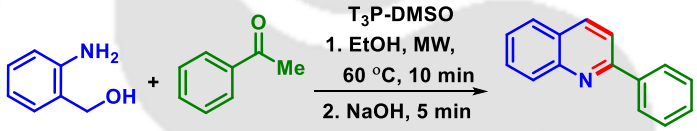

Scheme II.3.2. *Microwave-assisted synthesis of 2-Phenylquinolines.*

In 2016, Jiang et al. established a new regioselective approach to synthesize 2,3-disubstituted quinolines via a Pd-catalyzed intermolecular oxidative cyclization of *o*-vinylanilines and alkynes, assisted by Cu and O_2 (Scheme II.3.3).[23]. This protocol is proposed to proceed through sequential intermolecular amination of the alkyne, olefin insertion, and oxidative cleavage of the C–C bond.

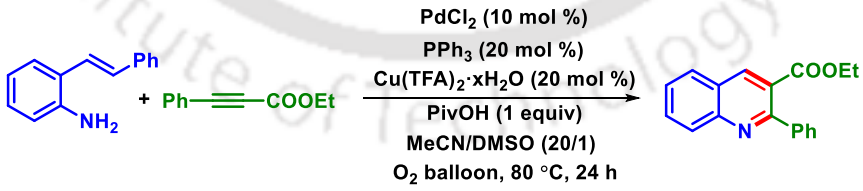

Scheme II.3.3. *Aerobic annulation to synthesize 2,3-disubstituted quinolines.*

In 2017, a regioselective Cu(I)-catalyzed synthesis of pharmaceutically important 2-arylthio quinolines was demonstrated by Volla's group (Scheme II.3.4).[24] The reaction progressed *via* the intermolecular annulation of aryl isothiocyanates, alkynes, and iodonium salts, yielding diversely functionalized quinolines in good to excellent yields.

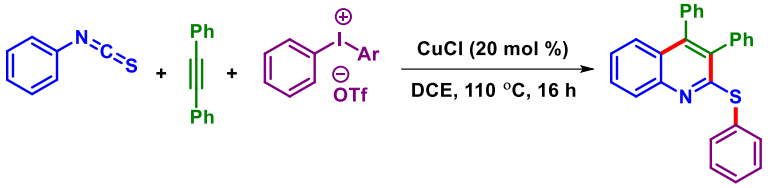

Scheme II.3.4. *Cu-catalyzed regioselective synthesis of 2-arylthio quinolines.*

Chen *et al.* introduced a $[IrCp^*Cl_2]_2$/KOH-catalyzed tandem approach to the synthesis of quinolines via an isomerization/cyclization reaction of allylic alcohols with 2-aminobenzyl alcohol (Scheme II.3.5).[25]

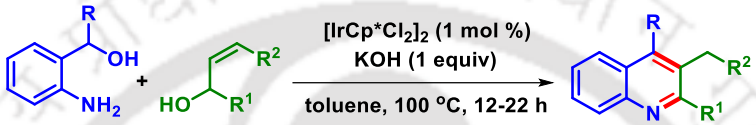

Scheme II.3.5. *Ir(III)-catalyzed synthesis of quinoline.*

In 2019, a Pd(II)-catalyzed tandem method was developed by Shao and Chen's group for the synthesis of 2-arylquinolines *via* the addition/cyclization of arylboronic acids to 2-aminostyryl nitriles through the formation of C−C, C−N bonds (Scheme II.3.6).[26] The mechanistic experiment reveals a nucleophilic addition of arylpalladium to the nitrile group followed by an intramolecular cyclization and dehydration to give the desired product.

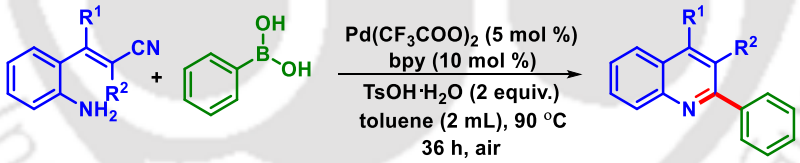

Scheme II.3.6. *Pd(II)-Catalyzed reaction of 2-aminostyryl nitrile with arylboronic acid.*

Later, in 2021, Li, Chen, and co-workers developed a new method for synthesizing poly-substituted quinolines using a Pd(II) catalyst under acidic conditions. This method involved a three-component tandem reaction of 2-aminobenzonitriles, arylboronic acids, and ketones (Scheme II.3.7).[27] The reaction has excellent chemoselectivity and avoids forming 4-aminoquinoline as a by-product *via* condensation-cyclization of 2-aminobenzonitriles with carbonyl compounds.

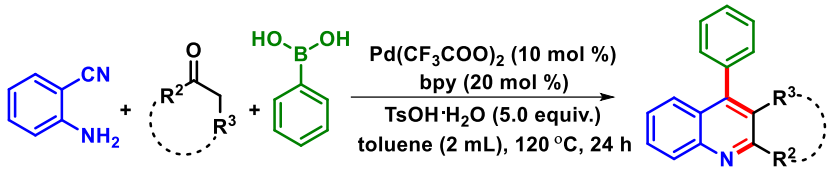

Scheme II.3.7. *Palladium(II)-catalyzed three-component tandem reactions.*

II.4. Present Work:

II.4.1. Optimization of the Reaction Conditions:

After successfully characterizing the two products (Section II.1), further screening was carried out to find out the optimal reaction conditions for selectively obtaining one of the products **3aa** or **4aa**. Initially, other solvents such as toluene (n.d/25%), dichloromethane (DCM) (n.d/38%), CH_3CN (n.d/n.d), dimethylformamide (DMF) (14%/n.d) were tested as alternatives to DCE, but none improved either the selectivity or the yield (Table II.4.1, entries 1–5). Fascinatingly, using EtOH as the solvent the product **3aa** was obtained in 64% along with a trace amount of **4aa** (5%), and some amount of unconsumed starting material after 24 h (Table II.4.1, entry 6). On prolonging the reaction time to 48 h the yield of **3aa** improved up to 72% and **4aa** (8%), (Table II.4.1, entry 7). However, similar improved selectivity between **3aa** and **4aa** could not be obtained with other alcoholic solvents such as MeOH (46%/30%), and ^{i}PrOH (57%/23%) (Table II.4.1, entries 8–9). A reaction performed in TFE showed an increase in the yield of **4aa** (15%/63%) (Table II.4.1, entry 10), demonstrating that the use of the fluorinated solvent (TFE) improved both the yield and selectivity in favor of **4aa**. The improved selectivity might be due to the strong hydrogen bonding ability of the fluorinated solvent. To further increase the yield and selectivity of **4aa** the loading of boronic acid and PTSA·H_2O was reduced to 3 equiv from 4 equiv, which results in the improved yield of **4aa** (71%) (Table II.4.1, entry 11). Interestingly, in a mixed solvent system of TFE/EtOH (1:1), the products **3aa** (37%) and **4aa** (35%) were obtained in nearly identical ratios under the same reaction parameters (Table II.4.1, entry 12). Thus, it was concluded that ethanol (EtOH) favouring the formation of pyridine (**3aa**) while 2,2,2-trifluoroethanol (TFE) predominately provides quinoline (**4aa**). Fixing the solvent to TFE and using boronic acid with PTSA·H_2O (3 equiv), alternative Pd(II)-catalyst and ligands were screened. The replacement of $Pd(OAc)_2$ with $Pd(TFA)_2$ resulted in a relatively lower yield of **3aa** (15%) and **4aa** (32%) (Table II.4.1, entry 13), while other Pd(II)-catalyst *viz.* $Pd(CH_3CN)_2Cl_2$ (n.d/n.d), $Pd(PPh_3)_2Cl_2$ (n.d/n.d), $PdBr_2$ (n.d/n.d)

were unable to deliver any of the products (Table II.4.1, entries 14–16). However, omitting either the catalyst {$Pd(OAc)_2$}, ligand (2,2'-bipyridine), or additive ($PTSA{\cdot}H_2O$) in TFE completely inhibits the reaction (Table II.4.1, entries 17–19). The variation of other bidentate ligands such as 1,10-phenanthroline (2%/29%), monodentate ligands like XPhos (3%/41%), PPh_3 (n.d/26%) (Table II.4.1, entries 20–22) was not beneficial for this reaction. Later on, performing the reaction in TFE with other additives (in place of $PTSA{\cdot}H_2O$) such as AcOH, trifluoroacetic acid, and *p*-toluic acid were found completely unsatisfactory (Table II.4.1, entries 23–25). The reaction was also completely silent in the absence of either catalyst $Pd(OAc)_2$ or additive $PTSA{\cdot}H_2O$ in EtOH (Table II.4.1, entries 26–27). In the absence of light, the reaction failed to give the product (**4aa**) in TFE, whereas, in EtOH, it gave a trace amount of (**3aa**, 10%) (Table II.4.1, entry 28). This suggests the requirement of a continuous supply of light, which facilitates the reaction via the MLCT process. Next, the feasibility of the reaction was evaluated under thermal conditions (80 °C) using the preferred solvent. It was observed that in TFE and EtOH, **3aa** was formed only in less amounts (trace, 20%), while **4aa** was not obtained at all (Table II.4.1, entry 29). Next, the fate of the reaction was checked under the light sources of variable wavelengths. It was observed that the use of 28 W (4 × 7 W) green light (513 nm) and 28 W (4 × 7 W) blue light (432 nm) fails to improve the formation of pyridine (**3aa**) and quinoline (**4aa**) in EtOH (41%/n.d), (36%/n.d), and TFE (10%/34%), (5%/40%), respectively (Table II.4.1, entry 30–33).

Table II.4.1. *Optimization of the reaction conditions*[a-j]

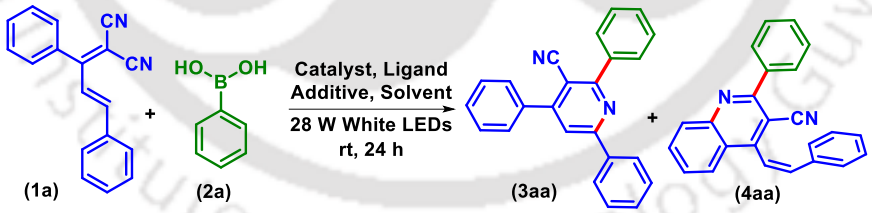

Entry	Catalyst (mol %)	Ligand (mol %)	Additive (equiv)	Solvent	Yield (%)[b] (3aa/4aa)
1	$Pd(OAc)_2$ (10)	2,2'-bipyridyl (20)	$PTSA{\cdot}H_2O$ (4)	1,2-DCE	20 / 31
2	$Pd(OAc)_2$ (10)	2,2'-bipyridyl (20)	$PTSA{\cdot}H_2O$ (4)	Toluene	n.d / 25
3	$Pd(OAc)_2$ (10)	2,2'-bipyridyl (20)	$PTSA{\cdot}H_2O$ (4)	DCM	n.d / 38
4	$Pd(OAc)_2$ (10)	2,2'-bipyridyl (20)	$PTSA{\cdot}H_2O$ (4)	CH_3CN	n.d / n.d
5	$Pd(OAc)_2$ (10)	2,2'-bipyridyl (20)	$PTSA{\cdot}H_2O$ (4)	DMF	14 / n.d

6	$Pd(OAc)_2$ (10)	2,2'-bipyridyl (20)	PTSA·H_2O (4)	EtOH	64 / 5
7	**$Pd(OAc)_2$ (10)**	**2,2'-bipyridyl (20)**	**PTSA·H_2O (4)**	**EtOH**	**72 / 8[c]**
8	$Pd(OAc)_2$ (10)	2,2'-bipyridyl (20)	PTSA·H_2O (4)	MeOH	46 / 30
9	$Pd(OAc)_2$ (10)	2,2'-bipyridyl (20)	PTSA·H_2O (4)	^{i}PrOH	57 / 23
10	$Pd(OAc)_2$ (10)	2,2'-bipyridyl (20)	PTSA·H_2O (4)	TFE	15 / 63
11	**$Pd(OAc)_2$ (10)**	**2,2'-bipyridyl (20)**	**PTSA·H_2O (3)**	**TFE**	**13 / 71[d]**
12	$Pd(OAc)_2$ (10)	2,2'-bipyridyl (20)	PTSA·H_2O (3)	TFE/EtOH (1:1)	37 / 35
13	$Pd(TFA)_2$ (10)	2,2'-bipyridyl (20)	PTSA·H_2O (3)	TFE	15 / 32
14	$Pd(CH_3CN)_2Cl_2$ (10)	2,2'-bipyridyl (20)	PTSA·H_2O (3)	TFE	n.d / n.d
15	$Pd(PPh_3)_2Cl_2$ (10)	2,2'-bipyridyl (20)	PTSA·H_2O (3)	TFE	n.d / n.d
16	$PdBr_2$ (10)	2,2'-bipyridyl (20)	PTSA·H_2O (3)	TFE	n.d / n.d
17	---	2,2'-bipyridyl (20)	PTSA·H_2O (3)	TFE	n.d / n.d
18	$Pd(OAc)_2$ (10)	---	PTSA·H_2O (3)	TFE	n.d / <18
19	$Pd(OAc)_2$ (10)	2,2'-bipyridyl (20)	---	TFE	n.d / n.d
20	$Pd(OAc)_2$ (10)	1,10-phen (20)	PTSA·H_2O (3)	TFE	trace / 29
21	$Pd(OAc)_2$ (10)	XPhos (20)	PTSA·H_2O (3)	TFE	trace / 41
22	$Pd(OAc)_2$ (10)	PPh_3 (20)	PTSA·H_2O (3)	TFE	n.d / 26
23	$Pd(OAc)_2$ (10)	2,2'-bipyridyl (20)	AcOH (3)	TFE	22 / n.d
24	$Pd(OAc)_2$ (10)	2,2'-bipyridyl (20)	CF_3COOH (3)	TFE	19 / 37
25	$Pd(OAc)_2$ (10)	2,2'-bipyridyl (20)	(Me)$PhCO_2H$ (3)	TFE	43 / n.d
26	---	2,2'-bipyridyl (20)	PTSA·H_2O (4)	EtOH	n.d /n.d
27	$Pd(OAc)_2$ (10)	2,2'-bipyridyl (20)	---	EtOH	n.d / n.d
28	$Pd(OAc)_2$ (10)	2,2'-bipyridyl (20)	PTSA·H_2O (3 & 4)	TFE & EtOH	n.d / n.d & 10 /n.d[e]
29	$Pd(OAc)_2$ (10)	2,2'-bipyridyl (20)	PTSA·H_2O (3 & 4)	TFE & EtOH	trace/n.d & 20/n.d[f]
30	$Pd(OAc)_2$ (10)	2,2'-bipyridyl (20)	PTSA·H_2O (4)	EtOH	41 / n.d[g]
31	$Pd(OAc)_2$ (10)	2,2'-bipyridyl (20)	PTSA·H_2O (3)	TFE	10 / 34[h]
32	$Pd(OAc)_2$ (10)	2,2'-bipyridyl (20)	PTSA·H_2O (4)	EtOH	36 / n.d[i]
33	$Pd(OAc)_2$ (10)	2,2'-bipyridyl (20)	PTSA·H_2O (3)	TFE	5 / 40[j]

[a]Reaction condition: (*E*)-2-(1,3-diphenylallylidene)malononitrile (**1a**) (0.25 mmol), phenylboronic acid (**2a**) (1.0 mmol), catalyst (mol %), ligand (mol %.), additive (equiv) at room temperature under 28 W white LEDs for 24 h in air. [b]Isolated yields. [c] reaction at rt for 48 h. [d] reaction with phenylboronic acids (0.75 mmol) and PTSA.H_2O (3 equiv). [e] reaction at rt (no light). [f]reaction at 80 [o]C. [g, h]Reaction performed using 28 W green LEDs light. [i,j]28 W blue LEDs light.

After a series of optimizations, the optimal condition for the synthesis of 2,4,6-triarylnicotinonitrile (**3aa**) was found to be the use of phenylboronic acid (**2a**, 1.0 mmol), $Pd(OAc)_2$ (10 mol %), 2,2′-bpy (20 mol %), PTSA·H_2O (1.0 mmol) in ethanol. For 2-aryl-4-styrylquinoline-3-carbonitriles (**4aa**) the best condition was the use of phenylboronic acid (**2a**, 0.75 mmol), $Pd(OAc)_2$ (10 mol %), 2,2′-bpy (20 mol %), PTSA.H_2O (0.75 mmol) in TFE.

II.4.2. Substrates Scope for the Synthesis of Pyridines:

Having the optimized reaction conditions, the synthesis of functionalized pyridines was pursued using various dicyanodienes (**1a**–**1n**) and phenylboronic acid (**2a**) (Scheme II.4.2). The unsubstituted dicyanodiene (**1a**) reacted with phenylboronic acid (**2a**) to afford the 2,4,6-triphenyl-pyridine-3-carbonitrile (**3aa**) in 72% yield. The R^1 and R^2 aryl ring having an electron-donating group (EDG) and electron-withdrawing group (EWG) reacted with phenylboronic acid (**2a**) to give their corresponding pyridines (**3ba–3fa**) in yields of 49%–79% and (**3ga**–**3ia**) in yields of 57%–62%. The protocol was further tested with dicyanodiene having various combinations of EDG/EWG in both R^1 and R^2 aryl rings such as *p*-Me/*p*-F (**1j**) and *p*-Cl/*p*-OMe (**1k**) with (**2a**) yielding their respective cyanopyridines (**3ja**, 59%) and (**3ka**, 73%). Next, the reaction was carried out with a substrate having a dioxolane ring (**1l**), giving the product (**3la**) in 78% yield. Furthermore, the reaction with monoheterocyclic (**1m**) and diheterocyclic (**1n**) containing dicyanodienes delivered the corresponding pyridines (**3ma**, 60%) and (**3na**, 47%) respectively (Scheme II.4.2).

The scope of this photochemical reaction was further evaluated by reacting dicyanodiene (**1a**) with various arylboronic acids (**2a**–**2m**) (Scheme II.4.2). Aryl boronic acids possessing different EDGs (**2b**–**2e**) and EWGs (**2f**–**2h**) responded positively affording respective cyanopyridines (**3ab**–**3ae**) in yields of 45–66% and (**3af**–**3ah**) in yields of 53%–59%. The reaction with phenylboronic acid containing a dioxolane group (**2j**) yielded the corresponding pyridine (**3aj**) with a 52% yield. This protocol with phenyl-1,4-diboronic acid (**2k**) provided cyanopyridines (**3ak**) in 63% yield, whereas the other boronic acid remained unreacted. Similarly, the reaction was successfully carried out with poly aromatic boronic acids such as 2-naphthylboronic acid (**2l**) and

pyrene-1-boronic acid (**2m**) and both provided their corresponding cyanopyridines (**3al**, 70%) and (**3am**, 64%) respectively (Scheme II.4.2).

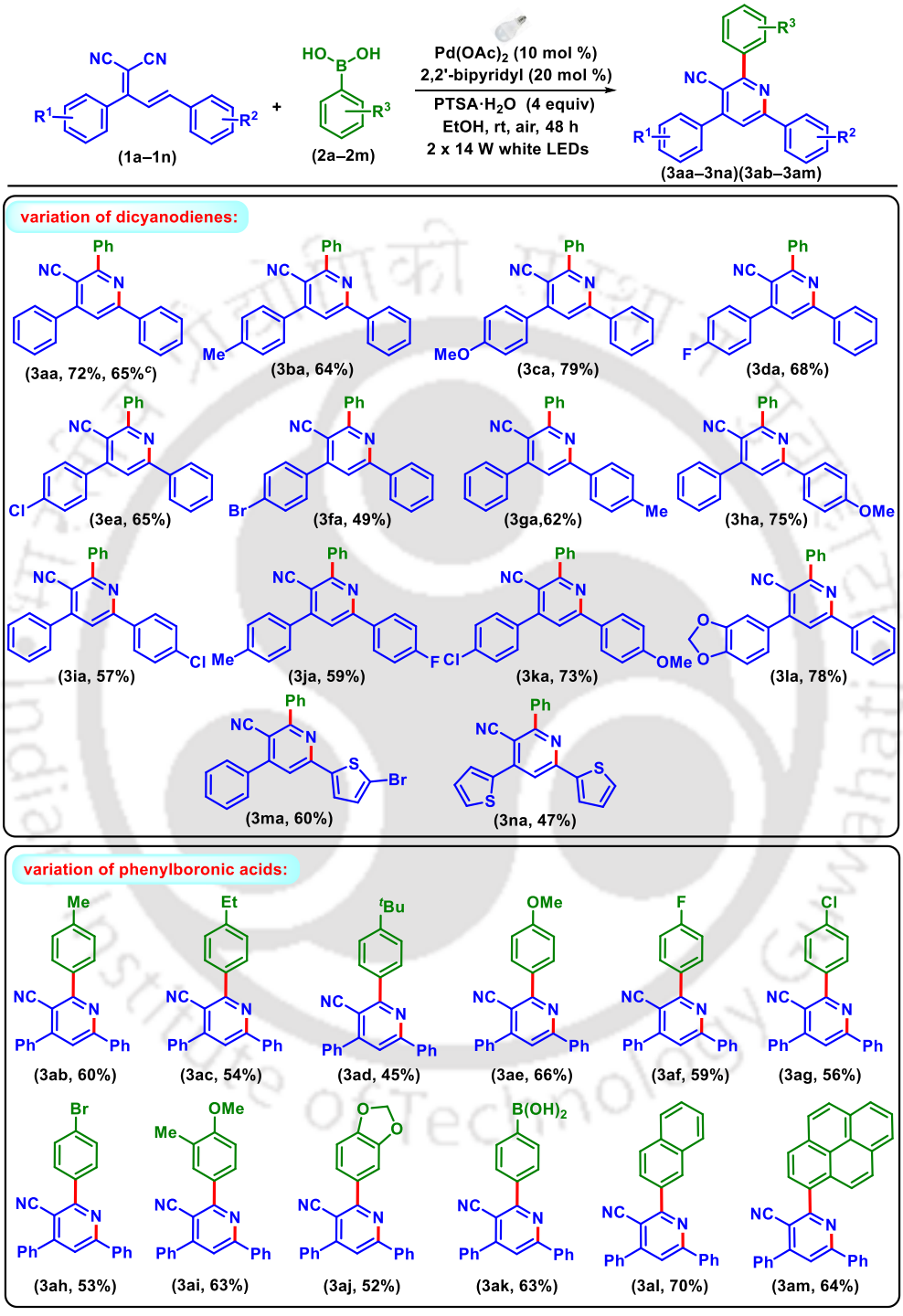

[a]Reaction conditions: (**1a–1n**) (0.25 mmol), (**2a**–**2m**) (1.0 mmol), $Pd(OAc)_2$ (0.025 mmol), 2,2′-bipyridyl (0.05 mmol), PTSA·H_2O (1.0 mmol), and EtOH (2 mL) at rt for 48 h in the air under two 14 W white LEDs. [b]Isolated yields. [c]Reaction performed on a 5 mmol scale.

Scheme II.4.2. *Substrate scope for the synthesis of pyridines.*[a,b,c]

II.4.3. Substrates Scope for the Synthesis of Quinolines:

As observed during the optimization process, the use of TFE completely alters the product selectivity giving quinolines (see Table II.4.1). Thus, after accomplishing the synthesis of a library of pyridines (Scheme II.4.2) using EtOH, the solvent system was switched to TFE to synthesize various substituted quinolines using a variety of dicyanodienes (**1a**–**1f**) and **2a** (Scheme II.4.3). The unsubstituted dicyanodiene (**1a**) reacted with **2a** to give the corresponding quinoline (**4aa**) in 71% yield with a ratio 97:3 of *Z*/*E*-isomer. Next, dicyanodiene containing EDG *p*-Me (**1b** and **1g**) and EWG *p*-Cl (**1e** and **1i**) groups in the R^1 and R^2 aryl ring reacted with (**2a**) affording quinolines (**4ba**–**4ia**) yields ranging from 59% to 69%. Furthermore, a furan containing heterocyclic dicyanodiene (**1o**) provided the corresponding product **4oa** in 54% yield (*Z*/*E* 99:1). Next, various arylboronic acids (**2b**–**2j**) with (**1a**) were explored. Phenylboronic acids possessing EDGs (**2b**–**2d**) and EWGs (**2g**–**2p**) also experienced efficient addition/cyclization to afford their respective quinolines (**4ab**–**4ad**) in 54–66% and (**4ag**–**4ap**) in 52–64% yields. Disubstituted phenylboronic acid having both EDG- and EWG *viz. p*-OMe-*m*-F (**2q**) also reacted smoothly to deliver the corresponding quinoline (**4aq**) in 63% yield (*Z*/*E* 86:14). From the yield pattern obtained in Scheme 3, no noticeable electronic effect of substituents in either of the reacting partner was observed. This is further confirmed by carrying out the reaction of boronic acids and dicyanodienes possessing a combination of EDG(*o*-Me)/EWG(*p*-Cl), EWG(*p*-Br)/EWG(*p*-Cl), and EWG(*p*-Cl)/EDG(*p*-^{t}Bu) groups affording their respective quinolines (**4in**, 62%, *Z*/*E* 94:6), (**4ih**, 54%, *Z*/*E* 87:13) and (**4pg**, 46%, *Z*/*E* 94:6) (Scheme II.4.3).

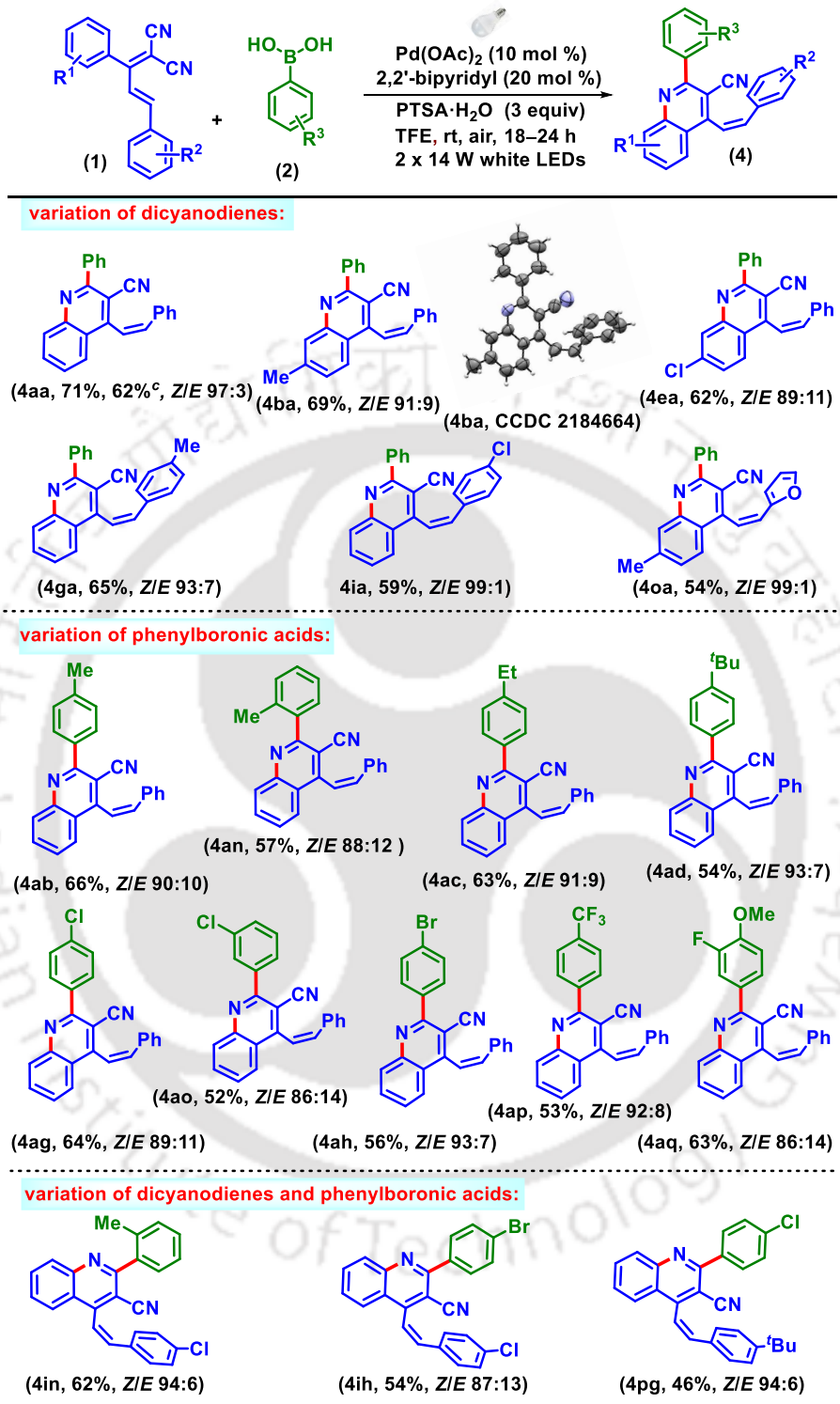

[a]Reaction conditions: **1** (0.25 mmol), **2** (0.75 mmol), $Pd(OAc)_2$ (0.025 mmol), 2,2'-bipyridyl (0.05 mmol), PTSA·H_2O (0.75 mmol), and TFE (2 mL) at rt for 18–24 h in air under two 14 W white LEDs. [b]Isolated yields and the ratio is determined from ^1H NMR. [c]Reaction performed on a 5 mmol scale.

Scheme II.4.3. *Substrates scope for the synthesis of quinolines.*[a,b,c]

II.5. Control Experiments:

After synthesizing the library of pyridines and quinoline derivatives, a few control experiments were carried out to understand the mechanistic path, as shown in Scheme II.5.1. Treatment of the *E* isomer of **1a** in the absence of **2a** under the standard condition gave no *Z*-isomer, suggesting no photoisomerization at the initial stage [Scheme II.5.1 (i)]. In the absence of light in TFE the reaction failed to give quinoline (**4aa**), whereas, in EtOH, the pyridine (**3aa**) was obtained in a yield of <15% after 48 h [Scheme II.5.1 (ii)a] suggesting the essential role of light in both these transformations. The reaction progress was unaffected in the presence of a radical scavenger TEMPO, suggesting the non-radical paths for both these transformations [Scheme II.5.1 (ii)b]. The performed H/D exchange suggests the irreversible nature of the reaction [Scheme II.5.1 (iii) and (iv)]. Next, to check any involvement of C–H bond cleavage in the rate-limiting step, competitive and parallel kinetic isotope effect (KIE) experiments were performed between **1g** and **1g-d$_5$**. A k_H/k_D of 1.51, for the parallel and 1.78 for the competitive reaction, suggests the C–H bond cleavage might not be involved in the rate-determining step [Scheme II.5.1 (v)].

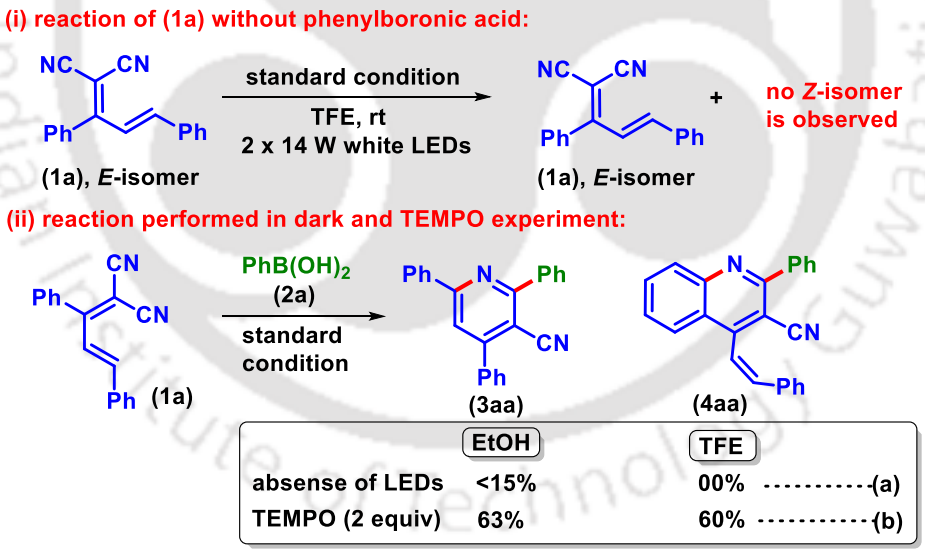

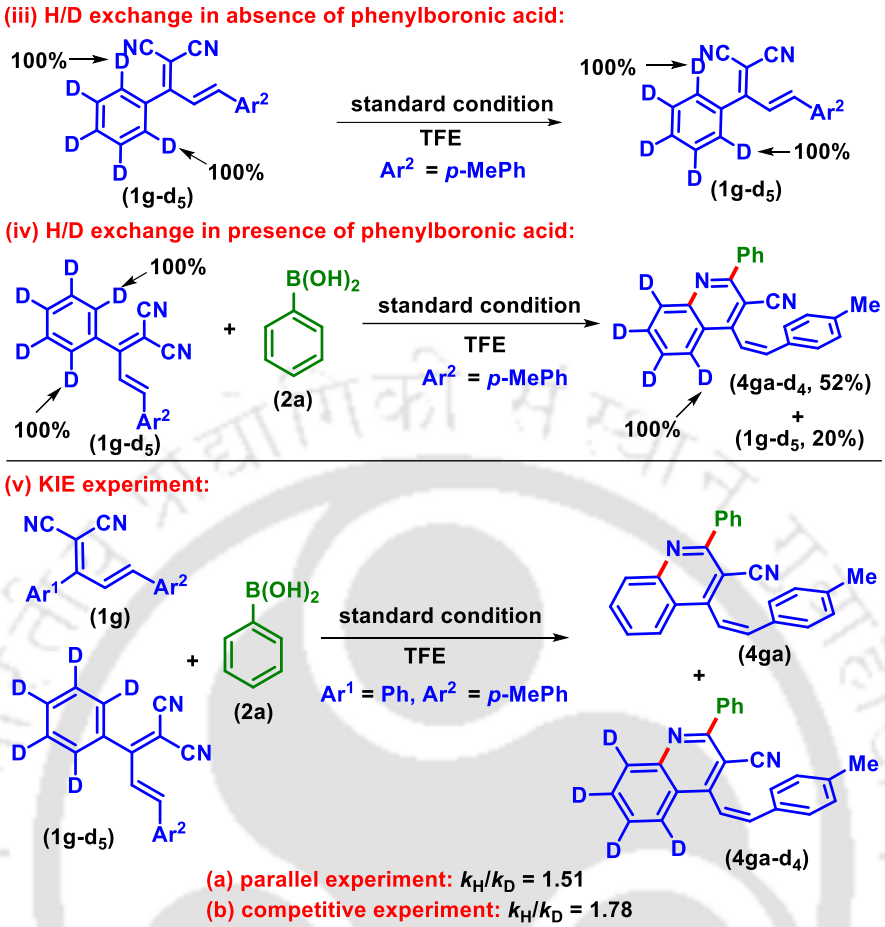

Scheme II.5.1. *Control experiments.*

To identify the visible-light absorbing species, UV-vis experiments were carried out by taking $Pd(OAc)_2$ (λ_{max} = 275 nm) and 2,2′-bpy (λ_{max} = 280 nm) independently. However, upon successive addition of 2,2′-bpy ligand the absorption maxima started appearing at ~420 nm. This confirms the MLCT between Pd(II) and 2,2′-bpy leading to $L_2Pd(0)$, which is the light-absorbing species (Figure II.5.1.a).[28] Next, to confirm the M→Z σ interaction between metal and ligands, a fluorescence quenching experiment was performed by taking $L_2Pd(0)$ as the probe and phenylboronic acid (**2a**) as the quencher. It was observed that the fluorescence intensity (λ_{max} = 466 nm) decreased upon successive addition of **2a** confirming the possible M-Z σ-interaction between them (Figure II.5.1.b–c).[13c] Next, an on-off experiment suggests that a continuous supply of visible light is essential for this photochemical transformation (Figure II.5.1.d).

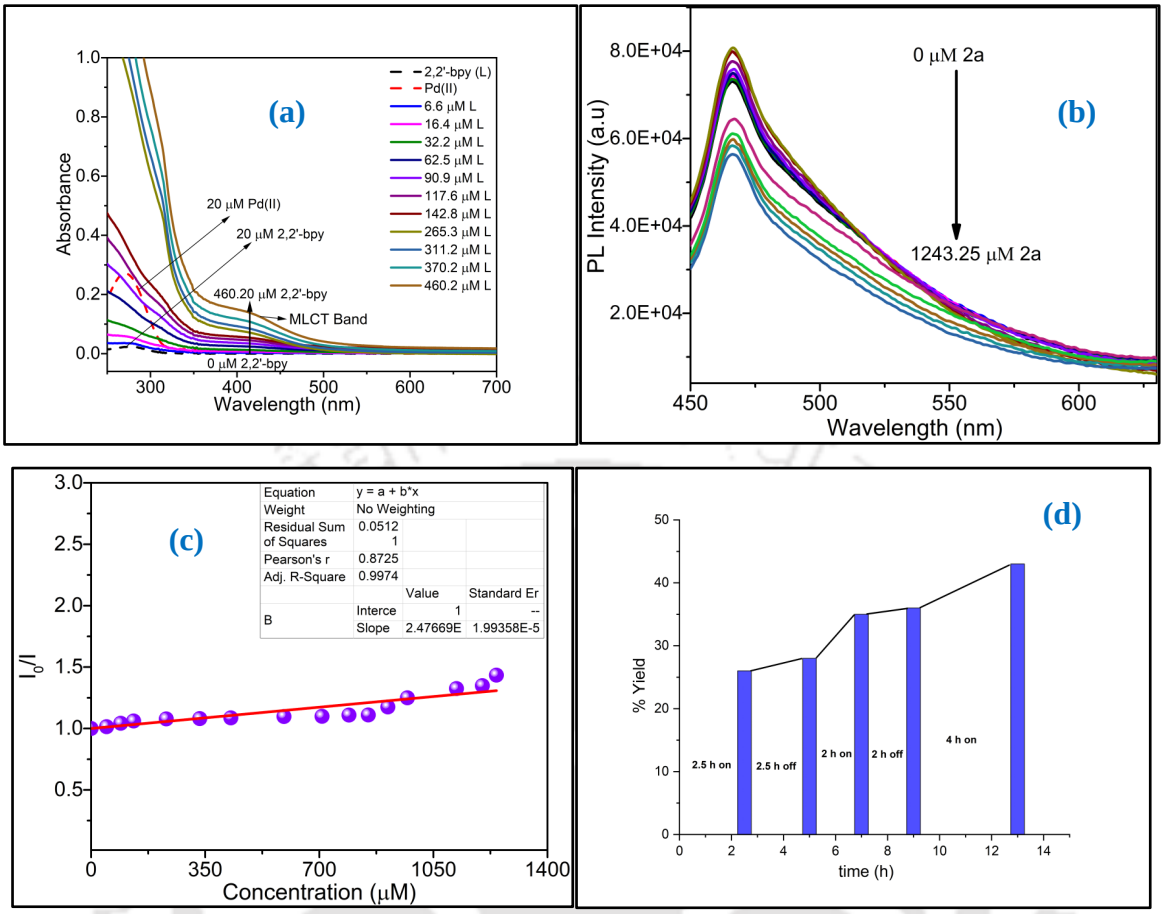

Figure II.5.1. *UV-vis spectra of (a) Pd(II), 2,2′-bpy and Pd-bpy complex in EtOH. (b) Fluorescence emission spectra of $L_2Pd(0)$ at varied conc. of quencher phenylboronic acid (**2a**) when excited at 420 nm (c) Stern-Volmer experiments (d) On-off experiment.*

II.6. Plausible Reaction Mechanism:

Based on the control experiments and previous literature reports a plausible mechanism is depicted (Scheme II.6.1 and II.6.2). Initially, $Pd(OAc)_2$ combines with ligand 2,2′-bpy (L) to form a $Pd(II)(bpy)(OAc)_2$ complex. Next, the reduction of this Pd(II)-complex in the presence of phenylboronic acid and 2,2′-bpy generates $[L_2Pd(0)]$ species[29a-b] (detected from HRMS) which *via* photoexcitation (a MLCT process confirmed by UV-experiments, see section II.9.6) [8b, 28] form a $[L_2Pd(0)]^*$ species[7a] under visible-light irradiation. Furthermore, in the presence of air (O_2), $[L_2Pd(0)]^*$ undergoes oxidation followed by transmetalation with phenylboronic acid producing an aryl-Pd(II) intermediate (A) which is facilitated through M → Z σ-interaction between the Pd and the boron center. (confirmed by quenching experiments).[8b,29c-d] The Pd(II) center of

intermediate **A** coordinates with the nitrile group proximate to the phenyl ring of **1a** to give intermediate **B**. Next, the aryl ring migrates to the nitrile via an intramolecular carbopalladation to form a Pd-ketimine complex (**C**).[8a] Furthermore, the more electronegative TFE can accelerate the C–H metalation step via H-bonding and facilitate the metalation in polar acidic or fluorinated solvents (HFIP and TFE). Thus, the interaction of TFE enhances the electrophilicity of the *ortho* C–H bond through H-bonding[14c] thereby facilitating the cyclopalladation via the formation of a 7-membered metallacycle (**D**).[14a] This is then transformed to intermediate **E** with concurrent elimination of PTSA. Next, the reductive elimination of intermediate **E** delivers the *E*-alkenylated quinoline (**F**) and regenerates Pd(0). This *E*-alkenylated quinoline (**F**) undergoes photoisomerization in the presence of a Pd catalyst or induced by photoexcitation[30] to afford the *Z*-alkenylated quinolone (**4aa**). Thus, the predominant formation of *Z*-isomer may be due to the low rotational energy barrier of the C=C double bond in the excited state. The exact driving force for this (*E* → *Z*) isomerization could not be revealed from the density functional theory DFT studies, since both are found to differ by only 1 kcal/mol in energy.

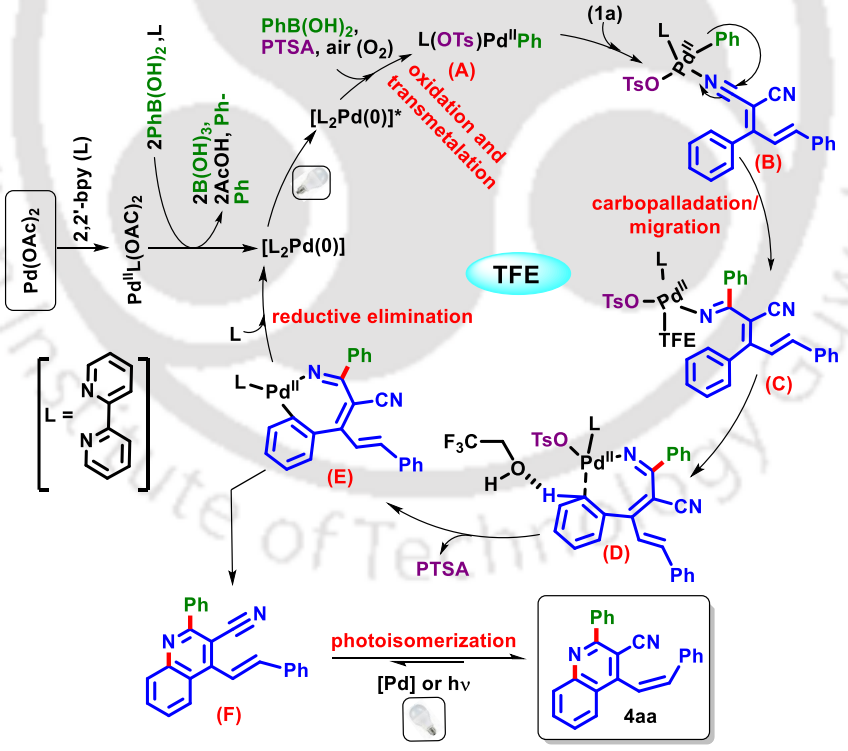

Scheme II.6.1. *Proposed mechanistic pathway in TFE.*

Similarly, for the formation of pyridine in EtOH, the aryl palladium (**A**) coordinates with the nitrile group toward the olefinic *E*-double bond of **1a** to give intermediate **K**. Next, migration of the phenyl ring via carbopalladation gives intermediate **L**, which is followed by an intramolecular cyclization giving a six-membered Pd-complex (**M**). Finally, β-H elimination of intermediate (**M**) delivers pyridine (**4aa**) with the generation of HPd(II)L(OTs), which is easily transformed to Pd(0) with the elimination of PTSA (Scheme II.5.2).

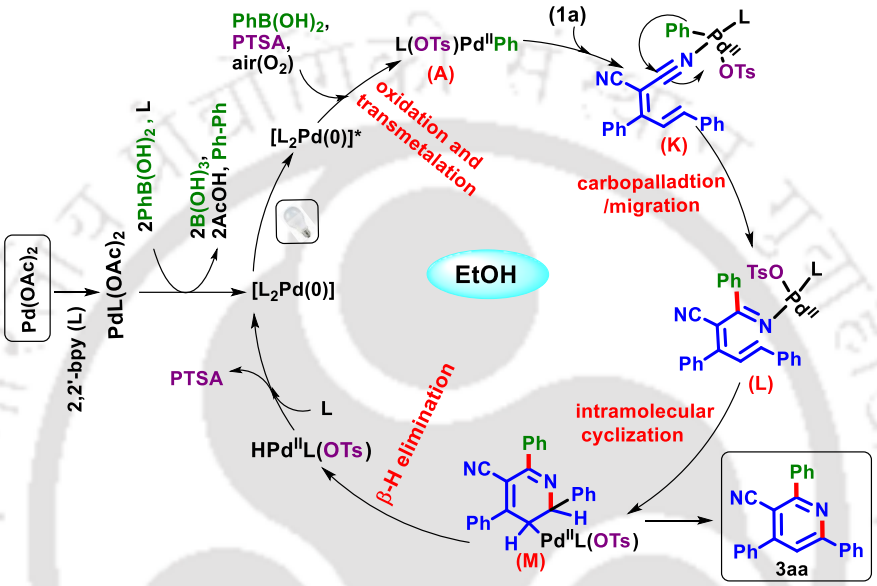

Scheme II.6.2. *Plausible mechanism in EtOH.*

II.7. Post-Synthetic Functionalizations:

To explore the synthetic utility, a few late-stage functionalizations were successfully carried out as shown in Scheme II.7.1. The cyano group of pyridine, 4-(4-methoxyphenyl)-2,6-diphenylnicotinonitrile (**3ca**) undergo a Pd(II)-catalyzed addition with phenylboronic acid (**2a**) to give keto product (**3caa**) in 65% yield.[31a] It may be mentioned here that under our photochemical conditions, the cyano group present in (**3ca**) did not react further to yield any trace of arylketone (**3caa**) even in the presence of Pd(II) and excess of boronic acid (**2a**) present in the medium, as this process is thermal one. Further, (**3ca**) undergoes a Ru(II)-catalyzed regioselective C–H/N annulation with diphenylacetylene (**r**) giving a highly fluorescence active annulated product (**3car**) in 76% yield.[31b] The annulation could have been taken with the other phenyl ring flanked between the –CN group and the pyridine nitrogen. As can be seen from the XRD analysis of **3aj** (an analog of **3ca**) the ring adjacent to the nitrile is out of the plane which is necessary for annulation. The

cyano group in **3ca** can be selectively hydrolyzed to an amidic group using ethanolic KOH, giving the amidic product (**3cab**) in 70% yield.[31c]

Similarly, the quinoline analog (**4ag**) having a nitrile and an olefinic moiety can undergo some useful transformations. In this context, when **4ag** was treated with phenylboronic acids (**2a**) in the presence of Pd(II) catalyst, a regioselective arylation at the olefinic site[31d] and concurrent hydrolysis of cyano to an amide took place, giving product **4aga** in 52% yield. Treatment of (**4ag**) with *m*-CPBA provided quinoline-*N*-oxide (**4ags**) in 75% yield[31e] without affecting the olefinic bond. Further, when **4ag** was treated with NaOH at 60 ^{o}C provided a cyclic amide (**4agb**, 61%).[31f] The cyclic amide was obtained via selective hydrolysis of nitrile to an amide followed by an intramolecular cyclization (Scheme II.7.1).

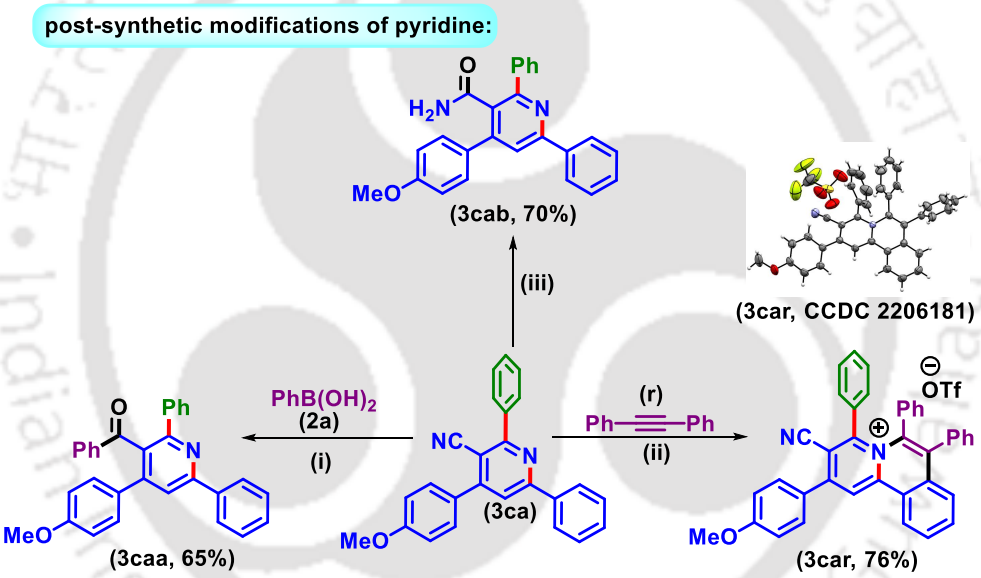

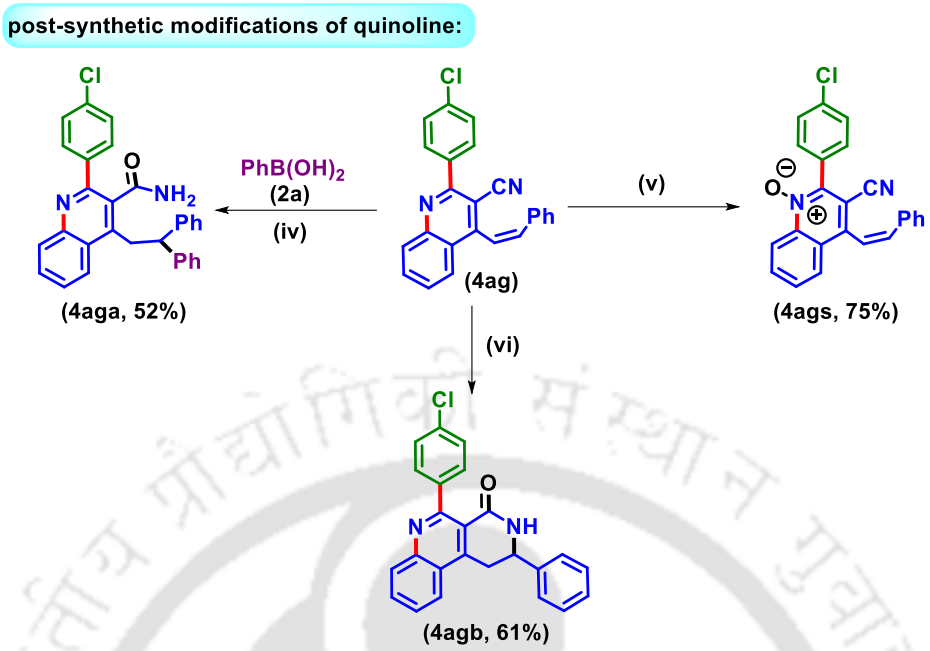

[a]Reaction conditions: [i] **3ca** (0.20 mmol), (**2a**) (0.60 mmol), $Pd(OAc)_2$ (10 mol %), 2,2′-bpy (20 mol %), PTSA. H_2O (10 equiv) and toluene (2 mL) at 120 °C in 24 h. [ii] **3ca** (0.20 mmol), diphenylacetylene (**r**) (0.40 mmol), [Ru(*p*-cymene)Cl_2]$_2$ (0.01 mmol), $Cu(OAc)_2 \cdot H_2O$ (0.44 mmol), TfOH (0.30 mmol) and DCE (2 mL) at 120 °C 12 h in pressure tube. [iii] **3ca** (0.20 mmol), KOH (5 equiv.), EtOH (2 mL), 80 °C, 6 h. [iv] **4ag** (0.20 mmol), (**2a**) (0.60 mmol), $Pd(OAc)_2$ (10 mol %), 2,2′-bpy (20 mol %), PTSA.H_2O (10 equiv.) and toluene (2 mL) at 120 °C in 24 h. [v] **4ag** (0.20 mmol), mCPBA (**s**) (5 equiv.) and DCM (2 mL) at rt in 12 h. [vi] **4ag** (0.20 mmol), NaOH (4–5 equiv.), ^{i}PrOH (2 mL), 60 °C, 24 h.

Scheme II.7.1. *Post Synthetic Functionalizations.*

II.8. Conclusion:

In conclusion, we have devised a visible-light irradiated solvent-dependent synthesis of polysubstituted quinolines and pyridines from (*E*)-2-(1,3-diarylallylidene)malononitriles by employing a Pd(II)-catalyst. Extreme solvent dependency is observed for the same substrate and catalytic combinations. Strongly H-bonding TFE solvent, yielded polysubstituted *Z*-alkenylated quinolines while ethanolic solvent provided functionalized pyridines. The in-situ-generated [L_2Pd(0)] acts as an exogenous photosensitizer by virtue of MLCT. The developed protocol proceeds under mild conditions and methods are scalable, having diverse substrate scopes. The obtained products can be further transformed to useful functionalities.

II.9. Experimental Section:

II.9.1. General Information:

All the reagents were commercial grade and purified according to the established procedures. All the reactions were carried out in oven-dried glassware. The highest commercial quality reagents were purchased and were used without further purification unless otherwise stated. Reactions were monitored by thin layer chromatography (TLC) on 0.25 mm silica gel plates ($60F_{254}$) visualized under UV illumination at 254 nm. Organic extracts were dried over anhydrous sodium sulfate (Na_2SO_4). Solvents were removed using a rotary evaporator under reduced pressure. Column chromatography was performed to purify the crude product on silica gel 60–120 mesh using a mixture of hexane and ethyl acetate as eluent. The isolated compounds were characterized by spectroscopic [^1H, $^{13}C\{1H\}$ NMR, and IR] techniques and HRMS analysis. NMR spectra were recorded in deuterochloroform ($CDCl_3$) deuterated acetonitrile (CD_3CN) and deuterated dimethyl sulfoxide (DMSO-d_6). ^1H, $^{13}C\{^1H\}$ were recorded in 500 (125) or 400 (100) MHz spectrometer and were calibrated using tetramethylsilane or residual undeuterated solvent for ^1H NMR, deuterochloroform for ^{13}C NMR as an internal reference {$Si(CH_3)_4$: 0.00 ppm or $CHCl_3$: 7.260 ppm for ^1H NMR, 77.230 ppm for ^{13}C NMR, CH_3CN: 1.94 ppm for ^1H NMR, 118.69 ppm for ^{13}C NMR and $(CH_3)_2SO$: 2.50 ppm for ^1H NMR, 39.50 ppm for ^{13}C NMR}. ^{19}F NMR was calibrated without any internal standard in $CDCl_3$ in a 500 MHz spectrometer. The chemical shifts are quoted in δ units, parts per million (ppm). ^1H NMR data is represented as follows: Chemical shift, multiplicity (s = singlet, d = doublet, t = triplet, q = quartet, m = multiplet), integration and coupling constant(s) *J* in hertz (Hz). High-resolution mass spectra (HRMS) were recorded on a mass spectrometer using electrospray ionization-time of flight (ESI-TOF) reflection experiments. FT-IR spectra were recorded in KBr or neat and reported in the frequency of absorption (cm^{-1}). All UV experiments were performed in 1 mL quartz cuvettes of path length 1 cm at 25 ^oC in UV/Vis spectrometer in HPLC grade solvent.

II.9.2. Light Information and Reaction Setup:

Philips 2 x 14 W white LED (flux 46 mW/cm^2) bulb was used as the light source for this light-promoted reaction and no filter was used. Borosilicate round bottom glass was used as the reaction vessel. The distance from the light source to the irradiation vessel was ~6–8 cm. Regular

fan was used to ventilate the area to maintain the room temperature (27–30 °C). The reaction set-up for this photochemical reaction is shown below (Figure II.9.2.1).

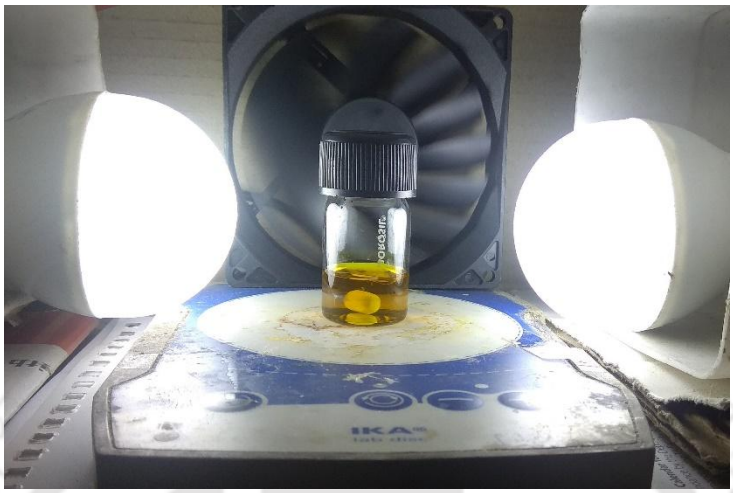

Figure II.9.2.1. *Photochemical reaction set-up.*

II.9.3. General Procedure:

II.9.3.1. General Procedure for the Synthesis of (*E*)-2-(1,3-Diarylallylidene)malononitriles (1a–1n):

Compounds **1a**–**1n** were synthesized in slightly modified literature procedures[32]

(i) General Procedure for the Synthesis of 2-(1-Phenylethylidene)malononitrile:

To an oven-dried 50 mL round bottom flask fitted with a reflux condenser was added acetophenone (1.20 g, 10 mmol), malononitrile (1.30 g, 20 mmol) and ammonium acetate (0.164 g, 2.16 mmol) in 5 mL of toluene and glacial acetic acid (2.0 mL). The reaction mixture was refluxed vigorously in a preheated oil bath for 12 h. Progress of the reaction was monitored by TLC. After completion of the reaction the mixture was cooled to room temperature, admixed with ethyl acetate (50 mL) and the organic layer was washed with saturated bicarbonate solution (20 mL). The organic layer was dried over anhydrous sodium sulfate (Na_2SO_4), and the solvent was evaporated under reduced pressure. The crude product so obtained was purified over a column of silica gel using hexane/ethyl acetate = 98:2 to give pure 2-(1-phenylethylidene)malononitrile (Scheme II.9.3.1.1).

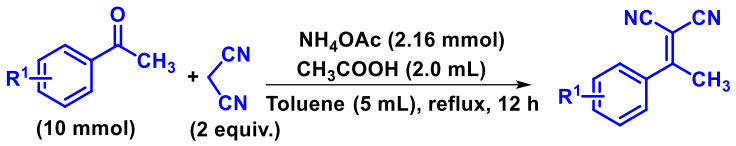

Scheme II.9.3.1.1. *Synthesis of 2-(1-arylethylidene)malononitriles.*

(ii) General Procedure for the Synthesis of (*E*)-2-(1,3-Diphenylallylidene)malononitrile:

To an oven-dried 50 mL round bottom flask was added 2-(1-phenylethylidene)malononitrile (1.68 g, 10 mmol), benzaldehyde (1.06 g, 10 mmol), and piperidine (0.085 g, 1 mmol) in ^{i}PrOH (3 mL). The reaction mixture was stirred at 65-70 ^{o}C in a preheated oil bath for 24 h. Completion of the reaction was monitored by TLC. Then the reaction mixture was cooled to room temperature, admixed with ethyl acetate (50 mL) and the organic layer was washed with brine (20 mL). The organic layer was dried over anhydrous sodium sulfate (Na_2SO_4), and the solvent was evaporated under reduced pressure. The crude product so obtained was purified over a column of silica gel using hexane/ethyl acetate = 99:1 to give pure (*E*)-2-(1,3-diphenylallylidene)malononitrile in 60% yield. (Scheme II.9.3.1.2).

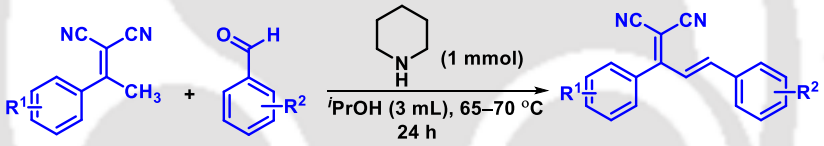

Scheme II.9.3.1.2. *Synthesis of (E)-2-(1,3-diarylallylidene)malononitriles (**1a–1n**).*

II.9.3.2. General Procedure for the Synthesis of 2,4,6-Triphenylnicotinonitriles (3aa) from (*E*)-2-(1,3-Diphenylallylidene)malononitrile (1a) and Phenylboronic Acid (2a):

To an oven-dried 10 mL vial was added (*E*)-2-(1,3-diphenylallylidene)malononitrile (**1a**) (0.0640 g, 0.25 mmol), phenylboronic acid (**2a**) (0.121 g, 1.0 mmol), $Pd(OAc)_2$ (0.0056 g, 0.025 mmol), 2,2′-bipyridine (0.0078 g, 0.05 mmol), and PTSA·H_2O (0.19 g, 1.0 mmol) in EtOH (2 mL). The reaction mixture was stirred at room temperature, maintaining an approximate distance of ~6–8 cm from two 14 W white LED bulbs. After completion of the reaction (monitored by TLC analysis), the reaction mixture was admixed with ethyl acetate (25 mL) and the organic layer was washed with saturated sodium bicarbonate solution (10 mL). The organic layer was dried over anhydrous sodium sulfate (Na_2SO_4), and the solvent was evaporated under reduced pressure. The crude product so obtained was purified over a column of silica gel using 2% ethyl acetate in hexane

to give pure 2,4,6-triphenylnicotinonitrile (**3aa**) in 72% yield (Scheme II.9.3.2.1). The identity and purity of the product were confirmed by spectroscopic analysis.

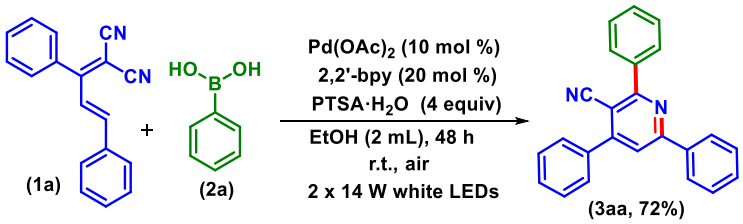

Scheme II.9.3.2.1. *Synthesis of 2,4,6-triphenylnicotinonitriles (**3aa**).*

II.9.3.3. Gram-scale Synthesis of 2,4,6-Triphenylnicotinonitriles (3aa) from (*E*)-2-(1,3-Diphenylallylidene)malononitrile (1a) and Phenylboronic Acid (2a):

To an oven-dried 50 mL round bottom flask was added (*E*)-2-(1,3-diphenylallylidene)malononitrile (**1a**) (1.24 g, 5.0 mmol), phenylboronic acid (**2a**) (2.42 g, 20.0 mmol), $Pd(OAc)_2$ (0.112 g, 0.5 mmol), 2,2′-bipyridine (0.156 g, 1.0 mmol), and PTSA·H_2O (3.8 g, 20.0 mmol) in EtOH (5 mL). The reaction mixture was stirred at room temperature, maintaining an approximate distance of ~6–8 cm from two 14 W white LED bulbs. After completion of the reaction (monitored by TLC analysis), the reaction mixture was admixed with ethyl acetate (50 mL) and the organic layer was washed with saturated sodium bicarbonate solution (20 mL). The organic layer was dried over anhydrous sodium sulfate (Na_2SO_4), and the solvent was evaporated under reduced pressure. The crude product so obtained was purified over a column of silica gel using 2% ethyl acetate in hexane to give pure 2,4,6-triphenylnicotinonitrile (**3aa**) (1.08 g, 65% yield) (Scheme II.9.3.3.1). The identity and purity of the product were confirmed by spectroscopic analysis.

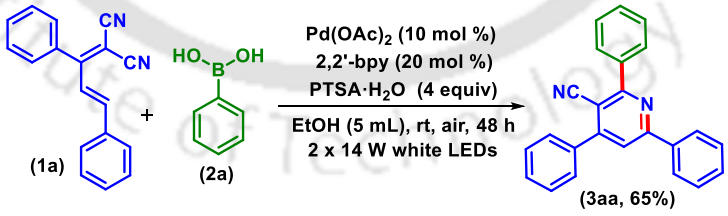

Scheme II.9.3.3.1. *Gram-scale synthesis of 2,4,6-Triphenylnicotinonitriles (**3aa**).*

II.9.3.4. (i) General Procedure for the Synthesis of (*Z*)-2-Phenyl-4-styrylquinoline-3-carbonitriles (4aa) from (*E*)-2-(1,3-Diphenylallylidene)malononitrile (1a) and Phenylboronic acid (2a):

To an oven-dried 10 mL vial was added (*E*)-2-(1,3-diphenylallylidene)malononitrile (**1a**) (0.064 g, 0.25 mmol), phenylboronic acid (**2a**) (0.0907 g, 0.75 mmol), $Pd(OAc)_2$ (0.0056 g, 0.025 mmol), 2,2′-bipyridine (0.0078 g, 0.05 mmol), and PTSA·H_2O (0.142 g, 0.75 mmol) in 2,2,2-trifluoroethanol (TFE) (2 mL). The reaction mixture was stirred at room temperature for 24 h maintaining an approximate distance of ~6–8 cm from two 14 W white LED bulbs. After completion of the reaction (monitored by TLC analysis), the reaction mixture was admixed with ethyl acetate (25 mL) and the organic layer was washed with saturated sodium bicarbonate solution (10 mL). The organic layer was dried over anhydrous sodium sulfate (Na_2SO_4), and the solvent was evaporated under reduced pressure. The crude product so obtained was purified over a column of silica gel using 2% ethyl acetate in hexane to give pure (*Z*)-2-phenyl-4-styrylquinoline-3-carbonitriles (**4aa**) in 71% yield with *Z*/*E* 97:3 (Scheme II.9.3.4.1). The identity and purity of the product were confirmed by spectroscopic analysis.

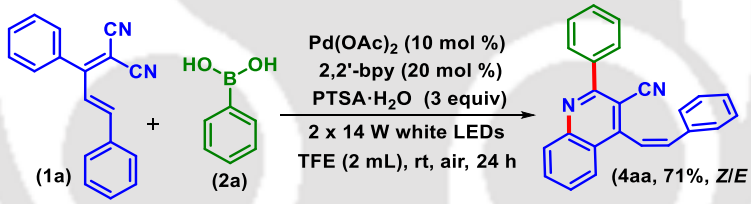

Scheme II.9.3.4.1. *Synthesis of (Z)-2-Phenyl-4-styrylquinoline-3-carbonitriles (**4aa**).*

II.9.3.5. Gram-scale Synthesis of (*Z*)-2-Phenyl-4-styrylquinoline-3-carbonitriles (4aa) from (*E*)-2-(1,3-Diphenylallylidene)malononitrile (1a) and Phenylboronic acid (2a):

To an oven-dried 50 mL round bottom flask was added (*E*)-2-(1,3-diphenylallylidene)malononitrile (**1a**) (1.24 g, 5.0 mmol), phenylboronic acid (**2a**) (1.815 g, 15.0 mmol), $Pd(OAc)_2$ (0.112 g, 0.5 mmol), 2,2′-bipyridine (0.156 g, 1.0 mmol), and PTSA·H_2O (2.85 g, 15.0 mmol) in 2,2,2-trifluoroethanol (TFE) (5 mL). The reaction mixture was stirred at room temperature for 24 h maintaining an approximate distance of ~6–8 cm from two 14 W white LED bulbs. After completion of the reaction (monitored by TLC analysis), the reaction mixture was admixed with ethyl acetate (50 mL) and the organic layer was washed with saturated sodium bicarbonate solution (20 mL). The organic layer was dried over anhydrous sodium sulfate (Na_2SO_4),

and the solvent was evaporated under reduced pressure. The crude product so obtained was purified over a column of silica gel using 2% ethyl acetate in hexane to give pure (*Z*)-2-phenyl-4-styrylquinoline-3-carbonitriles (**4aa**) (1.03 g, 62% yield, *Z*/*E* 97:3) (Scheme II.9.3.5.1). The identity and purity of the product were confirmed by spectroscopic analysis.

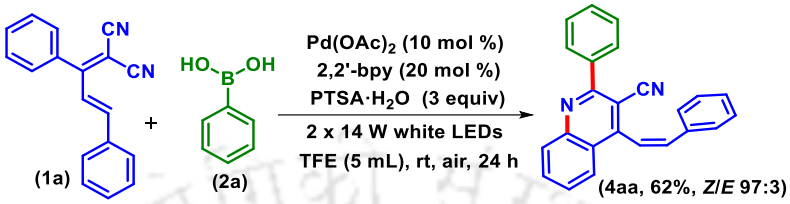

Scheme II.9.3.5.1. *Gram-scale synthesis of (Z)-2-Phenyl-4-styrylquinoline-3-carbonitriles (**4aa**).*

II.9.4. Mechanistic Investigations:

II.9.4.1. Reaction of (*E*)-2-(1,3-Diphenylylallylidene)malononitrile (1a) in the Absence of Phenylboronic acid (2a):

To an oven-dried 10 mL vial was added (*E*)-2-(1,3-diphenylylallylidene)malononitrile (**1a**) (0.064 g, 0.25 mmol), $Pd(OAc)_2$ (0.0056 g, 0.025 mmol), 2,2′-bipyridyl (0.0078 g, 0.05 mmol), and $PTSA{\cdot}H_2O$ (0.142 g, 0.75 mmol) in TFE (2 mL). The reaction mixture was stirred at room temperature for 24 h maintaining an approximate distance of ~6-8 cm from two 14W white LED bulbs. After completion of the reaction (monitored by TLC analysis), the reaction mixture was admixed with ethyl acetate (25 mL) and the organic layer was washed with saturated sodium bicarbonate solution (10 mL). The organic layer was dried over anhydrous sodium sulfate (Na_2SO_4), and the solvent was evaporated under reduced pressure. The crude product so obtained was purified over a column of silica gel using 1% ethyl acetate in hexane (Scheme II.9.4.1.1). The identity and purity of the product were confirmed by spectroscopic analysis. It was observed from the ^1H NMR analysis that there is no change in the configuration of the starting material which suggested that the *Z*-isomer is not formed initially (Figure II.9.4.1.1 and Figure II.9.4.1.2).

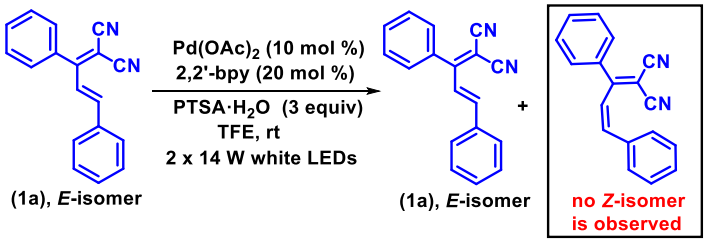

Scheme II.9.4.1.1. *Reaction of **1a** without phenylboronic acid (**2a**).*

^{1}H NMR of **1a** ($CDCl_3$, 500 MHz): δ 7.63–7.53 (m, 6H), 7.44–7.38 (m, 5H), 6.90 (d, 1H, J = 15.5 Hz).

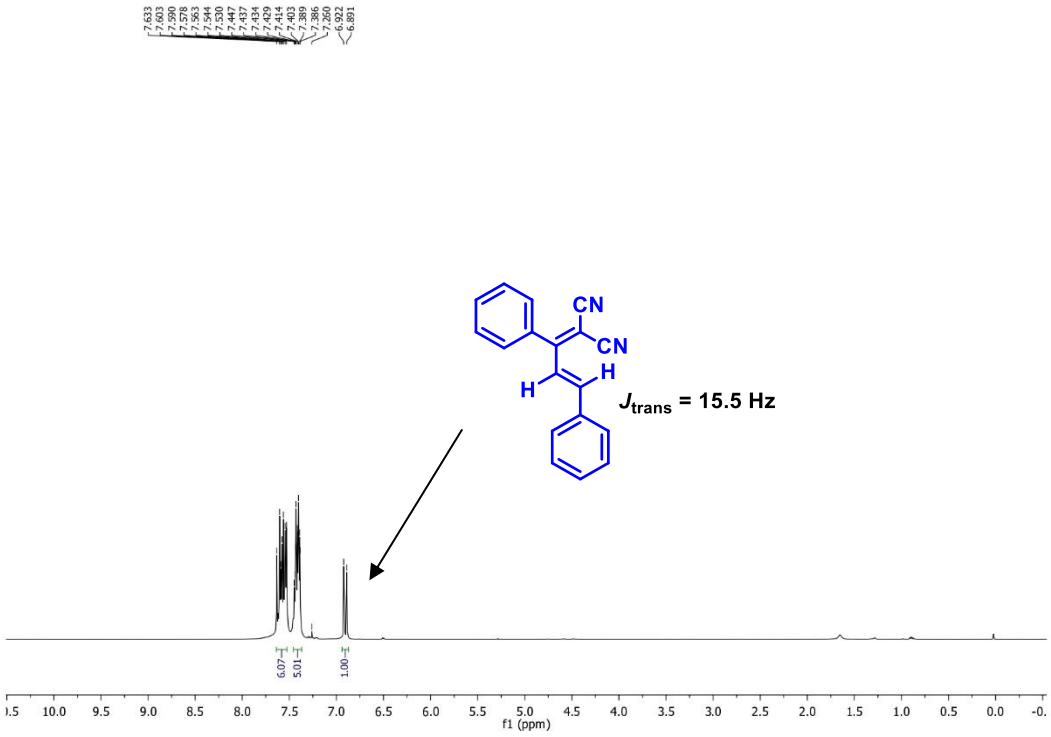

Figure II.9.4.1.1. *^{1}H NMR of **1a**.*

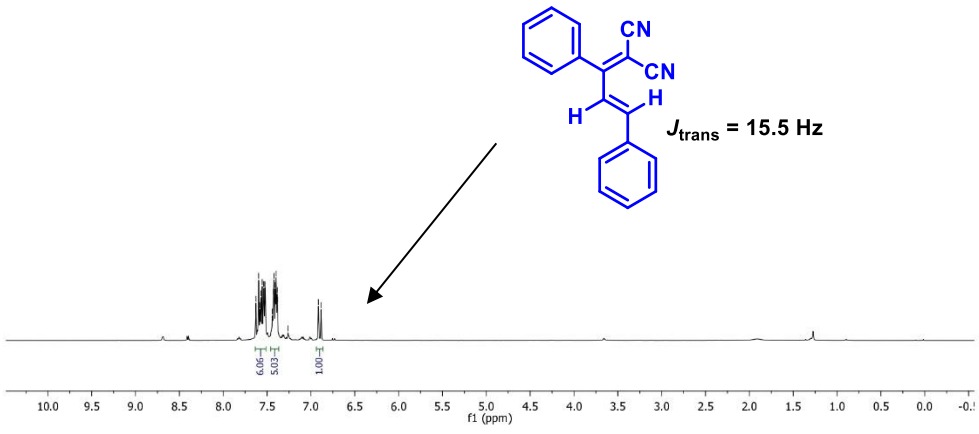

Figure II.9.4.1.2. *1H NMR of 1a after reaction without **2a**.*

II.9.4.2. Reaction In the Absence of LEDs:

(i) To an oven-dried 10 mL vial was added (*E*)-2-(1,3-diphenylylallylidene)malononitrile (**1a**) (0.064 g, 0.25 mmol), phenylboronic acid (**2a**) (0.121 g, 1.00 mmol), $Pd(OAc)_2$ (0.0056 g, 0.025 mmol), 2,2′-bipyridyl (0.0078 g, 0.05 mmol), and PTSA·H_2O (0.19 g, 0.75 mmol) in EtOH (2 mL). The reaction mixture was stirred at room temperature for 48 h in absence of white LEDs. After which, the reaction mixture was admixed with ethyl acetate (25 mL) and the organic layer was washed with saturated sodium bicarbonate solution (10 mL). The organic layer was dried over anhydrous Na_2SO_4, and the solvent was evaporated under reduced pressure. The crude product so obtained was purified over a column of silica gel using 2% ethyl acetate in hexane giving pure 2,4,6-triphenylnicotinonitriles (**3aa**) very less amount (<15%) (Scheme II.9.4.2.1). The identity and purity of the product were confirmed by spectroscopic analysis.

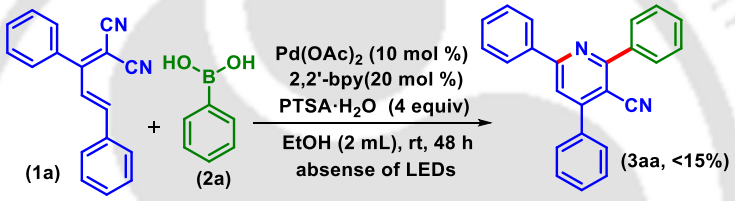

Scheme II.9.4.2.1. *Reaction in the absence of LEDs in EtOH.*

(ii) To an oven-dried 10 mL vial was added (*E*)-2-(1,3-diphenylylallylidene)malononitrile (**1a**) (0.064 g, 0.25 mmol), phenylboronic acid (**2a**) (0.0906 g, 0.75 mmol), $Pd(OAc)_2$ (0.0056 g, 0.025 mmol), 2,2′-bipyridyl (0.0078 g, 0.05 mmol), and PTSA·H_2O (0.142 g, 0.75 mmol) in TFE (2 mL). The reaction mixture was stirred at room temperature for 24 h in absence of white LEDs. From TLC it was observed that no trace of (*Z*)-2-phenyl-4-styrylquinoline-3-carbonitrile (**4aa**) is formed and the starting material (**1a**) remains unconsumed (Scheme II.9.4.2.2). From the dark experiments (absence of light) it is clear that light has a necessary role for this transformation.

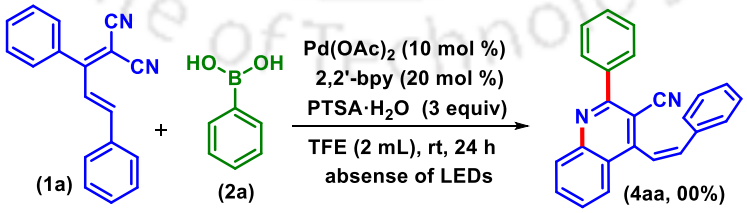

Scheme II.9.4.2.2. *Reaction in the absence of LEDs in TFE.*

II.9.4.3. Reaction in the Presence of TEMPO:

(i) To an oven-dried 10 mL vial was added (*E*)-2-(1,3-diphenylylallylidene)malononitrile (**1a**) (0.064g, 0.25 mmol), phenylboronic acid (**2a**) (0.121 g, 1.0 mmol), $Pd(OAc)_2$ (0.0056 g, 0.025 mmol), 2,2′-bipyridyl (0.0078 g, 0.05 mmol), PTSA·H_2O (0.19 g, 1.0 mmol), and (2,2,6,6-tetramethylpiperidin-1-yl)oxyl (TEMPO) (0.078 g, 0.5 mmol) in EtOH (2 mL). The reaction mixture was stirred at room temperature for 48 h maintaining an approximate distance of ~6-8 cm from two 14W white LED bulbs. After completion of the reaction (monitored by TLC analysis), the reaction mixture was admixed with ethyl acetate (25 mL) and the organic layer was washed with saturated sodium bicarbonate solution (10 mL). The organic layer was dried over anhydrous Na_2SO_4, and the solvent was evaporated under reduced pressure. The crude product so obtained was purified over a column of silica gel using 2% ethyl acetate in hexane to give pure 2,4,6-triphenylnicotinonitriles (**3aa**) (52 mg, 63% yield) (Scheme II.9.4.3.1). The identity and purity of the product were confirmed by spectroscopic analysis.

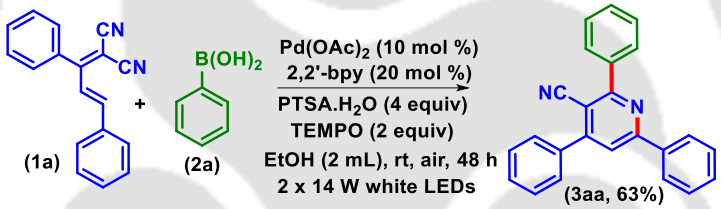

Scheme II.9.4.3.1. *Reaction in the presence of TEMPO in EtOH.*

(ii) To an oven-dried 10 mL vial was added (*E*)-2-(1,3-diphenylylallylidene)malononitrile (**1a**) (0.064g, 0.25 mmol), phenylboronic acid (**2a**) (0.0906 g, 0.75 mmol), $Pd(OAc)_2$ (0.0056 g, 0.025 mmol), 2,2′-bipyridyl (0.0078 g, 0.05 mmol), PTSA·H_2O (0.142 g, 0.75 mmol), and (2,2,6,6-tetramethylpiperidin-1-yl)oxyl (TEMPO) (0.078 g, 0.5 mmol) in TFE (2 mL). The reaction mixture was stirred at room temperature for 24 h maintaining an approximate distance of ~6-8 cm from two 14W white LED bulbs. After completion of the reaction (monitored by TLC analysis), the reaction mixture was admixed with ethyl acetate (25 mL), and the organic layer was washed with saturated sodium bicarbonate solution (10 mL). The organic layer was dried over anhydrous Na_2SO_4, and the solvent was evaporated under reduced pressure. The crude product so obtained was purified over a column of silica gel using 2% ethyl acetate in hexane to give pure (*Z*)-2-phenyl-4-styrylquinoline-3-carbonitriles (**4aa**) (50 mg, 63% yield) (Scheme II.9.4.3.2). The identity and purity of the product were confirmed by spectroscopic analysis. From the yield pattern of the pyridines (in EtOH) and quinolines (in TFE), it is clear that the reaction does not go through a radical intermediate.

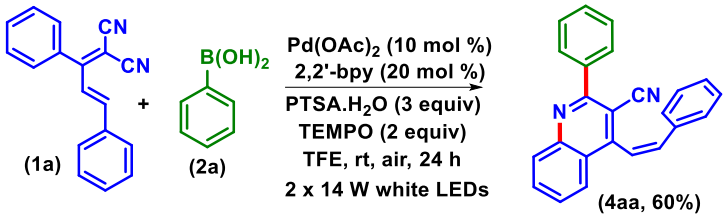

Scheme II.9.4.3.2. *Reaction in the presence of TEMPO in TFE.*

II.9.4.4. Isotope Labeling Experiments:

(i) H/D Exchange in the Absence of Phenylboronic acid (2a):

To an oven-dried 10 mL vial was added (*E*)-2-(1-(phenyl-d5)-3-(*p*-tolyl)allylidene)malononitrile (**1g-d$_5$**) (0.068 g, 0.25 mmol), $Pd(OAc)_2$ (0.0056 g, 0.025 mmol), 2,2′-bipyridyl (0.0078 g, 0.05 mmol), and $PTSA{\cdot}H_2O$ (0.142 g, 0.75 mmol) in 2,2,2-trifluoroethanol (TFE) (2 mL). The reaction mixture was stirred at room temperature for 24 h, maintaining an approximate distance of ~6-8 cm from two 14W white LED bulbs. After completion of the reaction (monitored by TLC analysis), the reaction mixture was admixed with ethyl acetate (25 mL) and the organic layer was washed with saturated sodium bicarbonate solution (10 mL). The organic layer was dried over anhydrous sodium sulfate (Na_2SO_4), and the solvent was evaporated under reduced pressure. The crude product so obtained was purified over a column of silica gel using 1% ethyl acetate in hexane (Scheme II.9.4.4.1). From the ^{1}H NMR, no H/D exchange is observed, suggesting the irreversible nature of the reaction (Figure II.9.4.4.1 and Figure II.9.4.4.2).

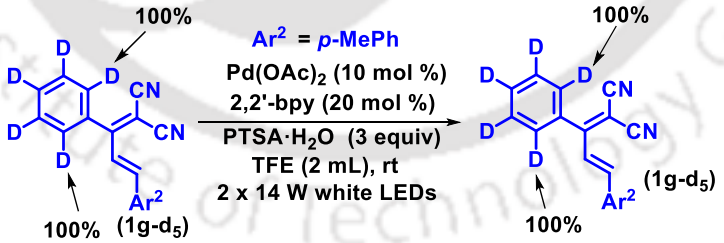

Scheme II.9.4.4.1. *H/D exchange without phenylboronic acid (**2a**).*

^{1}H NMR of **1g-d$_5$** ($CDCl_3$, 500 MHz): δ 7.57 (d, 1H, *J* = 16 Hz), 7.43 (d, 2H, *J* = 8.0 Hz), 7.21 (d, 2H, *J* = 7.5 Hz), 6.87 (d, 1H, *J* = 15.5 Hz), 2.39 (s, 3H).

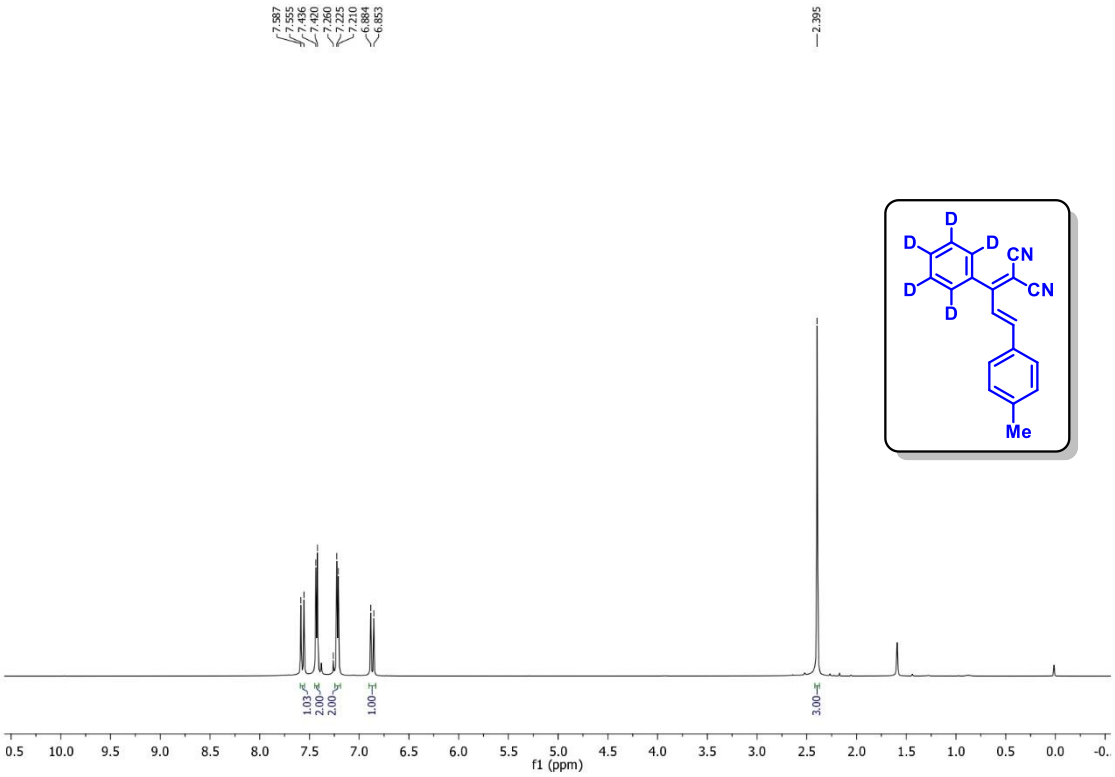

Figure II.9.4.4.1. *^{1}H NMR of* ***1g-d$_5$****.*

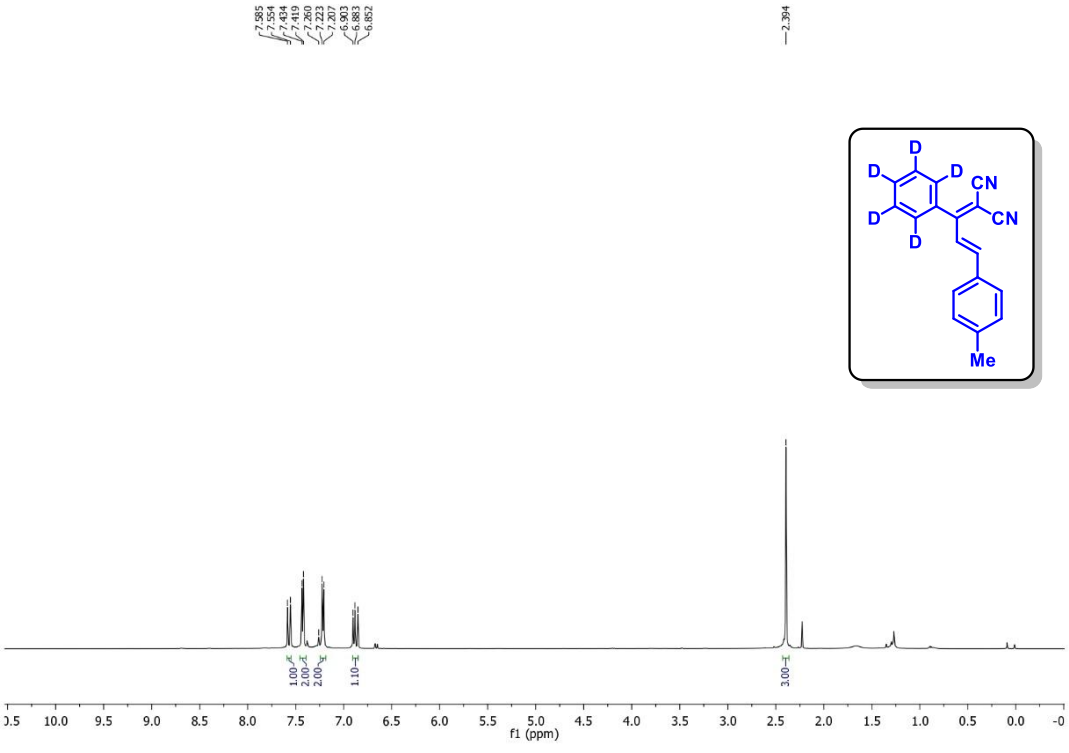

Figure II.9.4.4.2. *^{1}H NMR of* ***1g-d$_5$*** *after reaction without phenylboronic acid (****2a****).*

(ii) H/D Exchange in the Presence of Phenylboronic acid (2a):

To an oven-dried 10 mL vial was added (*E*)-2-(1-(phenyl-d5)-3-(*p*-tolyl)allylidene)malononitrile (**1g-d$_5$**) (0.068 g, 0.25 mmol), phenylboronic acid **(2a)** (0.0906 g, 0.75 mmol), $Pd(OAc)_2$ (0.0056 g, 0.025 mmol), 2,2′-bipyridyl (0.0078 g, 0.05 mmol), and PTSA·H_2O (0.142 g, 0.75 mmol) in 2,2,2-trifluoroethanol (TFE) (2 mL). The reaction mixture was stirred at room temperature for 24 h, maintaining an approximate distance of ~6-8 cm from two 14 W white LED bulbs. After completion of the reaction (monitored by TLC analysis), the reaction mixture was admixed with ethyl acetate (25 mL) and the organic layer was washed with saturated sodium bicarbonate solution (10 mL). The organic layer was dried over anhydrous sodium sulfate (Na_2SO_4), and the solvent was evaporated under reduced pressure. The crude product so obtained was purified over a column of silica gel using 1% ethyl acetate in hexane to give pure (**4ga-d$_4$**) in 52% yield and 2% ethyl acetate in hexane to give unconsumed (**1g-d$_5$**) in 20% yield (Scheme II.9.4.4.2). From the ^{1}H NMR, no H/D exchange is observed in the final product (**4ga-d$_4$**). This result also suggests that the reaction is irreversible.

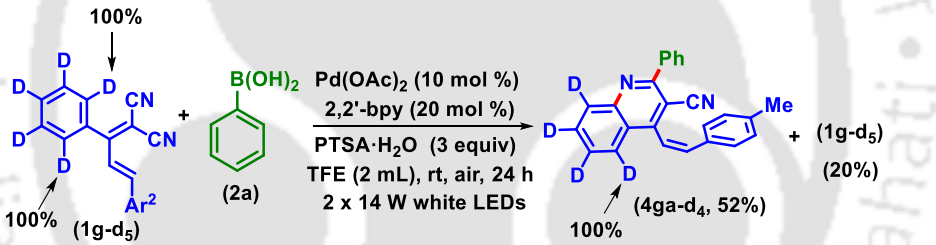

Scheme II.9.4.4.2. *H/D exchange with phenylboronic acid (**2a**).*

II.9.4.5. Kinetic Isotope Effect (KIE) Experiments:

(i) Parallel reaction:

To an oven-dried 10 mL vial was added (*E*)-2-(1-phenyl-3-(*p*-tolyl)allylidene)malononitrile (**1g**) (0.067 g, 0.25 mmol), phenylboronic acid (**2a**) (0.0906 g, 0.75 mmol), $Pd(OAc)_2$ (0.0056 g, 0.025 mmol), 2,2′-bipyridyl (0.0078 g, 0.05 mmol), and PTSA·H_2O (0.142 g, 0.75 mmol) in 2,2,2-trifluoroethanol (TFE) (2 mL). On the other hand, in another oven-dried 10 mL vial was added (*E*)-2-(1-(phenyl-d5)-3-(*p*-tolyl)allylidene)malononitrile (**1g-d$_5$**) (0.068 g, 0.25 mmol), phenylboronic acid (**2a**) (0.0906 g, 0.75 mmol), $Pd(OAc)_2$ (0.0056 g, 0.025 mmol), 2,2′-bipyridyl (0.0078 g, 0.05 mmol), and PTSA·H_2O (0.142 g, 0.75 mmol) in 2,2,2-trifluoroethanol (TFE) (2 mL). Then, these two mixtures were stirred at room temperature maintaining an approximate distance of ~6-8 cm

from two 14W white LED bulbs. Next, after 60 min an equal amount (100 μL) of reaction mixture was taken from both the vials and dissolved in 1 mL ethyl acetate separately and filtered off the residue. Then ethyl acetate was removed under reduced pressure and was taken for ^{1}H NMR using nitromethane as the internal standard. This process was repeated after 120, 180, and 240 min (Scheme II.9.4.5.1).

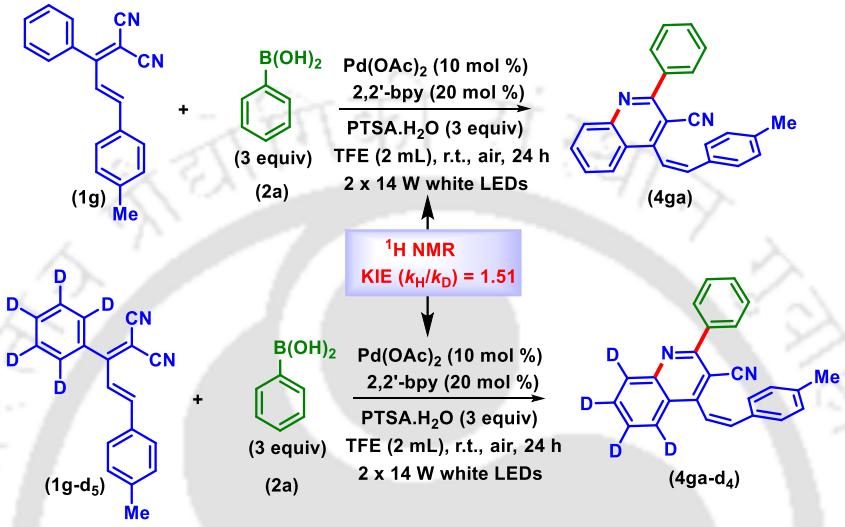

Scheme II.9.4.5.1. *Parallel KIE experiment.*

The k_H/k_D value for the parallel experiment is determined by ^{1}H NMR by plotting NMR yield (%) vs time (min). The corresponding graph has been plotted to determine the KIE value (Figure II.9.4.5.1). From the plot, the slope for the conversion of **4ga** is 0.1033, and for **4ga-d4** is 0.0683. Finally, the parallel kinetic isotope effect (KIE) is determined as 1.51 (k_H/k_D = 0.1033/0.0683), suggesting the C–H bond cleavage might not be involved in the rate-limiting step.

Time (min)	60	120	180	240
The yield of **4ga** (%)	17	24	29	36
The yield of **4ga-d$_4$** (%)	15	19	25	30

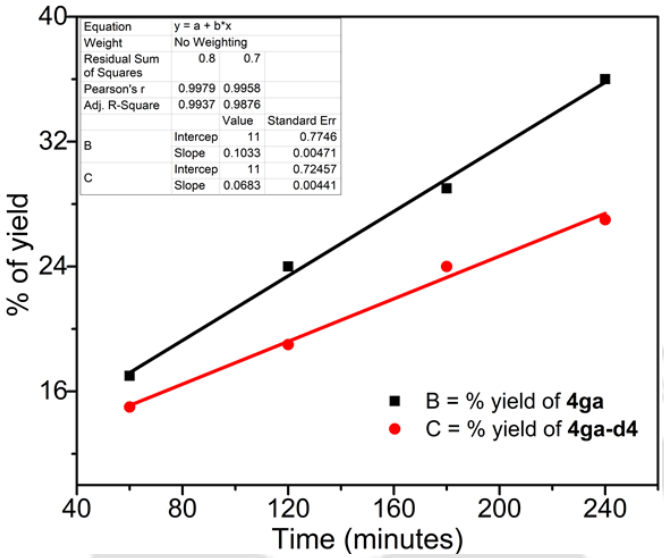

Figure II.9.4.5.1. *Plot of % yield vs time (min) for Parallel KIE Experiment.*

(ii) Competitive Reaction:

To an oven-dried 10 mL vial was added (*E*)-2-(1-phenyl-3-(*p*-tolyl)allylidene)malononitrile (**1g**) (0.067 g, 0.25 mmol) and (*E*)-2-(1-(phenyl-d5)-3-(*p*-tolyl)allylidene)malononitrile (**1g-d$_5$**) (0.068 g, 0.25 mmol), Phenylboronic acid (**2a**) (0.0906 g, 0.75 mmol), $Pd(OAc)_2$ (0.0056 g, 0.025 mmol), 2,2′-bipyridyl (0.0078 g, 0.05 mmol), and PTSA·H_2O (0.142 g, 0.75 mmol) in 2,2,2-trifluoroethanol (TFE) (2 mL). The reaction mixture was stirred at room temperature for 24 h, maintaining an approximate distance of ~6-8 cm from two 14 W white LED bulbs. After completion of the reaction (monitored by TLC analysis), the reaction mixture was admixed with ethyl acetate (25 mL), and the organic layer was washed with saturated sodium bicarbonate solution (10 mL). The organic layer was dried over anhydrous sodium sulfate (Na_2SO_4), and the solvent was evaporated under reduced pressure. The crude product so obtained was purified over a column of silica gel using 2% ethyl acetate in hexane to give mixture of (*Z*)-4-(4-methylstyryl)-2-phenylquinoline-3-carbonitrile (**4ga**) and (*Z*)-4-(4-methylstyryl)-2-phenylquinoline-3-carbonitrile-5,6,7,8-d$_4$ (**4ga-d$_4$**) respectively (Scheme II.9.4.5.2).

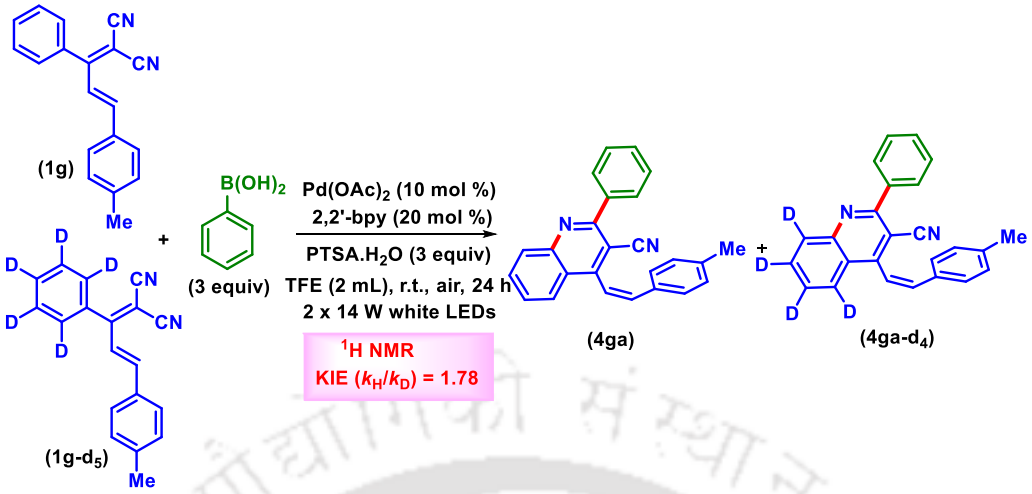

Scheme II.9.4.5.2. *Competitive Experiment.*

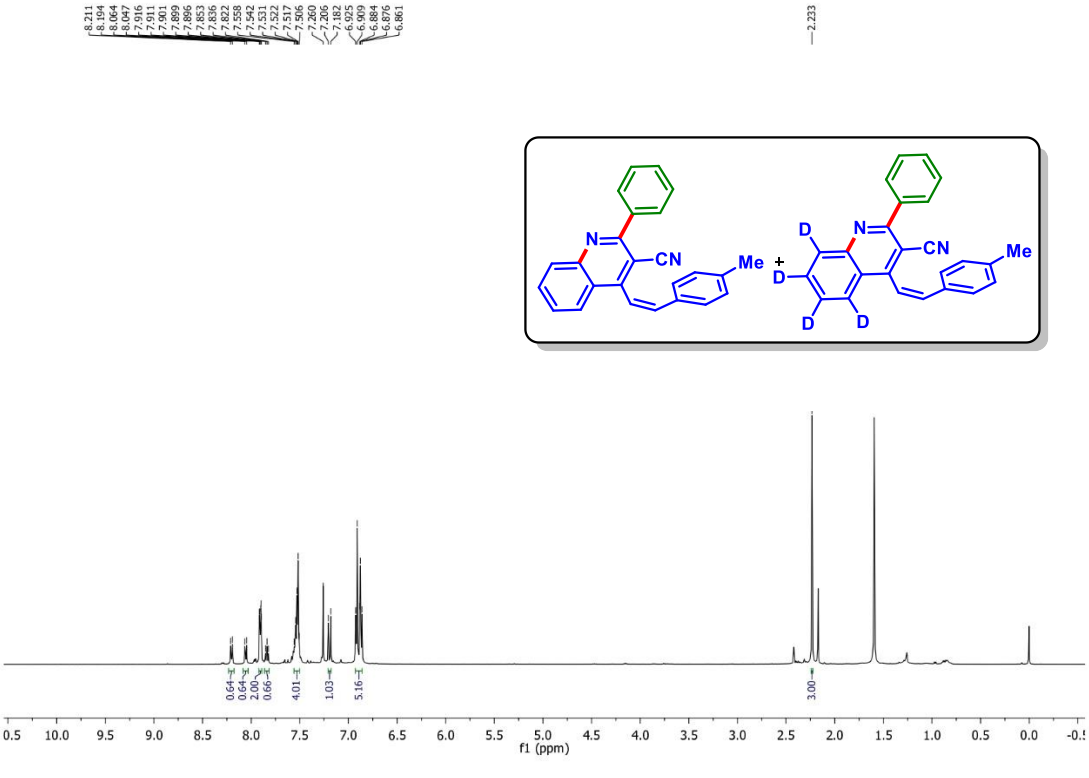

Figure II.9.4.5.2. *^{1}H NMR of the mixture of* ***4ga*** *and* ***4ga-d$_4$****.*

Calculation:

^{1}H NMR (Figure II.9.4.5.2) of the mixture of **4ga** and **4ga-d$_4$** ($CDCl_3$, 500 MHz): δ 8.20 (d, 0.64H, J = 8.5 Hz), 8.05 (d, 0.64H, J = 8.5 Hz), 7.91–7.89 (m, 2H), 7.83 (t, 0.66H, J = 7.75 Hz), 7.56–7.50 (m, 4H), 7.19 (d, 1H, J = 12.0 Hz), 6.92–6.86 (m, 5H), 2.23 (s, 3H).

By analyzing the ^{1}H NMR data of the mixture of **4ga** and **4ga-d$_4$** as shown in Figure II.9.4.5.2, the ratio of **4ga** and **4ga-d$_4$** was determined to be 0.64

Thus the k_H/k_D for the competitive KIE experiment is 0.64/(1 – 0.64) = 0.64/0.36 = 1.78

Therefore, from the KIE experiment, the k_H/k_D is 1.51 for parallel and 1.78 for competitive reaction, which suggests that the C–H bond cleavage might not be involved in the rate-determining step.

II.9.4.6 ESI-MS Studies for the Reaction Mixtures:

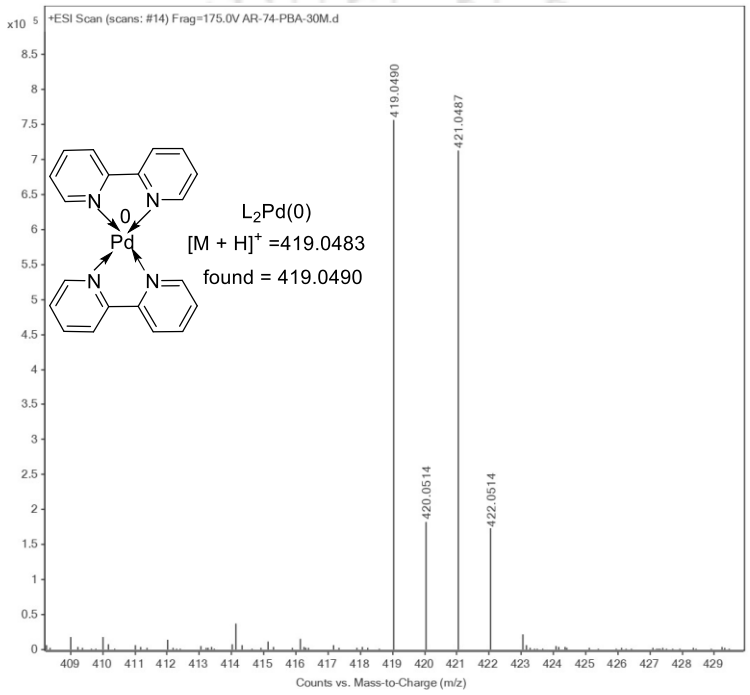

Figure II.9.4.6.1. *HRMS spectrum of $L_2Pd(0)$ after 30 min.*

II.9.5. On-off Experiments:

To an oven-dried 10 mL vial was added (*E*)-2-(1-phenyl-3-(*p*-tolyl)allylidene)malononitrile (**1g**) (0.067 g, 0.25 mmol), Phenylboronic acid (**2a**) (0.0906 g, 0.75 mmol), $Pd(OAc)_2$ (0.0056 g, 0.025 mmol), 2,2′-bipyridyl (0.0078 g, 0.05 mmol), and PTSA·H_2O (0.142 g, 0.75 mmol) in 2,2,2-trifluoroethanol (TFE) (2 mL). The reaction mixture was stirred and irradiated by 2 x 14 W white LEDs at room temperature for 2.5 h. Then the reaction mixture was taken (100 μL) and dissolved in 1 mL ethyl acetate and filtered off the residue. Then ethyl acetate was removed under reduced pressure and taken for ^{1}H NMR using $CDCl_3$ as solvent and nitromethane as internal standard. The

^{1}H NMR yield of corresponding product (**4ga**) was found to be 26% (Figure II.9.5.1). Then the reaction mixture was continuously stirred in the absence of light for 2.5 h and repeating the same steps, the ^{1}H NMR yield of **4ga** was obtained as 28% (Figure II.9.5.2). Again the reaction mixture was continuously stirred in presence of light for 2 h and repeating the same steps, the ^{1}H NMR yield of **4ga** was obtained as 35% (Figure II.9.5.3) and after 2 h in absence of light, the yield was 36% (Figure II.9.5.4). Finally, when the reaction mixture was again stirred in the presence of 2 x 14 W white LEDs for 4 h, the desired product (**4ga**) was obtained with 43% yield as shown from ^{1}H NMR (Figure II.9.5.5). These results suggested that continuous visible light irradiation is essential for this transformation (Scheme II.9.5.1).

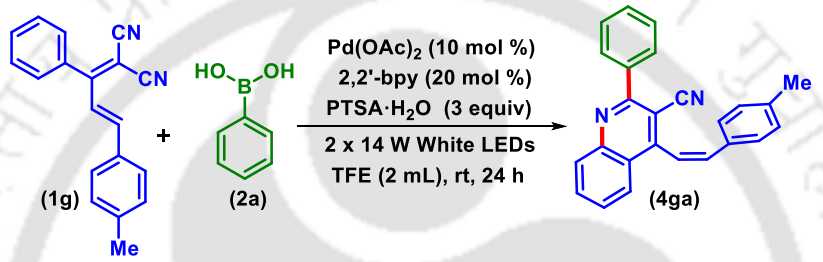

Scheme II.9.5.1. *On-off experiment.*

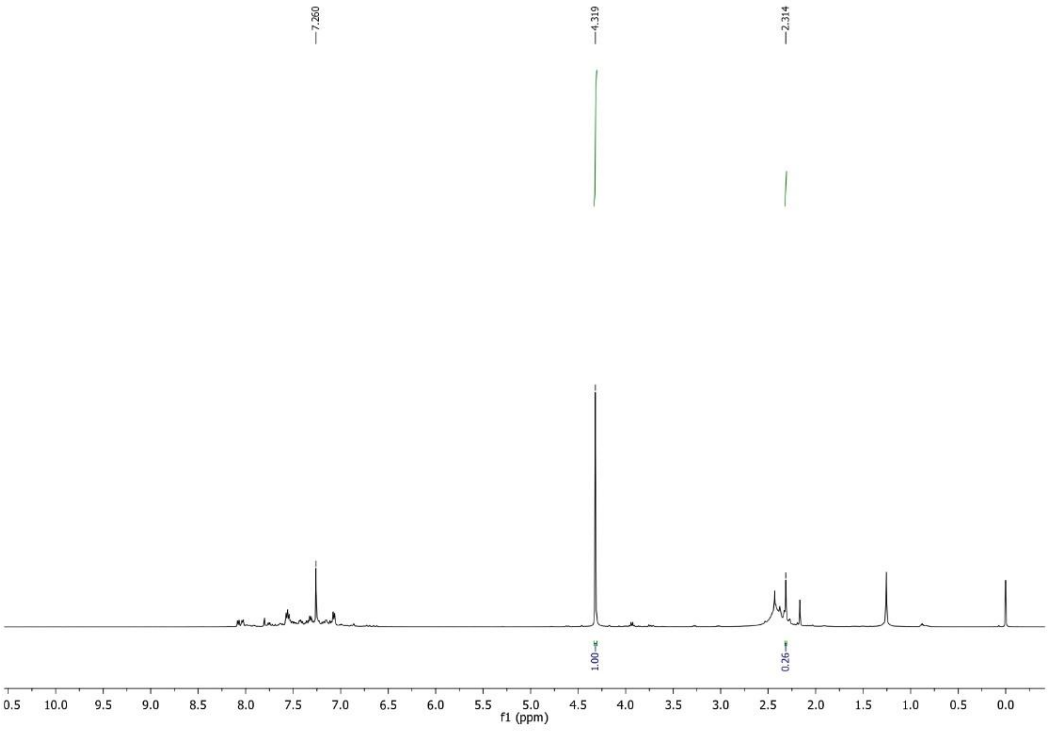

Figure II.9.5.1. *^{1}H NMR of the reaction mixture after 2.5 h light on.*

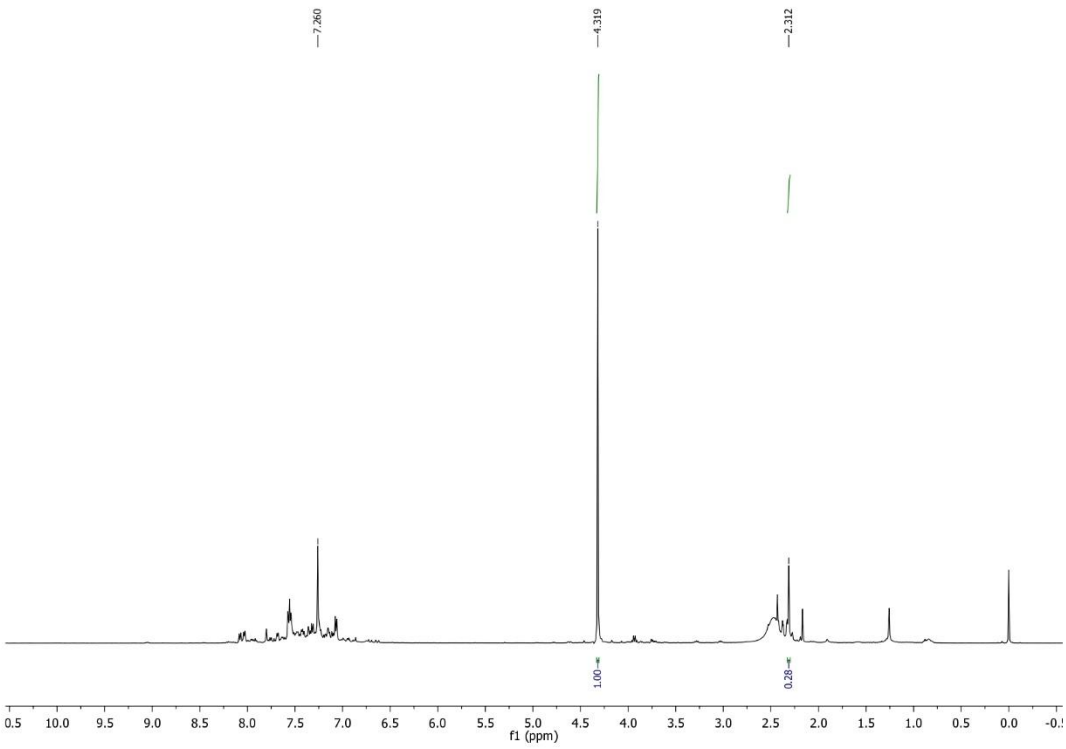

Figure II.9.5.2. *^{1}H NMR of the reaction mixture after 2.5 h light off.*

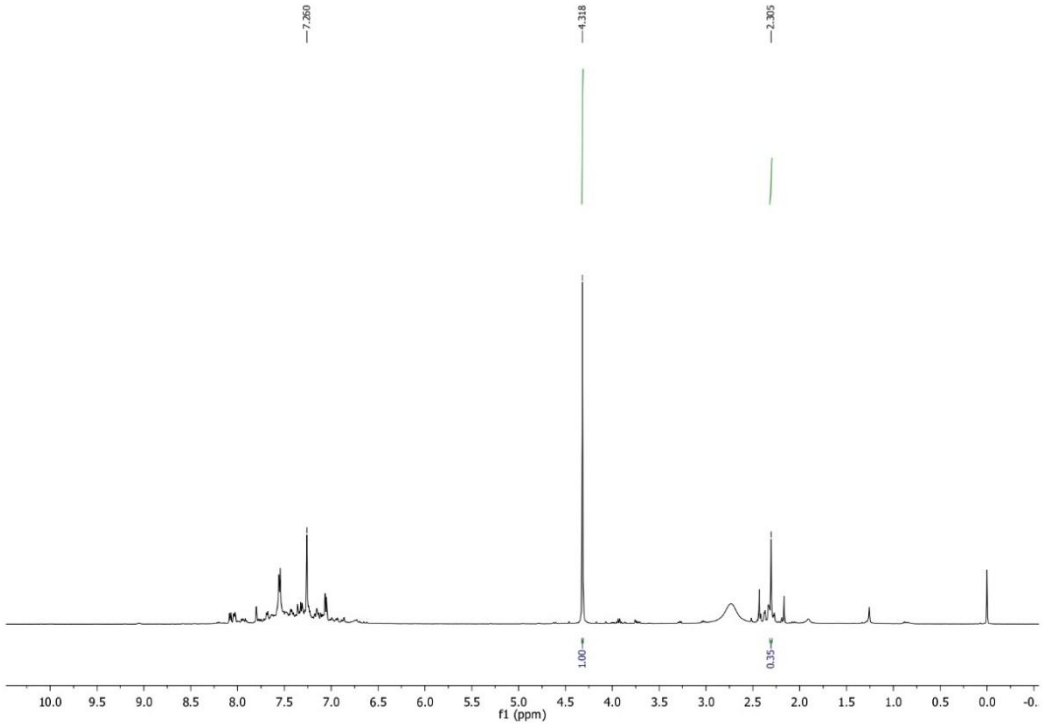

Figure II.9.5.3. *^{1}H NMR of the reaction mixture after 2.0 h light on.*

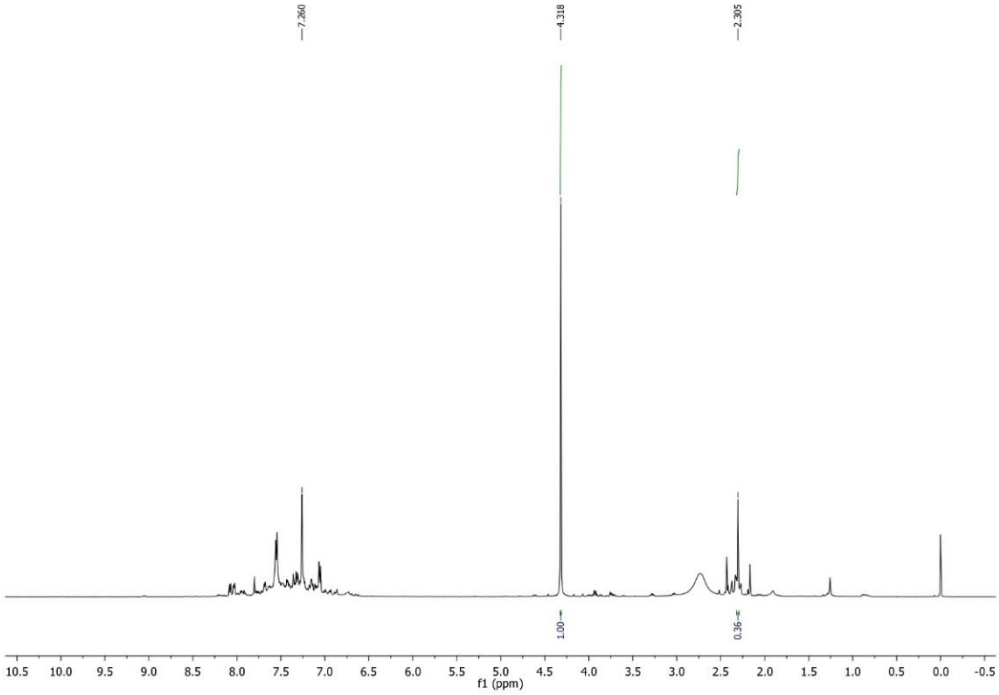

Figure II.9.5.4. *^{1}H NMR of the reaction mixture after 2.0 h light off.*

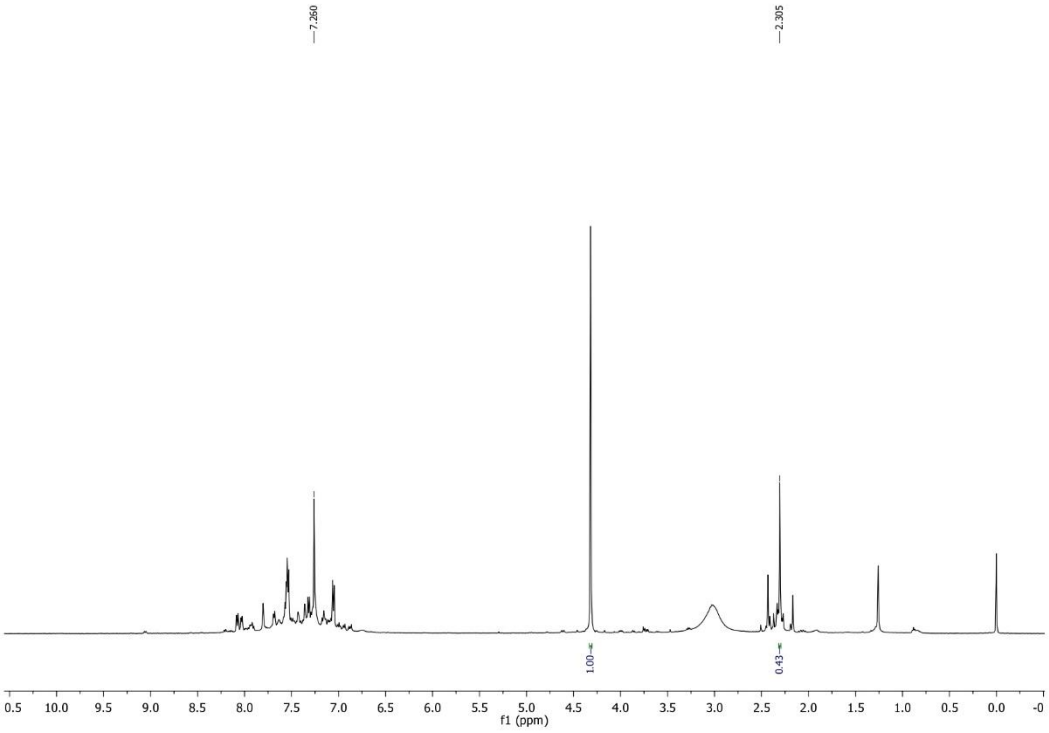

Figure II.9.5.5. *^{1}H NMR of the reaction mixture after 4.0 h light on.*

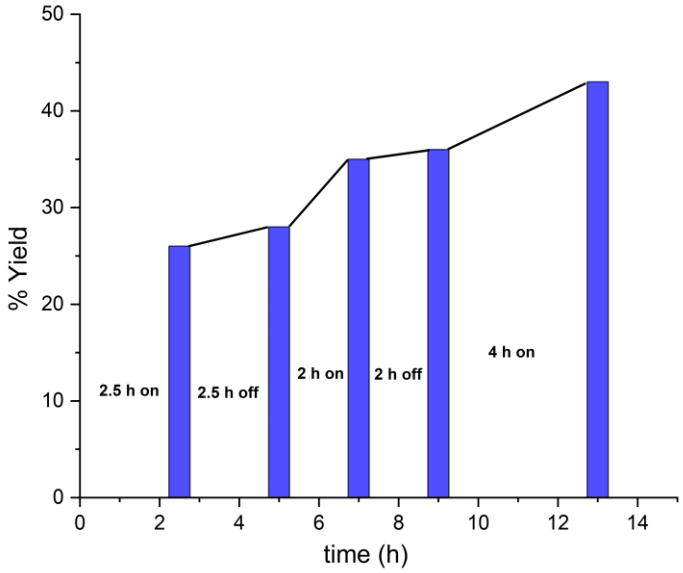

Figure II.9.5.6. *Plot %yield vs time (h) for On-off experiments in TFE.*

II.9.6. UV-vis Experiments:

A 1 mM 10 mL stock solution of $Pd(OAc)_2$, 2,2′-bipyridyl (L), and phenylboronic acid (**2a**) was prepared separately in EtOH. At first, the UV absorption of only $Pd(OAc)_2$ (20 μM) and 2,2′-bipyridyl (20 μM) was taken absorption maxima (λ_{max}) was found at 275 nm and 280 nm respectively. Next after successive addition of ligand 2,2′-bipyridyl (6.6 μM, 16.4 μM, 32.2 μM… so on) from 1mM stock solution to the existing solution of $Pd(OAc)_2$ (20 μM) then the absorption maxima of $Pd(OAc)_2$ (275 nm) undergo a red shift towards the visible region (420 nm) (Figure II.9.6.1). Further, the intensity was also increased successively, upon excessive addition of the 2,2′-bipyridyl to the same existing solution. This clearly indicates the complex formation occurs between 2,2′-bipyridyl and Pd(II) leading to $L_2Pd(0)$, thereby confirming the MLCT process due to $L_2Pd(0)$ which is the light-absorbing species. (Figure II.9.6.1).

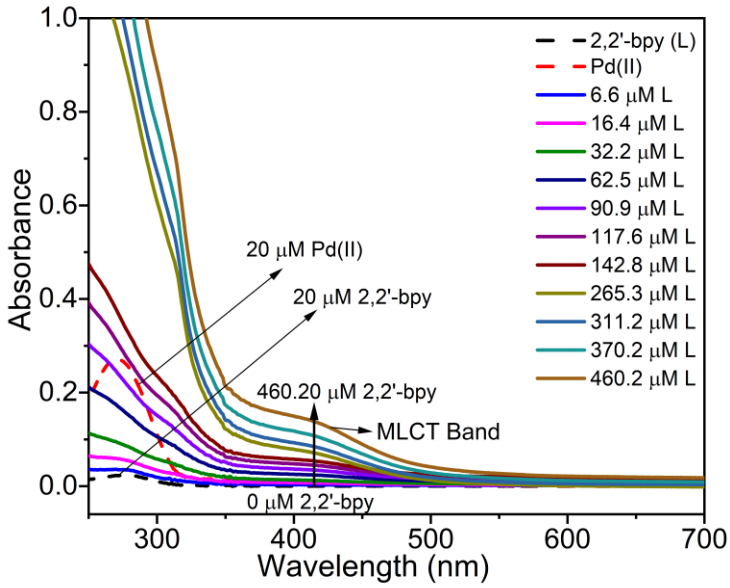

Figure II.9.6.1. *UV-vis spectra in EtOH.*

Next, a fluorescence quenching experiment was performed to confirm the M→Z σ-interaction between $L_2Pd(0)$ and phenylboronic acid (**2a**). A 1 mM stock solution was prepared by mixing **2a** in EtOH by an appropriate dilution. In UV-vis spectroscopy the MLCT band of the light-absorbing species [$L_2Pd(0)$] was observed at 420 nm. For the fluorescence measurement, the sample was excited at 420 nm, and the emission was observed at 466 nm. For each fluorescence quenching experiment, a 20 μL (1 mM) solution of phenylboronic acid (**2a**) was added to the existing solution of Pd-bpy solution (20 μM Pd + 460.20 μM 2,2′-bpy) taken in a fluorescence cuvette, and fluorescence emission spectra were recorded after each addition. As evident from Figure II.9.6.2, a decrease in emission intensity was observed after each addition of phenylboronic acid (**2a**) concentration (0−1250 μM). This suggests a possible M→Z σ-interaction between the $L_2Pd(0)$ and the quencher **2a** (Figure II.9.6.2). With these data, the Stern−Volmer graph was plotted using the equation $I_0/I = 1 + K_{SV}[Q]$, where I_0 and I are the integrated emission intensity in the absence and presence of quencher and Ksv is the quenching constant. A linear quenching was observed (Figure II.9.6.3).

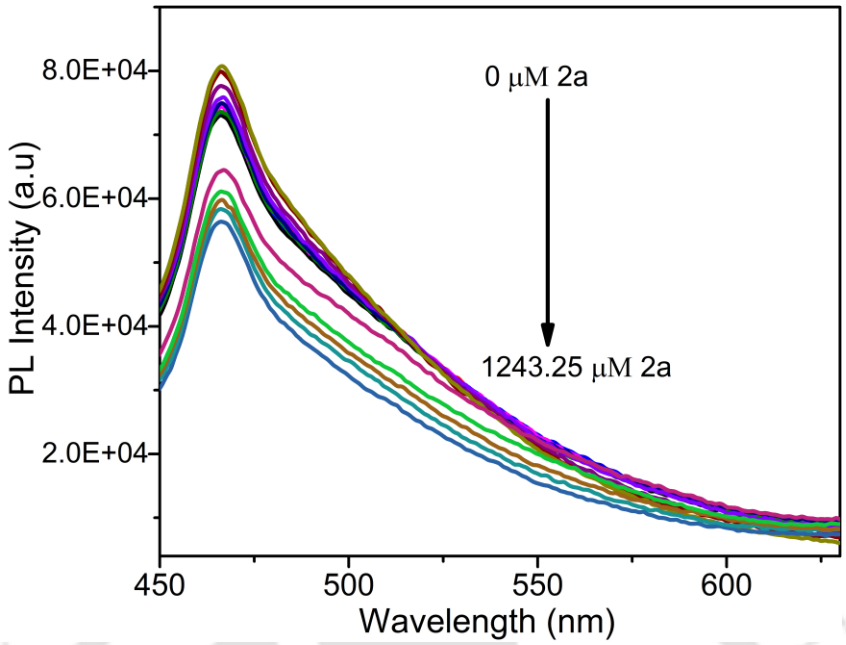

Figure II.9.6.2. *Fluorescence emission spectra of $L_2Pd(0)$ at varied conc. of quencher phenylboronic acid (**2a**) when excited at 420 nm.*

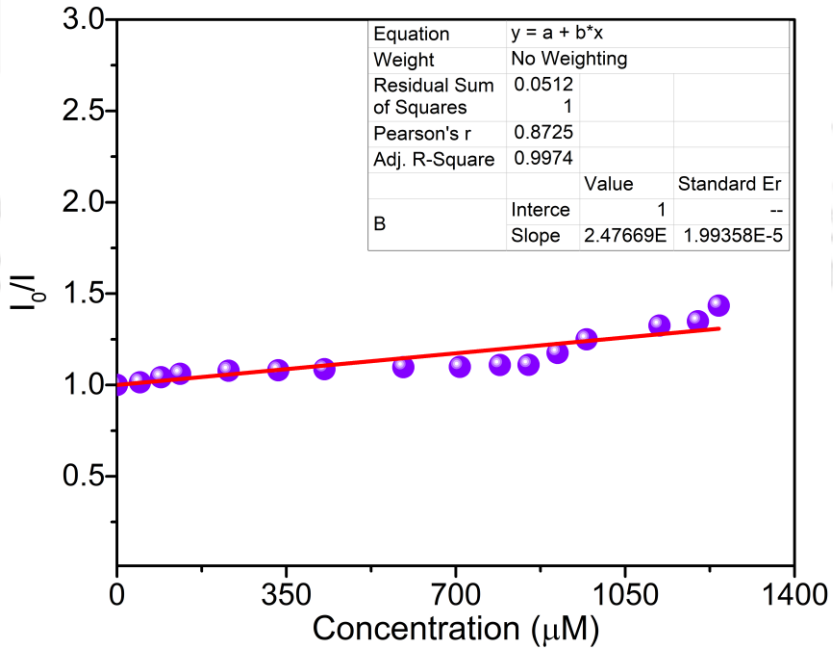

Figure II.9.6.3. *Stern-Volmer experiments.*

II.9.7. Procedure of Post-Synthetic Functionalizations:

II.9.7.1. General Procedure for the Synthesis of (4-(4-Methoxyphenyl)-2,6-diphenylpyridin-3-yl)(phenyl)methanone (3caa) from 4-(4-Methoxyphenyl)-2,6-diphenylnicotinonitrile (3ca) and Phenylboronic acid (2a):

To an oven-dried round bottom flask containing a magnetic bar was added 4-(4-Methoxyphenyl)-2,6-diphenylnicotinonitrile (**3ca**) (0.072 g, 0.20 mmol), phenylboronic acid (**2a**) (0.0724 g, 0.6 mmol), $Pd(OAc)_2$ (0.0045 g, 0.02 mmol), 2,2′-bipyridyl (0.0062 g, 0.04 mmol), and $PTSA{\cdot}H_2O$ (0.38 g, 2.0 mmol) in toluene (2 mL). The reaction mixture was stirred in an oil bath preheated at 120 °C for 24 h. After completion of the reaction (monitored by TLC analysis), the reaction mixture was admixed with ethyl acetate (25 mL) and the organic layer was washed with saturated sodium bicarbonate solution (10 mL). The organic layer was dried over anhydrous sodium sulfate (Na_2SO_4), and the solvent was evaporated under reduced pressure. The crude product so obtained was purified over a column of silica gel using 5% ethyl acetate in hexane to give pure (4-(4-methoxyphenyl)-2,6-diphenylpyridin-3-yl)(phenyl)methanone (**3caa**) in 65% yield (Scheme II.9.7.1.1). The identity and purity of the product were confirmed by spectroscopic analysis.

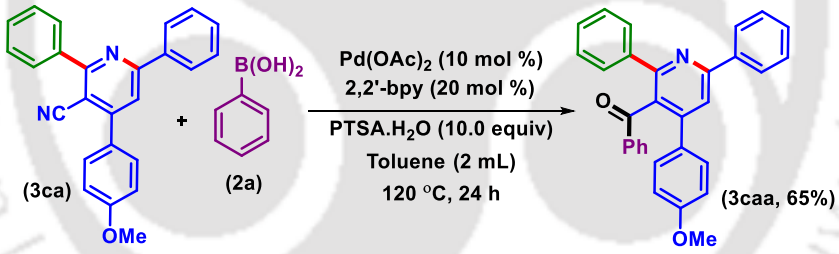

Scheme II.9.7.1.1. *Synthesis of keto compound (**3caa**).*

II.9.7.2 General Procedure for the Synthesis of 3-Cyano-2-(4-methoxyphenyl)-4,6,7-triphenylpyrido[2,1-*a*]isoquinolin-5-ium (3car) from 4-(4-Methoxyphenyl)-2,6-diphenylnicotinonitrile (3ca) and Diphenylacetylene (r):

To an oven-dried pressure tube (20.3 cm x 19 mm, 21 mL) containing a magnetic bar was added 4-(4-Methoxyphenyl)-2,6-diphenylnicotinonitrile (**3ca**) (0.0724 g, 0.20 mmol), diphenylacetylene (**r**) (0.043 g, 0.24 mmol), $[Ru(p\text{-cymene})Cl_2]_2$ (0.0061 g, 0.01 mmol), $Cu(OAc)_2{\cdot}H_2O$ (0.084 g, 0.44 mmol), and TfOH (0.045 g, 0.30 mmol) in DCE (2 mL). The reaction mixture was stirred in an oil bath preheated at 120 °C for 24 h. After completion of the reaction

(monitored by TLC analysis), the reaction mixture was admixed with ethyl acetate (25 mL) and the organic layer was washed with saturated sodium bicarbonate solution (10 mL). The organic layer was dried over anhydrous sodium sulfate (Na_2SO_4), and the solvent was evaporated under reduced pressure. The crude product so obtained was purified over a column of silica gel using 3% methanol in dichloromethane to give pure 3-cyano-2-(4-methoxyphenyl)-4,6,7-triphenylpyrido[2,1-*a*]isoquinolin-5-ium (**3car**) in 76% yield (Scheme II.9.7.2.1). The identity and purity of the product were confirmed by spectroscopic analysis.

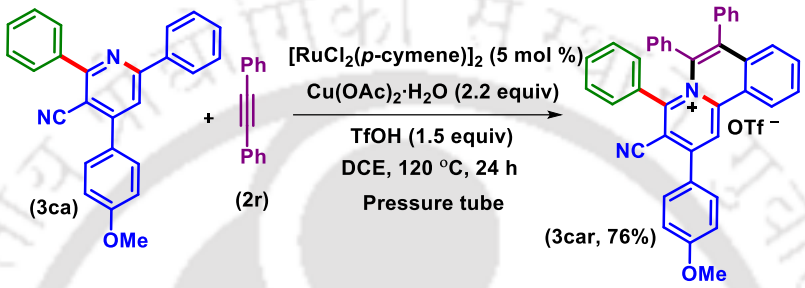

Scheme II.9.7.2.1. *Ru(II)-catalyzed C–H/N annulation of* ***3ca*** *with diphenylacetylene (**r**).*

II.9.7.3 General Procedure for the Synthesis of 4-(4-Methoxyphenyl)-2,6-diphenylnicotinamide (3cab) from 4-(4-Methoxyphenyl)-2,6-diphenylnicotinonitrile (3ca):

To an oven-dried round bottom flask containing a magnetic bar and fitted with a reflux condenser was added 4-(4-Methoxyphenyl)-2,6-diphenylnicotinonitrile (**3ca**) (0.0724 g, 0.20 mmol), and KOH (0.056 g, 1 mmol) in ethanol (2 mL). The reaction mixture was stirred in an oil bath preheated at 80 °C for 24 h. After completion of the reaction (monitored by TLC analysis), the reaction mixture was admixed with ethyl acetate (25 mL) and the organic layer was washed with brine (10 mL). The organic layer was dried over anhydrous sodium sulfate (Na_2SO_4), and the solvent was evaporated under reduced pressure. The crude product so obtained was purified over a column of silica gel using 20% ethyl acetate in hexane to give pure 4-(4-methoxyphenyl)-2,6-diphenylnicotinamide (**3cab**) in 70% yield (Scheme II.9.7.3.1). The identity and purity of the product were confirmed by spectroscopic analysis.

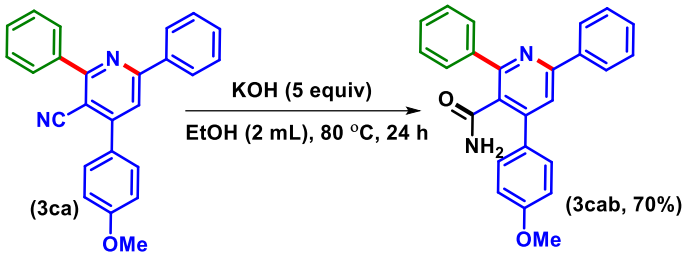

Scheme II.9.7.3.1. *Synthesis of nicotinamide analog (**3cab**).*

II.9.7.4 General Procedure for the Synthesis of 2-(4-Chlorophenyl)-4-(2,2-diphenylethyl)quinoline-3-carboxamide (4aga) and from (*Z*)-2-(4-Chlorophenyl)-4-styrylquinoline-3-carbonitrile (4ag):

To an oven-dried round bottom flask a magnetic bar was added (*Z*)-2-(4-chlorophenyl)-4-styrylquinoline-3-carbonitrile (**4ag**) (0.0732 g, 0.20 mmol), phenylboronic acid (**2a**) (0.072 g, 0.6 mmol), $Pd(OAc)_2$ (0.0045 g, 0.02 mmol), 2,2′-bipyridyl (0.0062 g, 0.04 mmol), and $PTSA{\cdot}H_2O$ (0.38 g, 2.0 mmol) in toluene (2 mL). The reaction mixture was stirred in an oil bath preheated at 120 °C for 24 h. After completion of the reaction (monitored by TLC analysis), the reaction mixture was admixed with ethyl acetate (25 mL), and the organic layer was washed with saturated sodium bicarbonate solution (10 mL). The organic layer was dried over anhydrous sodium sulfate (Na_2SO_4), and the solvent was evaporated under reduced pressure. The crude product so obtained was purified over a column of silica gel using 5% ethyl acetate in hexane to give pure 5-(4-chlorophenyl)-2-phenyl-2,3-dihydrobenzo[*c*][2,7]naphthyridin-4(1*H*)-one (**4aga**) and 2-(4-chlorophenyl)-4-(2,2-diphenylethyl)quinoline-3-carboxamide (**4aga**) in 52% yield (Scheme II.9.7.4.1). The identity and purity of the product were confirmed by spectroscopic analysis.

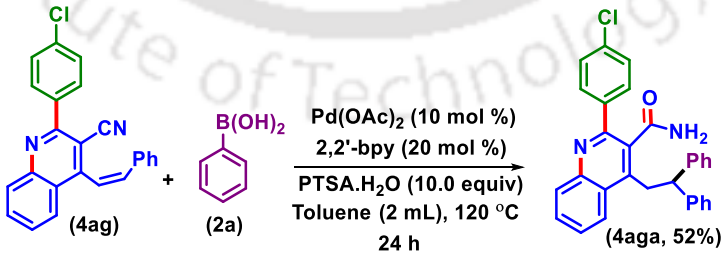

Scheme II.9.7.4.1. *Pd(II)-catalyzed regioselective hydroarylation of **4ag**.*

II.9.7.5 General Procedure for the Synthesis of (*Z*)-2-(4-Chlorophenyl)-3-cyano-4-styrylquinoline 1-oxide (4ags) from (*Z*)-2-(4-Chlorophenyl)-4-styrylquinoline-3-carbonitrile (4ag):

To an oven-dried round bottom flask containing a magnetic bar was added (*Z*)-2-(4-chlorophenyl)-4-styrylquinoline-3-carbonitrile (**4ag**) (0.0732 g, 0.20 mmol), and *m*-CPBA (**s**) (0.172 g, 1 mmol) in dichloromethane (2 mL). The reaction mixture was stirred at room temperature for 12 h. After completion of the reaction (monitored by TLC analysis), the reaction mixture was admixed with ethyl acetate (20 mL) and the organic layer was washed with saturated sodium bicarbonate solution (10 mL). The organic layer was dried over anhydrous sodium sulfate (Na_2SO_4), and the solvent was evaporated under reduced pressure. The crude product so obtained was purified over a column of silica gel using 20% ethyl acetate in hexane to give pure (*Z*)-2-(4-chlorophenyl)-3-cyano-4-styrylquinoline 1-oxide (**4ags**) in 75% yield (Scheme II.9.7.5.1). The identity and purity of the product were confirmed by spectroscopic analysis.

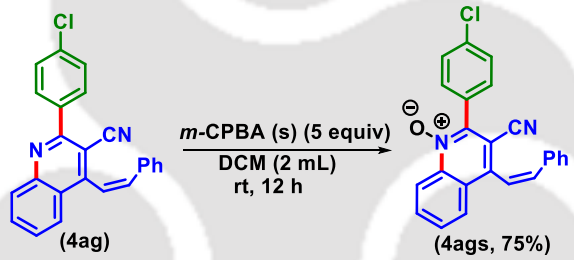

Scheme II.9.7.5.1. *Synthesis of quinoline N-oxide (**4ags**).*

II.9.7.6 General Procedure for the Synthesis of 5-(4-Chlorophenyl)-2-phenyl-2,3-dihydrobenzo[*c*][2,7]naphthyridin-4(1*H*)-one (4agb) from (*Z*)-2-(4-Chlorophenyl)-4-styrylquinoline-3-carbonitrile (4ag):

To an oven-dried round bottom flask containing a magnetic bar and fitted with a reflux condenser was added 4-(4-Methoxyphenyl)-2,6-diphenylnicotinonitrile (**3ca**) (0.0732 g, 0.20 mmol), and NaOH (0.056 g, 1 mmol) in ethanol (2 mL). The reaction mixture was stirred in an oil bath preheated at 80 ^{o}C for 24 h. After completion of the reaction (monitored by TLC analysis), the reaction mixture was admixed with ethyl acetate (25 mL) and the organic layer was washed with brine (10 mL). The organic layer was dried over anhydrous sodium sulfate (Na_2SO_4), and the solvent was evaporated under reduced pressure. The crude product so obtained was purified over a

column of silica gel using 30% ethyl acetate in hexane to give pure 5-(4-chlorophenyl)-2-phenyl-2,3-dihydrobenzo[*c*][2,7]naphthyridin-4(1*H*)-one (**4agb**) in 61% yield (Scheme II.9.7.6.1). The identity and purity of the product were confirmed by spectroscopic analysis.

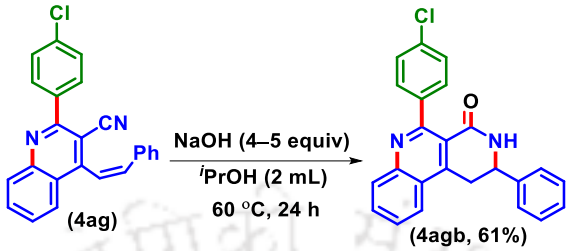

Scheme II.9.7.6.1. *Basic hydrolysis of* ***4ag*** *for the formation of cyclic amide (****4agb****).*

II.9.8. Crystallographic Information:

II.9.8.1. Crystallographic Information of 2-(Benzo[*d*][1,3]dioxol-5-yl)-4,6-diphenylnicotinonitrile (3aj):

(i) Sample Preparation: The single crystal of compound **3aj** was prepared by the slow evaporation method for which 10 mg of the compound (**3aj**) was dissolved in 1 mL of DCM in a clean and dry 10 mL glass vial. MeOH (0.5 mL) was added to this solution slowly with a dropper. The mouth of the glass vial was covered with a cap having a small hole and kept for slow evaporation at room temperature. Crystals of **3aj** were obtained as a transparent white needle-like crystal after around 2–3 days.

(ii) Data Collection: Diffraction data were collected at 298 K with MoKα radiation (λ = 0.71073 Å) using a Bruker Nonius SMART APEX CCD diffractometer equipped with a graphite monochromator and Apex CD camera. The SMART software was used for data collection and for indexing the reflections and determining the unit cell parameters. Data reduction and cell refinement were performed using SAINT[1,2] software and the space groups of these crystals were determined from systematic absences by XPREP and further justified by the refinement results. The structures were solved by direct methods and refined by full-matrix least-squares calculations using SHELXTL-97[3] software. All the non-H atoms were refined in the anisotropic approximation against F^2 of all reflections.

1. G. M. Sheldrick, SADABS, 1996, based on the method described in: R. H. Blessing, *Acta Crystallogr*. 1995, **A51**, 33–38.

2. SMART and SAINT, Siemens Analytical X-ray Instruments Inc., Madison, WI, 1996.

3. G. M. Sheldrick, *Acta Crystallogr.*, 2008, **A64**, 112–122.

(iii) Crystallographic description of 2-(benzo[*d*][1,3]dioxol-5-yl)-4,6-diphenylnicotinonitrile (3aj):

$C_{25}H_{16}N_2O_2$, crystal dimensions 0.25 x 0.22 x 0.16 mm, M_r = 376.40, Triclinic, space group P -1, a = 7.6584 (14), b = 10.3894 (19), c = 13.063 (2) Å, α = 99.628 (6)°, β = 101.770 (6)°, γ = 109.338 (6)°, V = 928.6 (3) Å^3, Z = 2, ρ_{calcd} = 1.346 g/cm^3, μ = 0.087 mm^{-1}, F(000)= 392.0, reflection collected / unique = 4682 / 2941, refinement method = full-matrix least-squares on F^2, final R indices [I> 2\s(I)]:R_1 = 0.0951, wR_2 = 0.1448, R indices (all data): R_1 = 0.0541, wR_2 = 0.1258, goodness of fit = 1.052. **CCDC-2184661** for 2-(benzo[d][1,3]dioxol-5-yl)-4,6-diphenylnicotinonitrile (**3aj**) contains the supplementary crystallographic data for this paper. These data can be obtained free of charge from The Cambridge Crystallographic Data Centre via www.ccdc.cam.ac.uk/data_request/cif.

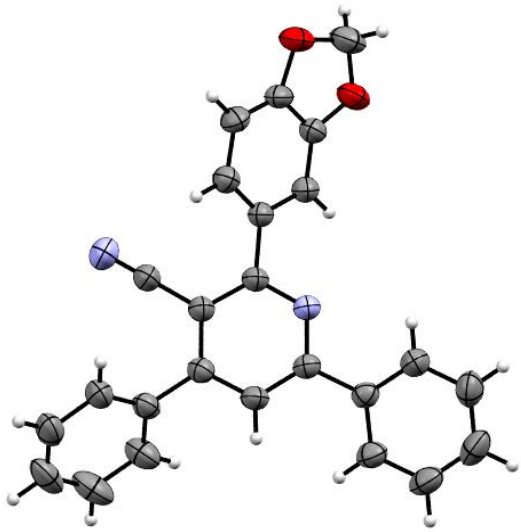

Figure II.9.8.1.1. *ORTEP diagram of 2-(benzo[d][1,3]dioxol-5-yl)-4,6-diphenylnicotinonitrile (**3aj**) with 40% ellipsoid probability (CCDC 2184661).*

II.9.8.2. Crystallographic information of (*Z*)-7-methyl-2-phenyl-4-styrylquinoline-3-carbonitrile (4ba):

(i) Sample Preparation: The single crystal of compound **4ba** was prepared by the slow evaporation method for which 10 mg of the compound (**4ba**) was dissolved in 1 mL of DCM in a clean and dry 10 mL glass vial. MeOH (0.5 mL) was added to this solution slowly with a dropper. The mouth of the glass vial was covered with a cap having a small hole and kept it for slow

evaporation at room temperature. Single crystals of **4ba** were obtained as a transparent white needle-like crystal after around 2–3 days.

(ii) Data Collection: Diffraction data were collected at 293 K with MoKα radiation (λ = 0.71073 Ǻ) using a Bruker Nonius SMART APEX CCD diffractometer equipped with graphite monochromator and Apex CD camera. The SMART software was used for data collection and for indexing the reflections and determining the unit cell parameters. Data reduction and cell refinement were performed using SAINT[1,2] software and the space groups of these crystals were determined from systematic absences by XPREP and further justified by the refinement results. The structures were solved by direct methods and refined by full-matrix least-squares calculations using SHELXTL-97[3] software. All the non-H atoms were refined in the anisotropic approximation against F^2 of all reflections.

1. G. M. Sheldrick, SADABS, 1996, based on the method described in: R. H. Blessing, *Acta Crystallogr*. 1995, **A51**, 33–38.

2. SMART and SAINT, Siemens Analytical X-ray Instruments Inc., Madison, WI, 1996.

3. G. M. Sheldrick, *Acta Crystallogr*., 2008, **A64**, 112–122.

(iii) Crystallographic description of (*Z*)-7-methyl-2-phenyl-4-styrylquinoline-3-carbonitrile (4ba):

$C_{25}H_{18}N_2$, crystal dimensions 0.10 x 0.06 x 0.04 mm, M_r = 379.83, Monoclinic, space group P 1 21/n1, a = 9.9296 (5), b = 15.4700 (5), c = 13.2136 (7) Å, α = 90, β = 111.910 (6)º, γ = 90, V = 1883.15 (17) Å^3, Z = 4, ρ_{calcd} = 1.222 g/cm^3, μ = 0.072 mm^{-1}, F(000)= 728.0, reflection collected / unique = 4041 / 1787, refinement method = full-matrix least-squares on F^2, final R indices [I> 2\s(I)]:R_1 = 0.1352, wR_2 = 0.1674, R indices (all data): R_1 = 0.0542, wR_2 = 0.1330, goodness of fit = 1.023. **CCDC-2184664** for (*Z*)-7-methyl-2-phenyl-4-styrylquinoline-3-carbonitrile **(4ba)** contains the supplementary crystallographic data for this paper. These data can be obtained free of charge from The Cambridge Crystallographic Data Centre via www.ccdc.cam.ac.uk/data_request/cif.

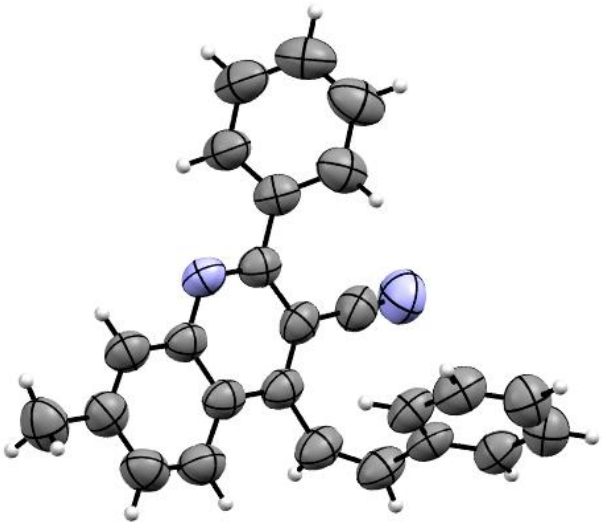

Figure II.9.8.2.1. *ORTEP diagram of (Z)-7-methyl-2-phenyl-4-styrylquinoline-3-carbonitrile (**4ba**) with 40% ellipsoid probability (CCDC 2184664).*

II.9.8.3. Crystallographic information of 3-cyano-2-(4-methoxyphenyl)-4,6,7-triphenylpyrido[2,1-*a*]isoquinolin-5-ium (3car):

(i) Sample Preparation: The single crystal of compound **3car** was prepared by the slow evaporation method. In a dry 10 mL glass vial, 10 mg of the compound (**3car**) was dissolved in 1 mL of DCM and then MeOH (0.5 mL) was added to this solution slowly with a dropper. The mouth of the glass vial was covered with a cap having a small hole and kept it for slow evaporation at room temperature. Single crystals of **3car** were obtained as a transparent white needle-like crystal after around 2-3 days.

(ii) Data Collection: Diffraction data were collected at 298 K with MoKα radiation (λ = 0.71073 Å) using a Bruker Nonius SMART APEX CCD diffractometer equipped with graphite monochromator and Apex CD camera. The SMART software was used for data collection and for indexing the reflections and determining the unit cell parameters. Data reduction and cell refinement were performed using SAINT[1,2] software and the space groups of these crystals were determined from systematic absences by XPREP and further justified by the refinement results. The structures were solved by direct methods and refined by full-matrix least-squares calculations using SHELXTL-97[3] software. All the non-H atoms were refined in the anisotropic approximation against F^2 of all reflections.

1. G. M. Sheldrick, SADABS, 1996, based on the method described in: R. H. Blessing, *Acta Crystallogr*. 1995, **A51**, 33–38.

2. SMART and SAINT, Siemens Analytical X-ray Instruments Inc., Madison, WI, 1996.

3. G. M. Sheldrick, *Acta Crystallogr*., 2008, **A64**, 112–122.

(iii) Crystallographic description of 3-cyano-2-(4-methoxyphenyl)-4,6,7-triphenylpyrido[2,1-*a*]isoquinolin-5-ium (3car):

$C_{40}H_{28}F_3N_2O_4S$, crystal dimensions 0.25 x 0.22 x 0.16 mm, M_r = 689.70, Monoclinic, space group P 21/n, a = 10.7433 (4), b = 28.9225 (10), c = 11.9569 (4) Å, α = 90 , β = 116.530 (1)^o, γ = 90, V = 3324.1 (2) Å^3, Z = 4, ρ_{calcd} = 1.378 g/cm^3, μ = 0.160 mm^{-1}, F(000)= 1428.0, reflection collected / unique = 5824 / 4698, refinement method = full-matrix least-squares on F^2, final R indices [I> 2\s(I)]:R_1 = 0.0668, wR_2 = 0.1676, R indices (all data): R_1 = 0.0544, wR_2 = 0.1575, goodness of fit = 0.985. **CCDC-2206181** for 3-cyano-2-(4-methoxyphenyl)-4,6,7-triphenylpyrido[2,1-*a*]isoquinolin-5-ium (**3car**) contains the supplementary crystallographic data for this paper. These data can be obtained free of charge from The Cambridge Crystallographic Data Centre via www.ccdc.cam.ac.uk/data_request/cif.

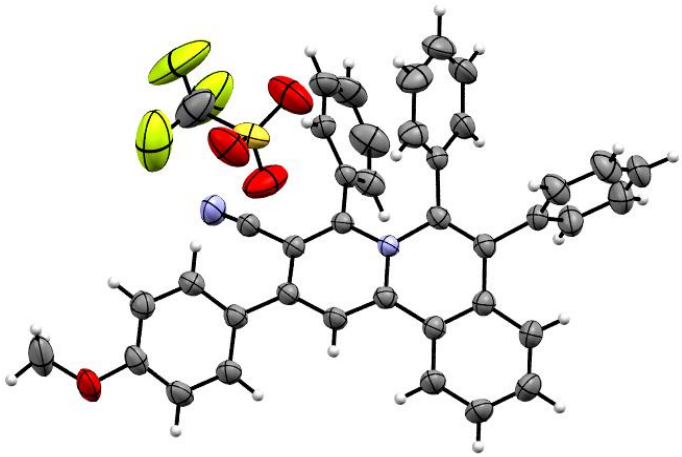

Figure II.9.8.3.1. *ORTEP diagram of 3-cyano-2-(4-methoxyphenyl)-4,6,7-triphenylpyrido[2,1-a]isoquinolin-5-ium (**3car**) with 40% ellipsoid probability (CCDC 2206181).*

II.9.9. DFT:

The greater thermodynamic stability of *E*-disubstituted alkenes over the *Z*-isomer, and thermal or photo-isomerization between these two alkenes, are the two common concepts. The literature reports reveal that the *E*→*Z* isomerization of activated olefin proceeds *via* an energy transfer (E_T) and single electron transfer (SET) manifold.[30,33] In contrast to the ground-state reactivity, due to high rotational barriers, the C=C double bond rotation is impossible, which alleviates by an appropriate wavelength in photochemical excitation. Generally, this photoexcitation occurs *via* the excitation of an electron from a π→π* orbital, thereby reducing the bond order and allowing rotation and subsequent relaxation to the ground state.[30,33] Thus, the predominant formation of *Z*-isomer may be due to the low rotational energy barrier of the C=C double bond in the excited state which is isomerized from (*E* → *Z*) upon photoexcitation. However, calculations suggest that the *Z*-configuration is also preferred in the gas phase conditions.[30] In the current study we have optimized *E* and *Z* configurations of the product geometry and both are found to differ by only a kcal/mol in relative Gibbs free energy (Figure II.9.9.1. and Table II.9.9.1).

Computational Details

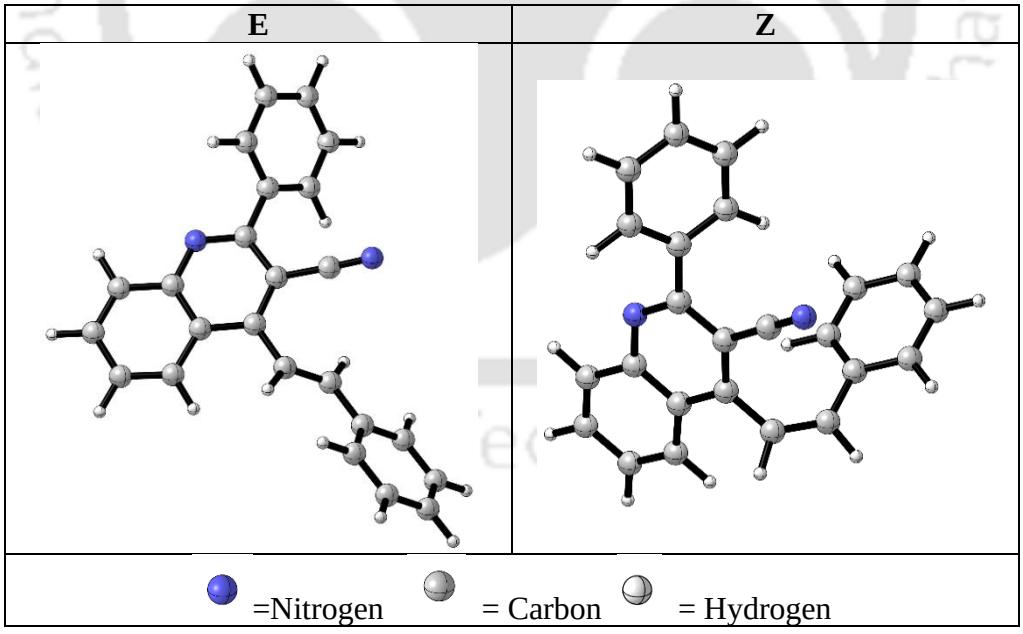

Figure II.9.9.1*. Optimized geometries of product using the Gaussian09 (Revision D.01) suite of quantum chemical program.[34] The effect of a solvent continuum, in TFE (2,2,2-Trifluoroethanol), was evaluated using the Cramer−Truhlar continuum solvation model that employs quantum*

mechanical charge densities of solutes, designated as SMD.[35] *The geometries were optimized using the B3LYPD3 hybrid density functional in conjunction with 6-31++G** basis set for all atoms.*[36]

Table II.9.9.1. *Relative Gibbs Free Energies (kcal/mol) for the E and Z geometries of product obtained at different Level of Theories*[a]

	L1	**L2**	**L3**
E isomer of product	0.0	0.0	0.0
Z isomer of product	1.1	1.5	1.4

[a]**L1** = $SMD_{(TFE)}$/B3LYP-D3/6-31G**; **L2** = $SMD_{(TFE)}$/B3LYP-D3/6-31+G**; **L3** = $SMD_{(TFE)}$/B3LYP-D3/6-31++G**

Cartesian Coordinates of the Optimized Geometries of Various Stationary Points Obtained at the $SMD_{(TFE)}$/B3LYP-D3/6-31++G** Level of Theory.

E geometry of product

Number of imaginary frequencies= 0
Eletcronic energy =-1033.8091701
Zero-point correction= 0.329014 (Hartree/Particle)
Thermal correction to Energy= 0.349264
Thermal correction to Enthalpy= 0.350208
Thermal correction to Gibbs Free Energy= 0.278086
Sum of electronic and zero-point Energies= -1033.480156
Sum of electronic and thermal Energies= -1033.459906
Sum of electronic and thermal Enthalpies= -1033.458962
Sum of electronic and thermal Free Energies= -1033.531084

Cartesian Coordinates

C,0,0.033008652,4.5436037475,0.2417572856
C,0,0.5646242573,3.2780582367,0.0990164543
C,0,-0.2842486409,2.1397246717,0.0249327078
C,0,-1.6978900105,2.3286514317,0.1358367159
C,0,-2.2175324836,3.6411625946,0.2780401092
C,0,-1.3686591832,4.7276204945,0.3248704545
H,0,0.6934255191,5.4039372094,0.2953766876
H,0,1.6405559655,3.1528086384,0.0513433667
C,0,0.2093529174,0.8051303312,-0.149738832
H,0,-3.2938989183,3.762296124,0.3544086551
H,0,-1.7738558846,5.72939707,0.4347140284
C,0,-2.1389021465,0.0555167527,-0.0023303053
C,0,-0.7387778593,-0.2274355171,-0.1872972251
N,0,-2.5857773059,1.2889557708,0.1341019564
C,0,-0.3454162753,-1.5543142409,-0.5469807114
N,0,-0.0518584187,-2.6313409264,-0.8809066335

C,0,1.6451191593,0.5696022697,-0.3292488013
H,0,2.1684321855,1.2934484757,-0.9476250288
C,0,2.3283138251,-0.4327679115,0.2638820984
C,0,-3.1567232244,-1.030458297,0.0176691403
C,0,-4.3276785246,-0.8959343672,-0.747082855
C,0,-2.9893572975,-2.1723015788,0.8183437191
C,0,-5.3043865245,-1.8930979547,-0.7246263792
H,0,-4.4617067539,-0.0139900623,-1.3658104421
C,0,-3.9729057946,-3.1636809325,0.8474662144
H,0,-2.1021852012,-2.2782906124,1.4353901086
C,0,-5.1297239597,-3.0297510584,0.0728431725
H,0,-6.2000907948,-1.7831231932,-1.3296264268
H,0,-3.8362345534,-4.0373888704,1.4784465176
H,0,-5.8913354645,-3.8044352062,0.0919530251
C,0,3.7592285139,-0.7194571198,0.1221727364
C,0,4.3391467576,-1.675776892,0.9795302536
C,0,4.58318278,-0.0905130146,-0.8351408808
C,0,5.698325528,-1.9850057296,0.8967492632
H,0,3.715230669,-2.1750156988,1.7168579883
C,0,5.9390751156,-0.4011656519,-0.9176120676
H,0,4.1621778205,0.6346789872,-1.5247530468
C,0,6.5040739824,-1.3472485501,-0.0511885059
H,0,6.126060781,-2.7231092331,1.5695789119
H,0,6.5583605398,0.0904453001,-1.6628621667
H,0,7.5615647504,-1.5866393693,-0.1201972981
H,0,1.7992625002,-1.0909841178,0.9503480356

Z geometry of product

Number of imaginary frequencies= 0
Eletcronic energy = -1033.8068179
Zero-point correction= 0.328861 (Hartree/Particle)
Thermal correction to Energy= 0.348986
Thermal correction to Enthalpy= 0.349930
Thermal correction to Gibbs Free Energy= 0.278068
Sum of electronic and zero-point Energies= -1033.477957
Sum of electronic and thermal Energies= -1033.457832
Sum of electronic and thermal Enthalpies= -1033.456888
Sum of electronic and thermal Free Energies= -1033.528749

Cartesian Coordinates

C,0,-1.534797864,4.5721247825,0.3976378691

C,0,-0.5958237428,3.7270778494,-0.1570152896
C,0,-0.8344371303,2.3268842879,-0.2204565129
C,0,-2.0481670005,1.8047240726,0.3288348472
C,0,-2.9976351337,2.6977997157,0.8892678869
C,0,-2.7469542051,4.0542295867,0.9179504566
H,0,-1.3443058498,5.6403888053,0.4392211546
H,0,0.3333314782,4.1305329474,-0.5454296144
C,0,0.088166074,1.4087310026,-0.8080299604
H,0,-3.9148927273,2.2843416195,1.2975555212
H,0,-3.4780753878,4.7317324373,1.3495762057
C,0,-1.4660067583,-0.3876006348,-0.1559106124
C,0,-0.2588327776,0.0545830026,-0.8019926799
N,0,-2.3259508155,0.4668088873,0.3653769904
C,0,0.5486700867,-0.8878893263,-1.5109712396
N,0,1.1842551947,-1.6524511916,-2.1174897153
C,0,1.3215651641,1.8984188504,-1.4542931113
H,0,1.169488922,2.6649477453,-2.211613466
C,0,2.5880420816,1.5063362086,-1.2065064277
H,0,3.3591002776,1.9315343317,-1.847459171
C,0,3.0793922686,0.5682265109,-0.1821168193
C,0,2.4615372085,0.4125956471,1.0739389682
C,0,4.2216325457,-0.2033841923,-0.4680219098
C,0,2.9496242977,-0.5130457227,1.9965848078
H,0,1.6061449367,1.0265396163,1.3356368754
C,0,4.7049156251,-1.1354753351,0.4525127141
H,0,4.7207916383,-0.0809742939,-1.4260307779
C,0,4.0668399037,-1.2979721023,1.6866465916
H,0,2.4609551785,-0.6174349714,2.9614926969
H,0,5.5800581442,-1.7312489794,0.2079884693
H,0,4.4436776672,-2.0194811758,2.4062888447
C,0,-1.7995927088,-1.8331494101,-0.0480067065
C,0,-3.0868675838,-2.2804726859,-0.3880286262
C,0,-0.8552658555,-2.7564981963,0.4307147194
C,0,-3.4178698581,-3.6314526775,-0.2682251378
H,0,-3.819118125,-1.5684684181,-0.756567635
C,0,-1.1931505559,-4.1054195096,0.5609178051
H,0,0.1348830486,-2.4197315495,0.7234034052
C,0,-2.4721486941,-4.5472268004,0.2067008323
H,0,-4.4123155954,-3.9689728335,-0.5467454458
H,0,-0.4583877935,-4.8087518418,0.9425707968
H,0,-2.731122579,-5.5981020586,0.3020024006

II.10. Spectral Data:

2,4,6-Triphenylnicotinonitrile (3aa):

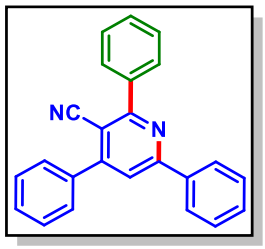

As a white solid (60 mg, 72% yield, mp 208–210 °C); Purification over a column of silica gel (2% EtOAc in hexane); ^{1}H NMR ($CDCl_3$, 500 MHz): δ 8.18 (d, 2H, J = 7.75 Hz), 8.05 (d, 2H, J = 8.0 Hz), 7.82 (s, 1H), 7.69 (d, 2H, J = 7.75 Hz), 7.57–7.50 (m, 9H); ^{13}C{^{1}H} NMR ($CDCl_3$, 125 MHz): δ 162.6, 159.3, 155.6, 138.2, 137.7, 137.0, 130.7, 130.2, 130.1, 129.6, 129.2, 129.1, 128.9, 128.7, 127.7, 118.8, 117.9, 104.5; IR (KBr, cm^{-1}): 2924, 2858, 2215, 1727, 1571, 1488, 1276, 1171, 1073, 873; HRMS (ESI/Q-TOF) (m/z) calcd for $C_{24}H_{17}N_2$ [M + H]$^+$ 333.1386; found 333.1395.

2,6-Diphenyl-4-(p-tolyl)nicotinonitrile (3ba):

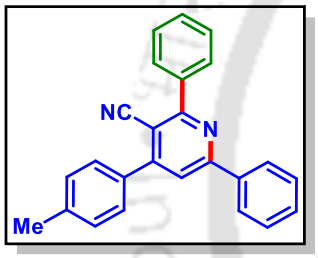

As a white solid (55 mg, 64% yield, mp 150–152 °C); Purification over a column of silica gel (2% EtOAc in hexane); ^{1}H NMR ($CDCl_3$, 400 MHz): δ 8.19–8.17 (m, 2H), 8.06–8.03 (m, 2H), 7.81 (s, 1H), 7.61−7.50 (m, 8H), 7.38 (d, 2H, J = 7.6 Hz), 2.46 (s, 3H); ^{13}C{1H} NMR ($CDCl_3$, 100 MHz): δ 162.5, 159.2, 155.6, 140.3, 138.2, 137.8, 134.0, 130.6, 130.2, 129.8, 129.5, 129.1, 128.7, 128.6, 127.7, 118.7, 118.1, 104.4, 21.5; IR (KBr, cm^{-1}): 2925, 2862, 2214, 1578, 1290, 1247, 1172, 1074, 877; HRMS (ESI/Q-TOF) (m/z) calcd for $C_{25}H_{19}N_2$ [M + H]$^+$ 347.1543; found 347.1552.

4-(4-Methoxyphenyl)-2,6-diphenylnicotinonitrile (3ca):

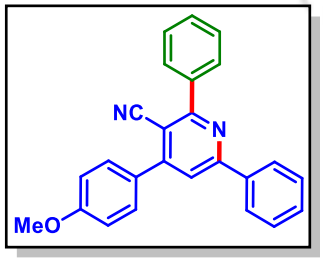

As a white solid (71 mg, 79% yield, mp 176–178 °C); Purification over a column of silica gel (4% EtOAc in hexane); ^{1}H NMR ($CDCl_3$, 500 MHz): δ 8.18 (d, 2H, J = 8 Hz), 8.04 (d, 2H, J = 7.75 Hz), 7.79 (s, 1H), 7.66 (d, 2H, J = 8.5 Hz), 7.56–7.50 (m, 6H), 7.08 (d, 2H, J = 9.0 Hz), 3.89 (s, 3H); ^{13}C{^{1}H} NMR ($CDCl_3$, 125 MHz): δ 162.6, 161.2, 159.2, 155.2, 138.3, 137.8, 130.6, 130.3, 130.1, 129.5, 129.2, 129.1, 128.6, 127.7, 118.5, 118.2, 114.6, 104.3, 55.6; IR (KBr, cm^{-1}): 2925, 2860, 2218, 1669, 1582, 1459, 1253, 1173, 1027, 819; HRMS

(ESI/Q-TOF) (m/z) calcd for $C_{25}H_{19}N_2O$ $[M + H]^+$ 363.1492; found 363.1495.

4-(4-Fluorophenyl)-2,6-diphenylnicotinonitrile (3da):

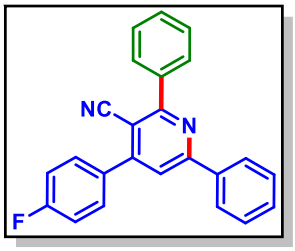

As a white solid (59 mg, 68% yield, mp 222–224 °C); Purification over a column of silica gel (2% EtOAc in hexane); ^{1}H NMR ($CDCl_3$, 500 MHz): δ 8.19 (d, 2H, J = 7.5 Hz), 8.06 (d, 2H, J = 7 Hz), 7.80 (s, 1H), 7.70–7.68 (m, 2H), 7.57–7.52 (m, 6H), 7.29–7.25 (m, 2H); ^{13}C{^{1}H} NMR ($CDCl_3$, 125 MHz): δ 163.9 (d, J = 249.3 Hz), 162.6, 159.4, 154.5, 138.1, 137.6, 133.0 (d, J = 3.5 Hz), 130.9, 130.8 (d, J = 7.3 Hz), 130.3, 129.5, 129.2, 128.7, 127.7, 118.6, 117.8, 116.3 (d, J = 21.8 Hz), 104.4; ^{19}F NMR ($CDCl_3$, 471 MHz): δ –110.6 (s); IR (KBr, cm^{-1}): 2925, 2851, 2216, 1645, 1576, 1451, 1225, 1163, 1096, 876; HRMS (ESI/Q-TOF) (m/z) calcd for $C_{24}H_{16}FN_2$ $[M + H]^+$ 351.1292; found 351.1303.

4-(4-Chlorophenyl)-2,6-diphenylnicotinonitrile (3ea):

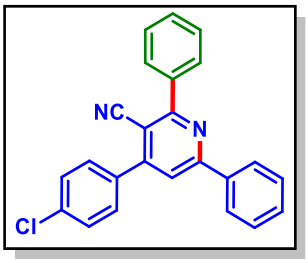

As a white solid (60 mg, 65% yield, mp 219–221 °C); Purification over a column of silica gel (2% EtOAc in hexane); ^{1}H NMR ($CDCl_3$, 500 MHz): δ 8.17 (d, 2H, J = 7.5 Hz), 8.04 (d, 2H, J = 7.25 Hz), 7.78 (s, 1H), 7.62 (d, 2H, J = 8.5 Hz), 7.56–7.51 (m, 8H); ^{13}C{^{1}H} NMR ($CDCl_3$, 125 MHz): δ 162.6, 159.5, 154.4, 138.0, 137.6, 136.5, 135.3, 130.8, 130.3, 130.2, 129.6, 129.5, 129.2, 128.7, 127.7, 118.5, 117.7, 104.3; IR (KBr, cm^{-1}): 2921, 2857, 2216, 1677, 1575, 1484, 1260, 1172, 1087, 822; HRMS (ESI/Q-TOF) (m/z) calcd for $C_{24}H_{16}ClN_2$ $[M + H]^+$ 367.0997; found 367.0997.

4-(4-Bromophenyl)-2,6-diphenylnicotinonitrile (3fa):

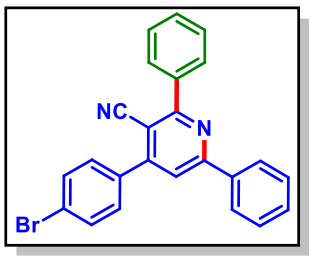

As a white solid (50 mg, 49% yield, mp 238–240 °C); Purification over a column of silica gel (2% EtOAc in hexane); ^{1}H NMR ($CDCl_3$, 500 MHz): δ 8.17 (d, 2H, J = 7.25 Hz), 8.03 (d, 2H, J = 7.5 Hz), 7.78 (s, 1H), 7.71 (d, 2H, J = 8.5 Hz), 7.57–7.51 (m, 8H); ^{13}C{^{1}H} NMR ($CDCl_3$, 125 MHz): δ 162.7, 159.5, 154.4, 138.0, 137.5, 135.3, 132.4,

130.8, 130.5, 130.4, 129.5, 129.2, 128.7, 127.7, 124.8, 118.4, 117.7, 104.2; IR (KBr, cm^{-1}): 2924, 2858, 2219, 1679, 1573, 1484, 1261, 1172, 1089, 823; HRMS (ESI/Q-TOF) (m/z) calcd for $C_{24}H_{16}BrN_2$ $[M + H]^+$ 411.0491; found 411.0499.

2,4-Diphenyl-6-(p-tolyl)nicotinonitrile (3ga):

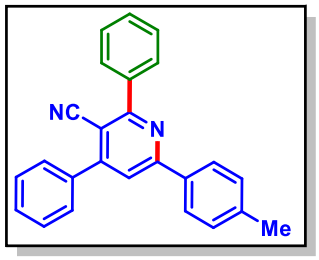

As a white solid (54 mg, 62% yield, mp 165–167 °C); Purification over a column of silica gel (2% EtOAc in hexane); ^1H NMR ($CDCl_3$, 400 MHz): δ 8.09 (d, 2H, J = 8.0 Hz), 8.05 (d, 2H, J = 7.8 Hz), 7.79 (s, 1H), 7.69 (d, 2H, J = 7.6 Hz), 7.59–7.54 (m, 6H), 7.32 (d, 2H, J = 7.6 Hz), 2.44 (s, 3H); $^{13}C\{^1H\}$ NMR ($CDCl_3$, 100 MHz): δ 162.4, 159.2, 155.4, 141.1, 138.2, 137.0, 134.9, 130.1, 130.0, 129.8, 129.5, 129.1, 128.8, 128.6, 127.6, 118.3, 118.0, 104.0, 21.6; IR (KBr, cm^{-1}): 2923, 2856, 2216, 1574, 1452, 1532, 1260, 1079, 881; HRMS (ESI/Q-TOF) (m/z) calcd for $C_{25}H_{19}N_2$ $[M + H]^+$ 347.1543; found 347.1550.

6-(4-Methoxyphenyl)-2,4-diphenylnicotinonitrile (3ha):

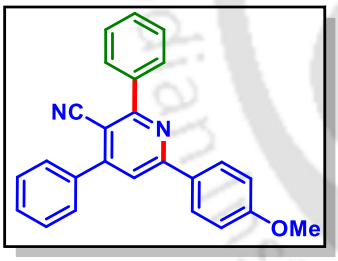

As a white solid (68 mg, 75% yield, mp 164–166 °C); Purification over a column of silica gel (4% EtOAc in hexane); ^1H NMR ($CDCl_3$, 500 MHz): δ 8.16 (d, 2H, J = 9.0 Hz), 8.05 (d, 2H, J = 7.75 Hz), 7.74 (s, 1H), 7.68 (d, 2H, J = 8.25 Hz), 7.56–7.54 (m, 6H), 7.02 (d, 2H, J = 9.0 Hz), 3.87 (s, 3H); $^{13}C\{^1H\}$ NMR ($CDCl_3$, 125 MHz): δ 162.4, 161.9, 158.8, 155.3, 138.3, 137.1, 130.2, 130.1, 129.9, 129.5, 129.2, 129.1, 128.8, 128.6, 118.0, 117.8, 114.5, 103.6, 55.6; IR (KBr, cm^{-1}): 2923, 2857, 2212, 1574, 1456, 1251, 1025, 878; HRMS (ESI/Q-TOF) (m/z) calcd for $C_{25}H_{19}N_2O$ $[M + H]^+$ 363.1492; found 363.1500.

6-(4-Chlorophenyl)-2,4-diphenylnicotinonitrile (3ia):

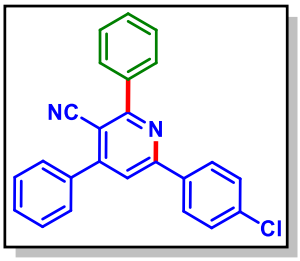

As a white solid (52 mg, 57% yield, mp 212–214 °C); Purification over a column of silica gel (2% EtOAc in hexane); ^{1}H NMR ($CDCl_3$, 500 MHz): δ 8.13 (d, 2H, J = 8.5 Hz), 8.03 (d, 2H, J = 7.5 Hz), 7.78 (s, 1H), 7.68 (d, 2H, J = 7.5 Hz), 7.57–7.55 (m, 6H), 7.48 (d, 2H, J = 9.0 Hz); ^{13}C{^{1}H} NMR ($CDCl_3$, 125 MHz): δ 162.6, 158.0, 155.8, 138.0, 137.0, 136.7, 136.1, 130.3, 130.2, 129.5, 129.4, 129.2, 129.0, 128.8, 128.7, 118.5, 117.7, 104.8; IR (KBr, cm^{-1}): 2924, 2860, 2218, 1652, 1575, 1485, 1260, 1172, 1092, 824; HRMS (ESI/QTOF) (m/z) calcd for $C_{24}H_{16}ClN_2$ $[M + H]^+$ 367.0997; found 367.0988.

6-(4-Fluorophenyl)-2-phenyl-4-(p-tolyl)nicotinonitrile (3ja):

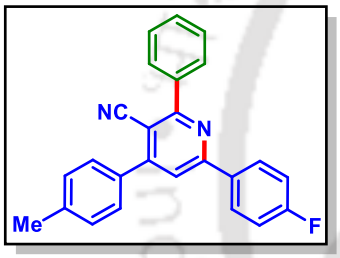

As a yellow solid (54 mg, 59% yield, mp 211–213 °C); Purification over a column of silica gel (2% EtOAc in hexane); ^{1}H NMR ($CDCl_3$, 500 MHz): δ 8.18 (d, 2H, J = 8.75 Hz), 8.02 (d, 2H, J = 7.0 Hz), 7.75 (s, 1H), 7.59−7.54 (m, 5H), 7.37 (d, 2H, J = 8.0 Hz), 7.19 (t, 2H, J = 8.5 Hz), 2.48 (s, 3H); ^{13}C{^{1}H} NMR ($CDCl_3$, 125 MHz): δ 164.5 (d, J = 249.75 Hz), 162.6, 158.1, 155.8, 140.4, 138.2, 134.04, 134.02, 130.6, 130.2, 129.9, 129.7 (d, J = 8.6 Hz), 129.5, 128.7 (d, J = 8.75 Hz), 118.3, 117.9, 116.1 (d, J = 21.75 Hz), 104.4, 21.5; ^{19}F NMR ($CDCl_3$, 471 MHz): δ –110.2 (s); IR (KBr, cm^{-1}): 2957, 2923, 2854, 2215, 1640, 1587, 1454, 1275, 1200, 1155, 819; HRMS (ESI/Q-TOF) (m/z) calcd for $C_{25}H_{18}FN_2$ $[M + H]^+$ 365.1449; found 365.1447.

4-(4-Chlorophenyl)-6-(4-methoxyphenyl)-2-phenylnicotinonitrile (3ka):

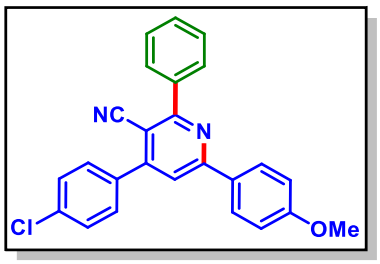

As a white solid (72 mg, 73% yield, mp 214–216 °C); Purification over a column of silica gel (4% EtOAc in hexane); ^{1}H NMR ($CDCl_3$, 500 MHz): δ 8.15 (d, 2H, J = 9.0 Hz), 8.02 (d, 2H, J = 7.25 Hz), 7.69 (s, 1H), 7.61 (d, 2H, J = 8.5 Hz), 7.55–7.52 (m, 5H), 7.02 (d, 2H, J = 9.0 Hz), 3.88 (s, 3H); ^{13}C{^{1}H} NMR ($CDCl_3$, 125 MHz): δ 162.5, 162.1, 159.0, 154.1, 138.2, 136.4, 135.5, 130.3, 130.2, 130.0, 129.5,

129.4, 129.3, 128.7, 117.9, 117.6, 114.6, 103.4, 55.6; IR (KBr, cm^{-1}): 2925, 2858, 2216, 1727, 1574, 1459, 1177, 1259, 1088, 820; HRMS (ESI/Q-TOF) (m/z) calcd for $C_{25}H_{18}ClN_2O$ $[M + H]^+$ 397.1102; found 397.1103.

4-(Benzo[d][1,3]dioxol-5-yl)-2,6-diphenylnicotinonitrile (3la):

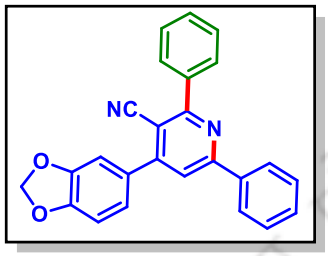

As a white solid (73 mg, 78% yield, mp 237–239 °C); Purification over a column of silica gel (2% EtOAc in hexane); ^1H NMR ($CDCl_3$, 500 MHz): δ 8.17 (d, 2H, J = 7.5 Hz), 8.03 (d, 2H, J = 7.5 Hz), 7.77 (s, 1H), 7.55–7.50 (m, 6H), 7.19–7.15 (m, 2H), 6.98 (d, 1H, J = 8.5 Hz), 6.07 (s, 2H); $^{13}C\{^1H\}$ NMR ($CDCl_3$, 125 MHz): δ 162.7, 159.3, 155.2, 149.4, 148.4, 138.2, 137.8, 130.8, 130.7, 130.2, 129.5, 129.1, 128.6, 127.7, 123.3, 118.6, 118.0, 109.2, 109.0, 104.4, 101.9; IR (KBr, cm^{-1}): 2930, 2853, 2218, 1650, 1595, 1480, 1256, 1106, 1039, 810; HRMS (ESI/Q-TOF) (m/z) calcd for $C_{25}H_{17}N_2O_2$ $[M + H]^+$ 377.1285; found 377.1294.

6-(5-Bromothiophen-2-yl)-2,4-diphenylnicotinonitrile (3ma):

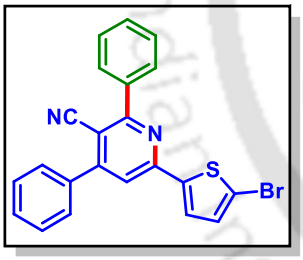

As a white solid (63 mg, 60% yield, mp 260–262 °C); Purification over a column of silica gel (2% EtOAc in hexane); ^1H NMR ($CDCl_3$, 400 MHz): δ 8.01–7.99 (m, 2H), 7.66–7.63 (m, 2H), 7.58 (s, 1H), 7.56–7.53 (m, 6H), 7.48 (d, 1H, J = 4.0 Hz), 7.12 (d, 1H, J = 4.0 Hz); $^{13}C\{^1H\}$ NMR ($CDCl_3$, 100 MHz): δ 162.6, 155.7, 153.5, 145.1, 137.4, 136.6, 131.6, 130.5, 130.2, 129.5, 129.2, 128.8, 128.7, 127.1, 118.6, 117.7, 116.3, 104.0; IR (KBr, cm^{-1}): 2955, 2923, 2850, 2218, 1643, 1571, 1432, 1275, 1260, 764; HRMS (ESI/Q-TOF) (m/z) calcd for $C_{22}H_{14}BrN_2S$ $[M + H]^+$ 417.0056; found 417.0046.

2-Phenyl-4,6-di(thiophen-2-yl)nicotinonitrile (3na):

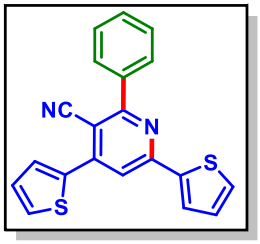

As a white solid (40 mg, 47% yield, mp 196–198 °C); Purification over a column of silica gel (2% EtOAc in hexane); ^1H NMR ($CDCl_3$, 500 MHz): δ 8.00–7.98 (m, 2H), 7.91 (d, 1H, J = 3.5 Hz), 7.79 (d, 1H, J = 3.5 Hz), 7.75 (s, 1H), 7.58–7.53 (m, 5H), 7.24 (t, 1H, J =

4.25 Hz), 7.17 (t, 1H, *J* = 4.25 Hz); $^{13}C\{^{1}H\}$ NMR ($CDCl_3$, 125 MHz): δ 163.4, 154.6, 147.1, 143.4, 137.8, 137.7, 130.6, 130.4, 129.9, 129.6, 129.3, 128.9, 128.7, 128.6, 127.4, 118.3, 116.0, 102.0; IR (KBr, cm^{-1}): 2921, 2852, 2216, 1640, 1590, 1494, 1288, 1111, 1069, 885; HRMS (ESI/Q-TOF) (m/z) calcd for $C_{20}H_{13}N_2S_2$ $[M + H]^+$ 345.0515; found 345.0525.

4,6-Diphenyl-2-(p-tolyl)nicotinonitrile (3ab):

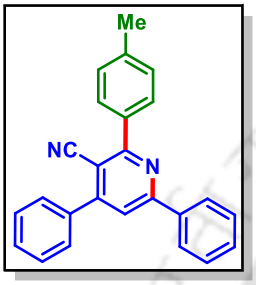

As a white solid (52 mg, 60% yield, mp 178–180 °C); Purification over a column of silica gel (2% EtOAc in hexane); ^{1}H NMR ($CDCl_3$, 500 MHz): δ 8.18 (d, 2H, *J* = 7.75 Hz), 7.96 (d, 2H, *J* = 8.5 Hz), 7.79 (s, 1H), 7.68 (d, 2H, *J* = 7.75 Hz), 7.57–7.49 (m, 6H), 7.36 (d, 2H, *J* = 8.0 Hz), 2.46 (s, 3H); $^{13}C\{^{1}H\}$ NMR ($CDCl_3$, 125 MHz): δ 162.6, 159.3, 155.6, 140.5, 137.9, 137.1, 135.5, 130.6, 130.0, 129.5, 129.4, 129.2, 129.1, 128.9, 127.7, 118.5, 118.0, 104.3, 21.6; IR (KBr, cm^{-1}): 2924, 2856, 2213, 1571, 1450, 1231, 1176, 1084, 874; HRMS (ESI/Q-TOF) (m/z) calcd for $C_{25}H_{19}N_2$ $[M + H]^+$ 347.1543; found 347.1548.

2-(4-Ethylphenyl)-4,6-diphenylnicotinonitrile (3ac):

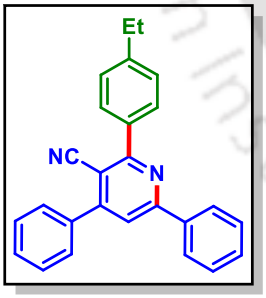

As a white solid (48 mg, 54% yield, mp 173–175 °C); Purification over a column of silica gel (2% EtOAc in hexane); ^{1}H NMR ($CDCl_3$, 500 MHz): δ 8.19 (d, 2H, *J* = 7.75 Hz), 8.00 (d, 2H, *J* = 8.0 Hz), 7.80 (s, 1H), 7.69 (d, 2H, *J* = 8.25 Hz), 7.58–7.50 (m, 6H), 7.39 (d, 2H, *J* = 8.0 Hz), 2.76 (q, 2H, *J* = 7.5 Hz), 1.32 (t, 3H, *J* = 7.5 Hz); $^{13}C\{^{1}H\}$ NMR ($CDCl_3$, 125 MHz): δ 162.5, 159.2, 155.6, 146.7, 137.8, 137.1, 135.6, 130.6, 130.0, 129.6, 129.2, 129.1, 128.8, 128.2, 127.7, 118.5, 118.0, 104.3, 29.0, 15.5; IR (KBr, cm^{-1}): 2925, 2864, 2214, 1570, 1450, 1262, 1184, 1075, 874; HRMS (ESI/Q-TOF) (m/z) calcd for $C_{26}H_{21}N_2$ $[M + H]^+$ 361.1699; found 361.1709.

2-(4-(tert-Butyl)phenyl)-4,6-diphenylnicotinonitrile (3ad):

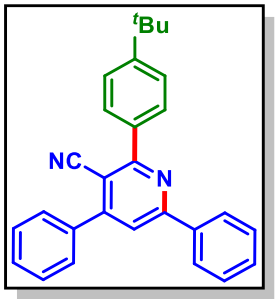

As a white solid (43 mg, 45% yield, mp 138–140 °C); Purification over a column of silica gel (2% EtOAc in hexane); ^{1}H NMR ($CDCl_3$, 500 MHz): δ 8.19 (d, 2H, J = 7.75 Hz), 8.02 (d, 2H, J = 8.5 Hz), 7.80 (s, 1H), 7.69 (d, 2H, J = 7.75 Hz), 7.59–7.56 (m, 5H), 7.52–7.49 (m, 3H), 1.40 (s, 9H); ^{13}C{^{1}H} NMR ($CDCl_3$, 125 MHz): δ 162.4, 159.2, 155.6, 153.5, 137.8, 137.1, 135.3, 130.6, 130.0, 129.3, 129.16, 129.13, 128.9, 127.7, 125.7, 118.5, 118.0, 104.2, 35.0, 31.4; IR (KBr, cm^{-1}): 2924, 2857, 2222, 1576, 1531, 1456, 1262, 1102, 1024, 804; HRMS (ESI/Q-TOF) (m/z) calcd for $C_{28}H_{25}N_2$ $[M + H]^+$ 389.2012 found 389.2033.

2-(4-Methoxyphenyl)-4,6-diphenylnicotinonitrile (3ae):

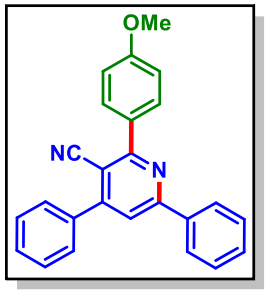

As a white solid (60 mg, 66% yield, mp 180–182 °C); Purification over a column of silica gel (3% EtOAc in hexane); ^{1}H NMR ($CDCl_3$, 500 MHz): δ 8.18 (d, 2H, J = 7.75 Hz), 8.07 (d, 2H, J = 9.0 Hz), 7.76 (s, 1H), 7.69 (d, 2H, J = 8.0 Hz), 7.56–7.49 (m, 6H), 7.08 (d, 2H, J = 8.5 Hz), 3.90 (s, 3H); ^{13}C{^{1}H} NMR ($CDCl_3$, 125 MHz): δ 162.0, 161.4, 159.1, 155.7, 137.8, 137.1, 131.1, 130.7, 130.6, 130.0, 129.1, 128.8, 127.7, 118.3, 118.2, 114.1, 103.8, 55.6; IR (KBr, cm^{-1}): 2924, 2862, 2216, 1664, 1581, 1455, 1253, 1175, 1017, 819; HRMS (ESI/Q-TOF) (m/z) calcd for $C_{25}H_{19}N_2O$ $[M + H]^+$ 363.1492; found 363.1490.

2-(4-Fluorophenyl)-4,6-diphenylnicotinonitrile (3af):

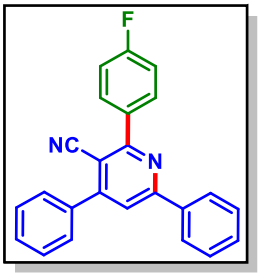

As a white solid (52 mg, 59% yield, mp 222–224 °C); Purification over a column of silica gel (2% EtOAc in hexane); ^{1}H NMR ($CDCl_3$, 500 MHz): δ 8.21–8.19 (m, 2H), 8.11–8.08 (m, 2H), 7.85 (s, 1H), 7.72–7.70 (m, 2H), 7.60–7.54 (m, 6H), 7.28 (d, 2H, J = 8.0 Hz); ^{13}C{^{1}H} NMR ($CDCl_3$, 125 MHz): δ 164.2 (d, J = 249.0 Hz), 161.4, 159.4, 155.7, 137.6, 136.9, 134.3 (d, J = 3.3 Hz), 131.7 (d, J = 8.6 Hz), 130.8, 130.2, 129.2, 128.8, 127.7, 118.8, 117.8, 115.9 (d, J =

21.6 Hz), 104.4; ^{19}F NMR ($CDCl_3$, 471 MHz): δ –110.6 (s); IR (KBr, cm^{-1}): 2923, 2856, 2216, 1662, 1594, 1480, 1260, 1153, 1078, 879; HRMS (ESI/Q-TOF) (m/z) calcd for $C_{24}H_{16}FN_2$ $[M + H]^+$ 351.1292; found 351.1299.

2-(4-Chlorophenyl)-4,6-diphenylnicotinonitrile (3ag):

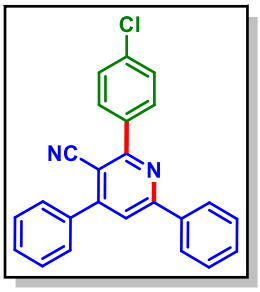

As a white solid (51 mg, 56% yield, mp 220–222 °C); Purification over a column of silica gel (2% EtOAc in hexane); ^{1}H NMR ($CDCl_3$, 500 MHz): δ 8.18–8.16 (m, 2H), 8.00 (d, 2H, J = 8.4 Hz), 7.83 (s, 1H), 7.69–7.66 (m, 2H), 7.58–7.51 (m, 8H); ^{13}C{^{1}H} NMR ($CDCl_3$, 125 MHz): δ 161.3, 159.4, 155.7, 137.5, 136.8, 136.6, 136.5, 135.4, 130.9, 130.8, 130.2, 129.2, 129.0, 128.8, 127.7, 119.0, 117.7, 104.4; IR (KBr, cm^{-1}): 2923, 2856, 2216, 1578, 1529, 1454, 1264, 1092, 1028, 804; HRMS (ESI/Q-TOF) (m/z) calcd for $C_{24}H_{16}ClN_2$ $[M + H]^+$ 367.0997; found 367.0995.

2-(4-Bromophenyl)-4,6-diphenylnicotinonitrile (3ah):

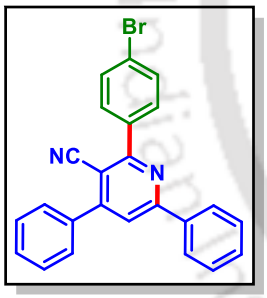

As a white solid (54 mg, 53% yield, mp 244–246 °C); Purification over a column of silica gel (2% EtOAc in hexane); ^{1}H NMR ($CDCl_3$, 500 MHz): δ 8.17–8.15 (m, 2H), 7.93 (d, 2H, J = 8.5 Hz), 7.83 (s, 1H), 7.70–7.67 (m, 4H), 7.57–7.51 (m, 6H); ^{13}C{^{1}H} NMR ($CDCl_3$, 125 MHz): δ 161.4, 159.5, 155.7, 137.5, 137.0, 136.8, 131.9, 131.1, 130.8, 130.2, 129.2, 128.8, 127.8, 125.0, 119.0, 117.7, 104.4; IR (KBr, cm^{-1}): 2923, 2855, 2214, 1732, 1571, 1485, 1266, 1174, 1073, 825; HRMS (ESI/Q-TOF) (m/z) calcd for $C_{24}H_{16}BrN_2$ $[M + H]^+$ 411.0491; found 411.0493.

2-(4-Methoxy-3-methylphenyl)-4,6-diphenylnicotinonitrile (3ai):

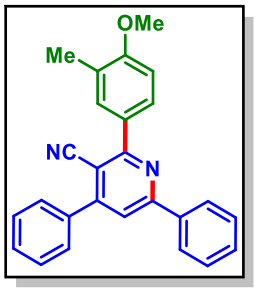

As a white solid (59 mg, 63% yield, mp 168–170 °C); Purification over a column of silica gel (3% EtOAc in hexane); ^{1}H NMR ($CDCl_3$, 500 MHz): δ 8.18 (d, 2H, J = 7.75 Hz), 7.93 (d, 1H, J = 8.4 Hz), 7.88 (s, 1H), 7.75 (s, 1H), 7.68 (d, 2H, J = 7.75 Hz), 7.58–7.49 (m, 6H), 6.98 (d, 1H, J = 8.5 Hz), 3.92 (s, 3H), 2.35 (s, 3H); ^{13}C{^{1}H} NMR

($CDCl_3$, 125 MHz): δ 162.3, 159.7, 159.1, 155.6, 137.9, 137.2, 131.9, 130.5, 130.2, 129.9, 129.1, 128.8, 128.5, 127.7, 127.1, 118.3, 118.1, 109.8, 103.9, 55.6, 16.5; IR (KBr, cm^{-1}): 2924, 2858, 2214, 1574, 1496, 1246, 1172, 1131, 1027, 879; HRMS (ESI/Q-TOF) (m/z) calcd for $C_{26}H_{21}N_2O$ $[M + H]^+$ 377.1648; found 377.1652.

2-(Benzo[d][1,3]dioxol-5-yl)-4,6-diphenylnicotinonitrile (3aj):

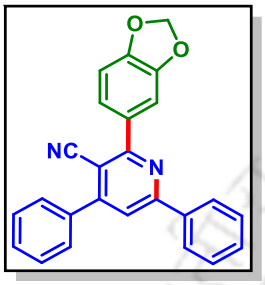

As a white solid (49 mg, 52% yield, mp 214–216 °C); Purification over a column of silica gel (2% EtOAc in hexane); ^1H NMR ($CDCl_3$, 500 MHz): δ 8.17–8.15 (m, 2H), 7.78 (s, 1H), 7.68–7.66 (m, 2H), 7.61 (d, 1H, J = 8.25 Hz), 7.56–7.50 (m, 7H), 6.97 (d, 1H, J = 8.0 Hz), 6.06 (s, 2H); $^{13}C\{^1H\}$ NMR ($CDCl_3$, 125 MHz): δ 161.8, 159.2, 155.8, 149.5, 148.1, 137.7, 137.0, 132.2, 130.7, 130.1, 129.1, 128.8, 127.7, 124.2, 118.5, 118.0, 110.0, 108.4, 104.0, 101.7; IR (KBr, cm^{-1}): 2926, 2854, 2218, 1572, 1496, 1248, 1173, 1026, 879; HRMS (ESI/Q-TOF) (m/z) calcd for $C_{25}H_{17}N_2O_2$ $[M + H]^+$ 377.1285; found 377.1288.

(4-(3-Cyano-4,6-diphenylpyridin-2-yl)phenyl)boronic acid (3ak):

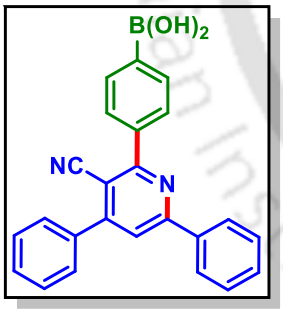

As a white solid (59 mg, 63% yield, mp 238–240 °C); Purification over a column of silica gel (25% EtOAc in hexane); ^1H NMR (DMSO-d_6, 500 MHz): δ 8.33–8.30 (m, 2H), 8.25 (d, 1H, J = 2.0 Hz), 8.17 (s, 1H), 7.98 (q, 4H, J_1 = 15.5, J_2 = 8.0 Hz), 7.85–7.83 (m, 2H), 7.62–7.54 (m, 5H); $^{13}C\{^1H\}$ NMR (DMSO-d_6, 125 MHz): δ 161.6, 158.3, 154.8, 139.2, 136.9, 136.3, 134.1, 134.0, 130.6, 129.9, 129.0, 128.9, 128.7, 128.2, 127.6, 118.8, 117.6, 104.2; ^{11}B NMR (DMSO-d_6, 213 MHz): δ –6.04 (s); IR (KBr, cm^{-1}): 3392, 2960, 2924, 2855, 2219, 1574, 1533, 1366, 1275, 1021, 846, 749; HRMS (ESI/Q-TOF) (m/z) calcd for $C_{24}H_{17}BN_2O_2K$ $[M + K]^+$ 415.1015; found 415.1023.

2-(Naphthalen-2-yl)-4,6-diphenylnicotinonitrile (3al):[10]

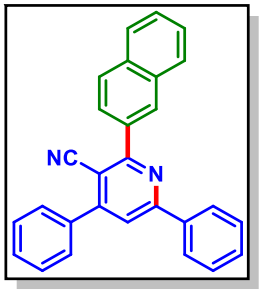

As a white solid (67 mg, 70% yield, mp 205–207 °C); Purification over a column of silica gel (2% EtOAc in hexane); ^{1}H NMR ($CDCl_3$, 500 MHz): δ 8.57 (s, 1H), 8.23–8.21 (m, 2H), 8.17–8.15 (m, 1H), 8.03–8.00 (m, 2H), 7.94–7.92 (m, 1H), 7.85 (s, 1H), 7.73–7.71 (m, 2H), 7.59–7.51 (m, 8H); ^{13}C{^{1}H} NMR ($CDCl_3$, 125 MHz): δ 162.5, 159.4, 155.7, 137.7, 137.0, 135.5, 134.2, 133.1, 130.7, 130.1, 129.7, 129.2, 129.1, 128.9, 128.5, 127.9, 127.8, 127.4, 126.7, 126.6, 118.8, 117.9, 104.8; IR (KBr, cm^{-1}): 2924, 2851, 2216, 1657, 1572, 1468, 1264, 1226, 1153, 1092, 873; HRMS (ESI/Q-TOF) (m/z) calcd for $C_{28}H_{19}N_2$ $[M + H]^+$ 383.1543; found 383.1545.

4,6-Diphenyl-2-(pyren-1-yl)nicotinonitrile (3am):

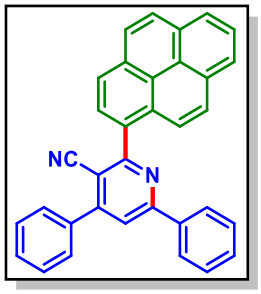

As a white solid (73 mg, 64% yield, mp 237–239 °C); Purification over a column of silica gel (2% EtOAc in hexane); δ ^{1}H NMR ($CDCl_3$, 400 MHz): δ 8.32 (q, 2H, J_1 = 18.8 and J_2 = 8.0 Hz), 8.26–8.19 (m, 5H), 8.17–8.15 (m, 3H), 8.05 (t, 1H, J = 7.6 Hz), 8.00 (s, 1H), 7.81–7.79 (m, 2H), 7.63–7.56 (m, 3H), 7.53–7.50 (m, 3H); ^{13}C{^{1}H} NMR ($CDCl_3$, 100 MHz): δ 163.9, 159.3, 155.0, 137.7, 136.7, 132.9, 132.5, 131.5, 131.0, 130.7, 130.2, 129.4, 129.3, 129.2, 128.9, 128.6, 127.8, 127.7, 127.5, 126.3, 125.9, 125.7, 125.2, 124.9, 124.8, 124.6, 118.9, 117.3, 107.7; IR (KBr, cm^{-1}): 3040, 2928, 2860, 2220, 1572, 1493, 1381, 1243, 1179, 1077, 885, 761; HRMS (ESI/Q-TOF) (m/z) calcd for $C_{34}H_{21}N_2$ $[M + H]^+$ 457.1699; found 457.1704.

(Z)-2-Phenyl-4-styrylquinoline-3-carbonitrile (4aa):

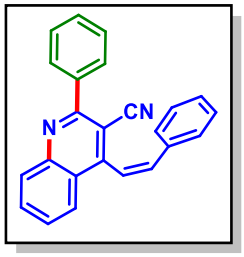

As a white solid (59 mg, 71% yield, *Z*/*E* 97:3, mp 144–146 °C); Purification over a column of silica gel (2% EtOAc in hexane); ^{1}H NMR ($CDCl_3$, 500 MHz): δ ^{1}H NMR ($CDCl_3$, 500 MHz): δ 8.23 (d, 1H, J = 8.5 Hz), 8.07 (d, 1H, J = 8.25 Hz), 7.92 (d, 2H, J = 7.25 Hz), 7.86 (t, 1H, J = 7.75 Hz), 7.58–7.54 (m, 4H), 7.28 (s, 1H), 7.20–7.12 (m, 3H), 7.02–6.98 (m, 3H); ^{13}C{^{1}H} NMR ($CDCl_3$, 125 MHz): δ

158.8, 153.4, 148.5, 138.2, 138.0, 135.4, 132.9, 130.5, 130.1, 129.4, 129.0, 128.8, 128.7, 128.6, 128.1, 126.2, 123.8, 122.3, 117.2, 105.3; IR (KBr, cm^{-1}): 3060, 2923, 2849, 2222, 1612, 1547, 1488, 1347, 1275, 1261, 1090, 765; HRMS (ESI/Q-TOF) (m/z) calcd for $C_{24}H_{17}N_2$ $[M + H]^+$ 333.1386; found 333.1390.

(Z)-7-Methyl-2-phenyl-4-styrylquinoline-3-carbonitrile (4ba):

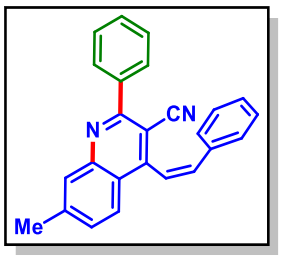

As a white solid (60 mg, 69% yield, *Z*/*E* 91:9, mp 119–121 °C); Purification over a column of silica gel (2% EtOAc in hexane); ^1H NMR ($CDCl_3$, 400 MHz): δ 7.98 (s, 1H), 7.92 (d, 1H, *J* = 8.8 Hz), 7.89–7.87 (m, 2H), 7.52–7.49 (m, 3H), 7.36 (d, 1H, *J* = 8.6 Hz), 7.21 (d, 1H, *J* = 12.4 Hz), 7.16–7.09 (m, 3H), 6.99–6.93 (m, 3H), 2.57 (s, 3H); $^{13}C\{^1H\}$ NMR ($CDCl_3$, 100 MHz): δ 158.7, 152.8, 148.6, 143.7, 138.1, 137.5, 135.3, 130.2, 129.8, 129.3, 129.1, 128.8, 128.5, 128.48, 128.45, 125.6, 122.3, 121.6, 117.3, 104.1, 22.0; IR (KBr, cm^{-1}): 3060, 2921, 2856, 2222, 1612, 1546, 1488, 1348, 1260, 1181, 1026, 770; HRMS (ESI/Q-TOF) (m/z) calcd for $C_{25}H_{19}N_2$ $[M + H]^+$ 347.1543; found 347.1550.

(Z)-7-Chloro-2-phenyl-4-styrylquinoline-3-carbonitrile (4ea):

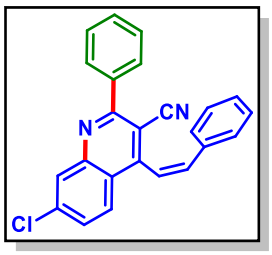

As a white solid (57 mg, 62% yield, *Z*/*E* 89:11, mp 124–126 °C); Purification over a column of silica gel (2% EtOAc in hexane); ^1H NMR ($CDCl_3$, 500 MHz): δ 8.19 (s, 1H), 7.95 (d, 1H, *J* = 9.0 Hz), 7.91–7.89 (m, 2H), 7.53–7.52 (m, 3H), 7.45 (d, 1H, *J* = 8.75 Hz), 7.25 (d, 1H, *J* = 12.5 Hz), 7.19–7.16 (m, 1H), 7.12 (t, 2H, *J* = 7.5 Hz), 6.97–6.92 (m, 3H); $^{13}C\{^1H\}$ NMR ($CDCl_3$, 125 MHz): δ 159.9, 153.4, 149.0, 139.1, 138.4, 137.8, 135.2, 130.4, 129.5, 129.4, 129.1, 129.0, 128.9, 128.85, 128.80, 127.6, 122.1, 121.9, 117.0, 105.5; IR (KBr, cm^{-1}): 3071, 2930, 2849, 2222, 1632, 1547, 1489, 1348, 1260, 1090, 835; HRMS (ESI/Q-TOF) (m/z) calcd for $C_{24}H_{16}ClN_2$ $[M + H]^+$ 367.0997; found 367.1001.

(Z)-4-(4-Methylstyryl)-2-phenylquinoline-3-carbonitrile (4ga):

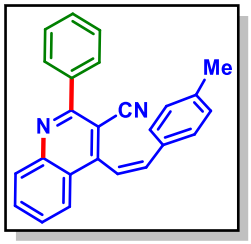

As a white solid (56 mg, 65% yield, *Z*/*E* 93:7, mp 162–164 °C); Purification over a column of silica gel (2% EtOAc in hexane); ^{1}H NMR ($CDCl_3$, 400 MHz): δ 8.20 (d, 1H, *J* = 8.4 Hz), 8.05 (d, 1H, *J* = 8.4 Hz), 7.91–7.89 (m, 2H), 7.83 (t, 1H, *J* = 7.8 Hz), 7.56–7.50 (m, 4H), 7.19 (d, 1H, *J* = 12.4 Hz), 6.92–6.85 (m, 5H), 2.23 (s, 3H); ^{13}C{^{1}H} NMR ($CDCl_3$, 100 MHz): δ 158.8, 153.7, 148.5, 138.7, 138.2, 137.8, 132.9, 132.6, 130.5, 130.1, 129.43, 129. 41, 128.9, 128.7, 128.1, 126.3, 123.8, 121.3, 117.3, 105.2, 21.4; IR (KBr, cm^{-1}): 3065, 2921, 2857, 2222, 1611, 1546, 1488, 1347, 1183, 1028, 827; HRMS (ESI/Q-TOF) (m/z) calcd for $C_{25}H_{19}N_2$ $[M + H]^+$ 347.1543; found 347.1547.

(Z)-4-(4-Chlorostyryl)-2-phenylquinoline-3-carbonitrile (4ia):

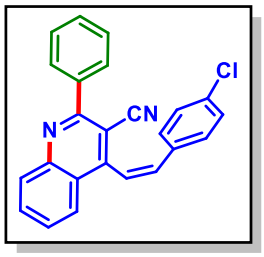

As a white solid (54 mg, 59% yield, *Z*/*E* 99:1, mp 191–193 °C); Purification over a column of silica gel (2% EtOAc in hexane); ^{1}H NMR ($CDCl_3$, 500 MHz): δ 8.21 (d, 1H, *J* = 8.5 Hz), 8.01 (d, 1H, *J* = 8.5 Hz), 7.90 (d, 2H, *J* = 7.75 Hz), 7.85 (t, 1H, *J* = 7.75 Hz), 7.58–7.51 (m, 4H), 7.18 (d, 1H, *J* = 12.5 Hz), 7.09 (d, 2H, *J* = 8.5 Hz), 6.99 (d, 1H, *J* = 12.5 Hz), 6.91 (d, 2H, *J* = 8.5 Hz); ^{13}C{^{1}H} NMR ($CDCl_3$, 125 MHz): δ 158.8, 152.8, 148.6, 138.0, 136.6, 134.6, 133.9, 133.0, 130.6, 130.3, 130.2, 129.4, 128.9, 128.8, 128.3, 125.9, 123.6, 123.0, 117.2, 105.2; IR (KBr, cm^{-1}): 3071, 2931, 2224, 1633, 1548, 1489, 1396, 1275, 1090, 835, 767; HRMS (ESI/Q-TOF) (m/z) calcd for $C_{24}H_{16}ClN_2$ $[M + H]^+$ 367.0997; found 367.0994.

(Z)-4-(2-(Furan-2-yl)vinyl)-7-methyl-2-phenylquinoline-3-carbonitrile (4oa):

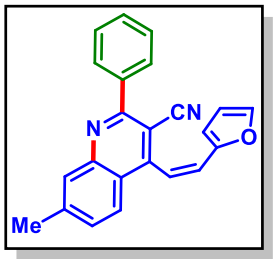

As a white solid (45 mg, 54% yield, *Z*/*E* 99:1, mp 119–121 °C); Purification over a column of silica gel (2% EtOAc in hexane); ^{1}H NMR ($CDCl_3$, 400 MHz): δ 8.83 (d, 1H, *J* = 4.8 Hz), 7.92–7.90 (m, 2H), 7.55–7.52 (m, 6H), 7.39–7.34 (m, 4H), 2.44 (s, 3H); ^{13}C{^{1}H} NMR ($CDCl_3$, 100 MHz): δ 163.0, 154.9, 152.0, 140.5, 137.9, 133.5,

130.2, 129.9, 129.4, 128.78, 128.75, 122.3, 117.5, 106.5, 21.5; IR (KBr, cm^{-1}): 2928, 2851, 2215, 1635, 1510, 1460, 1262, 1026, 832; HRMS (ESI/Q-TOF) (m/z) calcd for $C_{23}H_{17}N_2O$ $[M + H]^+$ 337.1335; found 337.1338.

(Z)-4-Styryl-2-(p-tolyl)quinoline-3-carbonitrile (4ab):

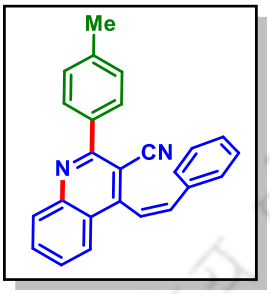

As a white solid (57 mg, 66% yield, *Z*/*E* 90:10 mp 144–146 °C); Purification over a column of silica gel (2% EtOAc in hexane); ^1H NMR ($CDCl_3$, 500 MHz): δ 8.18 (d, 1H, *J* = 8.5 Hz), 8.03 (d, 1H, *J* = 8.5 Hz), 7.83–7.79 (m, 3H), 7.52 (t, 1H, *J* = 7.5 Hz), 7.32 (d, 2H, *J* = 7.5 Hz), 7.23 (d, 1H, *J* = 12.5 Hz), 7.17–7.09 (m, 3H), 6.99–6.94 (m, 3H), 2.43 (s, 3H); $^{13}C\{^1H\}$ NMR ($CDCl_3$, 125 MHz): δ 158.8, 153.3, 148.6, 140.3, 137.9, 135.5, 135.4, 132.8, 130.5, 129.5, 129.3, 129.0, 128.68, 128.67, 127.9, 126.2, 123.7, 122.4, 117.4, 105.2, 21.6; IR (KBr, cm^{-1}): 3058, 2923, 2852, 2223, 1616, 1551, 1488, 1449, 1347, 1275, 1072, 826, 764; HRMS (ESI/Q-TOF) (m/z) calcd for $C_{25}H_{19}N_2$ $[M + H]^+$ 347.1543; found 347.1550.

(Z)-4-Styryl-2-(o-tolyl)quinoline-3-carbonitrile (4an):

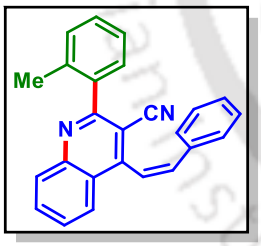

As a white solid (49 mg, 57% yield, *Z*/*E* 88:12, mp 128–132 °C); Purification over a column of silica gel (2% EtOAc in hexane); ^1H NMR ($CDCl_3$, 500 MHz): δ 8.21 (d, 1H, *J* = 8.5 Hz), 8.12 (d, 1H, *J* = 8.0 Hz), 7.87 (t, 1H, *J* = 7.75 Hz), 7.62 (t, 1H, *J* = 7.6 Hz), 7.38–7.33 (m, 2H), 7.29 (t, 2H, *J* = 7.75 Hz), 7.25 (d, 1H, *J* = 12.5 Hz), 7.18–7.10 (m, 3H), 7.00–6.97 (m, 3H), 2.12 (s, 3H); $^{13}C\{^1H\}$ NMR ($CDCl_3$, 125 MHz): δ 160.6, 152.2, 148.2, 138.2, 136.1, 135.5, 132.8, 130.8, 130.5, 129.6, 129.1, 129.0, 128.7, 128.6, 128.2, 126.1, 126.0, 124.2, 122.3, 116.4, 107.3, 19.7; IR (KBr, cm^{-1}): 3059, 2924, 2852, 2224, 1612, 1551, 1488, 1345, 1276, 1076, 827, 762; HRMS (ESI/Q-TOF) (m/z) calcd for $C_{25}H_{19}N_2$ $[M + H]^+$ 347.1543; found 347.1552.

(Z)-2-(4-Ethylphenyl)-4-styrylquinoline-3-carbonitrile (4ac):

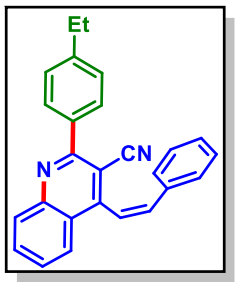

As a white solid (56 mg, 63% yield, *Z*/*E* 91:9, mp 144–146 °C); Purification over a column of silica gel (2% EtOAc in hexane); ^{1}H NMR ($CDCl_3$, 400 MHz): δ 8.18 (d, 1H, *J* = 8.4 Hz), 8.03 (d, 1H, *J* = 8.4 Hz), 7.84–7.80 (m, 3H), 7.52 (t, 1H, *J* = 7.7 Hz), 7.35 (d, 2H, *J* = 8.4 Hz), 7.23 (d, 1H, *J* = 12.4 Hz), 7.18–7.09 (m, 3H), 6.99–6.95 (m, 3H), 2.72 (q, 2H, J_1 = 15.2, J_2 = 7.6 Hz), 1.27 (t, 3H, *J* = 7.8 Hz); ^{13}C{^{1}H} NMR ($CDCl_3$, 125 MHz): δ 158.8, 153.3, 148.6, 146.6, 137.9, 135.6, 135.4, 132.8, 130.5, 129.4, 129.0, 128.6, 128.3, 127.9, 126.1, 123.7, 122.4, 117.4, 105.2, 29.0, 15.6; IR (KBr, cm^{-1}): 2967, 2931, 2221, 1637, 1544, 1488, 1275, 1261, 840, 764; HRMS (ESI/Q-TOF) (m/z) calcd for $C_{26}H_{21}N_2$ $[M + H]^+$ 361.1699; found 361.1705.

(Z)-2-(4-(tert-Butyl)phenyl)-4-styrylquinoline-3-carbonitrile (4ad):

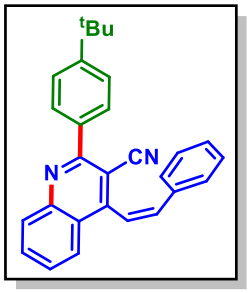

As a white solid (53 mg, 54% yield, *Z*/*E* 93:7, mp 150–152 °C); Purification over a column of silica gel (2% EtOAc in hexane); ^{1}H NMR ($CDCl_3$, 500 MHz): δ 8.18 (d, 1H, *J* = 8.5 Hz), 8.04 (d, 1H, *J* = 8.0 Hz), 7.86–7.80 (m, 3H), 7.55–7.51 (m, 3H), 7.24 (d, 1H, *J* = 12.5 Hz), 7.17–7.09 (m, 3H), 6.99–6.96 (m, 3H), 1.36 (s, 9H); ^{13}C{^{1}H} NMR ($CDCl_3$, 125 MHz): δ 158.8, 153.4, 153.3, 148.6, 137.9, 135.5, 135.3, 132.8, 130.5, 129.1, 129.0, 128.6, 127.9, 126.1, 125.8, 123.7, 122.5, 117.4, 105.2, 35.0, 31.4; IR (KBr, cm^{-1}): 3065, 2962, 2865, 2222, 1611, 1542, 1488, 1361, 1108, 838, 765; HRMS (ESI/Q-TOF) (m/z) calcd for $C_{28}H_{25}N_2$ $[M + H]^+$ 389.2012; found 389.2010.

(Z)-2-(4-Chlorophenyl)-4-styrylquinoline-3-carbonitrile (4ag):

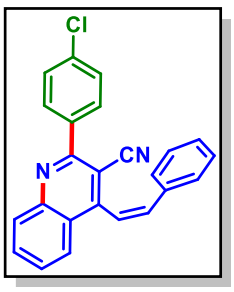

As a yellow solid (58 mg, 64% yield, *Z*/*E* 89:11, mp 156–158 °C); Purification over a column of silica gel (2% EtOAc in hexane); ^{1}H NMR ($CDCl_3$, 500 MHz): δ 8.18 (d, 1H, *J* = 8.5 Hz), 8.04 (d, 1H, *J* = 8.0 Hz), 7.85–7.83 (m, 3H), 7.55 (t, 1H, *J* = 7.5 Hz), 7.49 (d, 2H, *J* = 8.0 Hz), 7.24 (d, 1H, *J* = 10 Hz), 7.18–7.09 (m, 3H), 6.98–6.94

(m, 3H); ^{13}C NMR ($CDCl_3$, 125 MHz): δ 157.5, 153.5, 148.5, 138.2, 136.6, 136.5, 135.4, 133.1, 130.8, 130.5, 129.1, 129.0, 128.8, 128.7, 128.3, 126.2, 123.9, 122.2, 117.1, 105.0; IR (KBr, cm^{-1}): 2960, 2920, 2847, 2219, 1634, 1544, 1489, 1275, 1260, 1092, 830, 764; HRMS (ESI/Q-TOF) (m/z) calcd for $C_{24}H_{16}ClN_2$ $[M + H]^+$ 367.0997; found 367.1003.

(Z)-2-(3-Chlorophenyl)-4-styrylquinoline-3-carbonitrile (4ao):

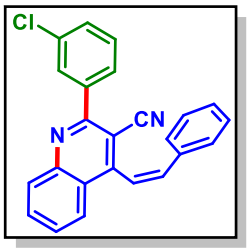

As a white solid (48 mg, 52% yield, *Z*/*E* 86:14, mp 121–123 °C); Purification over a column of silica gel (2% EtOAc in hexane); ^{1}H NMR ($CDCl_3$, 400 MHz): δ 8.20 (d, 1H, *J* = 8.4 Hz), 8.05 (d, 1H, *J* = 8.4 Hz), 7.91 (s, 1H), 7.85 (t, 1H, *J* = 7.7 Hz), 7.75 (d, 1H, *J* = 7.4 Hz), 7.56 (t, 1H, *J* = 7.8 Hz), 7.50–7.42 (m, 2H), 7.25 (d, 1H, *J* = 12.4 Hz), 7.17–7.10 (m, 3H), 6.98–6.94 (m, 3H); ^{13}C{^{1}H} NMR ($CDCl_3$, 100 MHz): δ 157.2, 153.6, 148.4, 139.7, 138.2, 135.3, 134.9, 133.1, 130.5, 130.2, 129.9, 129.5, 128.9, 128.8, 128.7, 128.4, 127.5, 126.2, 123.9, 122.1, 116.9, 105.0; IR (KBr, cm^{-1}): 2956, 2924, 2847, 2218, 1636, 1542, 1480, 1278, 1261, 1091, 832, 765; HRMS (ESI/Q-TOF) (m/z) calcd for $C_{24}H_{16}ClN_2$ $[M + H]^+$ 367.0997; found 367.0993.

(Z)-2-(4-Bromophenyl)-4-styrylquinoline-3-carbonitrile (4ah):

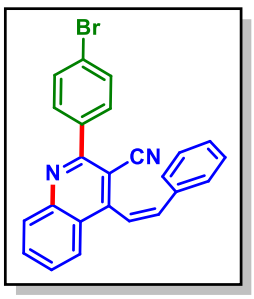

As a white solid (58 mg, 56% yield, *Z*/*E* 93:7, mp 153–155 °C); Purification over a column of silica gel (2% EtOAc in hexane); ^{1}H NMR ($CDCl_3$, 500 MHz): δ 8.18 (d, 1H, *J* = 8.5 Hz), 8.04 (d, 1H, *J* = 8.5 Hz), 7.84 (t, 1H, *J* = 7.5 Hz), 7.77 (d, 2H, *J* = 7.5 Hz), 7.65 (d, 2H, *J* = 7.0 Hz), 7.55 (t, 1H, *J* = 7.75 Hz), 7.24 (d, 1H, *J* = 11.5 Hz), 7.17–7.09 (m, 3H), 6.97–6.94 (m, 3H); ^{13}C{^{1}H} NMR ($CDCl_3$, 125 MHz): δ 157.5, 153.5, 148.5, 138.2, 137.0,135.4, 133.1, 132.0, 131.0, 130.5, 129.0, 128.8, 128.7, 128.3, 126.2, 124.9, 123.9, 122.2, 117.1, 105.0; IR (KBr, cm^{-1}): 3007, 2956, 2848, 2220, 1634, 1541,

1488, 1260, 1092, 830, 764; HRMS (ESI/Q-TOF) (m/z) calcd for $C_{24}H_{16}BrN_2$ $[M + H]^+$ 411.0491; found 411.0499.

(Z)-2-(4-Trifluoromethylphenyl)-4-styrylquinoline-3-carbonitrile (4ap):

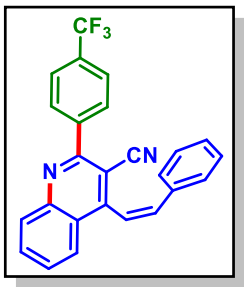

As a white solid (53 mg, 53% yield, *Z*/*E* 92:8, mp 139–141 °C); Purification over a column of silica gel (2% EtOAc in hexane); ^{1}H NMR ($CDCl_3$, 500 MHz): δ 8.18 (d, 1H, *J* = 8.5 Hz), 8.05 (d, 1H, *J* = 8.5 Hz), 7.98 (d, 2H, *J* = 8.0 Hz), 7.84 (t, 1H, *J* = 7.75 Hz), 7.75 (d, 2H, *J* = 8.0 Hz), 7.56 (t, 1H, *J* = 7.75 Hz), 7.23 (s, 1H), 7.16–7.08 (m, 3H), 6.96–6.94 (m, 3H); ^{13}C{^{1}H} NMR ($CDCl_3$, 125 MHz): δ 157.3, 153.6, 148.5, 141.5, 138.4, 135.4, 133.2,130.6, 129.8, 129.0, 128.8, 128.7, 128.6, 126.2, 125.7 (q, *J* = 3.8 Hz), 124.1, 122.1, 116.9, 105.1; ^{19}F NMR ($CDCl_3$, 471 MHz): δ –62.8 (s); IR (KBr, cm^{-1}): 2960, 2921, 2855, 2223, 1633, 1546, 1489, 1323, 1275, 1260, 1126, 1071, 852, 765; HRMS (ESI/Q-TOF) (m/z) calcd for $C_{25}H_{16}F_3N_2$ $[M + H]^+$ 401.1260; found 401.1259.

(Z)-2-(3-Fluoro-4-methoxyphenyl)-4-styrylquinoline-3-carbonitrile (4aq):

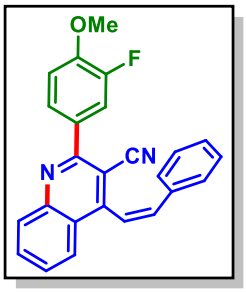

As a white solid (60 mg, 63% yield, *Z*/*E* 86:14, mp 208–210 °C); Purification over a column of silica gel (3% EtOAc in hexane); ^{1}H NMR ($CDCl_3$, 500 MHz): δ 8.26 (d, 1H, *J* = 8.5 Hz), 8.18 (d, 1H, *J* = 8.5 Hz), 7.87 (t, 1H, *J* = 7.75 Hz), 7.80–7.77 (m, 2H), 7.68–7.64 (m, 4H), 7.47–7.38 (m, 4H), 7.13 (t, 1H, *J* = 8.75 Hz), 3.98 (s, 3H); ^{13}C{^{1}H} NMR ($CDCl_3$, 125 MHz): δ 157.2 (d, J = 2.0 Hz), 153.4, 152.2, 151.5, 149.5 (d, *J* = 10.5 Hz),148.7, 141.9, 135.8, 132.8, 131.3 (d, *J* = 6.5 Hz), 130.6, 129.9, 129.2, 128.0, 127.6, 125.8 (d, *J* = 3.6 Hz), 125.6, 124.0, 121.1, 117.9, 117.5 (d, *J* = 19.7 Hz), 113.2 (d, J = 2.1 Hz), 103.3, 56.5; ^{19}F NMR ($CDCl_3$, 471 MHz): δ –134.4; IR (KBr, cm^{-1}): 3023, 2935, 2839, 2218, 1632, 1519, 1437, 1353, 1274, 1204, 1118, 1028, 972, 874, 763; HRMS (ESI/Q-TOF) (m/z) calcd for $C_{25}H_{18}FN_2O$ $[M + H]^+$ 381.1398; found 381.1403.

(Z)-4-(4-Chlorostyryl)-2-(o-tolyl)quinoline-3-carbonitrile (4in):

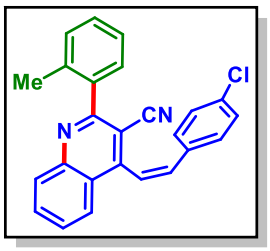

As a white solid (59 mg, 62% yield, *Z*/*E* 94:6, mp 175–178 °C); Purification over a column of silica gel (2% EtOAc in hexane); ^{1}H NMR ($CDCl_3$, 500 MHz): δ 8.21 (d, 1H, *J* = 8.5 Hz), 8.09 (d, 1H, *J* = 8.0 Hz), 7.89 (t, 1H, *J* = 7.5 Hz), 7.64 (t, 1H, *J* = 7.5 Hz), 7.39–7.29 (m, 4H), 7.19 (d, 1H, *J* = 12.0 Hz), 7.10 (d, 2H, *J* = 8.0 Hz), 7.01 (d, 1H, *J* = 12.5 Hz), 6.91 (d, 2H, *J* = 8.5 Hz), 2.12 (s, 3H); ^{13}C{^{1}H} NMR ($CDCl_3$, 125 MHz): δ 160.6, 151.6, 148.2, 138.1, 136.9, 136.1, 134.5, 133.9, 133.0, 130.8, 130.6, 130.2, 129.7, 129.1, 128.9, 128.4, 126.2, 125.8, 124.0, 123.0, 116.4, 107.2, 19.6; IR (KBr, cm^{-1}): 3063, 2959, 2924, 2224, 1611, 1552, 1488, 1396, 1261, 1090, 815, 766; HRMS (ESI/Q-TOF) (m/z) calcd for $C_{25}H_{18}ClN_2$ $[M + H]^+$ 381.1153; found 381.1159.

(Z)-2-(4-Bromophenyl)-4-(4-chlorostyryl)quinoline-3-carbonitrile (4ih):

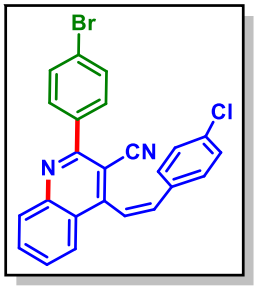

As a white solid (60 mg, 54% yield, *Z*/*E* 87:13, mp 227–229 °C); Purification over a column of silica gel (2% EtOAc in hexane); ^{1}H NMR ($CDCl_3$, 500 MHz): δ 8.19 (d, 1H, *J* = 8.5 Hz), 8.01 (d, 1H, *J* = 8.0 Hz), 7.86 (t, 1H, *J* = 7.25 Hz), 7.79 (d, 2H, *J* = 7.5 Hz), 7.66 (d, 2H, *J* = 8.0 Hz), 7.58 (t, 1H, *J* = 7.5 Hz), 7.19 (d, 1H, *J* = 12.0 Hz), 7.09 (d, 2H, *J* = 7.5 Hz), 6.98 (d, 1H, *J* = 12.5 Hz), 6.90 (d, 2H, *J* = 7.5 Hz); ^{13}C{^{1}H} NMR ($CDCl_3$, 125 MHz): δ 157.5, 153.0, 148.5, 136.9, 136.8, 134.6, 133.8, 133.2, 132.0, 131.0, 130.6, 130.1, 129.0, 128.5, 126.0, 125.0, 123.7, 122.8, 117.0, 104.8; IR (KBr, cm^{-1}): 3007, 2928, 2852, 2221, 1632, 1542, 1489, 1275, 1091, 1011, 832, 750; HRMS (ESI/Q-TOF) (m/z) calcd for $C_{24}H_{15}BrClN_2$ $[M + H]^+$ 445.0102; found 445.0111.

(Z)-4-(4-(tert-Butyl)styryl)-2-(4-chlorophenyl)quinoline-3-carbonitrile (4pg):

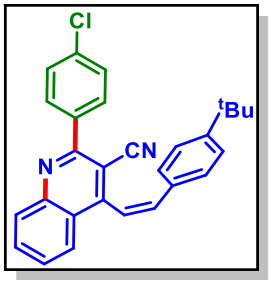

As a white solid (48 mg, 46% yield, *Z*/*E* 94:6, mp 164–166 °C); Purification over a column of silica gel (2% EtOAc in hexane); ^{1}H NMR ($CDCl_3$, 400 MHz): δ 8.19 (d, 1H, *J* = 8.0 Hz), 8.07 (d, 1H, *J* = 8.0 Hz), 7.87–7.82 (m, 3H), 7.56 (t, 1H, *J* = 7.6 Hz), 7.49 (d, 2H, *J* = 8.8 Hz), 7.20 (d, 1H, *J* = 12.8 Hz), 7.13 (d, 2H, *J* = 8.4 Hz), 6.89 (dd, 3H, J_1 = 10.6 Hz, J_2 = 2.2 Hz), 1.21 (s, 9H); ^{13}C{^{1}H} NMR ($CDCl_3$, 100 MHz): δ 157.6, 154.0, 151.9,148.4, 137.9, 136.6, 136.5, 133.1, 132.4, 130.7, 130.4, 129.0, 128.9, 128.3, 126.3, 125.6, 124.0, 121.3, 117.2, 105.0, 34.8, 31.2; IR (KBr, cm^{-1}): 3067, 2962, 2865, 2222, 1610, 1543, 1489, 1361, 1274, 1092, 835, 749; HRMS (ESI/Q-TOF) (m/z) calcd for $C_{28}H_{24}ClN_2$ $[M + H]^+$ 423.1623; found 423.1631.

(4-(4-Methoxyphenyl)-2,6-diphenylpyridin-3-yl)(phenyl)methanone (3caa):

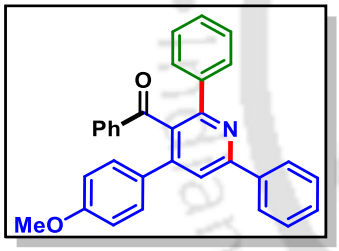

As a white solid (57 mg, 65% yield, mp 197–199 °C); Purification over a column of silica gel (5% EtOAc in hexane); ^{1}H NMR ($CDCl_3$, 400 MHz): δ 8.19–8.16 (m, 2H), 7.76 (s, 1H), 7.60–7.58 (m, 2H), 7.52–7.45 (m, 5H), 7.26–7.23 (m, 6H), 7.18 (t, 2H, *J* = 7.4 Hz), 6.79 (d, 2H, *J* = 8.8 Hz), 3.75 (s, 3H); ^{13}C{^{1}H} NMR ($CDCl_3$, 100 MHz): δ 176.6, 159.7, 157.1, 156.8, 149.7, 140.1, 138.9, 138.8, 132.2, 131.0, 130.7, 130.0, 129.5, 129.4, 128.9, 128.4, 128.2, 128.1, 127.9, 127.3, 120.2, 114.0, 55.4; IR (KBr, cm^{-1}): 3059, 2963, 2837, 1608, 1572, 1494, 1348, 1250, 1178, 1028, 829, 757; HRMS (ESI/Q-TOF) (m/z) calcd for $C_{31}H_{24}NO_2$ $[M + H]^+$ 442.1802; found 442.1812.

4-(4-Methoxyphenyl)-2,6-diphenylnicotinamide (3cab):

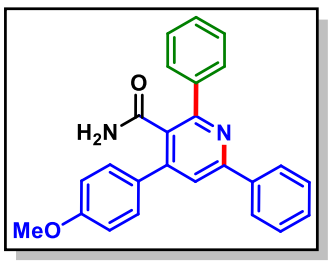

As a white solid (53 mg, 70% yield, mp 202–204 °C); Purification over a column of silica gel (15% EtOAc in hexane); ^{1}H NMR ($CDCl_3$, 400 MHz): δ 8.12–8.09 (m, 2H), 7.85–7.83 (m, 2H), 7.68 (s, 1H), 7.51–7.42 (m, 8H), 6.97 (d, 2H, *J* = 8.8 Hz), 5.53 (d, 2H, *J* = 51.6 Hz), 3.84 (s, 3H); ^{13}C{^{1}H} NMR ($CDCl_3$, 100 MHz): δ 170.7,

160.2, 157.2, 156.1, 149.0, 139.9, 138.7, 130.7, 129.8, 129.6, 129.1, 128.99, 128.95, 128.6, 128.4, 127.3, 119.9, 114.3, 55.5; IR (KBr, cm^{-1}): 3453, 3318, 3171, 3060, 2929, 2838, 1658, 1608, 1513, 1367, 1250, 1180, 1028, 833, 764; HRMS (ESI/Q-TOF) (m/z) calcd for $C_{25}H_{21}N_2O_2$ $[M + H]^+$ 381.1598; found 381.1597.

3-Cyano-2-(4-methoxyphenyl)-4,6,7-triphenylpyrido[2,1-a]isoquinolin-5-ium (3car):

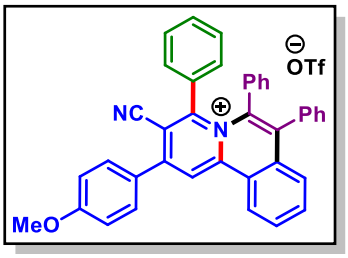

As a white solid (82 mg, 76% yield, mp 315–317 °C); Purification over a column of silica gel (3% MeOH in DCM); ^1H NMR (CD_3CN, 400 MHz): δ 9.37 (s, 1H), 9.21 (d, 1H, J = 8.4 Hz), 8.14 (d, 2H, J = 9.2 Hz), 8.11–8.08 (m, 1H), 8.04 (t, 1H, J = 7.7 Hz), 7.56 (d, 1H, J = 8.4 Hz), 7.34–7.28 (m, 6H), 7.22 (t, 2H, J = 7.8 Hz), 7.16–7.10 (m, 4H), 7.00 (t, 1H, J = 7.4 Hz), 6.85 (t, 2H, J = 7.8 Hz), 6.56 (d, 2H, J = 8.4 Hz), 3.96 (s, 3H); $^{13}C\{^1H\}$ NMR (CD_3CN, 100 MHz): δ 164.6, 157.9, 153.7, 150.4, 140.8, 139.6, 137.0, 136.9, 136.2, 135.4, 135.1, 133.2, 132.6, 132.3, 131.4, 131.2, 130.3, 130.2, 129.8, 129.6, 129.4, 129.1, 129.0, 128.2, 127.0, 126.3, 121.8, 116.3, 116.2, 114.6, 56.9; IR (KBr, cm^{-1}): 3057, 2936, 2847, 2243, 1592, 1446, 1261, 1163, 1029, 773; HRMS (ESI/Q-TOF) (m/z) calcd for $C_{39}H_{28}N_2O$ $[M + H]^+$ 540.2196; found 540.2192.

2-(4-Chlorophenyl)-4-(2,2-diphenylethyl)quinoline-3-carboxamide (4aga):

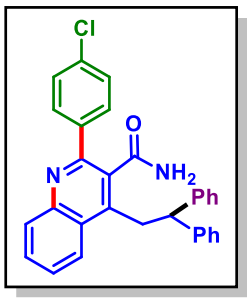

As a white solid (48 mg, 52% yield, mp 240–243 °C); Purification over a column of silica gel (15% EtOAc in hexane); ^1H NMR ($CDCl_3$, 400 MHz): δ 8.19 (d, 1H, J = 8.4 Hz), 8.01 (d, 1H, J = 8.4 Hz), 7.79 (t, 1H, J = 7.6 Hz), 7.66 (d, 2H, J = 8.8 Hz), 7.59 (t, 1H, J = 7.7 Hz), 7.38 (d, 2H, J = 8.4 Hz), 7.26–7.17 (m, 7H), 7.05 (d, 3H, J = 7.2 Hz), 4.90 (s, 1H), 4.57 (t, 1H, J = 7.4 Hz), 3.95 (d, 2H, J = 7.6 Hz), 3.81 (s, 1H); $^{13}C\{^1H\}$ NMR ($CDCl_3$, 100 MHz): δ 170.3, 154.2, 147.8, 144.6, 143.8, 138.5, 135.3, 130.9, 130.5, 130.2, 129.9, 128.8, 128.7, 128.6, 127.7, 127.1, 125.6, 124.4, 51.8, 36.4; IR (KBr, cm^{-1}): 3445, 3295, 3162, 2924, 1664, 1597, 1491, 1262, 1090, 1014,

836, 758; HRMS (ESI/Q-TOF) (m/z) calcd for $C_{30}H_{24}ClN_2O$ $[M + H]^+$ 463.1572; found 463.1576.

(Z)-2-(4-Chlorophenyl)-3-cyano-4-styrylquinoline 1-oxide (4ags):

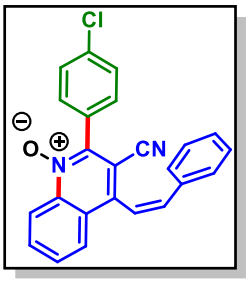

As a yellow solid (57 mg, 85% yield, mp 190–192 °C); Purification over a column of silica gel (20% EtOAc in hexane); ^{1}H NMR ($CDCl_3$, 400 MHz): δ 8.84 (d, 1H, J = 8.8 Hz), 8.08 (d, 1H, J = 8.4 Hz) 7.90 (t, 1H, J = 7.8 Hz), 7.67 (t, 1H, J = 7.7 Hz), 7.58–7.56 (m, 2H), 7.53–7.50 (m, 2H), 7.22–7.13 (m, 4H), 7.02–6.99 (m, 2H), 6.87 (d, 1H, J = 12.4 Hz); ^{13}C{^{1}H} NMR ($CDCl_3$, 100 MHz): δ 146.6, 143.4, 140.4, 139.0, 136.9, 135.2, 133.7, 131.5, 130.1, 129.2, 129.0, 128.9, 128.8, 128.7, 127.5, 126.9, 121.2, 121.0, 114.8, 108.4; IR (KBr, cm^{-1}): 3060, 2924, 2855, 2228, 1596, 1491, 1331, 1275, 1146, 1092, 812, 767; HRMS (ESI/Q-TOF) (m/z) calcd for $C_{24}H_{16}ClN_2O$ $[M + H]^+$ 383.0946; found 383.0925.

5-(4-Chlorophenyl)-2-phenyl-2,3-dihydrobenzo[c][2,7]naphthyridin-4(1H)-one (4agb):

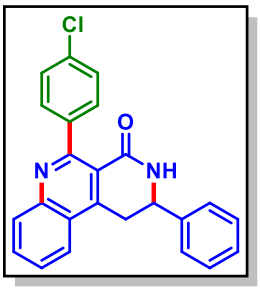

As a white solid (47 mg, 61% yield, mp 205–207 °C); Purification over a column of silica gel (15% EtOAc in hexane); ^{1}H NMR ($CDCl_3$, 400 MHz): δ 8.16 (d, 1H, J = 8.8 Hz), 7.96 (d, 1H, J = 8.4 Hz) 7.81 (t, 1H, J = 7.6 Hz), 7.62–7.58 (m, 3H), 7.51–7.39 (m, 7H), 6.32 (s, 1H), 5.02 (dd, 1H, J = 11.1 and 4.3 Hz), 3.75 (dd, 1H, J = 16.6, 4.2 Hz), 3.47 (dd, 1H, J = 16.8, 10.8 Hz); ^{13}C{^{1}H} NMR ($CDCl_3$, 100 MHz): δ 164.8, 158.1, 148.1, 147.3, 140.2, 139.9, 134.5, 131.8, 130.6, 130.3, 129.4, 129.0, 128.2, 127.6, 126.8, 124.3, 123.9, 120.7, 55.0, 34.1; IR (KBr, cm^{-1}): 3396, 3243, 2925, 2873, 1670, 1553, 1491, 1349, 1275, 1261, 1088, 832, 763; HRMS (ESI/Q-TOF) (m/z) calcd for $C_{24}H_{18}ClN_2O$ $[M + H]^+$ 385.1102; found 385.1106.

II.11. Representative NMR Spectra:

2,4,6-Triphenylnicotinonitrile (3aa): ^{1}H NMR ($CDCl_3$, 500 MHz)

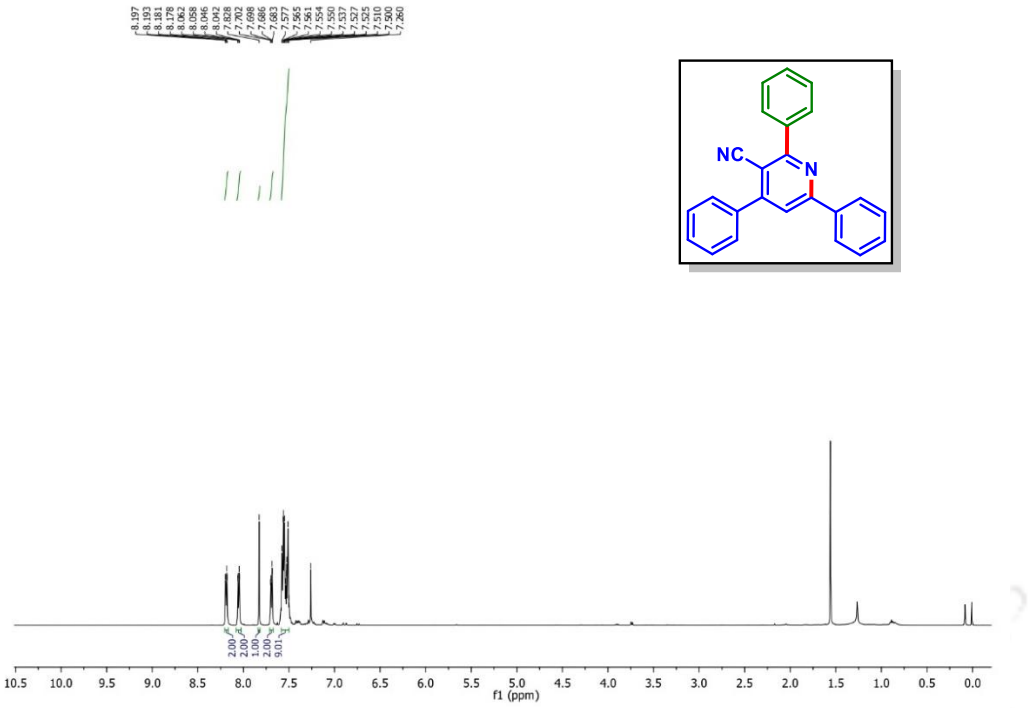

2,4,6-Triphenylnicotinonitrile (3aa):$^{13}C\{^{1}H\}$ NMR ($CDCl_3$, 125 MHz)

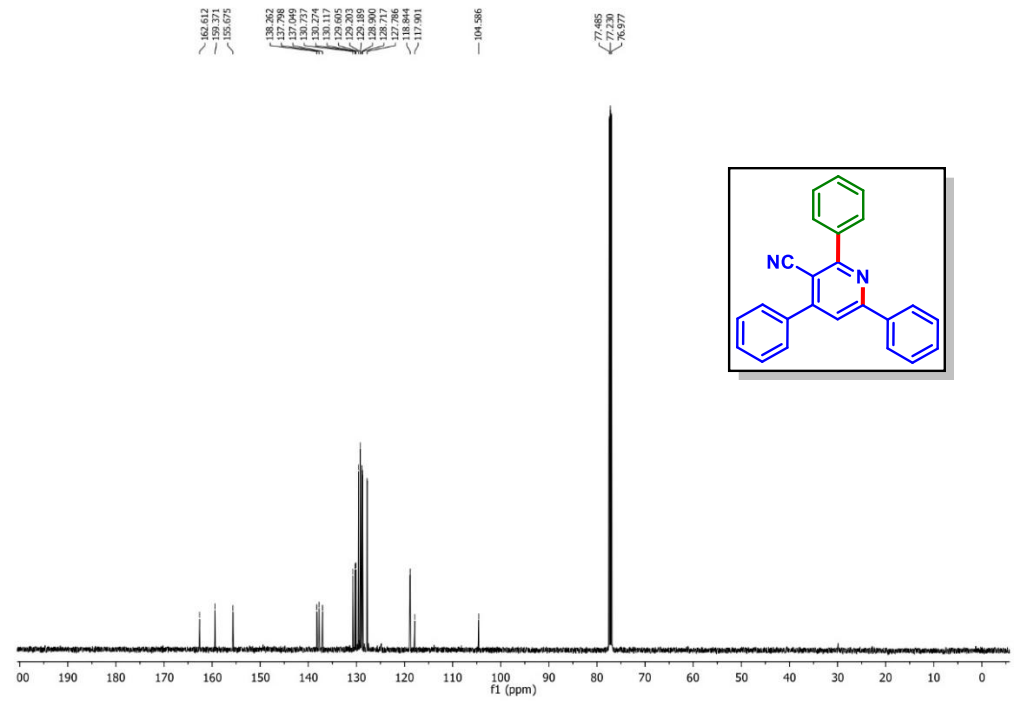

2,6-Diphenyl-4-(p-tolyl)nicotinonitrile (3ba): ^{1}H NMR ($CDCl_3$, 400 MHz)

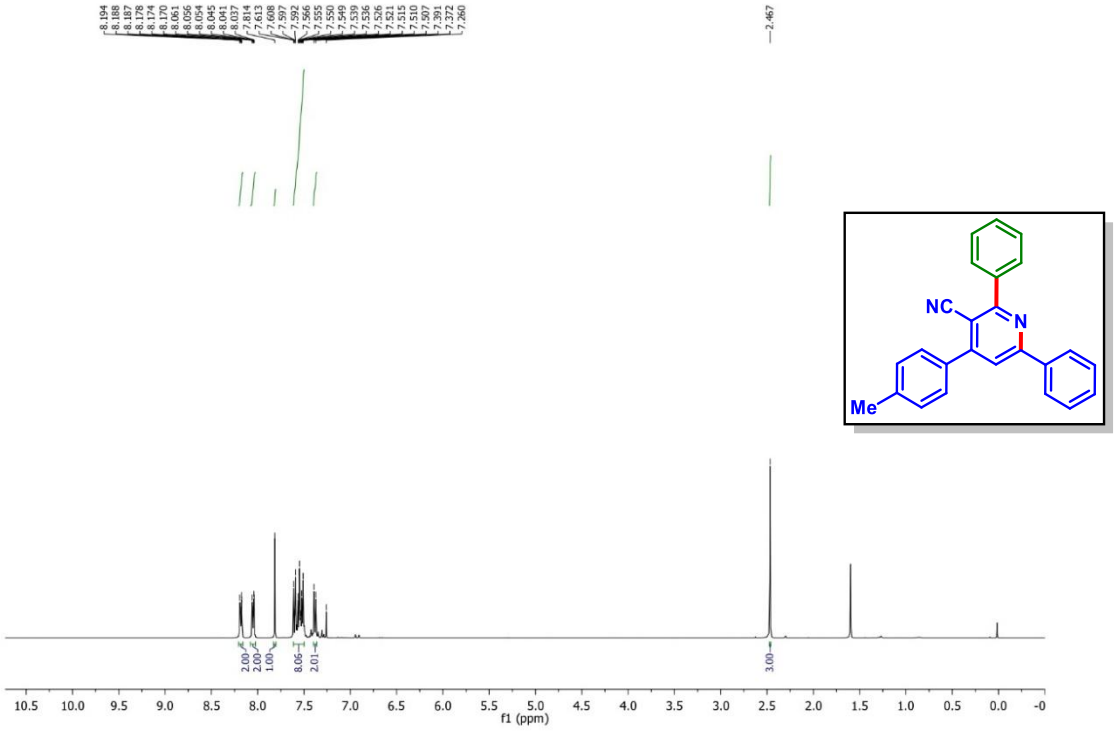

2,6-Diphenyl-4-(p-tolyl)nicotinonitrile (3ba): $^{13}C\{^{1}H\}$ NMR ($CDCl_3$, 100 MHz)

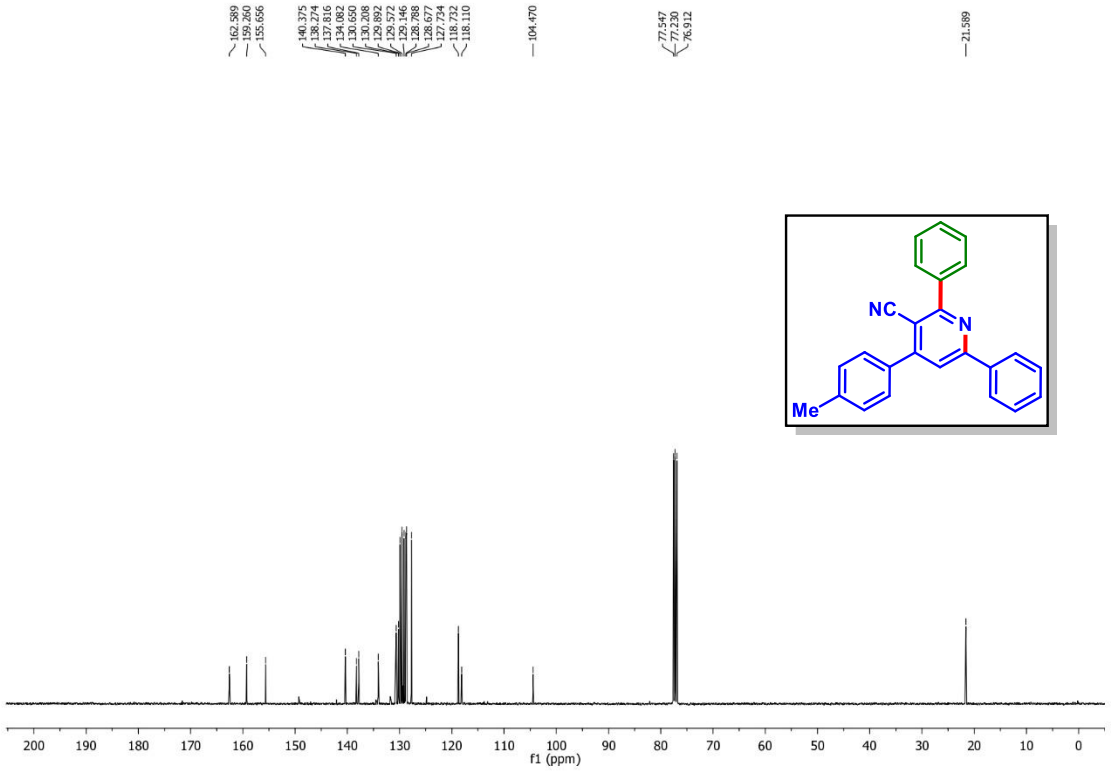

4-(4-Chlorophenyl)-2,6-diphenylnicotinonitrile (3ea): ^{1}H NMR ($CDCl_3$, 500 MHz)

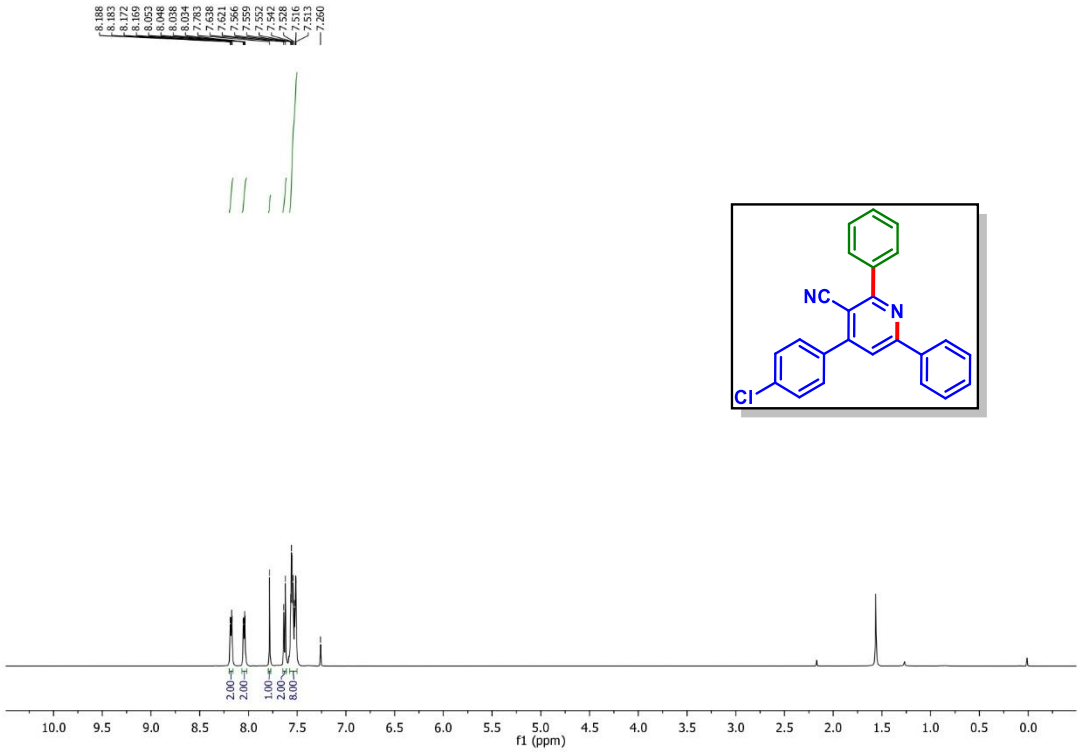

4-(4-Chlorophenyl)-2,6-diphenylnicotinonitrile (3ea): $^{13}C\{^{1}H\}$ NMR ($CDCl_3$, 125 MHz)

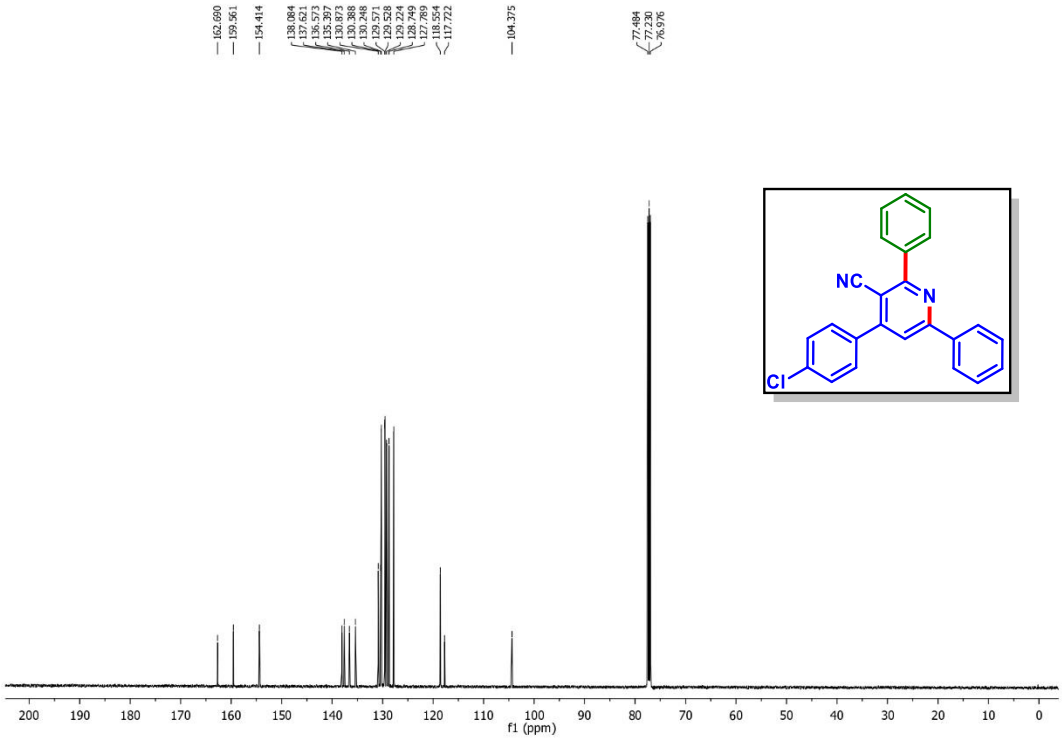

6-(4-Methoxyphenyl)-2,4-diphenylnicotinonitrile (3ha): ^{1}H NMR ($CDCl_3$, 500 MHz)

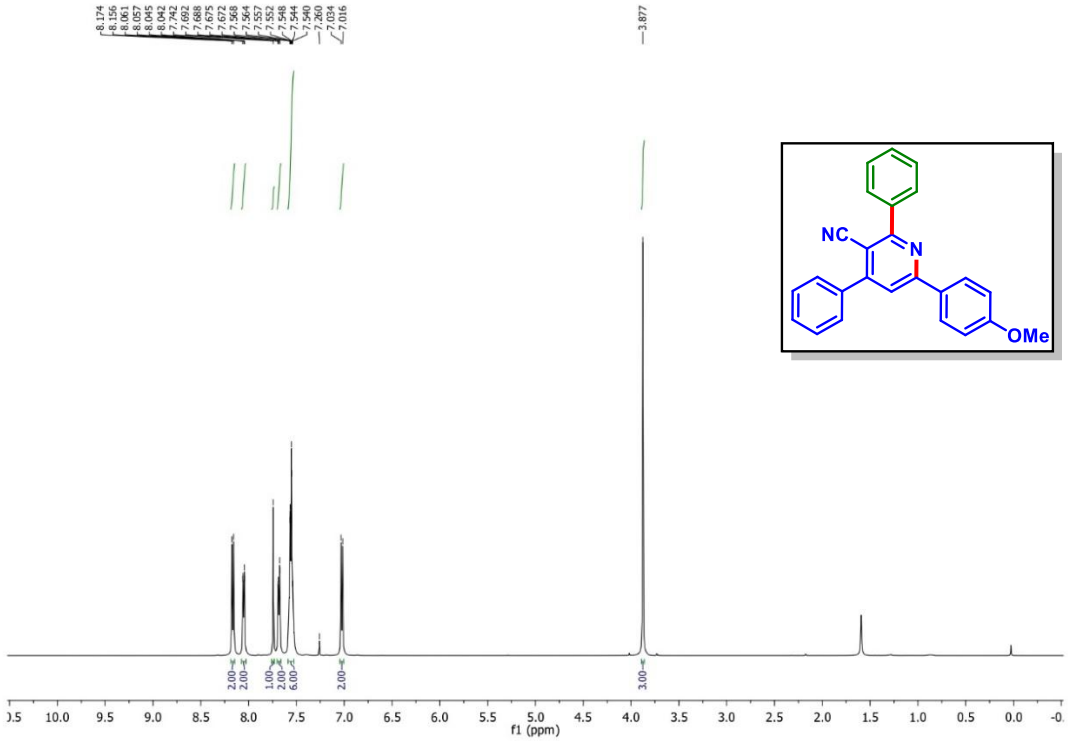

6-(4-Methoxyphenyl)-2,4-diphenylnicotinonitrile (3ha): $^{13}C\{^{1}H\}$ NMR ($CDCl_3$, 125 MHz)

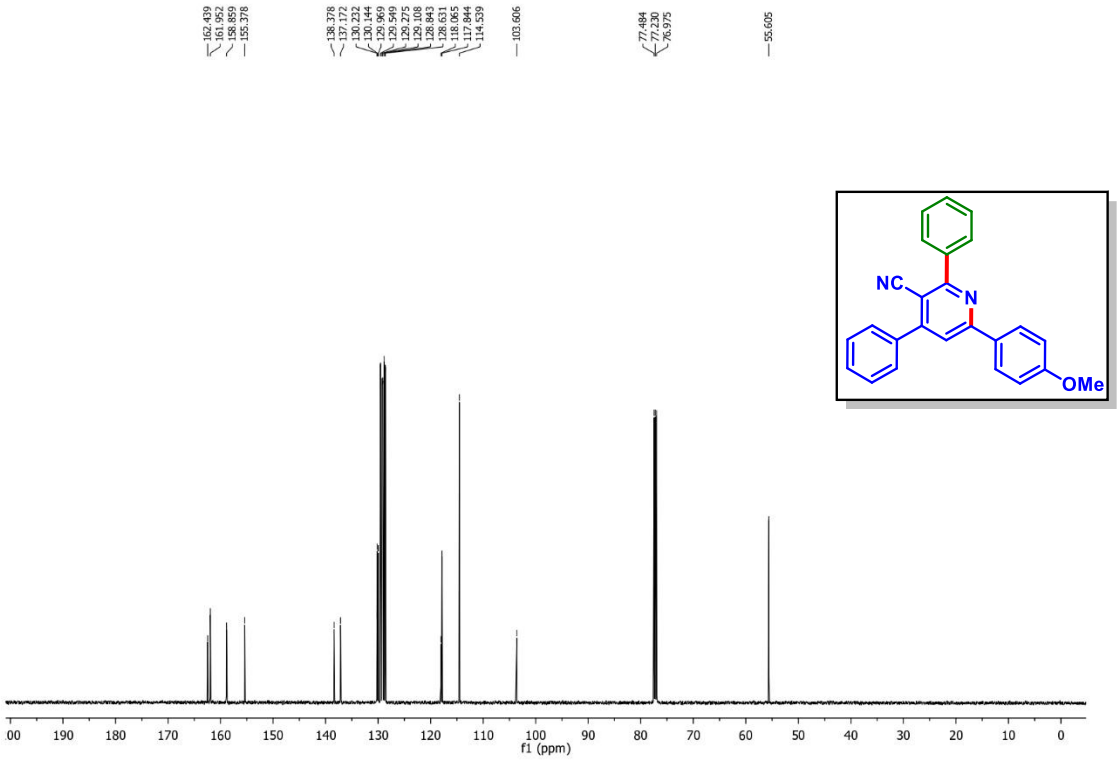

6-(4-Chlorophenyl)-2,4-diphenylnicotinonitrile (3ia): ^{1}H NMR ($CDCl_3$, 500 MHz)

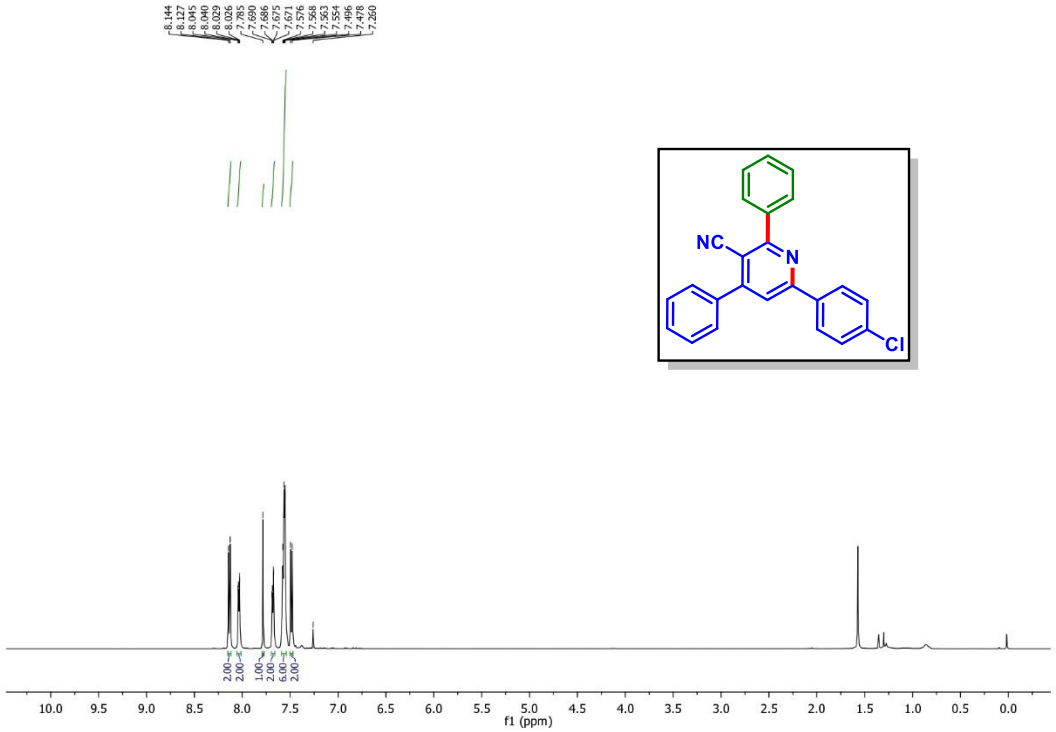

6-(4-Chlorophenyl)-2,4-diphenylnicotinonitrile (3ia): $^{13}C\{^{1}H\}$ NMR ($CDCl_3$, 125 MHz)

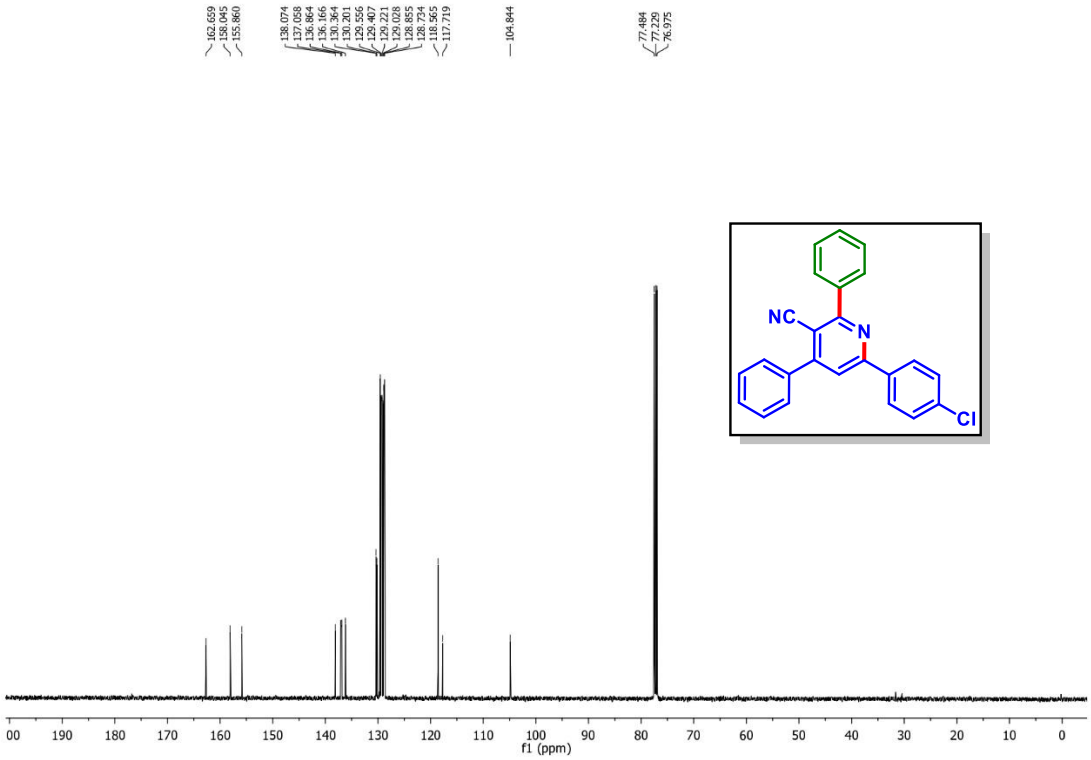

4-(4-Chlorophenyl)-6-(4-methoxyphenyl)-2-phenylnicotinonitrile (3ka): ^{1}H NMR ($CDCl_3$, 500 MHz)

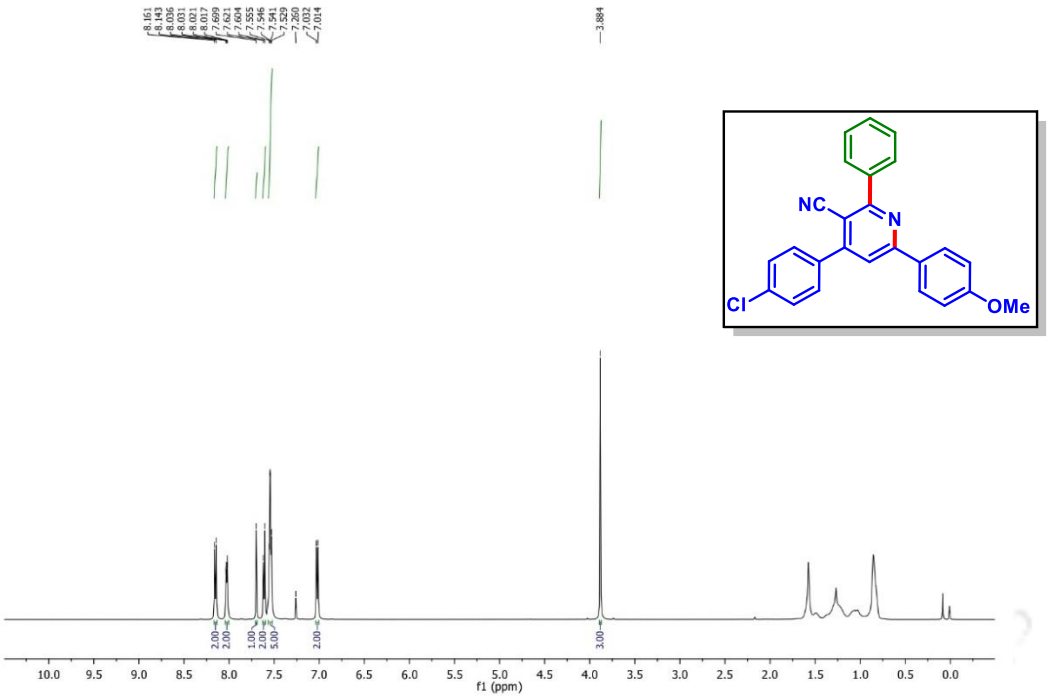

4-(4-Chlorophenyl)-6-(4-methoxyphenyl)-2-phenylnicotinonitrile (3ka): $^{13}C\{^{1}H\}$ NMR ($CDCl_3$, 125 MHz)

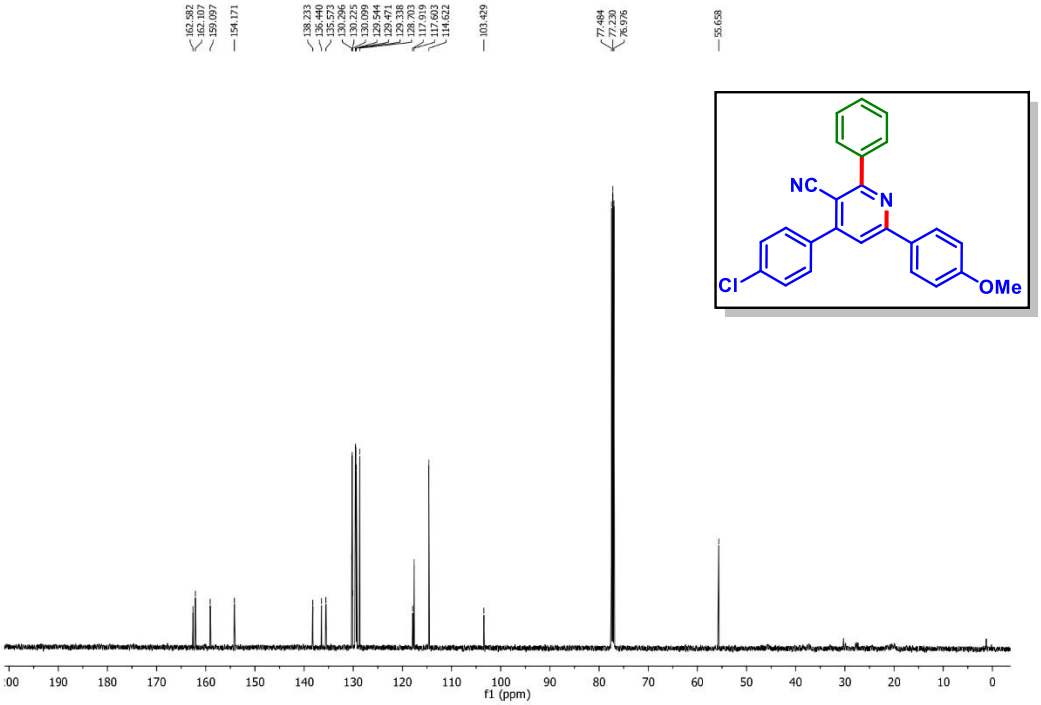

2-Phenyl-4,6-di(thiophen-2-yl)nicotinonitrile (3na): ^{1}H NMR ($CDCl_3$, 400 MHz)

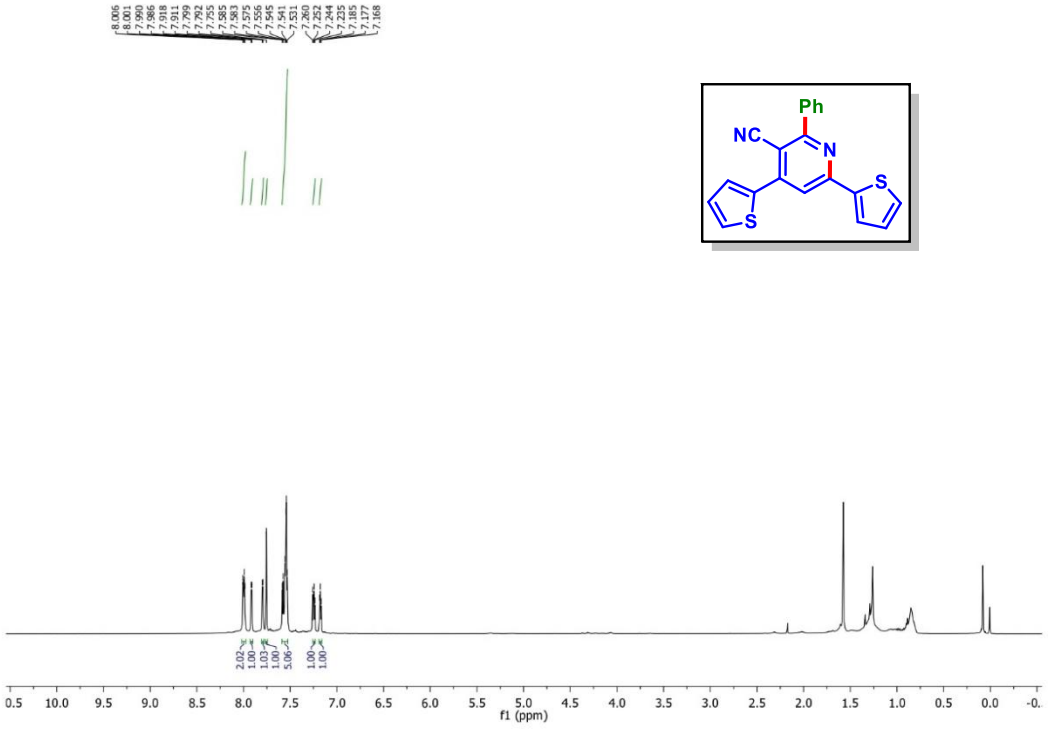

2-Phenyl-4,6-di(thiophen-2-yl)nicotinonitrile (3na): $^{13}C\{^{1}H\}$ NMR ($CDCl_3$, 100 MHz)

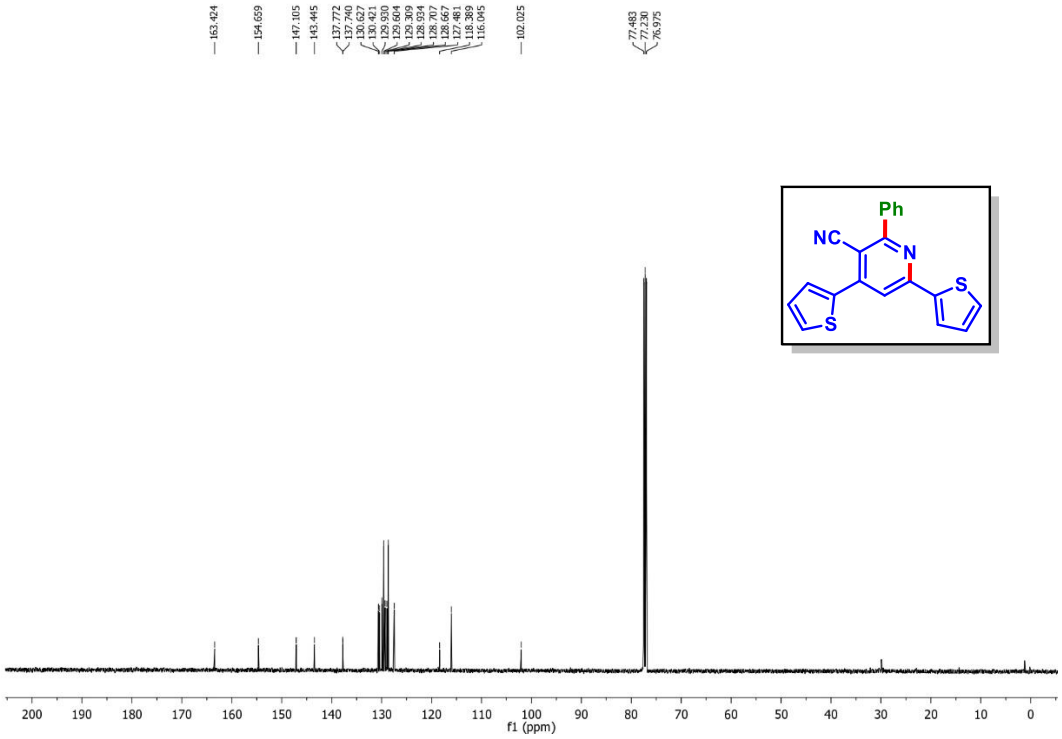

4,6-Diphenyl-2-(p-tolyl)nicotinonitrile (3ab): ^{1}H NMR ($CDCl_3$, 400 MHz)

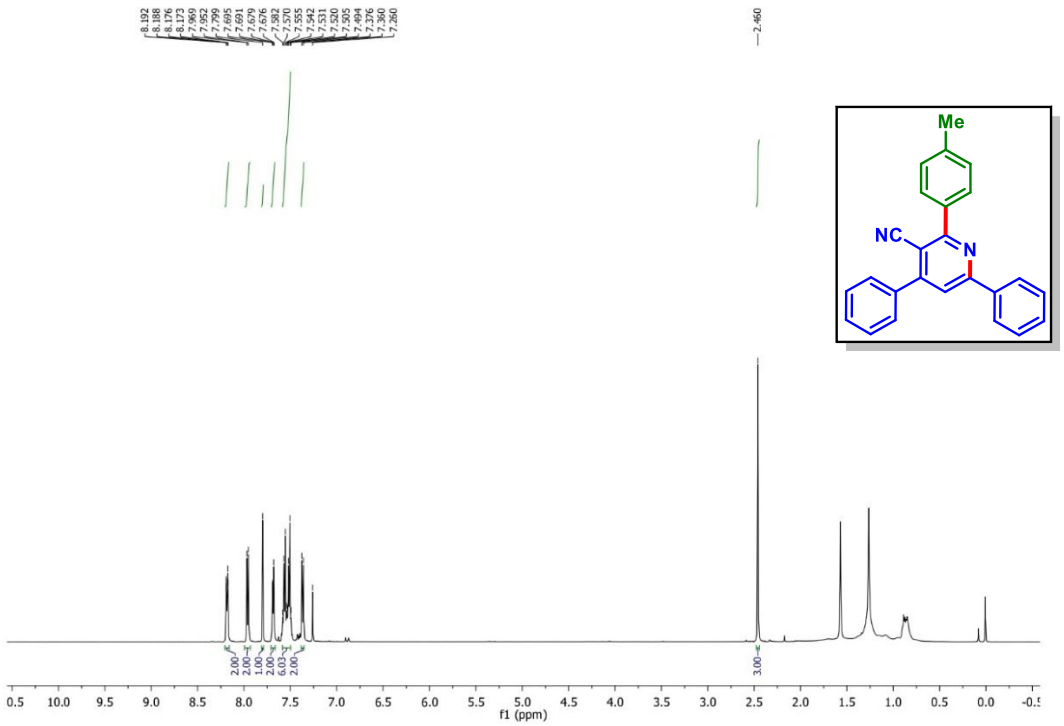

4,6-Diphenyl-2-(p-tolyl)nicotinonitrile (3ab): $^{13}C\{^{1}H\}$ NMR ($CDCl_3$, 100 MHz)

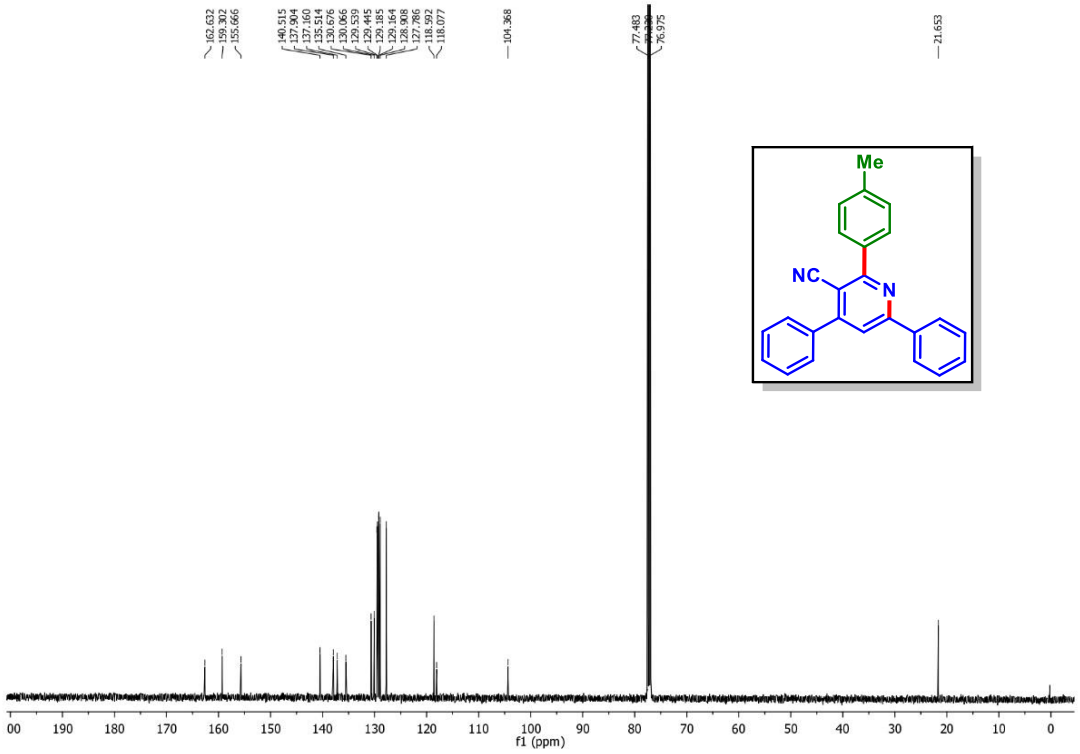

2-(4-Bromophenyl)-4,6-diphenylnicotinonitrile (3ah): ^{1}H NMR ($CDCl_3$, 500 MHz)

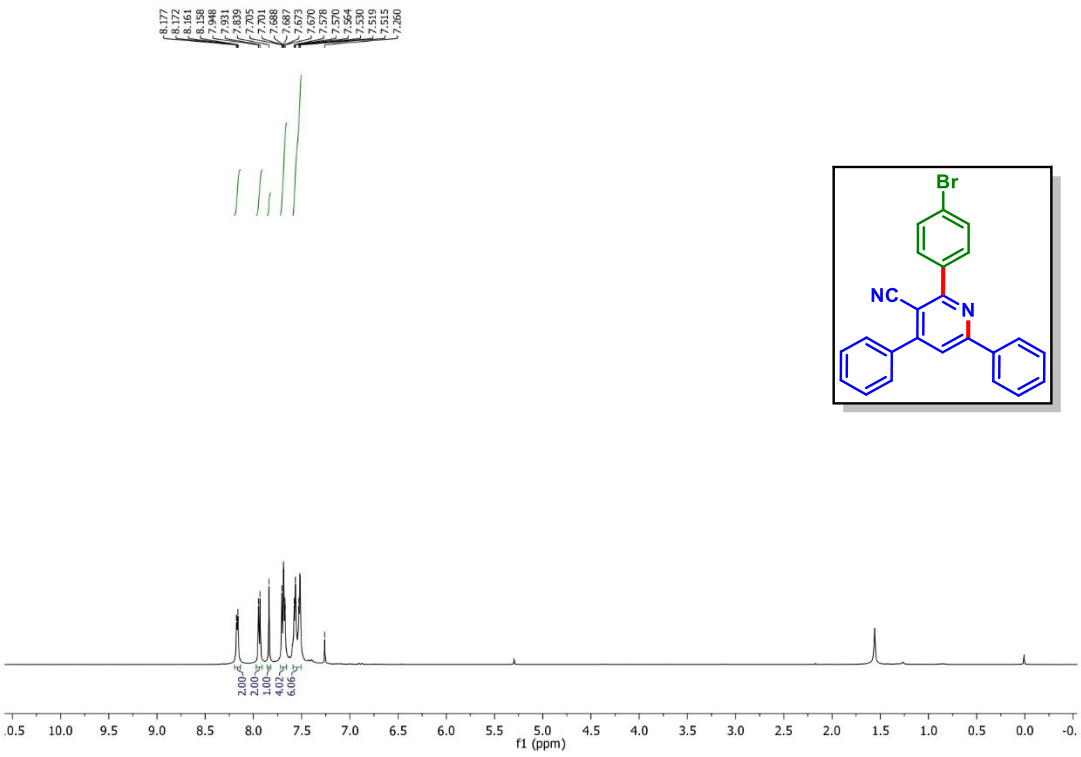

2-(4-Bromophenyl)-4,6-diphenylnicotinonitrile (3ah): ^{13}C NMR ($CDCl_3$, 125 MHz)

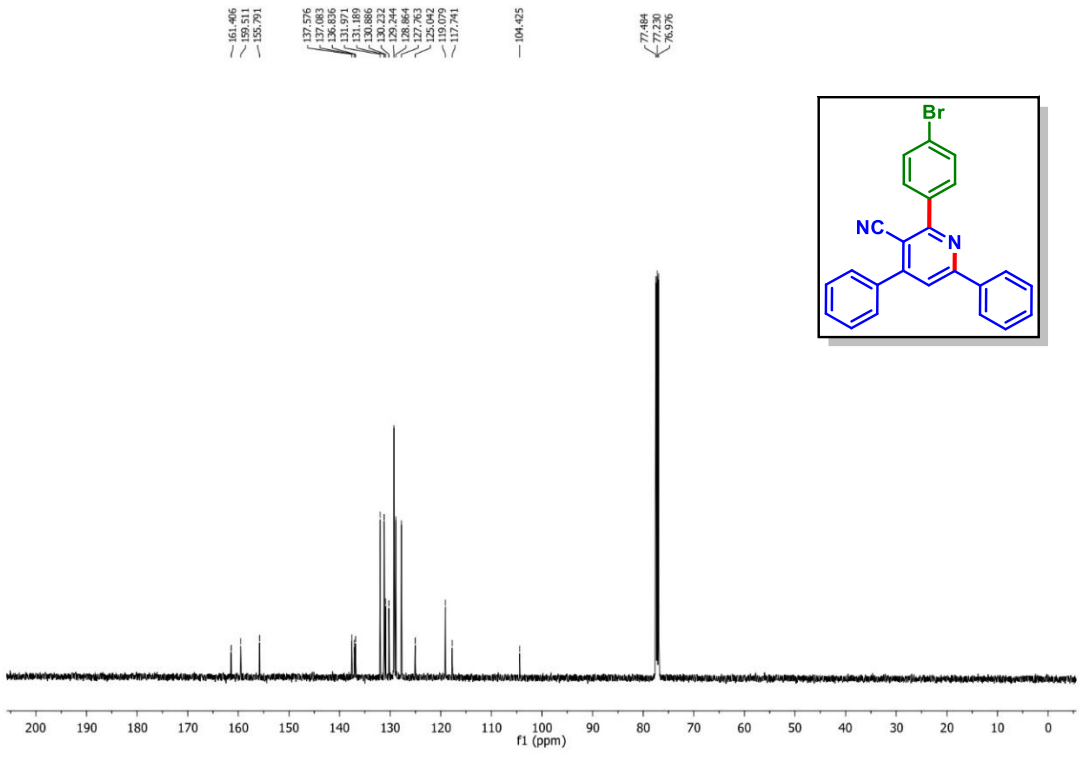

4,6-Diphenyl-2-(pyren-1-yl)nicotinonitrile (3am): ^{1}H NMR ($CDCl_3$, 400 MHz)

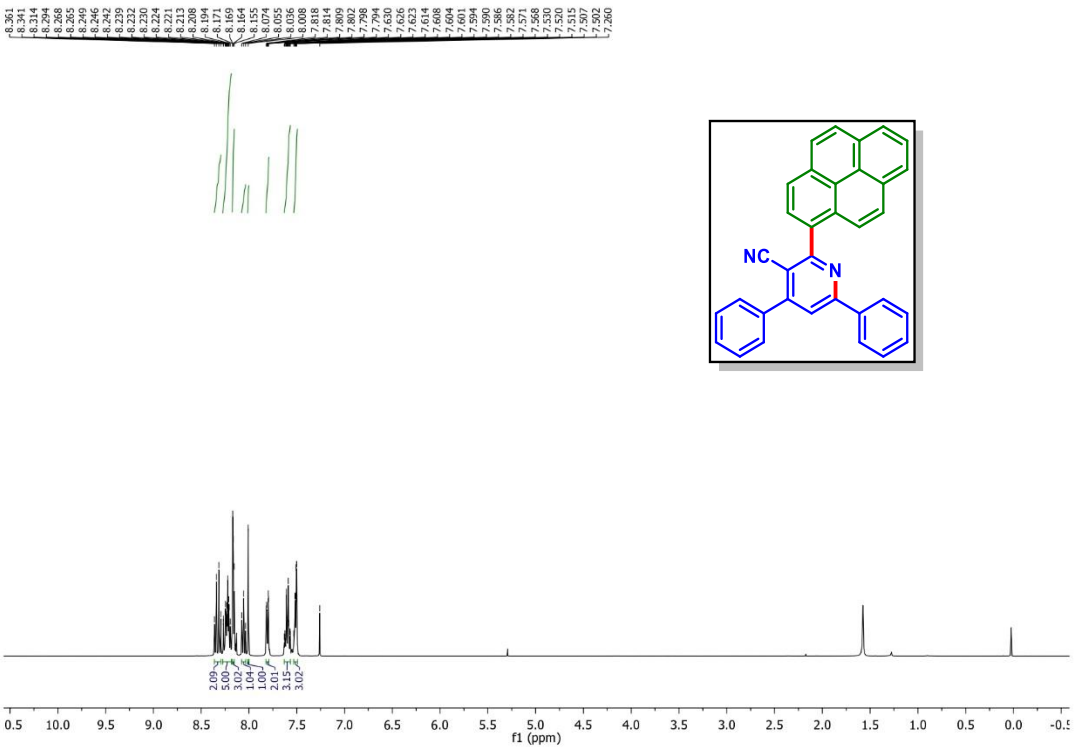

4,6-Diphenyl-2-(pyren-1-yl)nicotinonitrile (3am): ^{13}C NMR ($CDCl_3$, 100 MHz)

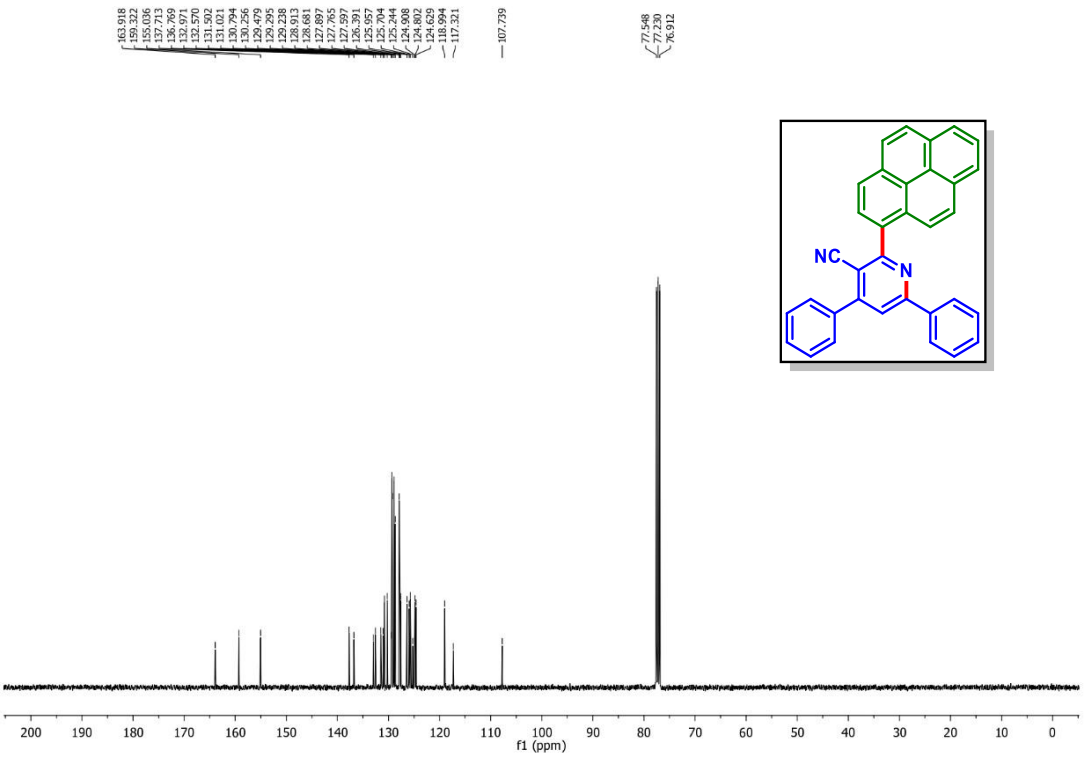

(Z)-2-Phenyl-4-styrylquinoline-3-carbonitrile (4aa): ^{1}H NMR ($CDCl_3$, 500 MHz)

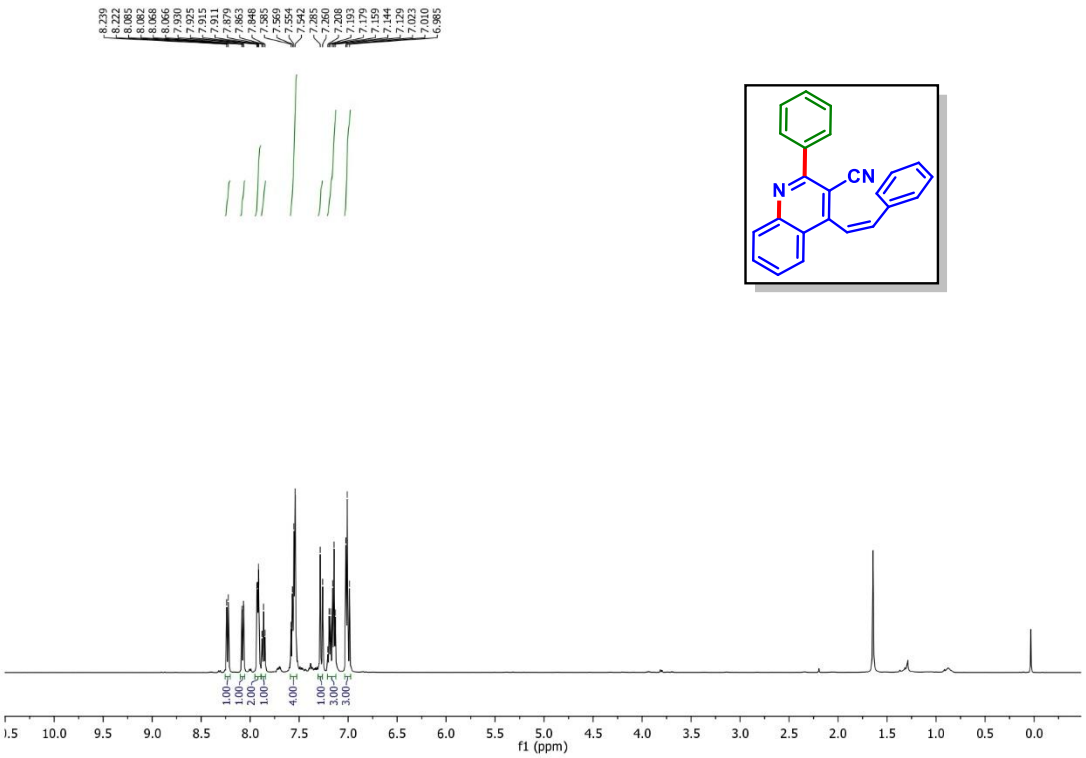

(Z)-2-Phenyl-4-styrylquinoline-3-carbonitrile (4aa): $^{13}C\{^1H\}$ NMR ($CDCl_3$, 125 MHz)

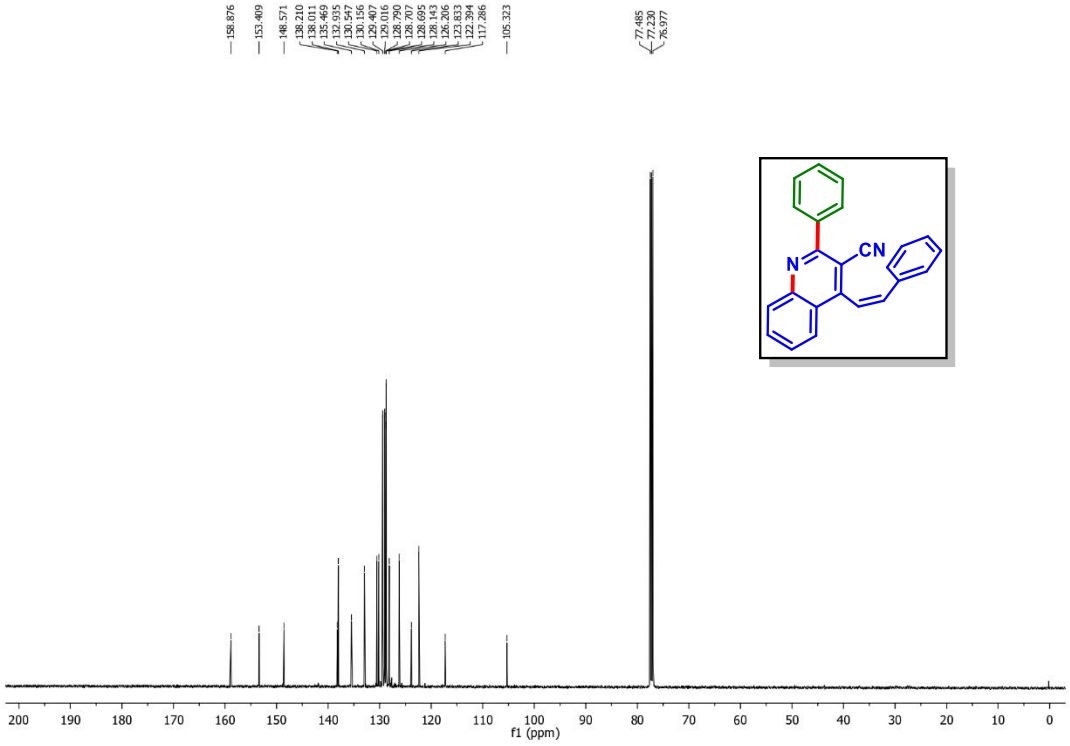

(Z)-7-Methyl-2-phenyl-4-styrylquinoline-3-carbonitrile (4ba): ^1H NMR ($CDCl_3$, 400 MHz)

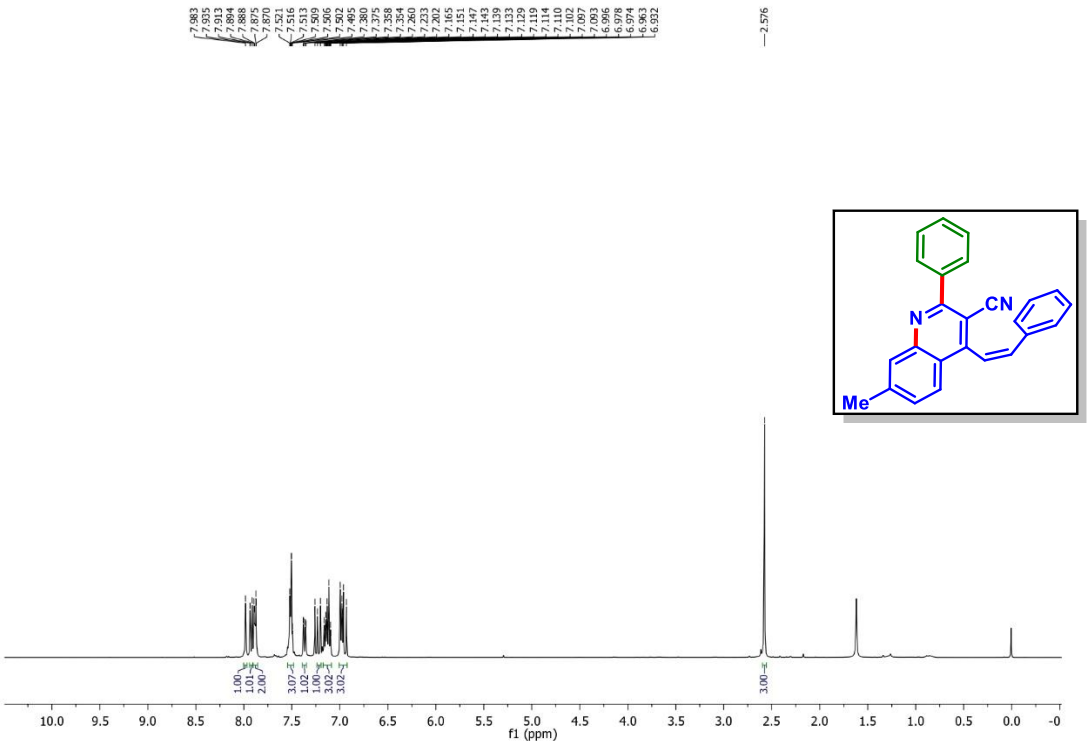

(Z)-7-Methyl-2-phenyl-4-styrylquinoline-3-carbonitrile (4ba): $^{13}C\{^{1}H\}$ NMR ($CDCl_3$, 100 MHz)

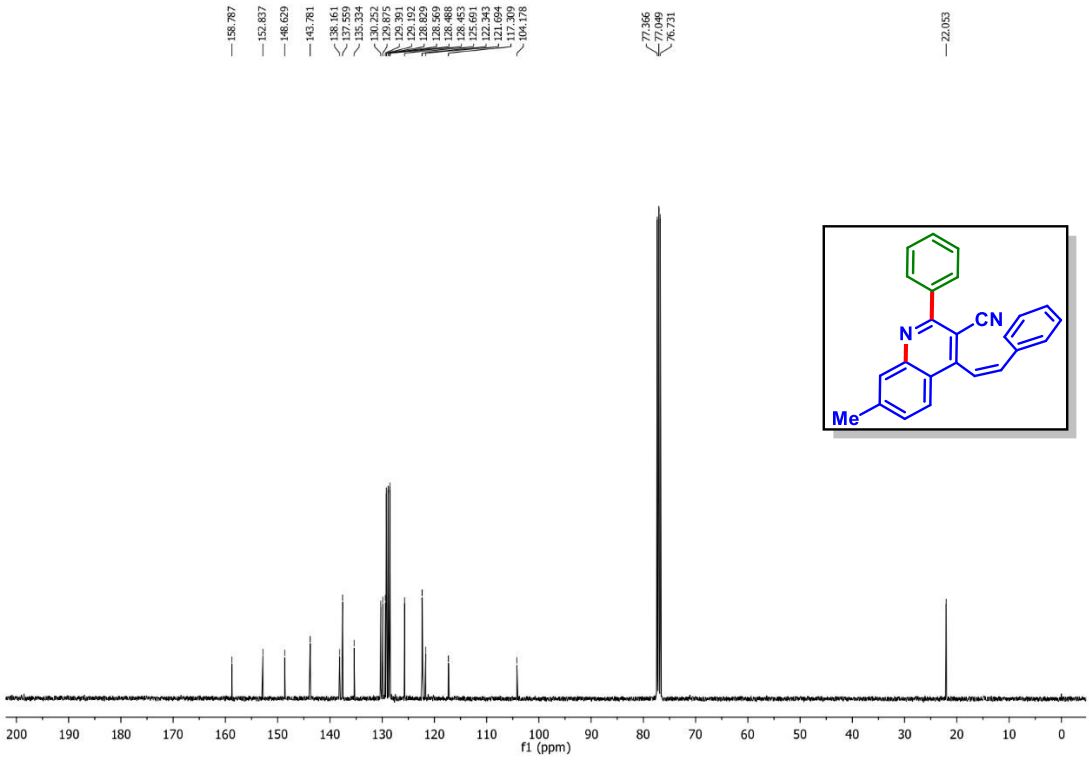

(Z)-7-Chloro-2-phenyl-4-styrylquinoline-3-carbonitrile (4ea): ^{1}H NMR ($CDCl_3$, 500 MHz)

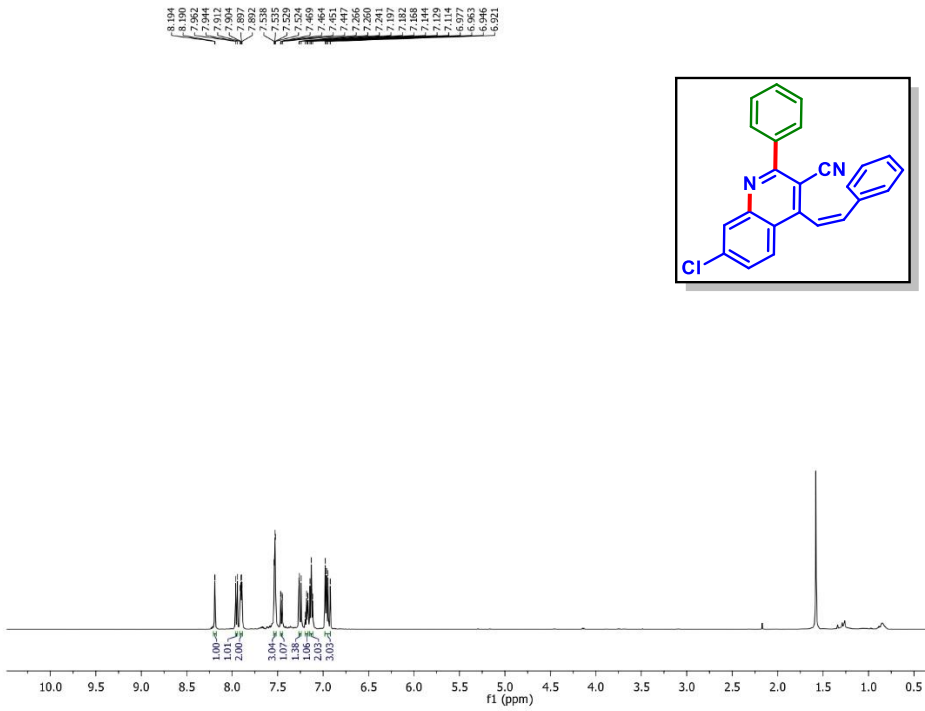

(Z)-7-Chloro-2-phenyl-4-styrylquinoline-3-carbonitrile (4ea): $^{13}C\{^{1}H\}$ NMR ($CDCl_3$, 125 MHz)

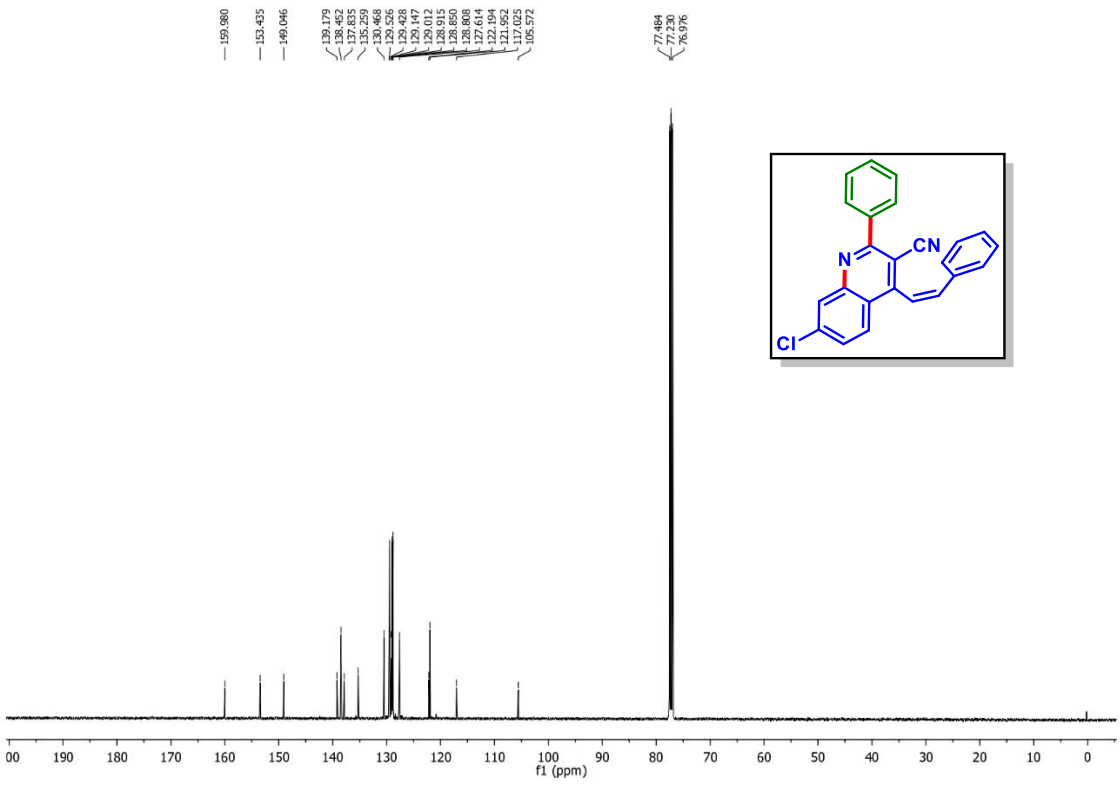

(Z)-4-(4-Methylstyryl)-2-phenylquinoline-3-carbonitrile (4ga): ^{1}H NMR ($CDCl_3$, 400 MHz)

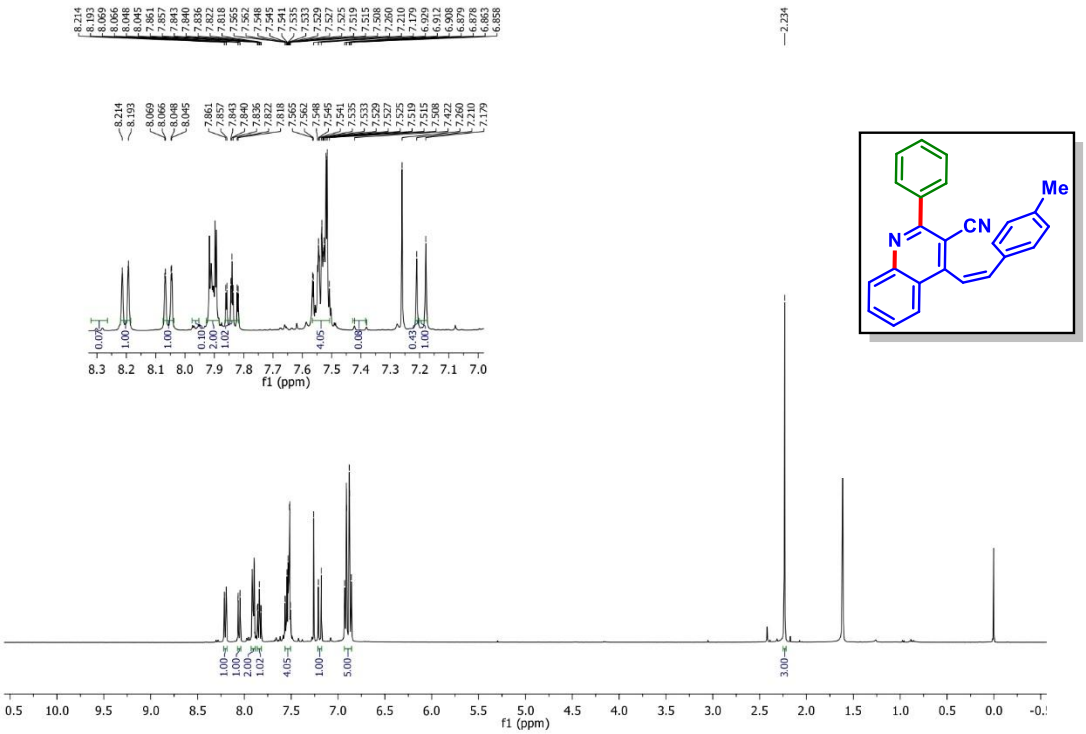

(Z)-4-(4-Methylstyryl)-2-phenylquinoline-3-carbonitrile (4ga): $^{13}C\{^{1}H\}$ NMR ($CDCl_3$, 100 MHz)

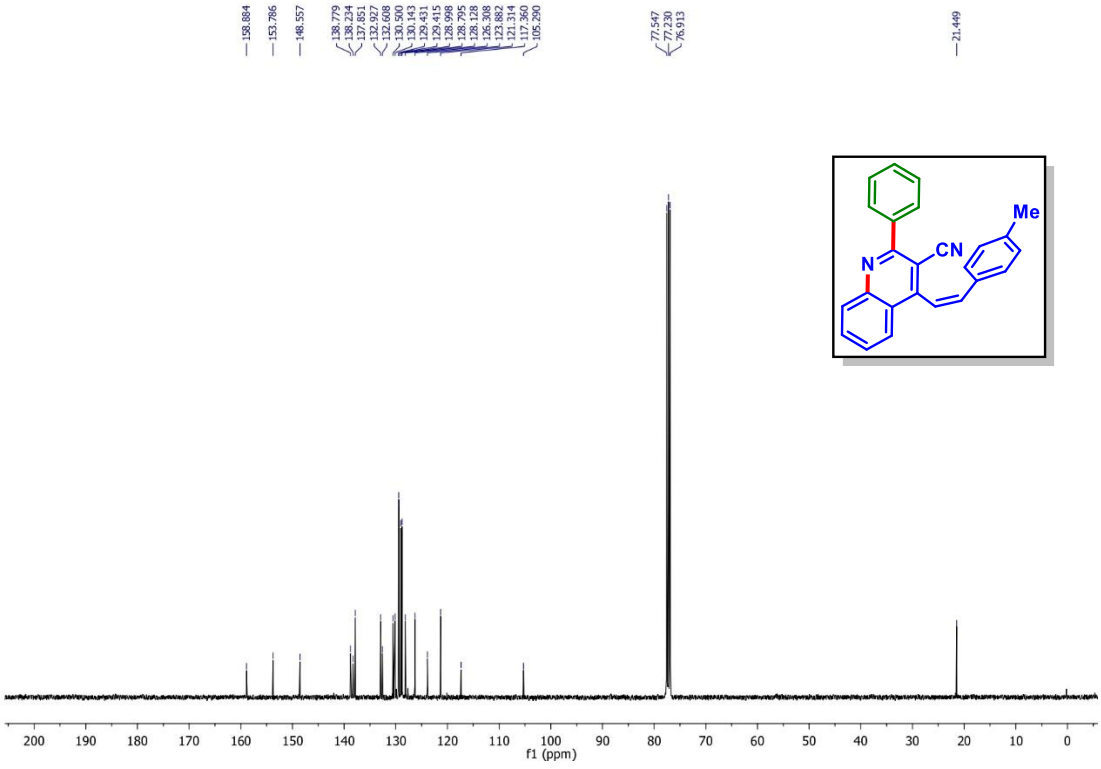

(Z)-4-(4-Chlorostyryl)-2-phenylquinoline-3-carbonitrile (4ia): ^{1}H NMR (CDCl$_3$, 500 MHz)

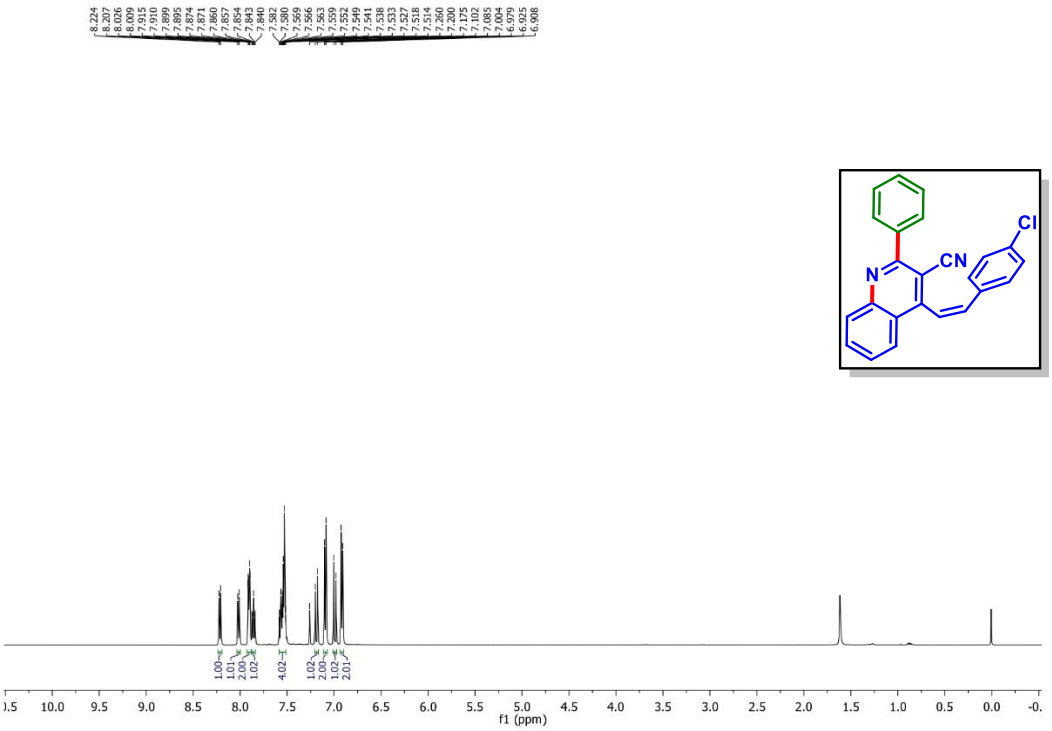

(Z)-4-(4-Chlorostyryl)-2-phenylquinoline-3-carbonitrile (4ia): ^{13}C{^{1}H} NMR (CDCl$_3$, 125 MHz)

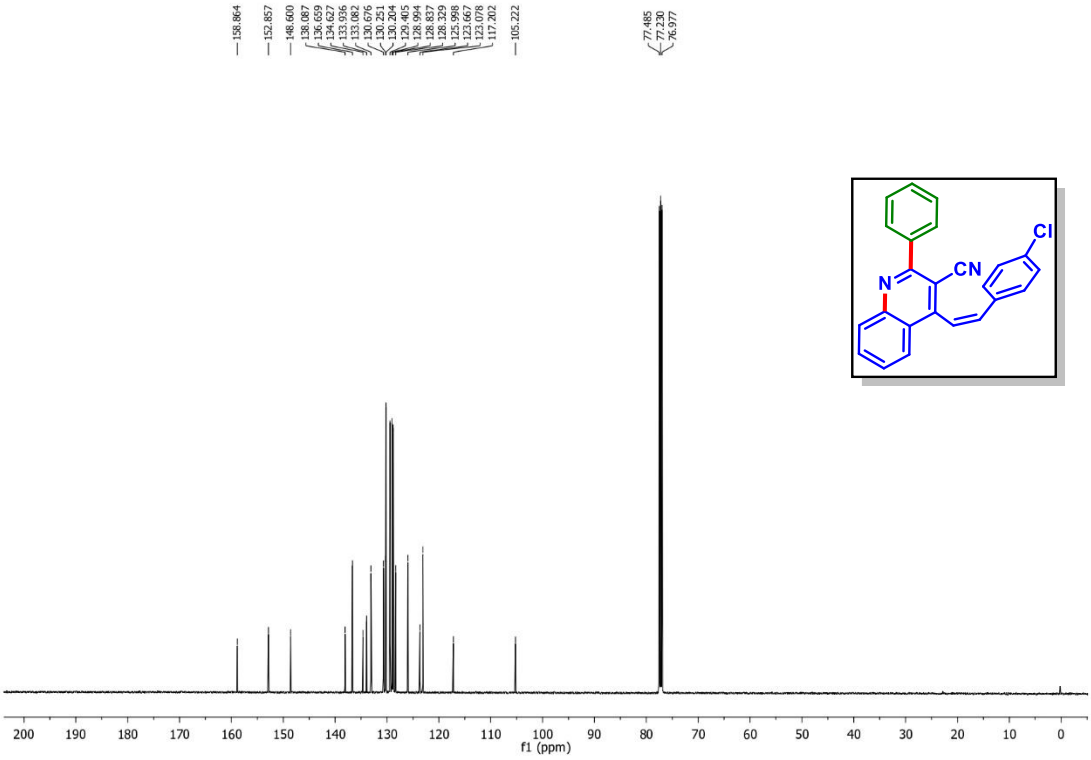

(Z)-4-Styryl-2-(p-tolyl)quinoline-3-carbonitrile (4ab): ^{1}H NMR ($CDCl_3$, 500 MHz)

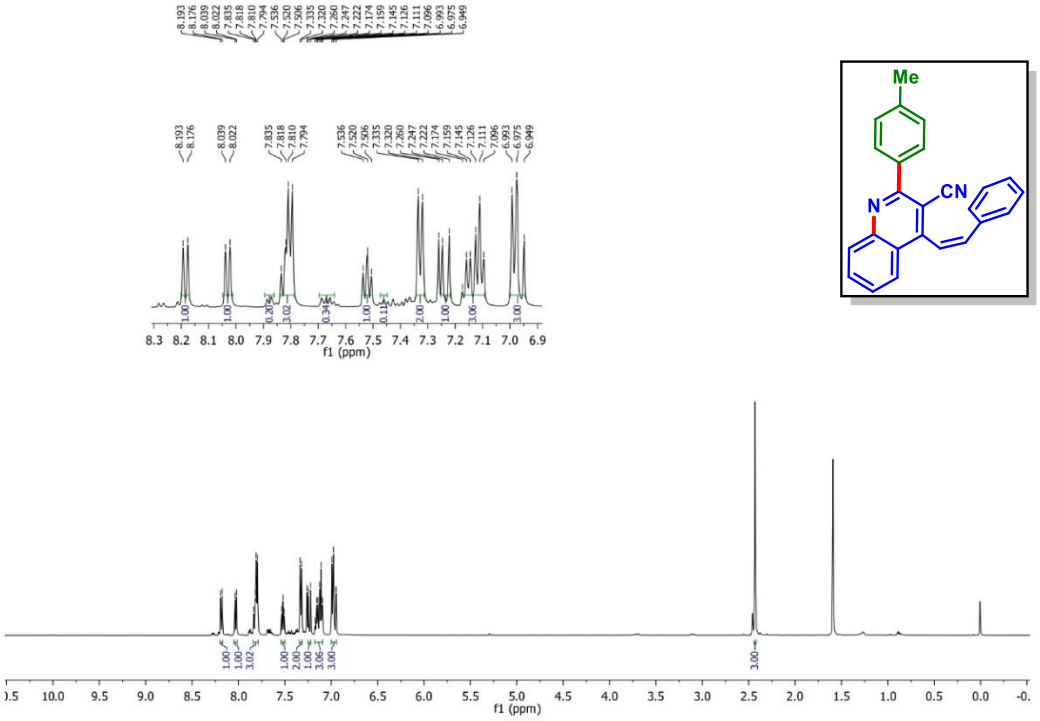

(Z)-4-Styryl-2-(p-tolyl)quinoline-3-carbonitrile (4ab): $^{13}C\{^{1}H\}$ NMR ($CDCl_3$, 125 MHz)

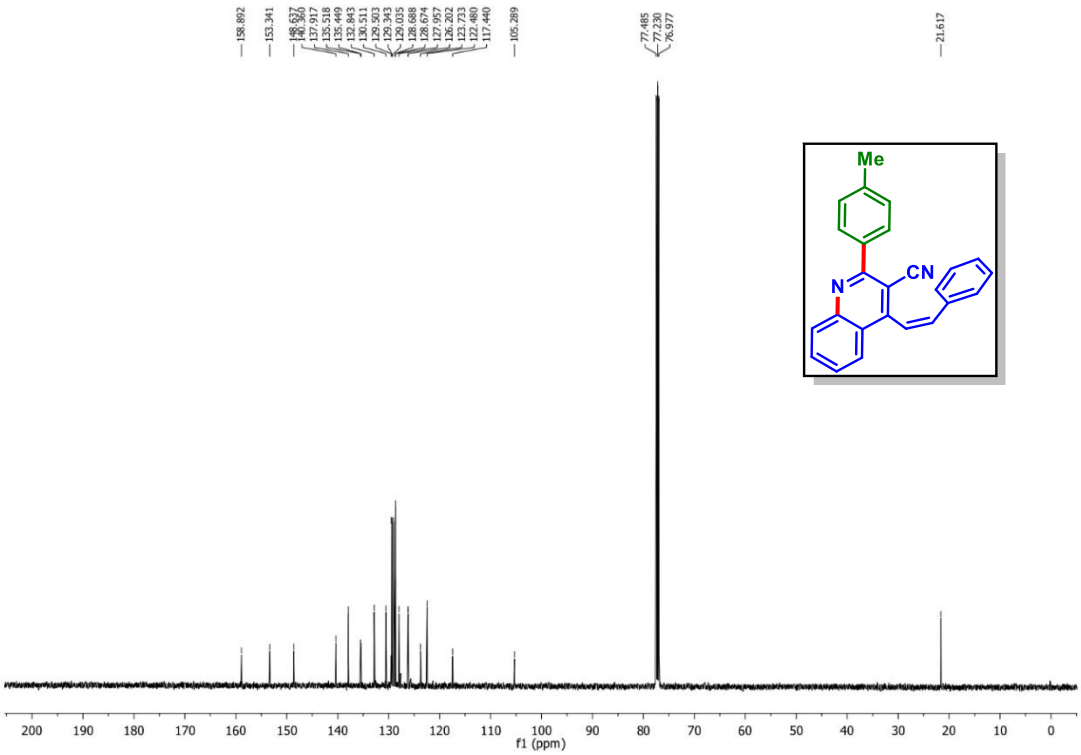

(Z)-2-(3-Chlorophenyl)-4-styrylquinoline-3-carbonitrile (4ao): ^{1}H NMR (CDCl$_3$, 500 MHz)

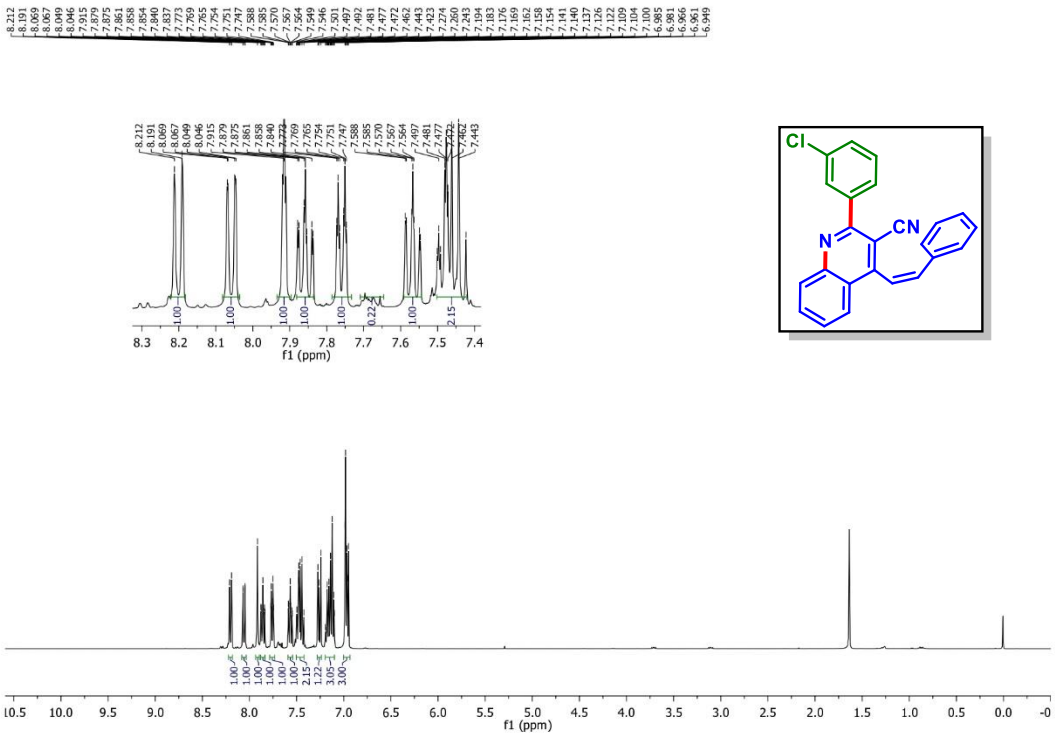

(Z)-2-(3-Chlorophenyl)-4-styrylquinoline-3-carbonitrile (4ao): ^{13}C{^{1}H} NMR (CDCl$_3$, 125 MHz)

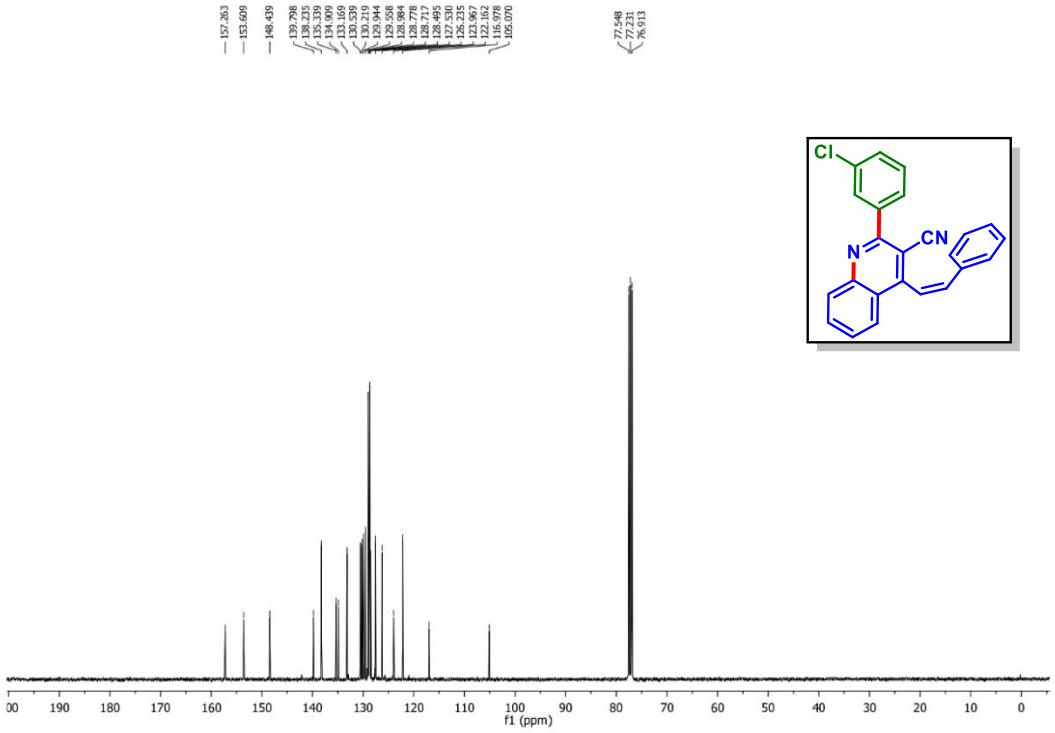

II.12. References:

[1] (a) Michael, J. P. *Nat. Prod. Rep.* **2008**, *25*, 166–187. (b) Solomon, V. R.; Lee, H. *Curr. Med. Chem.* **2011**, *18*, 1488–1508. (c) Mu, L.; Shi, W.; Chang, J. C.; Lee, S. T. *Nano Lett.* **2008**, *8*, 104–109. (d) Henry, G. D. *Tetrahedron* **2004**, *60*, 6043–6061.

[2] (a) Portela, C.; Afonso, C. M. M.; Pinto, M. M. M.; Ramos, M. J. *Bioorg. Med. Chem.* **2004**, *12*, 3313–3321. (b) Ali, S.; Khan, A. T. *Org. Biomol. Chem.* **2021**, *19*, 7041–7050. (c) Karki, R.; Thapa, P.; Yoo, H. Y.; Kadayat, T. M.; Park, P.-H.; Na, Y.; Lee, E.; Jeon, K.-H.; Cho, W.-J.; Choi, H.; Kwon, Y.; Lee, E.-S. *Eur. J. Med. Chem.* **2012**, *49*, 219–228. (d) Singh, B.; Ryan, H.; Kredo, T.; Chaplin, M.; Fletcher, T. *Cochrane Database of Systematic Reviews*, **2021**, DOI: 10.1002/14651858.CD013587.pub2. (e) Schwartz, I. S., Boulware, D. R., Lee, T. C. doi: 10.1016/j.lana.2022.100268.

[3] (a) Kraup, S. *Berichte* **1880**, *13*, 2080–2086. (b) Henze, H. R.; Carroll, D. W. *J. Am. Chem. Soc.* **1954**, *76*, 4580–4584. (c) Denmark, S. E.; Venkatraman, S. *J. Org. Chem.* **2006**, *71*, 1668–1676. (d) Hantzsch, A. *Ber. Dtsch. Chem. Ges.* **1881**, *14*, 1637–1638. (e) Kröhnke, F. *Synthesis* **1976,** *1*, 1–24.

[4] (a) Saunthwal, R. K.; Patel, M.; Verma, A. K. *Org. Lett.* **2016**, *18*, 2200–2203. (b) Kumar, G. R.; Kumar, R.; Rajesh, M.; Reddy, M. S. *Chem. Commun.* **2018**, *54*, 759–762. (c) Gulevich, A. V.; Dudnik, A. S.; Chernyak, N.; Gevorgyan, V. *Chem. Rev.* **2013**, *113*, 3084–3213.

[5] (a) Jiang, H.; An, X.; Tong, K.; Zheng, T.; Zhang, Y.; Yu, S. *Angew. Chem., Int. Ed.* **2015**, *54*, 4055–4059. (b) Sahoo, B.; Hopkinson, M. N.; Glorius, F. *Angew. Chem., Int. Ed.* **2015**, *54*, 15545–15549. (c) Das, A.; Ghosh, I.; König, B. *Chem. Commun.* **2016**, *52*, 8695–8698.

[6] (a) Wang, C.; Dong, G. *J. Am. Chem. Soc.* **2018**, *140*, 6057–6061. (b) Chen, S.; Meervelt, L. V.; Eycken, E. V. V.; Sharma, U. K. *Org. Lett.* **2022**, *24*, 1213–1218. (c) Feng, Z.; Min, Q.-Q.; Xiao, Y.-L.; Zhang, B.; Zhang, X. *Angew. Chem., Int. Ed.* **2014**, *53*, 1669–1673.

[7] (a) Chuentragool, P.; Kurandina, D.; Gevorgyan, V. *Angew. Chem., Int. Ed.* **2019**, *58*, 11586–11598. (b) Cheung, K. P. S.; Sarkar, S.; Gevorgyan, V. *Chem. Rev.* **2022**, *122*, 1543−1625. (c) Parasram, M.; Gevorgyan, V. *Chem. Soc. Rev.* **2017**, *46*, 6227–6240.

[8] (a) Dhara, H. N.; Rakshit, A.; Alam, T.; Patel, B. K. *Org. Biomol. Chem.* **2022**. *20*, 4243–4277. (b) Rakshit, A.; Kumar, P.; Alam, T.; Dhara, H.; Patel, B. K. *J. Org. Chem.* **2020**, *85*, 12482–12504. (c) Rakshit, A.; Dhara, H. N.; Sahoo, A. K.; Patel, B. K. *Chem Asian J.* **2022**, *17*, e202200792.

[9] Xu, T.; Shao, Y.; Dai, L.; Yu, S.; Cheng, T.; Chen, J. *J. Org. Chem.* **2019**, *84*, 13604–13614.

[10] Zhao, Z.; Zeng, G.; Chen, Y.; Zheng, J.; Chen, Z.; Shao, Y.; Zhang, F.; Chen, J.; Li, R. *Org. Lett.* **2021**, *23*, 7955–7960.

[11] Sheng, J.; Wang, Y.; Su, X.; He, R.; Chen, C. *Angew. Chem., Int. Ed.* **2017**, *56*, 4824–4828.

[12] Onodera, G.; Shimizu, Y.; Kimura, J.; Kobayashi, J.; Ebihara, Y.; Kondo, K.; Sakata, K.; Takeuchi, R. *J. Am. Chem. Soc.* **2012**, *134*, 10515–10531.

[13] (a) Li, H.; Wu, X.; Hao, W.; Li, H.; Zhao, Y.; Wang, Y.; Lian, P.; Zheng, Y.; Bao, X.; Wan, X. *Org. Lett.* **2018**, *20*, 5224–5227. (b) Youn, S. W.; Lee, E. M. *Org. Lett.* **2016**, *18*, 5728–5731. (c) Sahoo, A. K.; Rakshit, A.; Dahiya, A.; Pan, A.; Patel, B. K. *Org. Lett.* **2022**, *24*, 1918–1923.

[14] (a) Bhattacharya, T.; Ghosh, A.; Maiti, D. *Chem. Sci.* **2021**, *12*, 3857–3870. (b) Li, G.; Wan, L.; Zhang, G.; Leow, D.; Spangler, J.; Yu, J.-Q. *J. Am. Chem. Soc.* **2015**, *137*, 4391–4397. (c) Ghosh, S.; Khandelia, T.; Patel, B. K. *Org. Lett.* **2021**, *23*, 7370–7375. (d) Nunewar, S.; Kumar, S.; Priyanka, P.; Girase, P.; Kanchupalli, V. *Chem. Commun.* **2022**, *58*, 6140–6143.

[15] (a) Stout, D. M.; Meyers, A. I. *Chem. Rev.* **1982**, *82*, 223–243. (b) Allais, C.; Liéby-Muller, F.; Rodriguez, J.; Constantieux, T. *Eur. J. Org. Chem.* **2013**, *19*, 4131–4145. (c) Kelly, T. R.; Lebedev, R. L. *J. Org. Chem.* **2002**, *67*, 2197–2205. (d) Adib, M.; Tahermansouri, H.; Koloogani, S. A.; Mohammadia, B.; Bijanzadeh, H. R. *Tet. Lett.* **2006**, *47*, 5957–5960.

[16] K. R. Roesch, R. C. Larock, *J. Org. Chem.* **2002**, *67*, 86–94.

[17] (a) Neely, J. M.; Rovis, T. *Org. Chem. Front.* **2014**, *1*, 1010–1015. (b) Boger, D. L. *Chem. Rev.* **1986**, *86*, 781–793. (c) Wu, J.; Xu, W.; Yu, Z.-X.; Wang, J. *J. Am. Chem. Soc.* **2015**, *137*, 9489–9496. (d) Monbaliu, J.-C. M.; Masschelein, K. G. R.; Stevens, C. V. *Chem. Soc. Rev.* **2011**, *40*, 4708–4739. (e) Foster, R. A. A.; Willis, M. C. *Chem. Soc. Rev.* **2012**, *42*, 63–76. (f) Parthasarathy, K.; Jeganmohan, M.; Cheng, C.-H. *Org. Lett.* **2008**, *10*, 325–328.

[18] (a) McCormick, M. M.; Duong, H. A.; Zuo, G.; Louie, J. *J. Am. Chem. Soc.* **2005**, *127*, 5030–5031. (b) Heller, B.; Hapke, M. *Chem. Soc. Rev.* **2007**, *36*, 1085–1094. (c) Kumar, P.; Prescher, S.; Louie, J. *Angew. Chem., Int. Ed.* **2011**, *50*, 10694–10698. (d) Onodera, G.; Shimizu, Y.; Kimura, J.; Kobayashi, J.; Ebihara, Y.; Kondo, K.; Sakata, K.; Takeuchi, R. *J. Am. Chem. Soc.* **2012**, *134*, 10515–10531. (e) Karad, S. N.; Liu, R.-S. *Angew. Chem. Int. Ed.* **2014**, *53*, 9072–9076. (f) Sakai, T.; Danheiser, R. L. *J. Am. Chem. Soc.* **2010**, *132*, 13203–13205. (g) Xie, L.-G.; Shaaban, S.; Chen, X.; Maulide, N. *Angew. Chem. Int., Ed.* **2016**, *55*, 12864–12867.

[19] Yao, X.; Qi, L.; Li, R.; Zhen, Q.; Liu, J.; Zhao, Z.; Shao, Y.; Hu, M.; Chen, J. *ACS Comb. Sci*. **2020**, *22*, 114–119.

[20] Zhen, Q.; Li, R.; Qi, L.; Hu, K.; Yao, X.; Shao, Y.; Chen, J. *Org. Chem. Front.* **2020**, *7*, 286–291.

[21] (a) Kouznetsov, V.; Mendez, L. Y.; Gomez, C. M. *Curr. Org. Chem.* **2005**, *9*, 141–161. (b) Batista, V. F.; Pinto, D. C. G. A.; Silva, A. M. S. *ACS Sustainable Chem. Eng.* **2016**, *4*, 4064–4078. (c) Prajapati, S. M.; Patel, K. D.; Vekariya, R. H.; Panchal, S. N.; Patel, H. D. *RSC Adv.* **2014**, *4*, 24463–24476.

[22] Bharathkumar, H.; Mohan, C. D.; Ananda, H.; Fuchs, J. E.; Li, F.; Rangappa, S.; Surender, M.; Bulusu, K. C.; Girish, K. S.; Sethi, G.; Bender, A.; Basappa; Rangappa, K. S. *Bioorg. Med. Chem. Lett.* **2015**, *25*, 1804–1807.

[23] Zheng, J.; Li, Z.; Huang, L.; Wu, W.; Li, J.; Jiang, H. *Org. Lett.* **2016**, *18*, 3514–3517.

[24] Khan, S.; Volla, C. M. R. *Chem. Eur. J.* **2017**, *23*, 12462–12466.

[25] Chen, S.-J.; Lu, G.-P.; Cai, C. *Synthesis* **2015**, *47*, 976–984.

[26] Xu, T.; Shao, Y.; Dai, L.; Yu, S.; Cheng, T.; Chen, J. *J. Org. Chem.* **2019**, *84*, 13604–13614.

[27] Zhang, Y.; Chen, L.; Shao, Y.; Zhang, F.; Chen, Z.; Lv, N.; Chen, J.; Li, R. *Org. Chem. Front.* **2021**, *8*, 254–259.

[28] Anbalagan, V. *J. Coord. Chem.* **2003**, *56*, 161–172.

[29] (a) Li, Z.; García-Domínguez, A.; Nevado, C. *J. Am. Chem. Soc.* **2015**, *137*, 11610–11613. (b) Fredricks, M. A.; Drees, M.; Köhler, K. *ChemCatChem* **2010**, *2*, 1467–1476. (c) Morris, J. H.; Gysling, H. J.; Reed, D. *Chem. Rev.* **1985**, *85*, 51–76. (d) Amgoune, A.; Bourissou, D. *Chem. Commun.* **2011**, *47*, 859–871.

[30] (a) Rahman, S. M. A.; Sonoda, M.; Ono, M.; Miki, K.; Tobe; Y. *Org. Lett.* **2006**, *8*, 1197–1200. (b) Chen, C.; Voss, T.; Fröhlich, R.; Kehr, G.; Erker. G. *Org. Lett.* **2011**, *13*, 62–65. (c) Xu, K.; Fang, Y.; Yan, Z.; Zha, Z.; Wang, Z. *Org. Lett.* 2013, *15*, 2148–2151.

[31] (a) Zeng, G.; Liu, J.; Shao, Y.; Zhang, F.; Chen, Z.; Lv, N.; Chen, J.; Li, R. *J. Org. Chem.* **2021**, *86*, 861–867. (b) Ghosh, S.; Pal, S.; Rajamanickam, S.; Shome, R.; Mohanta, P. R.; Ghosh, S. S.; Patel, B. K. *ACS Omega* **2019**, *4*, 5565–5577. (c) Hall, J. H.; Gisler, M. *J. Org. Chem*. **1976**, *41*, 3769–3770. (d) Zheng, J.; Huang, L.; Huang, C.; Wu, W.; Jiang, H. *J. Org. Chem.* **2015**, *80*, 1235–1242. (e) Palav, A.; Misal, B.; Ernolla, A.; Parab, V.; Waske, P.; Khandekar, D.; Chaudhary, V.; Chaturbhuj, G. *Org. Process Res. Dev.* **2019**, *23*, 244–251. (f) Reddy, N. N. K.; Rao, S. N.; Patil, R. D.; Adimurthy, S. *Adv. Mater. Sci.* **2018**, *3*, 1–7.

[32] (a) Li, E.; Huang, Y. *Chem. Commun.* **2014**, *50*, 948–950. (b) Tian, J.; Sun, H.; Zhou, R.; He, Z. *Chin. J. Chem.* **2013**, *31*, 1348−1351. (c) Kang, T.-R.; Chen, L.-M. *Acta Cryst.* **2009**, *65*, o3164.

[33] (a) Metternich, J. B. Gilmour, R. *Synlett*, 2016, **27**, 2541–2552. (b) T. Nevesely, M. Wienhold, J. J. Molloy and R. Gilmour, *Chem. Rev.*, 2022, **122**, 2650−2694.

[34] Frisch, M. J.; Trucks, G. W.; Schlegel, H. B.; Scuseria, G. E.; Robb, M. A.; Cheeseman, J. R.; Scalmani, G.; Barone, V.; Mennucci, B.; Petersson, G. A.; Nakatsuji, H.; Caricato, M.; Li, X.; Hratchian, H. P.; Izmaylov, A. F.; Bloino, J.; Zheng, G.; Sonnenberg, J. L.; Hada, M.; Ehara, M.; Toyota, K.; Fukuda, R.; Hasegawa, J.; Ishida, M.; Nakajima, T.;

Honda, Y.; Kitao, O.; Nakai, H.; Vreven, T.; Montgomery, J. A., Jr.; Peralta, J. E.; Ogliaro, F.; Bearpark, M.; Heyd, J. J.; Brothers, E.; Kudin, K. N.; Staroverov, V. N.; Kobayashi, R.; Normand, J.; Raghavachari, K.; Rendell, A.; Burant, J. C.; Iyengar, S. S.; Tomasi, J.; Cossi, M.; Rega, N.; Millam, N. J.; Klene, M.; Knox, J. E.; Cross, J. B.; Bakken, V.; Adamo, C.; Jaramillo, J.; Gomperts, R.; Stratmann, R. E.; Yazyev, O.; Austin, A. J.; Cammi, R.; Pomelli, C.; Ochterski, J. W.; Martin, R. L.; Morokuma, K.; Zakrzewski, V. G.; Voth, G. A.; Salvador, P.; Dannenberg, J. J.; Dapprich, S.; Daniels, A. D.; Farkas, Ö .; Foresman, J. B.; Ortiz, J. V.; Cioslowski, J.; Fox, D. J. Gaussian 09, Revision D.01; Gaussian, Inc.: Wallingford, CT, 2013.

[35] Marenich, A. V.; Cramer, C. J.; Truhlar, D. G. *J. Phys. Chem. B.* **2009**, *113*, 6378–6396.

[36] Grimme, S.; Antony, J.; Ehrlich, S.; Krieg, H. *J. Chem. Phys*. **2010**, *132*, 154104–154119.

CHAPTER III

Pd(II)-Catalyzed Three-Component Synthesis of Furo[2,3-d]pyrimidines from β-Ketodinitriles, Boronic Acids, and Aldehydes

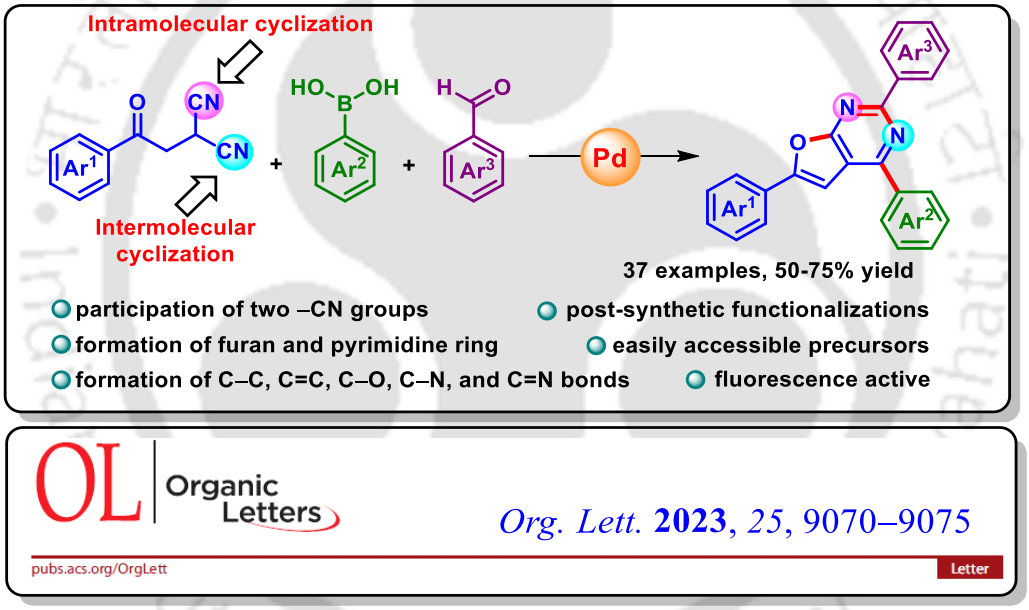

ABSTRACT: A Pd(II)-catalyzed three-component synthesis of 2,4,6-triarylfuro[2,3-*d*]pyrimidines from β-ketodinitriles, boronic acids, and aldehydes has been developed. The participation of both nitrile (–CN) groups led to the concurrent construction of furo-pyrimidine via the formation of C–C, C=C, C–O, C–N, and C=N bonds. The compounds show excellent photoluminescence properties with absorption maxima ranging from 348 to 387 nm and emission from 468 to 533 nm. The synthetic utility of the protocol was further demonstrated through a few postsynthetic manipulations.

भारतीय प्रौद्योगिकी संस्थान गुवाहाटी
Indian Institute of Technology Guwahati

CHAPTER III

Pd(II)-Catalyzed Three-Component Synthesis of Furo[2,3-*d*]pyrimidines from β-Ketodinitriles, Boronic Acids, and Aldehydes

III.1. Introduction:

The fused *N*-heterocyclic ring is a useful scaffold and plays a significant role in the design and discovery of new pharmacologically active molecules.[1] Specifically, the furan core is an essential five-membered *O*-heterocycle found in many natural products, biologically active molecules, pharmaceuticals, and functional materials.[2] The furo-pyrimidines are also identified as promising candidates in several bioactive compounds. Such a core has received attention due to its antitumor, analgesic, antihypertensive, and anti-inflammatory activities and as a potent adenosine kinase inhibitor even at very low concentrations (Figure III.1.1).[3] In addition, due to the π-extended features and remarkable photophysical properties, furopyrimidines have found their application as organic light-emitting diodes (OLED) and fluorescent dyes.[4]

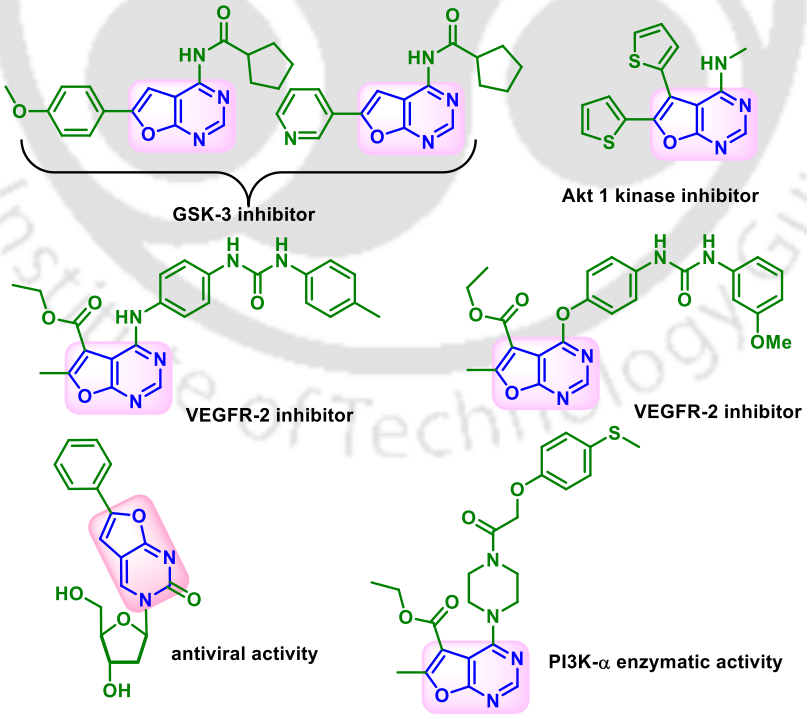

Figure III.1.1. *Representative bioactive furo[2,3-d]pyrimidines.*

Nitrile has been recognized as one of the most versatile and appreciated functional groups in organic chemistry.[5] Despite being stable and inherently inert, the nitrile group undergoes transition-metal-catalyzed alkyne insertion and annulations,[6a-6c] cycloadditions,[6d-6e] C–H bond functionalizations,[6f-6g,] and nucleophilic or radical cascade addition/cyclizations.[5c,6h-6i] Among these, the transition-metal-catalyzed cascade addition/cyclization opens up new exciting strategies for the synthesis of a large variety of functional molecules through the concomitant formation of C–C, C-N, C=O, and C=N bonds.[7] In the past decade, a series of Pd(II)-catalyzed reactions with nitrile have been developed and the concept of catalytic carbopalladation has been extended in the construction of *N*-heterocycles.[5b-5e] The reaction of various functionalized nitriles via a Pd(II)-catalyzed tandem cascade addition/cyclization with aryl boronic acids led to the synthesis of indoles, 2-arylquinolines, and pyrroles (Scheme III.1.1a–c).[8] The concept has recently been extended to visible-light mediated construction of pyridine and pyrrole from γ-ketodinitrile and β-ketodinitrile respectively, in which one of the nitrile groups participated and the other remained inert (Scheme III.1.1d).[9] However, in a Pd(II) catalyzed reaction between β-ketodinitrile and internal alkyne as coupling partners, both nitrile groups actively participated giving furo[2,3-*b*]pyridine.[6a] Apart from the nitriles and aryl boronic acids, aldehydes also play an important role as a coupling partner in a transition-metal-catalyzed addition/cyclization process for the construction of *N*-heterocycles.[10]

Our increasing interest in this domain and taking cues from the palladium-catalyzed addition reactions of the nitrile via carbopalladation, herein we report a Pd(II)-catalyzed addition of aryl boronic acids to β-ketodinitriles in the presence of aldehydes, providing an elegant protocol for the synthesis of a highly fluorescent furo[2,3-*d*]pyrimidines (Scheme III.1.1e). This cascade construction of furan and pyrimidine rings involves the concurrent participation of both the nitrile groups via the formation of C–C, C=C, C–O, C–N, and C=N bonds in one pot.

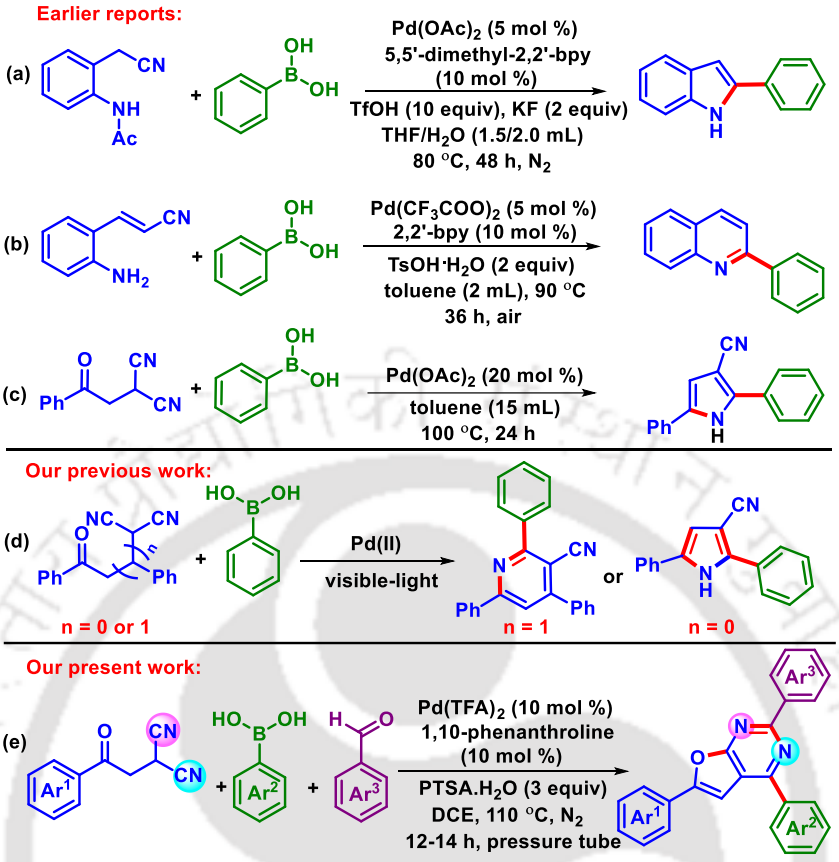

Scheme III.1.1. *Various approaches for the addition of boronic acid to nitriles.*

III.2. Strategies for the Synthesis of Furo[2,3-*d*]pyrimidine:

Fused furo[2,3-*d*]pyrimidines have shown remarkable biological properties such as antitumor, antibacterial, and antihypertensive activities.[4,11,12] Owing to the importance of this furo-pyrimidine core, numerous reactions have been established for their synthesis. Consequently, emerging an effective and mild process from easily available starting precursors to create furopyrimidine derivatives remains highly anticipated in modern organic chemistry.

III.2.1. Synthesis of the Furo[2,3-*d*]pyrimidine Derivatives from Furans:

Several groups have developed the synthesis of furopyrimidine derivatives from furan core unit, a few examples are listed below. In 2005, Lee *et al.* developed a synthesis of furo[2,3-*d*]pyrimidine starting from 1-amino-2-cyano-3,4-disubstituted furans (Scheme III.2.1.1).[4,11a] The reaction proceeds via formylation of the amino group, transformation of the cyano group to an amide, and the subsequent attack of the amino group on the carbonyl group.

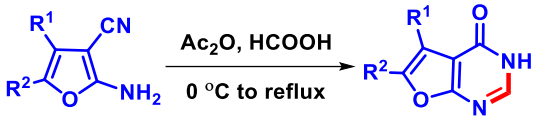

Scheme III.2.1.1. *Synthesis of furo[2,3-d]pyrimidines using Ac_2O.*

In 2007, Yoo and coworkers reported the synthesis of a series of furo[2,3-*d*]pyrimidines via the cyclization of 1-amino-2-cyano-3,4-disubstituted furans with acetic anhydride in formamide and with acetic anhydride in formic acid (Scheme III.2.1.2).[11b]

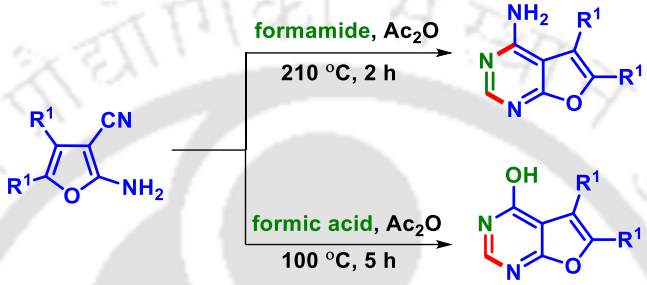

Scheme III.2.1.2. *Synthesis of furo[2,3-d]pyrimidines using formamide and formic acid.*

Later, in 2010, Hu and Ding's group developed an efficient iminophosphorane-mediated synthesis of ethyl 4-alkylamino-2-arylamino-6-methyl-furo[2,3-*d*]pyrimidine-5-carboxylate via aza-Wittig reactions (Scheme III.2.1.3).[11c] This two-step method involved the reaction of aromatic isocyanates with iminophosphorane to produce carbodiimides, which were then reacted with NH_3 to form ethyl 3,4-dihydro-6-methyl-4-oxo-2-arylaminofuro[2,3-*d*]pyrimidine-5-carboxylates.

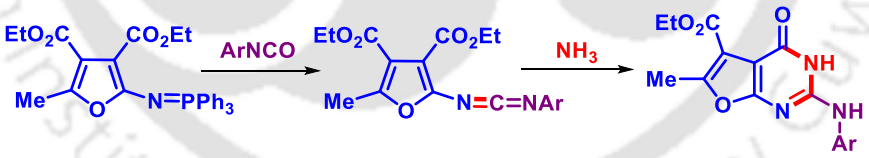

Scheme III.2.1.3. *Iminophosphorane-mediated synthesis of furo[2,3-d]pyrimidines.*

In 2017, Kaçan's group developed a multistep synthesis of 1,2-dihydrofuro[3,4-*d*]pyrimidines starting from dimethyl furan-3,4-dicarboxylate (Scheme III.2.1.4).[11d] The protocol involves the rearrangement of the azide group to the corresponding isocyanate at the ortho position, followed by cyclization with N, O, and S nucleophiles to yield the furopyrimidines.

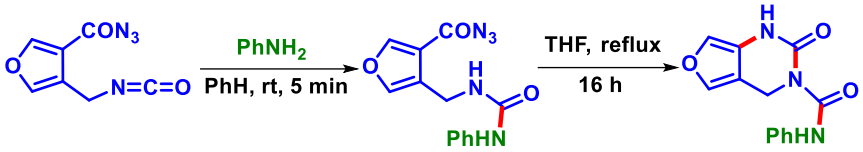

Scheme III.2.1.4. *Curtius rearrangement and intramolecular cyclization for synthesis of furopyrimidine.*

III.2.2. Synthesis of the Furo[2,3-*d*]pyrimidine Derivatives from Pyrimidines:

Furopyrimidines have also been synthesized from pyrimidine derivatives with a hydroxyl or keto group adjacent to the nitrogen of the pyrimidine ring. For example, in 2009, Zhao *et al.* established a method to access furopyrimidine derivatives by refluxing 1-chloro-1-nitroethene with 4,6-dihydroxy pyrimidines in ethanol (Scheme III.2.2.1).[12a]

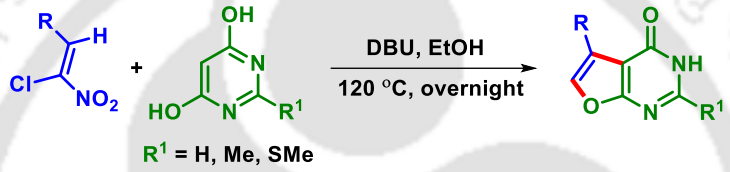

Scheme III.2.2.1. *Synthesis of furopyrimidine from 4,6-dihydroxy pyrimidines.*

Similarly, Zhang's group reported a catalyst-free approach for constructing furo[2,3-*d*]pyrimidine derivatives via a [3+2] cyclization of pyrimidine-4,6-diol with various nitroolefins. (Scheme III.2.2.2).[12b]

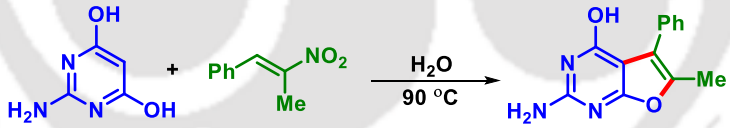

Scheme III.2.2.2. *Synthesis of furopyrimidine via [3 + 2] cyclization.*

A condensation method was developed to synthesize furopyrimidine by Gangjee *et al.* using 2-aminopyrimidin-4-ol and 2-chloroacetyl derivative in DMF at room temperature (Scheme III.2.2.3).[12c]

Scheme III.2.2.3. *Condensation method for synthesis of furopyrimidine.*

In 2007, Robins and co-workers established a one-pot approach to access furo[2,3-*d*]pyrimidine. This reaction involves two steps: the first step is the Sonogashira coupling of terminal alkynes with a 5-iodouracil derivative, followed by an *in situ* Cu(I)-promoted intramolecular cyclization, leading to furo[2,3-*d*]pyrimidine with excellent yields (Scheme III.2.2.4).[12d]

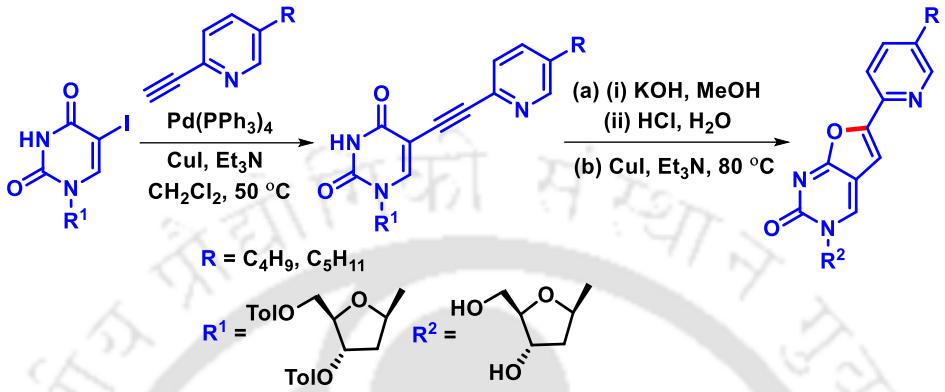

Scheme III.2.2.4. *Pd/Cu-catalyzed synthesis of furopyrimidine.*

Agrofoglio's group introduced a strategy for the synthesis of acyclic nucleosides featuring 5-alkynyl and 6-alkylfuro[2,3-*d*]pyrimidines via a 5-*endo-dig* electrophilic cyclization in the presence of $AgNO_3$ (Scheme III.2.2.5).[12e]

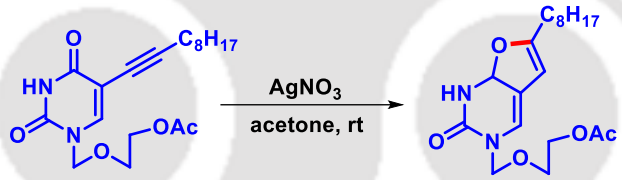

Scheme III.2.2.5. *Synthesis of furopyrimidine via 5-endo-dig cyclization.*

Later, Dembinski's group reported a 5-*endo-dig* cycloisomerization of 1,4- and 1,2,4-aryl-substituted but-3-yn-1-ones using a catalytic amount of zinc chloride etherate (10 mol %) in dichloromethane at room temperature, yielding substituted furo[2,3-*d*]pyrimidines (Scheme III.2.2.6).[12f]

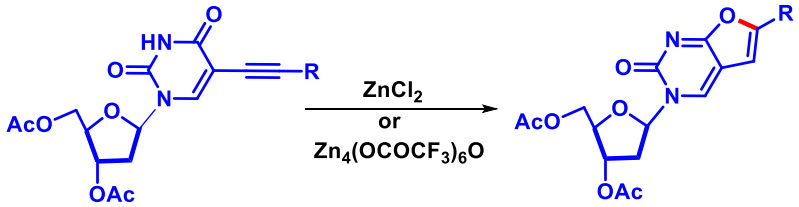

Scheme III.2.2.6. *Zn(II)-catalyzed synthesis of furopyrimidine.*

III.3. Present Work:

III.3.1. Optimization of the Reaction Conditions:

We began our investigation by anticipating a $Pd(OAc)_2$ (10 mol %) coupling of 2-(2-oxo-2-phenylethyl)malononitrile (**1**) (0.25 mmol), phenylboronic acid (**a**) (0.5 mmol, 2 equiv), and benzaldehyde (**a′**) (0.375 mmol, 1.5 equiv) in the presence of 1,10-phenanthroline (10 mol %) and *p*-toluenesulfonic acid ($PTSA{\cdot}H_2O$, 2 equiv) in 1,2-dichloroethane (DCE) (2 mL) at 110 °C under a N_2 atmosphere for 12 h. Gratifyingly, a new blue fluorescent spot (viewed under a 365 nm UV lamp) was observed and the isolated product was found to be furo[2,3-*d*]pyrimidine (**1aa′**, 54%) as confirmed from various spectroscopic analyses (Table III.3.1, entry 1). In addition, the formation of a furo-pyrimidine core skeleton was reconfirmed by the single-crystal X-ray diffraction of one of its derivatives [**1ea′** (Scheme III.3.2.1)]. After a series of reactions, the optimal condition for this protocol was found to be the use of β-ketodinitrile (**1**) (0.25 mmol), phenylboronic acid (**a**) (0.75 mmol, 3 equiv), benzaldehyde (**a′**) (0.375 mmol, 1.5 equiv), $Pd(TFA)_2$ (10 mol %), 1,10-phenanthroline (10 mol %) and $PTSA{\cdot}H_2O$ (3 equiv) in 1,2-dichloroethane (DCE) (2 mL) at 110 °C in a pressure tube under a N_2 atmosphere for 12 h.

To determine the best optimal reaction conditions, further screening of different reaction parameters was commenced. Initially, different solvents such as toluene (20%), dichloromethane (38%), CH_3CN (trace), DMF (48%), DMSO (43%), EtOH (n.d) instead of DCE were used but none could improve the yield of the product (Table III.3.1, entries 2–7). Increasing the loading of $PTSA{\cdot}H_2O$ from 2 to 3 equiv keeping all other parameters constant enhanced the yield of (**1aa′**) to 61% (Table III.3.1, entry 8). Maintaining the amount of $PTSA.H_2O$ to 3 equiv and increasing the loading of phenylboronic acid (**a**) from 2 to 3 equiv the product yield improved to 65% (Table III.3.1, entry 9). Next, diverse Pd-catalysts such as $Pd(TFA)_2$, $PdCl_2$ (30%), $Pd(PPh_3)_2Cl_2$ (25%), and $Pd(PPh_3)_4$ (trace) were screened, however, only $Pd(TFA)_2$ led to the anticipated product in 71% yield and all others were inefficient to improve the yield (Table III.3.1, entries 10-13). Screening of other bidentate as well as monodentate ligands *viz.* 2,2′-bipyridine (49%), Xphos (00%), and PPh_3 (trace) failed to improve the yield (Table III.3.1, entries 14–16). Replacement of $PTSA{\cdot}H_2O$ with other additives such as AcOH, CF_3SO_3H, and $PhCO_2H$ were found ineffective in improving the yield (Table III.3.1, entries 17–19). However, omitting either the catalyst {$Pd(TFA)_2$}, ligand (1,10-phenanthroline), or additive ($PTSA{\cdot}H_2O$) completely inhibited the reaction (Table III.3.1,

entries 20–22). The same reaction in an air atmosphere provided a slightly lower yield (66%) (Table III.3.1, entry 23). Lowering the reaction temperature to 80 °C, had a detrimental effect as the product yield dropped to 52% (Table III.3.1, entry 24). No significant improvement in the yield was observed even on prolonging the reaction to 24 h (72%) (Table III.3.1, entry 25). Additionally, upon reducing the Pd-catalyst loading from 10 mol % to 5 mol % a lower yield (60%) of the product was observed (Table III.3.1, entries 26).

After a series of reactions the best-optimized condition for this protocol was found to be the use of β-ketodinitrile (**1**) (0.25 mmol), phenylboronic acid (**a**) (0.75 mmol, 3 equiv), benzaldehyde (**a′**) (0.375 mmol, 1.5 equiv), $Pd(TFA)_2$ (10 mol %), 1,10-phenanthroline (10 mol %) and $PTSA{\cdot}H_2O$ (3 equiv) in 1,2-dichloroethane (DCE) (2 mL) at 110 °C in a pressure tube under N_2 atmosphere for 12 h (Table III.3.1, entry 10).

Table III.3.1. *Optimization of the Reaction Conditions*[a-g]

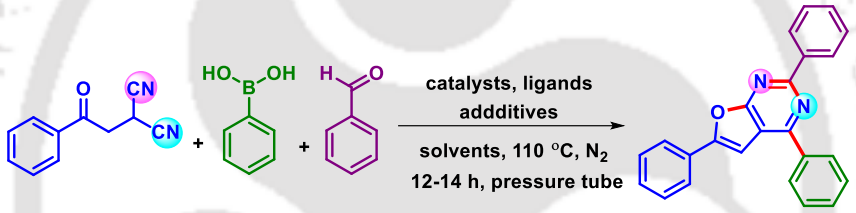

entry	catalyst (mol %)	ligand (mol %)	additive (equiv)	solvent	yield (%)[b]
1	$Pd(OAc)_2$ (10)	1,10-phenanthroline (10)	$PTSA{\cdot}H_2O$ (2)	1,2-DCE	54
2	$Pd(OAc)_2$ (10)	1,10-phenanthroline (10)	$PTSA{\cdot}H_2O$ (2)	Toluene	20
3	$Pd(OAc)_2$ (10)	1,10-phenanthroline (10)	$PTSA{\cdot}H_2O$ (2)	DCM	38
4	$Pd(OAc)_2$ (10)	1,10-phenanthroline (10)	$PTSA{\cdot}H_2O$ (2)	CH_3CN	trace
5	$Pd(OAc)_2$ (10)	1,10-phenanthroline (10)	$PTSA{\cdot}H_2O$ (2)	DMF	48
6	$Pd(OAc)_2$ (10)	1,10-phenanthroline (10)	$PTSA{\cdot}H_2O$ (2)	DMSO	43
7	$Pd(OAc)_2$ (10)	1,10-phenanthroline (10)	$PTSA{\cdot}H_2O$ (2)	EtOH	n.d
8	$Pd(OAc)_2$ (10)	1,10-phenanthroline (10)	$PTSA{\cdot}H_2O$ (3)	1,2-DCE	61
9	$Pd(OAc)_2$ (10)	1,10-phenanthroline (10)	$PTSA{\cdot}H_2O$ (3)	1,2-DCE	65[c]
10	**$Pd(TFA)_2$ (10)**	**1,10-phenanthroline (10)**	**$PTSA{\cdot}H_2O$ (3)**	**1,2-DCE**	**71**
11	$PdCl_2$ (10)	1,10-phenanthroline (10)	$PTSA{\cdot}H_2O$ (3)	1,2-DCE	30
12	$PdCl_2(PPh_3)_2$ (10)	1,10-phenanthroline (10)	$PTSA{\cdot}H_2O$ (3)	1,2-DCE	25
13	$Pd(PPh_3)_4$ (10)	1,10-phenanthroline (10)	$PTSA{\cdot}H_2O$ (3)	1,2-DCE	trace
14	$Pd(TFA)_2$ (10)	2,2'-bipyridyl (10)	$PTSA{\cdot}H_2O$ (3)	1,2-DCE	49
15	$Pd(TFA)_2$ (10)	XPhos (10)	$PTSA{\cdot}H_2O$ (3)	1,2-DCE	00

16	$Pd(TFA)_2$ (10)	PPh_3 (10)	PTSA·H_2O (3)	1,2-DCE	trace
17	$Pd(TFA)_2$ (10)	1,10-phenanthroline (10)	AcOH (3)	1,2-DCE	32
18	$Pd(TFA)_2$ (10)	1,10-phenanthroline (10)	CF_3SO_3H (3)	1,2-DCE	41
19	$Pd(TFA)_2$ (10)	1,10-phenanthroline (10)	$PhCO_2H$ (3)	1,2-DCE	16
20		1,10-phenanthroline (10)	PTSA·H_2O (3)	1,2-DCE	00
21	$Pd(TFA)_2$ (10)		PTSA·H_2O (3)	1,2-DCE	00
22	$Pd(TFA)_2$ (10)	1,10-phenanthroline (10)		1,2-DCE	00
23	$Pd(TFA)_2$ (10)	1,10-phenanthroline (10)	PTSA·H_2O (3)	1,2-DCE	66[d]
24	$Pd(TFA)_2$ (10)	1,10-phenanthroline (10)	PTSA·H_2O (3)	1,2-DCE	52[e]
25	$Pd(TFA)_2$ (10)	1,10-phenanthroline (10)	PTSA·H_2O (3)	1,2-DCE	72[f]
26	$Pd(TFA)_2$ (5)	1,10-phenanthroline (10)	PTSA·H_2O (3)	1,2-DCE	60[g]

[a]Reaction condition: 2-(2-oxo-2-phenylethyl)malononitrile (**1**) (0.25 mmol), phenylboronic acid (**a**) (0.5 mmol), benzaldehyde (**a′**) (0.375 mmol) catalyst (mol %), ligand (mol %), additives (equiv), solvent (2.0 mL) at 110 °C in a pressure tube for 12 h. [b]Isolated yields. [c]3.0 equiv of (**a**) was used. [d]Without N_2. [e]Temperature 80 °C. [f]Yield after 24 h. [g]lower Pd-catalyst loading.

III.3.2. Substrates Scopes for the Synthesis of Furo[2,3-*d*]pyrimidines:

With the optimized condition in hand, the effect of substituents on β-ketodinitriles (**1**–**13**) was scrutinized having phenylboronic acid (**a**) and benzaldehyde (**a′**) as the other reacting partners (Scheme III.3.2.1). The unsubstituted β-ketodinitrile (**1**) reacted with phenylboronic acid (**a**) and benzaldehyde (**a′**) to afford the 2,4,6-triphenylfuro[2,3-*d*]pyrimidine (**1aa′**) in 71% yield. The β-ketodinitriles have electron-donating substituents *viz*., *p*-Me (**2**), *p*-OMe (**3**), and *p*-^{i}Pr (**4**), that all reacted successfully with **a** and **a′**, providing their corresponding furo-pyrimidines (**2aa′**, 69%; **3aa′**, 62%; **4aa′**, 61%) in modest yields (Scheme 2). Similarly, substrates bearing electron-withdrawing groups such as *p*-F (**5**), *p*-Cl (**6**), *p*-Br (**7**), *o*-Br (**8**), and *p*-CF_3 (**9**) all provided their furo-pyrimidines in decent yields (**5aa′**, 64%; **6aa′**, 71%; **7aa′**, 62%; **8aa′**, 60%; **9aa′**, 56%). This methodology was equally successful when the phenyl ring of (**1**) was replaced with benzo[*d*][1,3]dioxole (**10**) and naphthyl (**11**) units giving their respective furo-pyrimidine (**10aa′**, 55%; **11aa′**, 74%). Unfortunately, the β-ketodinitriles having a thiophene (**12**) and tetralone (**13**) failed to give the corresponding products (**12aa′**, 0%; **13aa′**, 0%). This is possibly due to their competitive metal binding with the catalysts making it difficult to participate in the carbopalladation/migration process. The yield of product **1aa′** decreased from 71% to 60% by

performing a large-scale (3 mmol) reaction, suggesting the necessity of further fine-tuning of the reaction parameters (Scheme III.3.2.1).

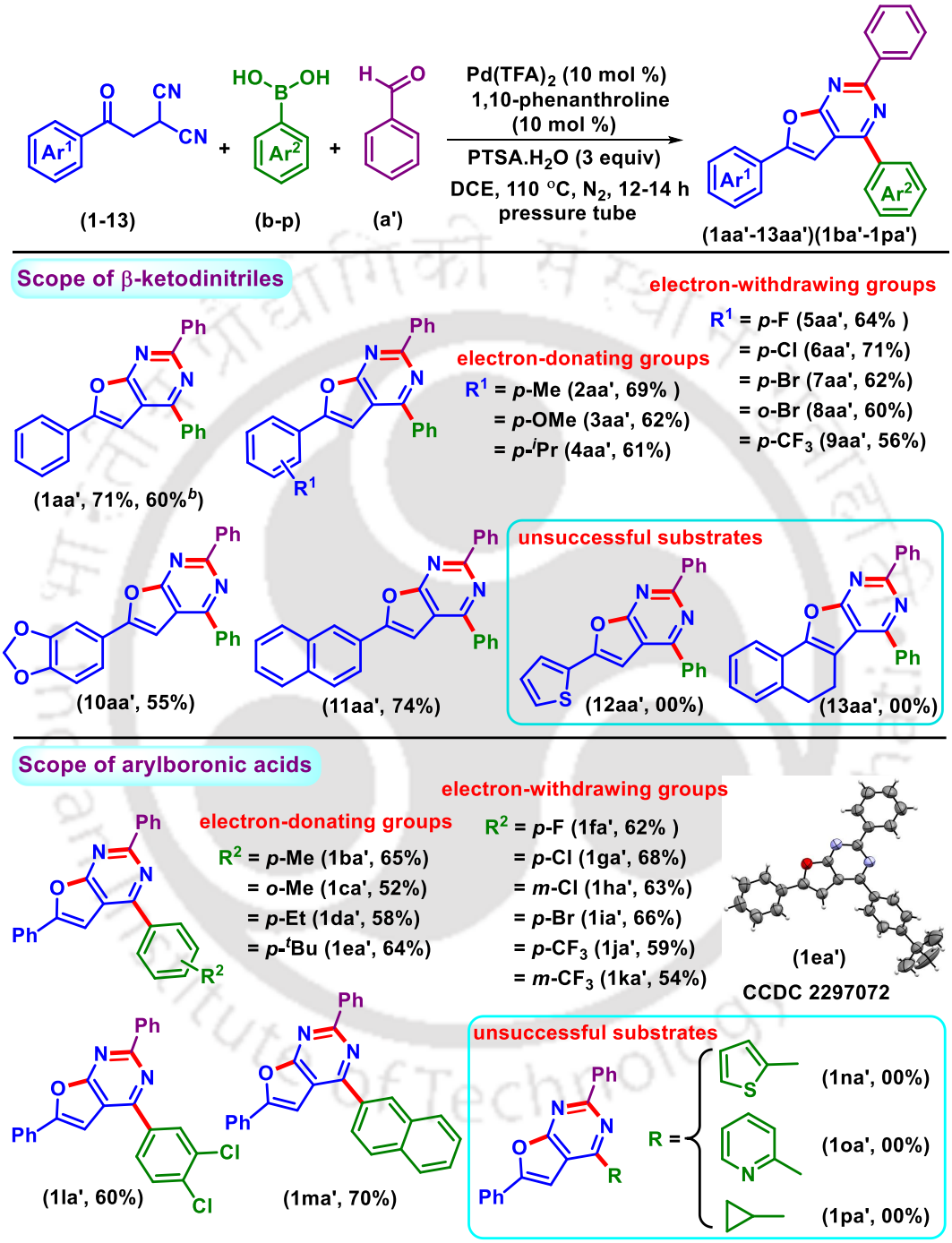

[a]Reaction conditions: **1**–**13** (0.25 mmol), **b-p** (0.75 mmol), benzaldehyde (**a′**, 0.375 mmol), $Pd(TFA)_2$ (0.025 mmol), 1,10-phenanthroline (0.025 mmol), $PTSA{\cdot}H_2O$ (0.75 mmol) and 1,2-DCE (2 mL) at 110 °C in a pressure tube under N_2 atmosphere for 12 h. [b]On a 3 mmol scale. [c]Isolated yield.

Scheme III.3.2.1. *Substrate scope for various β-ketodinitriles and boronic acids.*[a,b,c]

The protocol was further tested with various substituted phenylboronic acids (**b**–**p**), retaining β-ketodinitrile (**1**), and benzaldehyde (**a′**) (Scheme III.3.2.1) as the other partners. Phenylboronic acids possessing electron-donating groups such as *p*-Me (**b**), *o*-Me (**c**), *p*-Et (**d**), and *p*-^{t}Bu (**e**) responded positively affording their respective furopyrimidine (**1ba′**, 65%; **1ca′**, 52%; **1da′**, 58%; **1ea′**, 64%). Phenylboronic acids containing EWGs such as *p*-F (**f**), *p*-Cl **(g**), *m*-Cl **(h**), *p*-Br (**i**), *p*-CF_3 (**j**), and *m*-CF_3 (**k**) all experienced efficient cyclization with **1** and **a′** to yield their anticipated furo-pyrimidines (**1fa′**–**1ka′**) in moderate yields (54–68%). The reaction was also well tolerated with 3,4-dichlorophenylboronic acid (**l**) giving its furo-pyrimidine (**1la′**) in 60% yield. This protocol was also successful with a polyaromatic boronic acid; *viz.*, 2-naphthyl boronic acid (**m**) provides its furo-pyrimidine (**1ma′**) in 70% yield. Furthermore, the reactions with heterocyclic and aliphatic boronic acids such as thiophene-2-boronic acid (**n**), pyridine-2-boronic acid (**o**), and cyclopropyl boronic acid (**p**) all failed to yield their corresponding furo-pyrimidines. This may be due to their competitive metal binding with the Pd catalyst thereby preventing the further catalytic steps.

After successfully synthesizing a library of furo-pyrimidines using various substituted β-keto dinitriles (**1–13**) and boronic acids (**b**–**p**), we then extended the scope of this methodology to substituted aldehydes (**b′**–**p′**) (Scheme III.3.2.2). Aryl-aldehydes possessing electron-donating groups such as *p*-Me (**b′**), *p*-OMe (**c′**), *p*-^{t}Bu (**d′**), *p*-OBu (**e′**), and *p*-SMe (**f′**) positively responded to this protocol, providing their probable products (**1ab′**, 72%; **1ac′**, 70%; **1ad′**, 66%; **1ae′**, 75%; **1af′**, 73%). Aryl aldehydes bearing electron-withdrawing groups such as *p*-F (**g′**), *p*-Cl (**h′**), and *m*-Br (**i′**) underwent smooth heterocyclization upon reaction with β-ketodinitrile (**1**) and phenylboronic acid (**a**) delivering their furo-pyrimidines (**1ag′**, 65%; **1ah′**, 70%; **1ai′**, 66%). The reaction was also tested with 3,4-dimethoxy benzaldehyde (**j′**) and salicylaldehyde (**k′**), which yielded the furo-pyrimidine (**1aj′**, 62%; **1ak′**, 50%). In addition, polyaromatic aldehydes biphenyl-4-carboxaldehyde (**l′**) and 1-naphthyl aldehyde (**m′**) successfully yielded the corresponding furo-pyrimidines (**1al′**, 66%; **1am′**, 64%). Unlike in previous cases, in which thiophene bearing β-ketodinitrile (**12**) and boronic acid (**n**) failed to give the corresponding furopyrimidines, 4-bromothiophene-2-carboxaldehyde (**n′**) successfully provided its furopyrimidine (**1an′**) in 68% yield upon reaction with β-ketodinitrile (**1**) and boronic acid (**a**). Aliphatic aldehydes such as cyclohexane carboxaldehyde (**o′**) effectively delivered furopyrimidine (**1ao′**) in 53% yield. 4-Bromothiophene-2-carboxaldehyde (**n′**) was successful in this protocol, but pyridine-2-

carboxaldehyde (**p′**) failed to give the corresponding furo-pyrimidine (**1ap′**, 0%). This might be due to the competitive metal binding of the heteroatom with the Pd catalyst.

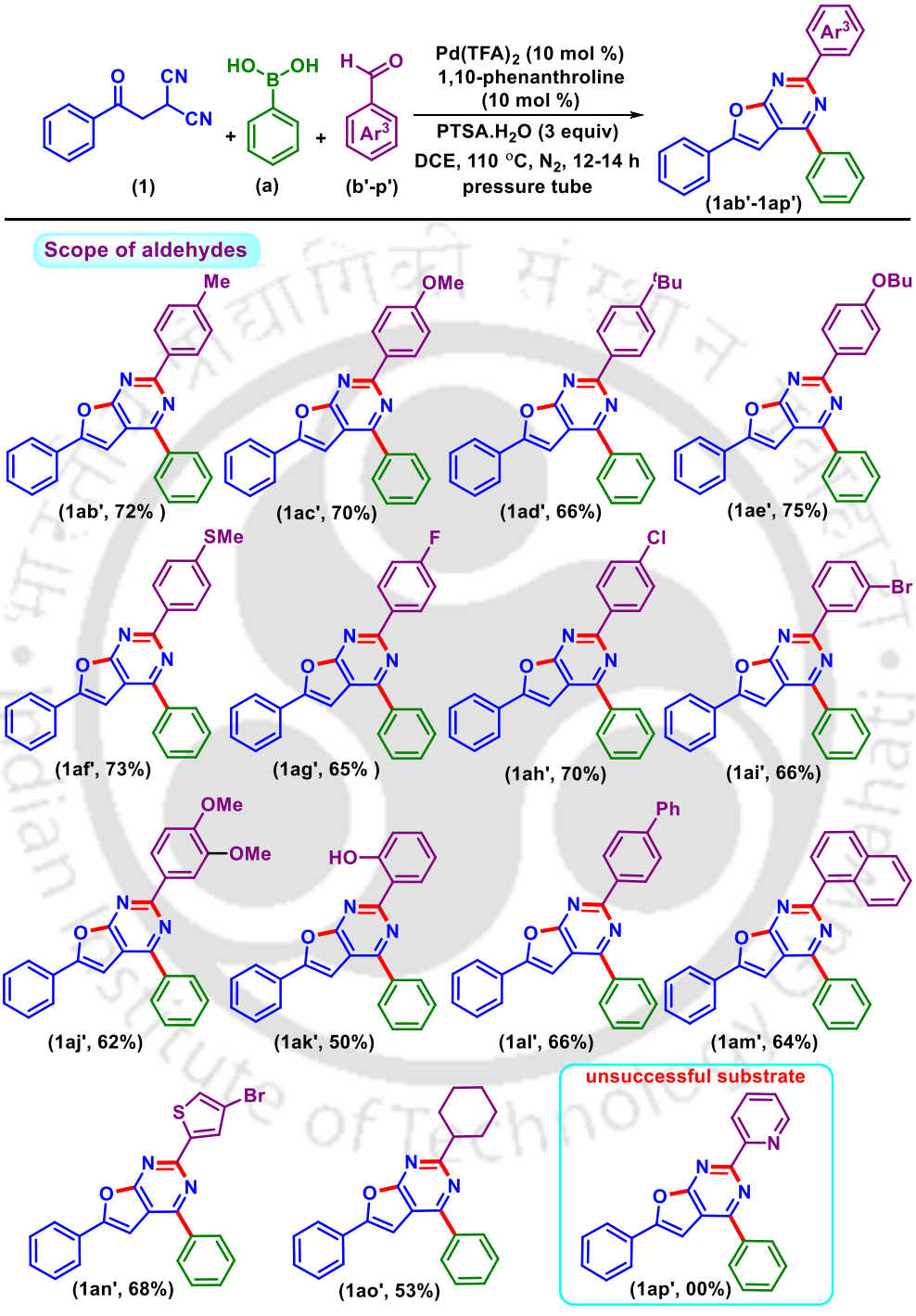

[a]Reaction conditions: **1** (0.25 mmol), **a** (0.75 mmol), (**b′–p′**) (0.375 mmol), $Pd(TFA)_2$ (0.025 mmol), 1,10-phenanthroline (0.025 mmol), $PTSA{\cdot}H_2O$ (0.75 mmol) and 1,2-DCE (2 mL) at 110 °C in a pressure tube under N_2 atmosphere for 12 h. [b]Isolated yield.

Scheme III.3.2.2. *Substrate scope for aldehydes.*[a,b]

III.4. Mechanistic Investigations:

III.4.1. Control Experiments:

Next, to illustrate a plausible reaction mechanism, a few control experiments were carried out for this Pd(II)-catalyzed cyclization reaction (Scheme 4). When β-ketodinitrile **1** was treated in the absence of phenylboronic acid (**a**) and benzaldehyde (**a′**), it yielded 2-amino-5-phenylfuran-3-carbonitrile **1′** in 80% yield [Scheme III.4.1.1], suggesting its intermediacy.

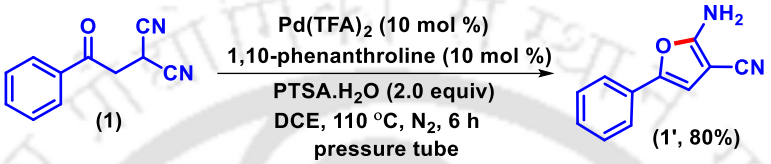

Scheme III.4.1.1. *Reaction in the absence of phenylboronic acid (**a**) and benzaldehyde (**a′**).*

The same product (**1′**) was obtained in 78% yield when the reaction was carried out even in the absence of the Pd catalyst and the ligand [Scheme III.4.1.2], thereby suggesting the non-involvement of Pd in the construction of the furan ring (**1′**), and its formation is a simple acid-catalyzed process.

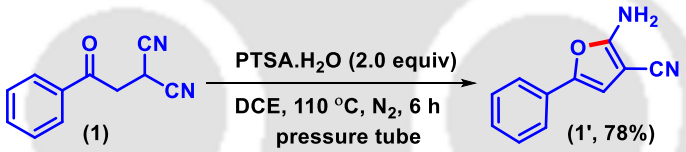

Scheme III.4.1.2. *Reaction in the absence of phenylboronic acid (**a**) and benzaldehyde (**a′**) and Pd(II)-catalyst.*

In addition, the reaction in the absence of a Pd catalyst and boronic acid **a**, i.e., between β-ketodinitrile **1** and benzaldehyde **a′** yielded imine **1a′** in 43% isolated yield [Scheme III.4.1.3].

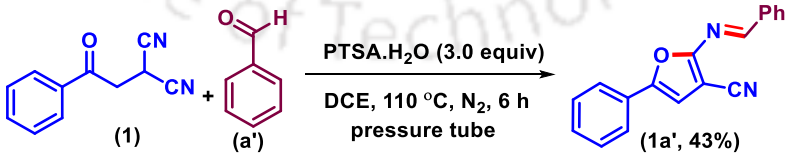

Scheme III.4.1.3. *Reaction in the absence of phenylboronic acid (a) and $Pd(TFA)_2$:*

Interestingly, the reaction of intermediate **1′** with phenylboronic acid **a** and benzaldehyde **a′** gave product **1aa′** in 90% yield [Scheme III.4.1.4]. This control experiment suggests **1′** as the possible intermediate.

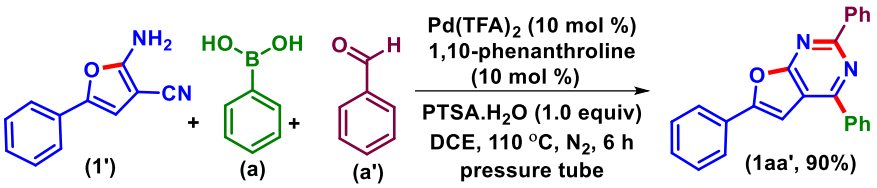

Scheme III.4.1.4. *Reaction with intermediate (**1'**) with phenylboronic acid (**a**) and benzaldehyde (**a'**).*

Subsequently, the reaction between imine **1a′** and phenylboronic acid **a** in the presence and absence of PTSA.H_2O afforded furo-pyrimidine **1aa′** (81% and 83%, respectively) after 6 h, thereby reconfirming the intermediacy of **1a′** [Scheme III.4.1.5]. The yields of **1aa′** in both cases remained unchanged, thereby suggesting the non-involvement of PTSA.H_2O in the catalytic cycle.

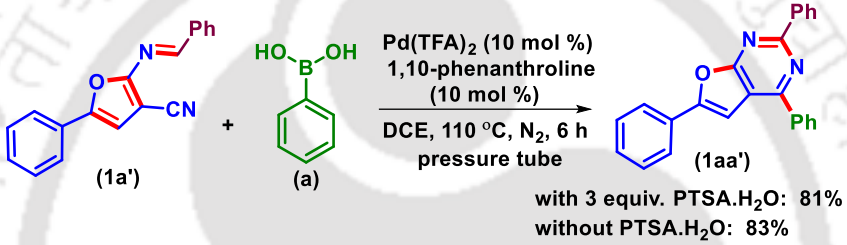

Scheme III.4.1.5. *Reaction between intermediate (**1a'**) and phenylboronic acid (**a**).*

III.4.2. Plausible Reaction Mechanism:

Based on these experimental findings and the literature reports, a plausible reaction pathway is depicted in Scheme III.4.2.1.[5b,6a] Initially, the β-ketodinitrile (**1**) undergoes an acid-catalyzed enolization in the presence of PTSA·H_2O to afford intermediate **I**. Intermediate **I** then undergoes further acid-catalyzed intramolecular cyclization to afford a five-membered cyclic intermediate **1′** that reacts with benzaldehyde **a′** to form imine intermediate **1a′**. The nitrile group of imine **1a′** then coordinates with aryl-Pd(II) complex (**B**) (which is formed via transmetalation of Pd catalyst **A** and phenylboronic acid **a**) to form an intermediate **C**. Carbopalladation of intermediate **C**, followed by migration of the phenyl group to the nitrile generates Pd-ketimine complex **D**, which underwent an intramolecular cyclization giving cyclic intermediate **E**. Finally, aromatization via β-H elimination of intermediate **E** afforded furo-pyrimidine **1aa′** and regenerates the Pd catalyst for the next catalytic cycle.

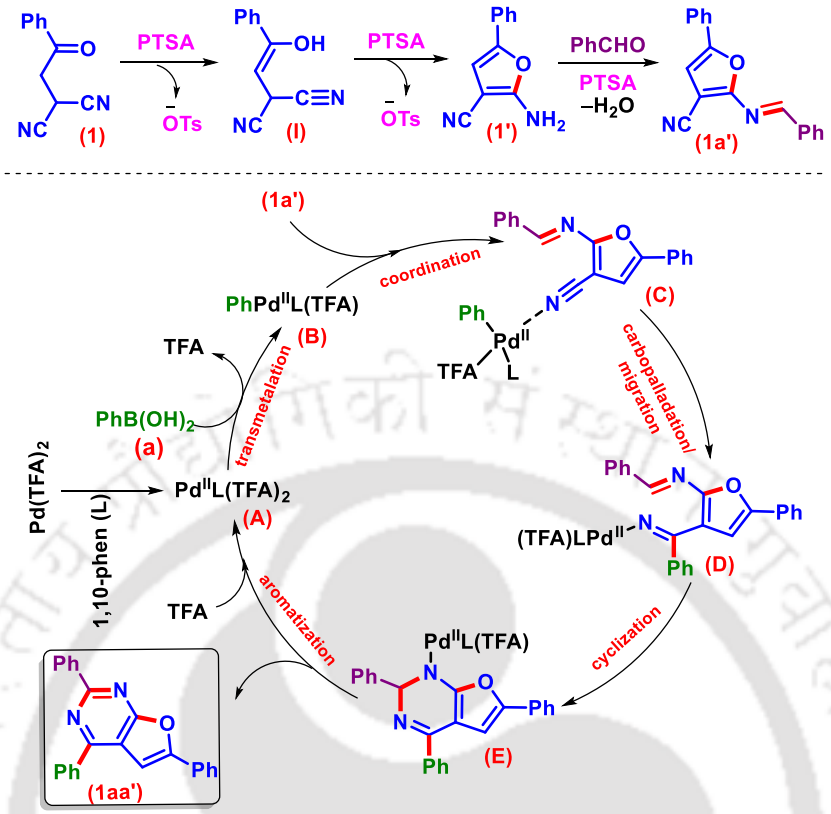

Scheme III.4.2.1. *Proposed reaction path.*

III.5. Post-Synthetic Applications:

To explore the synthetic utility of the synthesized furo-pyrimidines, a few late-stage functionalizations were carried out, as shown in Scheme III.5.1. The 2,4,6-triphenylfuro[2,3-*d*]pyrimidines (**1aa′**) undergo selective C–H, N annulation at one of the phenyl rings with diphenylacetylene (**x**) in the presence of a Ru(II)-catalyst giving annulated product **1x** in 72% yield.[6a] As one can see from the X-ray diffraction (XRD) structure of one of its derivatives [**1ea′** (Scheme III.3.2.1), the C-2 phenyl ring where the annulation is taking place is in the same plane, whereas the other phenyl (C-4) is out of the plane. In addition, *p*-Br-substituted furopyrimidine **8aa′** undergoes Pd(II)-catalyzed Suzuki coupling with phenylboronic acid **a**[13] and Heck coupling with 4-methylstyrene **z**[14] giving the corresponding cross-coupled products (**8y**, 80%; **8z**, 82%).

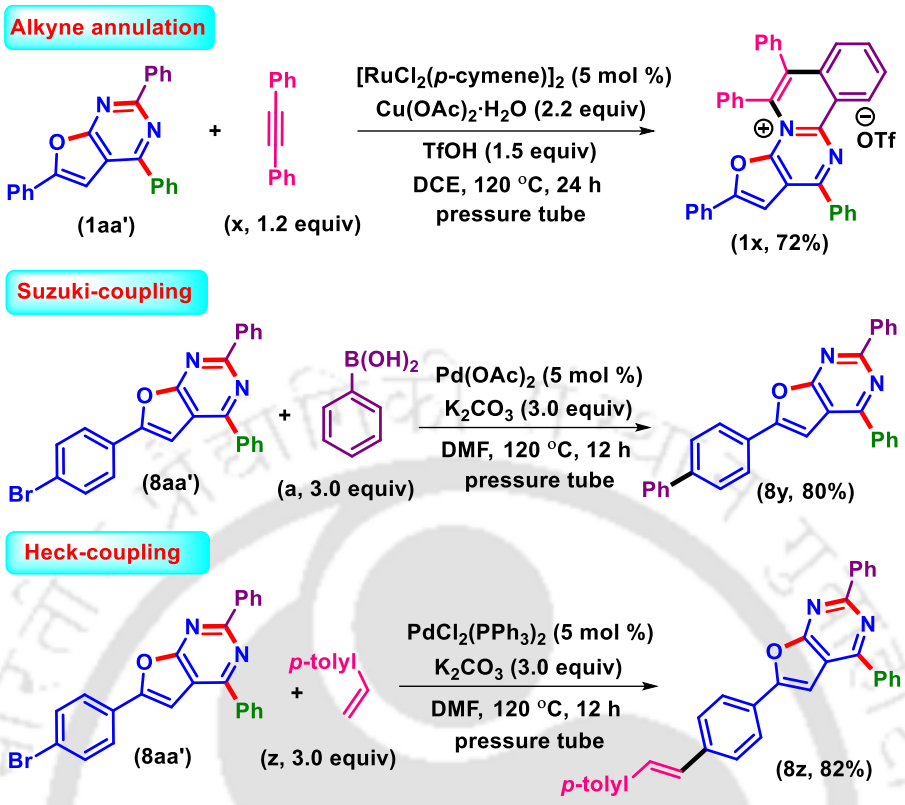

Scheme III.5.1. *Post-synthetic functionalizations.*

III.6. UV-vis Experiment:

Due to π-extended features, furo-pyrimidine derivatives show excellent luminogenic behavior under UV light.[4] The photophysical behavior of some of the synthesized compounds (**1aa′**, **2aa′**, **6aa′**, **11aa′**, **1da′**, **1ea′**, **1af′**, **1ak′**, **1al′**, **8y**, **8z**) was inspected. The absorption maxima were observed 348-387 nm and fluorescence emission was between 468 to 533 nm (Figure III.6.1. and Figure III.6.2). Therefore, they could be developed as good organic fluorophores have important applications in material sciences.

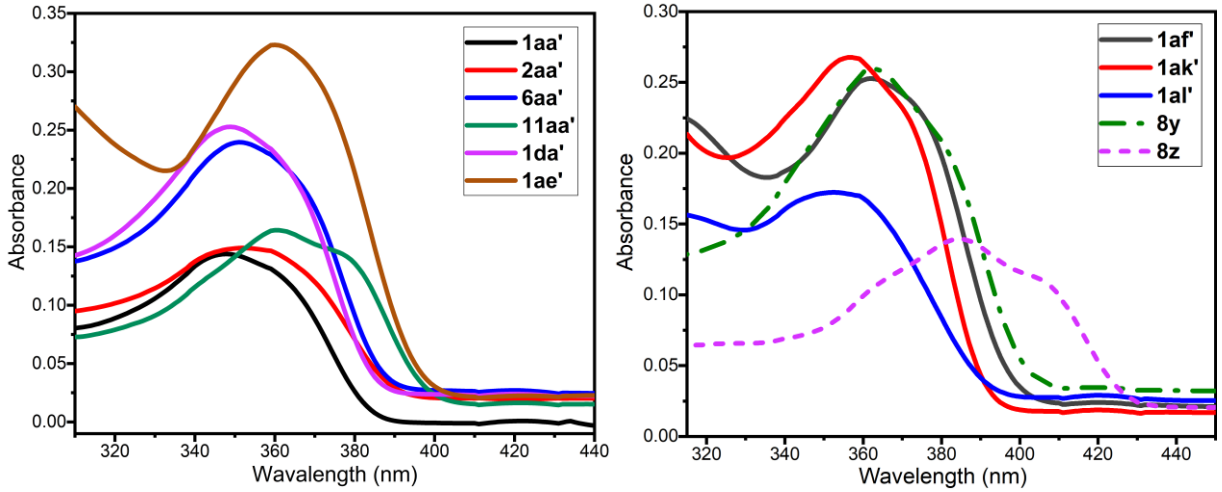

Figure III.6.1. *UV-Vis spectra of* ***1aa'***, ***2aa'***, ***6aa'***, ***11aa'***, ***1da'***, ***1ae'***, ***1af'***, ***1ak'***, ***1al'***, ***8y***, *and* ***8z*** *in* $CHCl_3$ *[concentrations: 1 x* 10^{-6} *M].*

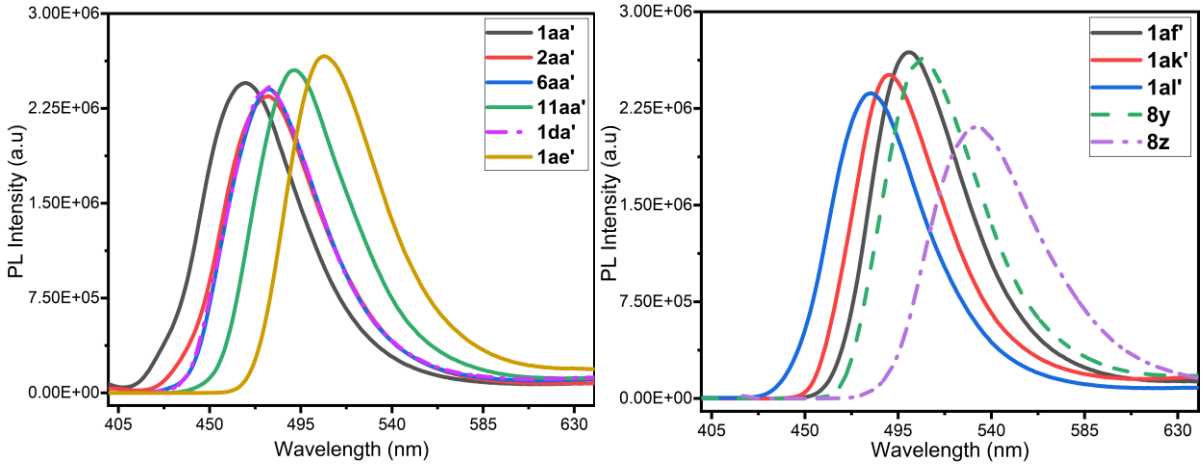

Figure III.6.2. *Photoluminescence spectra of* ***1aa'***, ***2aa'***, ***6aa'***, ***11aa'***, ***1da'***, ***1ae'***, ***1af'***, ***1ak'***, ***1al'***, ***8y***, *and* ***8z*** *in* $CHCl_3$ *[concentrations: 1 x* 10^{-6} *M].*

III.7. Conclusion:

In summary, a Pd(II)-catalyzed three-component synthesis of furo[2,3-*d*]pyrimidine has been established via the addition/cyclization cascade of β-ketodinitriles, phenylboronic acids, and benzaldehydes. Both nitrile groups of β-ketodinitriles participated, leading to the simultaneous construction of furan and pyrimidine. A diverse range of substrates were well tolerated giving moderate to good yields of the product. Additionally, the photoluminescence properties of furo-pyrimidines were confirmed by ultraviolet-visible spectroscopy having absorption maxima (λ_{max}) of 348–387 nm and fluorescence emission of 468–533 nm. Finally, to explore synthetic utility and

to expand the substrate scope, a large-scale synthesis, and a few post-synthetic functionalizations were also demonstrated.

III.8. Experimental Section:

III.8.1. General Information:

All the reagents were commercial grade and purified according to the established procedures. All the reactions were carried out in oven-dried glassware. The highest commercial quality reagents were purchased and were used without further purification unless otherwise stated. Reactions were monitored by thin layer chromatography (TLC) on 0.25 mm silica gel plates ($60F_{254}$) visualized under UV illumination at 254 nm. Organic extracts were dried over anhydrous sodium sulfate (Na_2SO_4). Solvents were removed using a rotary evaporator under reduced pressure. Column chromatography was performed to purify the crude product on silica gel 60–120 mesh using a mixture of hexane and ethyl acetate as eluent. The isolated compounds were characterized by spectroscopic [^1H, $^{13}C\{1H\}$ NMR, and IR] techniques and HRMS analysis. NMR spectra were recorded in deuterochloroform ($CDCl_3$). ^1H, $^{13}C\{^1H\}$ were recorded in 600 (150) or 500 (125) MHz spectrometer and were calibrated using tetramethylsilane or residual undeuterated solvent for ^1H NMR, deuterochloroform for ^{13}C NMR as an internal reference {$Si(CH_3)_4$: 0.00 ppm or $CHCl_3$: 7.260 ppm for ^1H NMR, 77.230 ppm for ^{13}C NMR}. ^{19}F NMR was calibrated without any internal standard in $CDCl_3$ and DMSO-d_6 in a 500 MHz spectrometer. The chemical shifts are quoted in δ units, parts per million (ppm). ^1H NMR data is represented as follows: Chemical shift, multiplicity (s = singlet, d = doublet, t = triplet, q = quartet, m = multiplet), integration and coupling constant(s) *J* in hertz (Hz). High-resolution mass spectra (HRMS) were recorded on a mass spectrometer using electrospray ionization-time of flight (ESI-TOF) reflection experiments. FT-IR spectra were recorded in KBr or neat and reported in the frequency of absorption (cm^{-1}). All UV experiments were performed in 1 mL quartz cuvettes of path length 1 cm at 25 ^oC in a UV/Vis spectrometer in HPLC grade Chloroform.

III.8.2. General Procedures:

III.8.2.1. General Procedure for the Synthesis of 2-(2-Oxo-2-arylylethyl)malononitriles (1–13):

Compounds **1**–**13** were synthesized in slightly modified literature procedures.[6i,15]

To an oven-dried 100 mL round bottom flask was added α-bromoacetophenone (10.0 mmol, 1.0 equiv, 1.97 g) and malononitrile (10.0 mmol, 1.0 equiv, 0.66 g) were dissolved in EtOH (20 mL). Then NaOH (0.4 g, 10.0 mmol, 1.0 eq.) in H_2O (20 mL) was added dropwise over 5 min. After letting the reaction mixture be stirred for 30 min at 0 °C, then stirred at room temperature for 30 min. After completion of the reaction (monitored by TLC analysis), the reaction mixture was admixed with ethyl acetate (40 mL), and the organic layer was washed with water (10 mL). The organic layer was dried over anhydrous Na_2SO_4, and the solvent was evaporated under reduced pressure. The crude product obtained was purified over a column of silica gel using 10% ethyl acetate in hexane to give pure 2-(2-oxo-2-phenylethyl)malononitriles (**1**) with 73% yield (1.35 g) (Scheme III.8.2.1.1).

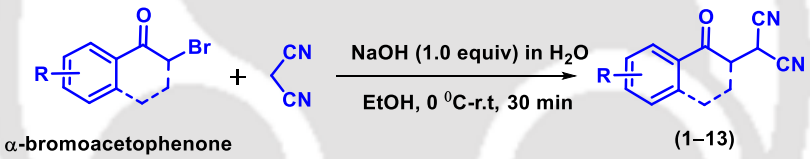

Scheme III.8.2.1.1. *Preparation of 2-(2-oxo-2-arylylethyl)malononitriles (**1–13**).*

III.8.2.2. General Procedure for the Synthesis of 2,4,6-Triphenylfuro[2,3-*d*]pyrimidine (1aa′) from 2-(2-Oxo-2-phenylethyl)malononitriles (1), Phenylboronic acid (a) and Benzaldehyde (a′):

To an oven-dried pressure tube (20.3 cm x 19 mm, 21 mL) containing a magnetic bar was added 2-(2-oxo-2-phenylethyl)malononitriles (**1**) (0.046 g, 0.25 mmol), phenylboronic acid (**a**) (0.090 g, 0.75 mmol), benzaldehyde (**a′**) (0.040 g, 0.375 mmol), $Pd(TFA)_2$ (0.0083 g, 0.025 mmol), 1,10-phenanthroline (0.0045 g, 0.025 mmol), PTSA·H_2O (0.142 g, 0.75 mmol) and 1,2-DCE (2 mL). After that, the reaction mixture was purged with N_2 using a needle and closed with the PTFE stopper. The reaction mixture was stirred at 110 °C in a preheated oil bath for 12 h. After completion of the reaction (monitored by TLC analysis), the reaction mixture was admixed with ethyl acetate (20 mL), and the organic layer was washed with saturated sodium bicarbonate solution (10 mL). The organic layer was dried over anhydrous Na_2SO_4, and the solvent was evaporated under reduced

pressure. The crude product obtained was purified over a column of silica gel using 1% ethyl acetate in hexane to give pure 2,4,6-triphenylfuro[2,3-*d*]pyrimidine (**1aa′**) with 71% yield (62 mg) (Scheme III.8.2.2.1). The identity and purity of the product were confirmed by spectroscopic analysis.

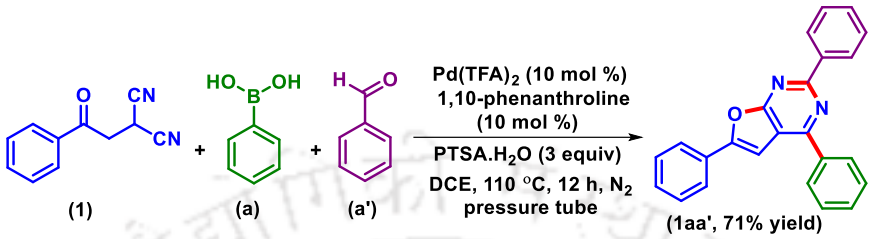

Scheme III.8.2.2.1. *Synthesis of 2,4,6-triphenylfuro[2,3-d]pyrimidine (**1aa'**).*

III.8.2.3. General Procedure for the Large-Scale Synthesis of 2,4,6-Triphenylfuro[2,3-*d*]pyrimidine (1aa′) from 2-(2-Oxo-2-phenylethyl)malononitriles (1) Phenylboronic acid (a) and Benzaldehyde (a′):

To a 10 mL round bottom flask containing a magnetic bar was added 2-(2-oxo-2-phenylethyl)malononitriles (**1**) (0.552 g, 3.0 mmol), phenylboronic acid (**a**) (1.089 g, 9.0 mmol), benzaldehyde (**a′**) (0.477 g, 4.5 mmol), $Pd(TFA)_2$ (0.0996 g, 0.3 mmol), 1,10-phenanthroline (0.054 g, 0.3 mmol), $PTSA{\cdot}H_2O$ (1.71 g, 9.0 mmol) and 1,2-DCE (5 mL). After that, the reaction mixture was purged with N_2 through a balloon and closed with the glass stopper. The reaction mixture was stirred at 110 °C in a preheated oil bath for 12 h. After completion of the reaction (monitored by TLC analysis), the reaction mixture was admixed with ethyl acetate (50 mL) and the organic layer was washed with saturated sodium bicarbonate solution (20 mL). The organic layer was dried over anhydrous Na_2SO_4, and the solvent was evaporated under reduced pressure. The crude product obtained was purified over a column of silica gel using 1% ethyl acetate in hexane to give pure 2,4,6-triphenylfuro[2,3-*d*]pyrimidine (**1aa′**) with 60% yield (625 mg) (Scheme III.8.2.3.1).

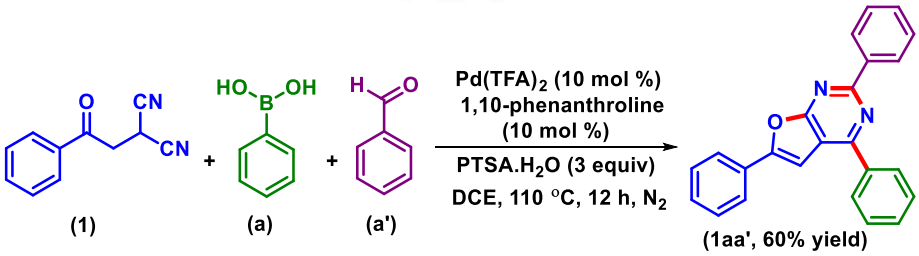

Scheme III.8.2.3.1. *Gram-scale synthesis of 2,4,6-triphenylfuro[2,3-d]pyrimidine (**1aa'**).*

III.8.3. Mechanistic Investigations:

III.8.3.1. In the Absence of Phenylboronic acid (a) and Benzaldehyde (a′):

To an oven-dried pressure tube (20.3 cm x 19 mm, 21 mL) containing a magnetic bar was added 2-(2-oxo-2-phenylethyl)malononitriles (**1**) (0.046 g, 0.25 mmol), $Pd(TFA)_2$ (0.0083 g, 0.025 mmol), 1,10-phenanthroline (0.0045 g, 0.025 mmol), $PTSA{\cdot}H_2O$ (0.095 g, 0.5 mmol) and 1,2-DCE (2 mL). After that, the reaction mixture was purged with N_2 using a needle and closed with the PTFE stopper. The reaction mixture was stirred at 110 ^oC in a preheated oil bath for 6 h. After completion of the reaction (monitored by TLC analysis), the reaction mixture was admixed with ethyl acetate (20 mL), and the organic layer was washed with saturated sodium bicarbonate solution (5 mL). The organic layer was dried over anhydrous Na_2SO_4, and the solvent was evaporated under reduced pressure. The crude product obtained was purified over a column of silica gel using 15% ethyl acetate in hexane to give pure 2-amino-5-phenylfuran-3-carbonitrile (**1′**) with 80% yield (37 mg) (Scheme III.8.3.1.1). The identity and purity of the product were confirmed by spectroscopic analysis.

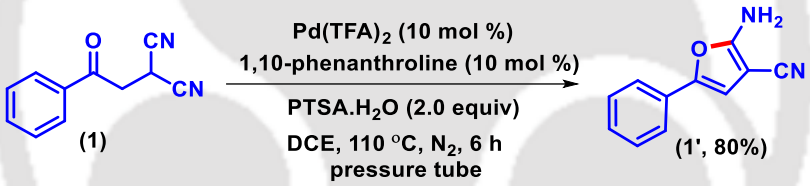

Scheme III.8.3.1.1. *Reaction in absence of phenylboronic acid (**a**) and benzaldehyde (**a′**).*

III.8.3.2. In the Absence of Phenylboronic acid (a), Benzaldehyde (a′) and $Pd(TFA)_2$:

To an oven-dried pressure tube (20.3 cm x 19 mm, 21 mL) containing a magnetic bar was added 2-(2-oxo-2-phenylethyl)malononitriles (**1**) (0.046 g, 0.25 mmol), $PTSA{\cdot}H_2O$ (0.095 g, 0.50 mmol) and 1,2-DCE (2 mL). After that, the reaction mixture was purged with N_2 using a needle and closed with the PTFE stopper. The reaction mixture was stirred at 110 ^oC in a preheated oil bath for 6 h. After completion of the reaction (monitored by TLC analysis), the reaction mixture was admixed with ethyl acetate (20 mL), and the organic layer was washed with saturated sodium bicarbonate solution (5 mL). The organic layer was dried over anhydrous Na_2SO_4, and the solvent was evaporated under reduced pressure. The crude product obtained was purified over a column of silica gel using 15% ethyl acetate in hexane to give pure 2-amino-5-phenylfuran-3-carbonitrile (**1′**)

with 82% yield (38 mg) (Scheme III.8.3.2.1). The identity and purity of the product were confirmed by spectroscopic analysis.

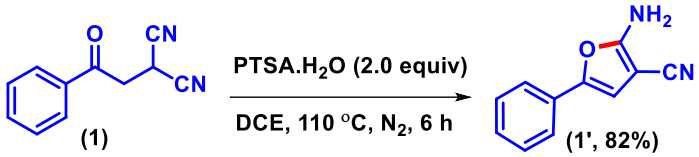

Scheme III.8.3.2.1. *Reaction in the absence of phenylboronic acid (**a**), benzaldehyde (**a′**), and Pd(TFA)2.*

III.8.3.3. In the Absence of Phenylboronic acid (a) and Pd(TFA)2:

To an oven-dried pressure tube (20.3 cm x 19 mm, 21 mL) containing a magnetic bar was added 2-(2-oxo-2-phenylethyl)malononitriles (**1**) (0.046 g, 0.25 mmol), benzaldehyde (**a′**), (0.040 g, 0.375 mmol), PTSA·H_2O (0.142 g, 0.75 mmol) and 1,2-DCE (2 mL). After that, the reaction mixture was purged with N_2 using a needle and closed with the PTFE stopper. The reaction mixture was stirred at 110 °C in a preheated oil bath for 6 h. After completion of the reaction (monitored by TLC analysis), the reaction mixture was admixed with ethyl acetate (20 mL), and the organic layer was washed with saturated sodium bicarbonate solution (5 mL). The organic layer was dried over anhydrous Na_2SO_4, and the solvent was evaporated under reduced pressure. The crude product obtained was purified over a column of silica gel using 2% ethyl acetate in hexane to give pure 2-(benzylideneamino)-5-phenylfuran-3-carbonitrile (**1a′**) with 43% yield (29 mg) (Scheme III.8.3.3.1). The identity and purity of the product were confirmed by spectroscopic analysis.

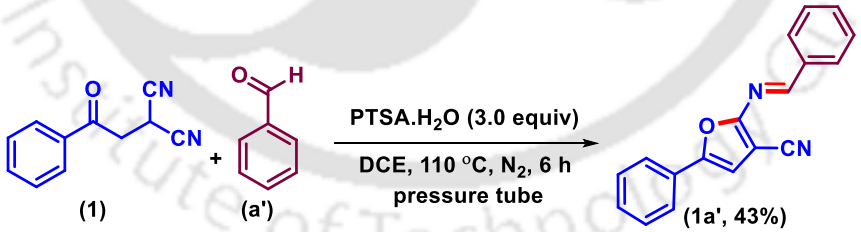

Scheme III.8.3.3.1. *Reaction in the absence of phenylboronic acid (**a**), and Pd(TFA)2.*

III.8.3.4. Reaction of 2-amino-5-phenylfuran-3-carbonitrile (1′) with Phenylboronic acid (a) and Benzaldehyde (a′):

To an oven-dried pressure tube (20.3 cm x 19 mm, 21 mL) containing a magnetic bar was added 2-amino-5-phenylfuran-3-carbonitrile (**1′**) (0.036 g, 0.20 mmol), phenylboronic acid (**a**) (0.072 g, 0.60 mmol), benzaldehyde (**a′**), (0.032 g, 0.30 mmol), $Pd(TFA)_2$ (0.0066 g, 0.02 mmol),

1,10-phenanthroline (0.0036 g, 0.02 mmol), PTSA·H_2O (0.038 g, 0.20 mmol) and 1,2-DCE (2 mL). After that, the reaction mixture was purged with N_2 using a needle and closed with the PTFE stopper. The reaction mixture was stirred at 110 °C in a preheated oil bath for 6 h. After completion of the reaction (monitored by TLC analysis), the reaction mixture was admixed with ethyl acetate (20 mL), and the organic layer was washed with saturated sodium bicarbonate solution (10 mL). The organic layer was dried over anhydrous Na_2SO_4, and the solvent was evaporated under reduced pressure. The crude product obtained was purified over a column of silica gel using 1% ethyl acetate in hexane to give pure 2,4,6-triphenylfuro[2,3-*d*]pyrimidine (**1aa′**) with 90% yield (63 mg) (Scheme III.8.3.4.1). The identity and purity of the product were confirmed by spectroscopic analysis.

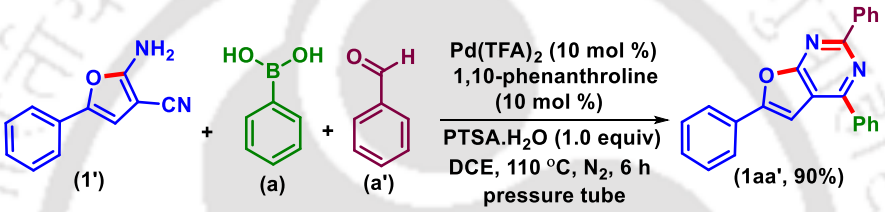

Scheme III.8.3.4.1. *Reaction of (1') with phenylboronic acid (**a**) and benzaldehyde (**a'**).*

III.8.3.5. Reaction of 2-(Benzylideneamino)-5-phenylfuran-3-carbonitrile (1a′) with Phenylboronic acid (a):

To two oven-dried pressure tubes (20.3 cm x 19 mm, 21 mL) containing magnetic bar was added 2-(benzylideneamino)-5-phenylfuran-3-carbonitrile (**1a′**) (0.054 g, 0.20 mmol), phenylboronic acid (**a**) (0.072 g, 0.60 mmol), $Pd(TFA)_2$ (0.0066 g, 0.02 mmol), 1,10-phenanthroline (0.0036 g, 0.02 mmol), 1,2-DCE (2 mL). In one pressure tube, PTSA·H_2O (0.114 g, 0.60 mmol) was added and another was without PTSA.H_2O. After that, both the reaction mixture was purged with N_2 using a needle and closed with the PTFE stopper. The reaction mixtures were stirred at 110 °C in a preheated oil bath for 6 h. After completion of the reaction (monitored by TLC analysis), the two reaction mixtures were admixed with ethyl acetate (20 mL), and the organic layer was washed with saturated sodium bicarbonate solution (10 mL). The organic layer was dried over anhydrous Na_2SO_4, and the solvent was evaporated under reduced pressure. The crude product obtained was purified over a column of silica gel using 1% ethyl acetate in hexane to give pure 2,4,6-triphenylfuro[2,3-*d*]pyrimidine (**1aa′**) with 81% yield (56 mg) in the presence of PTSA.H_2O and 83% yield (58 mg) without PTSA.H_2O (Scheme III.8.3.5.1).

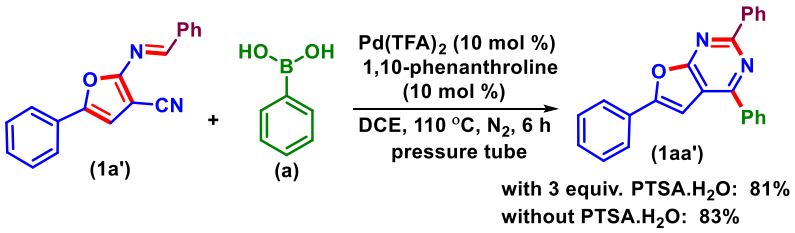

Scheme III.8.3.5.1. *Reaction of phenylboronic acid (**a**) with **1a′**.*

III.8.4. Procedure of Post-Synthetic Functionalizations:

III.8.4.1. General Procedure for the Synthesis of 2,5,6,12-Tetraphenylfuro[3',2':5,6]pyrimido[2,1-*a*]isoquinolin-4-ium (1x) from 2,4,6-Triphenylfuro[2,3-*d*]pyrimidine (1aa′) and Diphenylacetylene (x):[2a]

To an oven-dried pressure tube (20.3 cm x 19 mm, 21 mL) containing a magnetic bar was added 2,4,6-triphenylfuro[2,3-*d*]pyrimidine (**1aa′**) (0.069 g, 0.20 mmol), diphenylacetylene (**x**) (0.043 g, 0.24 mmol), [Ru(*p*-cymene)Cl_2]$_2$ (0.0061 g, 0.01 mmol), $Cu(OAc)_2 \cdot H_2O$ (0.084 g, 0.44 mmol), TfOH (0.045 g, 0.30 mmol) and DCE (2 mL). The reaction mixture was stirred in an oil bath preheated at 120 °C for 24 h. After completion of the reaction (monitored by TLC analysis), the reaction mixture was admixed with ethyl acetate (20 mL), and the organic layer was washed with saturated sodium bicarbonate solution (10 mL). The organic layer was dried over anhydrous sodium sulfate (Na_2SO_4), and the solvent was evaporated under reduced pressure. The crude product obtained was purified over a column of silica gel using 2% methanol in dichloromethane to give pure 2,5,6,12-tetraphenylfuro[3',2':5,6]pyrimido[2,1-*a*]isoquinolin-4-ium (**1x**) in 72% yield (76 mg) (Scheme III.8.4.1.1). The identity and purity of the product were confirmed by spectroscopic analysis.

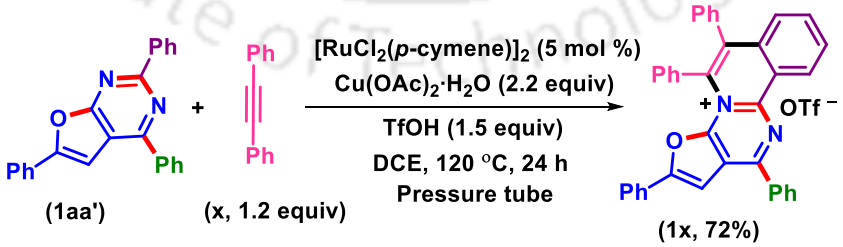

Scheme III.8.4.1.1. *Ru(II)-catalyzed annulation with diphenylacetylene.*

III.8.4.2. General Procedure for the Synthesis of 6-([1,1'-Biphenyl]-4-yl)-2,4-diphenylfuro[2,3-*d*]pyrimidine (8y) from 6-(4-Bromophenyl)-2,4-diphenylfuro[2,3-*d*]pyrimidine (8aa′) and Phenylboronic Acid (a):[2b]

To an oven-dried pressure tube (20.3 cm x 19 mm, 21 mL) containing a magnetic bar was added 6-(4-bromophenyl)-2,4-diphenylfuro[2,3-*d*]pyrimidine (**8aa′**) (0.085 g, 0.20 mmol), phenylboronic acid (**a**) (0.072 g, 0.60 mmol), $Pd(OAc)_2$ (0.0022 g, 0.01 mmol), K_2CO_3 (0.083 g, 0.60 mmol) and DMF (2 mL). The reaction mixture was stirred in an oil bath preheated at 120 °C for 12 h. After completion of the reaction (monitored by TLC analysis), the reaction mixture was admixed with ethyl acetate (20 mL), and the organic layer was washed with ice-cold water (5 mL). The organic layer was dried over anhydrous sodium sulfate (Na_2SO_4), and the solvent was evaporated under reduced pressure. The crude product obtained was purified over a column of silica gel using 10% ethyl acetate in hexane to give pure 6-([1,1'-biphenyl]-4-yl)-2,4-diphenylfuro[2,3-*d*]pyrimidine (**8y**) in 80% yield (68 mg) (Scheme III.8.4.2.1). The identity and purity of the product were confirmed by spectroscopic analysis.

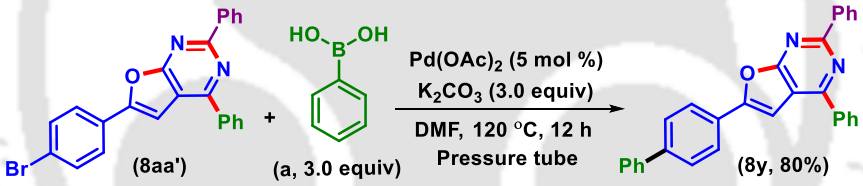

Scheme III.8.4.2.1. *Pd(II)-catalyzed Suzuki coupling.*

III.8.4.3. General Procedure for the Synthesis of (*E*)-6-(4-(4-Methylstyryl)phenyl)-2,4-diphenylfuro[2,3-*d*]pyrimidine (8z) from 6-(4-Bromophenyl)-2,4-diphenylfuro[2,3-*d*]pyrimidine (8aa′) and 4-Methylstyrene (z):[2c]

To an oven-dried pressure tube (20.3 cm x 19 mm, 21 mL) containing a magnetic bar was added 6-(4-bromophenyl)-2,4-diphenylfuro[2,3-d]pyrimidine (**8aa′**) (0.085 g, 0.20 mmol), 4-methylstyrene (**z**) (0.071 g, 0.60 mmol), $PdCl_2(PPh_3)_2$ (0.0070 g, 0.01 mmol), K_2CO_3 (0.083 g, 0.60 mmol) and DMF (2 mL). The reaction mixture was stirred in an oil bath preheated at 120 °C for 12 h. After completion of the reaction (monitored by TLC analysis), the reaction mixture was admixed with ethyl acetate (20 mL), and the organic layer was washed with ice-cold water (5 mL). The organic layer was dried over anhydrous sodium sulfate (Na_2SO_4), and the solvent was evaporated

under reduced pressure. The crude product obtained was purified over a column of silica gel using 10% ethyl acetate in hexane to give pure (*E*)-6-(4-(4-methylstyryl)phenyl)-2,4-diphenylfuro[2,3-*d*]pyrimidine (**8z**) in 82% yield (76 mg) (Scheme III.8.4.3.1). The identity and purity of the product were confirmed by spectroscopic analysis.

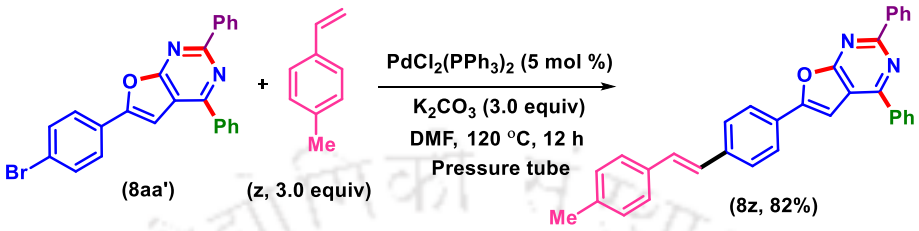

Scheme III.8.4.3.1. *Pd(II)-catalyzed Heck coupling.*

III.8.5. Crystallographic Information:

III.8.5.1 Crystallographic Information of 4-(4-(*tert*-Butyl)phenyl)-2,6-diphenylfuro[2,3-*d*]pyrimidine (1ea′):

(i) Sample Preparation: The single crystal of compound **1ea′** was prepared by the slow evaporation method for which 10 mg of the compound (**1ea′**) was dissolved in 1 mL ethyl acetate. The mouth of the glass vial was covered with a cap having a small hole and kept for slow evaporation at room temperature. Crystals of **1ea′** were obtained as a transparent white needle-like crystal after around 4–5 days.

(ii) Data Collection: Diffraction data were collected at 297 K with MoKα radiation (λ = 0.71073 Å) using a Bruker Nonius SMART APEX CCD diffractometer equipped with a graphite monochromator and Apex CD camera. The SMART software was used for data collection for indexing the reflections and determining the unit cell parameters. Data reduction and cell refinement were performed using SAINT[1,2] software and the space groups of these crystals were determined from systematic absences by XPREP and further justified by the refinement results. The structures were solved by direct methods and refined by full-matrix least-squares calculations using SHELXTL-97[3] software. All the non-H atoms were refined in the anisotropic approximation against F^2 of all reflections.

1. Blessing, R. H. *Acta Crystallogr.* **1995**, *A51*, 33.
2. SMART and SAINT, Siemens Analytical X-ray Instruments Inc., Madison, WI, 1996.
3. Sheldrick, G. M. *Acta Crystallogr.* **2008**, *A64*, 112.

(iii) Crystallographic Description of 4-(4-(*tert*-Butyl)phenyl)-2,6-diphenylfuro[2,3-*d*]pyrimidine (1ea′):

$C_{28}H_{24}N_2O$, crystal dimensions 0.22 x 0.18 x 0.14 mm, M_r = 404.49, Monoclinic, space group C 2/c, a = 25.597 (8), b = 10.938 (3), c = 17.667 (5) Å, α = 90°, β = 94.326 (13)°, γ = 90°, V = 4932 (2) Å^3, Z = 8, ρ_{calcd} = 1.089 g/cm^3, μ = 0.066 mm^{-1}, F(000)= 1712.0, reflection collected / unique = 4370 / 2816, refinement method = full-matrix least-squares on F^2, final R indices [I> 2\s(I)]:R_1 = 0.1137, wR_2 = 0.2541, R indices (all data): R_1 = 0.0760, wR_2 = 0.2046, goodness of fit = 1.045. **CCDC-2297072** for **4-(4-(*tert*-butyl)phenyl)-2,6-diphenylfuro[2,3-*d*]pyrimidine (1ea′)** contains the supplementary crystallographic data for this paper. These data can be obtained free of charge from The Cambridge Crystallographic Data Centre via www.ccdc.cam.ac.uk/data_request/cif.

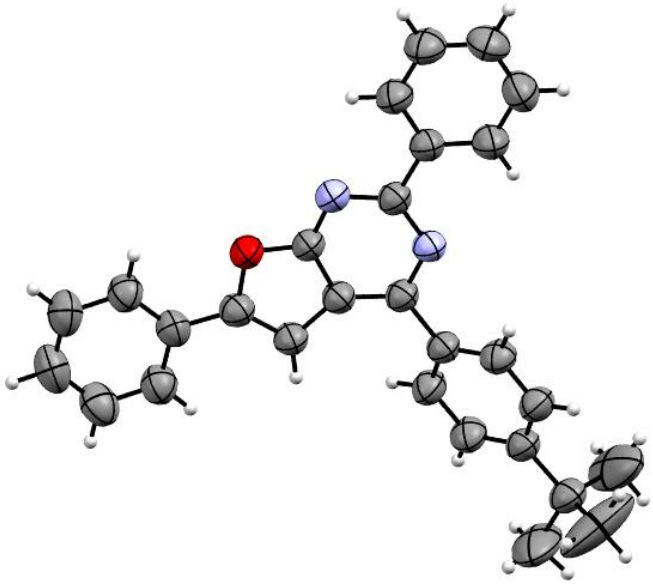

Figure III.8.5.1.1. *ORTEP Diagram of 4-(4-(tert-Butyl)phenyl)-2,6-diphenylfuro[2,3-d]pyrimidine (**1ea′**) with 50% ellipsoid probability (CCDC 2297072).*

III.8.6. UV-vis Experiment:

Due to π-extended features, furo-pyrimidine derivatives show excellent luminogenic behavior under UV light. The photophysical behavior of some of the synthesized compounds (**1aa′**, **2aa′**, **6aa′**, **11aa′**, **1da′**, **1ea′**, **1af′**, **1ak′**, **1al′**, **8y**, **8z**) was inspected. The absorption maxima were observed 348-387 nm and fluorescence emission was between 468 to 533 nm (Figure III.8.6.1 and Figure III.8.6.2). Therefore, they could be developed as good organic fluorophores having important applications in material sciences.

A 1mM stock solution in $CHCl_3$ of the selected compounds was prepared in a 10 mL volumetric flask. Then 10 µL of each of the 1 mM solutions was taken in another 10 mL volumetric flask and the volume was adjusted to 10 mL using $CHCl_3$ so that the final strength of the flasks was maintained 1µM. For the absorption and emission spectra measurement, 1.0 mL of 1 µM solution was taken in a 1 mL cuvette and the spectra of all compounds were recorded.

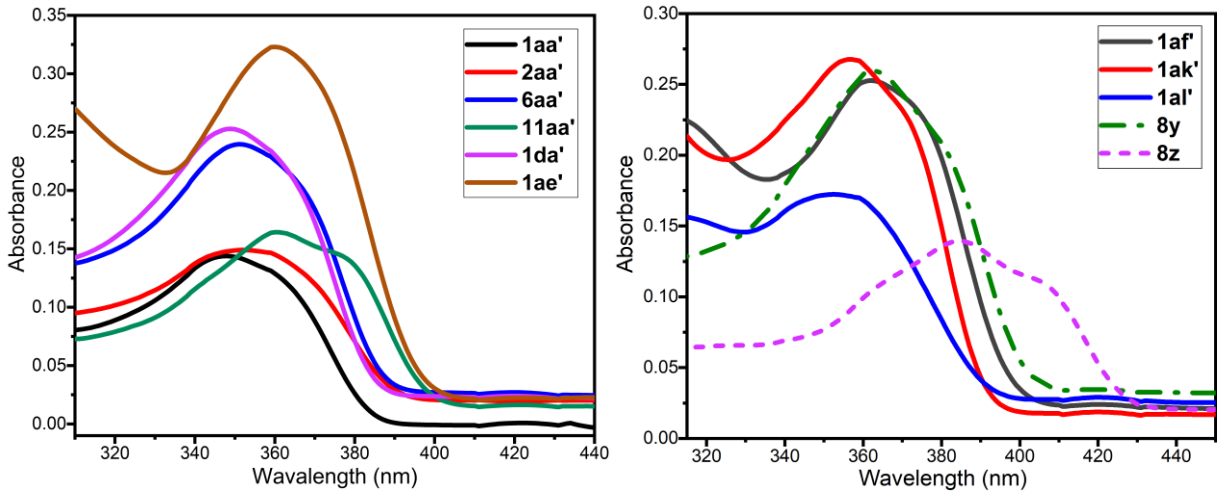

Figure III.8.6.1. *UV-Vis spectra of* ***1aa'***, ***2aa'***, ***6aa'***, ***11aa'***, ***1da'***, ***1ae'***, ***1af'***, ***1ak'***, ***1al'***, ***8y***, *and* ***8z*** *in* $CHCl_3$ *[concentrations: 1 x* 10^{-6} *M].*

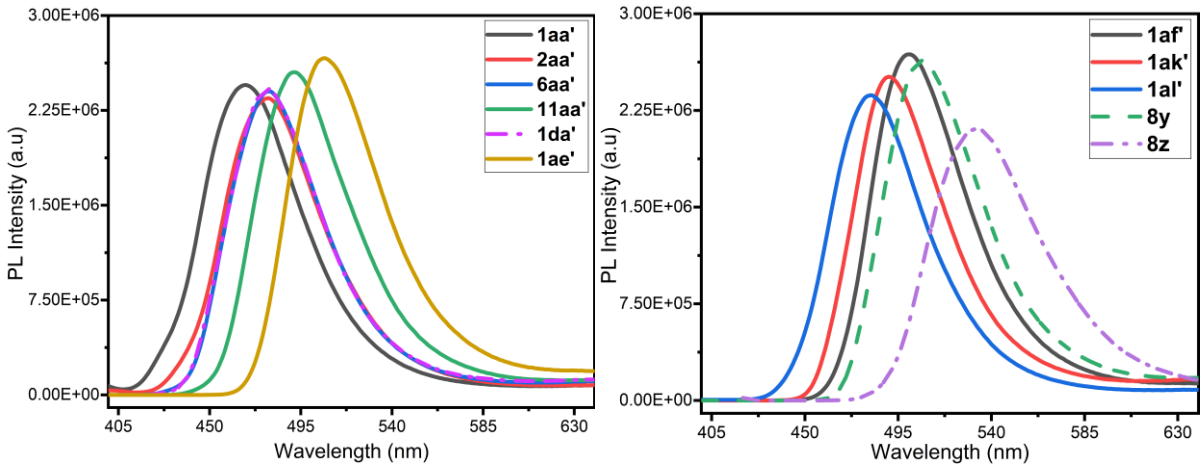

Figure III.8.6.2. *Photoluminescence spectra of* ***1aa'***, ***2aa'***, ***6aa'***, ***11aa'***, ***1da'***, ***1ae'***, ***1af'***, ***1ak'***, ***1al'***, ***8y***, *and* ***8z*** *in* $CHCl_3$ *[concentrations: 1 x* 10^{-6} *M].*

III.9. Spectral Data:

2,4,6-Triphenylfuro[2,3-d]pyrimidine (1aa'):

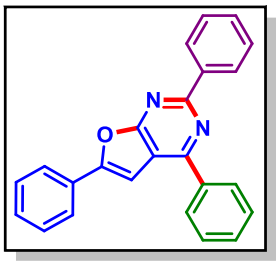

As a white solid (62 mg, 71% yield, mp 164–166 °C); Purification over a column of silica gel (1% EtOAc in hexane); ^{1}H NMR ($CDCl_3$, 500 MHz): δ 8.66 (d, 2H, J = 7.0 Hz), 8.27 (d, 2H, J = 7.5 Hz), 7.96 (d, 2H, J = 7.5 Hz), 7.63–7.57 (m, 3H), 7.54–7.48 (m, 5H), 7.43 (t, 1H, J = 7.5 Hz), 7.34 (s, 1H); ^{13}C{^{1}H} NMR ($CDCl_3$, 125 MHz): δ 168.8, 159.9, 158.3, 156.2, 137.9, 137.8, 130.8, 130.6, 130.0, 129.2, 129.1, 128.9, 128.7, 128.5, 125.5, 114.9, 99.5; IR (neat, cm^{-1}): 3062, 2925, 2852, 1593, 1552, 1489, 1362, 1272, 1021, 754, 689; HRMS (ESI/Q-TOF) (m/z) calcd for $C_{24}H_{17}N_2O$ [M + H]$^{+}$ 349.1335; found 349.1347.

2,4-Diphenyl-6-(p-tolyl)furo[2,3-d]pyrimidine (2aa'):

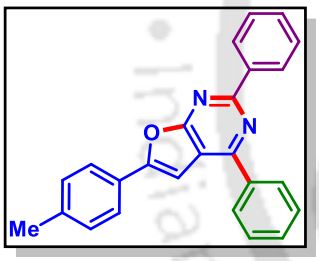

As a white solid (62 mg, 69% yield, mp 203–205 °C); Purification over a column of silica gel (1% EtOAc in hexane); ^{1}H NMR ($CDCl_3$, 500 MHz): δ 8.66 (d, 2H, J = 8.0 Hz), 8.26 (d, 2H, J = 7.5 Hz), 7.83 (d, 2H, J = 8.5 Hz), 7.62–7.56 (m, 3H), 7.54–7.49 (m, 3H), 7.28 (d, 2H, J = 8.0 Hz), 7.26 (s, 1H), 2.40 (s, 3H); ^{13}C{1H} NMR ($CDCl_3$, 125 MHz): δ 168.7, 159.6, 157.9, 156.5, 140.3, 137.9, 137.8, 130.7, 130.5, 129.9, 129.1, 128.8, 128.7, 128.4, 126.3, 125.4, 115.0, 98.6, 21.6; IR (neat, cm^{-1}): 3064, 2919, 2857, 1594, 1503, 1362, 1273, 1027, 759, 695; HRMS (ESI/Q-TOF) (m/z) calcd for $C_{25}H_{19}N_2O$ [M + H]$^{+}$ 363.1492; found 363.1508.

6-(4-Methoxyphenyl)-2,4-diphenylfuro[2,3-d]pyrimidine (3aa'):

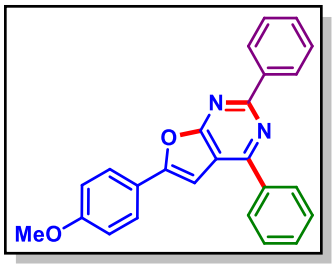

As a white solid (59 mg, 62% yield, mp 185–187 °C); Purification over a column of silica gel (4% EtOAc in hexane); ^{1}H NMR ($CDCl_3$, 500 MHz): δ 8.69 (d, 2H, J = 7.0 Hz), 8.31 (d, 2H, J = 7.5 Hz), 7.94 (d, 2H, J = 8.0 Hz), 7.67–7.64 (m, 2H), 7.61 (d, 1H, J = 7.0 Hz), 7.58–7.52 (m, 3H), 7.30 (s, 1H), 7.06 (d, 2H. J = 8.5 Hz), 3.92 (s, 3H); ^{13}C{^{1}H} NMR ($CDCl_3$, 125 MHz): δ 168.7, 161.2, 159.4, 157.7,

156.5, 138.0, 137.9, 130.7, 130.5, 129.1, 128.8, 128.7, 128.4, 127.2, 121.8, 115.2, 114.7, 97.7, 55.6; IR (neat, cm^{-1}): 2923, 2852, 1610, 1502, 1362, 1252, 1175, 1023, 759, 695; HRMS (ESI/Q-TOF) (m/z) calcd for $C_{25}H_{19}N_2O_2$ $[M + H]^+$ 379.1441; found 379.1448.

6-(4-Isopropylphenyl)-2,4-diphenylfuro[2,3-d]pyrimidine (4aa'):

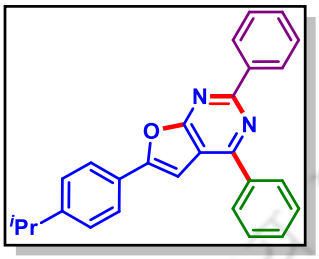

As a white solid (60 mg, 61% yield, mp 118–120 °C); Purification over a column of silica gel (1% EtOAc in hexane); ^1H NMR ($CDCl_3$, 500 MHz): δ 8.66 (d, 2H, J = 7.0 Hz), 8.27 (d, 2H, J = 7.0 Hz), 7.90 (d, 2H, J = 8.5 Hz), 7.63–7.56 (m, 3H), 7.55–7.47 (m, 3H), 7.36 (d, 2H, J = 8.0 Hz), 7.29 (s, 1H), 3.02–2.93 (m, 1H), 1.31 (s, 3H), 1.30 (s, 3H); $^{13}C\{1H\}$ NMR ($CDCl_3$, 125 MHz): δ 168.7, 159.6, 157.9, 156.5, 151.2, 137.9, 137.8, 130.7, 130.5, 129.1, 128.9, 128.7, 128.5, 127.3, 126.7, 125.6, 115.0, 98.7, 34.3, 24.0; IR (neat, cm^{-1}): 3062, 2960, 2869, 1594, 1495, 1273, 1026, 760, 694; HRMS (ESI/Q-TOF) (m/z) calcd for $C_{27}H_{23}N_2O$ $[M + H]^+$ 391.1805; found 391.1803.

6-(4-Fluorophenyl)-2,4-diphenylfuro[2,3-d]pyrimidine (5aa'):

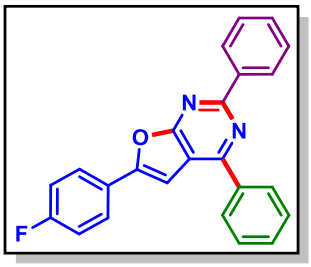

As a white solid (59 mg, 64% yield, mp 200–202 °C); Purification over a column of silica gel (1% EtOAc in hexane); ^1H NMR ($CDCl_3$, 500 MHz): δ 8.64 (d, 2H, J = 8.0 Hz), 8.23 (d, 2H, J = 8.25 Hz), 7.91–7.89 (m, 2H), 7.61–7.56 (m, 3H), 7.53–7.48 (m, 3H), 7.23 (s, 1H), 7.16 (t, 2H, J = 8.5 Hz); $^{13}C\{^1H\}$ NMR ($CDCl_3$, 125 MHz): δ 168.7, 163.7 (d, J = 249.5 Hz), 159.9, 158.2, 155.2, 137.7, 137.6, 130.7 (d, J = 21.8 Hz), 129.1, 128.8, 128.7, 128.5, 127.4 (d, J = 8.3 Hz), 125.4 (d, J = 3.25 Hz), 116.5, 116.3, 114.8, 99.1; ^{19}F NMR ($CDCl_3$, 471 MHz): δ –109.9 (s); IR (neat, cm^{-1}): 3053, 2922, 2852, 1607, 1500, 1396, 1228, 1025, 756, 689; HRMS (ESI/Q-TOF) (m/z) calcd for $C_{24}H_{16}FN_2O$ $[M + H]^+$ 367.1241; found 367.1239.

6-(4-Chlorophenyl)-2,4-diphenylfuro[2,3-d]pyrimidine (6aa'):

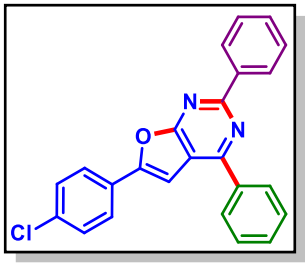

As a white solid (68 mg, 71% yield, mp 190–192 °C); Purification over a column of silica gel (1% EtOAc in hexane); ^{1}H NMR ($CDCl_3$, 500 MHz): δ 8.61 (dd, 2H, J_1 = 7.75 Hz, J_2 = 2.0 Hz), 8.20 (dd, 2H, J_1 = 8.0 Hz, J_2 = 1.5 Hz), 7.79 (d, 2H, J = 8.5 Hz), 7.60–7.55 (m, 3H), 7.52–7.48 (m, 3H), 7.40 (d, 2H, J = 8.5 Hz), 7.22 (s, 1H); ^{13}C{^{1}H} NMR ($CDCl_3$, 125 MHz): δ 168.6, 160.0, 158.3, 154.9, 137.7, 137.5, 135.8, 130.8, 130.6, 129.4, 129.1, 128.8, 128.6, 128.5, 127.5, 126.6, 114.6, 99.8; IR (neat, cm^{-1}): 3066, 2922, 1605, 1573, 1485, 1397, 1274, 1092, 759, 694; HRMS (ESI/Q-TOF) (m/z) calcd for $C_{24}H_{16}ClN_2O$ $[M + H]^+$ 383.0946; found 383.0955.

6-(4-Bromophenyl)-2,4-diphenylfuro[2,3-d]pyrimidine (7aa'):

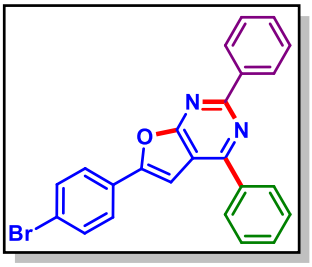

As a white solid (66 mg, 62% yield, mp 210–212 °C); Purification over a column of silica gel (1% EtOAc in hexane); ^{1}H NMR ($CDCl_3$, 500 MHz): δ 8.60 (d, 2H, J = 7.5 Hz), 8.20 (d, 2H, J = 7.5 Hz), 7.72 (d, 2H, J = 8.5 Hz), 7.57–7.48 (m, 8H), 7.24 (s, 1H); ^{13}C{^{1}H} NMR ($CDCl_3$, 125 MHz): δ 168.6, 160.0, 158.4, 154.9, 137.7, 137.5, 132.4, 130.8, 130.7, 129.1, 128.8, 128.7, 128.5, 127.9, 126.8, 124.1, 114.6, 99.9; IR (neat, cm^{-1}): 3062, 2924, 1594, 1480, 1361, 1271, 1070, 759, 697; HRMS (ESI/Q-TOF) (m/z) calcd for $C_{24}H_{16}BrN_2O$ $[M + H]^+$ 427.0441; found 427.0434.

6-(2-Bromophenyl)-2,4-diphenylfuro[2,3-d]pyrimidine (8aa'):

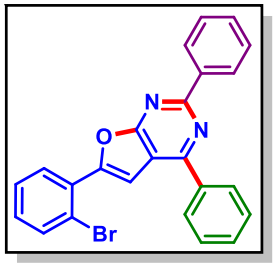

As a white solid (64 mg, 60% yield, mp 191–193 °C); Purification over a column of silica gel (1% EtOAc in hexane); ^{1}H NMR ($CDCl_3$, 500 MHz): δ 8.65 (d, 2H, J = 7.0 Hz), 8.26 (d, 2H, J = 7.5 Hz), 8.07 (d, 1H, J = 7.5 Hz), 7.89 (s, 1H), 7.71 (d, 1H, J = 8.0 Hz), 7.61–7.56 (m, 3H), 7.53–7.48 (m, 3H), 7.44 (t, 1H, J = 7.5 Hz), 7.24 (t, 1H, J = 7.25 Hz); ^{13}C{^{1}H} NMR ($CDCl_3$, 125 MHz): δ 168.2, 160.4, 159.0, 153.3, 137.8, 137.6, 134.7, 130.9, 130.7, 130.5, 130.4, 129.6, 129.2, 128.9, 128.7, 128.6, 127.9, 121.0, 114.3, 105.3; IR (neat, cm^{-1}):

3064, 2924, 2852, 1594, 1401, 1364, 1258, 1012, 754, 695; HRMS (ESI/Q-TOF) (m/z) calcd for $C_{24}H_{16}BrN_2O$ $[M + H]^+$ 427.0441; found 427.0442.

2,4-Diphenyl-6-(4-(trifluoromethyl)phenyl)furo[2,3-d]pyrimidine (9aa'):

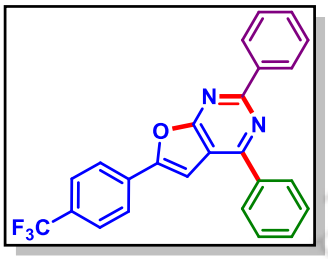

As a white solid (58 mg, 56% yield, mp 212–214 °C); Purification over a column of silica gel (1% EtOAc in hexane); ^{1}H NMR ($CDCl_3$, 500 MHz): δ 8.65 (d, 2H, J = 7.5 Hz), 8.25 (d, 2H, J = 7.0 Hz), 8.04 (d, 2H, J = 8.0 Hz), 7.74 (d, 2H, J = 8.0 Hz), 7.63–7.58 (m, 3H), 7.54–7.50 (m, 3H), 7.43 (s, 1H); ^{13}C{1H} NMR ($CDCl_3$, 125 MHz): δ 168.9, 160.6, 159.1, 154.3, 137.6, 137.5, 132.3, 131.0, 130.9, 129.2, 128.9, 128.7, 128.6, 126.2 (q, J_2 = 3.8 Hz), 125.6, 114.5, 101.5; ^{19}F NMR ($CDCl_3$, 471 MHz): δ –62.8 (s); IR (neat, cm^{-1}): 3064, 2925, 2854, 1595, 1399, 1323, 1127, 1068, 761, 698; HRMS (ESI/Q-TOF) (m/z) calcd for $C_{25}H_{16}F_3N_2O$ $[M + H]^+$ 417.1209; found 417.1205.

6-(Benzo[d][1,3]dioxol-5-yl)-2,4-diphenylfuro[2,3-d]pyrimidine (10aa'):

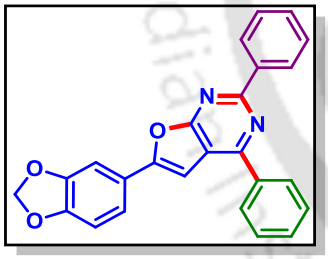

As a white solid (54 mg, 55% yield, mp 190–192 °C); Purification over a column of silica gel (4% EtOAc in hexane); ^{1}H NMR ($CDCl_3$, 500 MHz): δ 8.65 (d, 2H, J = 7.5 Hz), 8.26 (d, 2H, J = 7.0 Hz), 7.62–7.56 (m, 3H), 7.54–7.48 (m, 4H), 7.39 (s, 1H), 7.18 (s, 1H), 6.92 (d, 1H, J = 7.5 Hz), 6.04 (s, 2H); ^{13}C{1H} NMR ($CDCl_3$, 125 MHz): δ 168.6, 159.6, 157.8, 156.1, 149.3, 148.6, 137.9, 137.8, 130.7, 130.5, 129.1, 128.8, 128.7, 128.4, 123.3, 120.2, 115.1, 109.1, 105.8, 101.8, 98.2; IR (neat, cm^{-1}): 3060, 2917, 1594, 1483, 1366, 1264, 1039, 732, 702; HRMS (ESI/Q-TOF) (m/z) calcd for $C_{25}H_{17}N_2O_3$ $[M + H]^+$ 393.1234; found 393.1235.

6-(Naphthalen-2-yl)-2,4-diphenylfuro[2,3-d]pyrimidine (11aa'):

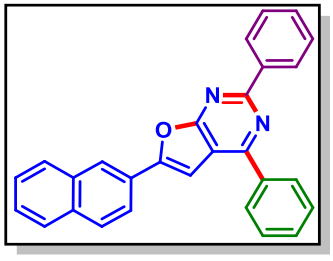

As a yellowish white solid (74 mg, 74% yield, mp 201–203 °C); Purification over a column of silica gel (2% EtOAc in hexane); ^{1}H NMR ($CDCl_3$, 500 MHz): δ 8.66 (d, 2H, J = 7.5 Hz), 8.43 (s, 1H), 8.26 (d, 2H, J = 8.0 Hz), 7.90–7.86 (m, 3H), 7.82–7.80 (m, 1H),

7.63–7.57 (m, 3H), 7.54–7.49 (m, 5H), 7.35 (s, 1H); $^{13}C\{1H\}$ NMR ($CDCl_3$, 125 MHz): δ 168.8, 159.8, 158.1, 156.1, 137.8, 137.7, 133.9, 133.4, 130.8, 130.6, 129.1, 129.0, 128.9, 128.8, 128.6, 128.5, 128.0, 127.3, 127.1, 126.2, 125.2, 122.5, 114.9, 99.9; IR (neat, cm^{-1}): 3057, 2925, 2854, 1594, 1548, 1399, 1240, 1026, 961, 758, 694; HRMS (ESI/Q-TOF) (m/z) calcd for $C_{28}H_{19}N_2O$ $[M + H]^+$ 399.1492; found 399.1502.

2,6-Diphenyl-4-(p-tolyl)furo[2,3-d]pyrimidine (1ba'):

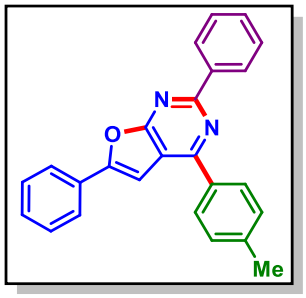

As a white solid (59 mg, 65% yield, mp 180–182 °C); Purification over a column of silica gel (1% EtOAc in hexane); ^1H NMR ($CDCl_3$, 500 MHz): δ 8.66 (d, 2H, J = 8.25 Hz), 8.18 (d, 2H, J = 8.5 Hz), 7.96 (d, 2H, J = 7.5 Hz), 7.54–7.48 (m, 5H), 7.44–7.40 (m, 3H), 7.34 (s, 1H), 2.49 (s, 3H); $^{13}C\{^1H\}$ NMR ($CDCl_3$, 125 MHz): δ 168.8, 159.8, 158.3, 156.0, 141.2, 138.0, 135.0, 130.5, 129.9, 129.8, 129.2, 128.8, 128.7, 128.5, 125.5, 114.6, 99.6, 21.7; IR (neat, cm^{-1}): 3047, 2921, 2852, 1593, 1397, 1264, 960, 749, 703; HRMS (ESI/Q-TOF) (m/z) calcd for $C_{25}H_{19}N_2O$ $[M + H]^+$ 363.1492; found 363.1501.

2,6-Diphenyl-4-(o-tolyl)furo[2,3-d]pyrimidine (1ca'):

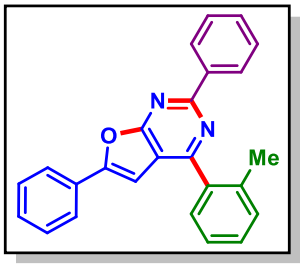

As a white solid (47 mg, 52% yield, mp 153–155 °C); Purification over a column of silica gel (1% EtOAc in hexane); ^1H NMR ($CDCl_3$, 500 MHz): δ 8.60 (d, 2H, J = 7.0 Hz), 7.92 (d, 2H, J = 7.5 Hz), 7.62 (d, 1H, J = 7.5 Hz), 7.52–7.46 (m, 5H), 7.44–7.39 (m, 4H), 7.00 (s, 1H), 2.55 (s, 3H); $^{13}C\{^1H\}$ NMR ($CDCl_3$, 125 MHz): δ 168.3, 161.1, 159.7, 156.1, 138.0, 137.2, 136.8, 131.7, 130.6, 130.0, 129.9, 129.8, 129.2, 128.7, 128.5, 126.1, 125.5, 116.9, 99.5, 20.7; IR (neat, cm^{-1}): 3063, 2919, 2852, 1593, 1488, 1399, 1265, 1018, 757, 689; HRMS (ESI/Q-TOF) (m/z) calcd for $C_{25}H_{19}N_2O$ $[M + H]^+$ 363.1492; found 363.1496.

4-(4-Ethylphenyl)-2,6-diphenylfuro[2,3-d]pyrimidine (1da'):

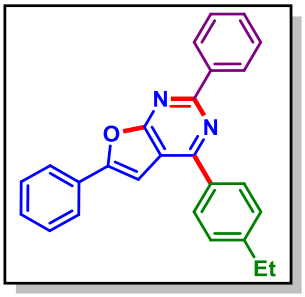

As a white solid (55 mg, 58% yield, mp 167–169 °C); Purification over a column of silica gel (1% EtOAc in hexane); ^{1}H NMR ($CDCl_3$, 500 MHz): δ 8.66 (d, 2H, J = 8.0 Hz), 8.20 (d, 2H, J = 7.5 Hz), 7.96 (d, 2H, J = 7.0 Hz), 7.54–7.43 (m, 8H), 7.35 (s, 1H), 2.79 (q, 2H, J_1 = 15 Hz, J_2 = 7.5 Hz), 1.33 (t, 3H, J = 7.5 Hz); ^{13}C{^{1}H} NMR ($CDCl_3$, 125 MHz): δ 168.8, 159.9, 158.4, 156.0, 147.5, 138.0, 135.3, 130.5, 129.9, 129.3, 129.2, 128.9, 128.72, 128.7, 128.5, 125.5, 114.6, 99.6, 29.1, 15.6; IR (neat, cm^{-1}): 2964, 2919, 2852, 1593, 1397, 1275, 750, 685; HRMS (ESI/Q-TOF) (m/z) calcd for $C_{26}H_{21}N_2O$ $[M + H]^+$ 377.1648; found 377.1650.

4-(4-(tert-Butyl)phenyl)-2,6-diphenylfuro[2,3-d]pyrimidine (1ea'):

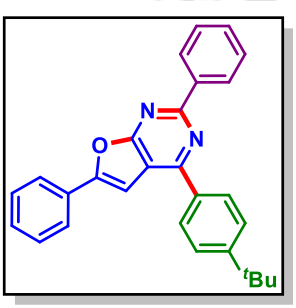

As a white solid (65 mg, 64% yield, mp 175–177 °C); Purification over a column of silica gel (1% EtOAc in hexane); ^{1}H NMR ($CDCl_3$, 500 MHz): δ 8.67 (d, 2H, J = 7.0 Hz), 8.21 (d, 2H, J = 8.5 Hz), 7.95 (d, 2H, J = 7.5 Hz), 7.64 (d, 2H, J = 8.5 Hz), 7.54–7.47 (m, 5H), 7.42 (t, 1H, J = 7.5 Hz), 7.35 (s, 1H), 1.42 (s, 9H); ^{13}C{^{1}H} NMR ($CDCl_3$, 125 MHz): δ 168.7, 159.8, 158.3, 155.9, 154.3, 137.9, 135.0, 130.5, 129.8, 129.2, 128.7, 128.6, 128.5, 126.1, 125.4, 114.7, 99.6, 35.1, 31.4; IR (neat, cm^{-1}): 3063, 2962, 2868, 1592, 1398, 1267, 1021, 963, 757, 689; HRMS (ESI/Q-TOF) (m/z) calcd for $C_{28}H_{25}N_2O$ $[M + H]^+$ 405.1961; found 405.1970.

4-(4-Fluorophenyl)-2,6-diphenylfuro[2,3-d]pyrimidine (1fa'):

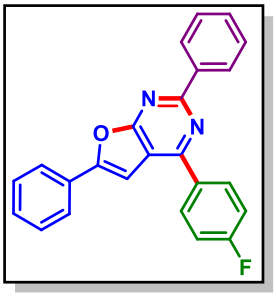

As a white solid (57 mg, 62% yield, mp 180–182 °C); Purification over a column of silica gel (1% EtOAc in hexane); ^{1}H NMR ($CDCl_3$, 500 MHz): δ 8.63 (d, 2H, J = 7.0 Hz), 8.29–8.26 (m, 2H), 7.95 (d, 2H, J = 7.5 Hz), 7.54–7.48 (m, 5H), 7.43 (t, 1H, J = 7.25 Hz), 7.31–7.27 (m, 3H); ^{13}C{^{1}H} NMR ($CDCl_3$, 125 MHz): δ 168.8, 164.5 (d, J = 250.1 Hz), 159.8, 157.0, 156.3, 137.7, 133.9 (d, J = 3.1 Hz), 130.9 (d, J = 8.6 Hz), 130.7, 130.1, 129.2, 129.0, 128.7, 128.5, 125.5, 116.2 (d, J = 21.7 Hz), 114.6, 99.2; ^{19}F NMR ($CDCl_3$, 471

MHz): δ –109.4 (s); IR (neat, cm^{-1}): 3064, 2923, 2854, 1593, 1508, 1398, 1232, 1154, 842, 751, 685; HRMS (ESI/Q-TOF) (m/z) calcd for $C_{24}H_{16}FN_2O$ $[M + H]^+$ 367.1241; found 367.1242.

4-(4-Chlorophenyl)-2,6-diphenylfuro[2,3-d]pyrimidine (1ga'):

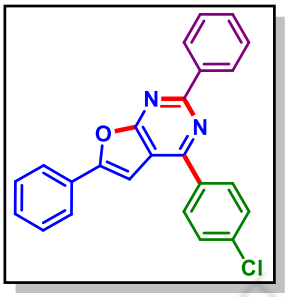

As a white solid (65 mg, 68% yield, mp 194–196 °C); Purification over a column of silica gel (1% EtOAc in hexane); ^1H NMR ($CDCl_3$, 500 MHz): δ 8.60 (d, 2H, J = 7.0 Hz), 8.18 (d, 2H, J = 8.0 Hz), 7.92 (d, 2H, J = 7.5 Hz), 7.55 (d, 2H, J = 8.0 Hz), 7.52–7.46 (m, 5H), 7.42 (t, 1H, J = 7.0 Hz), 7.24 (s, 1H); $^{13}C\{^1H\}$ NMR ($CDCl_3$, 125 MHz): δ 168.7, 159.8, 156.8, 156.4, 137.6, 137.0, 136.1, 130.7, 130.12, 130.11, 129.3, 129.2, 128.9, 128.7, 128.4, 125.5, 114.7, 99.1; IR (neat, cm^{-1}): 3059, 2921, 2857, 1591, 1489, 1396, 1275, 1092, 751, 685; HRMS (ESI/Q-TOF) (m/z) calcd for $C_{24}H_{16}ClN_2O$ $[M + H]^+$ 383.0946; found 383.0948.

4-(3-Chlorophenyl)-2,6-diphenylfuro[2,3-d]pyrimidine (1ha'):

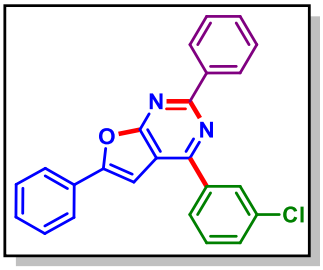

As a white solid (60 mg, 63% yield, mp 173–175 °C); Purification over a column of silica gel (1% EtOAc in hexane); ^1H NMR ($CDCl_3$, 500 MHz): δ 8.63 (d, 2H, J = 7.0 Hz), 8.25 (s, 1H), 8.13–8.11 (m, 1H), 7.96 (d, 2H, J = 7.5 Hz), 7.54–7.49 (m, 7H), 7.44 (t, 1H, J = 7.25 Hz), 7.30 (s, 1H); $^{13}C\{^1H\}$ NMR ($CDCl_3$, 125 MHz): δ 168.8, 159.9, 156.7, 156.6, 139.5, 137.6, 135.3, 130.8, 130.7, 130.3, 130.2, 129.2, 128.9, 128.8, 128.7, 128.5, 126.9, 125.6, 115.0, 99.0; IR (neat, cm^{-1}): 3057, 2925, 1569, 1400, 1264, 729, 702; HRMS (ESI/Q-TOF) (m/z) calcd for $C_{24}H_{16}ClN_2O$ $[M + H]^+$ 383.0946; found 383.0947.

4-(4-Bromophenyl)-2,6-diphenylfuro[2,3-d]pyrimidine (1ia'):

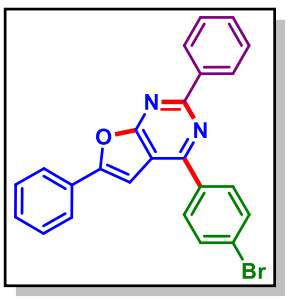

As a white solid (70 mg, 66% yield, mp 197–199 °C); Purification over a column of silica gel (1% EtOAc in hexane); ^1H NMR ($CDCl_3$, 500 MHz): δ 8.63 (d, 2H, J = 7.0 Hz), 8.15 (d, 2H, J = 8.5 Hz), 7.96 (d, 2H, J = 7.5 Hz), 7.74 (d, 2H, J = 8.5 Hz), 7.54–7.49 (m, 5H), 7.44 (t, 1H, J = 7.25 Hz), 7.30 (s, 1H); $^{13}C\{^1H\}$ NMR ($CDCl_3$, 125 MHz): δ 168.8, 159.9, 157.0, 156.5, 137.7, 136.6, 132.4, 130.7, 130.3,

130.1, 129.3, 128.9, 128.7, 128.5, 125.6, 125.4, 114.8, 99.1; IR (neat, cm^{-1}): 3059, 2920, 2852, 1589, 1486, 1358, 1264, 1070, 749, 703; HRMS (ESI/Q-TOF) (m/z) calcd for $C_{24}H_{16}BrN_2O$ $[M + H]^+$ 427.0441; found 427.0445.

2,6-Diphenyl-4-(4-(trifluoromethyl)phenyl)furo[2,3-d]pyrimidine (1ja'):

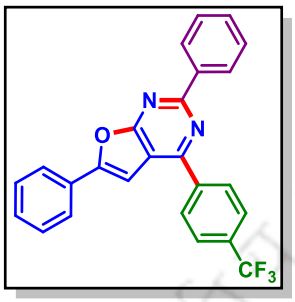

As a white solid (61 mg, 59% yield, mp 191–193 °C); Purification over a column of silica gel (1% EtOAc in hexane); ^1H NMR ($CDCl_3$, 500 MHz): δ 8.63 (d, 2H, J = 7.0 Hz), 8.35 (d, 2H, J = 8.0 Hz), 7.95 (d, 2H, J = 7.5 Hz), 7.86 (d, 2H, J = 8.0 Hz), 7.54–7.49 (m, 5H), 7.45 (t, 1H, J = 7.0 Hz), 7.29 (s, 1H); $^{13}C\{^1H\}$ NMR ($CDCl_3$, 125 MHz): δ 168.8, 160.0, 156.9, 156.5, 141.1, 137.5, 130.8, 130.3, 129.3, 129.1, 128.9, 128.8, 128.5, 126.0 (q, J_2 = 3.8 Hz), 125.6, 115.3, 98.9; ^{19}F NMR ($CDCl_3$, 471 MHz): δ –62.7 (s); IR (neat, cm^{-1}): 3062, 2923, 2852, 1592, 1490, 1324, 1122, 1066, 853, 755, 686; HRMS (ESI/Q-TOF) (m/z) calcd for $C_{25}H_{16}F_3N_2O$ $[M + H]^+$ 417.1209; found 417.1215.

2,6-Diphenyl-4-(3-(trifluoromethyl)phenyl)furo[2,3-d]pyrimidine (1ka'):

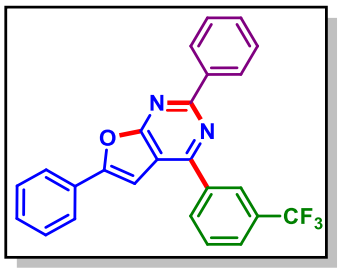

As a white solid (56 mg, 54% yield, mp 173–175 °C); Purification over a column of silica gel (1% EtOAc in hexane); ^1H NMR ($CDCl_3$, 500 MHz): δ 8.64 (d, 2H, J = 7.0 Hz), 8.53 (s, 1H), 8.44 (d, 1H, J = 7.5 Hz), 7.97 (d, 2H, J = 7.5 Hz), 7.83 (d, 1H, J = 7.5 Hz), 7.74 (t, 1H, J = 7.75 Hz), 7.56–7.50 (m, 5H), 7.46 (t, 1H, J = 7.25 Hz), 7.30 (s, 1H); $^{13}C\{^1H\}$ NMR ($CDCl_3$, 125 MHz): δ 168.9, 160.1, 156.9, 156.5, 138.6, 137.5, 132.0, 130.9, 130.3, 129.7, 129.3, 128.9, 128.8, 128.5, 127.3 (q, J_2 = 3.5 Hz), 125.7, 125.6 (q, J_2 = 4.2 Hz), 115.1, 98.8; ^{19}F NMR ($CDCl_3$, 471 MHz): δ –62.5 (s); IR (neat, cm^{-1}): 3063, 2924, 1591, 1400, 1326, 1265, 1125, 754, 691; HRMS (ESI/Q-TOF) (m/z) calcd for $C_{25}H_{16}F_3N_2O$ $[M + H]^+$ 417.1209; found 417.1211.

4-(3,4-Dichlorophenyl)-2,6-diphenylfuro[2,3-d]pyrimidine (1la'):

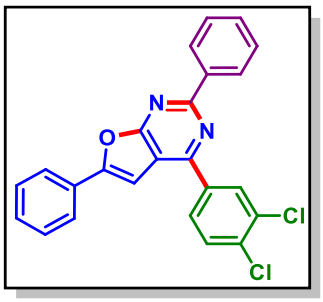

As a white solid (63 mg, 60% yield, mp 196–198 °C); Purification over a column of silica gel (1% EtOAc in hexane); ^{1}H NMR ($CDCl_3$, 500 MHz): δ 8.62 (d, 2H, J = 7.0 Hz), 8.38 (d, 1H, J = 2.0 Hz), 8.10 (dd, 1H, J_1 = 8.2 Hz, J_2 = 2.2 Hz), 7.97 (d, 2H, J = 7.5 Hz), 7.68 (d, 1H, J = 8.5 Hz), 7.55–7.50 (m, 5H), 7.46 (t, 1H, J = 7.25 Hz), 7.29 (s, 1H); ^{13}C{^{1}H} NMR ($CDCl_3$, 125 MHz): δ 168.9, 160.0, 156.9, 155.5, 137.7, 137.5, 135.1, 133.6, 131.1, 130.9, 130.6, 130.3, 129.3, 128.9, 128.8, 128.5, 127.9, 125.7, 114.9, 98.8; IR (neat, cm^{-1}): 2923, 2859, 1593, 1471, 1401, 1275, 1025, 750, 684; HRMS (ESI/Q-TOF) (m/z) calcd for $C_{24}H_{15}Cl_2N_2O$ $[M + H]^+$ 417.0556; found 417.0557.

4-(Naphthalen-2-yl)-2,6-diphenylfuro[2,3-d]pyrimidine (1ma'):

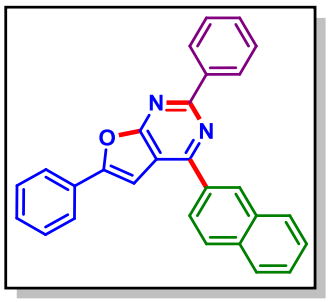

As a white solid (70 mg, 70% yield, mp 186–188 °C); Purification over a column of silica gel (1% EtOAc in hexane); ^{1}H NMR ($CDCl_3$, 500 MHz): δ 8.70–8.68 (m, 3H), 8.37 (d, 1H, J = 8.5 Hz), 8.04 (d, 2H, J = 8.5 Hz), 7.97 (d, 2H, J = 7.0 Hz), 7.95–7.93 (m, 1H), 7.60–7.58 (m, 2H), 7.56–7.49 (m, 5H), 7.44 (d, 1H, J = 7.5 Hz), 7.41 (s, 1H); ^{13}C{^{1}H} NMR ($CDCl_3$, 125 MHz): δ 168.8, 159.9, 158.2, 156.3, 137.9, 135.2, 134.5, 133.4, 130.6, 130.0, 129.2, 129.19, 129.16, 129.14, 128.9, 128.7, 128.5, 128.0, 127.6, 126.8, 125.7, 125.5, 115.1, 99.5; IR (neat, cm^{-1}): 3057, 2924, 2854, 1592, 1549, 1398, 1274, 1021, 748, 683; HRMS (ESI/Q-TOF) (m/z) calcd for $C_{28}H_{19}N_2O$ $[M + H]^+$ 399.1492; found 399.1503.

4,6-Diphenyl-2-(p-tolyl)furo[2,3-d]pyrimidine (1ab'):

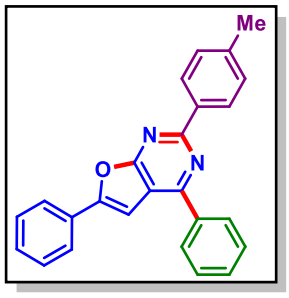

As a white solid (65 mg, 72% yield, mp 179–181 °C); Purification over a column of silica gel (1% EtOAc in hexane); ^{1}H NMR ($CDCl_3$, 500 MHz): δ 8.55 (d, 2H, J = 8.0 Hz), 8.27 (d, 2H, J = 7.5 Hz), 7.96 (d, 2H, J = 7.5 Hz), 7.63–7.55 (m, 3H), 7.49 (t, 2H, J = 7.5 Hz), 7.43 (t, 1H, J = 7.5 Hz), 7.34–7.32 (m, 3H), 2.44 (s, 3H); ^{13}C{^{1}H} NMR ($CDCl_3$, 125 MHz): δ 168.8, 160.1, 158.3, 156.0, 140.8, 137.9, 135.2,

130.7, 129.9, 129.5, 129.2, 129.1, 128.9, 128.5, 125.5, 114.6, 99.5, 21.7; IR (neat, cm^{-1}): 3065, 2921, 1596, 1490, 1398, 1272, 1019, 757, 688; HRMS (ESI/Q-TOF) (m/z) calcd for $C_{25}H_{19}N_2O$ $[M + H]^+$ 363.1492; found 363.1506.

2-(4-Methoxyphenyl)-4,6-diphenylfuro[2,3-d]pyrimidine (1ac'):

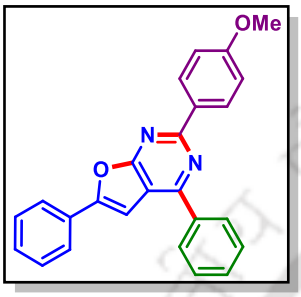

As a white solid (66 mg, 70% yield, mp 174–176 °C); Purification over a column of silica gel (1% EtOAc in hexane); ^1H NMR ($CDCl_3$, 500 MHz): δ 8.60 (d, 2H, J = 9.0 Hz), 8.25 (d, 2H, J = 7.0 Hz), 7.94 (d, 2H, J = 7.5 Hz), 7.62–7.54 (m, 3H), 7.48 (t, 2H, J = 7.5 Hz), 7.41 (t, 1H, J = 7.5 Hz), 7.31 (s, 1H), 7.03 (d, 2H, J = 9.0 Hz), 3.89 (s, 3H); $^{13}C\{^1H\}$ NMR ($CDCl_3$, 125 MHz): δ 168.8, 161.9, 159.8, 158..2, 155.7, 137.9, 130.7, 130.6, 130.1, 129.8, 129.3, 129.2, 129.1, 128.8, 125.4, 114.2, 114.0, 99.5, 55.5; IR (neat, cm^{-1}): 2957, 2926, 2857, 1594, 1400, 1252, 1164, 1022, 842, 752, 689; HRMS (ESI/Q-TOF) (m/z) calcd for $C_{25}H_{19}N_2O_2$ $[M + H]^+$ 379.1441; found 379.1447.

2-(4-(tert-Butyl)phenyl)-4,6-diphenylfuro[2,3-d]pyrimidine (1ad'):

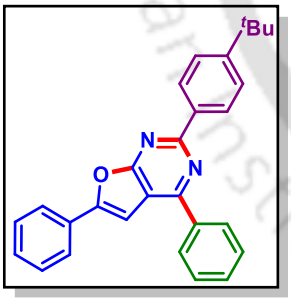

As a white solid (67 mg, 66% yield, mp 138–140 °C); Purification over a column of silica gel (1% EtOAc in hexane); ^1H NMR ($CDCl_3$, 500 MHz): δ 8.59 (d, 2H, J = 8.0 Hz), 8.26 (d, 2H, J = 7.5 Hz), 7.94 (d, 2H, J = 7.5 Hz), 7.60 (t, 2H, J = 7.0 Hz), 7.57–7.55 (m, 3H), 7.48 (t, 2H, J = 7.5 Hz), 7.41 (t, 1H, J = 7.5 Hz), 7.31 (s, 1H), 1.41 (s, 9H); $^{13}C\{^1H\}$ NMR ($CDCl_3$, 125 MHz): δ 168.8, 160.0, 158.1, 155.9, 153.9, 137.8, 135.2, 130.7, 129.8, 129.1, 129.0, 128.8, 128.3, 125.6, 125.4, 114.6, 99.5, 35.0, 31.4; IR (neat, cm^{-1}): 3059, 2961, 2867, 1593, 1547, 1360, 1266, 1175, 1017, 849, 749, 687; HRMS (ESI/Q-TOF) (m/z) calcd for $C_{28}H_{25}N_2O$ $[M + H]^+$ 405.1961; found 405.1969.

2-(4-Butoxyphenyl)-4,6-diphenylfuro[2,3-d]pyrimidine (1ae'):

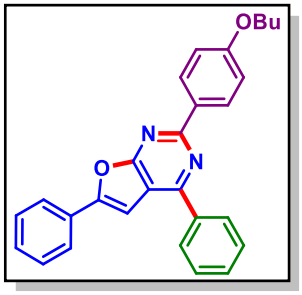

As a white solid (79 mg, 75% yield, mp 153–155 °C); Purification over a column of silica gel (1% EtOAc in hexane); ^{1}H NMR ($CDCl_3$, 600 MHz): δ 8.56 (d, 2H, J = 9.0 Hz), 8.22 (d, 2H, J = 7.8 Hz), 7.90 (d, 2H, J = 7.8 Hz), 7.58 (t, 2H, J = 7.8 Hz), 7.55–7.53 (m, 1H), 7.44 (t, 2H, J = 7.2 Hz), 7.38 (t, 1H, J = 7.2 Hz), 7.24 (s, 1H), 7.01 (d, 2H, J = 9.0 Hz), 4.03 (t, 2H, J = 6.6 Hz), 1.83–1.79 (m, 2H), 1.56–1.50 (m, 2H), 1.01 (t, 3H, J = 7.5 Hz); ^{13}C{^{1}H} NMR ($CDCl_3$, 150 MHz): δ 168.7, 161.4, 159.7, 158.0, 155.5, 137.8, 130.6, 130.3, 130.0, 129.7, 129.1, 129.09, 129.01, 128.8, 125.3, 114.4, 114.0, 99.4, 67.9, 31.4, 19.4, 14.0; IR (neat, cm^{-1}): 3060, 2957, 2871, 1592, 1400, 1361, 1247, 1164, 1022, 843, 758, 698; HRMS (ESI/Q-TOF) (m/z) calcd for $C_{28}H_{25}N_2O_2$ $[M + H]^+$ 421.1911; found 421.1914.

2-(4-(Methylthio)phenyl)-4,6-diphenylfuro[2,3-d]pyrimidine (1af'):

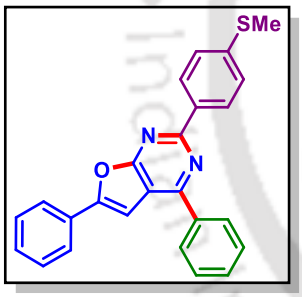

As a white solid (72 mg, 73% yield, mp 164–166 °C); Purification over a column of silica gel (1% EtOAc in hexane); ^{1}H NMR ($CDCl_3$, 500 MHz): δ 8.55 (d, 2H, J = 8.5 Hz), 8.23 (d, 2H, J = 7.5 Hz), 7.93 (d, 2H, J = 8.0 Hz), 7.61–7.54 (m, 3H), 7.48 (t, 2H, J = 7.25 Hz), 7.41 (t, 1H, J = 7.5 Hz), 7.35 (d, 2H, J = 8.5 Hz), 7.30 (s, 1H), 2.55 (s, 3H); ^{13}C{^{1}H} NMR ($CDCl_3$, 125 MHz): δ 168.7, 159.5, 158.2, 156.0, 141.9, 137.7, 134.4, 130.7, 129.9, 129.2, 129.1, 128.9, 128.8, 125.9, 125.4, 114.7, 99.5, 15.4; IR (neat, cm^{-1}): 3058, 2920, 2854, 1587, 1396, 1265, 1087, 960, 734, 699; HRMS (ESI/Q-TOF) (m/z) calcd for $C_{25}H_{19}N_2OS$ $[M + H]^+$ 395.1213; found 395.1218.

2-(4-Fluorophenyl)-4,6-diphenylfuro[2,3-d]pyrimidine (1ag'):

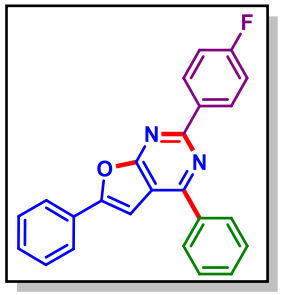

As a white solid (60 mg, 65% yield, mp 202–204 °C); Purification over a column of silica gel (1% EtOAc in hexane); ^{1}H NMR ($CDCl_3$, 500 MHz): δ 8.66–8.63 (m, 2H), 8.24 (d, 2H, J = 7.5 Hz), 7.95 (d, 2H, J = 7.5 Hz), 7.62–7.56 (m, 3H), 7.49 (t, 2H, J = 7.5 Hz), 7.43 (t, 1H, J = 7.25 Hz), 7.33 (s, 1H), 7.19 (t, 2H, J = 8.75 Hz); ^{13}C{^{1}H}

NMR ($CDCl_3$, 125 MHz): δ 168.7, 164.7 (d, J = 248.5 Hz), 159.0, 158.3, 156.2, 137.6, 134.1 (d, J = 2.8 Hz), 130.8, 130.6 (d, J = 8.6 Hz), 130.0, 129.2, 129.1, 129.0, 128.8, 125.5, 115.6 (d, J = 21.6 Hz), 114.8, 99.4; ^{19}F NMR ($CDCl_3$, 471 MHz): δ –110.7 (s); IR (neat, cm^{-1}): 2922, 2854, 1608, 1553, 1451, 1396, 1274, 1149, 848, 753, 691; HRMS (ESI/Q-TOF) (m/z) calcd for $C_{24}H_{16}FN_2O$ $[M + H]^+$ 367.1241; found 367.1241.

2-(4-Chlorophenyl)-4,6-diphenylfuro[2,3-d]pyrimidine (1ah'):

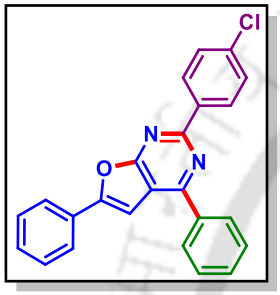

As a white solid (67 mg, 70% yield, mp 235–237 °C); Purification over a column of silica gel (1% EtOAc in hexane); ^1H NMR ($CDCl_3$, 500 MHz): δ 8.60 (d, 2H, J = 9.0 Hz), 8.25 (d, 2H, J = 7.5 Hz), 7.96 (d, 2H, J = 8.0 Hz), 7.63–7.56 (m, 3H), 7.52–7.43 (m, 5H), 7.35 (s, 1H); $^{13}C\{^1H\}$ NMR ($CDCl_3$, 125 MHz): δ 168.7, 158.9, 158.4, 156.5, 137.6, 136.8, 136.4, 130.9, 130.1, 129.8, 129.3, 129.2, 129.0, 128.95, 128.91, 125.5, 115.1, 99.5; IR (neat, cm^{-1}): 2918, 2850, 1589, 1490, 1364, 1275, 1088, 753, 693; HRMS (ESI/Q-TOF) (m/z) calcd for $C_{24}H_{16}ClN_2O$ $[M + H]^+$ 383.0946; found 383.0946.

2-(3-Bromophenyl)-4,6-diphenylfuro[2,3-d]pyrimidine (1ai'):

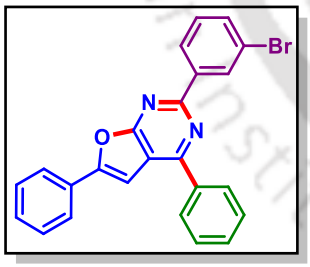

As a white solid (70 mg, 66% yield, mp 188–190 °C); Purification over a column of silica gel (1% EtOAc in hexane); ^1H NMR ($CDCl_3$, 600 MHz): δ 8.78 (s, 1H), 8.55 (d, 1H, J = 7.8 Hz), 8.22 (d, 2H, J = 7.2 Hz), 7.92 (d, 2H, J = 7.8 Hz), 7.61–7.57 (m, 4H), 7.48 (t, 2H, J = 7. 5 Hz), 7.42 (t, 1H, J = 7.2 Hz), 7.36 (t, 1H, J = 8.1 Hz), 7.30 (s, 1H); $^{13}C\{^1H\}$ NMR ($CDCl_3$, 150 MHz): δ 168.5, 158.3, 158.2, 156.5, 139.9, 137.4, 133.4, 131.4, 130.9, 130.2, 130.1, 129.2, 129.1, 128.9, 128.8, 127.0, 125.5, 123.0, 115.3, 99.4; IR (neat, cm^{-1}): 3063, 2923, 2851, 1598, 1489, 1362, 1263, 1021, 756, 697; HRMS (ESI/Q-TOF) (m/z) calcd for $C_{24}H_{16}BrN_2O$ $[M + H]^+$ 427.0441; found 427.0441.

2-(3,4-Dimethoxyphenyl)-4,6-diphenylfuro[2,3-d]pyrimidine (1aj'):

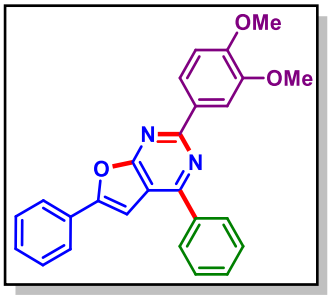

As a white solid (63 mg, 62% yield, mp 161–163 °C); Purification over a column of silica gel (1% EtOAc in hexane); ^{1}H NMR ($CDCl_3$, 500 MHz): δ 8.29 (d, 1H, J = 8.5 Hz), 8.25 (d, 2H, J = 7.5 Hz), 8.20 (s, 1H), 7.95 (d, 2H, J = 8.0 Hz), 7.63–7.57 (m, 3H), 7.49 (t, 2H, J = 7.5 Hz), 7.42 (t, 1H, J = 7.25 Hz), 7.32 (s, 1H), 7.01 (d, 1H, J = 8.5 Hz), 4.06 (s, 3H), 3.97 (s, 3H); ^{13}C{^{1}H} NMR ($CDCl_3$, 125 MHz): δ 168.8, 159.8, 158.2, 155.8, 151.4, 149.1, 137.8, 130.8, 130.7, 129.9, 129.2, 129.1, 128.8, 125.4, 121.9, 114.3, 111.2, 111.0, 99.5, 56.2, 56.1; IR (neat, cm^{-1}): 3057, 2932, 2834, 1594, 1515, 1401, 1361, 1265, 1132, 1024, 898, 759, 700; HRMS (ESI/Q-TOF) (m/z) calcd for $C_{26}H_{21}N_2O_3$ $[M + H]^+$ 409.1547; found 409.1552.

2-(4,6-Diphenylfuro[2,3-d]pyrimidin-2-yl)phenol (1ak'):

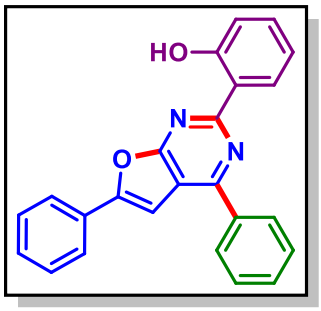

As a white solid (46 mg, 50% yield, mp 195–197 °C); Purification over a column of silica gel (3% EtOAc in hexane); ^{1}H NMR ($CDCl_3$, 600 MHz): δ 13.71 (s, 1H), 8.60 (dd, 1H, J_1 = 7.8 Hz, J_2 = 1.8 Hz), 8.10 (d, 2H, J = 7.2 Hz), 7.96 (d, 2H, J = 7.8 Hz), 7.65–7.61 (m, 3H), 7.51 (t, 2H, J = 7.5 Hz), 7.47–7.44 (m, 1H), 7.42–7.39 (m, 1H), 7.34 (s, 1H), 7.06 (d, 1H, J = 8.4 Hz), 7.01 (t, 1H, J = 6.9 Hz); ^{13}C{^{1}H} NMR ($CDCl_3$, 150 MHz): δ 167.8, 160.6, 160.5, 157.0, 156.8, 136.4, 133.1, 131.4, 130.3, 129.6, 129.3, 129.2, 128.7, 128.6, 125.6, 119.4, 119.2, 118.0, 114.8, 99.3; IR (neat, cm^{-1}): 3400, 2938, 2830, 1590, 1509, 1400, 1262, 1136, 1023, 756, 698; HRMS (ESI/Q-TOF) (m/z) calcd for $C_{24}H_{17}N_2O_2$ $[M + H]^+$ 365.1285; found 365.1295.

2-([1,1'-Biphenyl]-4-yl)-4,6-diphenylfuro[2,3-d]pyrimidine (1al'):

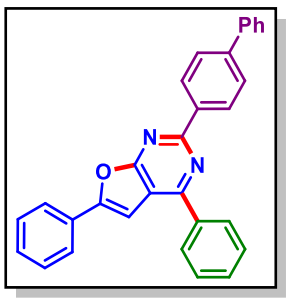

As a yellow solid (70 mg, 66% yield, mp 184–186 °C); Purification over a column of silica gel (2% EtOAc in hexane); ^{1}H NMR ($CDCl_3$, 500 MHz): δ 8.71 (d, 2H, J = 8.5 Hz), 8.27 (d, 2H, J = 7.0 Hz), 7.94 (d, 2H, J = 7.5 Hz), 7.75 (d, 2H, J = 8.0 Hz), 7.70 (d, 2H, J = 7.5 Hz), 7.62 (t, 2H, J = 7.25 Hz), 7.57 (t, 1H, J = 7.0 Hz), 7.48 (t, 4H, J = 7.25 Hz), 7.43 (d, 1H, J = 7.0 Hz), 7.39 (t, 1H, J = 7.5 Hz), 7.31 (s,

1H); $^{13}C\{^{1}H\}$ NMR ($CDCl_3$, 125 MHz): δ 168.7, 159.6, 158.2, 156.1, 143.2, 140.8, 137.7, 136.8, 130.8, 129.9, 129.2, 129.1, 129.0, 128.98, 128.91, 127.8, 127.3, 125.5, 114.8, 99.5; IR (neat, cm^{-1}): 3058, 3034, 1593, 1489, 1399, 1362, 1172, 1020, 756, 696; HRMS (ESI/Q-TOF) (m/z) calcd for $C_{30}H_{21}N_2O$ $[M + H]^+$ 425.1648; found 425.1658.

2-(Naphthalen-1-yl)-4,6-diphenylfuro[2,3-d]pyrimidine (1am'):

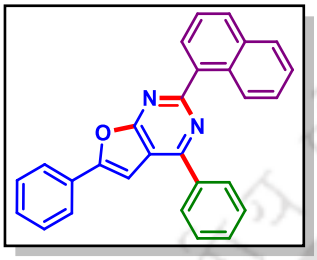

As a white solid (64 mg, 64% yield, mp 170–172 °C); Purification over a column of silica gel (2% EtOAc in hexane); ^{1}H NMR ($CDCl_3$, 500 MHz): δ 8.98 (d, 1H, *J* = 8.5 Hz), 8.32–8.28 (m, 3H), 8.00–7.97 (m, 3H), 7.95 (d, 1H, *J* = 8.0 Hz), 7.65–7.55 (m, 6H), 7.50 (t, 2H, *J* = 8.0 Hz), 7.45 (d, 1H, *J* = 7.5 Hz), 7.41 (s, 1H); $^{13}C\{^{1}H\}$ NMR ($CDCl_3$, 125 MHz): δ 168.4, 161.8, 158.2, 156.4, 137.6, 136.0, 134.4, 131.4, 130.8, 130.5, 130.0, 129.9, 129.3, 129.2, 129.0, 128.9, 128.6, 126.9, 126.4, 125.9, 125.6, 125.4, 114.6, 99.3; IR (neat, cm^{-1}): 3052, 2927, 2854, 1596, 1552, 1490, 1360, 1265, 1021, 949, 759, 700; HRMS (ESI/Q-TOF) (m/z) calcd for $C_{28}H_{19}N_2O$ $[M + H]^+$ 399.1492; found 399.1498.

2-(4-Bromothiophen-2-yl)-4,6-diphenylfuro[2,3-d]pyrimidine (1an'):

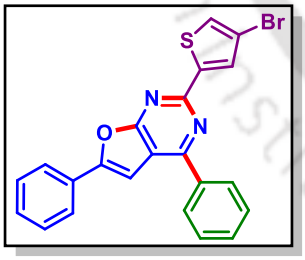

As a white solid (74 mg, 68% yield, mp 204–206 °C); Purification over a column of silica gel (2% EtOAc in hexane); ^{1}H NMR ($CDCl_3$, 500 MHz): δ 8.19 (d, 2H, *J* = 8.0 Hz), 8.02 (s, 1H), 7.92 (d, 2H, *J* = 7.5 Hz), 7.61–7.56 (m, 3H), 7.48 (t, 2H, *J* = 7.25 Hz), 7.43 (t, 1H, *J* = 7.0 Hz), 7.35 (s, 1H), 7.30 (s, 1H); $^{13}C\{^{1}H\}$ NMR ($CDCl_3$, 125 MHz): δ 168.2, 158.4, 156.5, 155.3, 144.5, 137.0, 131.1, 130.9, 130.1, 129.3, 129.2, 128.8, 126.7, 125.5, 115.1, 111.0, 99.6; IR (neat, cm^{-1}): 3052, 2924, 2859, 1578, 1490, 1435, 1365, 1240, 753, 686; HRMS (ESI/Q-TOF) (m/z) calcd for $C_{22}H_{14}BrN_2OS$ $[M + H]^+$ 433.0005; found 433.0005.

2-Cyclohexyl-4,6-diphenylfuro[2,3-d]pyrimidine (1ao'):

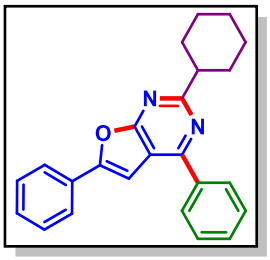

As a gummy liquid (47 mg, 53% yield); Purification over a column of silica gel (2% EtOAc in hexane); ^{1}H NMR ($CDCl_3$, 500 MHz): δ 8.15 (d, 2H, J = 7.0 Hz), 7.92 (d, 2H, J = 7.5 Hz), 7.59–7.52 (m, 3H), 7.47 (t, 2H, J = 7.75 Hz), 7.41 (t, 1H, J = 7.25 Hz), 7.29 (s, 1H), 3.09–3.03 (m, 1H), 2.16–2.13 (m, 2H), 1.92–1.88 (m, 2H), 1.84–1.76 (m, 3H), 1.52–1.43 (m, 3H); ^{13}C{^{1}H} NMR ($CDCl_3$, 125 MHz): δ 170.2, 168.5, 158.3, 155.5, 137.9, 130.6, 129.8, 129.3, 129.2, 129.1, 128.8, 125.4, 114.2, 99.1, 47.6, 32.3, 26.5, 26.3; IR (neat, cm^{-1}): 2920, 2856, 1560, 1490, 1262, 1355, 1080, 820, 752, 696; HRMS (ESI/Q-TOF) (m/z) calcd for $C_{24}H_{23}N_2O$ $[M + H]^+$ 355.1805; found 355.1811.

2-Amino-5-phenylfuran-3-carbonitrile (1'):

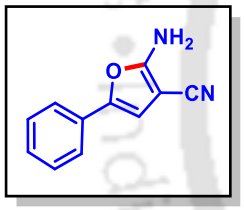

As a white solid (37 mg, 80% yield, mp 186–188 ^{o}C); Purification over a column of silica gel (15% EtOAc in hexane); ^{1}H NMR (DMSO-d_6, 500 MHz): δ 7.58 (s, 2H), 7.48 (d, 2H, J = 8.0 Hz), 7.36 (t, 2H, J = 8.0 Hz), 7.20 (t, 1H, J = 7.25 Hz), 6.96 (s, 1H); ^{13}C{^{1}H} NMR (DMSO-d_6, 125 MHz): δ 164.0, 141.8, 129.3, 128.8, 126.5, 122.0, 116.0, 106.7, 66.2; IR (neat, cm^{-1}): 3415, 3320, 2958, 2921, 2851, 2205, 1646, 1491, 1173, 1066, 882, 758; HRMS (ESI/Q-TOF) (m/z) calcd for $C_{11}H_9N_2O$ $[M + H]^+$ 185.0709; found 185.0704.

(E)-2-(Benzylideneamino)-5-phenylfuran-3-carbonitrile (1a'):

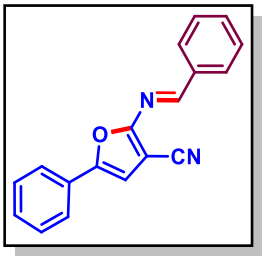

As a yellow solid (29 mg, 43% yield, mp 132–134 ^{o}C); Purification over a column of silica gel (2% EtOAc in hexane); ^{1}H NMR ($CDCl_3$, 500 MHz): δ 8.87 (s, 1H), 8.00 (d, 2H, J = 7.5 Hz), 7.69 (d, 2H, J = 7.5 Hz), 7.56–7.53 (m, 1H), 7.50 (t, 2H, J = 7.25 Hz), 7.44 (t, 2H, J = 7.5 Hz), 7.37 (t, 1H, J = 7.25 Hz), 6.84 (s, 1H); ^{13}C{^{1}H} NMR ($CDCl_3$, 125 MHz): δ 159.9, 159.8, 151.2, 135.4, 133.0, 129.9, 129.3, 129.2, 129.1, 128.8, 124.4, 113.8, 107.7, 92.5; IR (neat, cm^{-1}): 3062, 2924, 2231, 1566, 1449, 1209, 756, 685; HRMS (ESI/Q-TOF) (m/z) calcd for $C_{18}H_{13}N_2O$ $[M + H]^+$ 273.1022; found 273.1024.

2,5,6,12-Tetraphenylfuro[3',2':5,6]pyrimido[2,1-a]isoquinolin-4-ium (1x):

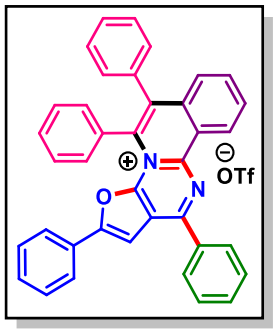

As a yellow solid (76 mg, 72% yield, mp 246–248 °C); Purification over a column of silica gel (2% MeOH in DCM); ^{1}H NMR (DMSO-d_6, 500 MHz): δ 9.71 (d, 1H, J = 8.5 Hz), 8.75 (d, 2H, J = 7.5 Hz), 8.54 (s, 1H), 8.21 (t, 1H, J = 7.5 Hz), 8.16 (t, 1H, J = 7.5 Hz), 7.92–7.85 (m, 3H), 7.61 (d, 2H, J = 7.5 Hz), 7.54 (t, 1H, J = 7.5 Hz), 7.51–7.45 (m, 4H), 7.42–7.37 (m, 5H), 7.27 (d, 2H, J = 6.5 Hz), 7.20 (d, 2H, J = 7.5 Hz); ^{13}C{^{1}H} NMR (DMSO-d_6, 125 MHz): δ 158.9, 156.5, 154.3, 144.1, 135.7, 135.2, 134.1, 134.0, 133.8, 133.63, 133.60, 133.5, 131.2, 131.0, 130.8, 130.4, 130.1, 129.9, 129.4, 128.9, 128.3, 128.2, 128.1, 126.6, 126.3, 125.2, 125.1, 117.8, 101.2; IR (neat, cm^{-1}): 3055, 2924, 1583, 1492, 1361, 1264, 1031, 731, 702; HRMS (ESI/Q-TOF) (m/z) calcd for $C_{38}H_{26}N_2O$ $[M + H]^+$ 526.2040; found 526.2016.

6-([1,1'-Biphenyl]-4-yl)-2,4-diphenylfuro[2,3-d]pyrimidine (8y):

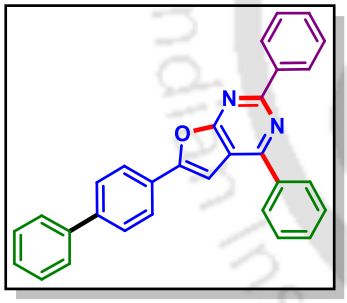

As a white solid (68 mg, 80% yield, mp 196–198 °C); Purification over a column of silica gel (1% EtOAc in hexane); ^{1}H NMR ($CDCl_3$, 500 MHz): δ 8.66 (d, 2H, J = 7.0 Hz), 8.26 (d, 2H, J = 7.0 Hz), 7.96 (d, 2H, J = 8.5 Hz), 7.68 (d, 2H, J = 8.0 Hz), 7.64–7.56 (m, 5H), 7.54–7.49 (m, 3H), 7.46 (t, 2H, J = 7.75 Hz), 7.38 (t, 1H, J = 7.25 Hz), 7.30 (s, 1H); ^{13}C{^{1}H} NMR ($CDCl_3$, 125 MHz): δ 168.7, 159.8, 158.1, 155.9, 142.5, 140.1, 137.8, 137.7, 130.7, 130.6, 129.1, 128.8, 128.6, 128.5, 128.0, 127.8, 127.7, 127.1, 125.8, 114.9, 99.4; IR (neat, cm^{-1}): 3058, 2925, 1594, 1484, 1362, 1264, 757, 696; HRMS (ESI/Q-TOF) (m/z) calcd for $C_{30}H_{21}N_2O$ $[M + H]^+$ 425.1648; found 425.1657.

(E)-6-(4-(4-Methylstyryl)phenyl)-2,4-diphenylfuro[2,3-d]pyrimidine (8z):

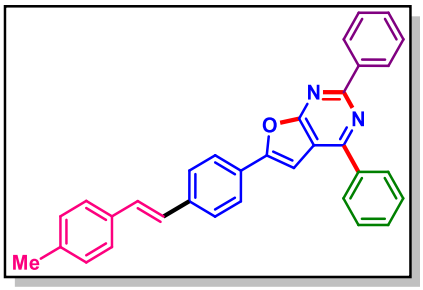

As a yellowish white solid (76 mg, 82% yield, mp 216–218 ^{o}C); Purification over a column of silica gel (1% EtOAc in hexane); ^{1}H NMR ($CDCl_3$, 500 MHz): δ 8.65 (d, 2H, J = 7.0 Hz), 8.25 (d, 2H, J = 7.0 Hz), 7.88 (d, 2H, J = 8.0 Hz), 7.61–7.48 (m, 8H), 7.41 (d, 2H, J = 7.5 Hz), 7.27 (s, 1H), 7.17 (d, 2H, J = 7.5 Hz), 7.15–7.01 (m, 2H), 2.37 (s, 3H); ^{13}C{^{1}H} NMR ($CDCl_3$, 125 MHz): δ 168.7, 159.7, 157.9, 156.0, 139.2, 138.2, 137.9, 137.8, 134.3, 130.7, 130.5, 130.1, 129.6, 129.1, 128.9, 128.6, 128.5, 127.7, 127.0, 126.9, 126.8, 125.7, 115.0, 99.2, 21.4; IR (neat, cm^{-1}): 3055, 2923, 2854, 1594, 1399, 1362, 1264, 961, 730, 702; HRMS (ESI/Q-TOF) (m/z) calcd for $C_{33}H_{25}N_2O$ $[M + H]^+$ 465.1961; found 465.1968.

III.10. Representative NMR Spectra:

2,4,6-Triphenylfuro[2,3-d]pyrimidine (1aa'): ^{1}H NMR (CDCl$_3$, 500 MHz)

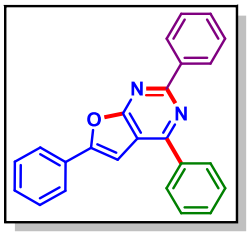

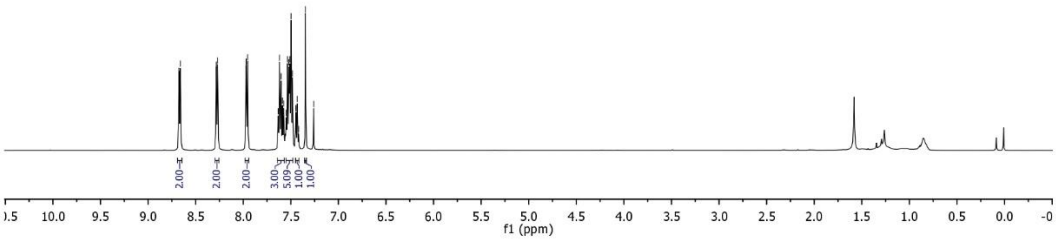

2,4,6-Triphenylfuro[2,3-d]pyrimidine (1aa'):^{13}C{^{1}H} NMR (CDCl$_3$, 125 MHz)

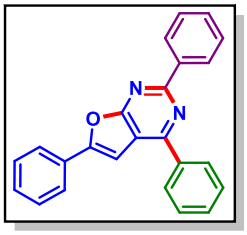

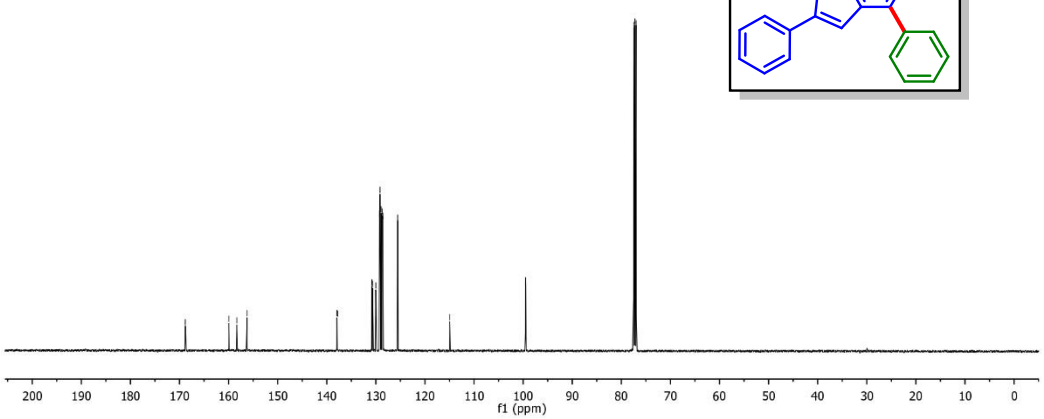

2,4-Diphenyl-6-(p-tolyl)furo[2,3-d]pyrimidine (2aa'): ^{1}H NMR (CDCl$_3$, 500 MHz)

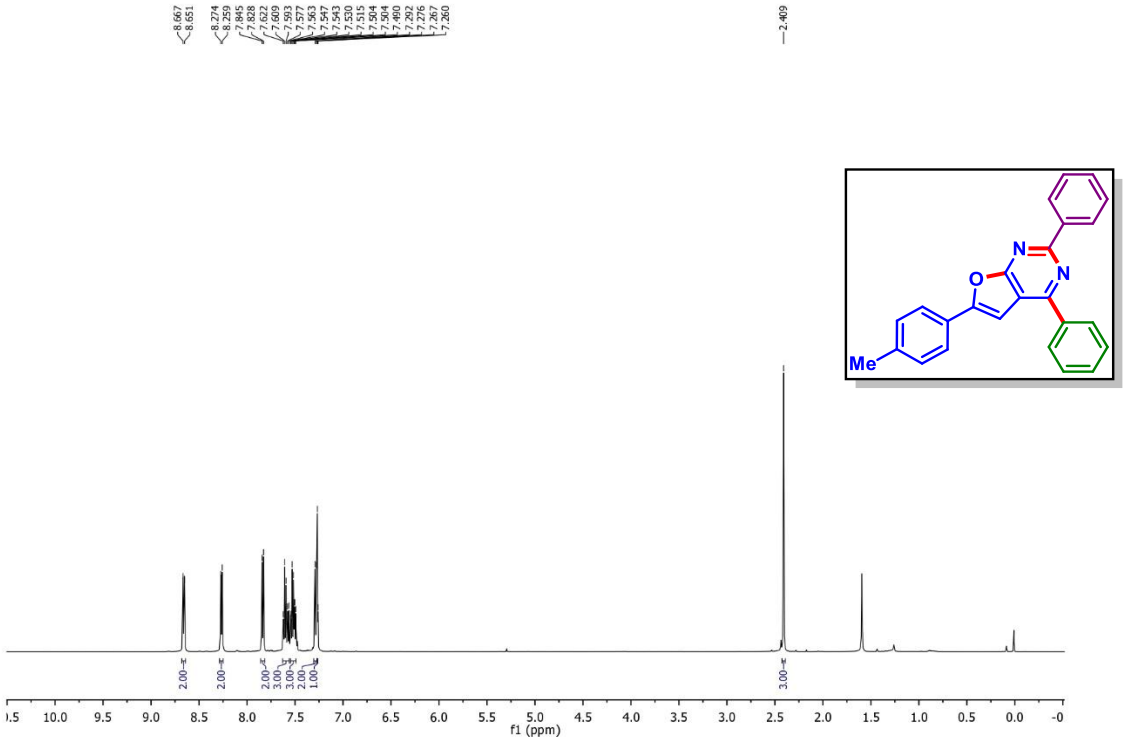

2,4-Diphenyl-6-(p-tolyl)furo[2,3-d]pyrimidine (2aa'): ^{13}C{^{1}H} NMR (CDCl$_3$, 125 MHz)

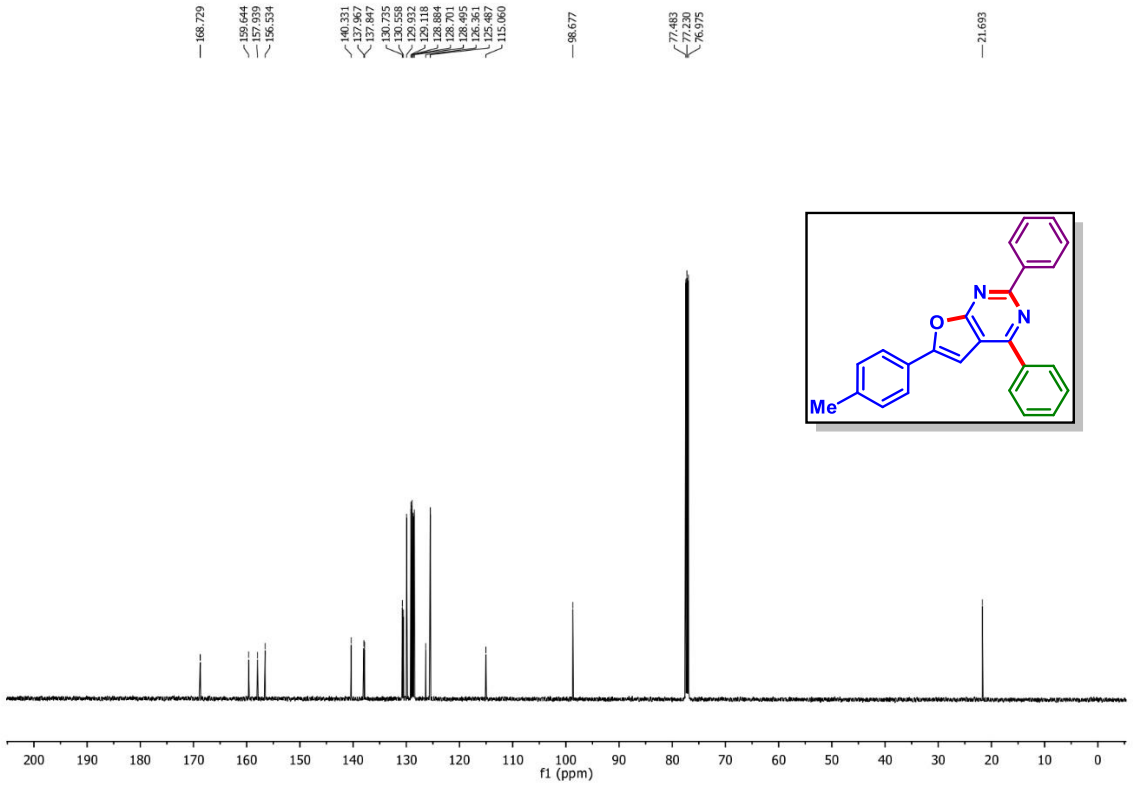

6-(4-Chlorophenyl)-2,4-diphenylfuro[2,3-d]pyrimidine (6aa'): ^{1}H NMR (CDCl$_3$, 500 MHz)

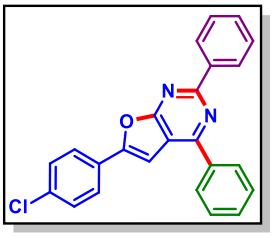

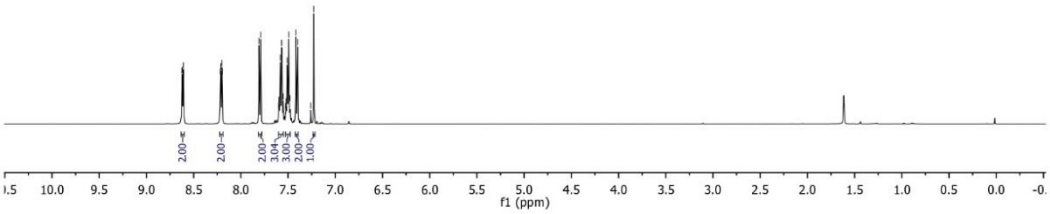

6-(4-Chlorophenyl)-2,4-diphenylfuro[2,3-d]pyrimidine (6aa'): ^{13}C{^{1}H} NMR (CDCl$_3$, 125 MHz)

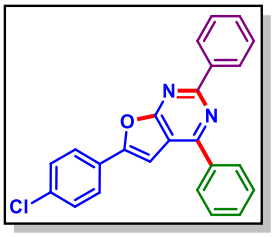

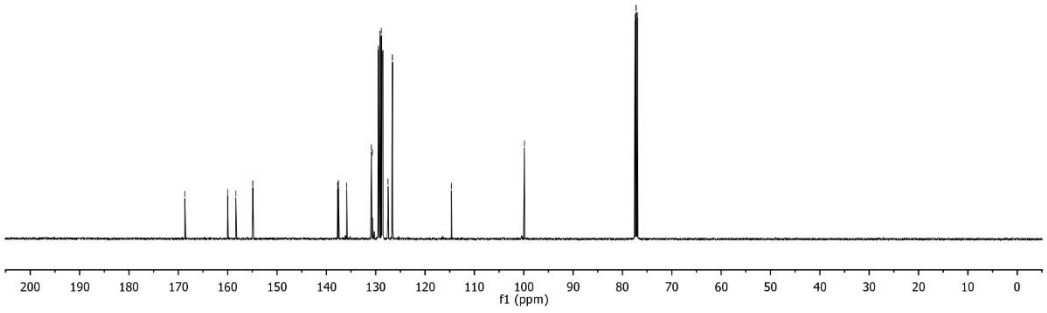

6-(Naphthalen-2-yl)-2,4-diphenylfuro[2,3-d]pyrimidine (11aa'): ^{1}H NMR (CDCl$_3$, 500 MHz)

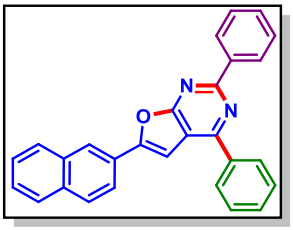

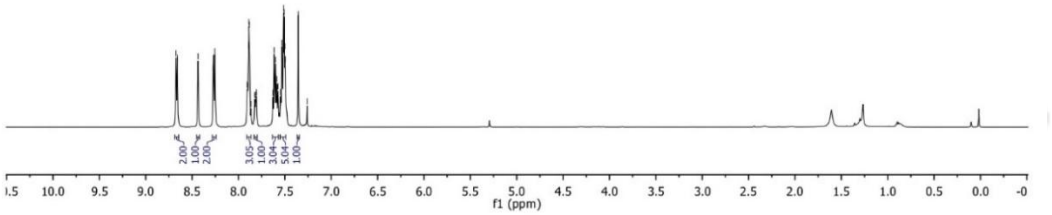

6-(Naphthalen-2-yl)-2,4-diphenylfuro[2,3-d]pyrimidine (11aa'): ^{13}C{^{1}H} NMR (CDCl$_3$, 125 MHz)

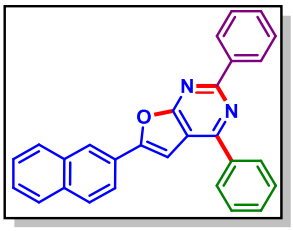

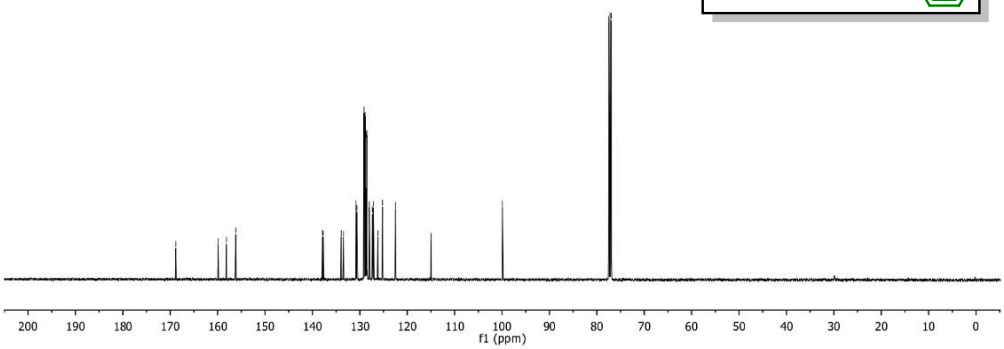

4-(4-Ethylphenyl)-2,6-diphenylfuro[2,3-d]pyrimidine (1da'):^{1}H NMR (CDCl$_3$, 500 MHz)

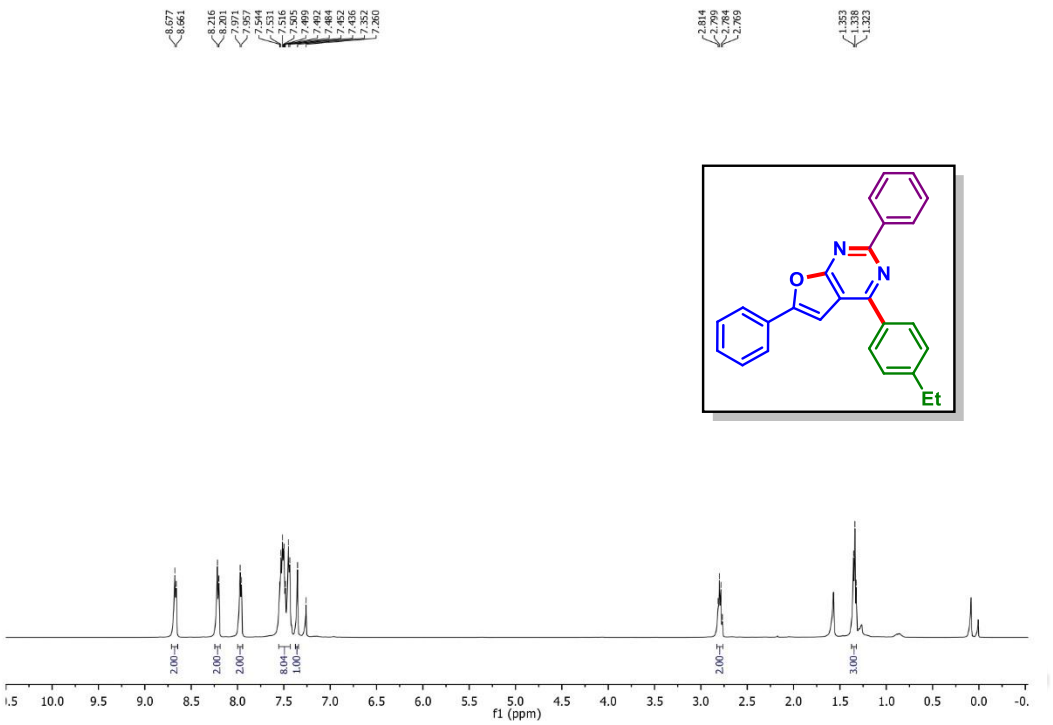

4-(4-Ethylphenyl)-2,6-diphenylfuro[2,3-d]pyrimidine (1da'): ^{13}C{^{1}H} NMR (CDCl$_3$, 125 MHz)

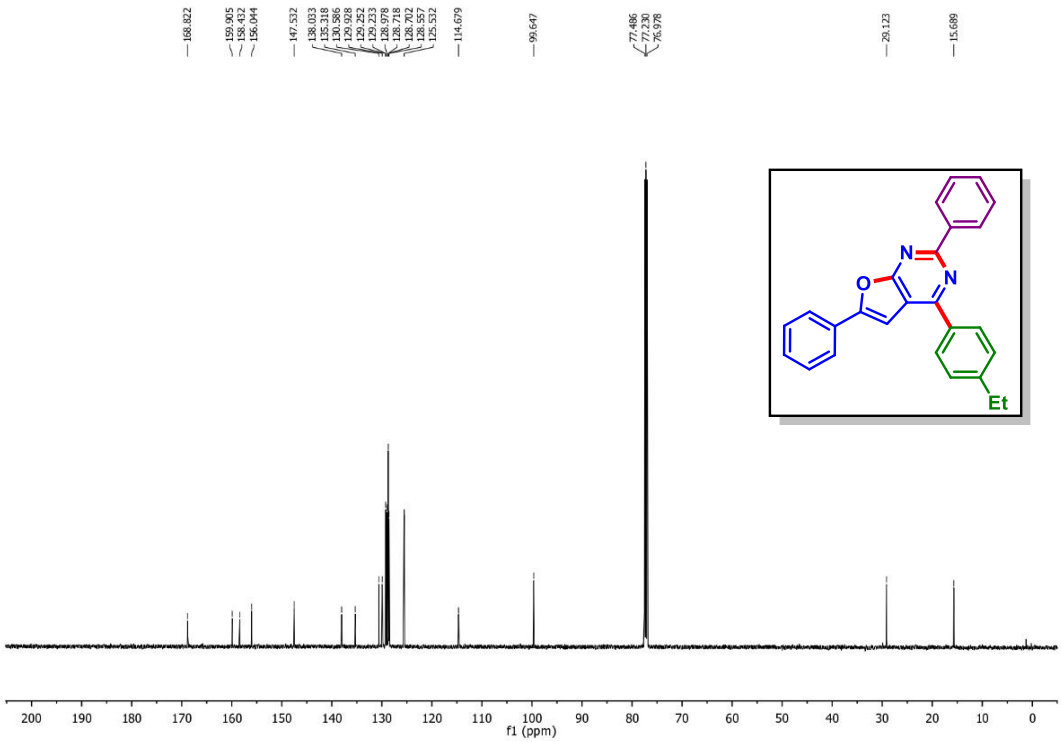

4-(3-Chlorophenyl)-2,6-diphenylfuro[2,3-d]pyrimidine (1ha'): ^{1}H NMR (CDCl$_3$, 500 MHz)

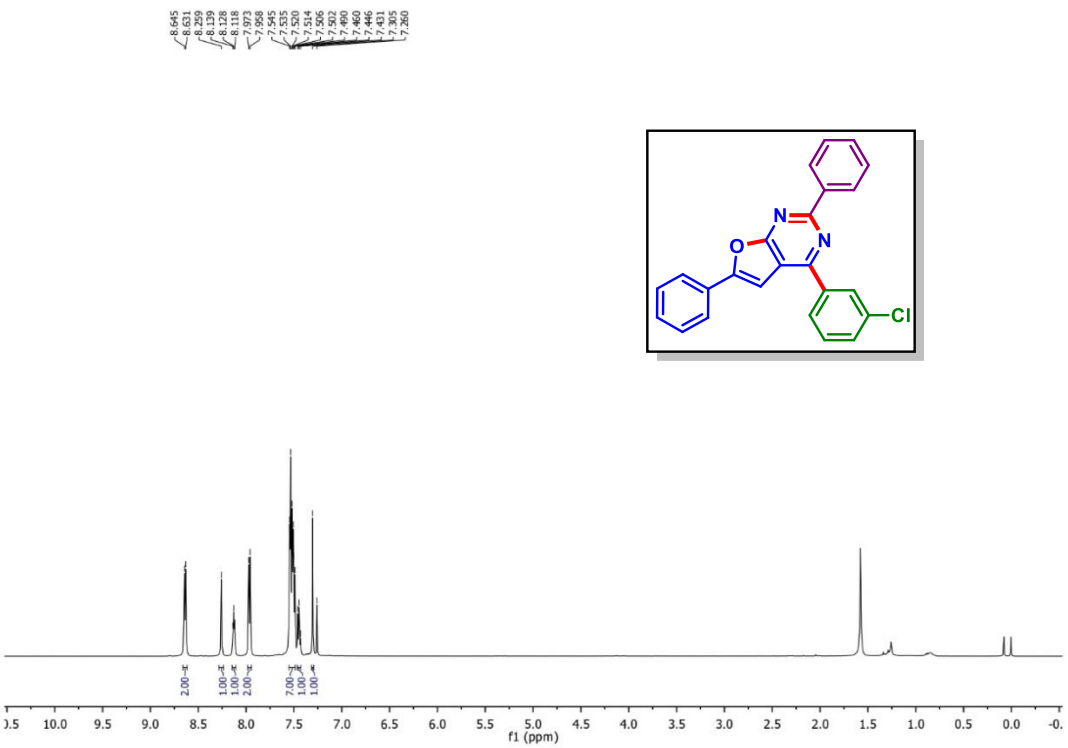

4-(3-Chlorophenyl)-2,6-diphenylfuro[2,3-d]pyrimidine (1ha'): ^{13}C{^{1}H} NMR (CDCl$_3$, 125 MHz)

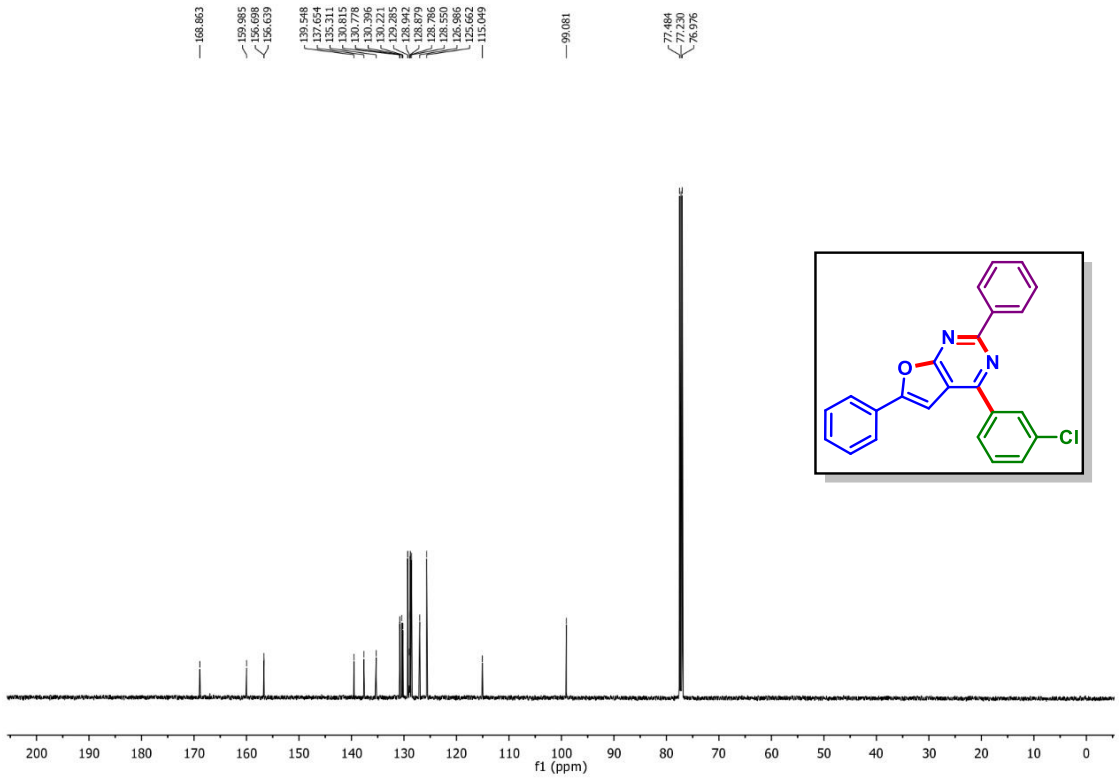

2-(4-Methoxyphenyl)-4,6-diphenylfuro[2,3-d]pyrimidine (1ac'): ^{1}H NMR (CDCl$_3$, 500 MHz)

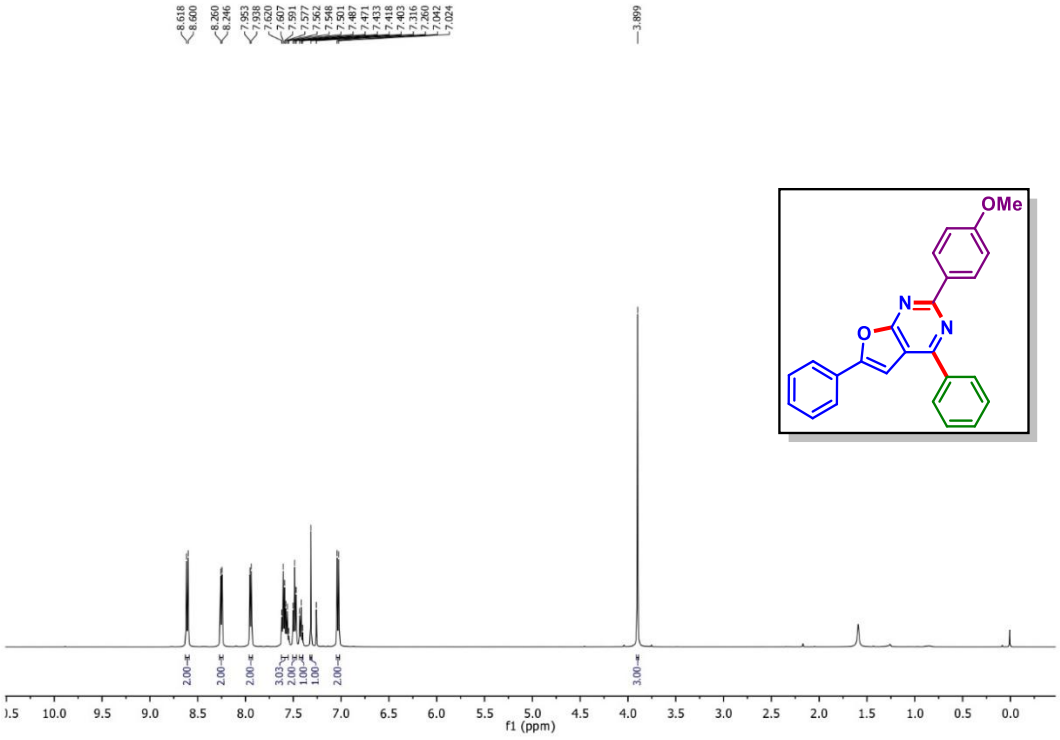

2-(4-Methoxyphenyl)-4,6-diphenylfuro[2,3-d]pyrimidine (1ac'): ^{13}C{^{1}H} NMR (CDCl$_3$, 125 MHz)

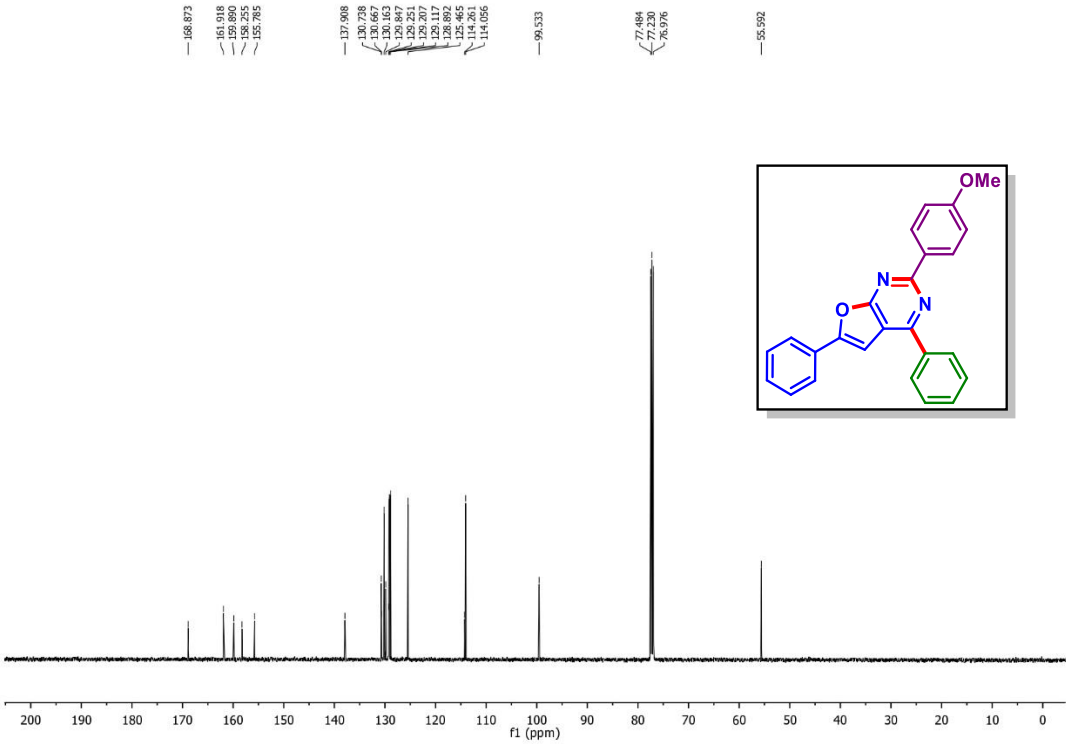

2-(4-Butoxyphenyl)-4,6-diphenylfuro[2,3-d]pyrimidine (1ae'): ^{1}H NMR (CDCl$_3$, 600 MHz)

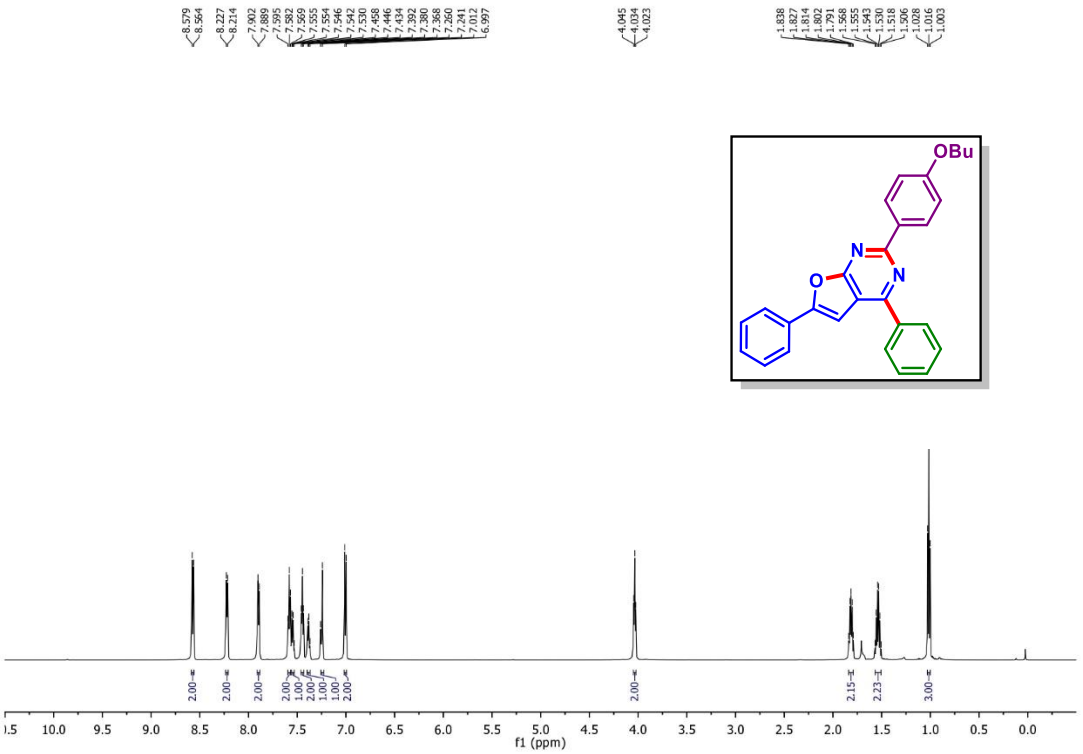

2-(4-Butoxyphenyl)-4,6-diphenylfuro[2,3-d]pyrimidine (1ae'): ^{13}C{^{1}H} NMR (CDCl$_3$, 150 MHz)

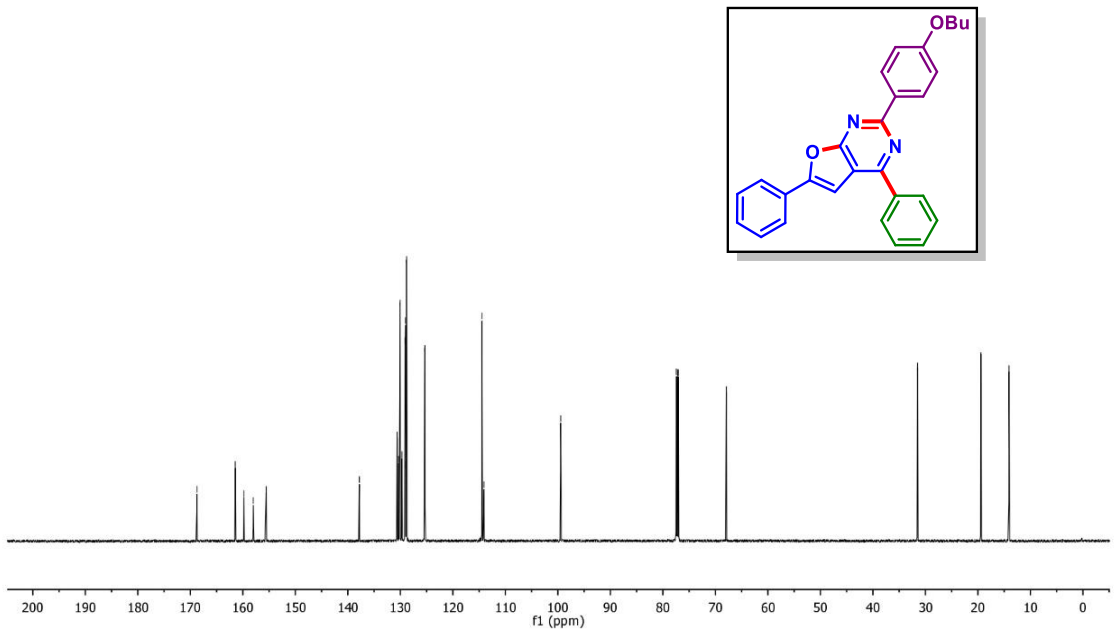

2-(4-Chlorophenyl)-4,6-diphenylfuro[2,3-d]pyrimidine (1ah'): ^{1}H NMR (CDCl$_3$, 500 MHz)

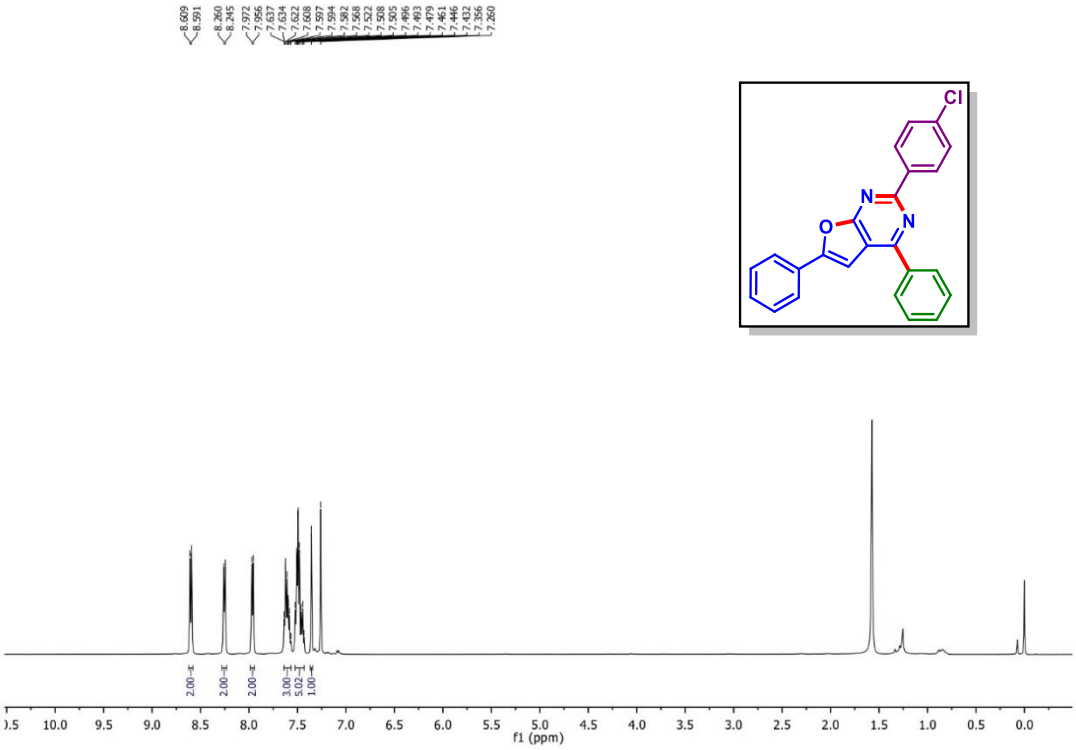

2-(4-Chlorophenyl)-4,6-diphenylfuro[2,3-d]pyrimidine (1ah'): ^{13}C{^{1}H} NMR (CDCl$_3$, 125 MHz)

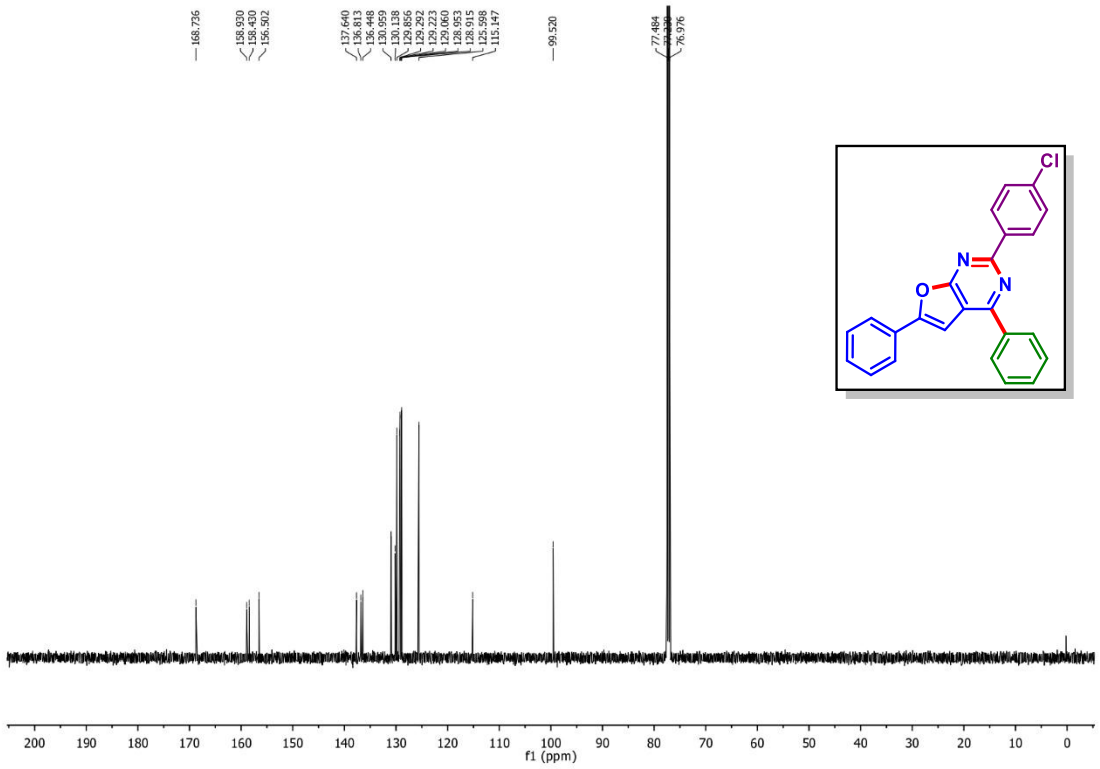

2-(4-Bromothiophen-2-yl)-4,6-diphenylfuro[2,3-d]pyrimidine (1an'): ^{1}H NMR (CDCl$_3$, 500 MHz)

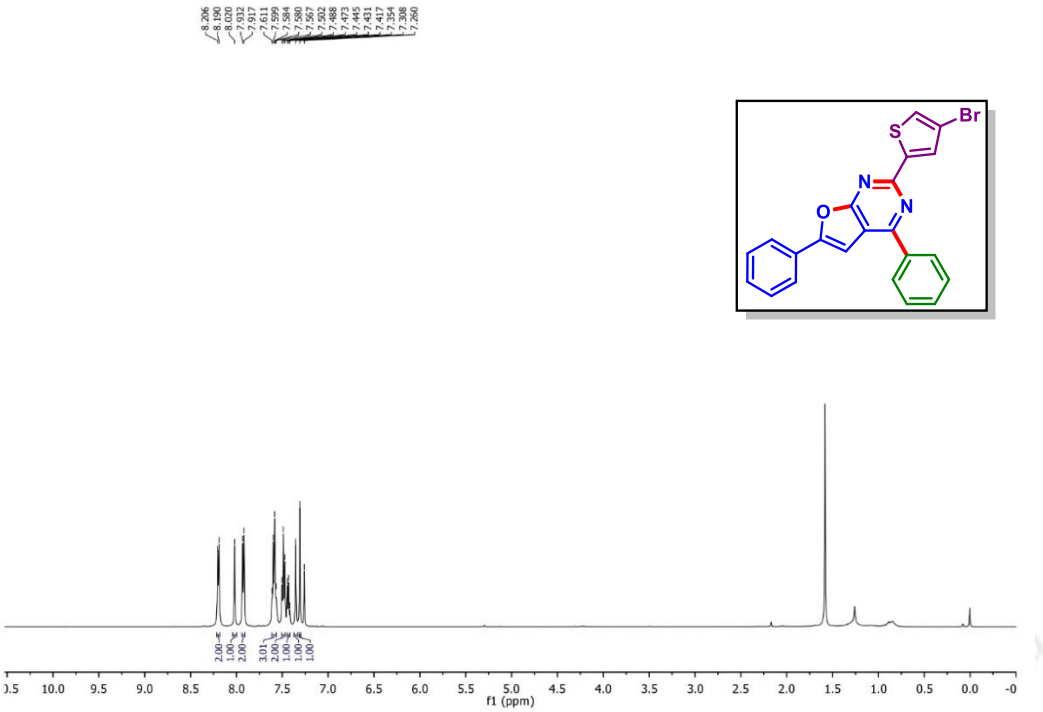

2-(4-Bromothiophen-2-yl)-4,6-diphenylfuro[2,3-d]pyrimidine (1an'): ^{13}C{^{1}H} NMR (CDCl$_3$, 125 MHz)

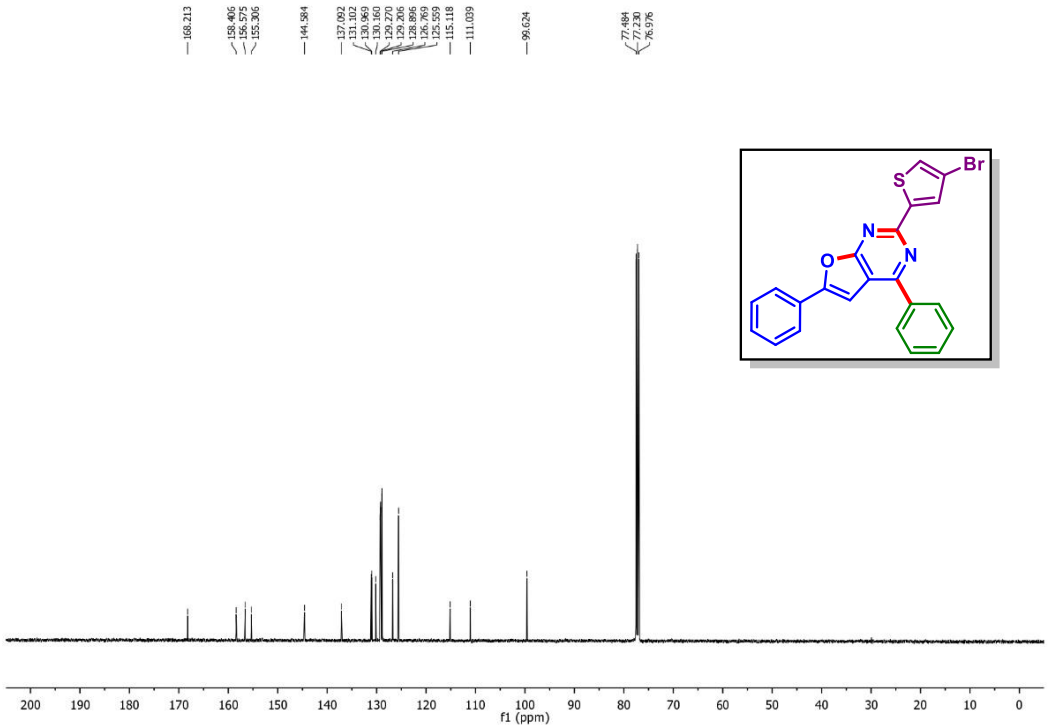

2-Cyclohexyl-4,6-diphenylfuro[2,3-d]pyrimidine (1ao'): ^{1}H NMR (CDCl$_3$, 500 MHz)

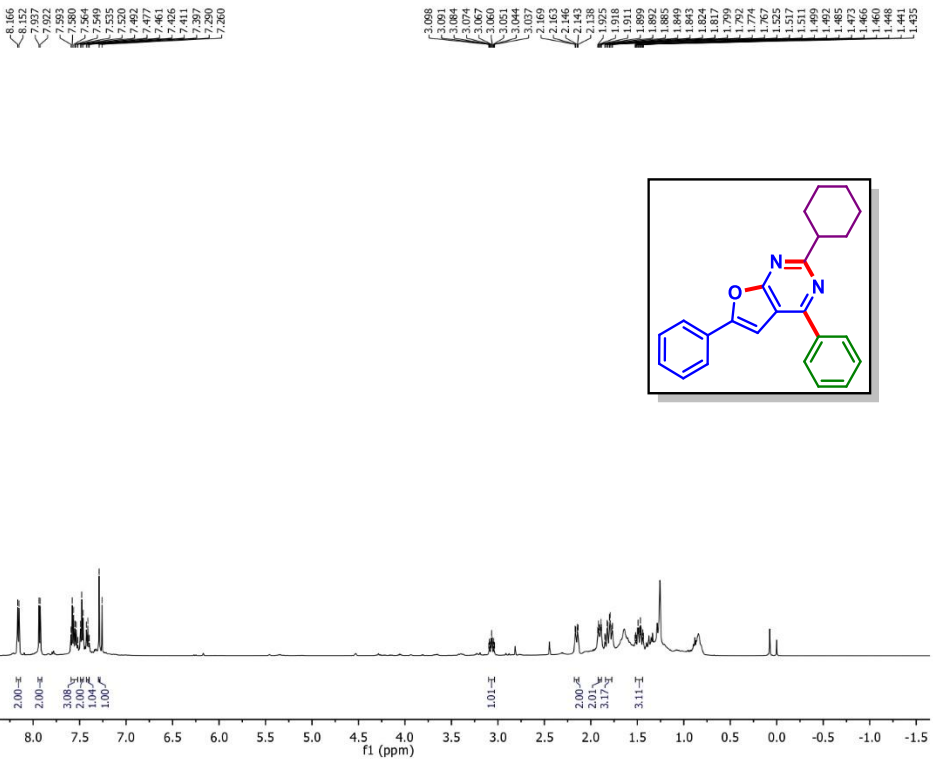

2-Cyclohexyl-4,6-diphenylfuro[2,3-d]pyrimidine (1ao'): ^{13}C{^{1}H} NMR (CDCl$_3$, 125 MHz)

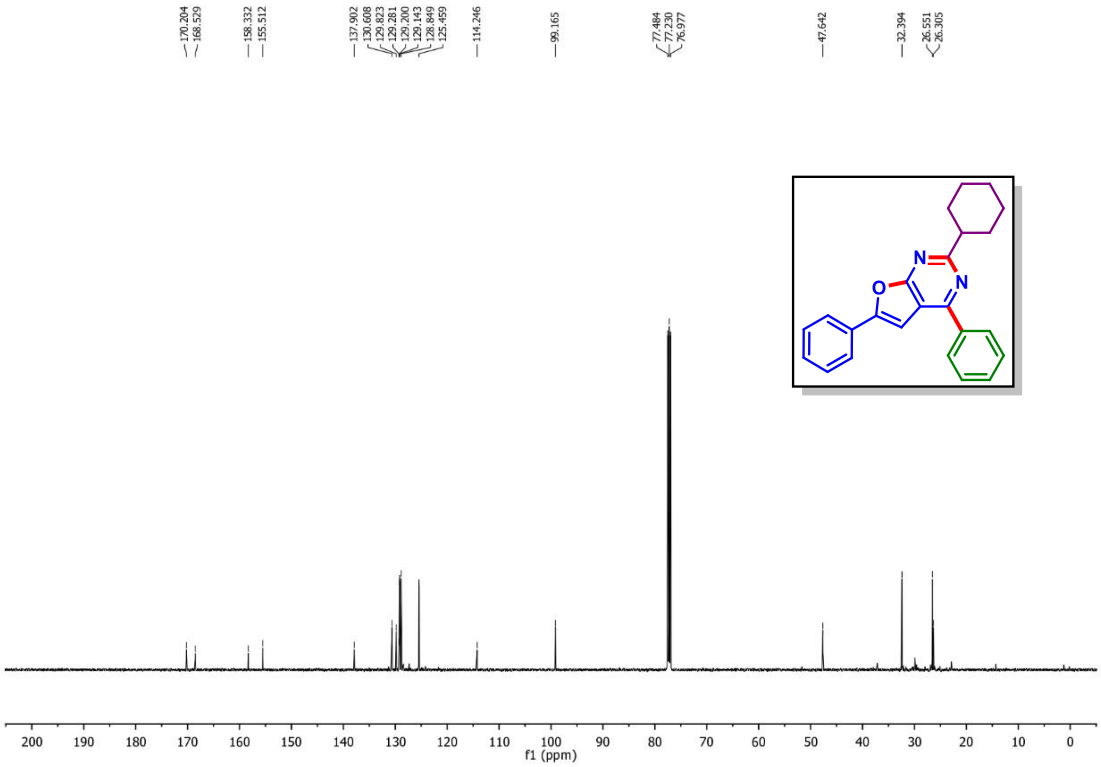

2-Amino-5-phenylfuran-3-carbonitrile (1'): ^{1}H NMR (DMSO-d$_6$, 500 MHz)

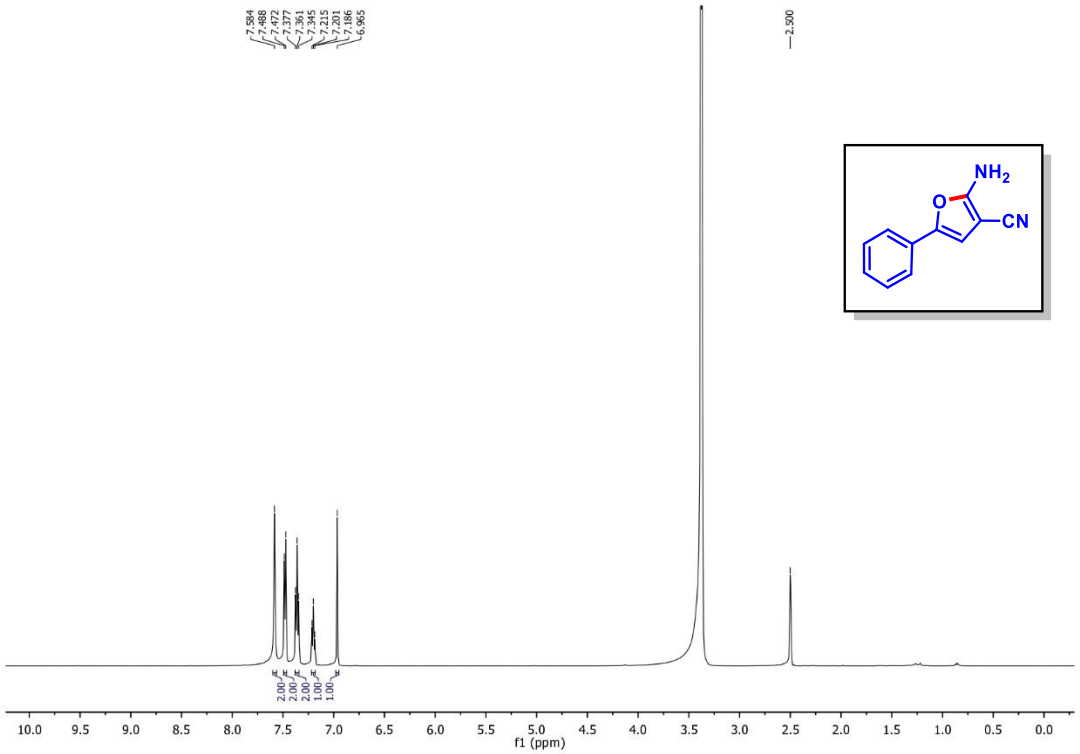

2-Amino-5-phenylfuran-3-carbonitrile (1'): ^{13}C{^{1}H} NMR (DMSO-d$_6$, 125 MHz)

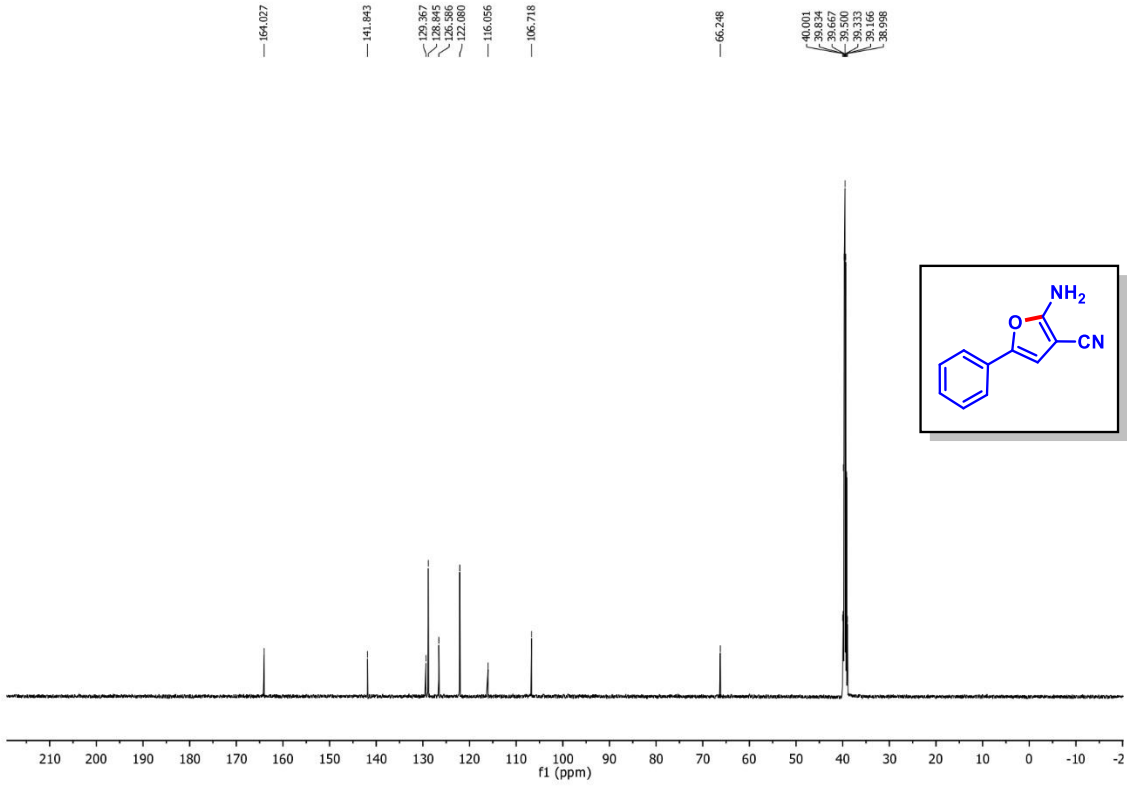

(E)-2-(Benzylideneamino)-5-phenylfuran-3-carbonitrile (1a'): ^{1}H NMR (CDCl$_3$, 500 MHz)

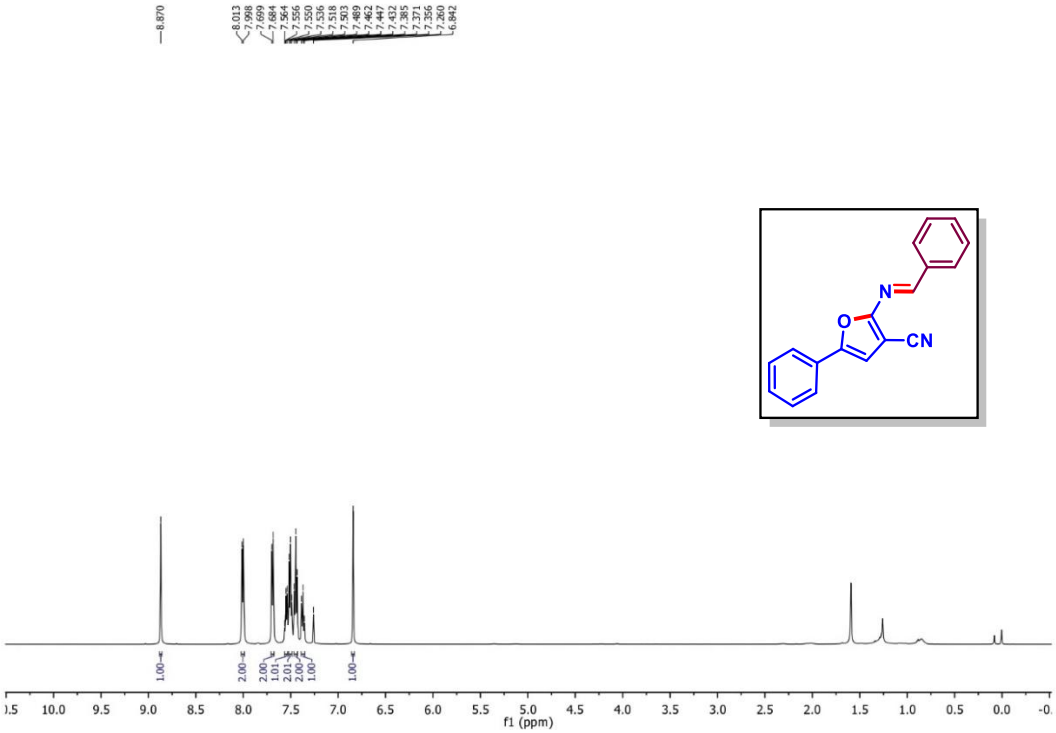

(E)-2-(Benzylideneamino)-5-phenylfuran-3-carbonitrile (1a'): ^{13}C{^{1}H} NMR (CDCl$_3$, 125 MHz)

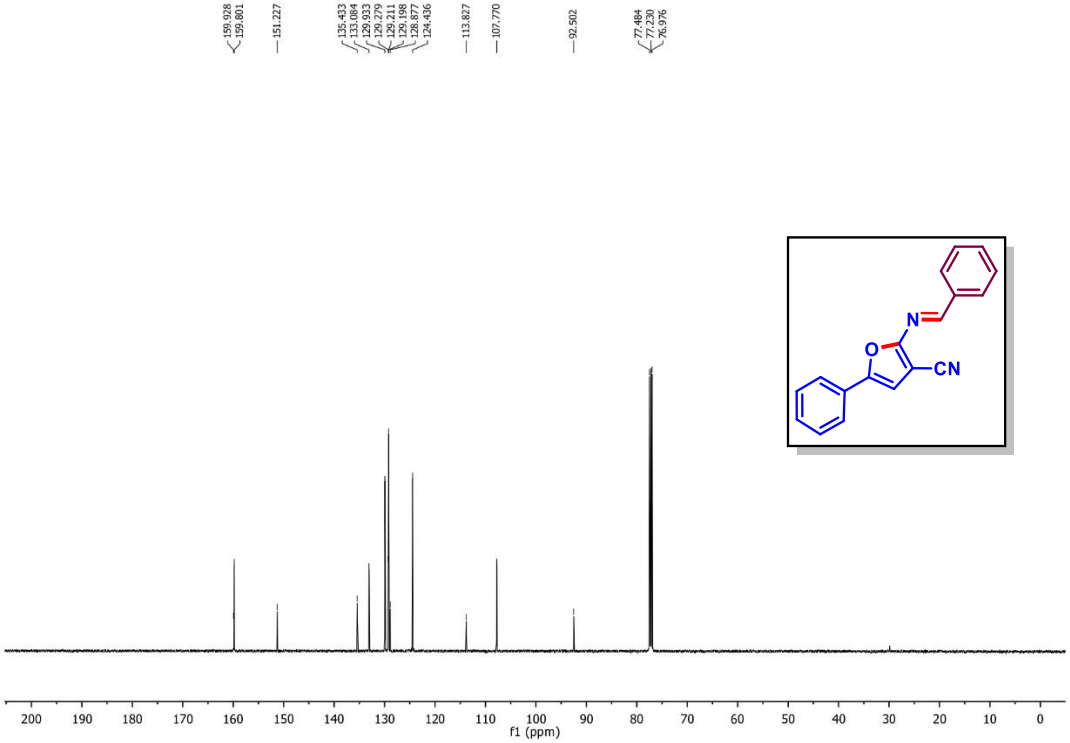

III.11. References:

[1] (a) Kochanowska-Karamyan, A. J.; Hamann, M. T. *Chem. Rev.* **2010**, *110*, 4489–4497. (b) Michael, J. P. *Nat. Prod. Rep.* **1995**, *12*, 465–475. (c) Smart, B. P.; Oslund, R. C.; Walsh, L. A.; Gelb, M. H. *J. Med. Chem.* **2006**, *49*, 2858–2860. (d) Kirilmis, C.; Ahmedzade, M.; Servi, S.; Koca, M.; Kizirgil, A.; Kazaz, C. *Eur. J. Med. Chem.* **2008**, *43*, 300–308. (e) Evarts, M. M.; Strong, Z. H.; Krische, M. J. *Org. Lett.* **2023**, *25*, 5907–5910.

[2] (a) Rassu, G.; Zanardi, F.; Battistini, L.; Casiraghi, G. *Chem. Soc. Rev.* **2000**, *29*, 109–118. (b) Moure, M. J.; SanMartin, R.; Dominguez, E. *Angew. Chem.* **2012**, *124*, 3274–3278. (c) Cai, S.-Z.; Ge, D.; Sun, L.-W.; Rao, W.; Wang, X.; Shen, Z.-L.; Chu, X.-Q. *Green Chem.* **2021**, *23*, 935–941.

[3] (a) Hossam, M.; Lasheen, D. S.; Ismail, N. S. M.; Esmat, A.; Mansour, A. M.; Singa, A. N. B.; Abouzid, K. A. M. *Eur. J. Med. Chem.*, **2018**, *144*, 330–348. (b) Zhao, A.; Gao, X.; Wang, Y.; Ai, J.; Wang, Y.; Chen, Y.; Geng, M.; Zhang, A. *Bioorg. Med. Chem.* **2011**, *19*, 3906–3918. (c) Kumar, R. N.; Poornachandra, Y.; Nagender, P.; Mallareddy, G.; Kumar, N. R.; Ranjithreddy, P.; Kumar, C. G.; Narsaiah, B. *Eur. J. Med. Chem.* **2016**, *108*, 68–78. (d) Devambatla, R. K. V.; Choudhary, S.; Ihnat, M.; Hamel, E.; Mooberry, S. L.; Gangjee, A. *Bioorg. Med. Chem. Lett.* **2018**, *28*, 3085–3093. (e) Abd El-Mageed, M. M. A.; Eissa, A. A. M.; El-Said Farag, A.; Osman, E. E. A. *Bioorg. Chem.* **2021**, *116*, 105336.

[4] Pyo, J. I.; Hwang, E. J.; Cheong, C. S.; Lee, S.-H.; Lee, S. W.; Kim, I. T.; Lee, S. H. *Synth. Met.* **2005**, *155*, 461–463.

[5] (a) Zhang, X.; Xie, X.; Liu, Y. *Chem. Sci.* **2016**, *7*, 5815–5820. (b) Dhara, H. N.; Rakshit, A.; Alam, T.; Patel, B. K. *Org. Biomol. Chem.* **2022**, *20*, 4243–4277. (c) Rakshit, A.; Dhara, H. N.; Sahoo, A. K.; Patel, B. K. *Chem. – Asian J.* **2022**, *17*, e202200792. (d) Dhara, H. N.; Rakshit, A.; Alam, T.; Sahoo, A. K.; Patel, B. K. *Org. Lett.* **2023**, *25*, 471–476. (e) Hu, K.; Zhen, Q.; Gong, J.; Cheng, T.; Qi, L.; Shao, Y.; Chen, J. *Org. Lett.* **2018**, *20*, 3083–3087. (f) Yu, H.; Xiao, L.; Yang, X.; Shao, L. *Chem. Commun.* **2017**, *53*, 9745–9748. (g) Lu, C.; Ye, M.; Li, M.; Zhang, Z.; He, Y.; Long,

L.; Chen, Z. *Chin. Chem. Lett.* **2021**, *32*, 3967–3971. (h) Dhara, H. N.; Rakshit, A.; Barik, D.; Ghosh, K.; Patel, B. K. *Chem. Commun.* **2023**, *59*, 7990–7993. (i) Xu, H.; Zhu, Y.; Chai, X.; Yang, J.; Dong, L. *Green Synth. Catal.* **2020**, *1*, 167–170.

[6] (a) Rakshit, A.; Dhara, H. N.; Sahoo, A. K.; Alam, T.; Patel, B. K. *Org. Lett.* ***2022***, *24*, 3741–3746. (b) Rakshit, A.; Sau, P.; Ghosh, S.; Patel, B. K. *Adv. Synth. Catal.* **2019**, *361*, 3824–3836. (c) Miura, T.; Murakami, M. *Org. Lett.* **2005**, *7*, 3339–3341. (d) Takahashi, T.; Tsai, F.-Y.; Li, Y.; Wang, H.; Kondo, Y.; Yamanaka, M.; Nakajima, K.; Kotora, M. *J. Am. Chem. Soc.* **2002**, *124*, 5059–5067. (e) Heller, B.; Hapke, M. *Chem. Soc. Rev.* **2007**, *36*, 1085–1094. (f) Maiti, S.; Li, Y.; Sasmal, S.; Guin, S.; Bhattacharya, T.; Lahiri, G. K.; Paton, R. S.; Maiti, D. *Nat. Commun.* **2022**, *13*, 3963–3972. (g) Wan, L.; Dastbaravardeh, N.; Li, G.; Yu, J.-Q. *J. Am. Chem. Soc.* **2013**, *135*, 18056-18059. (h) Li, X.; Fang, X.; Zhuang, S.; Liu, P.; Sun, P. *Org. Lett.* **2017**, *19*, 3580–3583. (i) Sahoo, A. K.; Rakshit, A.; Dahiya, A.; Pan, A.; Patel, B. K. *Org. Lett.* **2022**, *24*, 1918–1923.

[7] (a) Horneff, T.; Chuprakov, S.; Chernyak, N.; Gevorgyan, V.; Fokin, V. V. *J. Am. Chem. Soc.* **2008**, *130*, 14972–14974. (b) Li, X.; Huang, L.; Chen, H.; Wu, W.; Huang, H.; Jiang, H. *Chem. Sci.* **2012**, *3*, 3463–3467. (c) Bera, S.; Biswas, A.; Pal, J.; Roy, L.; Mondal, S.; Samanta, R. *Org. Lett.* **2023**, *25*, 1952–1957. (d) Mandal, D.; Roychowdhury, S.; Biswas, J. P.; Maiti, S.; Maiti, D. *Chem. Soc. Rev.* **2022**, *51*, 7358–7426.

[8] (a) Yu, S.; Qi, L.; Hu, K.; Gong, J.; Cheng, T.; Wang, Q.; Chen, J.; Wu, H. *J. Org. Chem.* **2017**, *82*, 3631–3638. (b) Xu, T.; Shao, Y.; Dai, L.; Yu, S.; Cheng, T.; Chen, J. *J. Org. Chem.* **2019**, *84*, 13604–13614. (c) Wang, Z.; Chen, W.; Luo, H.; He, C.; Zhang, G.; Yu, Y. *Synthesis* **2020**, *52*, 1659–1665.

[9] Rakshit, A.; Kumar, P.; Alam, T.; Dhara, H.; Patel, B. K. *J. Org. Chem.* **2020**, *85*, 12482–12504.

[10] (a) Kim, K.; Han, S. H.; Jeoung, D.; Ghosh, P.; Kim, S.; Kim, S. J.; Ku, J.-M.; Mishra, N. K.; Kim, I. S. *J. Org. Chem.* **2020**, *85*, 2520–2531. (b) Chun, R.; Kim, S.; Han, S. H.; Han, S.; Lee, S. H.; Mishra, N. K.; Jung, Y. H.; Kim, H. S, Kim, I. S. *Adv. Synth.*

Catal. **2019**, *361*, 1617–1626. (c) Choi, J. H.; Kim, K.; Oh, H.; Han, S.; Mishra, N. K.; Kim, I. S. *Org. Biomol. Chem.* **2020**, *18*, 9611–9622.

[11] (a) Aziz, M. A.; Serya, R. A. T.; Lasheen, D. S.; Abouzid, K. A. M. *Futur. J. Pharm. Sci.* **2016**, *2*, 1–8. (b) Kim, S. Y.; Kim, D. J.; Yang, B. S.; Yoo, K. H. *Bull. Korean Chem. Soc.* **2007**, *28*, 1114–1118. (c) Hu, Y.-G.; Wang, Y.; Du, S.-M.; Chen, X.-B.; Ding. M.-W. *Bioorg. Med. Chem. Lett.* **2010**, *20*, 6188–6190. (d) Yılmaz, A. S.; Kaçan, M. *Tetrahedron* **2017**, *73*, 4509–4512.

[12] (a) Zhao, A.; Gao, X.; Wang, Y.; Ai, J.; Wang, Y.; Chen, Y.; Geng, M.; Zhang, A.; *Bioorg. Med. Chem.* **2009**, *17*, 7324–7336. (b) Li, C.; Zhang, F. *Tet. Lett.* **2017**, *58*, 1572–1575. (c) Gangjee, A.; Li, W.; Lin, L.; Zeng, Y.; Ihnat, M.; Warnke, L. A.; Green, D. W.; Cody, V.; Pace, J.; Queener, S. F. *Bioorg. Med. Chem.* **2009**, *17*, 7324–7336. (d) Robins, M. J.; Nowak, I.; Rajwanshi, V. K.; Miranda, K.; Cannon, J. F.; Peterson, M. A.; Andrei, G.; Snoeck, R.; Clercq, E. D.; Balzarini, J. *J. Med. Chem.* **2007**, *50*, 3897–3905. (e) Amblard, F.; Aucagne, V.; Guenot, P.; Schinazic, R. F. Agrofoglio, L. A. *Bioorg. Med. Chem.* **2005**, *13*,1239–1248. (f) Sniady, A.; Durham, A.; Morreale, M. S.; Marcinek, A.; Szafert, S.; Lis, T.; Brzezinska, K. R.; Iwasaki, T.; Ohshima, T.; Mashima, K.; Dembinski, R. *J. Org. Chem.* **2008**, *73*, 5881–5889.

[13] Chen, X.; Sun, P.; Mo, B.; Chen, C.; Peng, J. *J. Org. Chem.* **2021**, *86*, 352–366.

[14] Kumar, A.; Mishra, P. K.; Saini, K. M.; Verma, A. K. *Adv. Synth. Catal.* **2021**, *363*, 2546–2551.

[15] (a) Abdelhamid, A. O.; Negm, A. M.; Abbas, I. M. *J. Prakt. Chem.* **1989**, *331*, 31–36. (b) Al-Mousawi, S. M.; Moustafa, M. S.; Meier, H.; Kolshorn, H.; Elnagdi, M. H. *Molecules* **2009**, *14*, 798–806.

भारतीय प्रौद्योगिकी संस्थान गुवाहाटी
Indian Institute of Technology Guwahati

CHAPTER IV

A Cascade Synthesis of Furo-Pyrrolo-Pyridines via Pd(II)-Catalyzed Dual N−H/C Annulative-Cyclization

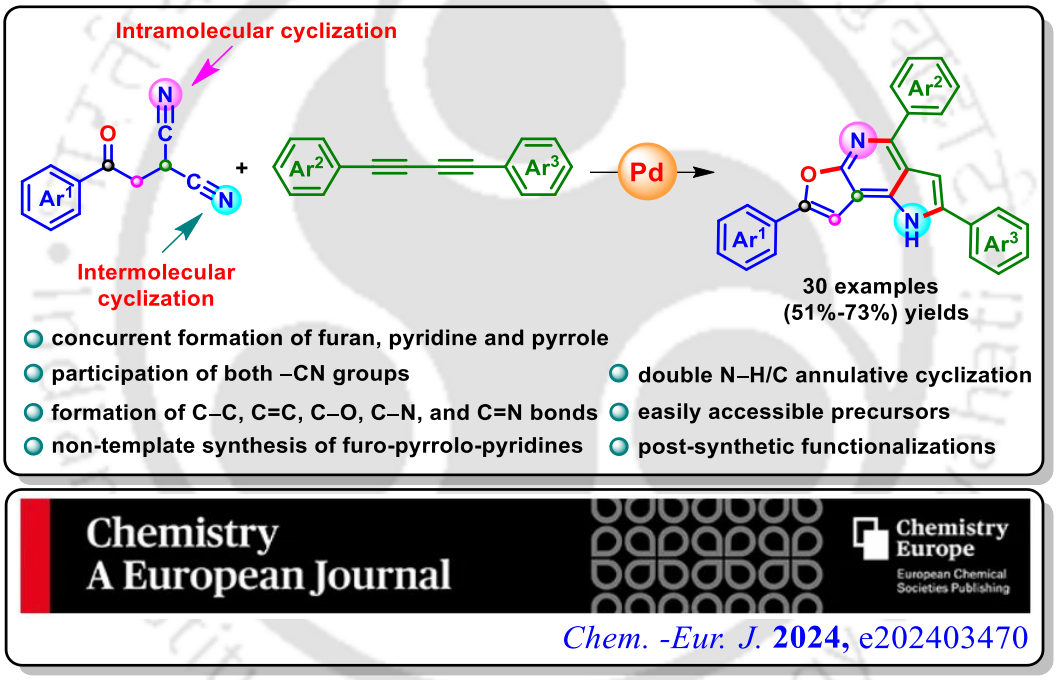

ABSTRACT: A Pd(II)-catalyzed non-template synthesis of furo[2,3-*b*]pyrrolo[2,3-*d*]pyridines from β-ketodinitriles and buta-1,3-diynes has been accomplished via dual annulative cyclization. The participation of both the nitrile (–CN) groups led to the concurrent construction of three heterocycles *viz.* furan, pyrrole, and pyridine forming C–C, C=C, C–O, C–N, and C=N bonds in one pot. The synthetic utility of the protocol was further demonstrated through a few post-synthetic manipulations.

भारतीय प्रौद्योगिकी संस्थान गुवाहाटी
Indian Institute of Technology Guwahati

CHAPTER IV

A Cascade Synthesis of Furo-Pyrrolo-Pyridines via Pd(II)-Catalyzed Dual N−H/C Annulative-Cyclization

IV.1. Introduction:

The fused nitrogen-containing heterocycles have been a subject of great interest due to their wide presence in pharmaceuticals and biologically important compounds.[1] In this regard, the fused heterocycle furo-pyridine is found in natural products and has drawn attention due to their biological activities such as anticancer, antiviral, agonists-antagonists, etc (Figure IV.1.1, I-V).[2] Further, the fusion of an π-excessive furan ring and a π-deficient pyridine ring renders these systems excellent organic fluorophores.[3] Similarly, fused pyrrolo-pyridine having biological activity are probed for pharmacological studies (Figure IV.1.1, VI-XIII).[4]

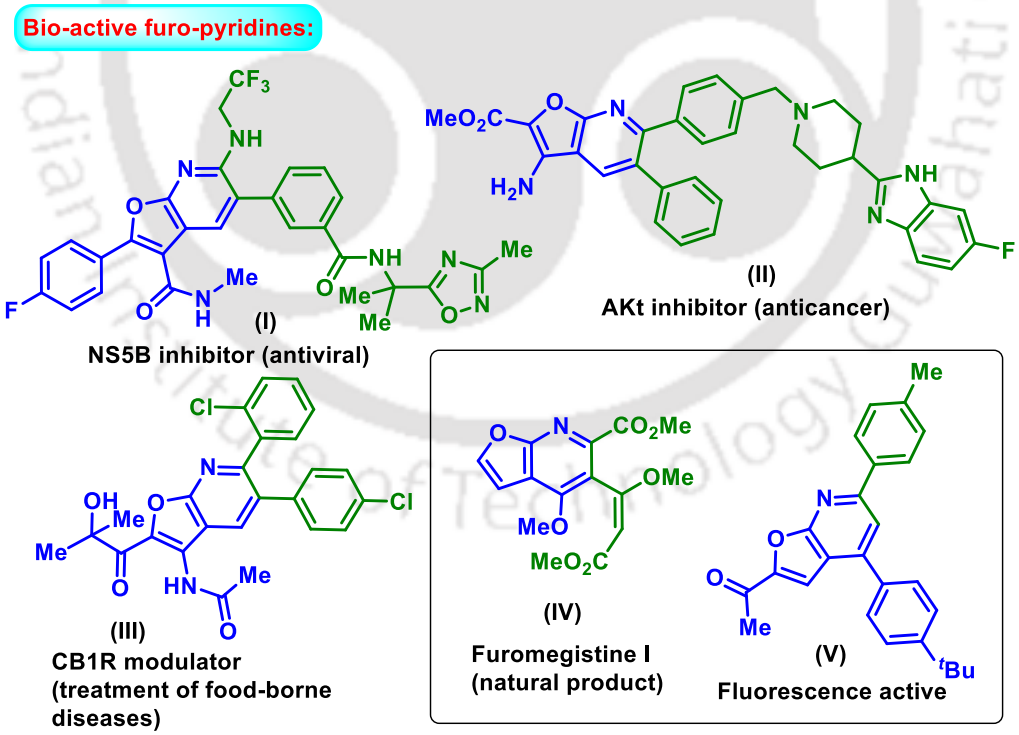

Figure IV.1.1. *Representative active furo-pyridines.*

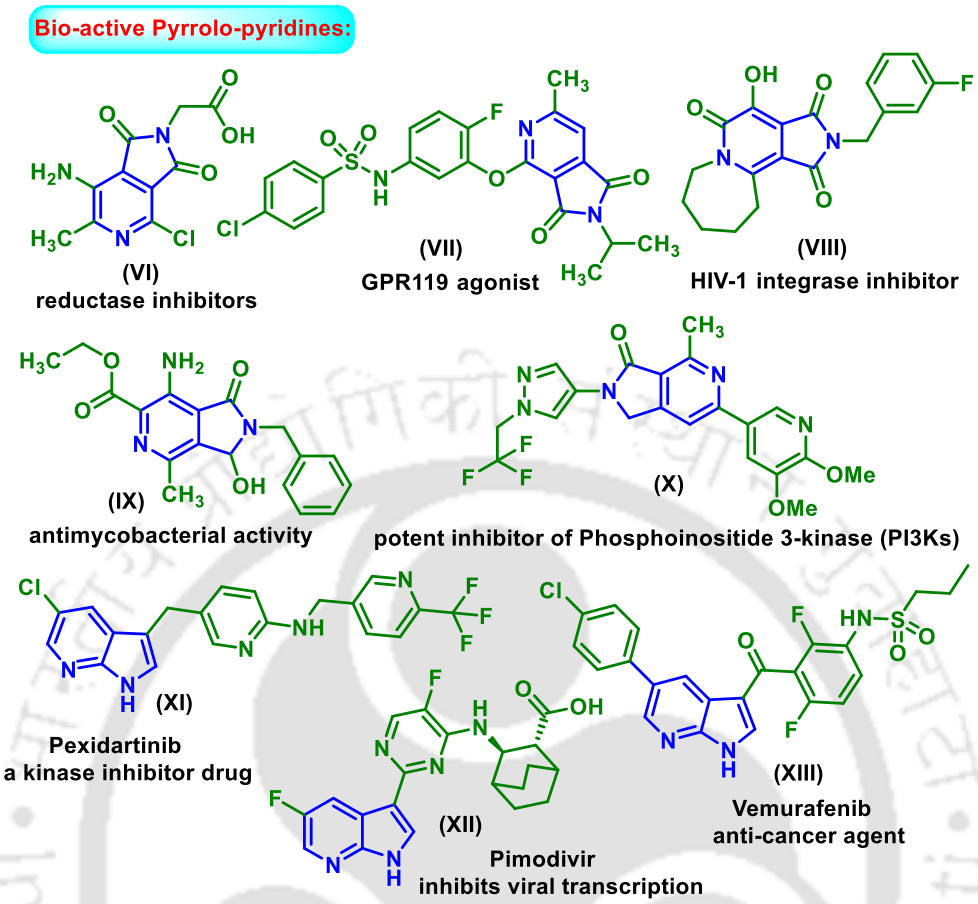

Figure IV.1.1. *Representative active pyrrolo-pyridine-containing drugs.*

Individually there are well-established methods for the synthesis of pyridine, pyrrole, and furan heterocycles. The conventional approach for synthesizing pyridine is centered around Hantzsch and Kröhnke synthesis.[5] The pyrrole synthesis is based on Knorr, Paal-Knorr, and Hantzsch approach[6a-6c] while furan synthesis is based on Paal-Knorr approach.[6d-6e] However, there is no well-defined strategy for the simultaneous construction of two or more fused heterocycles. A fused furo-pyridine is constructed over one of the pre-existed heterocyclic cores furan or a pyridine *i.e.* pyridine over furan or furan over pyridine.[7] Similarly, a pyrrolo-pyridine is constructed over the existing pyrrole or a pyridine ring.[8] However, the concomitant construction of three fused heterocycles *viz.* furan, pyridine, and pyrrole is unprecedented. Here, we disclose a strategy for the construction of three consecutive heterocycles without any pre-existing template from β-ketodinitriles and diynes in the presence of Pd(II) catalyst.

The nitrile group is no longer an inert functional group and lately turned out to be one of the most appreciated functional groups in many transition-metal-mediated alkyne insertions, annulation, cycloaddition, addition-cyclization, and C−H bond functionalizations.[9] In the last few years, the transition-metal-catalyzed alkyne insertion into C−H and N−H bonds has been exploited for the construction of fused *N*-heterocycles.[9a,9b] In most of the cases the activation of *ortho*-C–H bond participates via a coordinative functional group and subsequently cyclized with the internal alkyne leading to numerous heterocycles. In this rapidly growing realm of oxidative annulation with alkynes, the metal-catalyzed reactions involving the nitrile group have also been reported to access diverse carbocycles, heterocycles, and spirocycles.[10]

After the seminal discovery of Pd(II)-catalyzed oxidative alkyne annulation by Larock utilizing the nitrile moiety there has been a rapid upsurge in this area [Scheme IV.1.1 (i)].[11] Murakami and co-workers also reported a Rh(I)-catalyzed insertion of internal alkynes into 2-cyanophenylboronic acids leading to 2,3-indenones [Scheme IV.1.1 (ii)].[12] The transition metal-catalyzed [2 + 2 + 2] cycloaddition of a nitrile with alkyne-alkyne or alkyne-nitrile with an alkyne provides multi-substituted pyridine. In this context, Louie and co-workers reported a method for the synthesis of cyclopentane-fused pyridines from methyl-terminated tethered alkynes and alkyl or aryl nitriles in the presence of a Ni(0) catalyst [Scheme IV.1.1 (iii)].[13] Later in 2021, Yoshikai's group developed a Co(II)-catalyzed intermolecular [2 + 2 + 2] cycloaddition using unactivated nitriles and internal alkynes leading to penta-substituted pyridines [Scheme IV.1.1 (iv)].[14] Later on a Ru-catalyzed [4 + 2] C−H/N−H annulation was developed to access fused isoquinolines from γ-ketodinitriles and alkynes.[9b] Following this, a Pd(II)-catalyzed N−H/C annulation between β-ketodinitriles and alkynes provided access to furo[2,3-*b*]pyridines [Scheme IV.1.1 (v)].[9c] With the growing interest in alkyne annulation to nitrile, herein, we report a Pd(II)-catalyzed insertion of buta-1,3-diyne to β-ketodinitrile via dual N−H/C annulative-cyclization, providing a unique non-templated synthesis of a three-consecutive fused heterocycle furo[2,3-*b*]pyrrolo[2,3-*d*]pyridine [Scheme IV.1.1 (vi)].

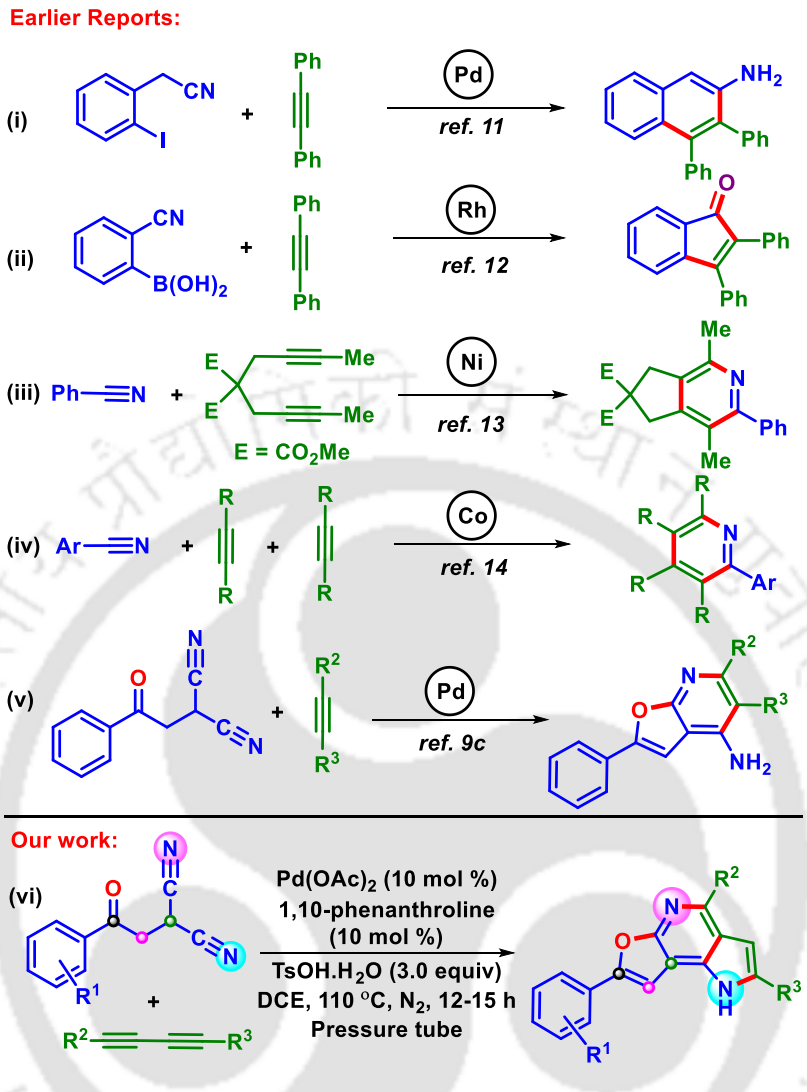

Scheme IV.1.1. *Various approaches for the insertion of alkynes to nitriles.*

IV.2. Strategies for the Synthesis of Furo-pyridine Heterocycles:

Furo-pyridine compounds are versatile and valuable in the development of new pharmaceuticals and advanced materials. Owing to the importance of the furopyridine core, numerous efforts have been made to construct these compounds.[7,15] However, there are limitations, as most existing strategies use functionalized pyridine or furan rings as precursors, which is undesirable. Therefore, developing an effective and mild process using easily available starting materials to produce furopyridine derivatives remains highly anticipated in modern organic chemistry.

IV.2.1. Synthesis of the Furo[2,3-*d*]pyridines from Pyridines:

In 2002, Arcadi and coworkers established a Pd(II)-catalyzed cross-coupling of 1-alkynes with *o*-iodoacetoxy- or *o*-iodobenzyloxypyridines to access 2,3-disubstituted furo[2,3-*b*]pyridines, followed by electrophilic cyclization by I_2 or $PdCl_2$/CO at room temperature (Scheme IV.2.1.1).[7a]

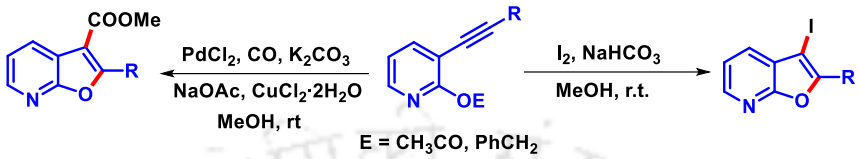

Scheme IV.2.1.1. *Synthesis of furo[2,3-b]pyridines via electrophilic cyclization.*

Rault and coworkers established a base-mediated synthesis of ethyl-3-aminofuropyridine-2-carboxylates from 1-halo-2-cyano or 1-hydroxy-2-cyano pyridines (Scheme IV.2.1.2).[16]

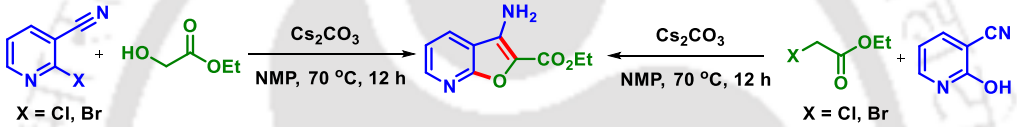

Scheme IV.2.1.2. *Base-mediated synthesis of furo[2,3-b]pyridines.*

In 2010, Sanford *et al.* developed a method to access furopyridine by reacting tetrafluoro-4-cyanopyridine with 1,3-dicarbonyl derivatives (Scheme IV.2.1.3).[17] The resulting fluorinated furopyridine scaffold was further subjected to nucleophilic addition to provide highly functionalized heteroaromatic systems.

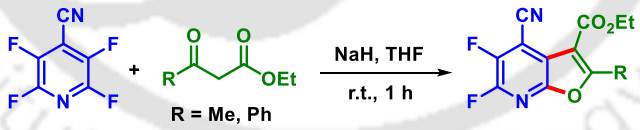

Scheme IV.2.1.3. *Synthesis of furo[2,3-b]pyridines from highly fluorinated pyridines.*

IV.2.2. Synthesis of the Furo[2,3-*d*]pyridines from Furans:

In most of the cases, the furo-pyridine ring was also synthesized from furan derivatives having an amino ($–NH_2$) group at the 2-position of the furan ring. For example, Villarroya *et al.* described a Lewis acid-mediated synthesis of furopyridine, featuring an amino group in the 4-position of the pyridine ring, starting from readily available 2-amino-4,5-diaryl-3-cyano furan derivatives. (Scheme IV.2.2.1).[7d]

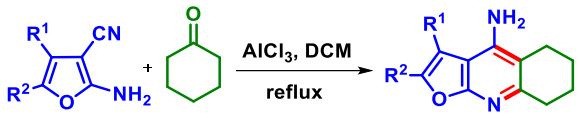

Scheme IV.2.2.1. *Synthesis of 4-amino-substituted furo[2,3-b]pyridines.*

Tverdokhlebov's group reported a condensation of 4,5-disubstituted 2-amino-3-furancarboxaldehyde with malononitrile in the presence of catalytic NH_4Cl to access substituted 6-aminofuro[2,3-*b*]pyridine-5-carbonitriles in excellent yields (Scheme IV.2.2.2).[7e]

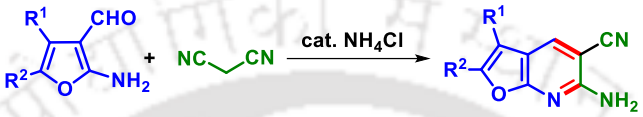

Scheme IV.2.2.2. *Synthesis of furo[2,3-b]pyridines from 2-amino-3-furancarboxaldehyde.*

IV.3. Strategies for the Synthesis of Pyrrolo-pyridine Heterocycles:

Pyrrolo-pyridines (also called aza-indoles) are a class of fused heterocyclic compounds consisting of a pyrrole ring fused to a pyridine ring. These structures are notable for their significant biological activities and potential therapeutic applications.[18] The combination of the electron-rich pyrrole and the electron-deficient pyridine rings often results in unique electronic properties, making them valuable scaffolds in medicinal chemistry.[8,19] Many classical methods for indole synthesis, such as Fischer and Madelung cyclizations, often cannot be effectively applied to the synthesis of corresponding azaindoles.[8a] Recent advances in organic chemistry have enabled efficient strategies for both azaindole formation and their further functionalization.

IV.3.1. Synthesis of the Pyrrolo-pyridines from Pyridines:

In 2011, Schmidt *et al.* disclosed an efficient Pd-catalyzed hetero-annulation strategy for the synthesis of functionalized 5-azaindoles through 4-acetamido-3-iodopyridines and diaryl alkynes (Scheme IV.3.1.1).[20] This method allows the synthesis of different 2,3-disubstituted azaindoles with various substitutions on the pyridine ring in good to excellent yields.

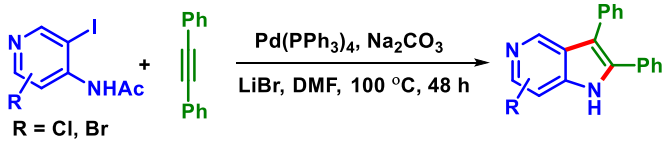

Scheme IV.3.1.1. *Synthesis of pyrrolo[3,2-c]pyridine via heteroannulation strategy.*

Yum and co-workers reported a Pd(II)-catalyzed cascade hetero-annulation reaction to access tetracyclic 5-azaindole analogues using benzylidene as the protecting group in aminoiodopyridine (Scheme IV.3.2.2).[21] This reaction demonstrated the potential for diversifying tetracyclic 5-azaindole analogues with various aryl imines.

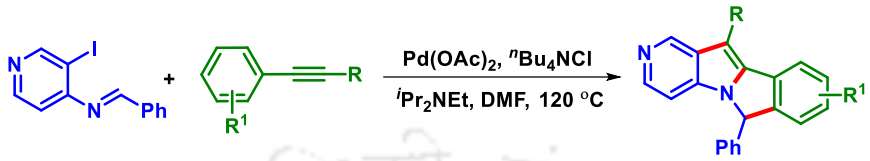

Scheme IV.3.1.2. *Pd(II)-catalyzed synthesis of pyrrolo[3,2-c]pyridine via heteroannulation.*

IV.3.2. Synthesis of the Pyrrolo-pyridines from Pyrroles:

In 2011, Kusurkar and coworkers established a condensation reaction of 2-(aryl)-2-(1*H*-pyrrol-2-yl)ethanamines for the formation of substituted-5-azaindoles using catalysts like TMSCl or TFA through Pictet-Spengler reaction (Scheme IV.3.2.1).[22] Nitro derivatives were prepared by Michael addition using pyrroles and nitro-olefins in the presence of silica gel at 150 °C.

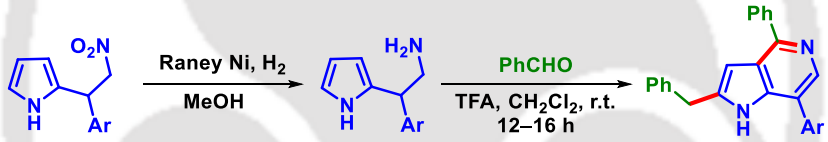

Scheme IV.3.2.1. *Synthesis of pyrrolo[3,2-c]pyridine via Pictet–Spengler condensation.*

In 2015, De Rosa and co-workers developed a regioselective reaction of 3-aminopyrrole with trifluoromethyl-β-diketones to produce 1*H*-pyrrolo[3,2-*b*]pyridines (Scheme IV.3.2.2).[8d] The formation of the γ-regioisomer is due to the increased electrophilicity of the adjacent carbonyl group and decreased basicity of the hydroxyl group of the CF_3 amino alcohol formed by the trifluoromethyl group, leading to the faster formation of the amino alcohol but slower subsequent dehydration to the β-enaminone.

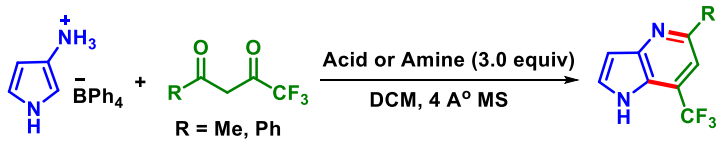

Scheme IV.3.2.2. *Synthesis of 1H-Pyrrolo[3,2-b]pyridine.*

IV.4. Present Work:

IV.4.1. Optimization of the Reaction Conditions:

We initiated our study by exploring a $Pd(OAc)_2$-catalyzed (10 mol %) coupling of 2-(2-oxo-2-phenylethyl)malononitrile (**1**) (0.20 mmol) with 1,4-diphenylbuta-1,3-diyne (**a**) (0.40 mmol, 2 equiv) in the presence of 1,10-phenanthroline (10 mol %) and *p*-toluenesulfonic acid (PTSA, $TsOH·H_2O$, 2 equiv) in 1,2-dichloroethane (DCE, 2 mL) at 110 °C under a nitrogen atmosphere for 12 hours. The formation of a new spot having blue fluorescent was observed under 365 nm UV light. The product was isolated and based on the spectroscopic analyses it was identified to be furo[2,3-*b*]pyrrolo[2,3-*d*]pyridine (**1a**, 62%) (Table S1, entry 1). The core skeletal structure was further confirmed by X-ray diffraction analysis of one of its derivatives (**1g**, CCDC 2350725). This one-pot reaction involves the participation of both the nitrile (–CN) groups, each serving as the source of heterocyclic nitrogen. While one of the nitrile groups participates in the construction of the pyrrole moiety, the other is involved in pyridine ring formation, leading to furo[2,3-*b*]pyrrolo[2,3-*d*]pyridine via the formation of C–C, C=C, C–O, C–N, and C=N bonds.

To identify the optimal reaction conditions for this transformation, extensive optimization studies were undertaken, utilizing a variety of catalysts, ligands, additives, and solvents. Initially, alternative solvents such as CH_3CN (28%), dichloromethane (32%), toluene (50%), DMF (n.d), DMSO (n.d), and EtOH (n.d) were tested, but none could improve the product yield (Table S1, entries 2-7). Further increasing the loading of $TsOH·H_2O$ from 2 to 3 equivalents, while keeping all other parameters constant, led to an improved yield of **1a** from 62% to 73% (Table S1, entry 8). Using DCE as the solvent and maintaining the loading of $TsOH·H_2O$ (3 equiv), Pd(II) catalysts and ligands were screened. Alternative catalysts such as $Pd(TFA)_2$ (55%), $PdCl_2$ (20%), $PdBr_2$ (15%), and $Pd(PPh_3)_2Cl_2$ (30%) were found inferiorcompared to $Pd(OAc)_2$ (Table S1, entries 9-12). The use of $Pd(OAc)_2$ (10 mol %) as the catalyst in combination with bidentate and monodentate ligands, such as 2,2′-bipyridine (50% yield), XPhos (trace yield), and PPh_3 (trace yield) all failed to enhance the yield (Table S1, entries 13-15). Further attempts to replace $TsOH·H_2O$ with other additives, such as $PhSO_3H$ (60%), AcOH (40%), and CF_3SO_3H (35%), were found ineffective in improving the yield (Table S1, entries 16-18). Notably, omitting any single component, either the catalyst [$Pd(OAc)_2$], ligand (1,10-phenanthroline), or additive ($TsOH·H_2O$), completely inhibited the product formation (Table S1, entries 19-21). Conducting the reaction in an air atmosphere produced

a lower yield of 64% (Table S1, entry 22). Next keeping all other parameters constant, reducing the loading of 1,4-diphenylbuta-1,3-diyne (**a**) from 2 equivalents to 1.5 equivalents led to a lower yield of 66% (Table S1, entry 23). A reduced yield of 63% and 67% of the product was observed when the reaction was performed at a lower temperature of 80 °C and 100 °C respectively (Table S1, entries 24-25). Even when the temperature was increased to 120°C, no further improvement in yield (72%) was observed (Table S1, entry 26). No significant improvement in the yield was observed even on prolonging the reaction time to 24 h (72%) (Table S1, entry 27). Reducing the Pd-catalyst loading from 10 mol % to 5 mol % also resulted in a lower yield of 62% (Table S1, entry 28).

After a series of reaction, the best-optimized condition for this protocol was found to be the use of β-ketodinitrile (**1**) (0.20 mmol), 1,4-diphenylbuta-1,3-diyne (**a**) (0.40 mmol, 2.0 equiv), $Pd(OAc)_2$ (10 mol %), 1,10-phenanthroline (10 mol %), and $TsOH{\cdot}H_2O$ (3 equiv) in 1,2-dichloroethane (DCE) (2 mL), at 110°C in a pressure tube under a nitrogen atmosphere for 12 hours (Table S1, entry 8).

Table IV.4.1. *Optimization of the Reaction Conditions*[a-i]

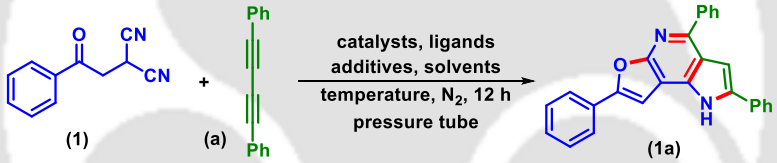

entry	catalyst (mol %)	ligand (mol %)	additive (equiv)	solvent	yield (%)[b]
1	$Pd(OAc)_2$ (10)	1,10-phenanthroline (10)	$TsOH{\cdot}H_2O$ (2)	1,2-DCE	62
2	$Pd(OAc)_2$ (10)	1,10-phenanthroline (10)	$TsOH{\cdot}H_2O$ (2)	CH_3CN	28
3	$Pd(OAc)_2$ (10)	1,10-phenanthroline (10)	$TsOH{\cdot}H_2O$ (2)	DCM	32
4	$Pd(OAc)_2$ (10)	1,10-phenanthroline (10)	$TsOH{\cdot}H_2O$ (2)	Toluene	50
5	$Pd(OAc)_2$ (10)	1,10-phenanthroline (10)	$TsOH{\cdot}H_2O$ (2)	DMF	n.d
6	$Pd(OAc)_2$ (10)	1,10-phenanthroline (10)	$TsOH{\cdot}H_2O$ (2)	DMSO	n.d
7	$Pd(OAc)_2$ (10)	1,10-phenanthroline (10)	$TsOH{\cdot}H_2O$ (2)	EtOH	n.d
8	**$Pd(OAc)_2$ (10)**	**1,10-phenanthroline (10)**	**$TsOH{\cdot}H_2O$ (3)**	**1,2-DCE**	**73**
9	$Pd(TFA)_2$ (10)	1,10-phenanthroline (10)	$TsOH{\cdot}H_2O$ (3)	1,2-DCE	55
10	$PdCl_2$ (10)	1,10-phenanthroline (10)	$TsOH{\cdot}H_2O$ (3)	1,2-DCE	20
11	$PdBr_2$ (10)	1,10-phenanthroline (10)	$TsOH{\cdot}H_2O$ (3)	1,2-DCE	15
12	$PdCl_2(PPh_3)_2$ (10)	1,10-phenanthroline (10)	$TsOH{\cdot}H_2O$ (3)	1,2-DCE	30
13	$Pd(OAc)_2$ (10)	2,2′-bipyridyl (10)	$TsOH{\cdot}H_2O$ (3)	1,2-DCE	50
14	$Pd(OAc)_2$ (10)	XPhos (10)	$TsOH{\cdot}H_2O$ (3)	1,2-DCE	trace

15	$Pd(OAc)_2$ (10)	PPh_3 (10)	$TsOH·H_2O$ (3)	1,2-DCE	trace
16	$Pd(OAc)_2$ (10)	1,10-phenanthroline (10)	$PhSO_3H$ (3)	1,2-DCE	60
17	$Pd(OAc)_2$ (10)	1,10-phenanthroline (10)	AcOH (3)	1,2-DCE	40
18	$Pd(OAc)_2$ (10)	1,10-phenanthroline (10)	CF_3SO_3H (3)	1,2-DCE	35
19		1,10-phenanthroline (10)	$TsOH·H_2O$ (3)	1,2-DCE	00
20	$Pd(OAc)_2$ (10)		$TsOH·H_2O$ (3)	1,2-DCE	00
21	$Pd(OAc)_2$ (10)	1,10-phenanthroline (10)		1,2-DCE	00
22	$Pd(OAc)_2$ (10)	1,10-phenanthroline (10)	$TsOH·H_2O$ (3)	1,2-DCE	64[c]
23	$Pd(OAc)_2$ (10)	1,10-phenanthroline (10)	$TsOH·H_2O$ (3)	1,2-DCE	66[d]
24	$Pd(OAc)_2$ (10)	1,10-phenanthroline (10)	$TsOH·H_2O$ (3)	1,2-DCE	63[e]
25	$Pd(OAc)_2$ (10)	1,10-phenanthroline (10)	$TsOH·H_2O$ (3)	1,2-DCE	67[f]
26	$Pd(OAc)_2$ (10)	1,10-phenanthroline (10)	$TsOH·H_2O$ (3)	1,2-DCE	72[g]
25	$Pd(OAc)_2$ (10)	1,10-phenanthroline (10)	$TsOH·H_2O$ (3)	1,2-DCE	72[h]
26	$Pd(OAc)_2$ (5)	1,10-phenanthroline (10)	$TsOH·H_2O$ (3)	1,2-DCE	62[i]

[a]Reaction condition: 2-(2-oxo-2-phenylethyl)malononitrile (**1**) (0.20 mmol), 1,4-diphenylbuta-1,3-diyne (**a**) (0.40 mmol), catalyst (mol %), ligand (mol %), additives (equiv), solvent (2.0 mL) at 110 °C in a pressure tube for 12 h. [b]Isolated yields. [c]Without N_2. [d]1.5 equiv of **a**. [e-g]Temperature 80, 100, 120 °C. [h]Yield after 24 h, [i]5 mol % $Pd(OAc)_2$.

IV.4.2. Substrates Scopes for the Synthesis of Fused Furo-pyrrolo-pyridines:

With the optimized conditions in hand, the effect of substituents on β-ketodinitriles (**1**–**17**) was scrutinized having 1,4-diphenylbuta-1,3-diyne (**a**) as the other reacting partner (Scheme 2). The unsubstituted β-ketodinitrile (**1**) with 1,4-diphenylbuta-1,3-diyne (**a**) under this condition afforded 2,4,7-triphenyl-1*H*-furo[2,3-*b*]pyrrolo[2,3-*d*]pyridine (**1a**) in 73% yield. The β-ketodinitriles having electron-donating groups (EDGs) *viz*. *p*-Me (**2**), *m*-Me (**3**), *o*-Me (**4**), *p*-^{i}Pr (**5**), *p*-^{t}Bu (**6**), and *m*-OMe (**7**) all reacted successfully with (**a**), providing their corresponding furo-pyrrolo-pyridines (**2a**, 68%), (**3a**, 65%), (**4a**, 54%), (**5a**, 66%), (**6a**, 63%), and (**7a**, 59%) in modest yields (Scheme 2). Similarly, substrates bearing electron-withdrawing groups (EWGs) such as *p*-F (**8**), *p*-Cl (**9**), *p*-Br (**10**), *o*-Br (**11**), *p*-CF_3 (**12**), and *m*-CF_3 (**13**) all provided their respective furo-pyrrolo-pyridine in decent yields (**8a**, 64%), (**9a**, 71%), (**10a**, 62%), (**11a**, 63%), (**12a**, 57%), and (**13a**, 55%), respectively. This protocol was equally successful when the phenyl ring of (**1**) was replaced with a polycyclic naphthyl (**14**) unit giving its furo-pyrrolo-pyridine (**14a**, 68%). Unfortunately, the β-ketodinitriles containing a thiophene ring (**15**) and a tetralone (**16**) both produced very low yields of the products (**15a**, trace) and (**16a**, trace), while the aliphatic

cyclohexane β-ketodinitrile failed to yield any product (**17a**, 00%). A reduced yield of 63% of the fused heterocycle (**1a**) from 73% was noticed when performed on a large scale (3 mmol) (Scheme IV.4.2.1).

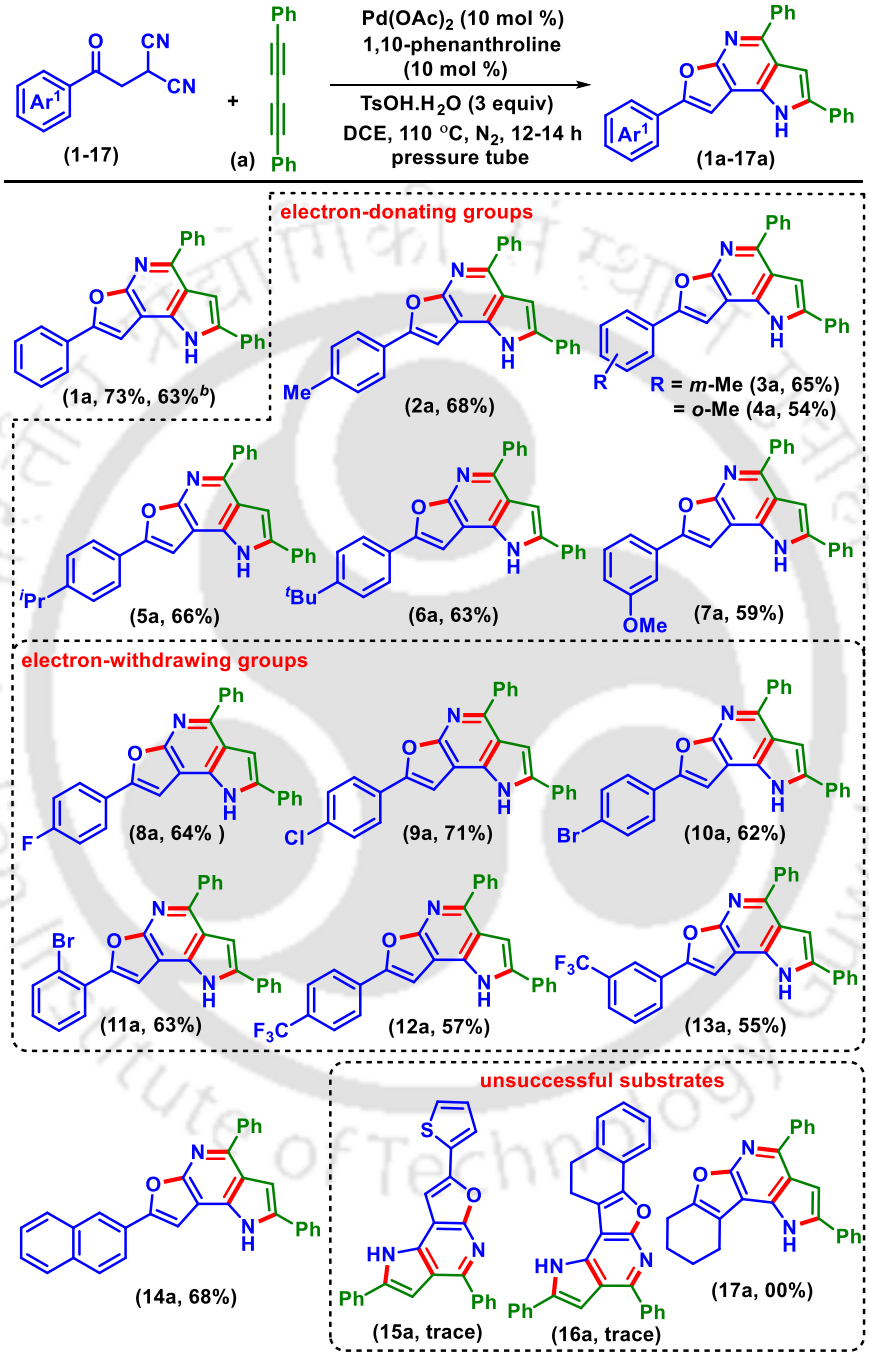

[a]Reaction conditions: **1–17** (0.20 mmol), 1,4-diphenylbuta-1,3-diyne (**a**) (0.40 mmol), $Pd(OAc)_2$ (0.020 mmol), 1,10-phenanthroline (0.020 mmol), $TsOH{\cdot}H_2O$ (0.60 mmol) and 1,2-DCE (2 mL) at 110 °C in a pressure tube under N_2 atmosphere for 12 h. [b]3 mmol scale. [c]Isolated yield.

Scheme IV.4.2.1. *Substrate scope for various β-ketodinitriles.*[a,b,c]

After successfully synthesizing a library of furo-pyrrolo-pyridines using various substituted β-ketodinitriles (**1–14**) the scope of this methodology was then extended to substituted 1,4-diphenylbuta-1,3-diyne (**b**–**r**) (Scheme IV.4.2.2). Butadiyne possessing EDGs such as *p*-Me (**b**), *m*-Me (**c**), *p*-Et (**d**), and *p*-^{t}Bu (**e**) responded positively providing the respective furo-pyrrolo-pyridines (**1b**, 65%), (**1c**, 66%), (**1d**, 62%), and (**1e**, 64%). Butadiyne containing EWGs such as *p*-F (**f**), *p*-Cl (**g**), *m*-Cl (**h**), *p*-Br (**i**), and *p*-CF_3 (**j**) all experienced efficient cyclization with (**1**) to yield their anticipated furo-pyrrolo-pyridines (**1f**–**1j**) in modest yields (51–70%). Furthermore, the diyne having *p*-*N*-pentyl group (**k**), efficiently participated in this protocol to give **1k** in 66% yield. The reaction with an unsymmetrical aromatic diyne having electron-donating *p*-Me and electron-withdrawing *p*-Cl (**l**) substituents provided an inseparable mixture of furo-pyrrolo-pyridine (**1l** and **1l′**) in a 2:1 ratio as determined by ^{1}H NMR. Here, in the major isomer (**1l**), the electron-rich phenyl ring possessing the *p*-Me group is oriented toward the pyridine site while the electron-deficient *p*-Cl ring is towards the pyrrole ring. To find out the reason behind the regioselectivity, atomic charge distribution calculation (6-31G+(d,p) basis set) on the substrate (**l**) was carried out. From the atomic charge distribution, the Mulliken charge difference between C1 and C4-center was found to be 0.012, and the C1-center (*i.e.* towards *p*-Me site) is comparatively more electrophilic than the C4 center (*i.e.* towards *p*-Cl bearing phenyl ring) (Scheme IV.4.2.2, for details, see section IV.8.6). An extreme regioselectivity was observed when the electronegativity between the two groups (*p*-Me and *p*-CF_3) in the diyne (**m**) are large. The reaction provided an exclusive regioisomeric furo-pyrrolo-pyridine (**1m**) in 64% yield. This is due to the large difference (0.048) in the Mulliken charge distribution between C1 and C4-center and the C1-center (*i.e.* towards *p*-Me bearing phenyl ring) is more electrophilic (Scheme 3, for details, see section IV.8.6). This protocol was equally successful with polyaromatic naphthalene containing diyne (**n**) providing its furo-pyrrolo-pyridine (**1n**) in 60% yield. However, the reaction with heterocyclic and aliphatic diyne such as thiophene diyne (**o**), 1-cyclohexynyl diyne (**p**), and cyclopropyl diyne (**q**) all failed to yield their corresponding furo-pyrrolo-pyridines. Further, *ortho*-substituted methyl-containing 1,4-diphenylbuta-1,3-diyne (**r**) failed to provide the expected product (**1r**). The failure may be attributed to the presence of two *o*-Me substituents that possibly hindered some of the reaction steps making it ineffective in this cascade cyclization. The protocol was further tested with β-ketodinitriles having EWGs *p*-F (**7**) and *o*-Br (**10**) with a diyne possessing *m*-Me group (**c**), both gave their respective furo-pyrrolo-pyridine (**7c**, 64% and **10c**, 59%) yields. Similarly, β-ketodinitrile having

an EWG *p*-Cl (**8**) reacted with a diyne bearing *p*-Et group (**d**) afforded the product (**8d**) in 55% yield.

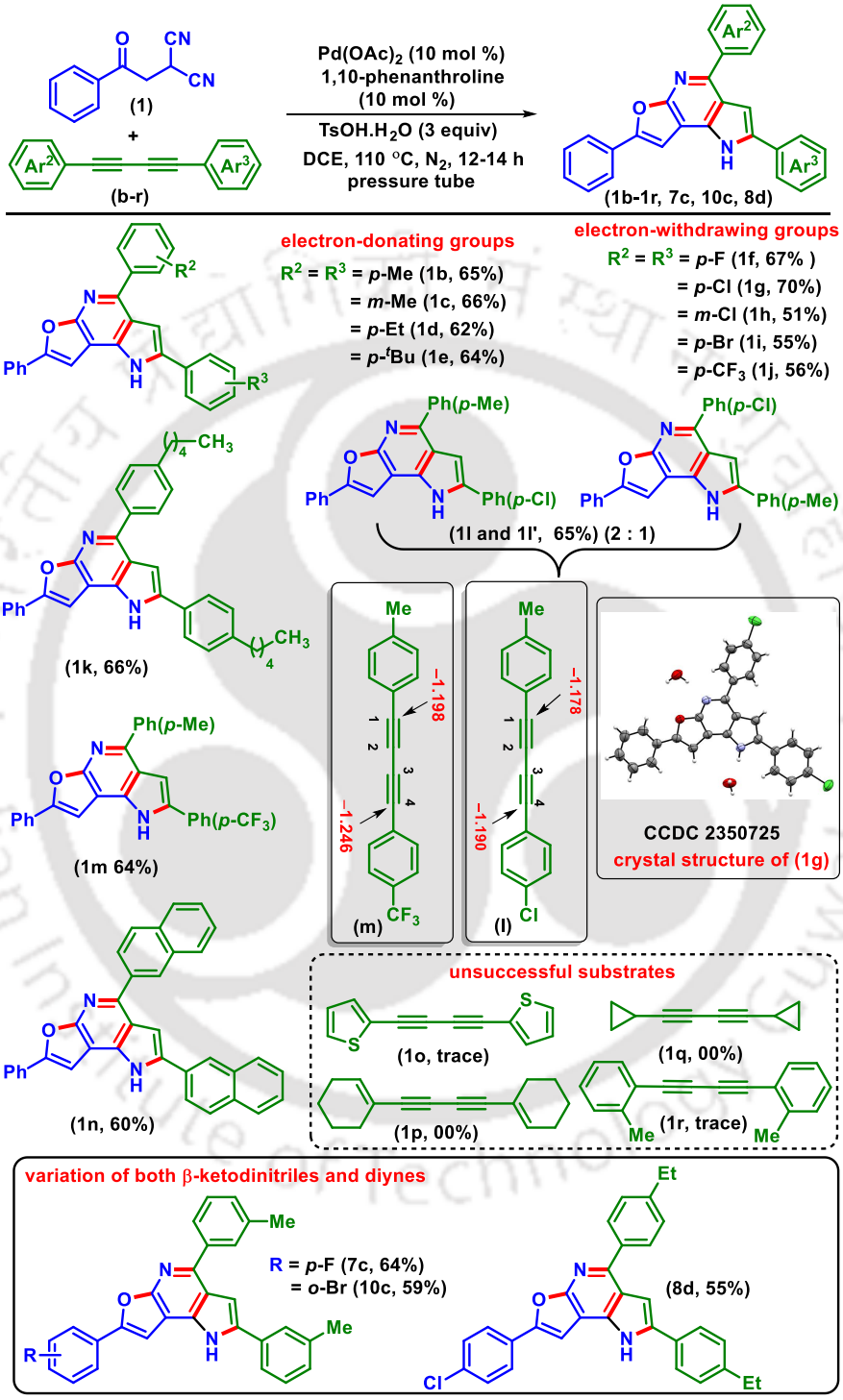

[a]Reaction conditions: **1** (0.20 mmol), **b–r** (0.40 mmol), $Pd(OAc)_2$ (0.020 mmol), 1,10-phenanthroline (0.020 mmol), $TsOH{\cdot}H_2O$ (0.60 mmol) and 1,2-DCE (2 mL) at 110 °C in a pressure tube under N_2 atmosphere for 12-14 h. [b]Isolated yield.

Scheme IV.4.2.2. *Substrate scope for buta-1,3-diynes.*[a,b]

IV.5. Mechanistic Investigations:

IV.5.1. Control Experiments:

Next, to propose a plausible reaction mechanism, a few control experiments were carried out for this Pd(II)-catalyzed synthesis of fused heterocycles (Scheme IV.5.1.1). Under identical reaction conditions in the absence of diyne (**a**), β-ketodinitrile (**1**) yielded 2-amino-5-phenylfuran-3-carbonitrile (**1′**) in 81% yield, suggesting its intermediacy [Scheme IV.5.1.1(i)]. The same product (**1′**) was obtained in 76% yield when the reaction was carried out even in the absence of Pd-catalyst and ligand [Scheme IV.5.1.1(ii)]. This suggests the non-involvement of Pd in the construction of the furan ring, thus the formation of (**1′**) is a simple acid-catalyzed process. The reaction of preformed 2-amino-5-phenylfuran-3-carbonitrile (**1′**) with diyne (**a**) afforded furo-pyrrolo-pyridine (**1a**) in 82% yield, thereby reconfirming its intermediacy (Scheme IV.5.1.1(iii)). To ascertain the role of Pd-catalyst and TsOH.H_2O in the catalytic cycle, two independent reactions were carried out between intermediate (**1′**) and diyne (**a**), one without $Pd(OAc)_2$, and the other without TsOH.H_2O [Scheme IV.5.1.1(iii)]. In both cases, the reaction failed to give the product (**1a**), confirming the necessity of $Pd(OAc)_2$ and TsOH.H_2O for the catalytic cycle [Scheme IV.5.1.1(iii)].

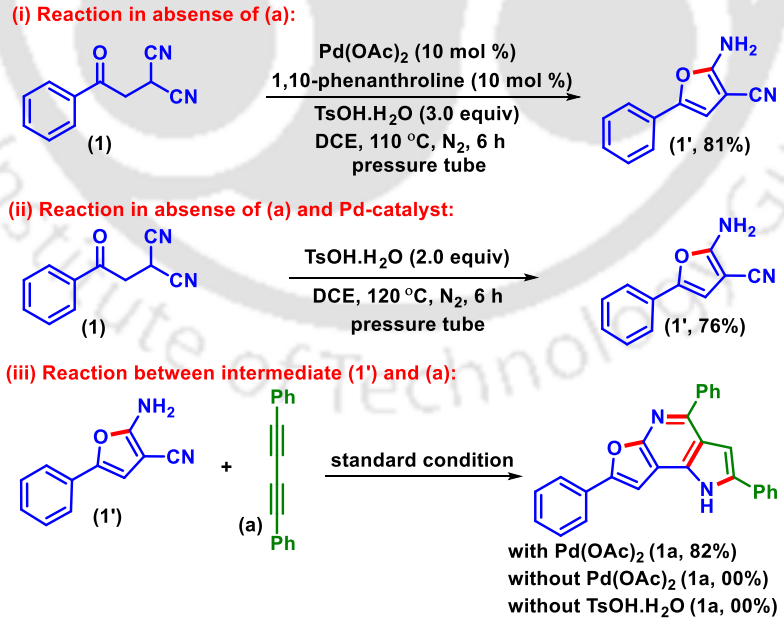

Scheme IV.5.1.1. *Control experiments.*

IV.5.2. Plausible Reaction Mechanism:

Based on these experimental findings and from the literature reports, a plausible mechanistic pathway has been depicted in Scheme IV.5.2.1.[9a,9b] In the presence of TsOH·H_2O, β-ketodinitrile (**1**) undergoes an acid-catalyzed enolization to afford an enol-intermediate (**I**) which on intramolecular cyclization (5-*exo-dig*) afforded a five-membered cyclic furan intermediate (**1′**). Next, the amino group of intermediate (**1′**) participates in a deprotonative coordination with the *in situ* generated Pd(II) complex (**A**) [which is formed via coordination of $Pd(OAc)_2$ with ligand 1,10-phenanthroline (L)] to form intermediate (**B**) with elimination of AcOH. Next, one of the alkyne sides of the diyne (**a**) is inserted into the N atom, giving an alkynyl Pd(II) intermediate (**C**). Subsequently, the intermediate (**C**) undergoes an intramolecular insertion (6-*exo-dig*) to the nitrile through a carbopalladation, giving an imine Pd complex to construct a pyridine ring (**D**). Next, the imine Pd-complex (**D**) endures an intramolecular 5-*endo-dig* cyclization via aminopalladation with another alkyne side to give a Pd-bound furo-pyrrolo-pyridine intermediate (**E**). Finally, protonolysis followed by aromatization of intermediate **E** afforded the furo-pyrrolo-pyridine (**1a**) and regenerated the Pd-catalyst (**F**) for the next catalytic cycle.

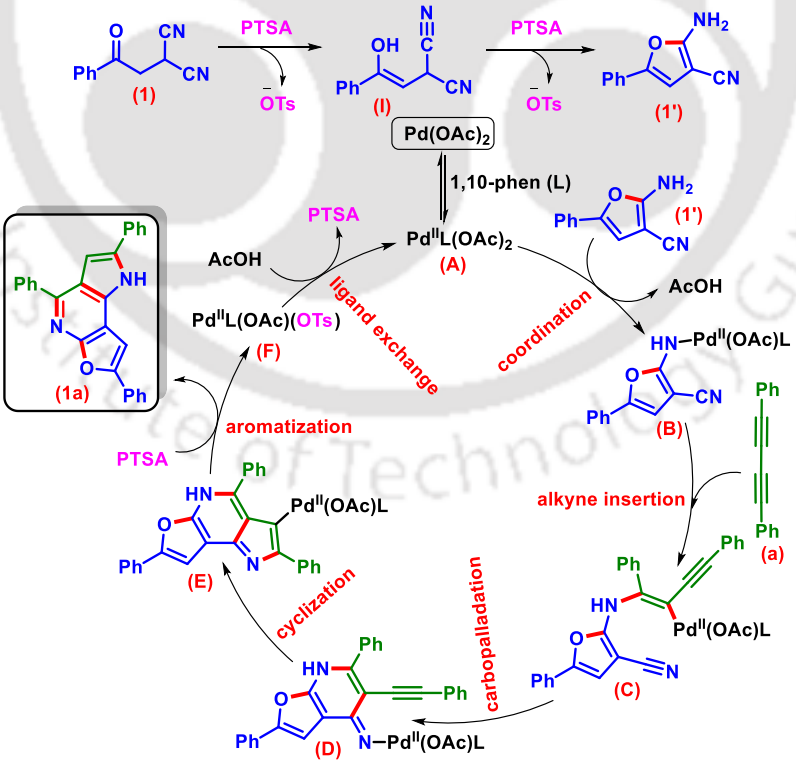

Scheme IV.5.2.1. *Plausible reaction pathway.*

IV.6. Post-Synthetic Applications:

To explore the synthetic utility of the synthesized furo-pyrrolo-pyridines, a few late-stage functionalizations were carried out as shown in Scheme IV.6.1. The furo-pyrrolo-pyridine (**7a**) undergoes selective C–H/N annulation at the phenyl ring adjacent to pyridine, with diphenylacetylene (**x**) in the presence of a Ru(II)-catalyst giving an annulated product (**1x**) in 73% yield.[9b] The formation of this regioselective annulated product is due to the presence of pyridine N-directing group adjacent to the peri-planner phenyl ring. Further, *p*-Br substituted furo-pyrrolo-pyridine (**8a**) undergoes Pd(II)-catalyzed Suzuki coupling with phenylboronic acid (**y**)[23] and Sonogashira coupling with 4-ethynyltoluene (**z**)[23] giving corresponding cross-coupled products (**8y**, 80%), and (**8z**, 78%), respectively.

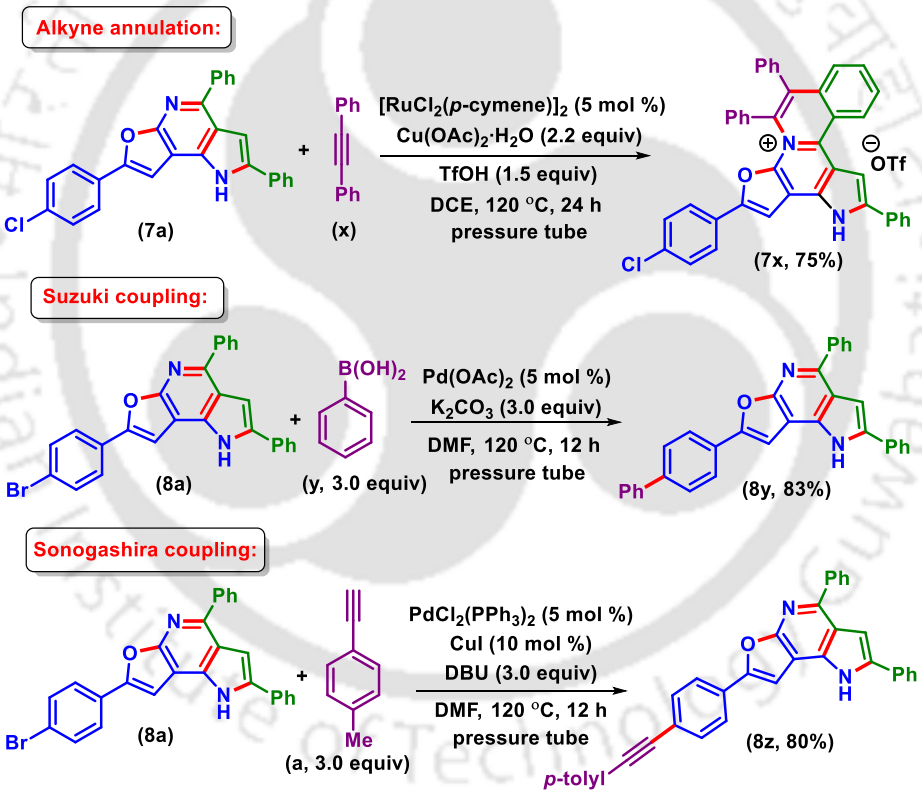

Scheme IV.6.1. *Post-synthetic functionalizations.*

IV.7. Conclusion:

In conclusion, a non-templated Pd(II)-catalyzed synthesis of furo[2,3-*b*]pyrrolo[2,3-*d*]pyridines has been established via addition/cyclization of β-ketodinitriles and diynes. While one of the nitrile groups participates in the formation of the pyridine ring the other in the construction of the pyrrole ring involves the formation of C–C, C=C, C–O, C–N, and C=N bonds. A diverse range of substrates were well tolerated, giving moderate to good yields of the product. The control experiment reveals the formation of a 2-amino-5-phenylfuran-3-carbonitrile intermediate in the absence of diyne. Finally, to explore synthetic utility as well as to expand the substrate scope, large-scale synthesis, and a few post-synthetic functionalizations were also demonstrated.

IV.8. Experimental Section:

IV.8.1. General Information:

All the reagents were commercial grade and purified according to the established procedures. All the reactions were carried out in oven-dried glassware. The highest commercial quality reagents were purchased and were used without further purification unless otherwise stated. Reactions were monitored by thin layer chromatography (TLC) on 0.25 mm silica gel plates ($60F_{254}$) visualized under UV illumination at 254 nm. Organic extracts were dried over anhydrous sodium sulfate (Na_2SO_4). Solvents were removed using a rotary evaporator under reduced pressure. Column chromatography was performed to purify the crude product on silica gel 60–120 mesh using a mixture of hexane and ethyl acetate as eluent. The isolated compounds were characterized by spectroscopic [^{1}H, ^{13}C{1H} NMR, and IR] techniques and HRMS analysis. NMR spectra were recorded in deuterochloroform ($CDCl_3$). ^{1}H, ^{13}C{^{1}H} were recorded in 600 (150) or 500 (125) MHz spectrometer and were calibrated using tetramethylsilane or residual undeuterated solvent for ^{1}H NMR, deuterochloroform for ^{13}C NMR as an internal reference {$Si(CH_3)_4$: 0.00 ppm or $CHCl_3$: 7.260 ppm for ^{1}H NMR, 77.230 ppm for ^{13}C NMR or $(CH_3)_2SO$: 2.500 ppm for ^{1}H NMR, 39.500 ppm for ^{13}C NMR }. ^{19}F NMR was calibrated without any internal standard in $CDCl_3$ and DMSO-d_6 in a 500 MHz spectrometer. The chemical shifts are quoted in δ units, parts per million (ppm). ^{1}H NMR data is represented as follows: Chemical shift, multiplicity (s = singlet, d = doublet, t = triplet, q = quartet, m = multiplet), integration and coupling constant(s) *J* in hertz (Hz). High-

resolution mass spectra (HRMS) were recorded on a mass spectrometer using electrospray ionization-time of flight (ESI-TOF) reflection experiments. FT-IR spectra were recorded in neat and reported in the frequency of absorption (cm^{-1}).

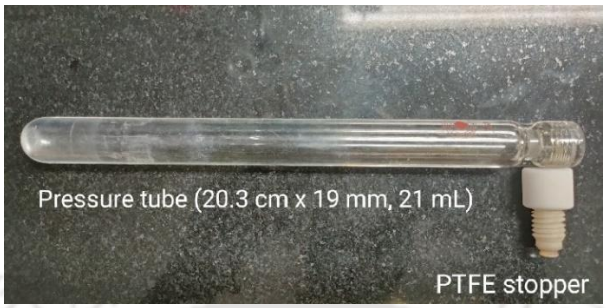

IV.8.2. General Procedures:

IV.8.2.1. General Procedure for the Synthesis of 2-(2-Oxo-2-arylethyl)malononitriles (1–15):

Compounds **1**–**15** were synthesized in slightly modified literature procedures.[24]

IV.8.2.2. General Procedure for the Synthesis of Symmetrical 1,3-Diynes (a–k, m–n):

Compounds **a–k**, **m–n** were synthesized by following the literature procedures.[25]

To an oven-dried 100 mL round bottom flask was added phenylacetylene (10 mmol), CuI (10 mmol), I_2 (10 mmol), and Na_2CO_3 (20 mmol) were dissolved in DMF (10 mL). The reaction mixture was stirred at 80 °C in a preheated oil bath for 4 h. After completion of the reaction (monitored by TLC analysis), the reaction mixture was admixed with ethyl acetate (50 mL), and the mixture was filtered through a pad of celite. The organic layer was washed with saturated aqueous $Na_2S_2O_3$ solution (20 mL) and ice-cold water (30 mL), dried over anhydrous Na_2SO_4, filtered, and concentrated under reduced pressure. The crude material was purified by column chromatography using hexane as eluant on silica gel to give the symmetrical 1,4-diphenylbuta-1,3-diyne (**a**) (1.71 g, 85%) (Scheme IV.8.2.2.1).

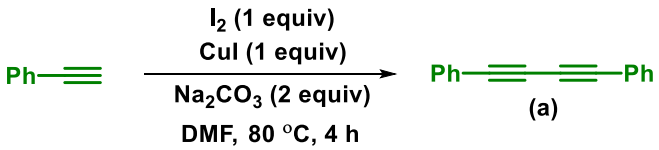

Scheme IV.8.2.2.1. *Synthesis of symmetrical 1,3-diynes (**b–k, m–n**).*

IV.8.2.3. General Procedure for the Synthesis of Unsymmetrical 1,3-diynes (l):

Compounds **l** were synthesized by following the literature procedures.[25]

To an oven-dried 100 mL round bottom flask containing 4-ethynyltoluene (1.16 g, 10 mmol) in acetone (10 mL) was added *N*-bromosuccinimide (NBS) (12 mmol, 1.2 equiv, 2.136 g,) and $AgNO_3$ (0.169 mg, 1 mmol). Then the reaction mixture was stirred at room temperature under the exclusion of light for 2 h. After completion of the reaction (monitored by TLC analysis), the solvent acetone was evaporated under reduced pressure. Then the reaction mixture was admixed with ethyl acetate (40 mL) and filtered through a pad of celite. The organic layer was washed with aqueous NaCl solution (30 mL), dried over anhydrous Na_2SO_4, and filtered and concentrated under reduced pressure. The crude material was further purified by column chromatography using hexane as the eluant on silica gel to give the 1-(bromoethynyl)-4-methylbenzene (**l′**) (1.65 g, 85%) (Scheme IV.8.2.3.1). The product was submitted to the next step.

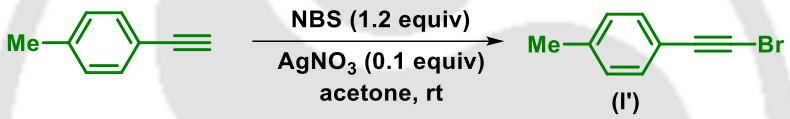

Scheme IV.8.2.3.1. *Synthesis of 1-(bromoethynyl)-4-methylbenzene (**l′**).*

To an oven-dried 100 mL round bottom flask containing 1-chloro-4-ethynylbenzene (**l″**) (5 mmol, 0.68 g) was added 1-(bromoethynyl)-4-methylbenzene (**l′**) (5.15 mmol, 1.3 equiv, 1.00 g), CuI (0.5 mmol, 10 mol %, 0.095 g), PPh_3 (1.0 mmol, 20 mol %, 0.262 g), K_2CO_3 (10 mmol, 2 equiv, 1.38 g), and ethanol (10 mL). The reaction was stirred at 100 ºC for 14 h in a pre-heated oil bath. After completion of the reaction (monitored by TLC analysis), the reaction mixture was cooled to room temperature and admixed with ethyl acetate (40 mL). The organic layer was washed with saturated aqueous $Na_2S_2O_3$ solution (20 mL) followed by ice-cold water (30 mL). Then the organic layer was dried over anhydrous Na_2SO_4, filtered, and concentrated under reduced pressure. The crude mixture was further purified by column chromatography (hexane : ethyl acetate 99:1) on silica gel to give the desired unsymmetrical 1,3-diynes 1-chloro-4-(*p*-tolylbuta-1,3-diyn-1-yl)benzene (**l**) (962 mg, 77%) (Scheme IV.8.2.3.2).

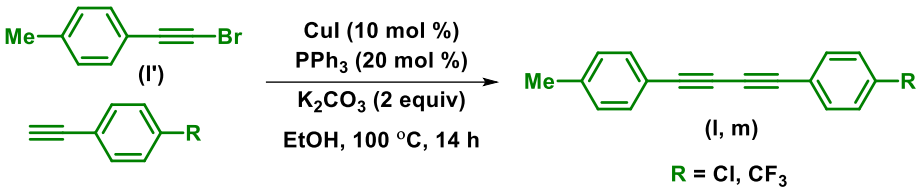

Scheme IV.8.2.3.2. *Synthesis of unsymmetrical 1,3-diynes (**l**, **m**).*

IV.8.2.4. General procedure for the Synthesis of Symmetrical 1,3-Diynes [1,4-Di(cyclohex-1-en-1-yl)buta-1,3-diyne (o)]:[25a]

In an oven-dried 100 mL round bottom flask containing 1-ethynylcyclohexene (5 mmol, 0.530 g), $PdCl_2(PPh_3)_2$ (0.15 mmol, 0.105 g), CuI (0.15 mmol, 0.0285 g), PPh_3 (0.45 mmol, 0.118 g) in Et_3N (3 mL) and MeCN (6 mL). The reaction was stirred at room temperature for 24 h. After completion of the reaction (monitored by TLC analysis), the reaction mixture was admixed with ethyl acetate (40 mL), and washed with aqueous HCl solution (1 mol/L) (2 x 20 ml) and water (30 ml). Then the organic layer was dried over anhydrous Na_2SO_4, filtered, and concentrated under reduced pressure. The crude mixture was purified by column chromatography (hexanes) on silica gel to give the respective symmetrical 1,3-diynes (**o**) (895 mg, 85%) (Scheme IV.8.2.4.1).

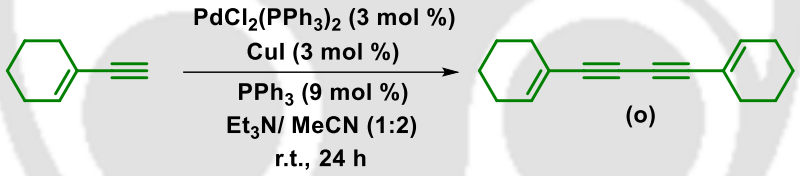

Scheme IV.8.2.4.1. *Synthesis of aliphatic symmetrical 1,3-diynes (**o**).*

IV.8.2.5. General procedure for the Synthesis of Aliphatic Symmetrical 1,3-Diynes [1,4-Dicyclopropylbuta-1,3-diyne (p)]:[25b]

To an oven-dried 100 mL round bottom flask containing cyclopropylacetylene (0.33 g, 5.0 mmol) was added CuI (0.0475 g, 0.25 mmol), TMEDA (0.058 g, 0.5 mmol), and Et_3N (1.515 g, 3 mmol) in 10 mL of acetone. The reaction flask was covered with a glass stopper and stirred at room temperature for 20 h. The progress of the reaction was monitored by TLC. After completion of the reaction, the solvent was removed under reduced pressure, and then the mixture was admixed with ethyl acetate (40 mL), and the organic layer was washed with aqueous HCl solution (1 mol/L) (2 x 20 ml) and water (30 ml). Then the organic layer was dried over anhydrous Na_2SO_4, filtered, and

again concentrated under reduced pressure. The crude product obtained was purified by column chromatography using hexane over silica gel to give 1,4-dicyclopropylbuta-1,3-diyne (**p**) as the liquid (494 mg, 76%) (Scheme IV.8.2.5.1).

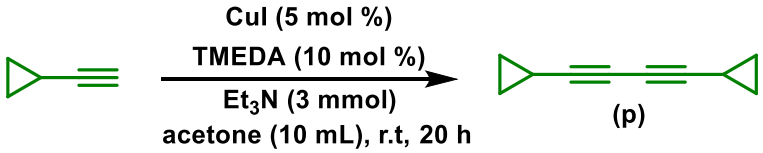

Scheme IV.8.2.5.1. *Synthesis of 1,4-dicyclopropylbuta-1,3-diyne (**p**).*

IV.8.2.6. General Procedure for the Synthesis of 2,4,7-Triphenyl-1*H*-furo[2,3-*b*]pyrrolo[2,3-*d*]pyridine (1a) from 2-(2-Oxo-2-phenylethyl)malononitrile (1) and 1,4-Diphenylbuta-1,3-diyne (a):

To an oven-dried pressure tube (20.3 cm x 19 mm, 21 mL) containing a magnetic bar was added 2-(2-oxo-2-phenylethyl)malononitrile (**1**) (0.037 g, 0.20 mmol), 1,4-diphenylbuta-1,3-diyne (**a**) (0.080 g, 0.40 mmol), $Pd(OAc)_2$ (0.0045 g, 0.02 mmol), 1,10-phenanthroline (0.0036 g, 0.025 mmol), $TsOH{\cdot}H_2O$ (0.114 g, 0.60 mmol) and 1,2-DCE (2 mL). After that, the reaction mixture was purged with N_2 using a needle and closed with a PTFE stopper. The reaction mixture was stirred at 110 ^oC in a preheated oil bath for 12 h. After completion of the reaction (monitored by TLC analysis), the reaction mixture was admixed with ethyl acetate (25 mL), and the organic layer was washed with saturated $NaHCO_3$ solution (10 mL). The organic layer was dried over anhydrous Na_2SO_4, and the solvent was evaporated under reduced pressure. The crude product so obtained was purified over a column of silica gel using 10% ethyl acetate in hexane to give pure 2,4,7-triphenyl-1*H*-furo[2,3-*b*]pyrrolo[2,3-*d*]pyridine (**1a**) with 73% yield (56 mg) (Scheme IV.8.2.6.1). The identity and purity of the product were confirmed by spectroscopic analysis.

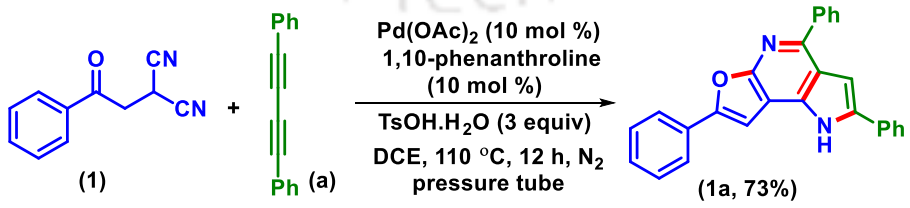

Scheme IV.8.2.6.1. *Synthesis of 2,4,7-triphenyl-1H-furo[2,3-b]pyrrolo[2,3-d]pyridine (**1a**).*

IV.8.2.7. General Procedure for the Large-Scale Synthesis of 2,4,7-Triphenyl-1*H*-furo[2,3-*b*]pyrrolo[2,3-*d*]pyridine (1a) between the Reaction of 2-(2-Oxo-2-phenylethyl)malononitrile (1), and 1,4-Diphenylbuta-1,3-diyne (a):

To an oven-dried pressure tube (20.3 cm x 19 mm, 21 mL) containing a magnetic bar was added 2-(2-oxo-2-phenylethyl)malononitriles (**1**) (0.552 g, 3.0 mmol), 1,4-diphenylbuta-1,3-diyne (**a**) (1.212 g, 6.0 mmol), $Pd(OAc)_2$ (0.0673 g, 0.3 mmol), 1,10-phenanthroline (0.054 g, 0.3 mmol), $TsOH{\cdot}H_2O$ (1.71 g, 9.0 mmol) and 1,2-DCE (6 mL). After that, the reaction mixture was purged with N_2 using a needle and closed with a PTFE stopper. The reaction mixture was stirred at 110 °C in a preheated oil bath for 12 h. After completion of the reaction (monitored by TLC analysis), the reaction mixture was admixed with ethyl acetate (50 mL), and the organic layer was washed with saturated $NaHCO_3$ solution (20 mL). The organic layer was dried over anhydrous Na_2SO_4, and the solvent was evaporated under reduced pressure. The crude product so obtained was purified over a column of silica gel using 10% ethyl acetate in hexane to give pure 2,4,7-triphenyl-1*H*-furo[2,3-*b*]pyrrolo[2,3-*d*]pyridine (**1a**) with 63% yield (725 mg) (Scheme IV.8.2.7.1).

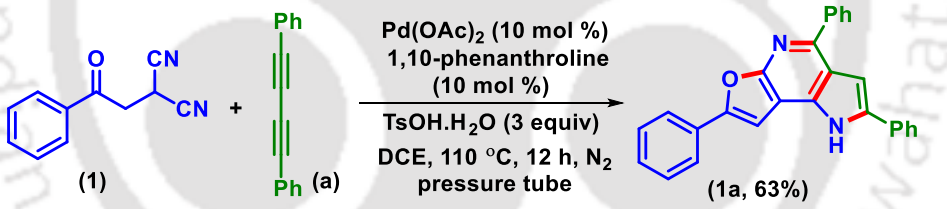

Scheme IV.8.2.7.1. *Large-scale synthesis of 2,4,7-triphenyl-1H-furo[2,3-b]pyrrolo[2,3-d]pyridine (**1a**).*

IV.8.3. Control Experiments:

IV.8.3.1. Reaction in the Absence of 1,4-Diphenylbuta-1,3-diyne (a):

To an oven-dried pressure tube (20.3 cm x 19 mm, 21 mL) containing a magnetic bar was added 2-(2-oxo-2-phenylethyl)malononitriles (**1**) (0.037 g, 0.20 mmol), $Pd(OAc)_2$ (0.0045 g, 0.020 mmol), 1,10-phenanthroline (0.0036 g, 0.020 mmol), $TsOH{\cdot}H_2O$ (0.114 g, 0.6 mmol) and 1,2-DCE (2 mL). After that, the reaction mixture was purged with N_2 using a needle and closed with a PTFE stopper. The reaction mixture was stirred at 110 °C in a preheated oil bath for 6 h. After completion of the reaction (monitored by TLC analysis), the reaction mixture was admixed with ethyl acetate

(25 mL), and the organic layer was washed with saturated $NaHCO_3$ solution (10 mL). The organic layer was dried over anhydrous Na_2SO_4, and the solvent was evaporated under reduced pressure. The crude product so obtained was purified over a column of silica gel using 15% ethyl acetate in hexane to give pure 2-amino-5-phenylfuran-3-carbonitrile (**1′**) with 81% yield (30 mg) (Scheme IV.8.3.1.1). The identity and purity of the product were confirmed by spectroscopic analyses.

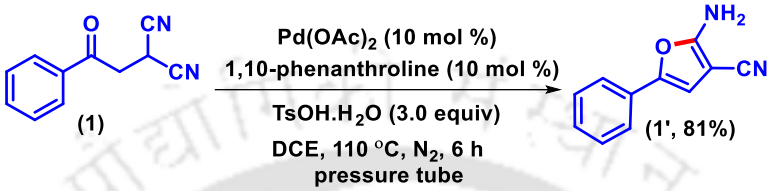

Scheme IV.8.3.1.1. *Reaction in the absence of 1,4-diphenylbuta-1,3-diyne (**a**).*

IV.8.3.2. Reaction in the Absence of 1,4-Diphenylbuta-1,3-diyne (a), and Pd-catalyst:

To an oven-dried pressure tube (20.3 cm x 19 mm, 21 mL) containing a magnetic bar was added 2-(2-oxo-2-phenylethyl)malononitriles (**1**) (0.037 g, 0.20 mmol), $TsOH{\cdot}H_2O$ (0.076 g, 0.40 mmol) and 1,2-DCE (2 mL). After that, the reaction mixture was purged with N_2 using a needle and closed with the PTFE stopper. The reaction mixture was stirred at 110 °C in a preheated oil bath for 6 h. After completion of the reaction (monitored by TLC analysis), the reaction mixture was admixed with ethyl acetate (25 mL), and the organic layer was washed with saturated $NaHCO_3$ solution (10 mL). The organic layer was dried over anhydrous Na_2SO_4, and the solvent was evaporated under reduced pressure. The crude product obtained was purified over a column of silica gel using 15% ethyl acetate in hexane to give pure 2-amino-5-phenylfuran-3-carbonitrile (**1′**) with 76% yield (28 mg) (Scheme IV.8.3.2.1). The identity and purity of the product were confirmed by spectroscopic analysis.

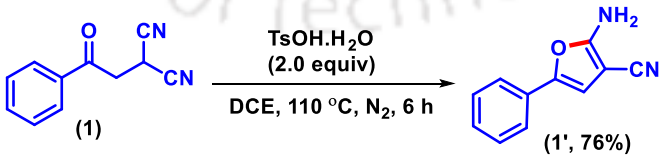

Scheme IV.8.3.2.1. *Reaction in the absence of 1,4-diphenylbuta-1,3-diyne (**a**), and $Pd(OAc)_2$.*

IV.8.3.3. Reaction between Intermediate 2-Amino-5-phenylfuran-3-carbonitrile (1') and 1,4-Diphenylbuta-1,3-diyne (a):

(i) To an oven-dried pressure tube (20.3 cm x 19 mm, 21 mL) containing a magnetic bar was added 2-amino-5-phenylfuran-3-carbonitrile (**1′**) (0.037 g, 0.20 mmol), 1,4-diphenylbuta-1,3-diyne (**a**) (0.067 g, 0.40 mmol), $Pd(OAc)_2$ (0.0045 g, 0.020 mmol), 1,10-phenanthroline (0.0036 g, 0.020 mmol), $TsOH{\cdot}H_2O$ (0.114 g, 0.60 mmol) and 1,2-DCE (2 mL). After that, the reaction mixture was purged with N_2 using a needle and closed with a PTFE stopper. The reaction mixture was stirred at 110 °C in a preheated oil bath for 6 h. After completion of the reaction (monitored by TLC analysis), the reaction mixture was admixed with ethyl acetate (25 mL), and the organic layer was washed with saturated $NaHCO_3$ solution (10 mL). The organic layer was dried over anhydrous Na_2SO_4, and the solvent was evaporated under reduced pressure. The crude product so obtained was purified over a column of silica gel using 10% ethyl acetate in hexane to give pure 2,4,7-triphenyl-1*H*-furo[2,3-*b*]pyrrolo[2,3-*d*]pyridine (**1a**) with 82% yield (63 mg) (Scheme IV.8.3.3.1). The identity and purity of the product were confirmed by spectroscopic analyses.

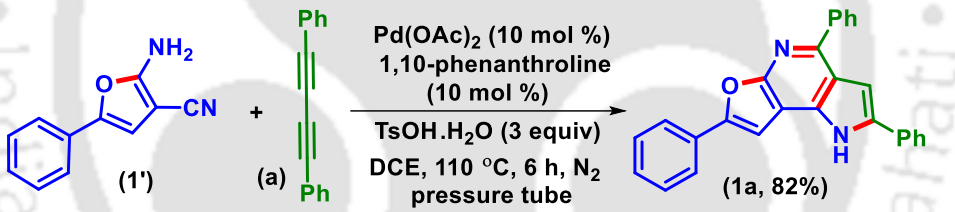

Scheme IV.8.3.3.1. *Reaction with Intermediate (1').*

(ii) Reaction between Intermediate 2-Amino-5-phenylfuran-3-carbonitrile (1') and 1,4-Diphenylbuta-1,3-diyne (a) in the Absence of $Pd(OAc)_2$ and Ligand:

To an oven-dried pressure tube (20.3 cm x 19 mm, 21 mL) containing a magnetic bar was added 2-amino-5-phenylfuran-3-carbonitrile (**1′**) (0.037 g, 0.20 mmol), 1,4-diphenylbuta-1,3-diyne (**a**) (0.067 g, 0.40 mmol), $TsOH{\cdot}H_2O$ (0.114 g, 0.60 mmol) and 1,2-DCE (2 mL). After that, the reaction mixture was purged with N_2 using a needle and closed with a PTFE stopper. The reaction mixture was stirred at 110 °C in a preheated oil bath for 6 h. The reaction failed to give the product (**1a**) monitored by TLC analysis and both the starting materials remained unreactive (Scheme IV.8.3.3.2).

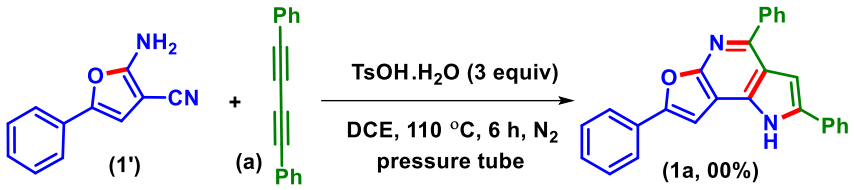

Scheme IV.8.3.3.2. *Reaction with intermediate (**1'**) in the absence of Pd-catalyst.*

(iii) Reaction between Intermediate 2-Amino-5-phenylfuran-3-carbonitrile (1') and 1,4-Diphenylbuta-1,3-diyne (a) in the Absence of TsOH·H_2O:

To an oven-dried pressure tube (20.3 cm x 19 mm, 21 mL) containing a magnetic bar was added 2-amino-5-phenylfuran-3-carbonitrile (**1′**) (0.037 g, 0.20 mmol), 1,4-diphenylbuta-1,3-diyne (**a**) (0.067 g, 0.40 mmol), $Pd(OAc)_2$ (0.0045 g, 0.020 mmol), 1,10-phenanthroline (0.0036 g, 0.020 mmol), and 1,2-DCE (2 mL). After that, the reaction mixture was purged with N_2 using a needle and closed with the PTFE stopper. The reaction mixture was stirred at 110 °C in a preheated oil bath for 6 h. The reaction failed to give the product (**1a**) monitored by TLC analysis and the starting materials were fully unconsumed (Scheme IV.8.3.3.3).

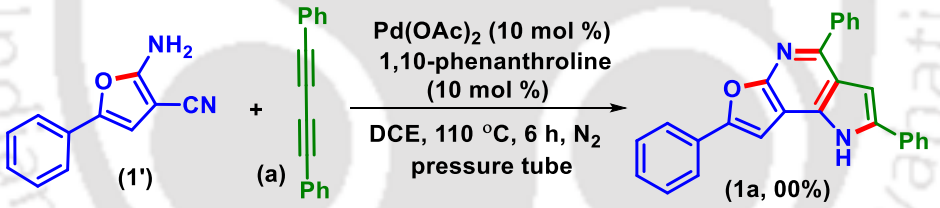

Scheme IV.8.3.3.3. *Reaction with intermediate (**1'**) in the absence of TsOH.H_2O.*

IV.8.4. Procedure of Post-Synthetic Functionalizations:

IV.8.4.1. General Procedure for the Synthesis of 2-(4-chlorophenyl)-5,6,12-triphenyl-13*H*-furo[3',2':5,6]pyrrolo[3',2':3,4]pyrido[2,1-*a*]isoquinolin-4-ium (7x) from 7-(4-chlorophenyl)-2,4-diphenyl-1*H*-furo[2,3-*b*]pyrrolo[2,3-*d*]pyridine (7a) and Diphenylacetylene (x):[2a]

To an oven-dried pressure tube (20.3 cm x 19 mm, 21 mL) containing a magnetic bar was added 7-(4-chlorophenyl)-2,4-diphenyl-1*H*-furo[2,3-*b*]pyrrolo[2,3-*d*]pyridine (**7a**) (0.084 g, 0.20 mmol), diphenylacetylene (**x**) (0.071 g, 0.40 mmol), $[Ru(p\text{-cymene})Cl_2]_2$ (0.0061 g, 0.01 mmol), $Cu(OAc)_2·H_2O$ (0.084 g, 0.44 mmol), TfOH (0.045 g, 0.30 mmol) and DCE (2 mL). The reaction

mixture was stirred in an oil bath preheated at 120 °C for 24 h. After completion of the reaction (monitored by TLC analysis), the reaction mixture was admixed with ethyl acetate (25 mL), and the organic layer was washed with saturated $NaHCO_3$ solution (10 mL). The organic layer was dried over anhydrous sodium sulfate (Na_2SO_4), and the solvent was evaporated under reduced pressure. The crude product obtained was purified over a column of silica gel using 2% methanol in dichloromethane to give pure 2-(4-chlorophenyl)-5,6,12-triphenyl-13*H*-furo[3',2':5,6]pyrrolo[3',2':3,4]pyrido[2,1-*a*]isoquinolin-4-ium (**7x**) in 73% yield (87 mg) (Scheme IV.8.4.1.1). The identity and purity of the product were confirmed by spectroscopic analyses.

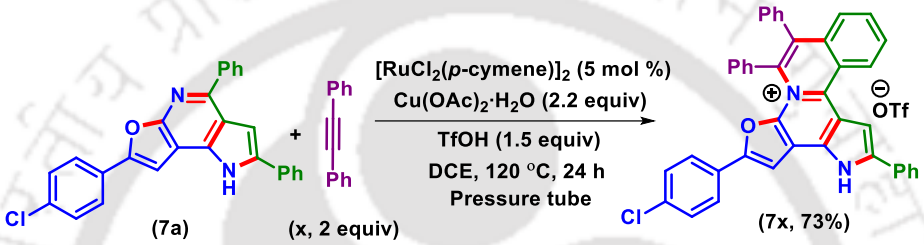

Scheme IV.8.4.1.1. *Ru(II)-catalyzed annulation with diphenylacetylene (**x**).*

IV.8.4.2. General Procedure for the Synthesis of 7-([1,1'-biphenyl]-4-yl)-2,4-diphenyl-1*H*-furo[2,3-*b*]pyrrolo[2,3-*d*]pyridine (8y) from 7-(4-bromophenyl)-2,4-diphenyl-1*H*-furo[2,3-*b*]pyrrolo[2,3-*d*]pyridine (8a) and Phenylboronic Acid (y):[2b]

To an oven-dried pressure tube (20.3 cm x 19 mm, 21 mL) containing a magnetic bar was added 7-(4-bromophenyl)-2,4-diphenyl-1*H*-furo[2,3-*b*]pyrrolo[2,3-*d*]pyridine (**8a**) (0.093 g, 0.20 mmol), phenylboronic acid (**y**) (0.072 g, 0.60 mmol), $Pd(OAc)_2$ (0.0022 g, 0.01 mmol), K_2CO_3 (0.083 g, 0.60 mmol) and DMF (2 mL). The reaction mixture was stirred in a preheated oil bath at 120 °C for 12 h. After completion of the reaction (monitored by TLC analysis), the reaction mixture was admixed with ethyl acetate (25 mL), and the organic layer was washed with ice-cold water (20 mL). The organic layer was dried over anhydrous sodium sulfate (Na_2SO_4), and the solvent was evaporated under reduced pressure. The crude product so obtained was purified over a column of silica gel using 10% ethyl acetate in hexane to give pure 7-([1,1'-biphenyl]-4-yl)-2,4-diphenyl-1*H*-furo[2,3-*b*]pyrrolo[2,3-*d*]pyridine (**8y**) in 80% yield (74 mg) (Scheme IV.8.4.2.1). The identity and purity of the product were confirmed by spectroscopic analyses.

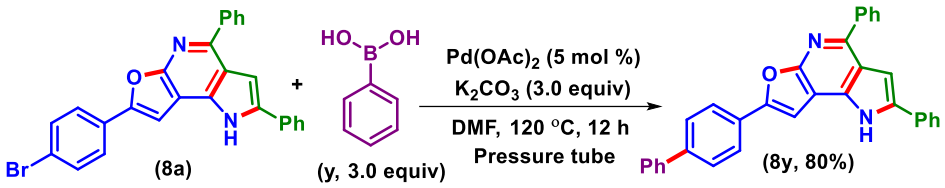

Scheme IV.8.4.2.1. *Pd(II)-catalyzed Suzuki coupling with phenylboronic acid (**y**).*

IV.8.4.3. General Procedure for the Synthesis of 2,4-Diphenyl-7-(4-(*p*-tolylethynyl)phenyl)-1*H*-furo[2,3-*b*]pyrrolo[2,3-*d*]pyridine (8z) from 7-(4-Bromophenyl)-2,4-diphenyl-1*H*-furo[2,3-*b*]pyrrolo[2,3-*d*]pyridine (8a) and 4-Ethynyltoluene (z):[2c]

To an oven-dried pressure tube (20.3 cm x 19 mm, 21 mL) containing a magnetic bar was added 7-(4-bromophenyl)-2,4-diphenyl-1*H*-furo[2,3-*b*]pyrrolo[2,3-*d*]pyridine (**8a**) (0.085 g, 0.20 mmol), 4-ethynyltoluene (**z**) (0.069 g, 0.60 mmol), $PdCl_2(PPh_3)_2$ (0.0070 g, 0.01 mmol), CuI (0.0038 g, 0.02 mmol), DBU (0.091 g, 0.60 mmol) and DMF (2 mL). The reaction mixture was stirred in a preheated oil bath at 120 °C for 12 h. After completion of the reaction (monitored by TLC analysis), the reaction mixture was admixed with ethyl acetate (25 mL), and the organic layer was washed with ice-cold water (20 mL). The organic layer was dried over anhydrous sodium sulfate (Na_2SO_4), and the solvent was evaporated under reduced pressure. The crude product so obtained was purified over a column of silica gel using 10% ethyl acetate in hexane to give pure 2,4-diphenyl-7-(4-(*p*-tolylethynyl)phenyl)-1*H*-furo[2,3-*b*]pyrrolo[2,3-*d*]pyridine (**8z**) in 78% yield (78 mg) (Scheme IV.8.4.3.1). The identity and purity of the product were confirmed by spectroscopic analyses.

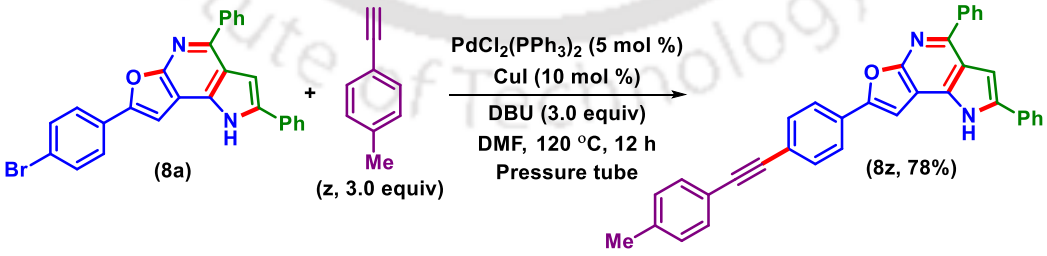

Scheme IV.8.4.3.1. *Pd(II)-catalyzed Sonogashira coupling with 4-ethynyltoluene (**z**).*

IV.8.5. Crystallographic Information:

IV.8.5.1. Crystallographic Information of 2,4-bis(4-chlorophenyl)-7-phenyl-1H-furo[2,3-*b*]pyrrolo[2,3-*d*]pyridine (1g):

(i) Sample Preparation: The single crystal of compound **1g** was prepared by the slow evaporation method for which 10 mg of the compound (**1g**) was dissolved in 1 mL dichloromethane. The mouth of the glass vial was covered with a cap having a small hole and kept for slow evaporation at room temperature. Crystals of **1g** were obtained as a transparent white needle-like crystal after around 4 to 5 days.

(ii) Data Collection: Diffraction data were collected at 299 K with MoKα radiation (λ = 0.71073 Ǻ) using a Bruker Nonius SMART APEX CCD diffractometer equipped with a graphite monochromator and Apex CD camera. The SMART software was used for data collection for indexing the reflections and determining the unit cell parameters. Data reduction and cell refinement were performed using SAINT[1,2] software and the space groups of these crystals were determined from systematic absences by XPREP and further justified by the refinement results. The structures were solved by direct methods and refined by full-matrix least-squares calculations using SHELXTL-97[3] software. All the non-H atoms were refined in the anisotropic approximation against F^2 of all reflections.

1. Blessing, R. H. *Acta Crystallogr.* **1995**, *A51*, 33.
2. SMART and SAINT, Siemens Analytical X-ray Instruments Inc., Madison, WI, 1996.
3. Sheldrick, G. M. *Acta Crystallogr.* **2008**, *A64*, 112.

(iii) Crystallographic Description of 2,4-bis(4-chlorophenyl)-7-phenyl-1*H*-furo[2,3-*b*]pyrrolo[2,3-*d*]pyridine (1g):

$C_{27}H_{16}Cl_2N_2O$, crystal dimensions 0.22 x 0.20 x 0.16 mm, M_r = 491.35, Monoclinic, space group P 1 21/n 1, a = 17.1257 (6), b = 7.4375 (2), c = 19.0948 (6) Å, α = 90°, β = 104.3750 (10)°, γ = 90°, V = 2356.00 (13) Å^3, Z = 4, ρ_{calcd} = 1.385 g/cm^3, μ = 0.308 mm^{-1}, $F(000)$= 1016.0, reflection collected / unique = 4104 / 3240, refinement method = full-matrix least-squares on F^2, final R indices [I> 2\s(I)]:R_1 = 0.0359, wR_2 = 0.0918, R indices (all data): R_1 = 0.0523, wR_2 = 0.1098, goodness of fit = 1.007. **CCDC-2350725** for **2,4-bis(4-chlorophenyl)-7-phenyl-1*H*-furo[2,3-*b*]pyrrolo[2,3-*d*]pyridine (1g)** contains the supplementary crystallographic data for this paper. These data can be obtained free of charge from The Cambridge Crystallographic Data Centre via www.ccdc.cam.ac.uk/data_request/cif.

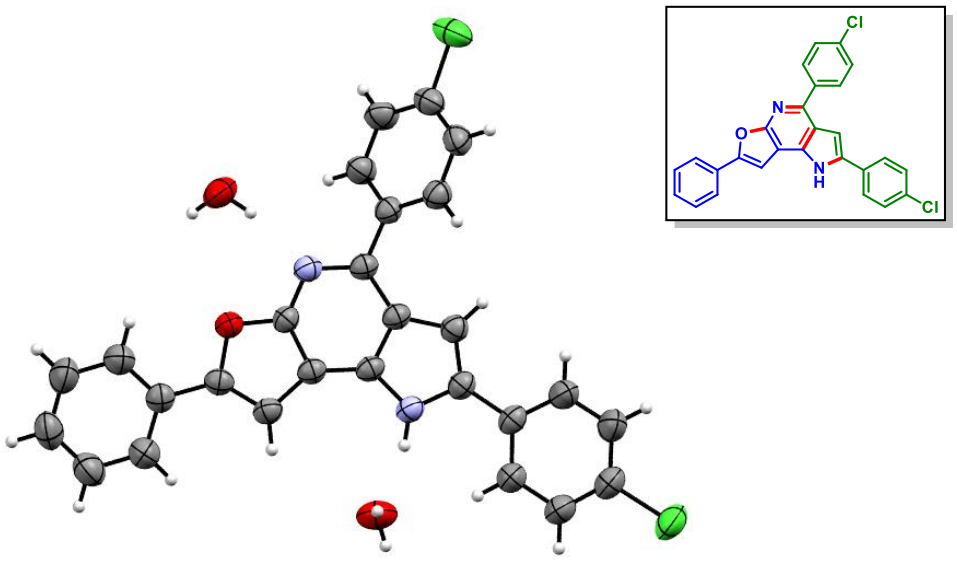

Figure IV.8.5.1.1. *ORTEP diagram of 2,4-bis(4-chlorophenyl)-7-phenyl-1H-furo[2,3-b]pyrrolo[2,3-d]pyridine (**1g**) with 50% ellipsoid probability (CCDC 2350725).*

IV.8.6. DFT Calculation:

(i) To find out the reason behind the regioselectivity, atomic charge distribution calculation (6-31G+(d,p) basis set) on the substrate (**l**) was carried out. From the atomic charge distribution, the Mulliken charges of the C1≡C2 bond were found to have −1.178 and 1.065, and for C3≡C4 are 1.108 and −1.190, respectively (Figure IV.8.6.1). The results confirm that the C1-center (i.e. towards *p*-Me bearing phenyl ring) is comparatively electrophilic as compared to the C4 center (i.e. towards *p*-Cl bearing phenyl ring).

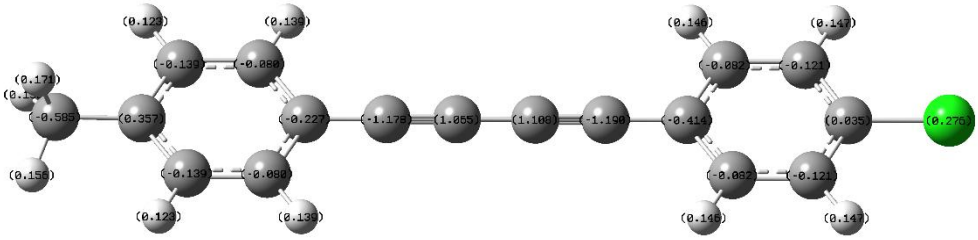

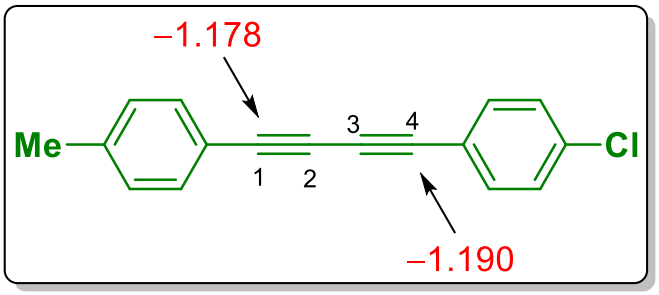

Figure IV.8.6.1. *Mulliken charge distribution of 1-chloro-4-(p-tolylbuta-1,3-diyn-1-yl)benzene* ***(l).***

XYZ Coordinates of Every Atom of 1-Chloro-4-(*p*-tolylbuta-1,3-diyn-1-yl)benzene (l):

Center Number	Atomic Number	Atomic Type	Coordinates (Angstroms) X	Y	Z
1	6	0	-5.927330	1.203179	-0.008200
2	6	0	-4.535323	1.211877	-0.006631
3	6	0	-3.813331	-0.000001	-0.004893
4	6	0	-4.535322	-1.211875	-0.007069
5	6	0	-5.927331	-1.203178	-0.008632
6	6	0	-6.650446	-0.000001	-0.006053
7	1	0	-6.463716	2.148790	-0.013052
8	1	0	-3.993806	2.152398	-0.010134
9	1	0	-3.993809	-2.152398	-0.010914
10	1	0	-6.463713	-2.148790	-0.013827
11	6	0	-2.391315	0.000002	-0.005454
12	6	0	-1.168430	0.000002	-0.004774
13	6	0	0.192061	-0.000003	-0.003776
14	6	0	1.414765	0.000012	-0.002605
15	6	0	2.836486	0.000000	-0.001048
16	6	0	3.556847	-1.213412	0.000036
17	6	0	3.556851	1.213414	-0.000400
18	6	0	4.949131	-1.215933	0.001733

19	1	0	3.015332	-2.153521	-0.000459
20	6	0	4.949134	1.215932	0.001299
21	1	0	3.015336	2.153522	-0.001235
22	6	0	5.635896	-0.000001	0.002361
23	1	0	5.498335	-2.151073	0.002568
24	1	0	5.498342	2.151071	0.001800
25	6	0	-8.160106	-0.000002	0.027292
26	1	0	-8.571381	-0.885982	-0.466059
27	1	0	-8.529409	-0.000272	1.060902
28	1	0	-8.571370	0.886239	-0.465597
29	17	0	7.392143	-0.000003	0.004523

(ii) Usually, a pyridine ring is more electron-deficient than a pyrrole ring. It is expected that in a *p*-Me-Ph, the -Me group should be more deshielded when attached to a pyridine system (as compared to a pyrrole ring system). But in the present case, the central pyridine ring is fused with two electron-rich pyrrole and furan rings. Thus, the central pyridine ring is more electron-rich than the pyrrole ring. Hence the *p*-Me-Ph attached to the pyridyl ring should be more shielded and appear in the upfield in ^{1}H NMR.

To further support our proposition, atomic charge distribution calculation was performed on regioisomers 2-(4-chlorophenyl)-7-phenyl-4-(*p*-tolyl)-1*H*-furo[2,3-*b*]pyrrolo[2,3-*d*]pyridine (**1l**) and 4-(4-chlorophenyl)-7-phenyl-2-(*p*-tolyl)-1*H*-furo[2,3-*b*]pyrrolo[2,3-*d*]pyridine (**1l′**) using the (6-31G+(d,p) basis set). The Mulliken charge on the *p*-Me group of the phenyl ring (i.e. adjacent to the pyridine ring) in compound (**1l**) was found to have –0.554, while for compound (**1l′**), it is –0.545 (Figure IV.8.6.2). This indicates that the *p*-Me group of the phenyl ring towards the pyridine site has a higher electron density and is more shielded (as compared to the pyrrole site) and should appear in the upfield in ^{1}H and ^{13}C NMR. The result also supports the observed regioselectivity in ^{13}C NMR spectra of the compound (**1l**) and (**1l′**), where the *p*-Me group of the phenyl ring towards pyridine appears in the upfield.

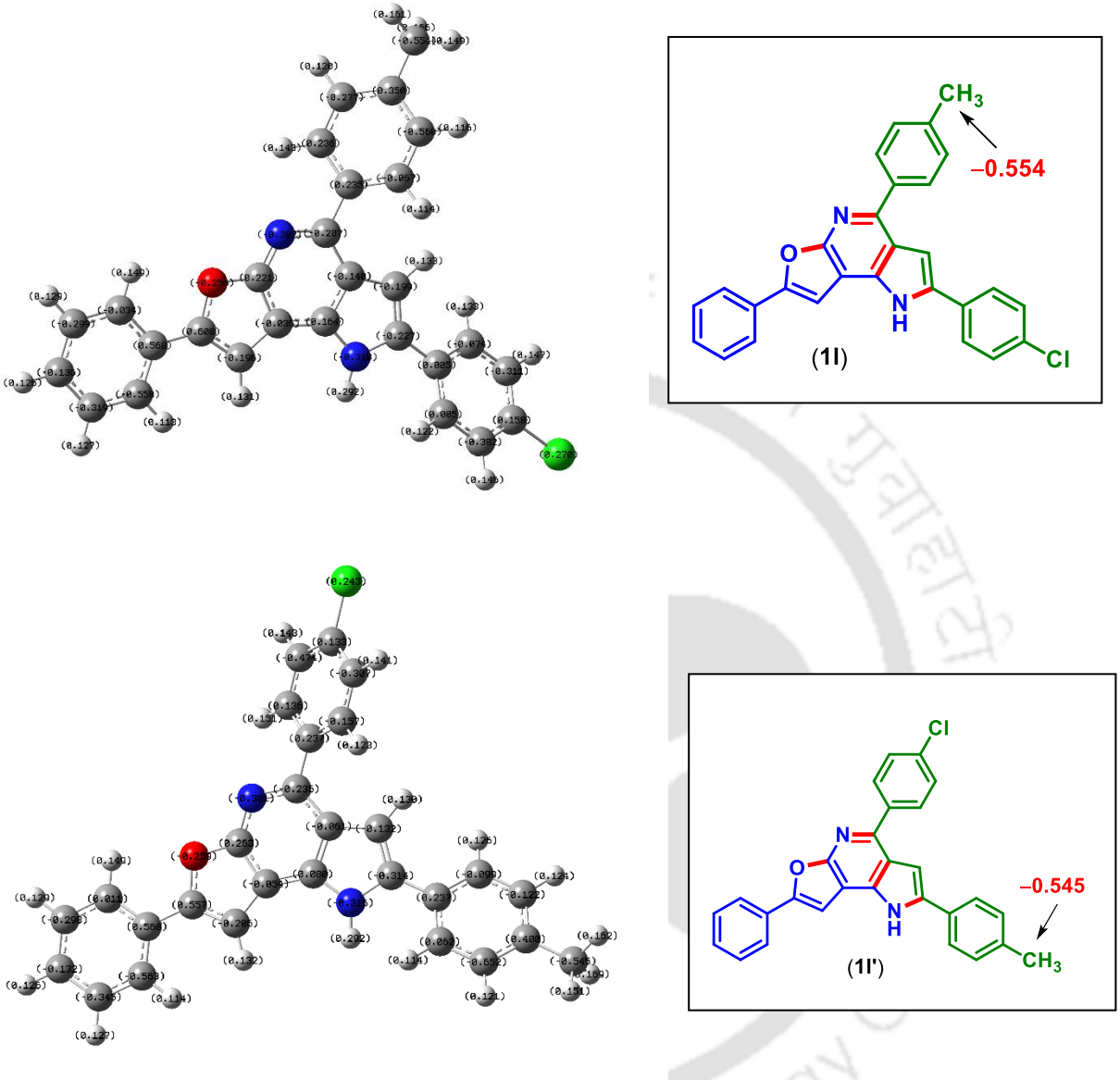

Figure IV.8.6.2. *Mulliken charge distribution of compounds (**1l**) and (**1l'**).*

XYZ Coordinates of Every Atom of 2-(4-chlorophenyl)-7-phenyl-4-(*p*-tolyl)-1*H*-furo[2,3-*b*]pyrrolo[2,3-*d*]pyridine (1l):

Center Number	Atomic Number	Atomic Type	Coordinates (Angstroms) X	Y	Z
1	6	0	1.522408	-0.829592	-0.073335

2	6	0	2.287105	0.348308	-0.016865
3	6	0	-0.357172	0.737139	-0.064589
4	6	0	0.139023	-0.596263	-0.093412
5	6	0	2.455789	-1.915596	-0.071716
6	1	0	2.242267	-2.973940	-0.109597
7	6	0	5.048884	-1.918745	0.013465
8	6	0	5.236863	-3.314371	-0.002495
9	6	0	6.181653	-1.084713	0.058353
10	6	0	6.518854	-3.857716	0.025277
11	1	0	4.377416	-3.976985	-0.035831
12	6	0	7.463061	-1.635196	0.086131
13	1	0	6.049265	-0.008691	0.070373
14	6	0	7.639810	-3.021191	0.069863
15	1	0	6.644401	-4.936534	0.012679
16	1	0	8.326371	-0.976967	0.120443
17	1	0	8.638674	-3.446602	0.091746
18	6	0	3.706070	-1.349852	-0.015441
19	6	0	0.131143	3.246363	-0.054630
20	6	0	0.876986	4.207330	0.652412
21	6	0	-0.989305	3.684967	-0.777942
22	6	0	0.497871	5.546349	0.653783
23	1	0	1.758873	3.885954	1.196282
24	6	0	-1.358400	5.031985	-0.779394
25	1	0	-1.554474	2.981402	-1.380270
26	6	0	-0.630338	5.986528	-0.058182
27	1	0	1.089611	6.265898	1.215253
28	1	0	-2.220969	5.345711	-1.362536

29	6	0	0.564050	1.828355	-0.049379
30	6	0	-1.041998	7.439885	-0.037188
31	1	0	-1.804761	7.649826	-0.792713
32	1	0	-1.456379	7.719951	0.939413
33	1	0	-0.187972	8.099546	-0.226495
34	6	0	-1.789335	0.627363	-0.008018
35	1	0	-2.499807	1.438591	0.021529
36	7	0	-0.934785	-1.448599	-0.101161
37	1	0	-0.877045	-2.446832	0.025637
38	6	0	-3.427442	-1.365551	0.011033
39	6	0	-3.629953	-2.639640	-0.551004
40	6	0	-4.528056	-0.725789	0.611918
41	6	0	-4.879843	-3.257699	-0.513301
42	1	0	-2.814949	-3.148739	-1.057575
43	6	0	-5.783336	-1.327440	0.645700
44	1	0	-4.394524	0.246445	1.075319
45	6	0	-5.951156	-2.595447	0.084969
46	1	0	-5.023256	-4.237441	-0.955674
47	1	0	-6.622004	-0.824923	1.115082
48	6	0	-2.117859	-0.711290	-0.022060
49	17	0	-7.529763	-3.365340	0.135203
50	7	0	1.888946	1.608962	-0.005705
51	8	0	3.617981	0.025212	0.017852

XYZ Coordinates of Every Atom of 4-(4-chlorophenyl)-7-phenyl-2-(*p*-tolyl)-1*H*-furo[2,3-*b*]pyrrolo[2,3-*d*]pyridine (1l′):

Center	Atomic	Atomic	Coordinates (Angstroms)		
Number	Number	Type	X	Y	Z

1	6	0	-1.562576	0.833931	-0.061378
2	6	0	-1.992802	-0.503279	-0.004870
3	6	0	0.663990	-0.182200	-0.045924
4	6	0	-0.167060	0.973469	-0.076798
5	6	0	-2.747700	1.637262	-0.065942
6	1	0	-2.817806	2.714566	-0.104272
7	6	0	-5.251273	0.963330	0.008120
8	6	0	-5.795709	2.261586	-0.030290
9	6	0	-6.127912	-0.136098	0.066574
10	6	0	-7.174931	2.453032	-0.010843
11	1	0	-5.137906	3.124132	-0.075889
12	6	0	-7.508502	0.062378	0.085685
13	1	0	-5.720121	-1.140282	0.096034
14	6	0	-8.039617	1.354278	0.047230
15	1	0	-7.576863	3.461620	-0.041341
16	1	0	-8.171088	-0.797089	0.130564
17	1	0	-9.114864	1.505306	0.061992
18	6	0	-3.806431	0.763923	-0.012969
19	6	0	0.845312	-2.732607	-0.040271
20	6	0	0.361231	-3.860154	0.646825
21	6	0	2.051996	-2.855262	-0.749727
22	6	0	1.066069	-5.061655	0.649632
23	1	0	-0.580270	-3.783080	1.179451
24	6	0	2.764462	-4.055408	-0.762859
25	1	0	2.424850	-2.020822	-1.333408
26	6	0	2.268297	-5.148877	-0.054656

27	1	0	0.688592	-5.922341	1.191084
28	1	0	3.687231	-4.143357	-1.326039
29	6	0	0.059664	-1.474638	-0.031700
30	6	0	2.016944	0.303103	0.009795
31	1	0	2.918688	-0.287893	0.043245
32	7	0	0.643967	2.077929	-0.083020
33	1	0	0.326546	3.027652	0.031552
34	6	0	3.067191	2.662560	0.028587
35	6	0	2.926102	3.940137	-0.540022
36	6	0	4.298079	2.345588	0.633946
37	6	0	3.972375	4.863307	-0.499439
38	1	0	2.007090	4.210006	-1.053662
39	6	0	5.339473	3.268189	0.660936
40	1	0	4.429773	1.373718	1.099715
41	6	0	5.198059	4.548764	0.100816
42	1	0	3.834865	5.840700	-0.955164
43	1	0	6.278162	2.993797	1.136441
44	6	0	1.979706	1.681085	-0.005347
45	7	0	-1.276665	-1.613735	0.009397
46	8	0	-3.362394	-0.540124	0.024717
47	17	0	3.164745	-6.663285	-0.056960
48	6	0	6.325660	5.551755	0.163392
49	1	0	6.441415	5.953919	1.177614
50	1	0	7.281878	5.095623	-0.114732
51	1	0	6.146619	6.396316	-0.508254

(iii) From the atomic charge distribution of diyne containing electron-donating *p*-Me and electron-withdrawing *p*-CF_3 (**m**), the Mulliken charges of the C1≡C2 bond were found to have –1.198 and 1.083, and for C3≡C4 are 1.117 and –1.246, respectively (Figure IV.8.6.3). The results confirm that the C1-center (i.e. towards *p*-Me bearing phenyl ring) is more electrophilic as compared to the C4 center (i.e. towards *p*-CF_3 bearing phenyl ring).

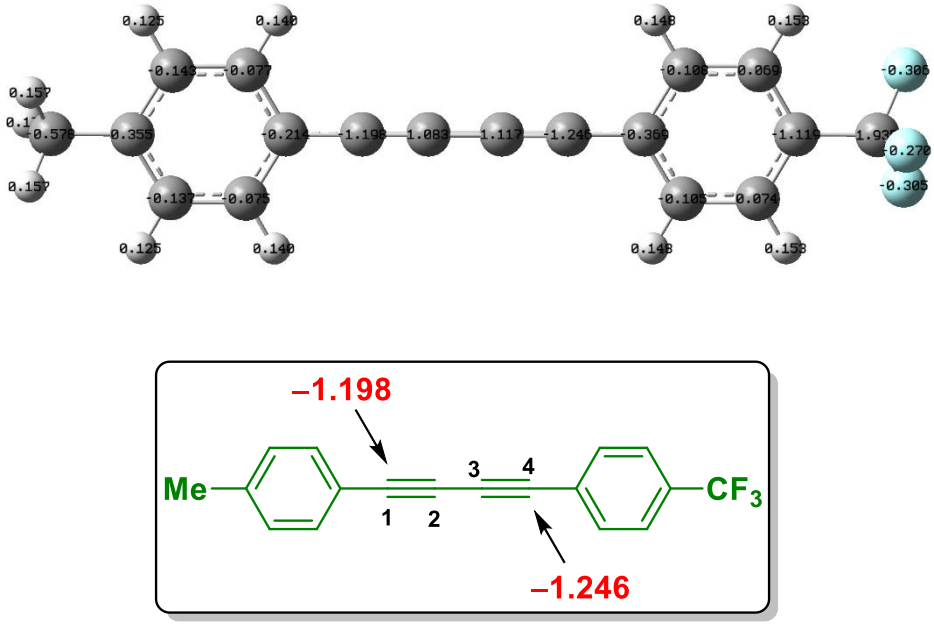

Figure IV.8.6.3. *Mulliken charge distribution of 1-methyl-4-((4-(trifluoromethyl)phenyl)buta-1,3-diyn-1-yl)benzene (**m**).*

XYZ Coordinates of Every Atom of 1-Methyl-4-((4-(trifluoromethyl)phenyl)buta-1,3-diyn-1-yl)benzene (m):

Center Number	Atomic Number	Atomic Type	Coordinates (Angstroms) X	Y	Z
1	6	0	6.775297	1.203685	0.015263
2	6	0	5.383464	1.212296	0.008890
3	6	0	4.662300	-0.000073	0.004175
4	6	0	5.383734	-1.212264	0.007956
5	6	0	6.775597	-1.203331	0.014322

6	6	0	7.498293	0.000248	0.015028
7	1	0	7.311599	2.149239	0.022492
8	1	0	4.841647	2.152612	0.011018
9	1	0	4.842125	-2.152700	0.009366
10	1	0	7.312139	-2.148745	0.020794
11	6	0	9.007890	0.000583	-0.011823
12	1	0	9.417064	-0.888504	0.477481
13	1	0	9.381287	0.007056	-1.043912
14	1	0	9.416853	0.883749	0.488341
15	6	0	3.240617	-0.000266	0.000394
16	6	0	2.017756	-0.000385	-0.003856
17	6	0	0.657764	-0.000523	-0.008733
18	6	0	-1.986346	-0.000605	-0.018125
19	6	0	-2.704579	-1.215573	-0.021872
20	6	0	-2.704544	1.214488	-0.022834
21	6	0	-4.095533	-1.213335	-0.029260
22	1	0	-2.160899	-2.154108	-0.021314
23	6	0	-4.095396	1.212268	-0.030255
24	1	0	-2.160767	2.152965	-0.023013
25	6	0	-4.794337	-0.000558	-0.035465
26	1	0	-4.638028	-2.152480	-0.036645
27	1	0	-4.637877	2.151451	-0.038433
28	6	0	-0.564814	-0.000590	-0.012856
29	6	0	-6.298404	0.000239	0.008161
30	9	0	-6.830518	1.087124	-0.604575
31	9	0	-6.831561	-1.095657	-0.587050
32	9	0	-6.768776	0.010937	1.287085

(iv) From the atomic charge distribution (6-31G+(d,p) basis set) of 7-Phenyl-2,4-di-*p*-tolyl-1*H*-furo[2,3-*b*]pyrrolo[2,3-*d*]pyridine (**1b**), it was found that the C-center of *p*-Me group of phenyl ring (i.e. towards the pyridine site) having charge –0.570 and the C-center of *p*-Me group of phenyl ring

(i.e. towards the pyrrole site) was found to have –0.533 (Figure IV.8.6.4). The results indicate that the *p*-Me group of phenyl ring (i.e. towards the pyridine site) is more electron-rich as compared to the *p*-Me group of phenyl ring (i.e. towards the pyrrole site).

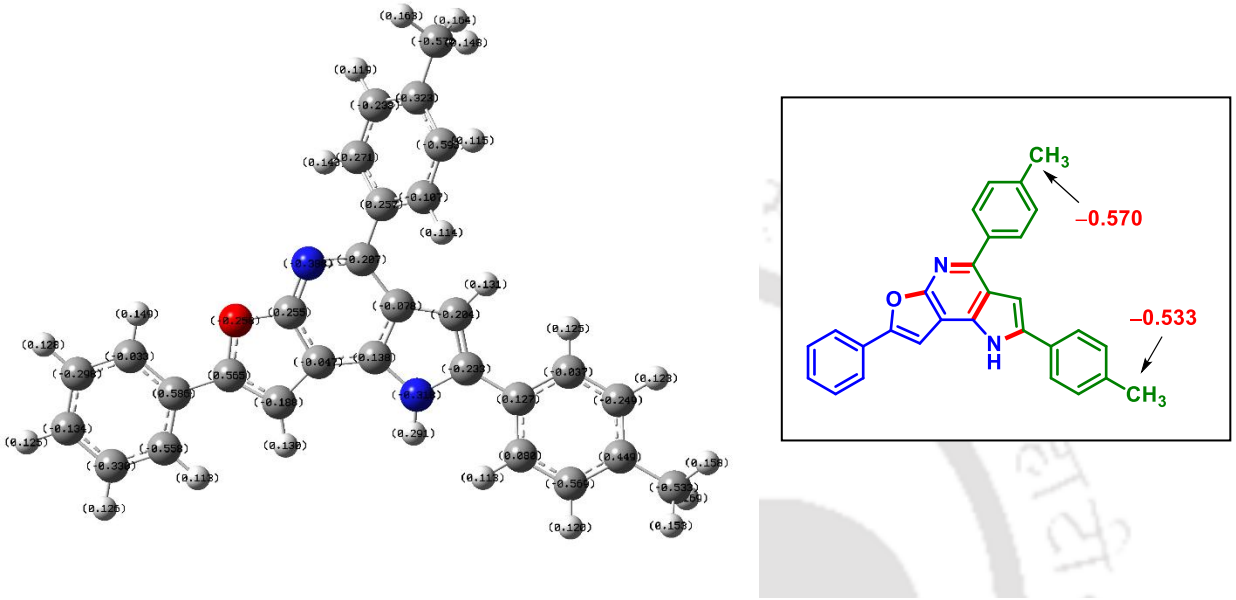

Figure IV.8.6.4. *Mulliken charge distribution of 7-phenyl-2,4-di-p-tolyl-1H-furo[2,3-b]pyrrolo[2,3-d]pyridine (**1b**).*

XYZ Coordinates of Every Atom of 7-Phenyl-2,4-di-*p*-tolyl-1*H*-furo[2,3-*b*]pyrrolo[2,3-*d*]pyridine (1b)

Center Number	Atomic Number	Atomic Type	Coordinates (Angstroms) X	Y	Z
1	6	0	1.365897	-0.761585	-0.056785
2	6	0	1.954594	0.513888	-0.010148
3	6	0	-0.719794	0.518392	-0.048947
4	6	0	-0.036611	-0.729933	-0.072267
5	6	0	2.445101	-1.702792	-0.056102
6	1	0	2.384356	-2.780976	-0.087766
7	6	0	5.012297	-1.335470	0.010437

8	6	0	5.397862	-2.690023	-0.005580
9	6	0	6.014745	-0.348166	0.046063
10	6	0	6.744609	-3.044217	0.012771
11	1	0	4.641843	-3.468837	-0.032060
12	6	0	7.361939	-0.709460	0.064375
13	1	0	5.729440	0.697751	0.058181
14	6	0	7.734897	-2.056025	0.047833
15	1	0	7.023191	-4.094034	-0.000048
16	1	0	8.122465	0.065556	0.091341
17	1	0	8.784444	-2.334448	0.062012
18	6	0	3.601989	-0.964077	-0.010263
19	6	0	-0.594086	3.072184	-0.053130
20	6	0	0.018527	4.137462	0.632766
21	6	0	-1.777337	3.339631	-0.759428
22	6	0	-0.547621	5.408496	0.630397
23	1	0	0.945378	3.950357	1.164394
24	6	0	-2.335554	4.620243	-0.764144
25	1	0	-2.247366	2.556031	-1.344231
26	6	0	-1.739034	5.676274	-0.064635
27	1	0	-0.055850	6.210502	1.176626
28	1	0	-3.244830	4.800858	-1.332565
29	6	0	0.035951	1.729861	-0.042113
30	6	0	-2.121768	0.202669	0.007400
31	1	0	-2.942321	0.902227	0.033750
32	7	0	-0.976443	-1.727322	-0.073628

33	1	0	-0.777150	-2.707646	0.048321
34	6	0	-3.453717	-2.010067	0.031718
35	6	0	-3.464311	-3.303570	-0.519677
36	6	0	-4.644079	-1.537046	0.615142
37	6	0	-4.616024	-4.090616	-0.483208
38	1	0	-2.579758	-3.691037	-1.018328
39	6	0	-5.791776	-2.324556	0.637509
40	1	0	-4.662001	-0.549683	1.066337
41	6	0	-5.801865	-3.620110	0.095701
42	1	0	-4.593987	-5.083117	-0.926619
43	1	0	-6.696073	-1.929865	1.094632
44	6	0	-2.254184	-1.169509	-0.000926
45	7	0	1.379506	1.703856	-0.003179
46	8	0	3.319011	0.384500	0.018090
47	6	0	-7.041242	-4.481392	0.158128
48	1	0	-7.131353	-4.974414	1.134523
49	1	0	-7.948885	-3.887398	0.009716
50	1	0	-7.021184	-5.265557	-0.604572
51	6	0	-2.347342	7.059121	-0.053222
52	1	0	-3.214880	7.119507	-0.716830
53	1	0	-2.678200	7.338977	0.954455
54	1	0	-1.623204	7.815867	-0.376326

IV.9. Spectral Data:

2,4,7-Triphenyl-1H-furo[2,3-b]pyrrolo[2,3-d]pyridine (1a):

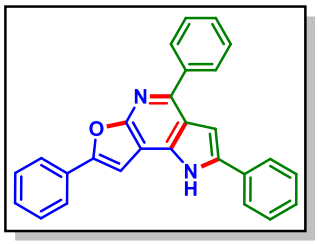

As a brown solid (56 mg, 73% yield, mp 149–151 °C); Purification over a column of silica gel (10% EtOAc in hexane); ^{1}H NMR ($CDCl_3$, 500 MHz): δ 9.37 (s, 1H), 8.09 (d, 2H, J = 7.5 Hz), 7.85 (d, 2H, J = 7.5 Hz), 7.71 (d, 2H, J = 7.5 Hz), 7.54 (t, 2H, J = 7.5 Hz), 7.44 (t, 2H, J = 7.75 Hz), 7.40 (t, 2H, J = 7.5 Hz), 7.35–7.30 (m, 3H), 7.19 (s, 1H), 7.13 (s, 1H); ^{13}C{^{1}H} NMR ($CDCl_3$, 125 MHz): δ 159.3, 153.6, 147.1, 140.1, 138.2, 135.9, 131.8, 130.3, 129.3, 129.2, 128.9, 128.7, 128.67, 128.64, 128.2, 125.3, 124.8, 121.0, 104.7, 101.0, 97.5; IR (neat, cm^{-1}): 3337, 3025, 2923, 2850, 1601, 1492, 1344, 1265, 1116, 754, 697; HRMS (ESI/Q-TOF) (m/z) calcd for $C_{27}H_{19}N_2O$ $[M + H]^+$ 387.1492; found 387.1505.

2,4-Biphenyl-7-(p-tolyl)-1H-furo[2,3-b]pyrrolo[2,3-d]pyridine (2a):

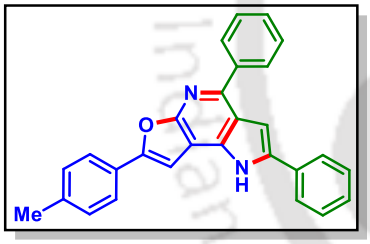

As a brown solid (54 mg, 68% yield, mp 142–144 °C); Purification over a column of silica gel (10% EtOAc in hexane); ^{1}H NMR ($CDCl_3$, 500 MHz): δ 9.37 (s, 1H), 8.08 (d, 2H, J = 7.5 Hz), 7.71 (t, 4H, J = 6.5 Hz), 7.53 (t, 2H, J = 7.5 Hz), 7.46–7.41 (m, 3H), 7.33 (t, 1H, J = 7.5 Hz), 7.20–7.18 (m, 3H), 7.05 (s, 1H), 2.36 (s, 3H); ^{13}C{1H} NMR ($CDCl_3$, 125 MHz): δ 159.1, 153.9, 146.7, 140.1, 138.7, 138.2, 135.9, 131.8, 129.6, 129.3, 129.2, 128.7, 128.5, 128.2, 127.6, 125.3, 124.8, 121.0, 104.8, 101.0, 96.7, 21.5; IR (neat, cm^{-1}): 3345, 3058, 2923, 2854, 1599, 1500, 1452, 1345, 1177, 756, 699; HRMS (ESI/Q-TOF) (m/z) calcd for $C_{28}H_{21}N_2O$ $[M + H]^+$ 401.1648; found 401.1655.

2,4-Diphenyl-7-(m-tolyl)-1H-furo[2,3-b]pyrrolo[2,3-d]pyridine (3a):

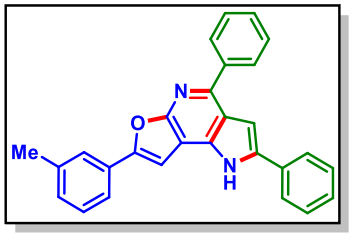

As a brown solid (52 mg, 65% yield, mp 148–150 °C); Purification over a column of silica gel (10% EtOAc in hexane); ^{1}H NMR ($CDCl_3$, 500 MHz): δ 9.79 (s, 1H), 8.09 (d, 2H, J = 7.5 Hz), 7.69 (d, 2H, J = 7.5 Hz), 7.62 (s, 1H), 7.53 (q, 3H, J = 7.3 Hz), 7.44 (t, 1H, J

= 7.5 Hz), 7.38 (t, 2H, *J* = 7.5 Hz), 7.28 (t, 1H, *J* = 7.25 Hz), 7.22 (t, 1H, *J* = 7.75 Hz), 7.16 (s, 1H), 7.08 (d, 1H. *J* = 7.5 Hz), 7.03 (s, 1H), 2.32 (s, 3H); $^{13}C\{^{1}H\}$ NMR ($CDCl_3$, 125 MHz): δ 159.1, 153.6, 146.8, 140.1, 138.5, 138.3, 136.0, 131.8, 130.2, 129.3, 129.1, 128.8, 128.7, 128.5, 128.0, 125.4, 125.3, 121.9, 121.0, 104.8, 100.8, 97.6, 21.6; IR (neat, cm^{-1}): 3337, 3057, 2923, 1601, 1492, 1264, 1028, 734, 700; HRMS (ESI/Q-TOF) (m/z) calcd for $C_{28}H_{21}N_2O$ $[M + H]^+$ 401.1648; found 401.1660.

2,4-Diphenyl-7-(o-tolyl)-1H-furo[2,3-b]pyrrolo[2,3-d]pyridine (4a):

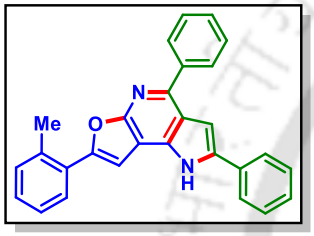

As a brown solid (43 mg, 54% yield, mp 138–140 °C); Purification over a column of silica gel (10% EtOAc in hexane); ^{1}H NMR ($CDCl_3$, 400 MHz): δ 9.49 (s, 1H), 8.09 (d, 2H, *J* = 7.6 Hz), 7.92 (d, 1H, *J* = 7.2 Hz), 7.72 (d, 2H, *J* = 8.0 Hz), 7.54 (t, 2H, *J* = 7.6 Hz), 7.47–7.41 (m, 5H), 7.33 (t, 2H, *J* = 7.4 Hz), 7.21 (s, 1H), 7.04 (s, 1H), 2.57 (s, 3H); $^{13}C\{^{1}H\}$ NMR ($CDCl_3$, 100 MHz): δ 158.9, 153.4, 147.2, 140.1, 138.1, 135.9, 135.6, 131.8, 131.5, 129.7, 129.3, 129.2, 128.7, 128.6, 128.5, 128.3, 128.2, 126.3, 125.3, 120.9, 104.6, 101.4, 101.0, 22.3; IR (neat, cm^{-1}): 3334, 2928, 2859, 1602, 1456, 1334, 1262, 1056, 731; HRMS (ESI/Q-TOF) (m/z) calcd for $C_{28}H_{21}N_2O$ $[M + H]^+$ 401.1648; found 401.1656.

7-(4-Isopropylphenyl)-2,4-diphenyl-1H-furo[2,3-b]pyrrolo[2,3-d]pyridine (5a):

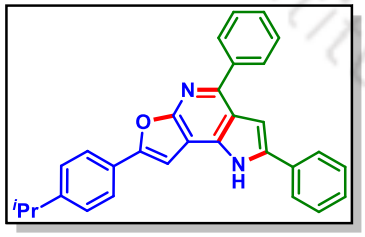

As a brown solid (56 mg, 66% yield, mp 145–147 °C); Purification over a column of silica gel (10% EtOAc in hexane); ^{1}H NMR ($CDCl_3$, 500 MHz): δ 9.29 (s, 1H), 8.01 (d, 2H, *J* = 7.5 Hz), 7.79 (d, 2H, *J* = 8.0 Hz), 7.72 (d, 2H, *J* = 8.0 Hz), 7.54 (t, 2H, *J* = 7.5 Hz), 7.44 (t, 2H, *J* = 7.75 Hz), 7.34 (t, 2H, *J* = 7.5 Hz), 7.28 (d, 2H, *J* = 8.0 Hz), 7.21 (s, 1H), 7.07 (s, 1H), 2.96–2.90 (m, 1H), 1.28 (s, 3H), 1.27 (s, 3H); $^{13}C\{1H\}$ NMR ($CDCl_3$, 125 MHz): δ 159.3, 154.0, 149.7, 146.8, 140.2, 138.2, 135.9, 131.9, 129.3, 129.2, 128.7, 128.5, 128.2, 128.0, 127.1, 125.3, 125.0, 121.0, 104.8, 101.1, 96.7, 34.2, 24.0; IR (neat, cm^{-1}): 3342, 3058, 2959, 2925, 1600, 1493, 1344,

1264, 1177, 735, 700; HRMS (ESI/Q-TOF) (m/z) calcd for $C_{30}H_{25}N_2O$ $[M + H]^+$ 429.1961; found 429.1964.

7-(4-(Tert-butyl)phenyl)-2,4-diphenyl-1H-furo[2,3-b]pyrrolo[2,3-d]pyridine (6a):

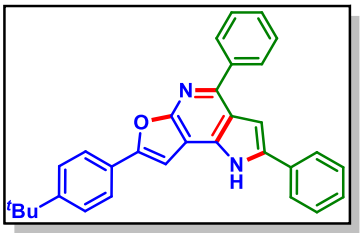

As a brown solid (56 mg, 63% yield, mp 180–182 °C); Purification over a column of silica gel (10% EtOAc in hexane); ^{1}H NMR ($CDCl_3$, 500 MHz): δ 9.26 (s, 1H), 8.01 (d, 2H, J = 7.5 Hz), 7.80 (d, 2H, J = 7.5 Hz), 7.72 (d, 2H, J = 7.5 Hz), 7.54 (t, 2H, J = 7.5 Hz), 7.45 (t, 4H, J = 7.75 Hz), 7.34 (t, 2H, J = 7.25 Hz), 7.21 (d, 1H, J = 2.0 Hz), 7.06 (s, 1H), 1.34 (s, 9H); ^{13}C{1H} NMR ($CDCl_3$, 125 MHz): δ 159.3, 153.9, 152.0, 146.9, 140.1, 138.1, 135.9, 131.9, 129.3, 129.2, 128.7, 128.5, 128.2, 127.6, 125.9, 125.3, 124.7, 121.0, 104.8, 101.1, 96.8, 34.9, 31.4; IR (neat, cm^{-1}): 3314, 3026, 2924, 1601, 1493, 1344, 1264, 1113, 733, 700; HRMS (ESI/Q-TOF) (m/z) calcd for $C_{31}H_{27}N_2O$ $[M + H]^+$ 443.2118; found 443.2115.

7-(3-Methoxyphenyl)-2,4-diphenyl-1H-furo[2,3-b]pyrrolo[2,3-d]pyridine (7a):

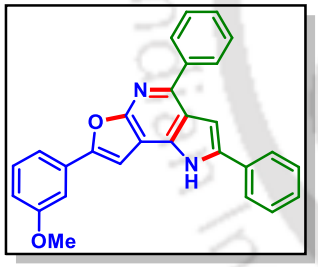

As a brown solid (49 mg, 59% yield, mp 148–150 °C); Purification over a column of silica gel (10% EtOAc in hexane); ^{1}H NMR ($CDCl_3$, 500 MHz): δ 9.51 (s, 1H), 8.08 (d, 2H, J = 7.0 Hz), 7.71 (d, 2H, J = 7.5 Hz), 7.53 (t, 2H, J = 7.5 Hz), 7.46–7.40 (m, 4H), 7.38 (d, 1H, J = 7.5 Hz), 7.33 (t, 1H, J = 7.5 Hz), 7.28 (d, 1H, J = 8.0 Hz), 7.19 (d, 1H, J = 2.0 Hz), 7.08 (s, 1H), 6.85 (dd, 1H, J_1 = 8.5 Hz, J_2 = 2.5 Hz) 3.80 (s, 3H); ^{13}C{1H} NMR ($CDCl_3$, 125 MHz): δ 160.1, 159.2, 153.4, 147.2, 140.1, 138.3, 135.9, 131.8, 131.6, 129.9, 129.3, 129.2, 128.7, 128.6, 128.2, 125.4, 121.1, 117.3, 115.0, 109.7, 104.7, 101.0, 97.8, 55.5; IR (neat, cm^{-1}): 3340, 3057, 2925, 2852, 1602, 1489, 1344, 1264, 1030, 733, 701; HRMS (ESI/Q-TOF) (m/z) calcd for $C_{28}H_{21}N_2O_2$ $[M + H]^+$ 417.1598; found 417.1604.

7-(4-Fluorophenyl)-2,4-diphenyl-1H-furo[2,3-b]pyrrolo[2,3-d]pyridine (8a):

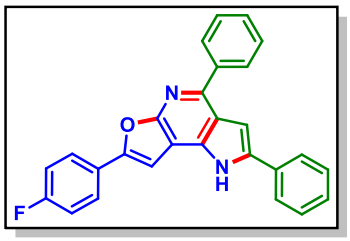

As a brown solid (52 mg, 64% yield, mp 170–172 °C); Purification over a column of silica gel (10% EtOAc in hexane); ^{1}H NMR ($CDCl_3$, 500 MHz): δ 9.43 (s, 1H), 8.08 (d, 2H, J = 7.5 Hz), 7.78–7.75 (m, 2H), 7.71 (d, 2H, J = 8.0 Hz), 7.53 (t, 2H, J = 7.25 Hz), 7.46–7.42 (m, 3H), 7.34 (t, 1H, J = 7.25 Hz), 7.18 (s, 1H), 7.06 (t, 2H, J = 8.25 Hz), 7.00 (s, 1H); ^{13}C{^{1}H} NMR ($CDCl_3$, 125 MHz): δ 163.0 (d, J = 247.5 Hz), 159.2, 152.7, 147.1, 140.0, 138.3, 135.9, 131.8, 129.3, 129.1, 128.8, 128.7, 128.3, 126.7, 126.6 (d, J = 8.0 Hz), 125.4, 121.1, 116.0 (d, J = 22 Hz), 104.7, 101.0, 97.2; ^{19}F NMR ($CDCl_3$, 471 MHz): δ –112.2 (s); IR (neat, cm^{-1}): 3345, 3026, 2923, 2851, 1600, 1497, 1344, 1264, 1116, 736, 698; HRMS (ESI/Q-TOF) (m/z) calcd for $C_{27}H_{18}FN_2O$ $[M + H]^+$ 405.1398; found 405.1391.

7-(4-Chlorophenyl)-2,4-diphenyl-1H-furo[2,3-b]pyrrolo[2,3-d]pyridine (9a):

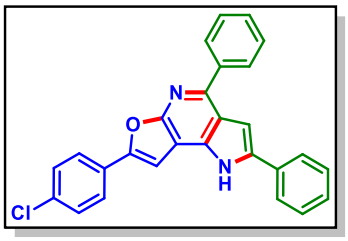

As a brown solid (60 mg, 71% yield, mp 155–157 °C); Purification over a column of silica gel (10% EtOAc in hexane); ^{1}H NMR ($CDCl_3$, 600 MHz): δ 10.0 (s, 1H), 8.08 (d, 2H, J = 7.8 Hz), 7.69 (d, 2H, J = 7.8 Hz), 7.52 (t, 3H, J = 7.8 Hz), 7.44 (t, 1H, J = 7.5 Hz), 7.38 (t, 2H, J = 7.5 Hz), 7.30 (t, 2H, J = 7.5 Hz), 7.21 (d, 2H, J = 8.4 Hz), 7.15 (s, 1H), 6.88 (s, 1H); ^{13}C{^{1}H} NMR ($CDCl_3$, 150 MHz): δ 159.1, 152.1, 147.1, 139.9, 138.5, 135.9, 134.1, 131.7, 129.2, 129.1, 129.0, 128.8, 128.7, 128.6, 128.1, 125.8, 125.3, 121.0, 104.7, 100.7, 98.1; IR (neat, cm^{-1}): 3342, 3059, 2924, 2849, 1600, 1484, 1342, 1263, 1092, 755, 699; HRMS (ESI/Q-TOF) (m/z) calcd for $C_{27}H_{18}ClN_2O$ $[M + H]^+$ 421.1102; found 421.1106.

7-(4-Bromophenyl)-2,4-diphenyl-1H-furo[2,3-b]pyrrolo[2,3-d]pyridine (10a):

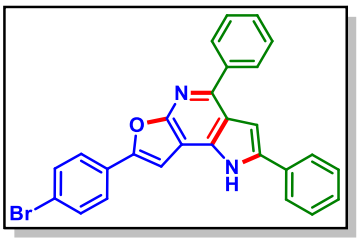

As a brown solid (58 mg, 62% yield, mp 158–160 °C); Purification over a column of silica gel (10% EtOAc in hexane); ^{1}H NMR ($CDCl_3$, 500 MHz): δ 9.48 (s, 1H), 8.06 (d, 2H, J = 7.5 Hz), 7.69 (d, 2H, J = 7.5 Hz), 7.59 (d, 2H, J = 8.0 Hz), 7.53 (t, 2H, J = 7.25 Hz), 7.46–7.42 (m, 5H), 7.34 (t, 1H, J = 7.5 Hz), 7.16 (s, 1H), 7.00 (s,

1H); $^{13}C\{^{1}H\}$ NMR ($CDCl_3$, 125 MHz): δ 159.2, 152.4, 147.4, 139.9, 138.4, 135.9, 132.1, 131.7, 129.3, 129.1, 128.8, 128.7, 128.3, 126.1, 125.4, 122.5, 121.1, 104.6, 101.0, 98.0; IR (neat, cm^{-1}): 3314, 3057, 2924, 2852, 1642, 1482, 1343, 1264, 1072, 733, 700; HRMS (ESI/Q-TOF) (m/z) calcd for $C_{27}H_{18}BrN_2O$ $[M + H]^+$ 465.0597; found 465.0606.

7-(2-Bromophenyl)-2,4-diphenyl-1H-furo[2,3-b]pyrrolo[2,3-d]pyridine (11a):

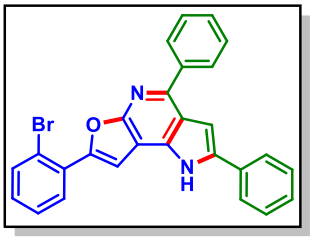

As a brown solid (59 mg, 63% yield, mp 150–152 °C); Purification over a column of silica gel (10% EtOAc in hexane); ^1H NMR ($CDCl_3$, 500 MHz): δ 9.87 (s, 1H), 8.09 (d, 2H, J = 7.5 Hz), 8.01 (d, 1H, J = 8.0 Hz), 7.74 (s, 1H), 7.71 (d, 2H, J = 8.0 Hz), 7.60 (d, 1H, J = 8.5 Hz), 7.53 (t, 2H, J = 7.5 Hz), 7.45 (t, 1H, J = 7.5 Hz), 7.40 (t, 2H, J = 7.5 Hz), 7.34–7.29 (m, 2H), 7.20 (s, 1H), 7.11 (t, 1H, J = 7.5 Hz); $^{13}C\{^{1}H\}$ NMR ($CDCl_3$, 125 MHz): δ 158.7, 150.6, 147.9, 140.0, 138.4, 136.2, 134.4, 131.8, 130.5, 129.9, 129.3, 129.2, 128.8, 128.7, 128.1, 127.7, 125.4, 121.1, 120.1, 104.4, 103.7, 100.9; IR (neat, cm^{-1}): 3355, 3026, 2923, 2852, 1601, 1452, 1343, 1262, 1027, 753, 698; HRMS (ESI/Q-TOF) (m/z) calcd for $C_{27}H_{18}BrN_2O$ $[M + H]^+$ 465.0597; found 465.0616.

2,4-Diphenyl-7-(4-(trifluoromethyl)phenyl)-1H-furo[2,3-b]pyrrolo[2,3-d]pyridine (12a):

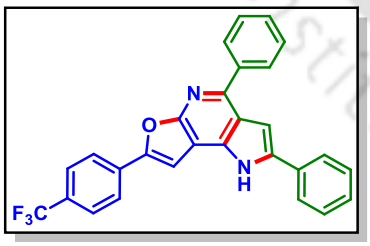

As a brown solid (52 mg, 57% yield, mp 143–145 °C); Purification over a column of silica gel (10% EtOAc in hexane); ^1H NMR ($CDCl_3$, 500 MHz): δ 9.86 (s, 1H), 8.06 (d, 2H, J = 7.5 Hz), 7.73 (d, 2H, J = 8.0 Hz), 7.67 (t, 2H, J = 7.5 Hz), 7.54–7.50 (m, 3H), 7.46 (d, 2H, J = 7.5 Hz), 7.38 (t, 2H, J = 7.5 Hz), 7.31 (d, 1H, J = 7.5 Hz), 7.13 (s, 1H), , 7.05 (s, 1H); $^{13}C\{1H\}$ NMR ($CDCl_3$, 125 MHz): δ 159.3, 151.5, 147.8, 139.8, 138.5, 136.0, 133.4, 131.6, 129.2, 129.1, 128.8, 128.7, 128.2, 125.8 (q, J = 3.5 Hz), 125.3, 124.6, 121.0, 104.5, 100.9, 99.7; ^{19}F NMR ($CDCl_3$, 471 MHz): δ –62.5 (s); IR (neat, cm^{-1}): 3350, 3059, 2925, 2852, 1615, 1492, 1322, 1122, 1069, 756,

700; HRMS (ESI/Q-TOF) (m/z) calcd for $C_{28}H_{18}F_3N_2O$ $[M + H]^+$ 455.1366; found 455.1366.

2,4-Diphenyl-7-(3-(trifluoromethyl)phenyl)-1H-furo[2,3-b]pyrrolo[2,3-d]pyridine (13a):

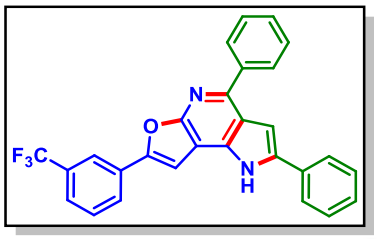

As a brown solid (50 mg, 55% yield, mp 136–138 °C); Purification over a column of silica gel (10% EtOAc in hexane); ^{1}H NMR ($CDCl_3$, 500 MHz): δ 9.65 (s, 1H), 8.07 (d, 2H, J = 7.5 Hz), 8.03 (s, 1H), 7.87 (d, 1H, J = 8.0 Hz), 7.68 (d, 2H, J = 8.0 Hz), 7.54–7.50 (m, 3H), 7.46–7.39 (m, 4H), 7.32 (t, 1H, J = 7.5 Hz), 7.16 (s, 1H), 7.10 (s, 1H); ^{13}C{1H} NMR ($CDCl_3$, 125 MHz): δ 159.2, 151.7, 147.7, 139.8, 138.5, 136.0, 131.6, 131.0, 129.4, 129.3, 129.2, 128.83, 128.80, 128.3, 127.7, 125.4, 124.9 (q, J = 3.87 Hz), 121.5 (q, J = 4.3 Hz), 121.1, 104.5, 101.0, 98.9; ^{19}F NMR ($CDCl_3$, 471 MHz): δ –62.8 (s); IR (neat, cm^{-1}): 3340, 3059, 2925, 2854, 1597, 1453, 1334, 1264, 1123, 1074, 755, 695; HRMS (ESI/Q-TOF) (m/z) calcd for $C_{28}H_{18}F_3N_2O$ $[M + H]^+$ 455.1366; found 455.1368.

7-(Naphthalen-2-yl)-2,4-diphenyl-1H-furo[2,3-b]pyrrolo[2,3-d]pyridine (14a):

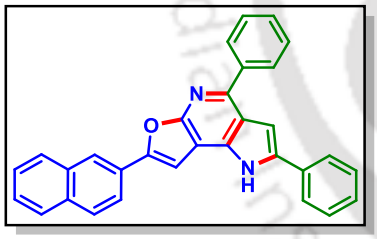

As a brown solid (59 mg, 68% yield, mp 168–170 °C); Purification over a column of silica gel (10% EtOAc in hexane); ^{1}H NMR ($CDCl_3$, 600 MHz): δ 9.52 (s, 1H), 8.32 (s, 1H), 8.09 (d, 2H, J = 7.8 Hz), 7.80–7.78 (m, 2H), 7.75 (d, 2H, J = 7.8 Hz), 7.70 (d, 2H, J = 7.8 Hz), 7.55 (t, 2H, J = 7.5 Hz), 7.47–7.43 (m, 3H), 7.41 (d, 2H, J = 7.2 Hz), 7.32 (t, 2H, J = 7.2 Hz), 7.17 (s, 1H); ^{13}C{1H} NMR ($CDCl_3$, 150 MHz): δ 159.3, 153.5, 147.0, 140.0, 138.2, 135.9, 133.5, 133.3, 131.8, 129.3, 129.2, 128.7, 128.65, 128.64, 128.5, 128.2, 127.8, 127.4, 126.7, 126.5, 125.3, 123.9, 122.4, 121.0, 104.8, 100.9, 98.2; IR (neat, cm^{-1}): 3337, 3056, 2924, 2854, 1599, 1492, 1264, 1176, 734, 701; HRMS (ESI/Q-TOF) (m/z) calcd for $C_{31}H_{21}N_2O$ $[M + H]^+$ 437.1648; found 437.1658.

7-Phenyl-2,4-di-p-tolyl-1H-furo[2,3-b]pyrrolo[2,3-d]pyridine (1b):

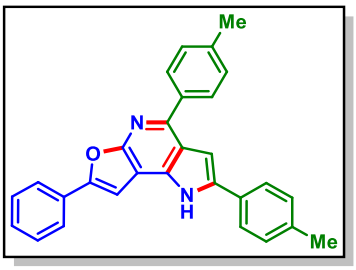

As a brown solid (54 mg, 65% yield, mp 164–166 °C); Purification over a column of silica gel (10% EtOAc in hexane); ^{1}H NMR ($CDCl_3$, 500 MHz): δ 9.55 (s, 1H), 7.98 (d, 2H, J = 8.0 Hz), 7.78 (d, 2H, J = 8.0 Hz), 7.60 (d, 2H, J = 7.5 Hz), 7.36–7.31 (m, 4H), 7.28 (d, 1H, J = 7.0 Hz), 7.21 (d, 2H, J = 8.0 Hz), 7.12 (s, 1H), 7.06 (s, 1H), 2.43 (s, 3H), 2.36 (s, 3H); ^{13}C{^{1}H} NMR ($CDCl_3$, 125 MHz): δ 159.1, 153.3, 146.9, 138.5, 138.4, 138.1, 137.3, 135.9, 130.4, 129.9, 129.4, 129.0, 128.9, 128.4, 125.2, 124.8, 120.9, 104.6, 100.4, 97.7, 21.5, 21.4; IR (neat, cm^{-1}): 3330, 3030, 2920, 2867, 1605, 1504, 1448, 1341, 1264, 1113, 758, 732, 702; HRMS (ESI/Q-TOF) (m/z) calcd for $C_{29}H_{23}N_2O$ [M + H]$^{+}$ 415.1805; found 415.1807.

7-Phenyl-2,4-di-m-tolyl-1H-furo[2,3-b]pyrrolo[2,3-d]pyridine (1c):

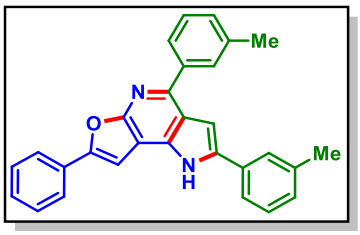

As a brown solid (55 mg, 66% yield, mp 149–151 °C); Purification over a column of silica gel (10% EtOAc in hexane); ^{1}H NMR ($CDCl_3$, 500 MHz): δ 9.67 (s, 1H), 7.89 (s, 1H), 7.86 (d, 1H, J = 8.0 Hz), 7.76 (d, 2H, J = 8.0 Hz), 7.53–7.50 (m, 2H), 7.38 (t, 1H, J = 7.5 Hz), 7.33 (t, 2H, J = 7.25 Hz), 7.29–7.22 (m, 3H), 7.15 (s, 1H), 7.11 (d, 1H, J = 7.0 Hz), 7.03 (s, 1H), 2.42 (s, 3H), 2.36 (s, 3H); ^{13}C{^{1}H} NMR ($CDCl_3$, 125 MHz): δ 159.2, 153.4, 147.2, 140.0, 138.9, 138.5, 138.4, 135.9, 131.8, 130.3, 129.8, 129.4, 129.1, 129.0, 128.9, 128.54, 128.52, 126.3, 126.1, 124.8, 122.5, 121.1, 104.7, 100.9, 97.6, 21.7, 21.6; IR (neat, cm^{-1}): 3332, 3060, 2923, 2878, 1603, 1491, 1342, 1264, 732, 701; HRMS (ESI/Q-TOF) (m/z) calcd for $C_{29}H_{23}N_2O$ [M + H]$^{+}$ 415.1805; found 415.1808.

2,4-Bis(4-ethylphenyl)-7-phenyl-1H-furo[2,3-b]pyrrolo[2,3-d]pyridine (1d):

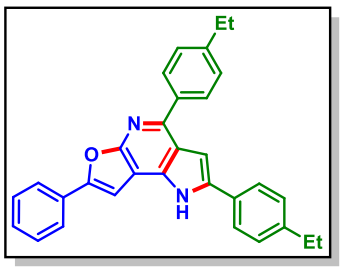

As a gummy liquid (55 mg, 62% yield); Purification over a column of silica gel (10% EtOAc in hexane); ^{1}H NMR ($CDCl_3$, 600 MHz): δ 9.34 (s, 1H), 8.01 (d, 2H, J = 7.8 Hz), 7.84 (d, 2H, J = 7.8 Hz), 7.64 (d, 2H, J = 8.4 Hz), 7.39 (t, 2H, J = 7.8 Hz), 7.36 (d, 2H, J = 8.4 Hz), 7.30 (t, 1H, J = 7.2 Hz), 7.27 (d, 2H, J = 7.8 Hz), 7.16–7.15 (m, 2H),

2.74 (q, 2H, *J* = 7.6 Hz), 2.68 (q, 2H, *J* = 7.6 Hz), 1.30 (t, 3H, *J* = 7.5 Hz), 1.26 (t, 3H, *J* = 7.5 Hz); $^{13}C\{^{1}H\}$ NMR ($CDCl_3$, 150 MHz): δ 153.4, 144.9, 144.5, 138.3, 135.8, 130.3, 129.2, 129.1, 128.9, 128.8, 128.5, 128.2, 125.3, 124.8, 120.9, 104.5, 100.6, 97.5, 28.9, 28.8, 15.7, 15.6; IR (neat, cm^{-1}): 3312, 3055, 2964, 2854, 1606, 1342, 1264, 1115, 732, 703; HRMS (ESI/Q-TOF) (m/z) calcd for $C_{31}H_{27}N_2O$ $[M + H]^+$ 443.2118; found 443.2108.

2,4-Bis(4-(tert-butyl)phenyl)-7-phenyl-1H-furo[2,3-b]pyrrolo[2,3-d]pyridine (1e):

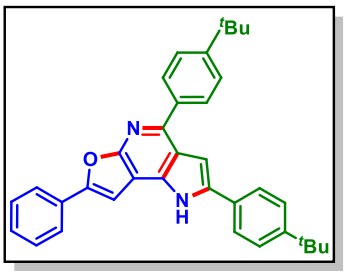

As a brownish solid (64 mg, 64% yield, mp 147–149 °C); Purification over a column of silica gel (10% EtOAc in hexane); ^{1}H NMR ($CDCl_3$, 500 MHz): δ 9.31 (s, 1H), 8.05 (d, 2H, *J* = 8.0 Hz), 7.84 (d, 2H, *J* = 7.0 Hz), 7.67 (d, 2H, *J* = 8.5 Hz), 7.55 (d, 2H, *J* = 7.5 Hz), 7.47 (d, 2H, *J* = 7.5 Hz), 7.40 (t, 2H, *J* = 7.0 Hz), 7.34–7.31 (m, 1H), 7.22 (s, 1H), 7.11 (s, 1H), 1.39 (s, 9H), 1.36 (s, 9H); $^{13}C\{^{1}H\}$ NMR ($CDCl_3$, 125 MHz): δ 159.4, 153.4, 151.7, 151.4, 147.1, 138.2, 137.3, 135.8, 130.5, 130.2, 129.0, 128.9, 128.5, 126.2, 125.7, 125.1, 124.8, 121.0, 104.5, 100.8, 97.5, 34.94, 34.92, 31.5, 31.4; IR (neat, cm^{-1}): 3317, 3058, 2961, 2867, 1605, 1426, 1341, 1264, 1118, 733, 702; HRMS (ESI/Q-TOF) (m/z) calcd for $C_{35}H_{35}N_2O$ $[M + H]^+$ 499.2744; found 499.2743.

2,4-Bis(4-fluorophenyl)-7-phenyl-1H-furo[2,3-b]pyrrolo[2,3-d]pyridine (1f):

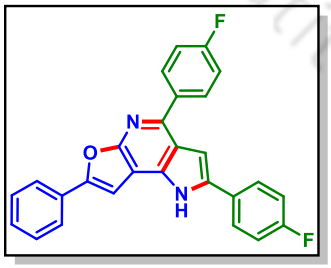

As a brown solid (57 mg, 67% yield, mp 168–170 °C); Purification over a column of silica gel (10% EtOAc in hexane); ^{1}H NMR ($CDCl_3$, 500 MHz): δ 9.55 (s, 1H), 8.00 (t, 2H, *J* = 6.25 Hz), 7.77 (d, 2H, *J* = 7.5 Hz), 7.65 (t, 2H, *J* = 6.5 Hz), 7.35 (t, 2H, *J* = 7.5 Hz), 7.29 (d, 1H, *J* = 7.5 Hz), 7.18 (t, 2H, *J* = 8.5 Hz), 7.12–7.09 (m, 3H), 7.01 (s, 1H); $^{13}C\{^{1}H\}$ NMR ($CDCl_3$, 125 MHz): δ 163.2 (d, *J* = 246.7 Hz), 162.8 (d, *J* = 243.7 Hz), 159.0, 153.7, 145.7, 137.6, 135.9, 130.8 (d, *J* = 8.2 Hz), 130.1, 128.9, 128.7, 128.0 (d, *J* = 3.2 Hz), 127.2 (d, *J* = 8.1 Hz), 124.8, 120.8, 116.3 (d, *J* = 21.6 Hz), 115.7 (d, *J* = 21.3 Hz), 104.8, 100.5, 97.5; ^{19}F NMR ($CDCl_3$, 471 MHz): δ –113.0 (s),

–113.1 (s); IR (neat, cm^{-1}): 3342, 3058, 2924, 2852, 1600, 1505, 1451, 1264, 1157, 837, 734, 700; HRMS (ESI/Q-TOF) (m/z) calcd for $C_{27}H_{17}F_2N_2O$ $[M + H]^+$ 423.1303; found 423.1310.

2,4-Bis(4-chlorophenyl)-7-phenyl-1H-furo[2,3-b]pyrrolo[2,3-d]pyridine (1g):

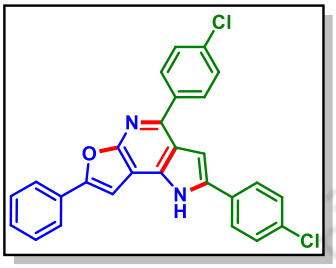

As a brown solid (64 mg, 70% yield, mp 144–146 °C); Purification over a column of silica gel (10% EtOAc in hexane); ^1H NMR ($CDCl_3$, 500 MHz): δ 9.43 (s, 1H), 7.96 (d, 2H, J = 8.5 Hz), 7.79 (d, 2H, J = 7.5 Hz), 7.60 (d, 2H, J = 8.5 Hz), 7.46 (d, 2H, J = 8.5 Hz), 7.40–7.36 (m, 4H), 7.31 (t, 1H, J = 7.25 Hz), 7.06 (s, 2H); $^{13}C\{^1H\}$ NMR ($CDCl_3$, 125 MHz): δ 159.2, 154.0, 145.7, 138.3, 137.4, 136.0, 134.7, 134.2, 130.3, 130.2, 130.1, 129.5, 129.0, 128.9, 128.8, 126.6, 124.8, 120.8, 105.0, 101.1, 97.4; IR (neat, cm^{-1}): 3302, 3063, 2924, 2857, 1595, 1488, 1344, 1264, 1092, 1013, 757, 734, 704; HRMS (ESI/Q-TOF) (m/z) calcd for $C_{27}H_{17}Cl_2N_2O$ $[M + H]^+$ 455.0712; found 455.0718.

2,4-Bis(3-chlorophenyl)-7-phenyl-1H-furo[2,3-b]pyrrolo[2,3-d]pyridine (1h):

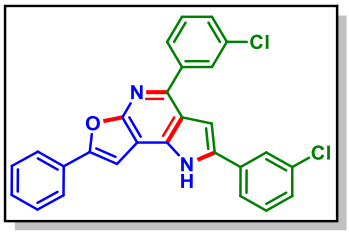

As a brown solid (46 mg, 51% yield, mp 139–141 °C); Purification over a column of silica gel (10% EtOAc in hexane); ^1H NMR ($CDCl_3$, 500 MHz): δ 9.41 (s, 1H), 8.05 (s, 1H), 7.93 (d, 1H, J = 7.5 Hz), 7.85 (d, 2H, J = 8.0 Hz), 7.68 (s, 1H), 7.58 (d, 1H, J = 7.5 Hz), 7.44 (d, 1H, J = 7.5 Hz), 7.41 (t, 3H, J = 7.5 Hz), 7.35 (t, 2H, J = 7.25 Hz), 7.30 (d, 1H, J = 8.0 Hz), 7.14 (d, 2H, J = 7.0 Hz); $^{13}C\{^1H\}$ NMR ($CDCl_3$, 125 MHz): δ 159.2, 154.1, 145.5, 141.7, 137.1, 136.1, 135.3, 134.8, 133.4, 130.6, 130.1, 130.0, 129.1, 129.0, 128.9, 128.7, 128.3, 127.2, 125.4, 124.9, 123.5, 120.8, 105.2, 101.5, 97.5; IR (neat, cm^{-1}): 3334, 3059, 2929, 1595, 1478, 1344, 1264, 1080, 731; HRMS (ESI/Q-TOF) (m/z) calcd for $C_{27}H_{17}Cl_2N_2O$ $[M + H]^+$ 455.0712; found 455.0721.

2,4-Bis(4-bromophenyl)-7-phenyl-1H-furo[2,3-b]pyrrolo[2,3-d]pyridine (1i):

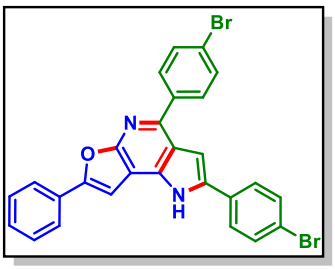

As a brown solid (60 mg, 55% yield, mp 124–126 °C); Purification over a column of silica gel (10% EtOAc in hexane); ^{1}H NMR ($CDCl_3$, 500 MHz): δ 9.78 (s, 1H), 7.88 (d, 2H, J = 8.0 Hz), 7.75 (d, 2H, J = 8.0 Hz), 7.63 (d, 2H, J = 8.0 Hz), 7.53 (d, 2H, J = 8.5 Hz), 7.48 (d, 2H, J = 8.5 Hz), 7.33 (t, 2H, J = 7.5 Hz), 7.28 (d, 1H, J = 7.0 Hz), 7.17 (s, 1H), 6.99 (s, 1H); ^{13}C{^{1}H} NMR ($CDCl_3$, 125 MHz): δ 158.9, 153.8, 145.3, 138.8, 137.5, 136.1, 134.0, 132.3, 131.9, 130.6, 130.0, 128.9, 128.7, 126.8, 124.8, 123.0, 122.2, 120.6, 105.0, 100.8, 97.8; IR (neat, cm^{-1}): 3350, 3065, 2925, 2854, 1721, 1587, 1486, 1344, 1262, 1176, 1009, 828, 758; HRMS (ESI/Q-TOF) (m/z) calcd for $C_{27}H_{17}Br_2N_2O$ $[M + H]^+$ 542.9702; found 542.9697.

7-Phenyl-2,4-bis(4-(trifluoromethyl)phenyl)-1H-furo[2,3-b]pyrrolo[2,3-d]pyridine (1j):

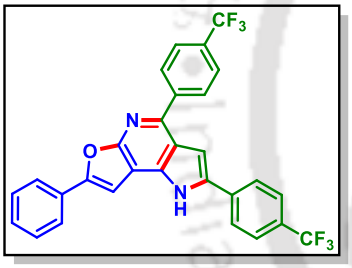

As a yellowish white solid (58 mg, 56% yield, mp 122–124 °C); Purification over a column of silica gel (10% EtOAc in hexane); ^{1}H NMR ($CDCl_3$, 500 MHz): δ 9.59 (s, 1H), 8.14 (d, 2H, J = 8.0 Hz), 7.83 (d, 2H, J = 7.5 Hz), 7.79 (d, 2H, J = 8.0 Hz), 7.76 (d, 2H, J = 8.5 Hz), 7.68 (d, 2H, J = 8.0 Hz), 7.40 (t, 2H, J = 7.25 Hz), 7.33 (t, 1H, J = 7.25 Hz), 7.19 (s, 1H), 7.16 (s, 1H); ^{13}C{^{1}H} NMR ($CDCl_3$, 125 MHz): δ 159.3, 154.4, 145.5, 143.1, 137.1, 136.3, 134.9, 129.9, 129.3, 129.1, 129.0, 126.3 (q, J = 3.6 Hz), 125.7 (q, J = 3.7 Hz), 125.5, 124.9, 121.0, 105.4, 102.1, 97.4; ^{19}F NMR ($CDCl_3$, 471 MHz): δ –62.4 (s), –62.6 (s); IR (neat, cm^{-1}): 3360, 3055, 2927, 2857, 1618, 1323, 1264, 1123, 1067, 735, 703; HRMS (ESI/Q-TOF) (m/z) calcd for $C_{29}H_{17}F_6N_2O$ $[M + H]^+$ 523.1240; found 523.1238.

2,4-Bis(4-pentylphenyl)-7-phenyl-1H-furo[2,3-b]pyrrolo[2,3-d]pyridine (1k):

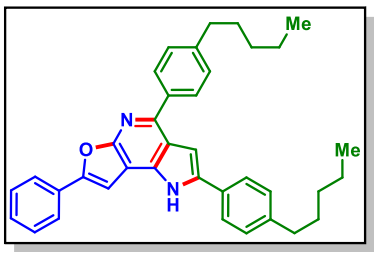

As a brownish gummy liquid (69 mg, 66% yield); Purification over a column of silica gel (10% EtOAc in hexane); ^{1}H NMR ($CDCl_3$, 500 MHz): δ 9.44 (s, 1H), 8.00 (d, 2H, J = 8.0 Hz), 7.81 (d, 2H, J = 8.0 Hz), 7.63 (d, 2H, J = 8.0 Hz), 7.37 (t, 2H, J = 7.75 Hz), 7.31 (d, 2H, J = 8.0 Hz), 7.29 (d, 1H, J = 7.5 Hz), 7.24 (d, 2H, J = 8.0 Hz), 7.15

(s, 1H), 7.11 (s, 1H), 2.68 (t, 2H, *J* = 7.75 Hz), 2.62 (t, 2H, *J* = 7.5 Hz), 1.69–1.62 (m, 5H), 1.38–1.33 (m, 7H), 0.93–0.89 (m, 6H); $^{13}C\{^{1}H\}$ NMR ($CDCl_3$, 125 MHz): δ 159.2, 153.4, 147.0, 143.6, 143.2, 138.4, 137.5, 135.8, 130.4, 129.33, 129.31, 129.0, 128.9, 128.8, 128.5, 125.3, 124.8, 121.0, 104.5, 100.6, 97.6, 36.0, 35.8, 31.75, 31.70, 31.3, 31.2, 22.8, 22.7, 14.3, 14.2; IR (neat, cm^{-1}): 3337, 3060, 2926, 2855, 1605, 1432, 1341, 1264, 1116, 733, 702; HRMS (ESI/Q-TOF) (m/z) calcd for $C_{37}H_{39}N_2O$ $[M + H]^+$ 527.3057; found 527.3049.

Mixture of 2-(4-chlorophenyl)-7-phenyl-4-(p-tolyl)-1H-furo[2,3-b]pyrrolo[2,3-d]pyridine (1l) and 4-(4-chlorophenyl)-7-phenyl-2-(p-tolyl)-1H-furo[2,3-b]pyrrolo[2,3-d]pyridine (1l'):

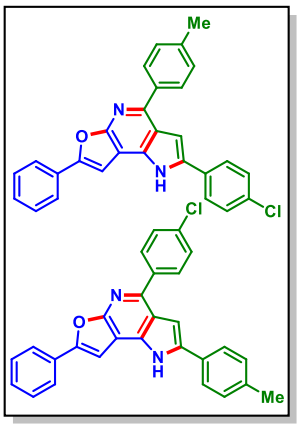

As a brown solid (56 mg, 65% yield, mp 155–157 °C); Purification over a column of silica gel (10% EtOAc in hexane); ^{1}H NMR ($CDCl_3$, 500 MHz): δ 9.54 (s, 1H), 9.42 (s, 0.50 H), 7.99 (d, 2H, *J* = 8.5 Hz), 7.97–7.93 (m, 2.25H), 7.80 (d, 2H, *J* = 8.0 Hz), 7.77–7.73 (m, 2.40H), 7.59 (d, 3H, *J* = 7.5 Hz), 7.47 (d, 3H, *J* = 8.0 Hz), 7.36 (q, 6.43H, *J* = 7.5 Hz), 7.33–7.28 (m, 7.50H), 7.22 (d, 2H, *J* = 7.5 Hz), 7.08 (s, 1.30H), 7.05–7.03 (m, 2.18H), 2.43 (s, 1.55H), 2.38 (s, 3H); $^{13}C\{^{1}H\}$ NMR ($CDCl_3$, 125 MHz): δ 159.0, 153.7, 153.3, 145.3, 138.7, 138.6, 138.3, 138.1, 135.9, 135.8, 134.5, 134.4, 130.4, 130.3, 130.2, 130.0, 129.9, 129.5, 129.4, 129.39, 129.37, 129.1, 129.0, 128.97, 128.93, 128.91, 128.8, 128.7, 128.5, 126.6, 126.5, 125.3, 125.2, 124.8, 124.7, 120.9, 105.0, 104.9, 100.4, 99.8, 97.63, 97.60, 21.5, 21.4; IR (neat, cm^{-1}): 3330, 3026, 2923, 2852, 1601, 1491, 1343, 1263, 1178, 1091, 758, 698; HRMS (ESI/Q-TOF) (m/z) calcd for $C_{28}H_{20}ClN_2O$ $[M + H]^+$ 435.1259; found 435.1269.

7-phenyl-4-(p-tolyl)-2-(4-(trifluoromethyl)phenyl)-1H-furo[2,3-b]pyrrolo[2,3-d]pyridine (1m):

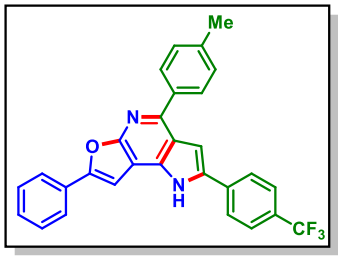

As a brown solid (60 mg, 64% yield, mp 137–139 °C); Purification over a column of silica gel (10% EtOAc in hexane); ^{1}H NMR ($CDCl_3$, 400 MHz): δ 9.58 (s, 1H), 8.14 (d, 2H, *J* = 8.0 Hz), 7.77 (d, 2H, *J* = 7.2 Hz), 7.73 (d, 2H, *J* = 8.0 Hz), 7.58 (d, 2H, *J* = 8.0 Hz),

7.35 (t, 3H, *J* = 7.4 Hz), 7.30 (d, 1H, *J* = 7.2 Hz), 7.22 (d, 2H, *J* = 8.0 Hz), 7.04 (s, 1H), 2.38 (s, 3H); $^{13}C\{^{1}H\}$ NMR [$CDCl_3$, 125 MHz (taken in 500 MHz)]: δ 159.0, 154.0, 144.7, 143.5, 139.1, 138.5, 135.9, 130.1, 130.0, 129.3, 129.0, 128.9, 128.8, 128.7, 125.5 (q, *J* = 3.5 Hz), 125.3, 124.8, 121.2, 105.4, 99.6, 97.5, 21.4; ^{19}F NMR ($CDCl_3$, 471 MHz): δ –62.3 (s); IR (neat, cm^{-1}): 3356, 2962, 2923, 1615, 1321, 1262, 1109, 1066, 758; HRMS (ESI/Q-TOF) (m/z) calcd for $C_{29}H_{20}F_3N_2O$ $[M + H]^+$ 469.1522; found 469.1524.

2,4-Di(naphthalen-2-yl)-7-phenyl-1H-furo[2,3-b]pyrrolo[2,3-d]pyridine (1n):

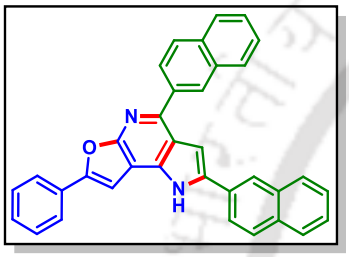

As a brown solid (58 mg, 60% yield, mp 159–161 °C); Purification over a column of silica gel (10% EtOAc in hexane); ^{1}H NMR ($CDCl_3$, 500 MHz): δ 9.50 (s, 1H), 8.54 (s, 1H), 8.24 (d, 1H, *J* = 8.5 Hz), 8.08 (s, 1H), 8.00–7.96 (m, 2H), 7.92–7.90 (m, 1H), 7.86 (t, 3H, *J* = 7.75 Hz), 7.80 (t, 3H, *J* = 7.75 Hz), 7.54–7.52 (m, 2H), 7.48–7.46 (m, 2H), 7.40 (t, 3H, *J* = 7.25 Hz), 7.32–7.31 (m, 1H), 7.15 (s, 1H); $^{13}C\{^{1}H\}$ NMR ($CDCl_3$, 125 MHz): δ 159.4, 153.7, 146.9, 138.3, 137.5, 136.1, 133.7, 133.6, 133.5, 133.1, 130.3, 129.2, 129.1, 129.0, 128.8, 128.7, 128.5, 128.3, 128.2, 128.0, 127.9, 127.0, 126.9, 126.6, 126.5, 126.3, 124.9, 123.7, 123.5, 121.3, 104.8, 101.6, 97.6; IR (neat, cm^{-1}): 3347, 3025, 2923, 2851, 1601, 1452, 1264, 1179, 817, 738, 698; HRMS (ESI/Q-TOF) (m/z) calcd for $C_{35}H_{23}N_2O$ $[M + H]^+$ 487.1805; found 487.1797.

7-(4-Fluorophenyl)-2,4-di-m-tolyl-1H-furo[2,3-b]pyrrolo[2,3-d]pyridine (7c):

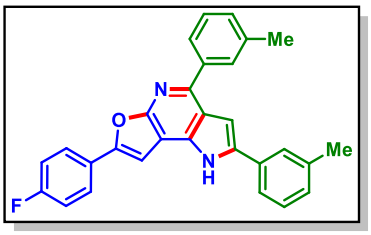

As a brown solid (55 mg, 64% yield, mp 132–134 °C); Purification over a column of silica gel (10% EtOAc in hexane); ^{1}H NMR ($CDCl_3$, 500 MHz): δ 9.66 (s, 1H), 7.88 (s, 1H), 7.85 (d, 1H, *J* = 8.0 Hz), 7.70 (t, 2H, *J* = 6.75 Hz), 7.53–7.50 (m, 2H), 7.38 (t, 1H, *J* = 7.75 Hz), 7.30 (t, 1H, *J* = 7.75 Hz), 7.24 (d, 1H, *J* = 8.0 Hz), 7.15–7.13 (m, 2H), 7.02 (t, 2H, *J* = 8.5 Hz), 6.94 (s, 1H); $^{13}C\{^{1}H\}$ NMR ($CDCl_3$, 125 MHz): δ 162.9 (d, *J* = 247.2 Hz), 159.1, 152.5, 147.2, 139.9, 138.9, 138.5, 138.4, 135.9, 131.7, 129.7, 129.4, 129.1,

129.0, 128.5, 126.6 (q, J = 3.2 Hz), 126.5 (q, J = 8.1 Hz), 126.3, 126.1, 122.5, 121.1, 116.0 (d, J = 21.8 Hz), 104.6, 100.8, 97.3, 21.7, 21.6; ^{19}F NMR ($CDCl_3$, 471 MHz): δ –112.4 (s); IR (neat, cm^{-1}): 3327, 3046, 2922, 2855, 1607, 1498, 1340, 1232, 1156, 1116, 837, 767; HRMS (ESI/Q-TOF) (m/z) calcd for $C_{29}H_{22}FN_2O$ $[M + H]^+$ 433.1711; found 433.1710.

7-(2-Bromophenyl)-2,4-di-m-tolyl-1H-furo[2,3-b]pyrrolo[2,3-d]pyridine (10c):

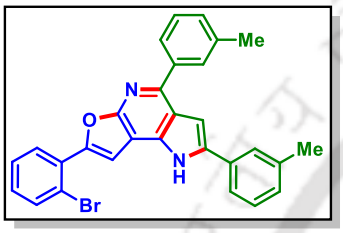

As a brown solid (58 mg, 59% yield, mp 136–138 ^oC); Purification over a column of silica gel (10% EtOAc in hexane); ^{1}H NMR ($CDCl_3$, 500 MHz): δ 9.73 (s, 1H), 8.05 (d, 1H, J = 8.0 Hz), 7.91 (s, 1H), 7.87 (d, 1H, J = 7.5 Hz), 7.80 (s, 1H), 7.62 (d, 1H, J = 8.0 Hz), 7.55–7.52 (m, 2H), 7.42 (t, 1H, J = 7.5 Hz), 7.35 (t, 1H, J = 7.5 Hz), 7.30 (t, 1H, J = 7.75 Hz), 7.27 (s, 1H), 7.17 (s, 1H), 7.13 (d, 2H, J = 7.5 Hz), 2.46 (s, 3H), 2.39 (s, 3H); ^{13}C{^{1}H} NMR ($CDCl_3$, 125 MHz): δ 158.7, 150.4, 148.1, 140.0, 138.9, 138.5, 138.4, 136.2, 134.4, 131.7, 130.6, 129.9, 129.8, 129.5, 129.2, 129.1, 128.9, 128.5, 127.7, 126.4, 126.1, 122.5, 121.1, 120.1, 104.3, 103.7, 100.9, 21.7, 21.6; IR (neat, cm^{-1}): 3335, 3054, 2987, 1592, 1452, 1343, 1264, 895, 731, 703; HRMS (ESI/Q-TOF) (m/z) calcd for $C_{29}H_{22}BrN_2O$ $[M + H]^+$ 493.0910; found 493.0903.

7-(4-Chlorophenyl)-2,4-bis(4-ethylphenyl)-1H-furo[2,3-b]pyrrolo[2,3-d]pyridine (8d):

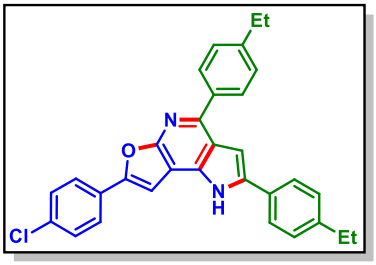

As a gummy liquid (52 mg, 55% yield); Purification over a column of silica gel (10% EtOAc in hexane); ^{1}H NMR ($CDCl_3$, 500 MHz): δ 9.48 (s, 1H), 8.00 (d, 2H, J = 8.0 Hz), 7.67 (d, 2H, J = 8.0 Hz), 7.63 (d, 2H, J = 7.5 Hz), 7.35 (d, 2H, J = 7.5 Hz), 7.31 (d, 2H, J = 8.5 Hz), 7.26 (d, 2H, J = 8.0 Hz), 7.15 (d, 1H, J = 2.0 Hz), 7.02 (s, 1H), 2.73 (q, 2H, J = 7.6 Hz), 2.68 (q, 2H, J = 7.6 Hz), 1.31–1.25 (m, 6H); ^{13}C{^{1}H} NMR ($CDCl_3$, 125 MHz): δ 159.1, 152.1, 147.3, 144.9, 144.6, 138.5, 137.4, 135.8, 134.2, 129.2, 129.17, 129.15, 128.9, 128.8, 128.3, 125.9, 125.4, 121.0, 104.4, 100.6, 98.0, 28.9, 28.8,

15.7, 15.6; IR (neat, cm^{-1}): 3388, 2964, 2928, 1483, 1340, 1264, 1178, 1091, 833, 733, 703; HRMS (ESI/Q-TOF) (m/z) calcd for $C_{31}H_{26}ClN_2O$ $[M + H]^+$ 477.1728; found 477.1732.

***2-Amino-5-phenylfuran-3-carbonitrile (1'):*[6]**

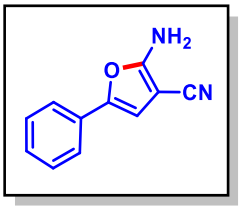

As a white solid (30 mg, 80% yield, mp 186–188 °C); Purification over a column of silica gel (15% EtOAc in hexane); ^1H NMR (DMSO-d_6, 600 MHz): δ 7.62 (s, 2H), 7.48 (d, 2H, J = 7.8 Hz), 7.35 (t, 2H, J = 7.2 Hz), 7.19 (t, 1H, J = 7.2 Hz), 6.97 (s, 1H); $^{13}C\{^1H\}$ NMR (DMSO-d_6, 150 MHz): δ 164.0, 141.8, 129.3, 128.8, 126.5, 122.0, 116.1 106.7, 66.2; IR (neat, cm^{-1}): 3415, 3320, 2958, 2921, 2851, 2205, 1646, 1491, 1173, 1066, 882, 758.

2-(4-Chlorophenyl)-5,6,12-triphenyl-13H-furo[3',2':5,6]pyrrolo[3',2':3,4]pyrido[2,1-a]isoquinolin-4-ium (7x):

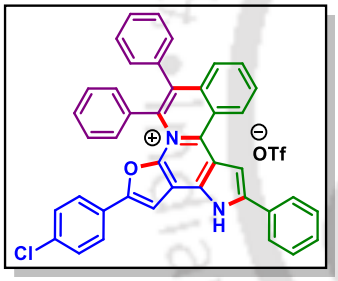

As a yellow solid (87 mg, 73% yield, mp 212–214 °C); Purification over a column of silica gel (2% MeOH in DCM); ^1H NMR (DMSO-d_6, 500 MHz): δ 13.70 (s, 1H), 9.44 (d, 1H, J = 8.5 Hz), 8.43 (s, 1H), 8.13 (d, 2H, J = 8.0 Hz), 8.05 (t, 1H, J = 7.75 Hz), 7.93 (t, 1H, J = 7.75 Hz), 7.62 (s, 1H), 7.59 (t, 2H, J = 7.75 Hz), 7.50 (t, 1H, J = 7.5 Hz), 7.46 (d, 2H, J = 7.5 Hz), 7.41–7.31 (m, 9H), 7.19 (d, 2H, J = 7.0 Hz), 6.93 (d, 2H, J = 8.0 Hz); $^{13}C\{^1H\}$ NMR (DMSO-d_6, 125 MHz): δ 153.0, 145.5, 142.6, 135.6, 135.2, 134.8, 134.7, 134.6, 134.4, 132.9, 132.7, 131.3, 130.7, 130.4, 130.3, 129.6, 129.4, 129.1, 128.9, 128.85, 128.82, 128.1, 127.94, 127.90, 126.6, 126.2, 125.9, 125.6, 124.7, 117.6, 109.5, 103.8, 99.3; IR (neat, cm^{-1}): 3347, 2958, 2925, 2856, 1728, 1462, 1379, 1272, 1122, 1072, 741, 699; HRMS (ESI/Q-TOF) (m/z) calcd for $C_{41}H_{27}ClN_2O$ $[M + H]^+$ 598.1806; found 598.1800.

7-([1,1'-Biphenyl]-4-yl)-2,4-diphenyl-1H-furo[2,3-b]pyrrolo[2,3-d]pyridine (8y):

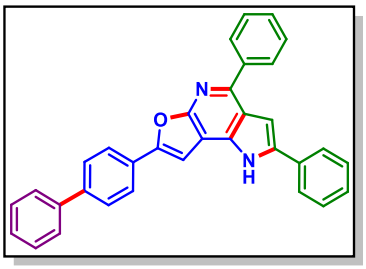

As a brown solid (74 mg, 80% yield, mp 152–154 °C); Purification over a column of silica gel (10% EtOAc in hexane); ^{1}H NMR ($CDCl_3$, 500 MHz): δ 9.44 (s, 1H), 8.09 (d, 2H, J = 7.5 Hz), 7.85 (d, 2H, J = 8.5 Hz), 7.72 (d, 2H, J = 7.5 Hz), 7.59 (t, 3H, J = 8.25 Hz), 7.53 (t, 2H, J = 7.5 Hz), 7.46–7.42 (m, 6H), 7.37–7.35 (m, 2H), 7.19 (s, 1H), 7.08 (s, 1H); ^{13}C{^{1}H} NMR ($CDCl_3$, 125 MHz): δ 159.3, 153.4, 147.1, 141.2, 140.5, 140.0, 138.3, 135.9, 131.8, 129.3, 129.2, 129.0, 128.7, 128.6, 128.2, 127.7, 127.5, 127.1, 125.4, 125.2, 121.1, 104.8, 101.0, 97.6; IR (neat, cm^{-1}): 3322, 3058, 2924, 2852, 1644, 1484, 1344, 1263, 1117, 755, 697; HRMS (ESI/Q-TOF) (m/z) calcd for $C_{33}H_{23}N_2O$ $[M + H]^+$ 463.1805; found 463.1800.

2,4-Diphenyl-7-(4-(p-tolylethynyl)phenyl)-1H-furo[2,3-b]pyrrolo[2,3-d]pyridine (8z):

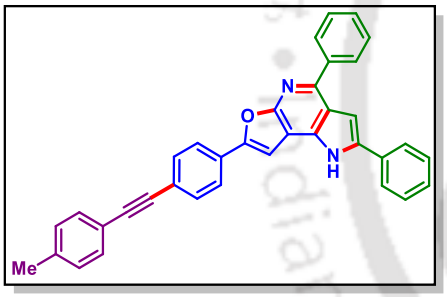

As a brown solid (78 mg, 78% yield, mp 157–159 °C); Purification over a column of silica gel (10% EtOAc in hexane); ^{1}H NMR ($CDCl_3$, 500 MHz): δ 9.71 (s, 1H), 8.07 (d, 2H, J = 7.5 Hz), 7.71 (d, 2H, J = 7.5 Hz), 7.67 (d, 2H, J = 8.0 Hz), 7.52 (t, 2H, J = 7.5 Hz), 7.45–7.40 (m, 7H), 7.32 (t, 1H, J = 7.5 Hz), 7.16–7.14 (m, 3H), 7.02 (s, 1H), 2.37 (s, 3H); ^{13}C{^{1}H} NMR ($CDCl_3$, 125 MHz): δ 159.2, 152.7, 147.2, 140.0, 138.7, 138.4, 135.9, 132.0, 131.8, 131.7, 129.6, 129.3, 129.2, 129.1, 128.8, 128.7, 128.2, 125.4, 124.5, 123.4, 121.0, 120.2, 104.8, 100.9, 98.4, 91.2, 88.9, 21.7; IR (neat, cm^{-1}): 3350, 3026, 2922, 2851, 1602, 1512, 1492, 1343, 1264, 1117, 1029, 815, 735, 698; HRMS (ESI/Q-TOF) (m/z) calcd for $C_{36}H_{25}N_2O$ $[M + H]^+$ 501.1961; found 501.1954.

IV.10. Representative NMR Spectra:

2,4,7-Triphenyl-1H-furo[2,3-b]pyrrolo[2,3-d]pyridine (1a): ^{1}H NMR ($CDCl_3$, 500 MHz)

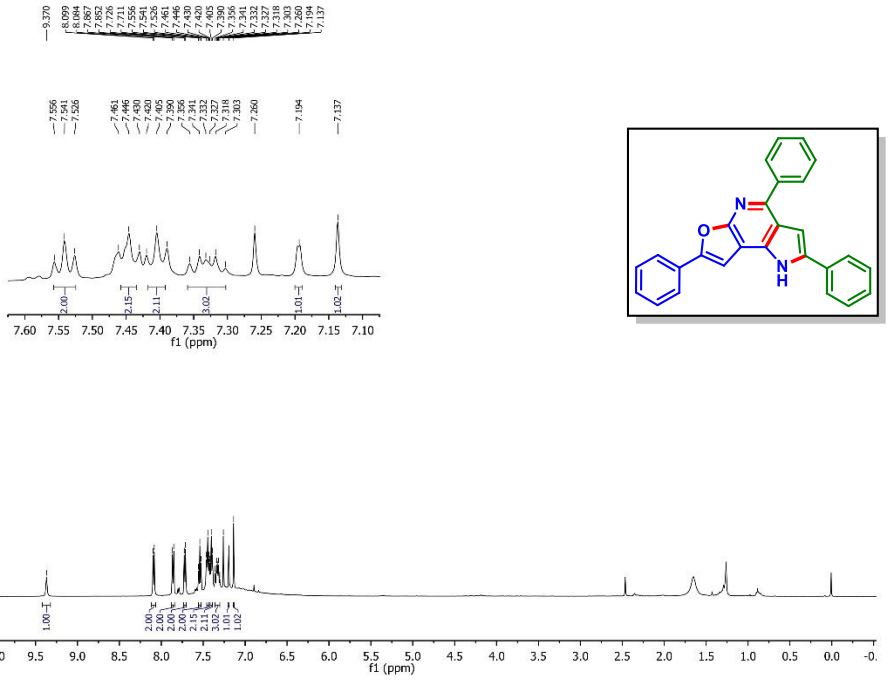

2,4,7-Triphenyl-1H-furo[2,3-b]pyrrolo[2,3-d]pyridine (1a): $^{13}C\{^{1}H\}$ NMR ($CDCl_3$, 125 MHz)

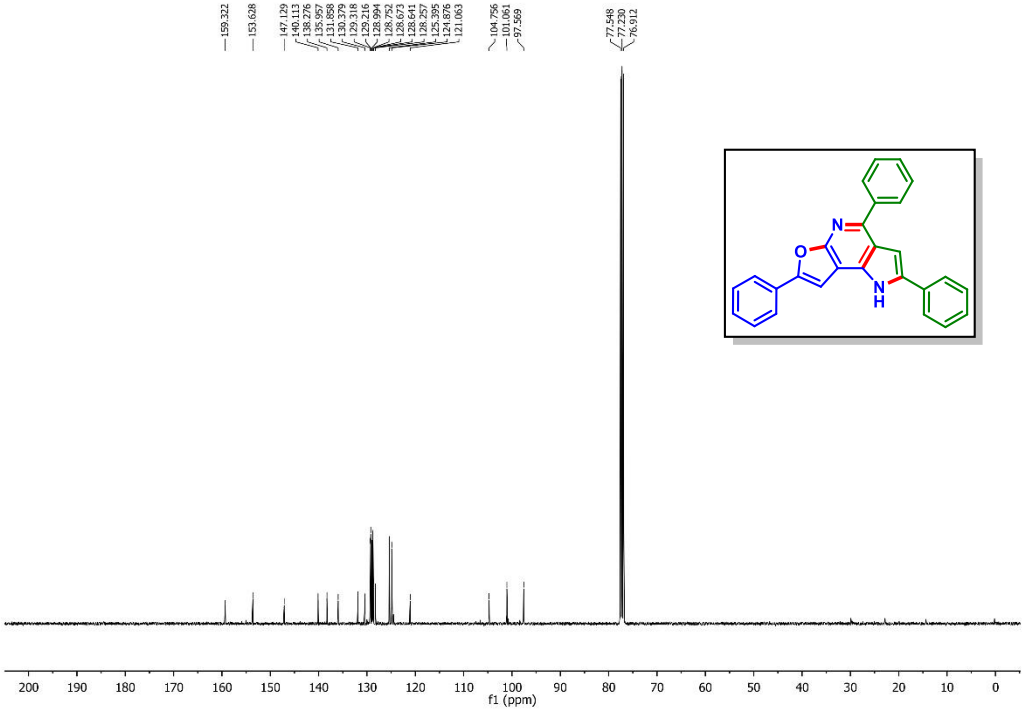

2,4-Diphenyl-7-(p-tolyl)-1H-furo[2,3-b]pyrrolo[2,3-d]pyridine (2a): ^{1}H NMR ($CDCl_3$, 500 MHz)

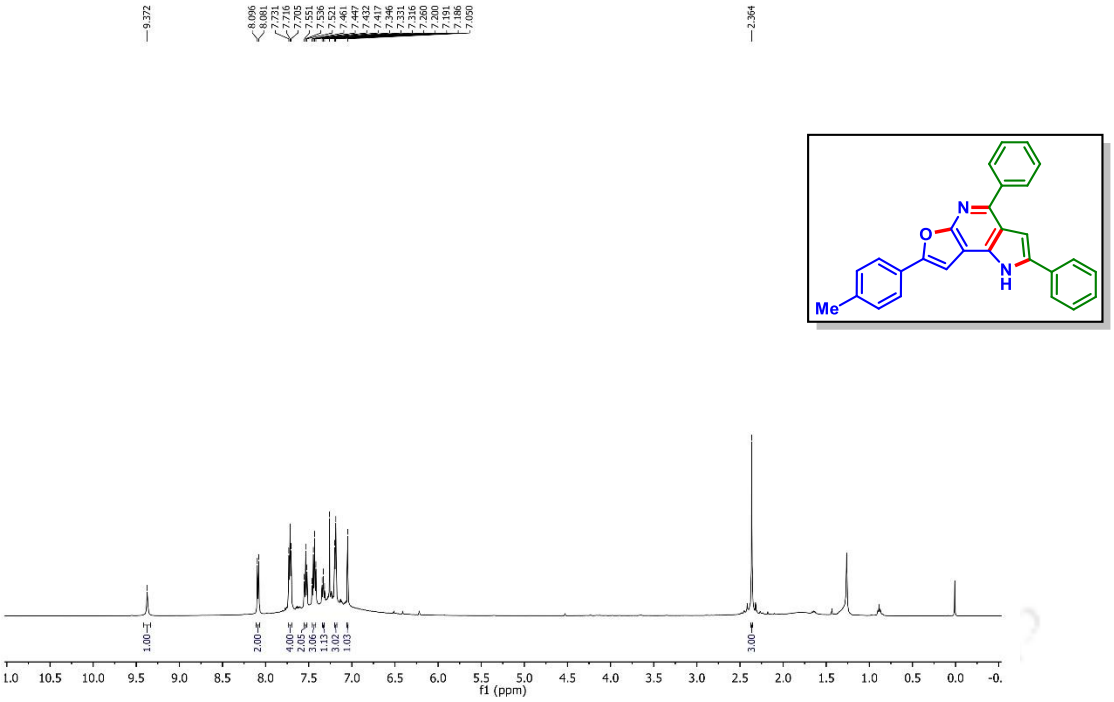

2,4-Diphenyl-7-(p-tolyl)-1H-furo[2,3-b]pyrrolo[2,3-d]pyridine (2a): $^{13}C\{^{1}H\}$ NMR ($CDCl_3$, 125 MHz)

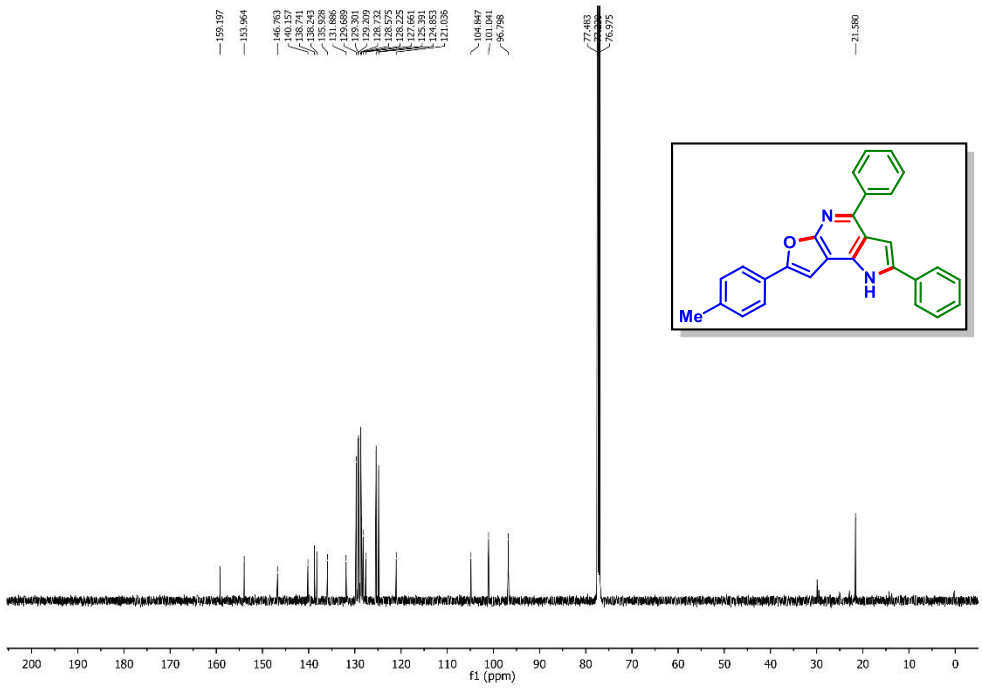

7-(4-(Tert-butyl)phenyl)-2,4-diphenyl-1H-furo[2,3-b]pyrrolo[2,3-d]pyridine (5a): ^{1}H NMR ($CDCl_3$, 500 MHz)

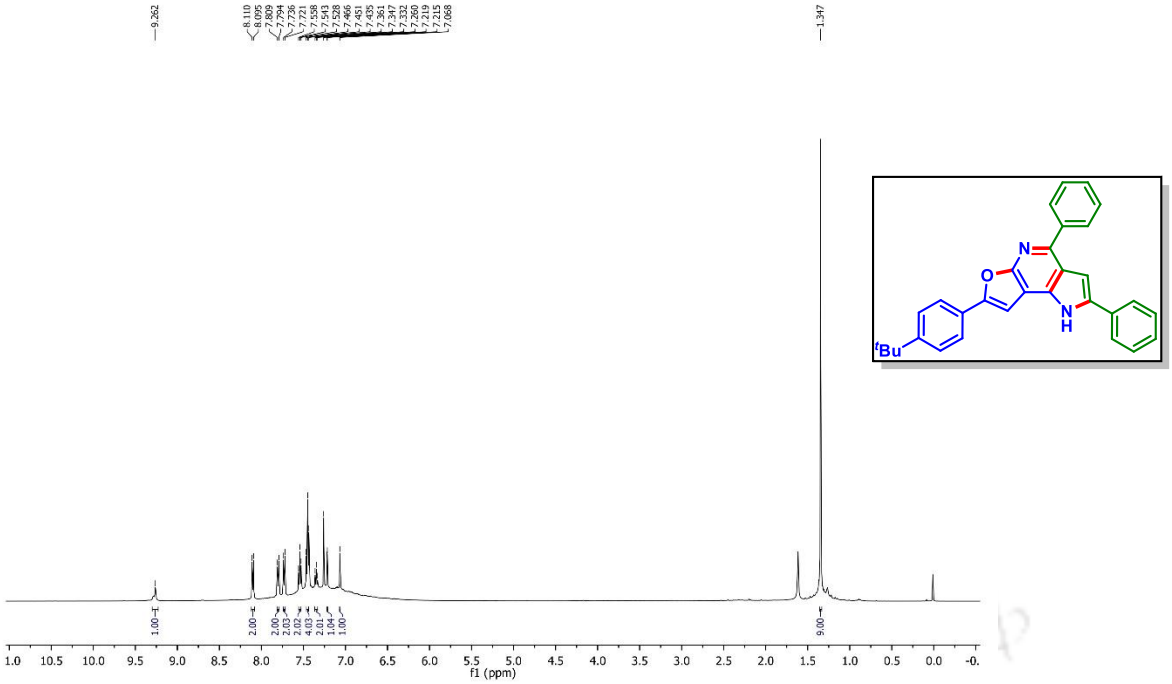

7-(4-(Tert-butyl)phenyl)-2,4-diphenyl-1H-furo[2,3-b]pyrrolo[2,3-d]pyridine (5a): $^{13}C\{^{1}H\}$ NMR ($CDCl_3$, 125 MHz)

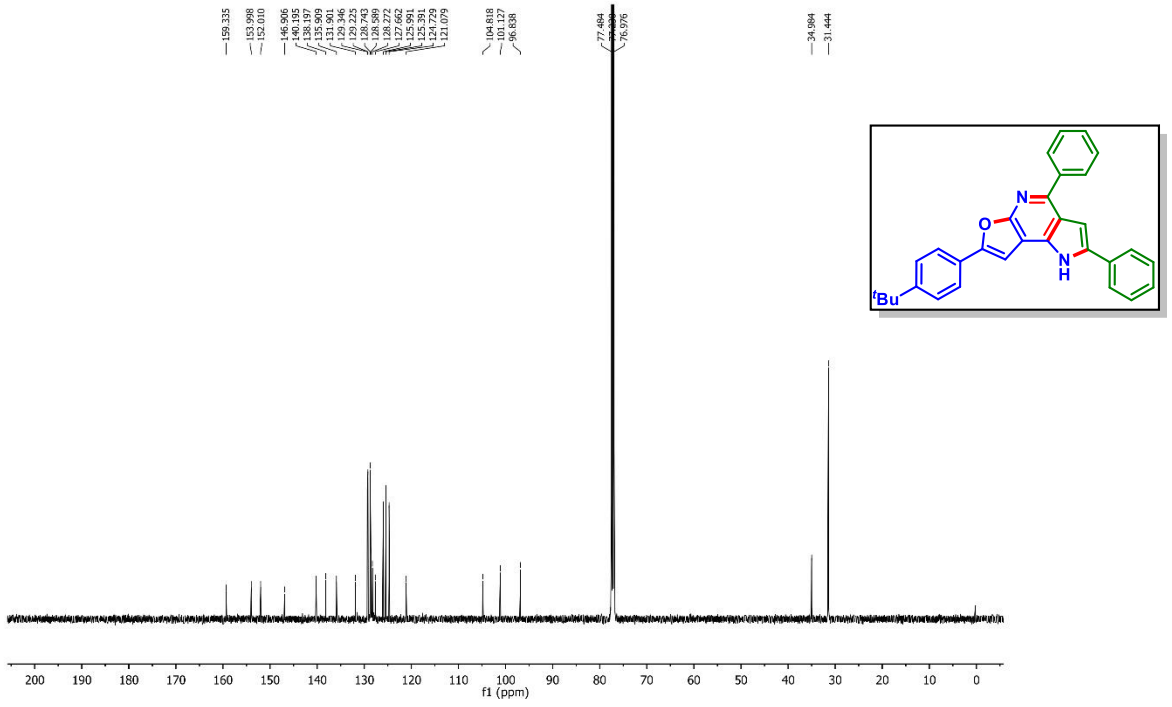

7-(4-Chlorophenyl)-2,4-diphenyl-1H-furo[2,3-b]pyrrolo[2,3-d]pyridine (8a): ^{1}H NMR ($CDCl_3$, 600 MHz)

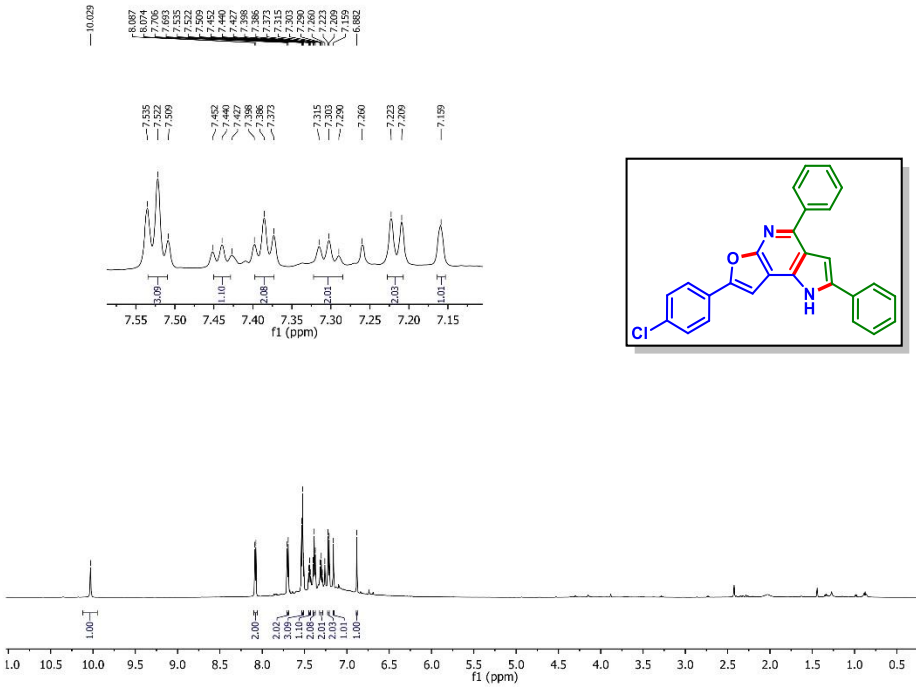

7-(4-Chlorophenyl)-2,4-diphenyl-1H-furo[2,3-b]pyrrolo[2,3-d]pyridine (8a): $^{13}C\{^{1}H\}$ NMR ($CDCl_3$, 150 MHz)

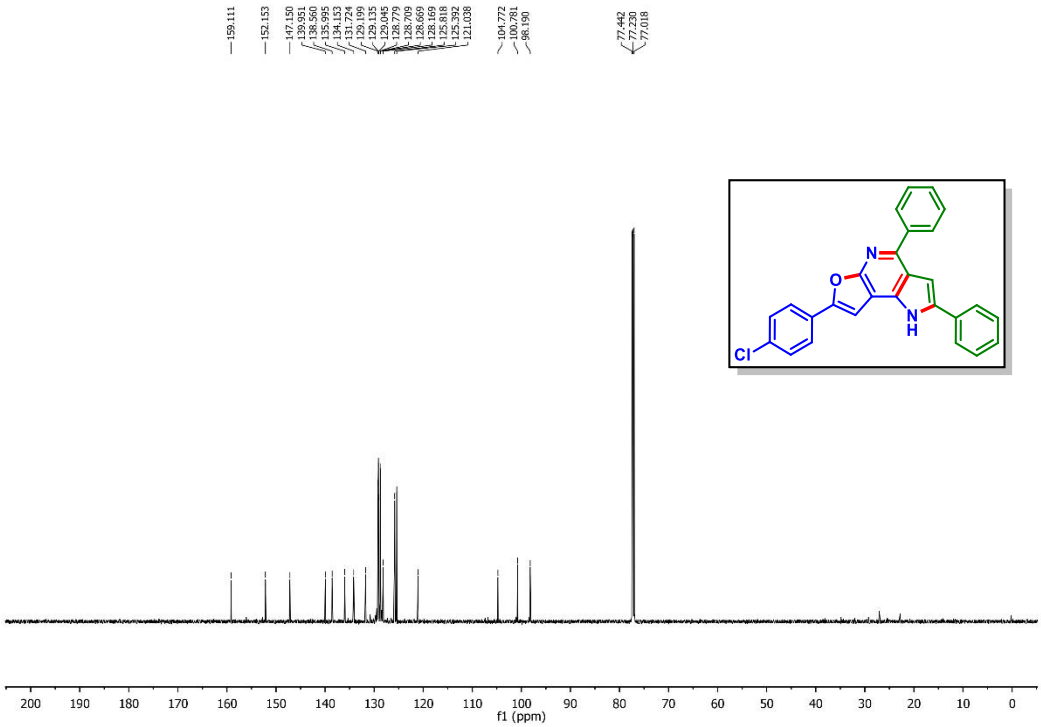

7-(4-Bromophenyl)-2,4-diphenyl-1H-furo[2,3-b]pyrrolo[2,3-d]pyridine (9a): ^{1}H NMR ($CDCl_3$, 500 MHz)

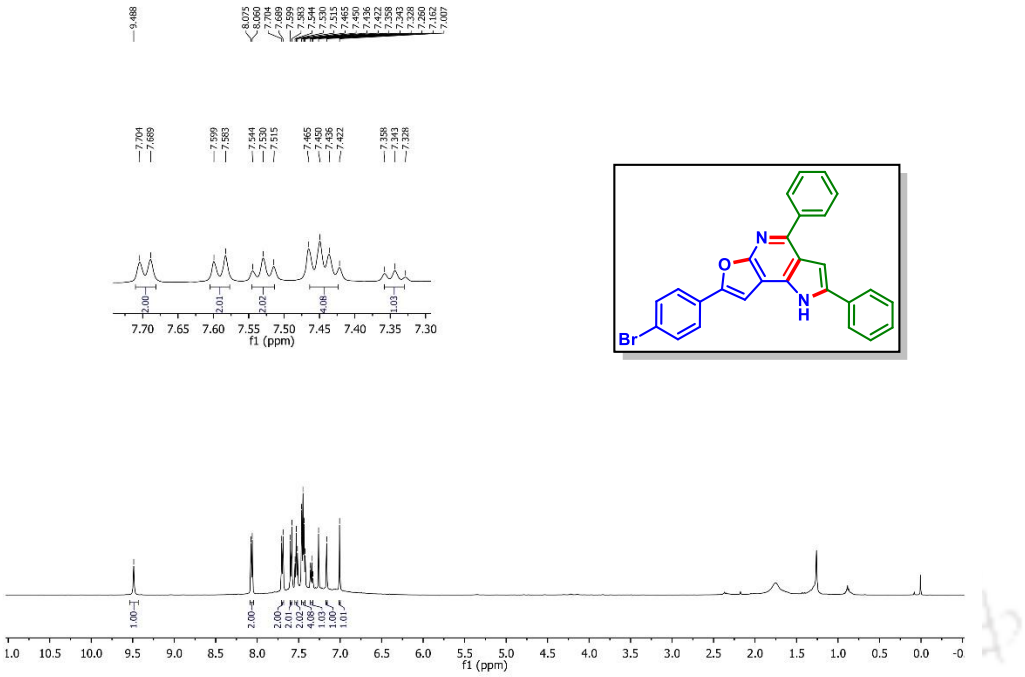

7-(4-Bromophenyl)-2,4-diphenyl-1H-furo[2,3-b]pyrrolo[2,3-d]pyridine (9a): $^{13}C\{^{1}H\}$ NMR ($CDCl_3$, 125 MHz)

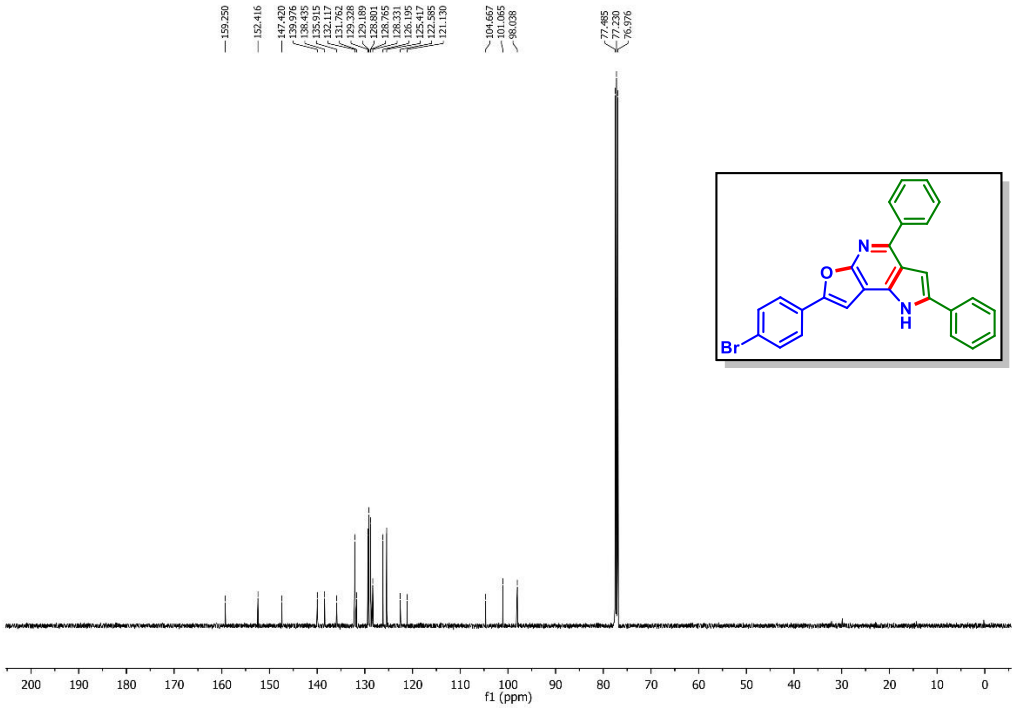

7-Phenyl-2,4-di-m-tolyl-1H-furo[2,3-b]pyrrolo[2,3-d]pyridine (1c): ^{1}H NMR ($CDCl_3$, 500 MHz)

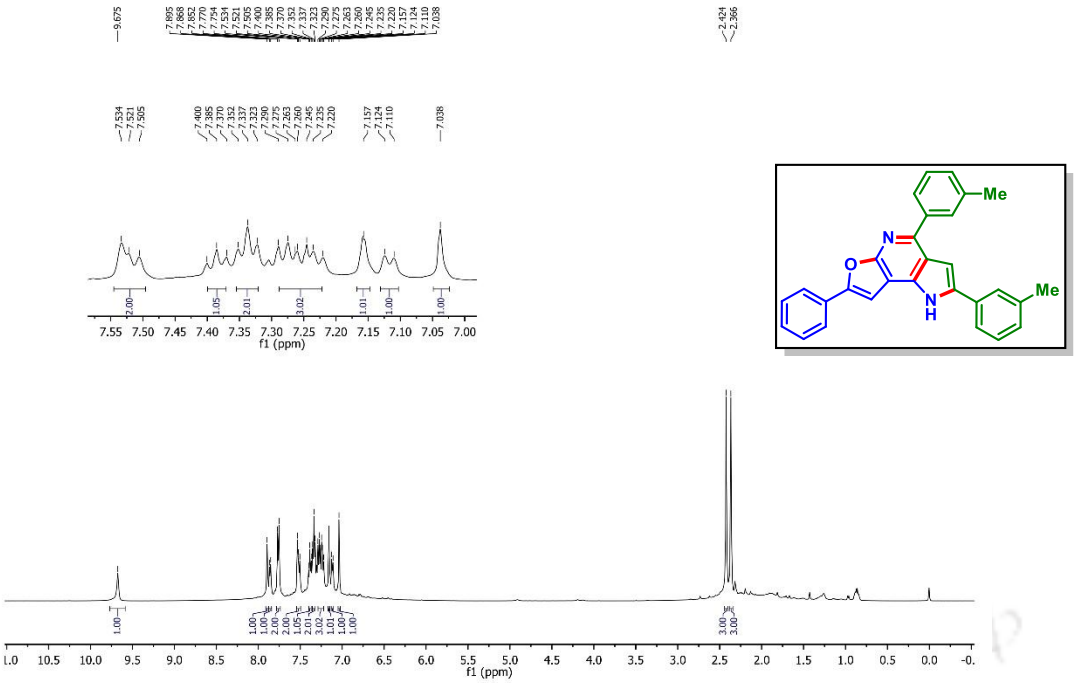

7-Phenyl-2,4-di-m-tolyl-1H-furo[2,3-b]pyrrolo[2,3-d]pyridine (1c): $^{13}C\{^{1}H\}$ NMR ($CDCl_3$, 125 MHz)

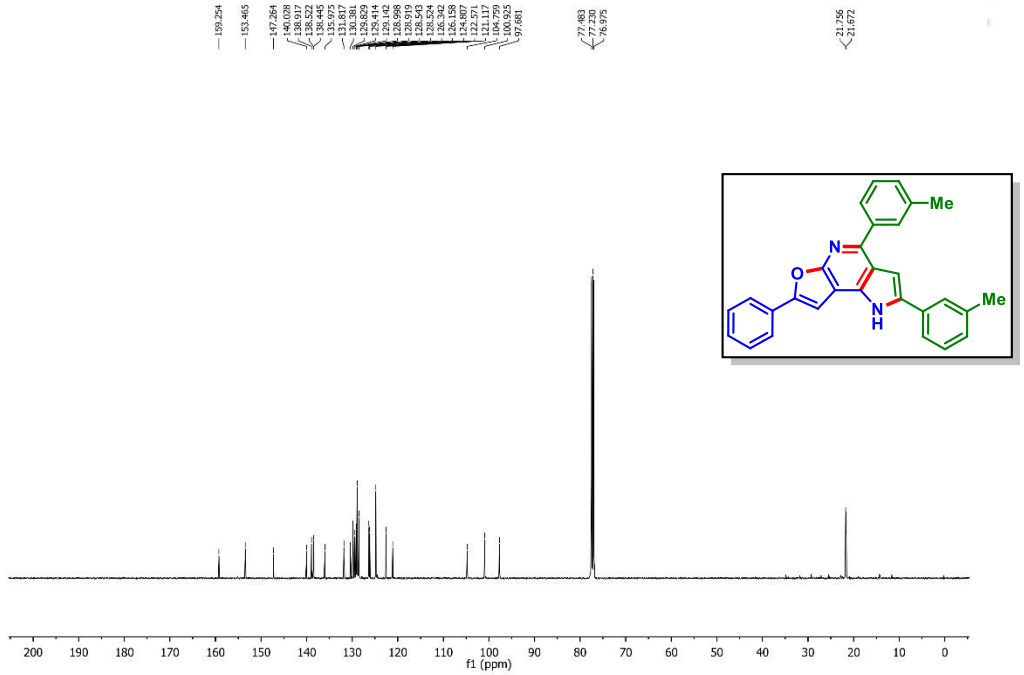

2,4-Bis(4-chlorophenyl)-7-phenyl-1H-furo[2,3-b]pyrrolo[2,3-d]pyridine (1g): ^{1}H NMR ($CDCl_3$, 500 MHz)

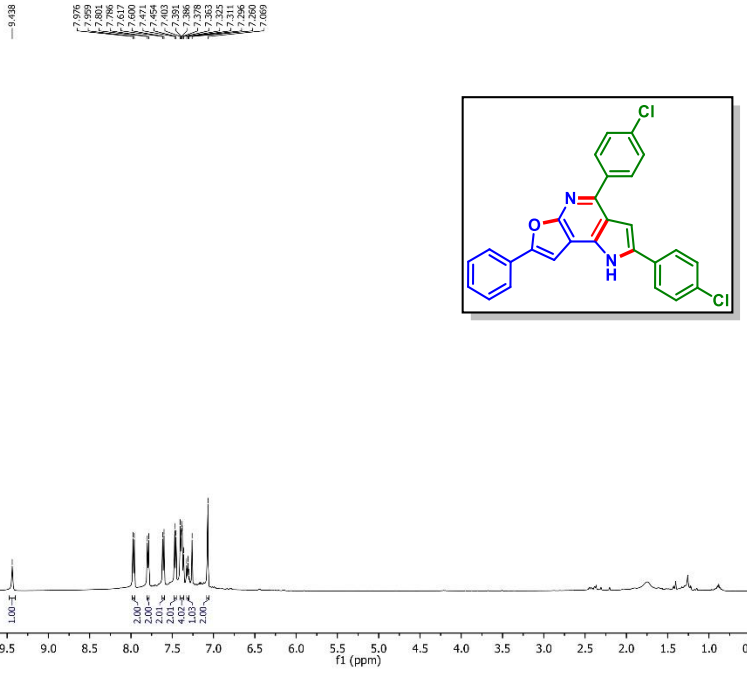

2,4-Bis(4-chlorophenyl)-7-phenyl-1H-furo[2,3-b]pyrrolo[2,3-d]pyridine (1g): $^{13}C\{^{1}H\}$ NMR ($CDCl_3$, 125 MHz)

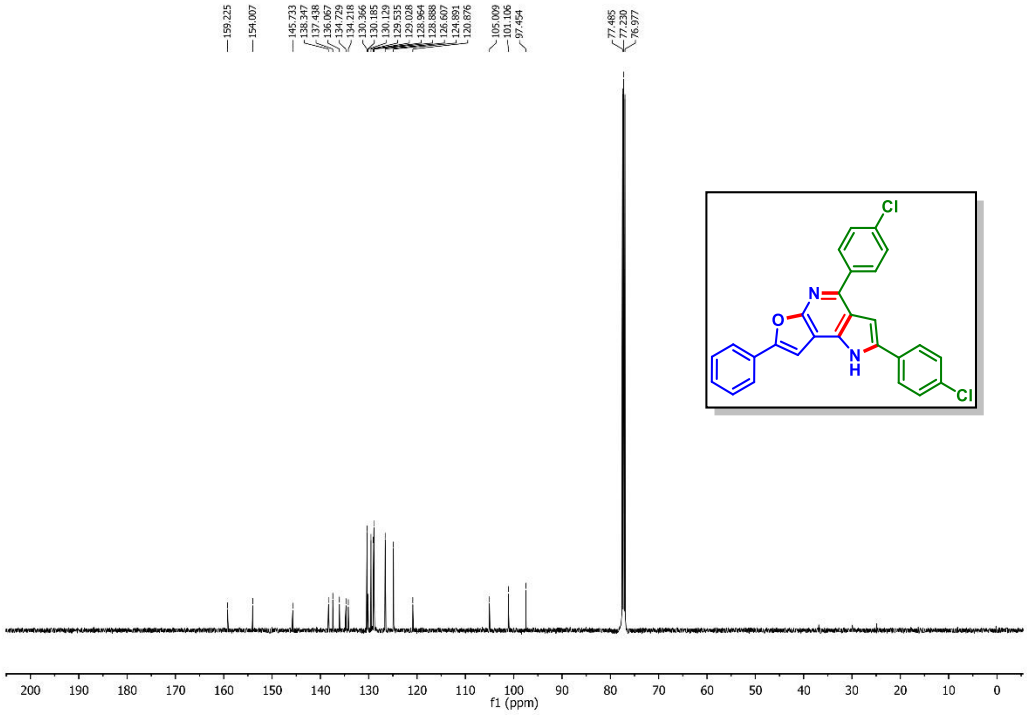

IV.11. References:

[1] (a) Zhang, B.; Studer, A. *Chem. Soc. Rev.* **2015**, *44*, 3505–3521. (b) Zeni, G.; Larock, R. C. *Chem. Rev.* **2004**, *104*, 2285–2309.

[2] (a) Martin, M. W.; Newcomb, J.; Nunes, J. J.; Bemis, J. E.; McGowan, D. C.; White, R. D.; Buchanan, J. L.; DiMauro, E. F.; Boucher, C.; Faust, T.; Hsieh, F.; Huang, X.; Lee, J. H.; Schneider, S.; Turci, S. M.; Zhu, X. *Bioorg. Med. Chem. Lett.* **2007**, *17*, 2299–2304. (b) Wu, Z.; Robinson, R. G.; Fu, S.; Barnett, S. F.; Defeo-Jones, D.; Jones, R. E.; Kral, A. M.; Huber, H. E.; Kohl, N. E.; Hartman, G. D.; Bilodeau, M. T. *Bioorg. Med. Chem. Lett.* **2008**, *18*, 2211–2214. (c) Rodriguez, A. L.; Williams, R.; Zhou, Y.; Lindsley, S. R.; Le, U.; Grier, M. D.; Weaver, C. D.; Conn, P. J.; Lindsley, C. W. *Bioorg. Med. Chem. Lett.* **2009**, *19*, 3209–3213. (d) Debenham, J. S.; Madsen-Duggan, C. B.; Toupence, R. B.; Walsh, T. F.; Wang, J.; Tong, X.; Kumar, S.; Lao, J.; Fong, T. M.; Xiao, J. C.; Huang, C. R. R. C.; Shen, C.-P.; Feng, Y.; Marsh, D. J.; Stribling, D. S.; Shearman, L. P.; Strack, A. M.; Goulet, M. T. *Bioorg. Med. Chem. Lett.* **2010**, *20*, 1448–1452.

[3] (a) Sirakanyan, S. N.; Hovakimyan, A. A.; Noravyan, A. S. Synthesis, *Russ. Chem. Rev.* **2015**, *84*, 441 454. (b) Ibrahim, M. M.; Al-Refai, M.; Al-Fawwaz, A.; Ali, B. F.; Geyer, A.; Harms, K.; Marsch, M.; Kruger, M.; Osman, H.; Azmi, M. N. *J. Fluoresc.* **2018**, *28*, 655–662.

[4] (a) Motati, D.R.; Amaradhi, R.; Ganesh, T. *Org. Chem. Front.* **2021**, *8*, 466–513. (b) Gordon, G.M.; Lagier, A.J.; Ponchel, C.; Bauskar, A.; Itakura, T.; Jeong, S.; Patel, N.; Fini, M. E. *Wound Repair Regen.* **2016**, *24*, 89–99. (c) Yu, M.; Ken, J.; Wang, Y.; Zhu, J.; Kayser, F.; Medina, J.C.; Siegler, K.; Conn, M.; Shan, B.; Grillo, M.P.; Coward, P.; Liu, J. *Bioorg. Med. Chem. Lett.* **2014**, *24*, 156–160. (d) Zhao, X.Z.; Maddali, K.; Metifiot, M.; Smith, S. J.; Vu, B. C.; Marchand, C.; Hughes, S. H.; Pommier, Y.; Burke, T. R. *Bioorg. Med. Chem. Lett.* **2011**, *21*, 2986–2990. (e) Collier, P.N.; Panchagnula, A.; O′Dowd, H.; Le Tiran, A.; Aronov, A.M. *ACS Med. Chem. Lett.* **2019**, *10*, 117–120.

[5] (a) Rakshit, A.; Kumar, P.; Alam, T.; Dhara, H.; Patel, B. K. *J. Org. Chem.* **2020**, *85*, 12482–12504. (b) Hantzsch, A. *Ber. Dtsch. Chem. Ges.* **1881**, *14*, 1637–1638. (c) Kröhnke, F. *Synthesis* **1976**, 1–24.

[6] (a) Knorr, L. *Ber. Dtsch. Chem. Ges.* **1884**, *17*, 1635-1642. (b) Paal, C. *Ber. Dtsch. Chem. Ges.* **1885**, *18*, 367–371. (c) Hantzsch, A. *Ber. Dtsch. Chem. Ges.* **1890**, *23*, 1474–1476. (d) Amarnath, V.; Amamath, K. *J. Org. Chem.* **1995**, *60*, 301–307. (e) Minetto, G.; Raveglia, L. F.; Sega, A.; Taddei, M. *Eur. J. Org. Chem.* **2005**, 5277–5288.

[7] (a) Arcadi, A.; Cacchi, S.; Di Giuseppe, S.; Fabrizi, G.; Marinelli, F. *Org. Lett.* **2002**, *4*, 2409–2412. (b) Bossharth, E.; Desbordes, P.; Monteiro, N.; Balme, G. *Org. Lett.* **2003**, *5*, 2441–2444. (d) de los Ríos, C.; Marco, J. L.; Carreiras, M. D. C.; Chinchón, P. M.; García, A. G.; Villarroya, M. *Bioorg. Med. Chem.* **2002**, *10*, 2077–2088. (e) Denisenko, A. V.; Tverdokhlebov, A. V.; Tolmachev, A. A.; Volovenko, Y. M.; Shishkina, S. V.; Shishkin, O. V. *Synthesis* **2010**, *6*, 1009–1013.

[8] (a) Song, J. J.; Reeves, J. T.; Gallou, F.; Tan, Z.; Yee, N. K.; Senanayake, C. H. *Chem. Soc. Rev.* **2007**, *36*, 1120–1132. (b) Motati, D. R.; Amaradhi, R.; Ganesh, T. *Org. Chem. Front.* **2021**, *8*, 466–513. (c) Mérour, J.-Y.; Routier, S.; Suzenet, F.; Joseph, B. *Tetrahedron* **2013**, *69*, 4767–4834. (d) De Rosa, M.; Arnold, D.; Hartline, D.; Truong, L.; Verner, R.; Wang, T.; Westin, C. *J. Org. Chem.* **2015**, *80*, 12288–12299.

[9] (a) Rakshit, A.; Dhara, H. N.; Sahoo, A. K.; Patel, B. K. *Chem. - Asian J.* **2022**, *17*, e202200792. (b) Rakshit, A.; Dhara, H. N.; Sahoo, A. K.; Alam, T.; Patel, B. K. *Org. Lett.* **2022**, *24*, 3741–3746. (c) Rakshit, A.; Sau, P.; Ghosh, S.; Patel, B. K. *Adv. Synth. Catal.* **2019**, *361*, 3824–3836. (d) Varela, J. A.; Saá, C. *Chem. Rev.* **2003**, *103*, 3787–3801. (e) Dhara, H. N.; Rakshit, A.; Alam, T.; Patel, B. K. *Org. Biomol. Chem.* **2022**, *20*, 4243–4277. (f) Dhara, H. N.; Rakshit, A.; Alam, T.; Sahoo, A. K.; Patel, B. K. *Org. Lett.* **2023**, *25*, 471–476. (g) Maiti, S.; Li, Y.; Sasmal, S.; Guin, S.; Bhattacharya, T.; Lahiri, G. K.; Paton, R. S.; Maiti, D. *Nat. Commun.* **2022**, *13*, 3963–3972. (h) Wan, L.; Dastbaravardeh, N.; Li, G.; Yu, J.-Q. *J. Am. Chem. Soc.* **2013**, *135*, 18056–18059. (i) Dhara, H. N.; Rakshit, A.; Barik, D.; Ghosh, K.; Patel, B. K. *Chem. Commun.* **2023**, *59*, 7990–7993. (j) Dhara, H. N.; Das, B.; Barik, D.; Manna, S.; Patel, B. K. *Org. Lett.* **2023**, *25*, 9070–9075.

[10] (a) Zhou, Y.; Zhou, L.; Jesikiewicz, L. T.; Liu, P.; Buchwald, S. L. *J. Am. Chem. Soc.* **2020**, *142*, 9908–9914. (b) Li, D.-A.; He, X.-H.; Tang, X.; Wu, Y.; Zhao, H.; He, G.; Peng, C.; Han, B.; Zhan, G. *Org. Lett.* **2022**, *24*, 6197–6201. (c) Su, L.; Xie, S.; Dong, J.; Liu, F.; Yin, S.-F.; Zhou, Y. *Org. Lett.* **2022**, *24*, 5994–5999. (d) Huvelle, S.; Matton, P.; Tran, C.; Rager, M.-N.; Haddad, M.; Ratovelomanana-Vidal, V. *Org. Lett.* **2022**, *24*, 5126–5131. (e) Hu, X.; Xie, X.; Gan, Y.; Wang, G.; Liu, Y. *Org. Lett.* **2021**, *23*, 1296–1301. (f) Bian, Q.; Wu, C.; Yuan, J.; Shi, Z.; Ding, T.; Huang, Y.; Xu, H.; Xu, Y. *J. Org. Chem.* **2020**, *85*, 4058–4066. (g) Takahashi, T.; Tsai, F.-Y.; Li, Y.; Wang, H.; Kondo, Y.; Yamanaka, M.; Nakajima, K.; Kotora, M. *J. Am. Chem. Soc.* **2002**, *124*, 5059–5067.

[11] (a) Tian, Q.; Pletnev, A. A.; Larock, R. C. *J. Org. Chem.* **2003**, *68*, 339–347.

[12] Miura, T.; Murakami, M. *Org. Lett.* 2005, *7*, 3339–3341.

[13] McCormick, M. M.; Duong, H. A.; Zuo, G.; Louie, J. *J. Am. Chem. Soc.* **2005**, *127*, 5030–5031.

[14] Wang, C.-S.; Sun, Q.; García, F.; Wang, C.; Yoshikai, N. *Angew. Chem., Int. Ed.* **2021**, *60*, 9627–9634.

[15] (a) Liu, J.; Zhu, L.; Wan, W.; Huang, X. *Org. Lett*. **2020**, *22*, 3279–3285. (b) Li, Z.; Ling, F.; Cheng, D.; Ma, C. *Org. Lett*. **2014**, *16*, 1822–1825. (c) Fumagalli, F.; da Silva Emery, F. *J. Org. Chem*. **2016**, *81*, 10339–10347. (d) Wan, Y.; Zheng, X.; Ma, C. *Angew. Chem., Int. Ed*. **2018**, *57*, 5482–5486. (e) Agasti, S.; Pal, T.; Achar, T. K.; Maiti, S.; Pal, D.; Mandal, S.; Daud, K.; Lahiri, G. K.; Maiti, D. *Angew. Chem., Int. Ed*. **2019**, *58*, 11039–11043.

[16] Cailly, T.; Lemaître, S.; Fabis, F.; Rault, S. *Synthesis*. **2007**, *20*, 3247–3251.

[17] Cartwright, M. W.; Parks, E. L.; Pattison, G.; Slater, R.; Sandford, G.; Wilson, I.; Yufit, D. S.; Howard, J. A. K.; Christopher, J. A.; Miller, D. D. *Tetrahedron*. **2010**, *66*, 3222–3227.

[18] (a) Zhao, S.-B.; Wang, S. *Chem. Soc. Rev.* **2010**, *39*, 3142–3156. (b) Cash, M. T.; Schreiner, P. R.; Phillips, R. S. *Org. Biomol. Chem.* **2005**, *3*, 3701–3706. (c) Zhang, Y.-P.; You, Y.; Zhao, J.-Q.; Zhou, X.-J.; Zhang, X.-M.; Xu, X.-Y.; Yuan, W.-C. *Org. Chem. Front.* **2019**, *6*, 1879–1884. (d) Meanwell, N. A.; Krystal, M. R.; Nowicka-Sans, B.;

Langley, D. R.; Conlon, D. A.; Eastgate, M. D.; Grasela, D. M.; Timmins, P.; Wang, T.; Kadow, J. F. *J. Med. Chem.* **2018**, *61*, 62−80.

[19] (a) Cincinelli, R.; Musso, L.; Merlini, L.; Giannini, G.; Vesci, L.; Milazzo, F. M.; Carenini, N.; Perego, P.; Penco, S.; Artali, R.; Zunino, F.; Pisano, C.; Dallavalle, S. *Bioorg. Med. Chem.* **2014**, *22*, 1089−1103. (b) Esteve, C.; Gonzalez, J.; Gual, S.; Vidal, L.; Alzina, S.; Sentellas, S.; Jover, I.; Horrillo, R.; De Alba, J.; Miralpeix, M.; Tarrason, G.; Vidal, B. *Bioorg. Med. Chem. Lett.* **2015**, *25*, 1217−1222. (c) Feneyrolles, C.; Guiet, L.; Singer, M.; Van Hijfte, N.; Dayde-Cazals, B.; Fauvel, B.; Cheve, G.; Yasri, A. *Bioorg. Med. Chem. Lett.* **2017**, *27*, 862−866.

[20] Calvet, G.; Livecchi, M.; Schmidt, F. *J. Org. Chem.* **2011**, *76*, 4734−4740.

[21] Sung, N.-D.; Yang, O.-K.; Kang, S. S.; Yum, E. K. *Bull. Korean Chem. Soc.* **2004**, *25*, 1351.

[22] Shumaila, A. M. A.; Puranik, V. G.; Kusurkar, R. S. *Tetrahedron* **2011**, *67*, 936−942.

[23] Chen, X.; Sun, P.; Mo, B.; Chen, C.; Peng, J. *J. Org. Chem.* **2021**, *86*, 352−366.

[24] (a) Sahoo, A. K.; Rakshit, A.; Dahiya, A.; Pan, A.; Patel, B. K. *Org. Lett.* **2022**, *24*, 1918−1923. (b) Abdelhamid, A. O.; Negm, A. M.; Abbas, I. M. *J. Prakt. Chem.* **1989**, *331*, 31−36. (c) Al-Mousawi, S. M.; Moustafa, M. S.; Meier, H.; Kolshorn, H.; Elnagdi, M. H. *Molecules* **2009**, *14*, 798−806.

[25] (a) Paixão, D. B.; Rampon, D. S.; Salles, H. D.; Soares, E. G. O.; Bilheri, F. N.; Schneider, P. H. *J. Org. Chem.* **2020**, *85*, 12922−12934. (b) Zhang, S.; Liu, X.; Wanga, T. *Adv. Synth. Catal.* **2011**, *353*, 1463−1466. (c) Sontakke, G. S.; Ghosh, C.; Pal, K.; Volla, C. M. R. *J. Org. Chem.* **2022**, *87*, 14103−14114. (d) Zatolochnaya, O. V.; Gevorgyan, V. *Org. Lett.* **2013**, *15*, 2562−2565.

भारतीय प्रौद्योगिकी संस्थान गुवाहाटी
Indian Institute of Technology Guwahati

CHAPTER V

Visible-Light Driven Electron-Donor-Acceptor (EDA) Complex Initiated Synthesis of Thio-functionalized Pyridines

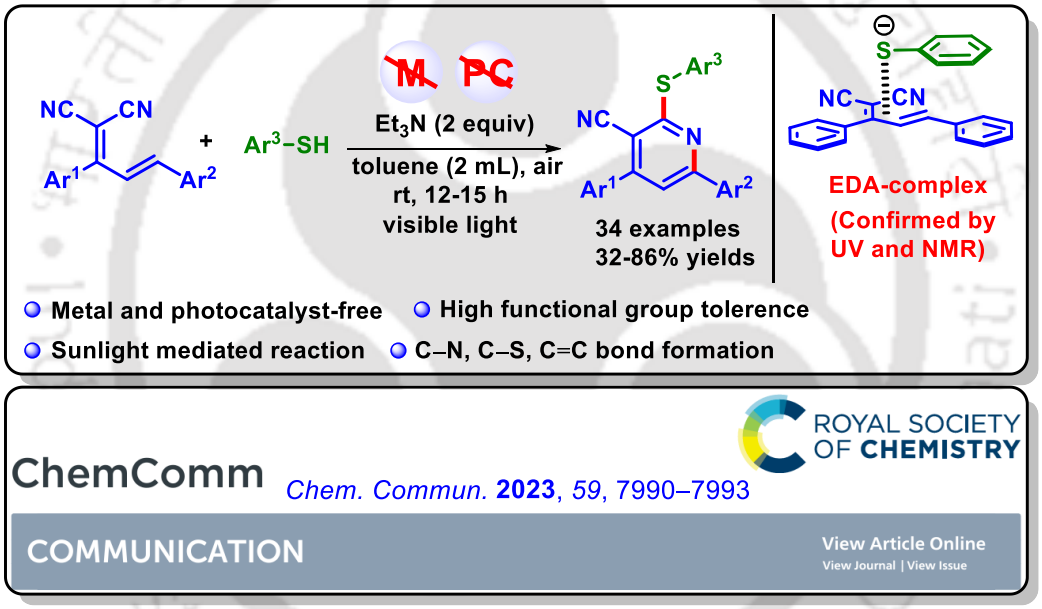

ABSTRACT: A visible/solar-light-induced electron-donor-acceptor (EDA) aggregated/mediated radical cyclization between (*E*)-2-(1,3-diarylallylidene)malononitriles and thiophenols lead to poly-functionalized pyridines. The two reacting partners form an EDA complex that absorbs light and triggers the single-electron transfer (SET) to generate thiol radical which undergoes addition/cyclization with dicyanodiene through the formation of C–S and C–N bonds.

भारतीय प्रौद्योगिकी संस्थान गुवाहाटी
Indian Institute of Technology Guwahati

CHAPTER V

Visible-Light Driven Electron-Donor-Acceptor (EDA) Complex Initiated Synthesis of Thio-functionalized Pyridines

V.1. Introduction:

The advancement of photochemical strategies by virtue of the single-electron transfer (SET) process to build molecular complexity is a sustainable approach because of their simplicity, efficiency, non-requirement of photosensitizer, and unique mode of activation.[1] However, due to the weak absorption of visible light, most of these transformations require the assistance of a transition-metal photocatalyst or an organic dye as the photosensitizer.[2] But in recent years, there has been an upsurge in organic photoreactions which expunge the use of exogenous photosensitizers.[3] In this context, any synthesis accomplished by an electron donor-acceptor (EDA)-complex brings a remarkable renaissance in the field of visible-light-driven radical chemistry.[4] Usually, most electron-rich and electron-deficient reacting partners do not absorb visible light individually. However, when they interact, a ground-state EDA complex results which absorbs the visible light and undergoes a SET process from the donor (D) to the acceptor (A), producing a charge-separated state and eliminating the necessity for any external photocatalyst.

If the electron transfer process has a sufficiently long lifetime, the charge-separated species can react through the *in situ* generation of reactive radical species. Generally, the formation of an EDA complex is via non-bonding interactions which show characteristic weak absorption or a charge-transfer band in the absorption spectrum.[4a] Although long ago in 1952, a quantum-mechanical theory was proposed by Mulliken for the formation of a colored EDA complex. Most of the pioneering work related to EDA complex photochemistry has traditionally been explored very recently. Some groups have developed this chemistry using readily accessible feedstocks for the atom-economical construction of diverse complex molecules through the formation of C–C, and C–heteroatom bonds.[4] Because of the easy generation of thiophenolate, it is a convenient donor forming EDA complex with various acceptors promoting a variety of photochemical reactions.[4a–f] For example, in 2021, Xia *et al.* reported a metal-free thiolation of C(sp^3)–H bond of ethereal,

allylic, and benzylic substrates through a photoexcited thiophenolate anion and iodobenzene EDA complex.[4a] Recently, Liu and co-workers developed a visible-light-driven synthesis of β-hydroxysulfides via the formation of an EDA complex using thiophenolate anion and alkene.[4b]

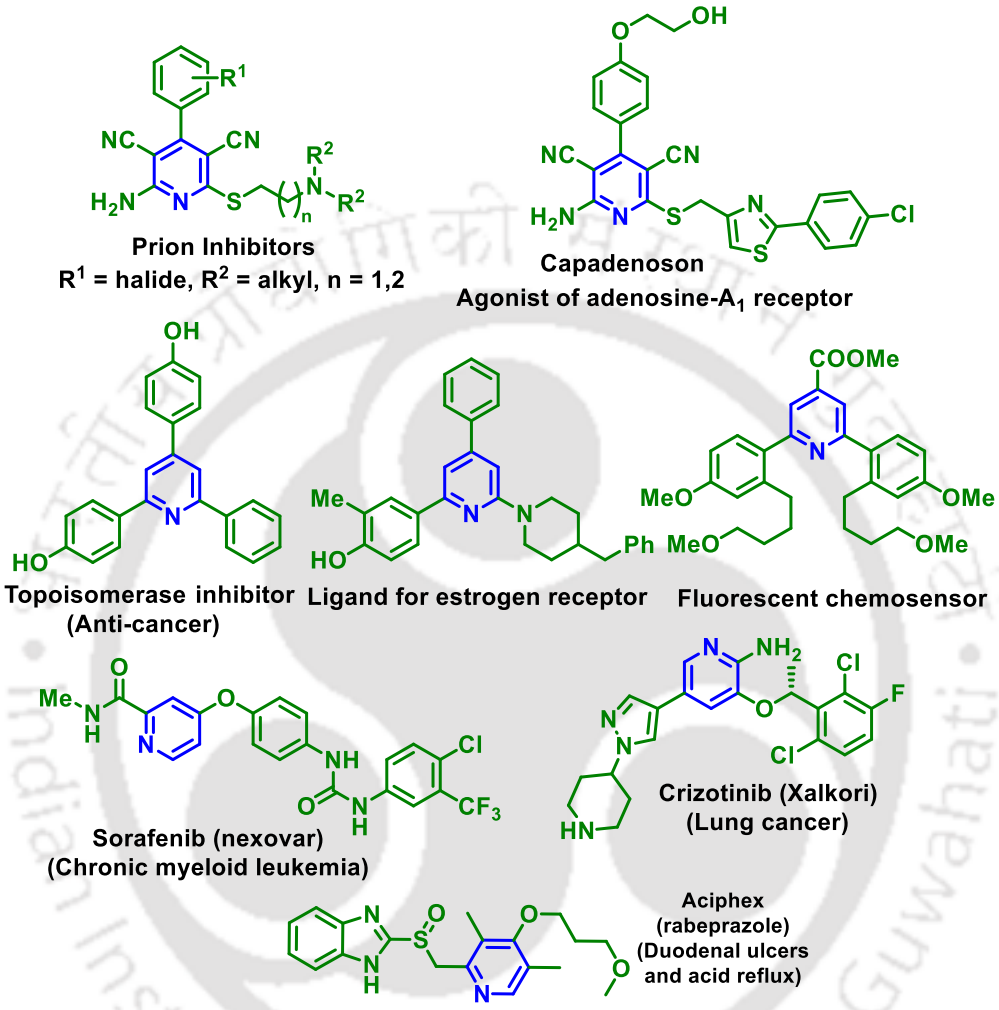

Figure V.1.1. *A few bio-active pyridine-containing drugs.*

Among the *N*-heterocycles, substituted pyridines have attracted the attention of synthetic chemists because of their biological activity and application in material sciences (Figure V.1.1)[5]. Although, several methods *viz*. Kröhnke, Hantzsch synthesis has been well documented in the literature[6] but still, there is a continuous thirst for highly efficient strategies to create this heterocyclic core. Owing to the presence of polar unsaturated –C≡N bond, the nitrile functionality has efficiently triggered the formation of pyridines and various *N*-heterocycles through cycloadditions or nucleophilic cascade processes.[7] Various groups have sporadically reported the

transition-metal-catalyzed (Ir, Fe, Co, Ru, Ni) [2 + 2 + 2] cycloaddition between nitriles and alkynes for the synthesis of highly functionalized pyridines [Scheme V.1.1 (i)].[8] In 2020, Chen and co-workers utilized the nitrile functionality to synthesize pyridines via transition-metal-catalyzed [Ni(II) and Pd(II)] addition of aryl boronic acid under thermal conditions [Scheme V.1.1 (ii)].[9] Our group also developed a Pd(II)-catalyzed addition of arylboronic acid to nitrile under a photochemical process. We have also successfully developed the synthesis of 3-cyanopyridines from γ-ketodinitriles and dicyanodienes under visible light irradiation without using any exogenous photosensitizer [Scheme V.1.1 (iii)].[10]

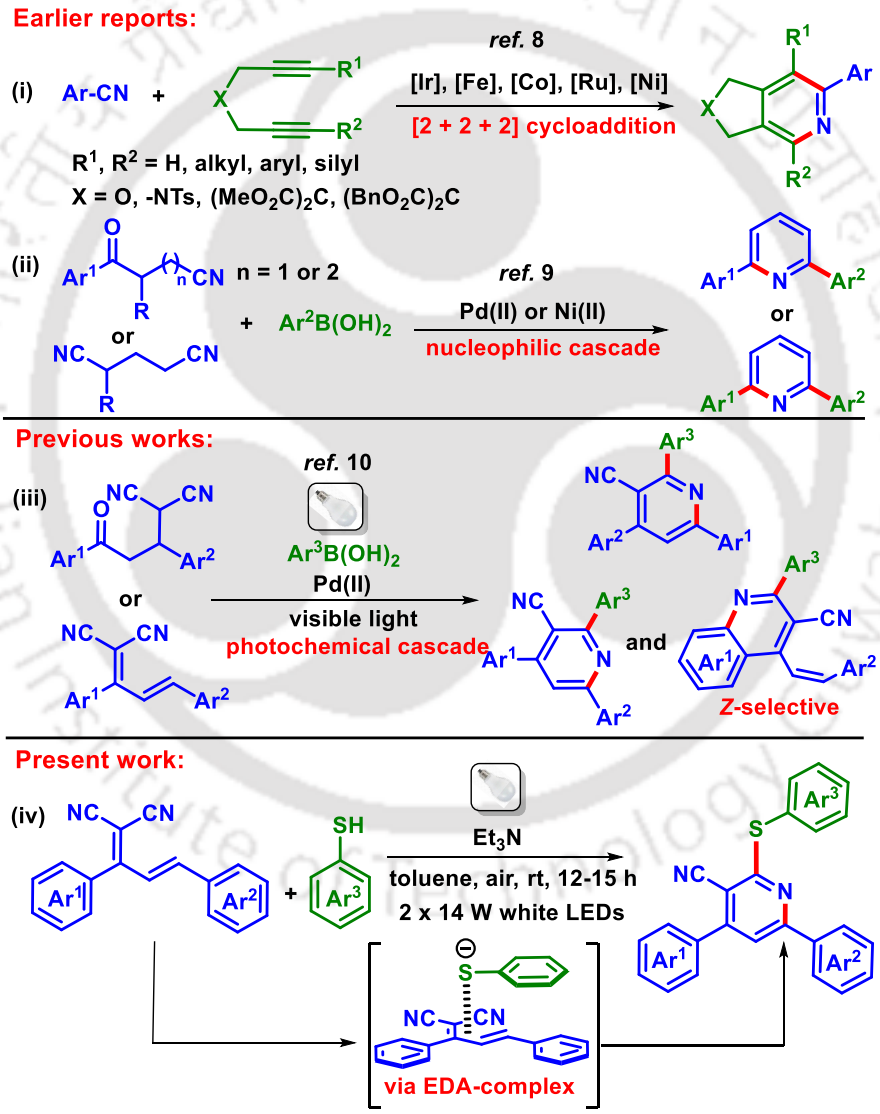

Scheme V.1.1. *Different approach for the synthesis of functionalized pyridines.*

Furthermore, the radical acceptability of the nitrile group has also been thoroughly investigated under visible-light irradiation in the presence of a suitable photocatalyst.[11] In this regard, thiophenol plays a vital radical source via the SET process to achieve thio-functionalized *N*-heterocycles.[11c-d,12] Inspired by this, our group reported the synthesis of thio-functionalized pyrroles and pyridines from β- and γ-ketodinitriles respectively using Eosin Y as an effective photocatalyst under green light irradiation.[11c-d]

Our continuous contribution in nitrile-triggered reactions to access various heterocycles[10,13] and taking cues from the previous literature reports, now we envision the synthesis of tetrasubstituted pyridines under metal- and photocatalyst-free conditions. Therefore, herein we disclose a visible-light-induced synthesis of thio-functionalized pyridine from (*E*)-2-(1,3-diphenylallylidene)malononitrile (**1**) and thiophenol (**a**) via the formation of an electron-donor-acceptor (EDA) complex. After a series of optimization, the best protocol was found to be the use of (*E*)-2-(1,3-diphenylallylidene)malononitrile (**1**, 0.25 mmol) and thiophenol (**a**, 0.75 mmol), Et_3N (0.5 mmol) in toluene (2 mL) in the air at room temperature for 12 h (Table V.3.1, entry 1).

V.2. Strategies for the Synthesis of Thio-functionalized Pyridines:

Owing to the several multifaceted applications of thio-functionalized pyridines, synthetic chemists have long endeavored to discover various pathways to achieve these important structural motifs. Several methods have been developed for the synthesis of thio-pyridine. For example, Zhao's group established a multi-component synthesis of 2-amino-3,5-dicarbonitrile-6-thio-pyridines using aldehydes, malononitrile, and thiophenols in the presence of a Zn(II) or Cd(II) metal-organic framework (MOF) as the heterogeneous catalyst (Scheme V.2.1).[14a] This reaction does not require any organic solvent, offering a convenient and green approach for synthesizing biologically significant 6-(alkylthio)-2-amino-pyridine-3,5-dicarbonitrile derivatives.

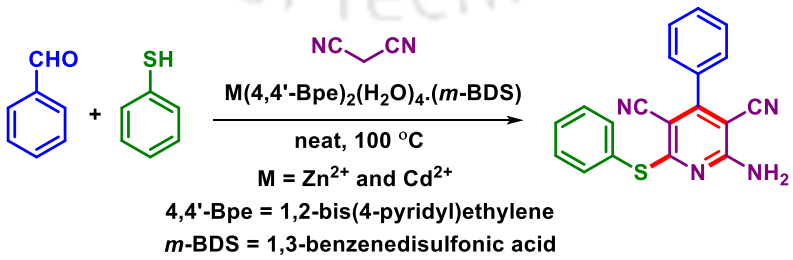

Scheme V.2.1. *Multi-component synthesis of thio-pyridine.*

Similarly, Sobhani's group developed a one-pot, three-component reaction of aryl/heteroaryl/alkyl aldehydes with aryl/alkyl thiols and malononitrile to synthesize thio-functionalized pyridines at room temperature (Scheme V.2.2).[14b] The reaction is promoted by 2-hydroxyethylammonium acetate (2-HEAA) as a task-specific ionic liquid, facilitating dual activation of substrates.

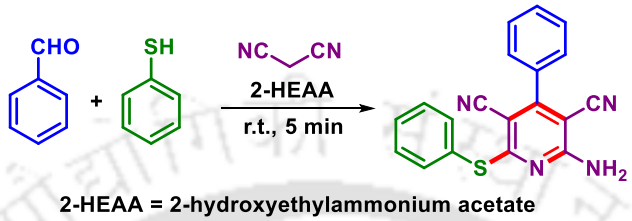

Scheme V.2.2. *Synthesis of thio-pyridine in the presence of 2HEAA.*

Sinha *et al.* developed a Montmorillonite K-10 clay-catalyzed one-pot, multicomponent condensation of aldehydes, malononitrile, and thiophenol, which afforded 2-amino-3,5-dicarbonitrile-6-thiopyridines in good to excellent yields (Scheme V.2.3).[14c] This protocol demonstrated that the product yield remained unaffected even after recycling the catalyst three times.

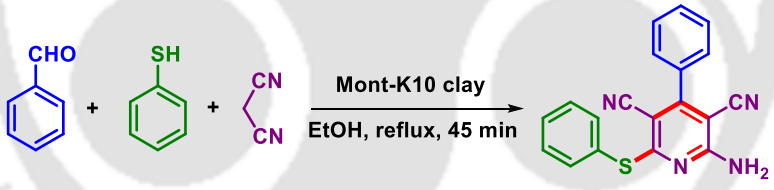

Scheme V.2.3. *Mont K-10 clay-catalyzed synthesis of thio-pyridine.*

In 2018, Shtyrlin's group achieved a base-mediated three-component reaction involving an aldehyde derivative of pyridoxine, malononitrile, and thiophenol (Scheme V.2.4).[14d] The results demonstrated the excellent potential of 2-amino-6-sulfanylpyridine-3,5-dicarbonitriles and 5-substituted pyridoxines (including their ammonium salts) for the design of novel pharmacological agents.

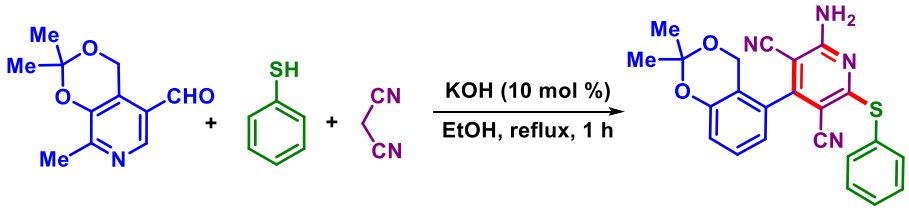

Scheme V.2.4. *Base-mediated synthesis of thio-functionalized pyridine.*

A few years back, Goswami and coworkers reported an efficient protocol for synthesizing 3-(2-thiopyridyl)indoles via a Ru(II)-catalyzed [2 + 2 + 2] cycloaddition reaction of α,ω-diynes with 3-thiocyanatoindoles under mild conditions (Scheme V.2.5).[14e] This atom-economical method provides efficient access to 3-(2-thiopyridyl)indole motifs, which have structural similarities to other pyridyl indole thioethers with potential medicinal importance.

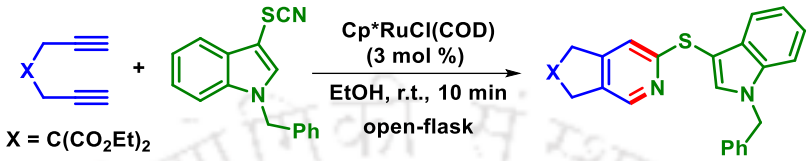

Scheme V.2.5. *Synthesis of thio-pyridine via [2 + 2 + 2] cycloaddition.*

Last year (2023), our group also developed a visible/solar-light-mediated synthesis of thio-functionalized pyridines using γ-ketodinitriles, thiophenol as coupling partners, and eosin Y as the photocatalyst (Scheme V.2.6).[14f] The reaction proceeds through *in situ* generation of a thiyl radical which selectively participated in radical cyclization with one of the nitrile groups to afford the thiopyridine as the product.

Scheme V.2.6. *Visible-light mediated synthesis of thio-pyridine.*

Recently, Dashyan's group developed a two-step method for constructing thio-functionalized pyridines (Scheme V.2.7).[14g] In the first step, 2-cyano-3-phenyl-2-butenoic acid ethyl ester was reacted with carbon disulfide in the presence of triethylamine in ethanol at room temperature to yield 6-amino-4-phenyl-2-thio-2*H*-thiopyran-5-carboxylic acid ethyl ester. In the second step, this thiopyran underwent a reaction with morpholine to produce ethyl 6-morpholin-4-yl-4-phenyl-2-thioxo-1,2-dihydropyridine-3-carboxylate.

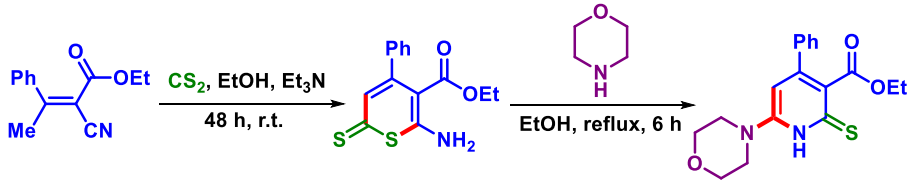

Scheme V.2.7. *Two-step method for synthesis of multi-substituted thio-pyridine.*

V.3. Present Work:

V.3.1. Optimization of the Reaction Conditions:

Initially, we selected (*E*)-2-(1,3-diphenylallylidene)malononitrile (**1**) and thiophenol (**a**) as the model substrates to explore the optimal reaction conditions for the formation of 4,6-diphenyl-2-(phenylthio)nicotinonitrile (**1a**) (Table V.3.1). To our delight, when a mixture of **1** (0.25 mmol), **a** (0.75 mmol, 76 μL), and Et_3N (2.0 equiv, 0.5 mmol, 70 μL) in toluene (2 mL) was irradiated with visible light [2 x 14 W white LEDs (flux 46 mW/cm^2)] at room temperature for12 h, it delivers the desired product **1a** in 86% isolated yield (Table V.3.1, entry 1). The use of other solvents such as 1,2-dichloroethane (DCE) (65%), CH_3CN (27%), 2,2,2-trifluoroethanol (TFE) (53%), MeOH (63%), and DMSO (52%) resulted in lower yields (Table V.3.1, entry 2). The reaction with inorganic bases *viz.* K_2CO_3 (trace), and KOAc (00%) didn't give the product whereas organic bases such as DBU (50%), DABCO (62%), and DIPEA (81%) failed to improve the yield (Table V.3.1, entry 3). Inorganic bases such as K_2CO_3 and KOAc being ionic in nature are insoluble in non-polar solvents such as toluene. Thus, the reaction medium is non-homogeneous and sufficiently basic to be able to deprotonate thiophenol to generate a thiophenolate anion which is necessary for the formation of the EDA complex. Next to confirm the role of the base this reaction was carried out in the absence of Et_3N (Table V.3.1, entry 4). A sharp decrease in the yield (10%), suggested base is necessary for this protocol. Further, no improvement in the yield (83%) was observed when the reaction was carried out with an increasing amount (3 equiv) of Et_3N (Table V.3.1, entry 5). Next, to investigate the role of air (O_2) a reaction was carried out under a nitrogen atmosphere (Table V.3.1, entry 6). The yield (13%) of product **1a** drops sharply, indicating that air (O_2) was critical for this cyclization. The reaction was also carried out under O_2 atmosphere which gave 87% yield of the product, suggesting an essential role of O_2 (Table V.3.1, entry 7). Further, the reaction in the absence of light produces **1a** with a very low yield (16%), suggesting the essential role of light in this transformation (Table V.3.1, entry 8). The reaction was also tested with light sources of different wavelengths such as green LEDs (513 nm) and blue LEDs (432 nm). Unfortunately, both light sources failed to improve the yield of **1a** (Table V.3.1, entry 9). So, the best-optimized conditions for this protocol were found to be the use of (*E*)-2-(1,3-diphenylallylidene)malononitrile (**1**, 0.25 mmol) and thiophenol (**a**, 0.75 mmol, 76 μL), Et_3N (0.5 mmol, 70 μL) in toluene (2 mL) in the presence of an aerial atmosphere at room temperature for 12 h.

Table V.3.1. *Optimization of the reaction conditions*

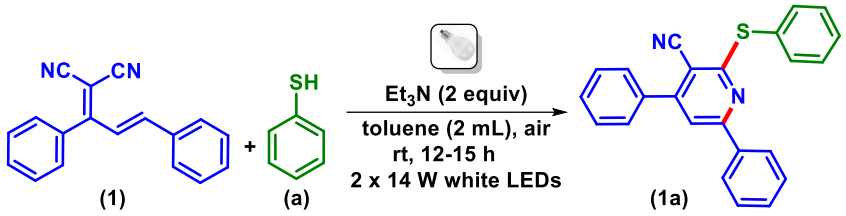

Entry	Variation from the standard condition	% yield of **1a**
1	None	86
2	DCE, CH_3CN, TFE, MeOH, DMSO instead of toluene	65, 27, 53, 63, 52
3	K_2CO_3, KOAc, DBU, DABCO, DIPEA instead of Et_3N	trace, 00, 50, 62, 81
4	Without Et_3N	10
5	3 equiv of Et_3N instead of 2 equiv of Et_3N	83
6	N_2 instead of air	13
7	O_2 instead of air	87
8	Without light	16
9	Green LEDs, blue LEDs instead of white LEDs	70, 67

V.3.2. Substrates Scopes of (*E*)-2-(1,3-diarylallylidene)malononitrile:

Having the optimized conditions, the scope and generality of this cyclization in different dicyanodienes containing electron-donating groups (EDGs) and electron-withdrawing groups (EWGs) were examined (Scheme V.3.2.1). The unsubstituted dicyanodiene (**1**) reacted with thiophenol (**a**) to afford the 4,6-diphenyl-2-(phenylthio)nicotinonitrile (**1a**) in 86% yield. The Ar^1 ring having EDGs such as *p*-Me (**2**), *p*-OMe (**3**), and EWGs *viz*. *p*-F (**4**), *p*-Cl (**5**), *p*-Br (**6**), and *o*-Br (**7**) substituents reacted with thiophenol (**a**) to give their corresponding thiopyridines (**2a**, 78%), (**3a**, 76%), (**4a**, 75%), (**5a**, 81%), (**6a**, 74%) and (**7a**, 72%) in moderate to good yields. Similarly, the Ar^2 ring of (*E*)-2-(1,3-diphenylallylidene)malononitriles bearing EDGs *p*-Me (**8**), *p*-OMe (**9**) *p*-^{t}Bu (**10**) and EWGs *p*-F (**11**) *p*-Cl (**12**) substituents reacted smoothly with (**a**) to afford corresponding nicotinonitriles (**8a**, 78%), (**9a**, 76%), (**10a**, 72%), (**11a**, 73%) and (**12a**, 77%), respectively. Dicyanodiene containing dioxolane ring (**13**) also smoothly takes part in this reaction to give pyridine (**13a**, 74%) yield.

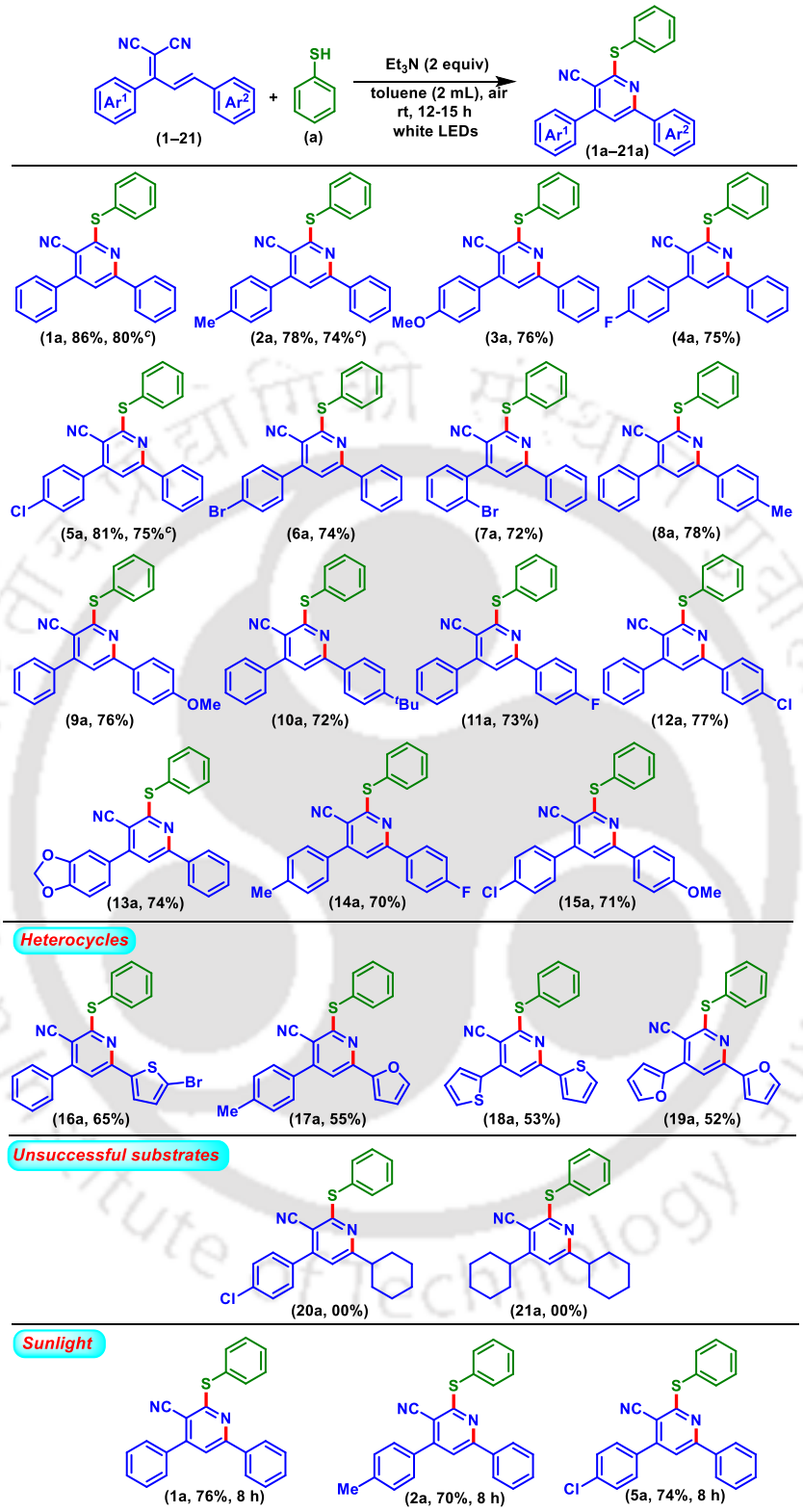

[a]Reaction conditions: (**1–21**) (0.25 mmol), **a** (0.75 mmol), Et_3N (0.5 mmol), and toluene (2 mL) at rt for 12–15 h in air under two 14 W white LEDs. [b]Isolated yields. [c]Reaction performed on a 5 mmol scale.

Scheme V.3.2.1. *Substrate scope of dicyanodienes.*[a,b,c]

The protocol was further tested with dicyanodiene having various combinations of EDGs/EWGs in both Ar^1 and Ar^2 rings such as *p*-Me/*p*-F (**14**) and *p*-Cl/*p*-OMe (**15**) with (**a**) yielded their respective cyanopyridines (**14a**, 70%) and (**15a**, 71%). Furthermore, the reaction is tested with mono-heterocyclic (**16** and **17**) and di-heterocyclic thiophene (**18**) and furan (**19**) containing dicyanodienes delivered the corresponding thiopyridines (**16a**, 65% and **17a**, 55%), and (**18a**, 53% and **19a**, 52%) respectively. In lieu of the phenyl-substituted substrates, alkyl-substituted dicyanodienes such as (**20**) and (**21**) both failed to react with thiophenol (**a**), which is perhaps due to their inability to form EDA complex. Next, as a more common and clean green light source, we have attempted this protocol under the sunlight taking dicyanodienes, **1**, **2**, and **5** with thiophenol (**a**). To our delight, the corresponding thio-functionalized pyridines (**1a**, 76%), (**2a**, 70%), and (**5a**, 74%) are obtained in good yields in 8 h. The yield obtained was 8–10% lower as the exposure time in sunlight was only 8 h compared to 12 h exposure time for white LED mediated reaction.

V.3.3. Substrates Scopes of Thiophenol:

The scope of this photochemical reaction was further evaluated with dicyanodiene (**1**) and various thiophenols (**b**–**q**) (Scheme V.3.3.1). Thiophenols possessing EDGs such as *p*-Me (**b**), *o*-Me (**c**), *p*-OMe (**d**), and *m*-OMe (**e**) responded positively affording respective cyanopyridines (**1b**, 78%), (**1c**, 74%), (**1d**, 76%), and (**1e**, 69%) in good yields. Thiophenols containing EWGs such as *p*-F (**f**), *m*-F (**g**), *p*-Cl (**h**), *m*-Cl (**i**), and *o*-Br (**j**) all experienced efficient cyclization with (**1**) to afford desired cyanopyridines (**1f**–**1j)** in moderate to good yields (64%–73%). This photochemical approach with poly-aromatic thiophenol *viz*. 2-naphthylthiol (**k**) successfully provided thiocyanopyridine (**1k**) in 80% yield. Further, the reaction was also tested with heterocyclic thiols such as 2-thiophene thiol (**l**) and pyridine-4-thiol (**m**) giving the product (**1l**, 71%) and (**2m**, 32%), respectively. The pyridine ring being electron-deficient is unable to form the EDA complex efficiently with (**2**), thereby giving a lower yield. The protocol was also effective for aliphatic thiophenols such as *p*-Cl benzyl mercaptan (**n**), and benzyl mercaptan (**o**), successfully giving the products (**1n**, 64%) (**2n**, 62%), and (**6o**, 52%), respectively. Whereas other aliphatic thiophenols *viz*. cyclohexyl (**p**) and *n*-butyl (**q**) failed to give the corresponding thiopyridines. The failure of these alkyl thiols is possibly due to their inability to form EDA complex and the subsequent thiol radical.[4b,c] Further, the dicyanodiene, **1** also reacted smoothly with *p*-Me (**b**) and *p*-F (**f**) substituted thiophenols to afford the pyridines (**1b**, 70%) and (**1f**, 61%), respectively under the sunlight in 8 h.

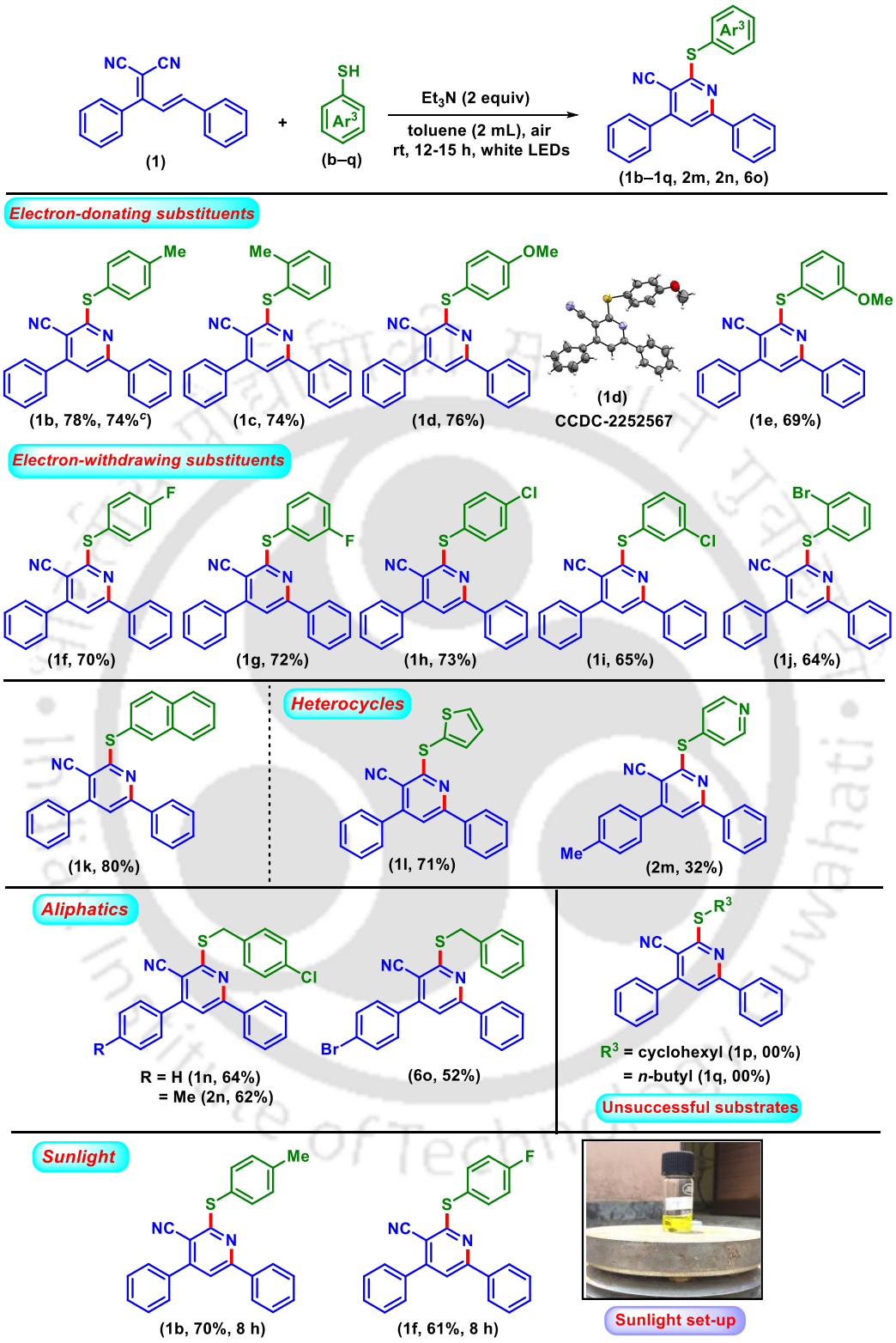

[a]Reaction conditions: **1** (0.25 mmol), **b–q** (0.75 mmol), Et_3N (0.5 mmol), and toluene (2 mL) at rt for 12–15 h in air. under two 14 W white LEDs. [b]Isolated yields. [c]Reaction performed on a 5 mmol scale.

Scheme V.3.3.1. *Substrate scope thiophenols.*[a,b,c]

V.4. Mechanistic Investigations:

V.4.1. Control Experiments:

A few experiments were conducted to depict a plausible mechanistic pathway. In the presence of 2,2,6,6-tetramethyl-1-piperidinyloxy (TEMPO) formation of **1a** sharply dropped, indicating a radical path. The detection of a TEMPO-thiophenol adduct (**X**) by HRMS analysis of the reaction aliquot further confirms the radical nature of the process (Scheme V.4.1.1a). The yield of **1a** decreases to 13% under the N_2 atmosphere, whereas it provided 87% yield under an O_2 atmosphere, suggesting the necessary role of air (O_2) (Scheme V.4.1.1b and Scheme V.4.1.1c).[4b]

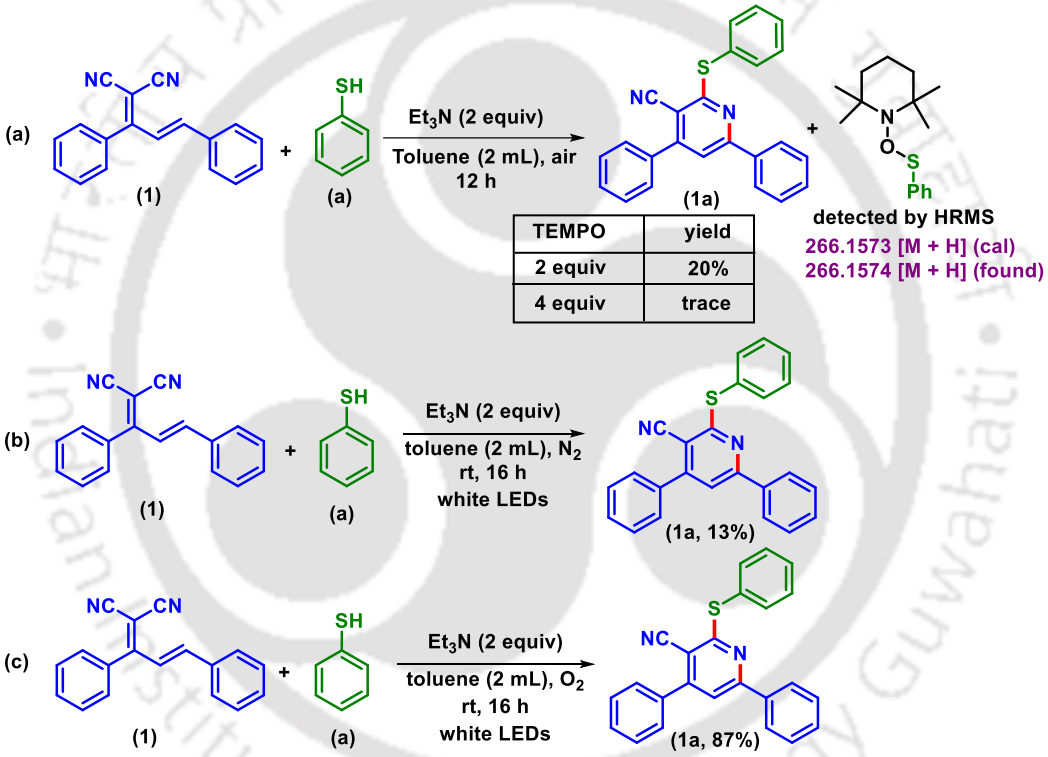

Scheme V.4.1.1. *Control experiments.*

Additionally, the necessity of visible light was confirmed by on/off experiments (Figure V.4.1.1a). The formation of EDA complex between (**1**), thiophenol (**a**), and Et_3N in toluene has been confirmed by the appearance of a light-yellow color upon mixing and a progressive red shift in the visible region (Figure V.4.1.1b).[4] A fluorescence quenching was performed taking dicyanodiene (**1**) as the probe and thiophenol (**a**) as the quencher. A decrease in the fluorescence intensity (λ_{max} = 432 nm) with an increase in the concentration of thiophenol (**a**) confirms the possible interaction between dicyanodiene (**1**) and thiophenol (**a**) (Figure V.4.1.1b and Figure

V.4.1.1c). To find further evidence for the EDA complex formation, ^{19}F nuclear magnetic resonance (^{19}F NMR) measurements were carried out between (*E*)-2-(1-(4-fluorophenyl)-3-phenylallylidene)malononitrile (**4**) and thiophenol (**a**).[4d,18] The chemical shift of the –F group of (**4**) distinctly moved downfield with increasing ratios of (**a**) and Et_3N (Figure V.4.1.1d and Figure V.4.1.1e). The binding constant (K_{EDA}) of the proposed EDA pair was determined using a spectrophotometric Benesi-Hilderbrand plot and was found to be 139.6 mM^{-1} (Figure V.6.7.1, for details, see section V.6.7).

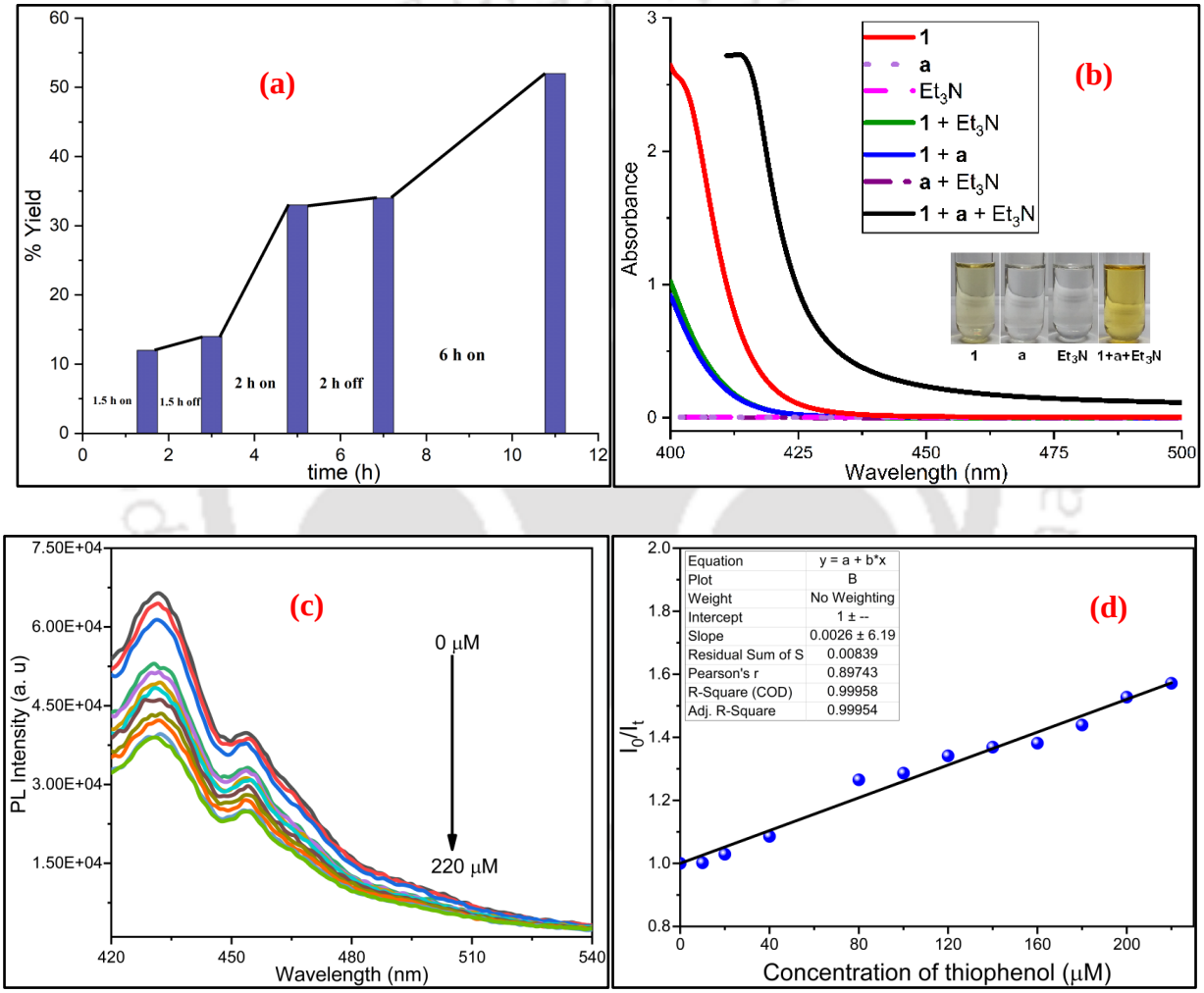

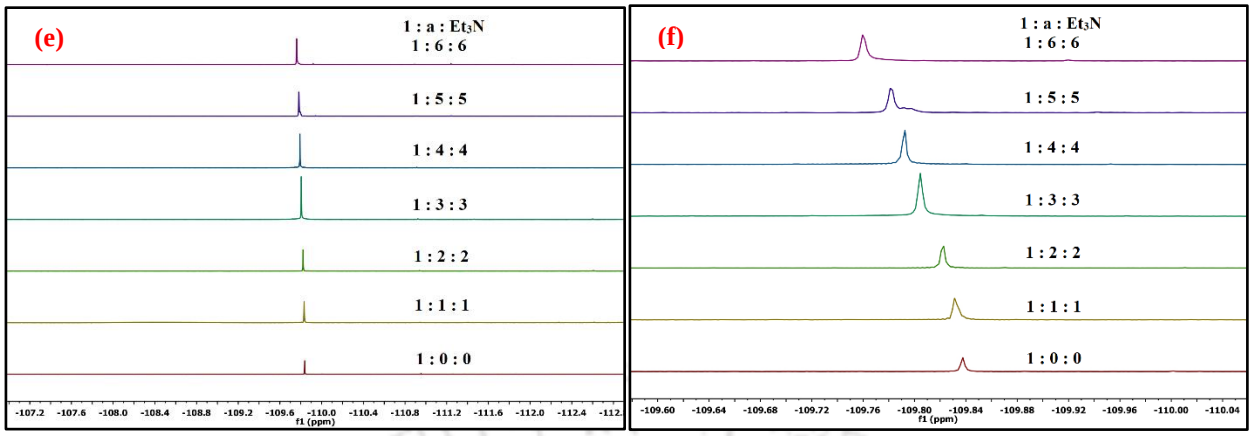

Figure V.4.1.1. *(a) Plot %yield vs time (hrs) for On-off experiments. (b) UV-vis spectra of EDA complex in toluene. (c) Fluorescence emission spectra of (**1**) at varied conc. of quencher thiophenol (**a**). (d) Stern-Volmer Plot. (e) ^{19}F-NMR of (E)-2-(1-(4-fluorophenyl)-3-phenylallylidene)malononitrile (**4**), thiophenol (**a**) and Et_3N with different ratios. (f) Evidence for the formation of the EDA complex through ^{19}F NMR.*

V.4.2. Plausible Reaction Mechanism:

Based on the above experimental results and previous reports a plausible mechanism is outlined in Scheme V.4.2.1.[4b] Initially, the thiolate ion (**A**) is formed in the presence of Et_3N, that interacts with the dicyanodienes (**1**) to generate an EDA complex (**B**), which exhibits strong absorption in the visible-light region (λ_{max} = 414 nm). Under visible-light irradiation, the EDA complex (**B**) is excited to complex (**B***) which transfers an electron to O_2 and generates a superoxide radical anion $O_2^{\bullet-}$ and a thiol radical (**C**) (detected from HRMS of its TEMPO-adduct). This radical anion $O_2^{\bullet-}$ reacts further with another molecule of thiophenol (**a**) to generate a thiolate anion (**A**) and $HO_2^{\bullet}$ radical.[4b] Next, the thiol radical (**C**) attacks one of the nitrile groups of **1** to produce an iminyl radical (**D**), which on intramolecular (6-*endo*-trig) cyclization generates a carbon-centered radical intermediate (**E**). The final product **1a** can be obtained by any of the two possible pathways. In path-i, aromatization of intermediate (**E**) through a proton abstraction by $HO_2^{\bullet}$ affords the thiopyridine **1a** (H_2O_2 detected by Mohr's salt).[15] In path-ii, the intermediate (**E**) reacts with the *in situ* generated $HO_2^{\bullet}$ radical to provide a hydroperoxide intermediate (**F**).[4b] This is then followed by cleavage of the peroxide bond and abstraction of a proton from thiophenol (**a**) to provide

intermediate (**G**).[4b] Finally, loss of water from intermediate **G** in the presence of the base leads to (**1a**).

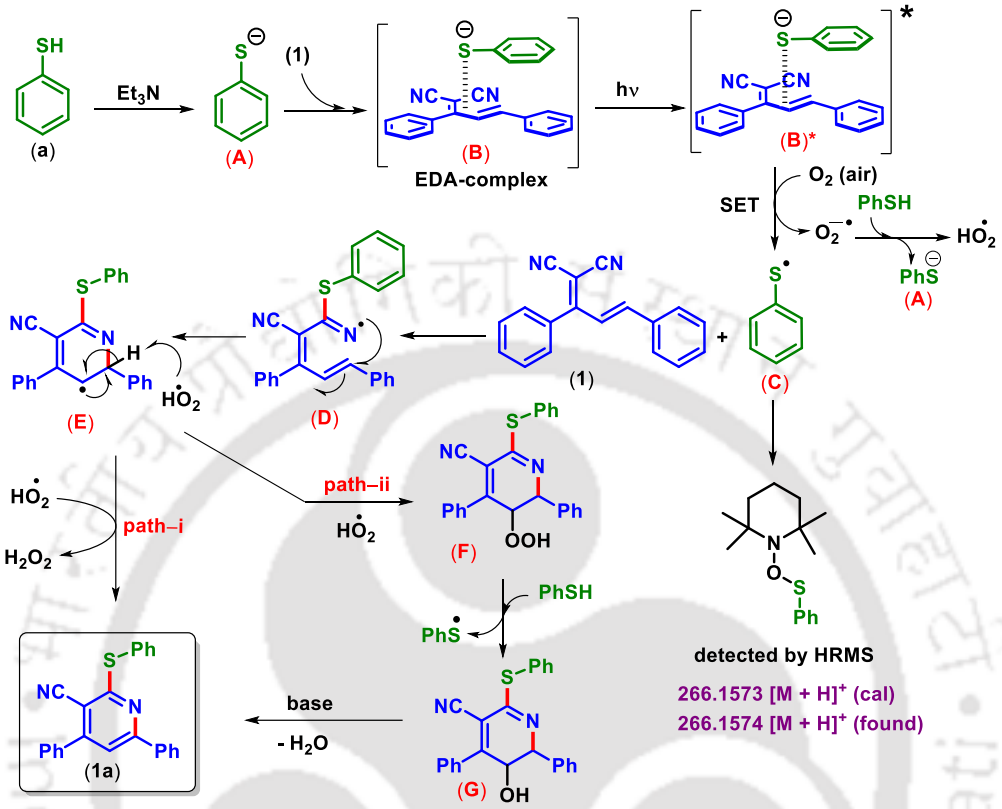

Scheme V.4.2.1. *Proposed mechanistic pathway.*

V.5. Conclusion:

In summary, we have developed a visible-light-driven EDA complex-promoted synthesis of thio-functionalized 3-cyanopyridine analouges. The protocol has been achieved via the cyclization of (*E*)-2-(1,3-diarylallylidene)malononitriles and thiophenols in the absence of photocatalyst, transition metal, and oxidant. The radical pathway for this transformation is proven by the radical trapping experiment and EDA complexation via UV-vis analysis, ^{19}F NMR, and fluorescence quenching experiments. The developed protocol proceeds under LEDs or sunlight and the method is scalable having diverse substrate scopes.

V.6. Experimental Section:

V.6.1. General Information:

All the reagents were commercial grade and purified according to the established procedures. All the reactions were carried out in oven-dried glassware. The highest commercial quality reagents were purchased and were used without further purification unless otherwise stated. Reactions were monitored by thin layer chromatography (TLC) on 0.25 mm silica gel plates ($60F_{254}$) visualized under UV illumination at 254 nm. Organic extracts were dried over anhydrous sodium sulfate (Na_2SO_4). Solvents were removed using a rotary evaporator under reduced pressure. Column chromatography was performed to purify the crude product on silica gel 60–120 mesh using a mixture of hexane and ethyl acetate as eluent. The isolated compounds were characterized by spectroscopic [^1H, $^{13}C\{1H\}$ NMR, and IR] techniques and HRMS analysis. NMR spectra were recorded in deuterochloroform ($CDCl_3$). ^1H, $^{13}C\{^1H\}$ were recorded in 500 (125) or 400 (100) MHz spectrometer and were calibrated using tetramethylsilane or residual undeuterated solvent for ^1H NMR, deuterochloroform for ^{13}C NMR as an internal reference {$Si(CH_3)_4$: 0.00 ppm or $CHCl_3$: 7.260 ppm for ^1H NMR, 77.230 ppm for ^{13}C NMR}. ^{19}F NMR was calibrated without any internal standard in $CDCl_3$ and DMSO-d_6 in a 500 MHz spectrometer. The chemical shifts are quoted in δ units, parts per million (ppm). ^1H NMR data is represented as follows: Chemical shift, multiplicity (s = singlet, d = doublet, t = triplet, q = quartet, m = multiplet), integration and coupling constant(s) *J* in hertz (Hz). High-resolution mass spectra (HRMS) were recorded on a mass spectrometer using electrospray ionization-time of flight (ESI-TOF) reflection experiments. FT-IR spectra were recorded in KBr or neat and reported in the frequency of absorption (cm^{-1}). All UV experiments were performed in 3 mL quartz cuvettes of path length 1 cm at 25 ^oC in UV/Vis spectrometer in HPLC grade toluene.

V.6.2. Light Information and Reaction Setup:

Philips 2 x 14 W white LED (flux 46 mW/cm^2) bulbs were used as the light source for this light-promoted reaction and no filter was used. A borosilicate 10 mL vial was used as the reaction vessel. The distance from the light source to the irradiation vessel was ~6–8 cm. Regular fan was used to ventilate the area to maintain the room temperature (27–30 ^oC). The reaction set-up for this photochemical reaction is shown below (Figure V.6.2.1).

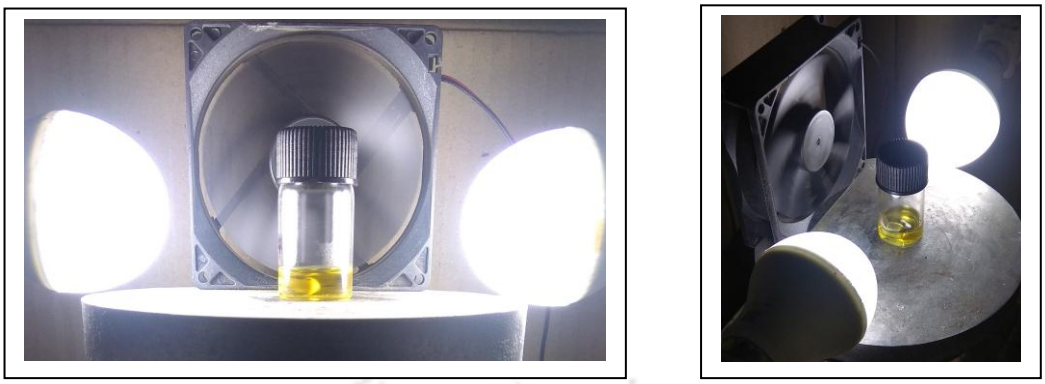

Figure V.6.2.1. *Photochemical reaction set-up.*

V.6.3. General Procedure:

V.6.3.1. General Procedure for the Synthesis of (*E*)-2-(1,3-Diarylallylidene)malononitriles (1–21):

Compounds **1**–**21** were synthesized in slightly modified literature procedures[16]

V.6.3.2. (i) General Procedure for the Synthesis of 4,6-Diphenyl-2-(phenylthio)nicotinonitrile (1a) from (*E*)-2-(1,3-Diphenylallylidene)malononitrile (1) and Thiophenol (a):

To an oven-dried 10 mL vial was added (*E*)-2-(1,3-diphenylallylidene)malononitrile (**1**) (0.0640 g, 0.25 mmol), thiophenol (**a**) (0.082 g/76 μL, 0.75 mmol), and Et_3N (0.050 g/70 μL, 0.5 mmol) in toluene (2 mL) in air atmosphere. The reaction mixture was stirred at room temperature for 12 h, maintaining an approximate distance of ~6–8 cm from two 14 W white LED bulbs. After completion of the reaction (monitored by TLC analysis), the reaction mixture was admixed with ethyl acetate (20 mL), and the organic layer was washed with water (20 mL). The organic layer was dried over anhydrous sodium sulfate (Na_2SO_4), and the solvent was evaporated under reduced pressure. The crude product so obtained was purified over a column of silica gel using 2% ethyl acetate in hexane to give pure 4,6-diphenyl-2-(phenylthio)nicotinonitrile (**1a**) in 86% yield (78 mg) (Scheme V.6.3.2.1). The identity and purity of the product were confirmed by spectroscopic analysis.

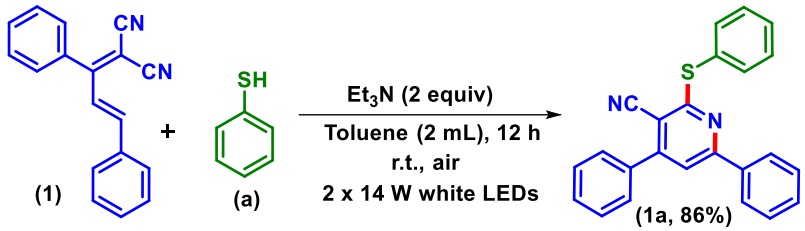

Scheme V.6.3.2.1. *Synthesis of 4,6-diphenyl-2-(phenylthio)nicotinonitrile (**1a**).*

V.6.3.3. Gram-scale Synthesis of 4,6-Diphenyl-2-(phenylthio)nicotinonitrile (1a) from (*E*)-2-(1,3-Diphenylallylidene)malononitrile (1) and Thiophenol (a):

To an oven-dried 50 mL round bottom flask was added (*E*)-2-(1,3-diphenylallylidene)malononitrile (**1**) (1.28 g, 5.0 mmol), thiophenol (**a**) (1.65 g/1.2 mL, 15.0 mmol,), and Et_3N (1.01 g/1.04 mL, 10.0 mmol,) in toluene (5 mL) in air atmosphere. The reaction mixture was stirred at room temperature for 12 h, maintaining an approximate distance of ~6–8 cm from two 14 W white LED bulbs. After completion of the reaction (monitored by TLC analysis), the reaction mixture was admixed with ethyl acetate (50 mL) and the organic layer was washed with water (2 x 20 mL). The organic layer was dried over anhydrous sodium sulfate (Na_2SO_4), and the solvent was evaporated under reduced pressure. The crude product so obtained was purified over a column of silica gel using 2% ethyl acetate in hexane to give pure 4,6-diphenyl-2-(phenylthio)nicotinonitrile (**1a**) in 80% yield (1.46 g) (Scheme V.6.3.3.1). The identity and purity of the product were confirmed by spectroscopic analysis.

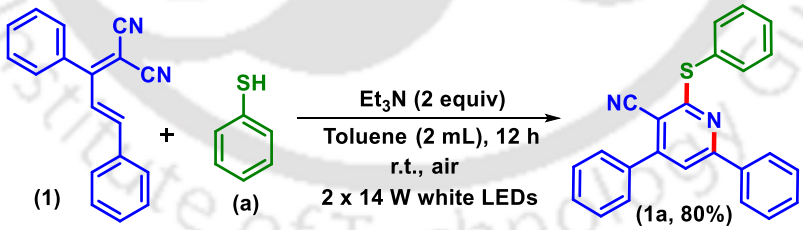

Scheme V.6.3.3.1. *Gram-scale synthesis of 4,6-diphenyl-2-(phenylthio)nicotinonitrile (**1a**).*

V.6.3.4. General Procedure for the Synthesis of 4,6-Diphenyl-2-(phenylthio)nicotinonitrile (1a) in the Presence of Sunlight:

To an oven-dried 10 mL vial was added (*E*)-2-(1,3-diphenylallylidene)malononitrile (**1**) (0.0640 g, 0.25 mmol), thiophenol (**a**) (0.082 g/76 µL, 0.75 mmol), and Et_3N (0.050 g/70 µL, 0.5 mmol) in toluene (2 mL) in air atmosphere. The reaction mixture was stirred under sunlight

with a surrounding temperature was 28-35 ^{o}C for 8 h. After completion of the reaction (monitored by TLC analysis), the reaction mixture was admixed with ethyl acetate (20 mL), and the organic layer was washed with water (20 mL). The organic layer was dried over anhydrous sodium sulfate (Na_2SO_4), and the solvent was evaporated under reduced pressure. The crude product so obtained was purified over a column of silica gel using 2% ethyl acetate in hexane to give pure 4,6-diphenyl-2-(phenylthio)nicotinonitrile (**1a**) in 76% yield (69 mg) (Scheme V.6.3.4.1). The identity and purity of the product were confirmed by spectroscopic analysis.

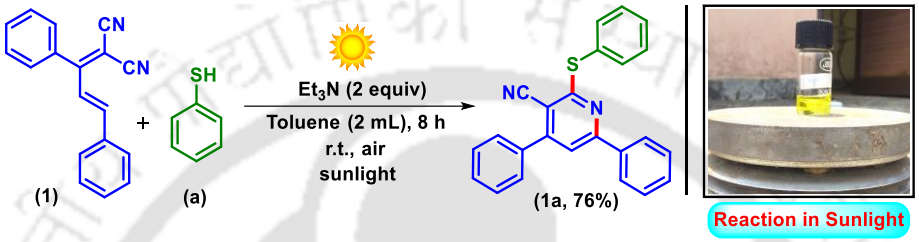

Scheme V.6.3.4.1. *Synthesis of 4,6-diphenyl-2-(phenylthio)nicotinonitrile (**1a**) in sunlight.*

V.6.4 Control Experiments:

V.6.4.1 Radical-trapping Experiments with TEMPO:

(I) Reaction in the Presence of 2 equiv of TEMPO:

To an oven-dried 10 mL vial was added (*E*)-2-(1,3-diphenylylallylidene)malononitrile (**1**) (0.064g, 0.25 mmol), thiophenol (**a**) (0.0825 g/76 µL, 0.75 mmol), Et_3N (0.0505 g/70 µL, 0.5 mmol,), and (2,2,6,6-tetramethylpiperidin-1-yl)oxyl (TEMPO) (0.078 g, 0.5 mmol) in toluene (2 mL). The reaction mixture was stirred at room temperature for 12 h maintaining an approximate distance of ~6-8 cm from two 14 W white LED bulbs. After completion of the reaction (monitored by TLC analysis), the reaction mixture was admixed with ethyl acetate (25 mL), and the organic layer was washed with water (20 mL). The organic layer was dried over anhydrous Na_2SO_4, and the solvent was evaporated under reduced pressure. The crude product so obtained was purified over a column of silica gel using 2% ethyl acetate in hexane to give pure 4,6-diphenyl-2-(phenylthio)nicotinonitrile (**1a**) (18 mg, 20% yield) (Scheme V.6.4.1.1). The identity and purity of the product were confirmed by spectroscopic analysis.

In another set of identical reactions formation of TEMPO-thiol adduct was monitored. Each time (10 µL) of reaction aliquot was taken at a time interval of 20 minutes and subjected to HRMS analysis. A TEMPO-thiophenol adduct (**X**) was detected after 1 h (Figure V.6.4.1.1).

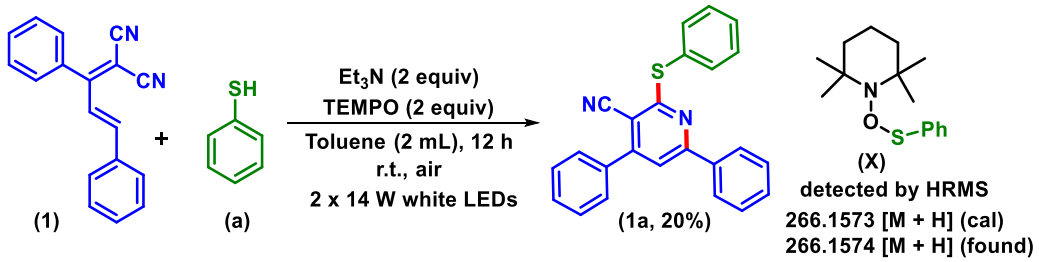

Scheme V.6.4.1.1. *Reaction in the presence of 2 equiv of TEMPO.*

(II) Reaction in the Presence of 4 equiv of TEMPO:

To an oven-dried 10 mL vial was added (*E*)-2-(1,3-diphenylylallylidene)malononitrile (**1**) (0.064g, 0.25 mmol), thiophenol (**a**) (0.0825 g/76 µL, 0.75 mmol), Et_3N (0.0505 g/70 µL, 0.5 mmol), and (2,2,6,6-tetramethylpiperidin-1-yl)oxyl (TEMPO) (0.156 g, 1.0 mmol) in toluene (2 mL). The reaction mixture was stirred at room temperature for 15 h maintaining an approximate distance of ~6-8 cm from two 14 W white LED bulbs. After 18 h of the reaction (monitored by TLC analysis), it was found that a trace amount of product 4,6-diphenyl-2-(phenylthio)nicotinonitrile (**1a**) was formed (Scheme V.6.4.1.2). The result suggests that the reaction goes through a radical pathway. However, the TEMPO-thiophenol adduct (**X**) cannot be isolated by column chromatography but it is detected from the HRMS analysis of the reaction mixture (Figure V.6.4.1.1).

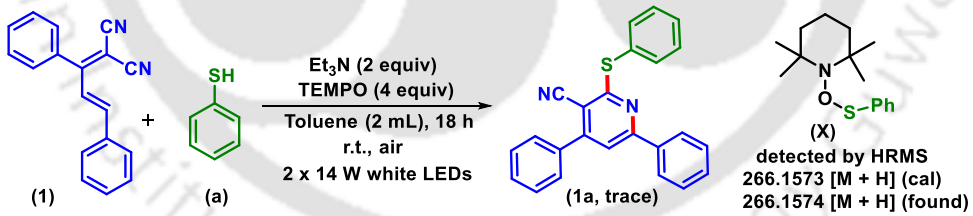

Scheme V.6.4.1.2. *Reaction in the presence of 4 equiv of TEMPO.*

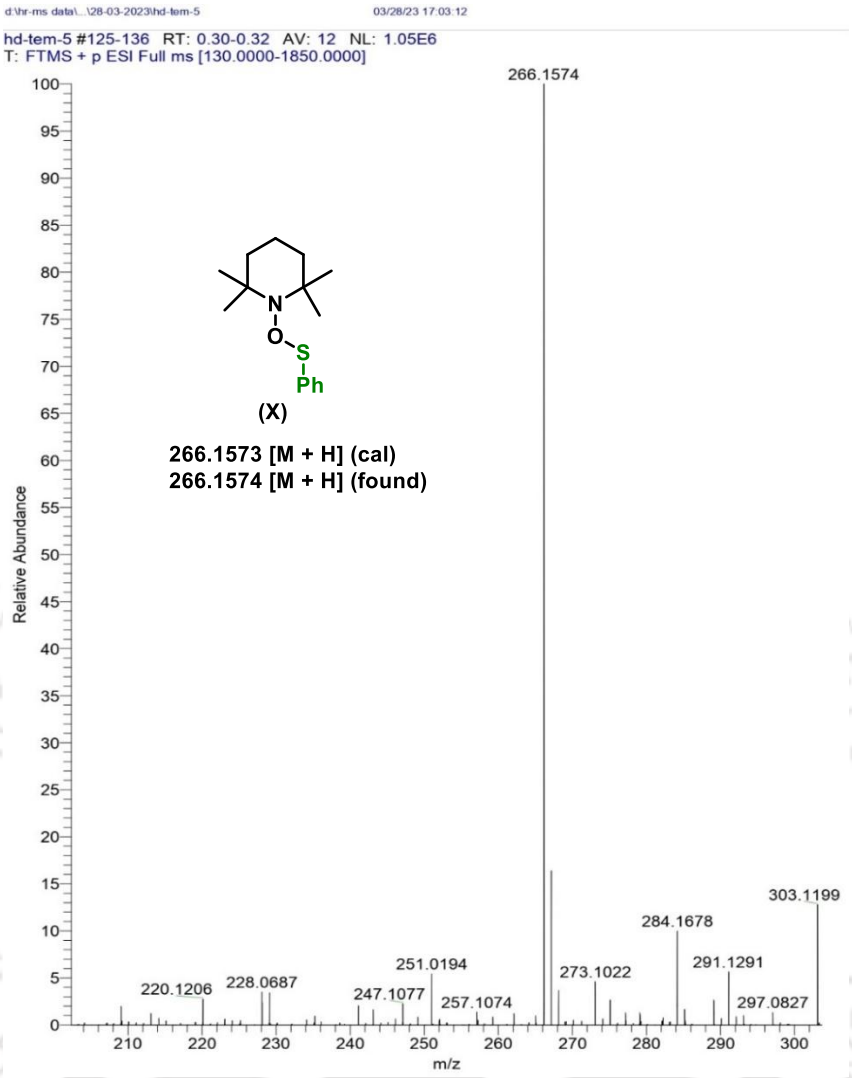

Figure V.6.4.1.1. *HRMS of TEMPO-thiophenol adduct (**X**).*

V.6.4.2. Reaction in the Presence of N_2 Atmosphere:

To an oven-dried 10 mL vial was added (*E*)-2-(1,3-diphenylallylidene)malononitrile (**1**) (0.0640 g, 0.25 mmol), thiophenol (**a**) (0.0825 g/76 μL, 0.75 mmol), and Et_3N (0.0505 g/70 μL, 0.5 mmol) in toluene (2 mL) in N_2 atmosphere. The reaction mixture was stirred at room temperature for 15 h, maintaining an approximate distance of ~6-8 cm from two 14 W white LED bulbs. After completion of the reaction (monitored by TLC analysis), the reaction mixture was admixed with ethyl acetate (25 mL) and the organic layer was washed with water (20 mL). The organic layer was dried over anhydrous Na_2SO_4, and the solvent was evaporated under reduced pressure. The crude product so obtained was purified over a column of silica gel using 2% ethyl acetate in hexane to

give pure 4,6-diphenyl-2-(phenylthio)nicotinonitrile (**1a**) (12 mg, 13%) (Scheme V.6.4.2.1). The identity and purity of the product were confirmed by spectroscopic analysis.

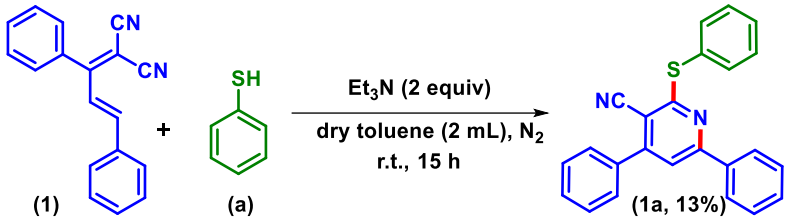

Scheme V.6.4.2.1. *Reaction in the presence of N_2 atmosphere.*

V.6.4.3. Reaction in the Presence of O_2 Atmosphere:

To an oven-dried 10 mL vial was added (*E*)-2-(1,3-diphenylallylidene)malononitrile (**1**) (0.0640 g, 0.25 mmol), thiophenol (**a**) (0.0825 g/76 µL, 0.75 mmol), and Et_3N (0.0505 g/70 µL, 0.5 mmol) in toluene (2 mL) in O_2 atmosphere. The reaction mixture was stirred at room temperature for 15 h, maintaining an approximate distance of ~6-8 cm from two 14 W white LED bulbs. After completion of the reaction (monitored by TLC analysis), the reaction mixture was admixed with ethyl acetate (25 mL) and the organic layer was washed with water (20 mL). The organic layer was dried over anhydrous sodium sulfate (Na_2SO_4), and the solvent was evaporated under reduced pressure. The crude product so obtained was purified over a column of silica gel using 2% ethyl acetate in hexane to give pure 4,6-diphenyl-2-(phenylthio)nicotinonitrile (**1a**) (79 mg, 87%) (Scheme V.6.4.3.1). The identity and purity of the product were confirmed by spectroscopic analysis.

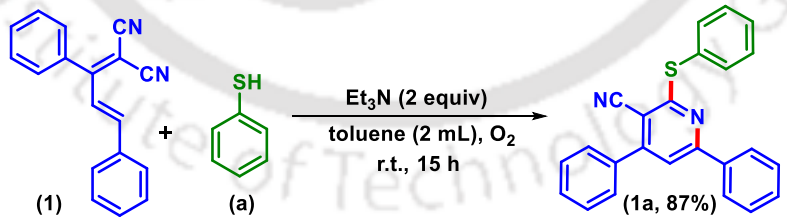

Scheme V.6.4.3.1. *Reaction in the presence of O_2 atmosphere.*

V.6.4.4. Reaction in the Absence of White LEDs:

To an oven-dried 10 mL vial was added (*E*)-2-(1,3-diphenylallylidene)malononitrile (**1**) (0.0640 g, 0.25 mmol), thiophenol (**a**) (0.0825 g/76 µL, 0.75 mmol), and Et_3N (0.0505 g/70 µL, 0.5 mmol) in toluene (2 mL) in air atmosphere. The reaction mixture was stirred in the absence of

light at room temperature for 15 h. After completion of the reaction (monitored by TLC analysis), the reaction mixture was admixed with ethyl acetate (25 mL), and the organic layer was washed with water (20 mL). The organic layer was dried over anhydrous sodium sulfate (Na_2SO_4), and the solvent was evaporated under reduced pressure. The crude product so obtained was purified over a column of silica gel using 2% ethyl acetate in hexane to give pure 4,6-diphenyl-2-(phenylthio)nicotinonitrile (**1a**) in 16% yield (15 mg) (Scheme V.6.4.4.1). The identity and purity of the product were confirmed by spectroscopic analysis.

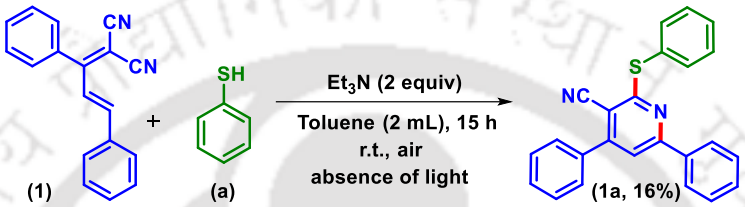

Scheme V.6.4.4.1. *Reaction in the absence of LEDs.*

V.6.4.5. H_2O_2 Detection in the Reaction Mixture[15]

(I) H_2O_2 Detection by Mohr's Salt:

In an oven-dried 10 mL borosilicate vial was added (*E*)-2-(1,3-diphenylallylidene)malononitrile (**1**) (0.0640 g, 0.25 mmol), thiophenol (**a**) (0.0825 g/76 µL, 0.75 mmol), and Et_3N (0.0505 g/70 µL, 0.5 mmol) in toluene (2 mL) in air atmosphere. The reaction mixture was stirred at room temperature, maintaining an approximate distance of ~6-8 cm from two 14 W white LED bulbs. After around 1 hour, a 100 µL solution of Mohr's Salt (10 mg in 100 µL H_2O + 1 mL CH_3CN) was added to the reaction mixture. After some time a rapid setting of $Fe(OH)_3$ floc was observed [Figure V.6.4.5.1 (b)]. The floc observed was because of the rapid oxidation of Fe(II) to Fe(III) due to the presence of hydrogen peroxide, H_2O_2 in the medium.

(a)  **(b)**  

Figure V.6.4.5.1. *(a) Reaction mixture before addition of Fe(II) solution (Mohr's Salt). (b) Reaction mixture after addition of Fe(II) solution (Mohr's Salt).*

V.6.5. On-off Experiments:

To an oven-dried 10 mL vial was added (*E*)-2-(1,3-diphenylallylidene)malononitrile (**1**) (0.0640 g, 0.25 mmol), thiophenol (**a**) (0.0825 g, 0.75 mmol), and Et_3N (0.0505 g, 0.5 mmol) in toluene (2 mL) in air atmosphere. The reaction mixture was stirred and irradiated by 2 x 14 W white LEDs at room temperature for 1.5 h. Then each 200 μL of the reaction aliquots was taken in a 5 mL pear-shaped round bottom flask and evaporated and co-evaporated with ethyl acetate (2 x 500μL) in a rotatory evaporator and dried under reduced pressure. The crude mixture was dissolved in 500 μL of $CDCl_3$ (containing 7% CH_3NO_2 as an internal standard.). The ^1H NMR yield of the corresponding product (**1a**) was found to be 14% (Figure V.6.5.1).

Then the reaction mixture was continuously stirred in the absence of light (under dark) for 1.5 h and the same steps were repeated, the ^1H NMR yield of **1a** was 15% (Figure V.6.5.2).

Again the reaction mixture was continuously stirred in the presence of 2 x 14 W light for 2 h and the same steps were repeated, the ^1H NMR yield of **1a** was found to be 33% (Figure V.6.5.3) and after 2 h in the absence of light, the yield was 34% (Figure V.6.5.4). Finally, when the reaction mixture was again stirred in the presence of 2 x 14 W white LEDs for 6 h, the desired product (**1a**) obtained in 52% yield as determined from ^1H NMR (Figure V.6.5.5). These results suggested that continuous irradiation of visible light is essential for this transformation.

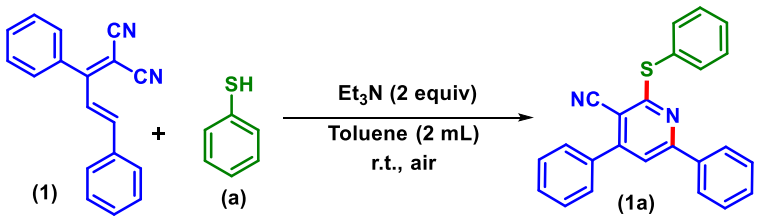

Scheme V.6.5.1. *On-off experiment.*

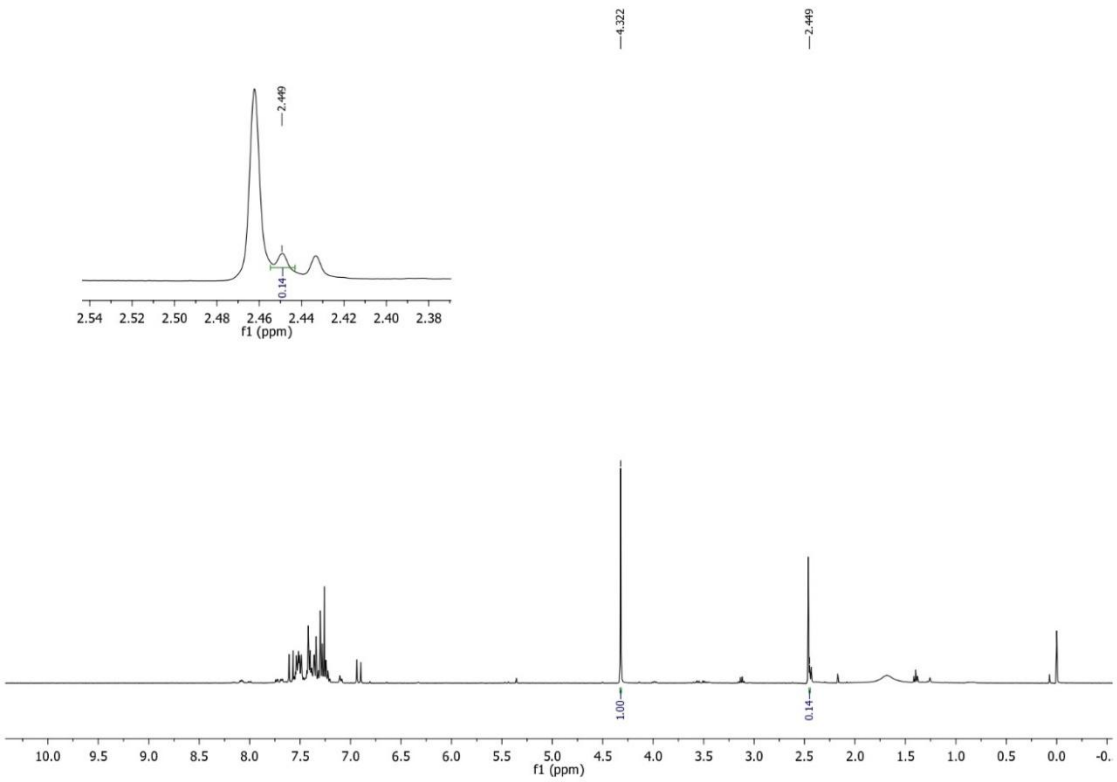

Figure V.6.5.1. *^{1}H NMR of the reaction mixture after 1.5 h light on.*

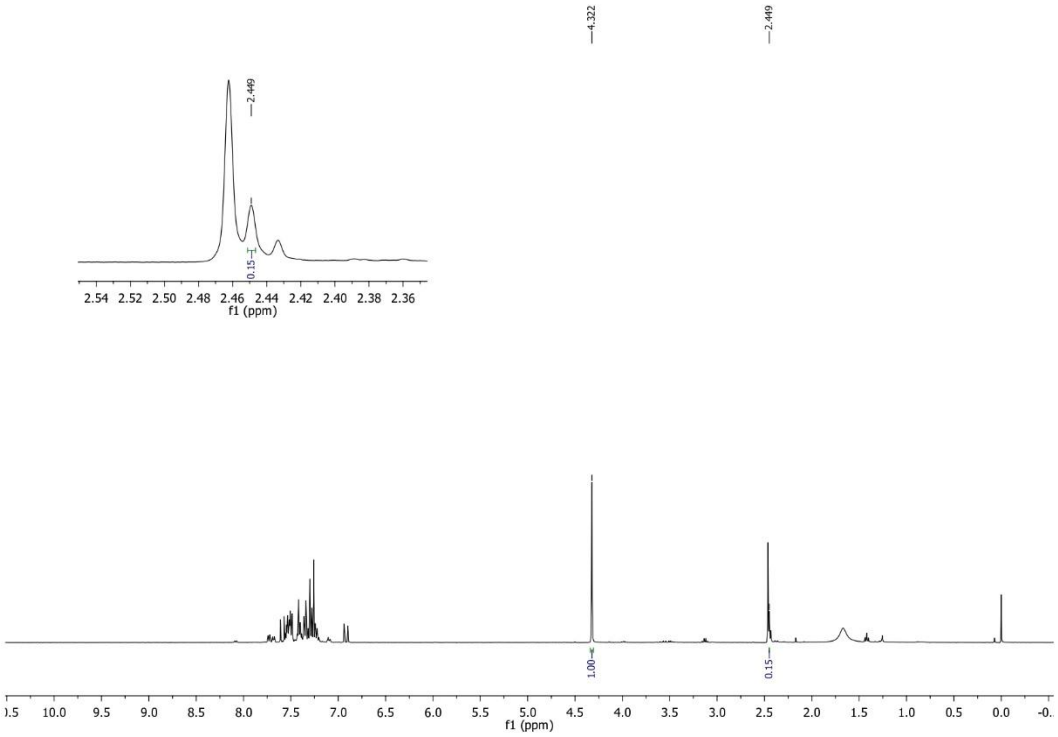

Figure V.6.5.2. *^{1}H NMR of the reaction mixture after 1.5 h light off.*

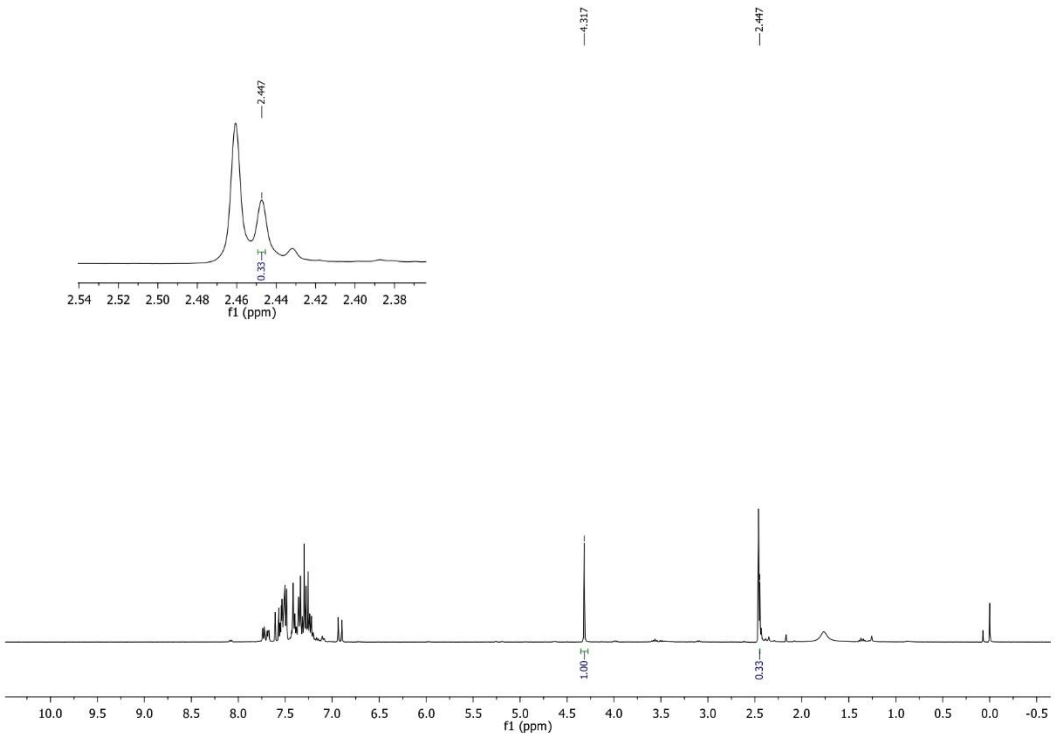

Figure V.6.5.3. *^{1}H NMR of the reaction mixture after 2.0 h light on.*

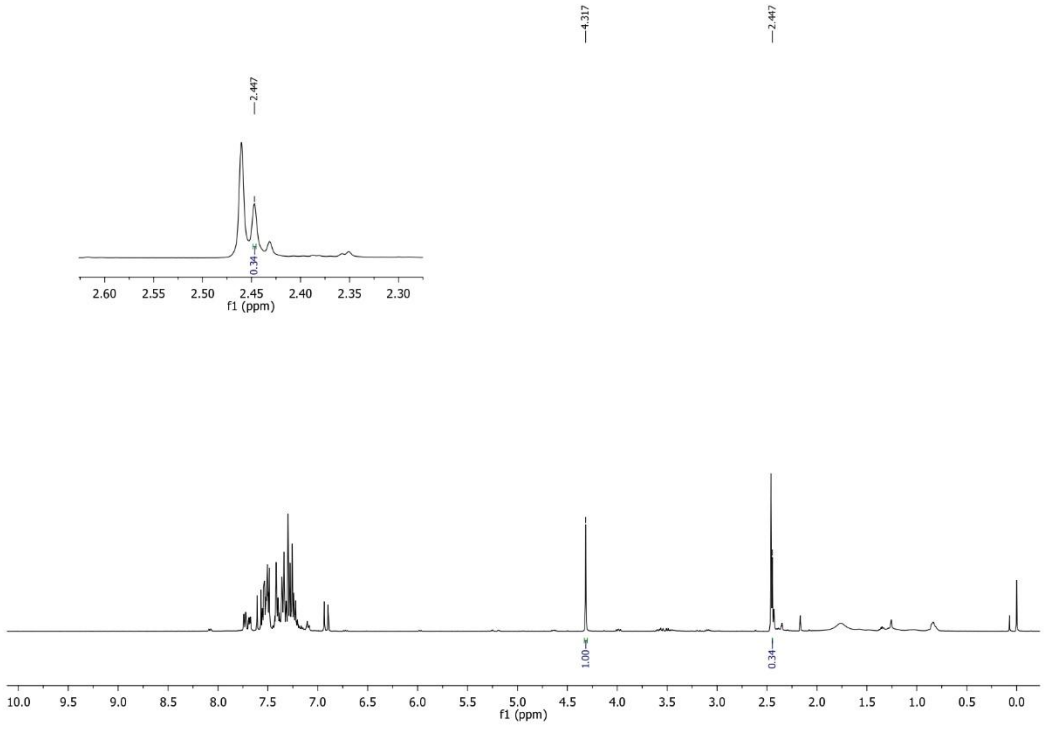

Figure V.6.5.4. *^{1}H NMR of the reaction mixture after 2.0 h light off.*

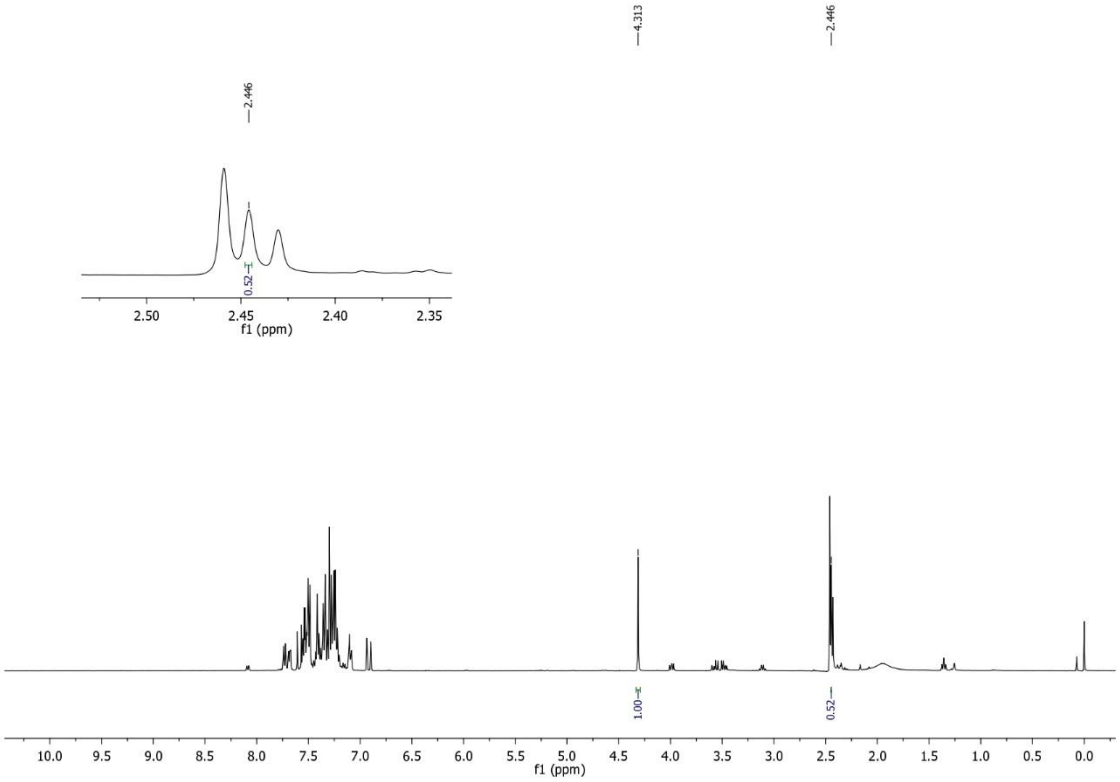

Figure V.6.5.5. *^{1}H NMR of the reaction mixture after 6.0 h light on.*

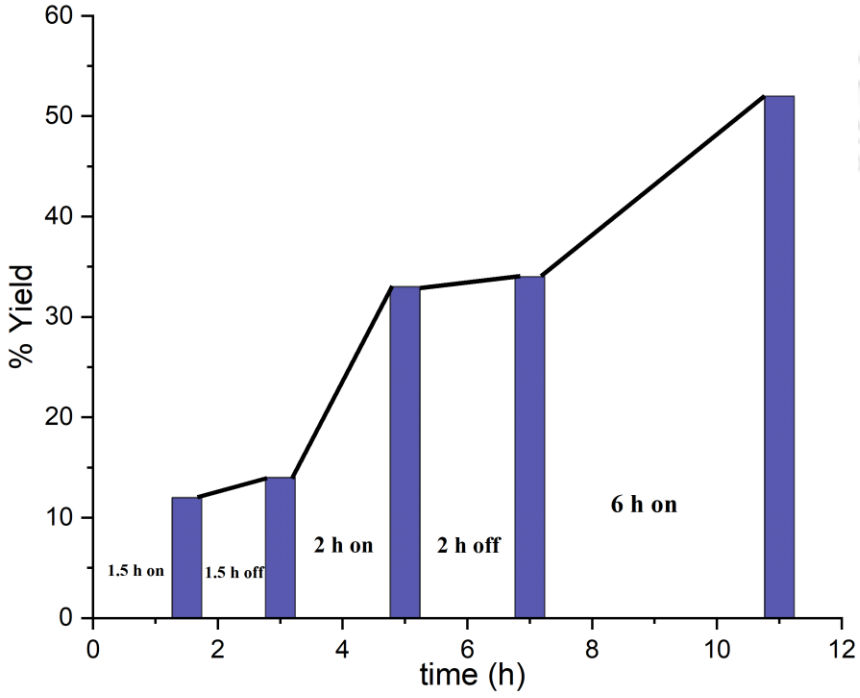

Figure V.6.5.6. *Plot %yield vs time (h) for On-off experiments.*

V.6.6. UV-vis Experiments:[4]

A 10 mL stock solution of (*E*)-2-(1,3-diphenylallylidene)malononitrile (**1**, 5 mM), thiophenol (**a**, 5 mM) and Et_3N (5 mM) were prepared separately in toluene. At first, the UV absorption of **1**, **a**, and Et_3N was taken individually none of which showed any absorption in the visible region (Figure V.6.6.1). Next, 1 mL each of **1**, **a**, and Et_3N was taken in a 3 mL UV cuvette and was then exposed to the light source (white LEDs) for 10 minutes, during this period the solution turned to light yellow with an absorption maximum shift towards the visible region (λ_{max} = 414 nm), suggesting the formation of an electron donor-acceptor complex (Figure V.6.6.1).

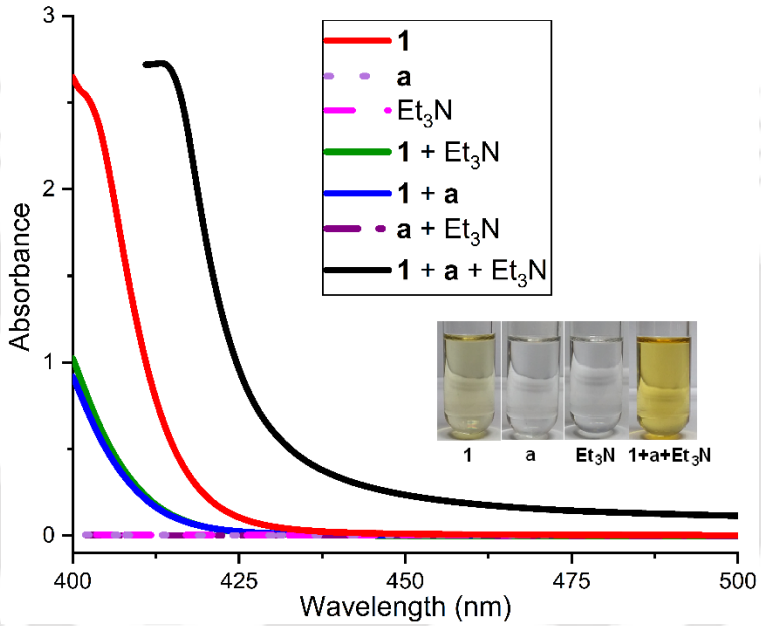

Figure V.6.6.1. *UV-vis spectra of EDA complex in toluene.*

(a) Fluorescence Studies:[17a]

In order to find further evidence for the formation of EDA pair between (*E*)-2-(1,3-diphenylallylidene)malononitrile (**1**) and PhSH (**a**), a fluorescence quenching experiment was performed. **Flask–I**. (*E*)-2-(1,3-diphenylallylidene)malononitrile (**1**) (2.56 mg) and Et_3N (1.5 µL) were taken in a 10 mL volumetric flask and the volume was adjusted to 10 mL using toluene so that the final strength of **1** and Et_3N was maintained 1 mM. **Flask–II**. In another 10 mL volumetric flask) (**1**) (2.56 mg), PhSH (**a**) (1.10 mg) and Et_3N (1.5 µL) were taken in a 10 mL volumetric flask and the volume was adjusted to 10 mL using toluene so that the final strength of (*E*)-2-(1,3-diphenylallylidene)malononitrile (**1**), PhSH (**a**) and Et_3N was maintained 1 mM. Then 200 µL of

each of the solutions (from **Flask-I** and **II**) was taken in another two 10 mL volumetric flasks (**Flask-III** and **IV**) and the volume was adjusted to 10 mL using toluene so that the final strength of both flasks was maintained 20 μM. Now **Flask-III** containing 20 μM of (*E*)-2-(1,3-diphenylallylidene)malononitrile (**1**) and Et_3N, and **Flask-IV** containing 20 μM of (*E*)-2-(1,3-diphenylallylidene)malononitrile (**1**) PhSH (**a**) and Et_3N.

For the fluorescence measurement, 2.0 mL solution from **Flask-III** was taken in a cuvette was excited at 400 nm, and the emission was observed at 432 nm. A 10 μL aliquot from **Flask-IV** [containing thiophenol (**a**)] was added sequentially and fluorescence emission was recorded each time after irradiation at regular intervals. As evident from Figure V.6.6.2, a decrease in emission intensity was observed after each addition of thiophenol (**a**) {concentration 0-220 μM}. This suggests a possible interaction between **1** and thiophenol (**a**).[17a]

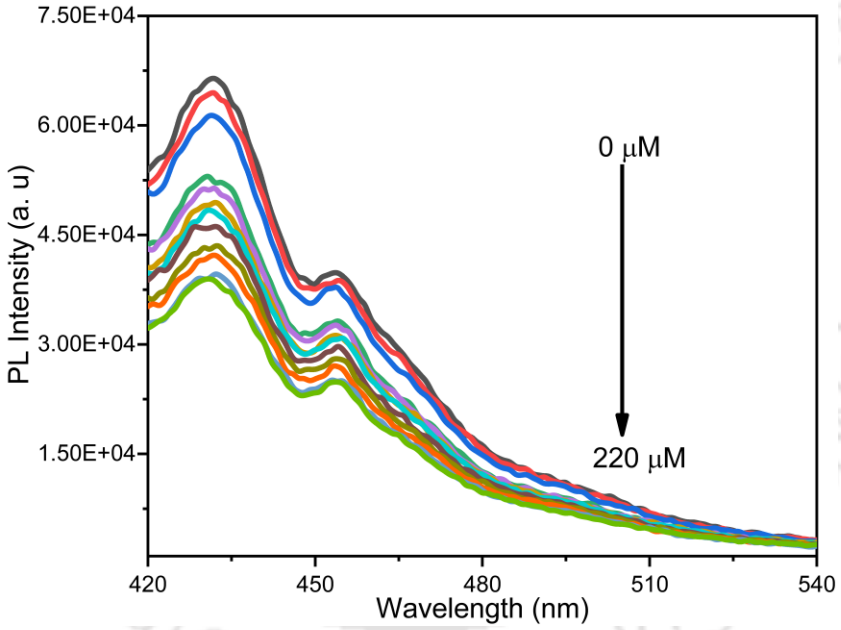

Figure V.6.6.2. *Fluorescence emission spectra of (**1**) at varied conc. of quencher thiophenol (**a**).*

With these data, the Stern–Volmer graph was plotted using the equation $I_0/I = 1 + K_{SV}[Q]$, where I_0 and I are the integrated emission intensity in the absence and presence of a quencher and K_{sv} is the quenching constant. A linear quenching was observed (Figure V.6.6.3).

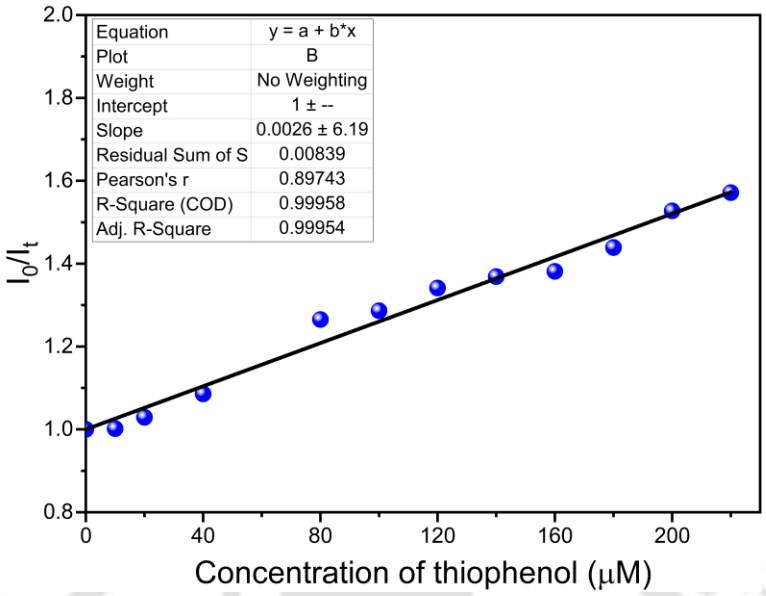

Figure V.6.6.3. *Stern-Volmer Plot.*

V.6.7. ^{19}F NMR Experiments:[4d,18]

Further to confirm the formation of the EDA complex a ^{19}F NMR experiments were performed by the preparation of DMSO-d_6 solutions containing (*E*)-2-(1-(4-fluorophenyl)-3-phenylallylidene)malononitrile (**4**), thiophenol (**a**) and Et_3N in different ratios, keeping constant the amount of (*E*)-2-(1-(4-fluorophenyl)-3-phenylallylidene)malononitrile (**4**) (0.1 mmol) and increasing the amount of **a** and Et_3N (**4** : **a** : Et_3N = 1 : 0 : 0; 1 : 1 : 1; 1 : 2 : 2; 1 : 3 : 3; 1 : 4 : 4; 1: 5 : 5, and 1 : 6 : 6). The Figure V.6.7.1 shows the ^{19}F recorded spectra. The evidence of interaction between **4** and **a** is highlighted in Figure V.6.7.1. and Figure V.6.7.2. Due to the interaction between F- containing substrate **4** and (**a**), the chemical shift of **4** progressively shifted downfield with increasing amounts of thiophenol (**a**) and Et_3N.

Table V.6.7.1: *^{19}F NMR δ (ppm) value for the ratio of **4**, **a**, **Et$_3$N***

Entry	**4** (mmol)	**a** (mmol)	**Et$_3$N** (mmol)	**4** : **a** : Et_3N	δ_F (ppm)
1	0.1	0	0	1 : 0 : 0	–109.8376
2	0.1	0.1	0.1	1 : 1 : 1	–109.8315
3	0.1	0.2	0.2	1 : 2 : 2	–109.8220

4	0.1	0.3	0.3	1 : 3 : 3	–109.8045
5	0.1	0.4	0.4	1 : 4 : 4	–109.7924
6	0.1	0.5	0.5	1 : 5 : 5	–109.7814
7	0.1	0.6	0.6	1 : 6 : 6	–109.7599

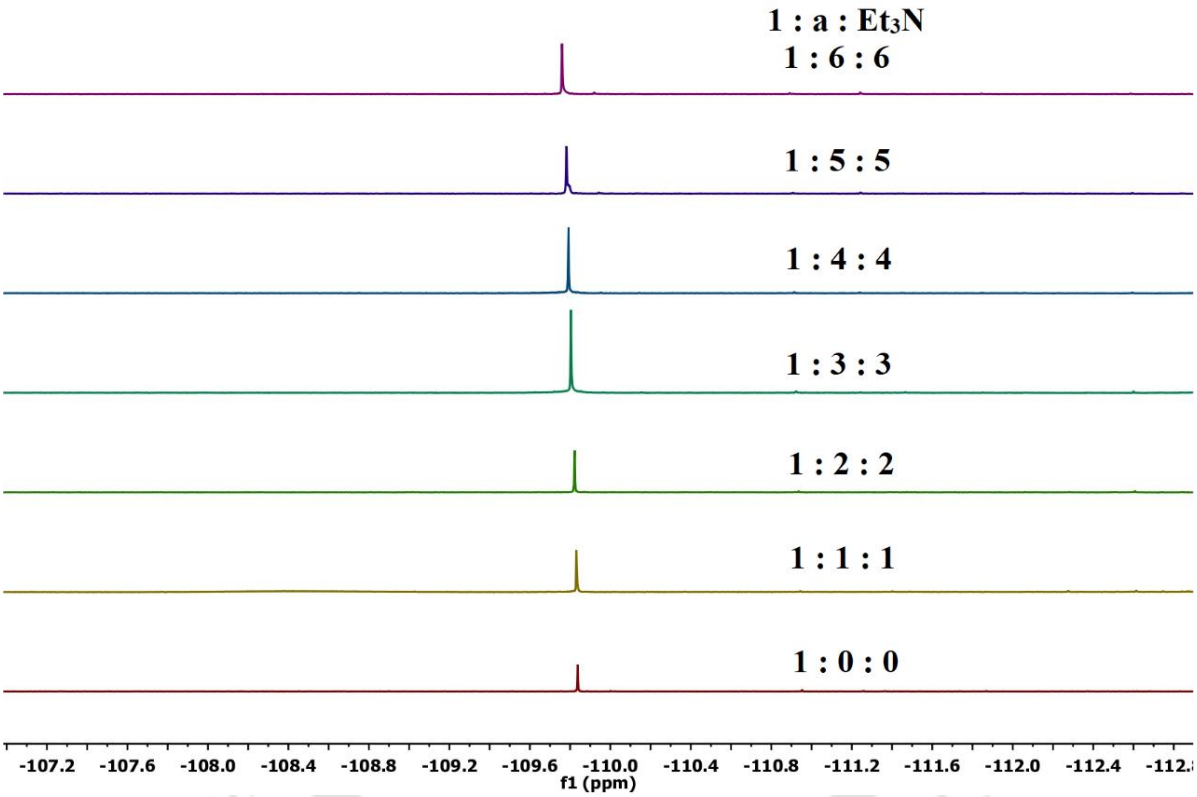

Figure V.6.7.1. *^{19}F-NMR of (E)-2-(1-(4-fluorophenyl)-3-phenylallylidene)malononitrile (**4**), thiophenol (**a**) and Et_3N with different ratios.*

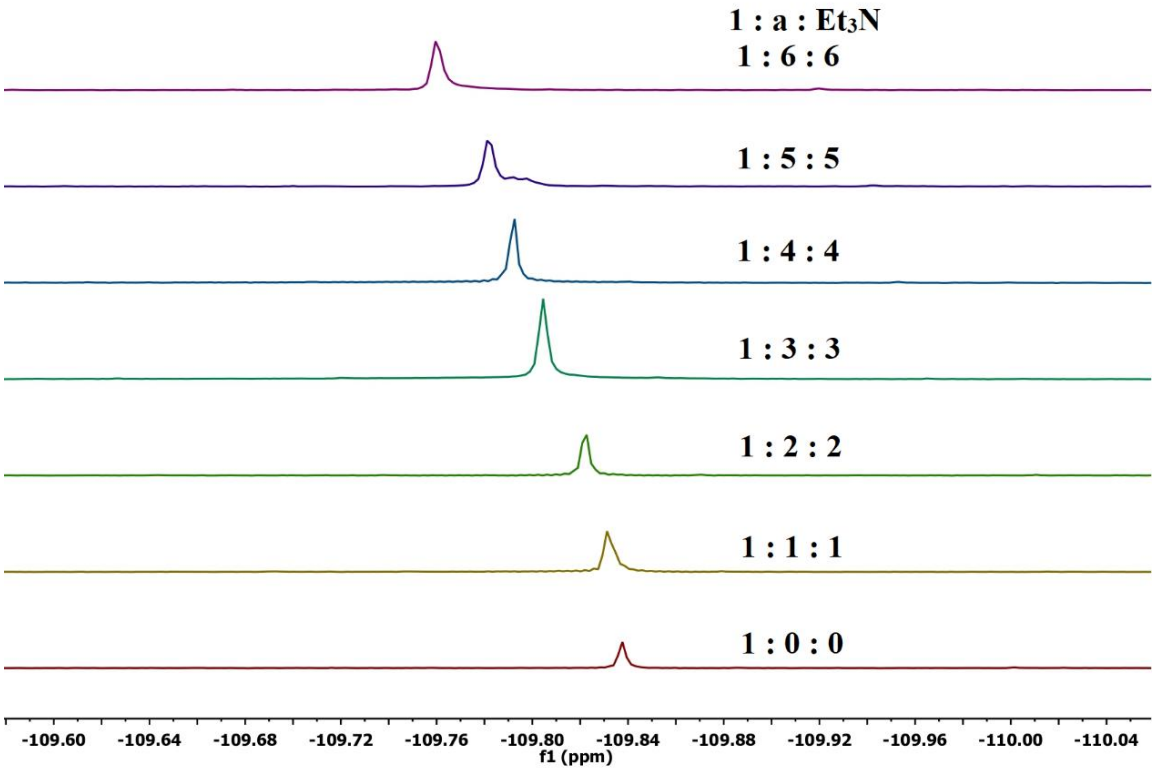

Figure V.6.7.2. *Evidence for the formation of the EDA complex through* ^{19}F *NMR.*

V.6.8. Determination of Binding Constant (K_{EDA}) of EDA Complex:[17]

The binding constant of the proposed EDA complex between (*E*)-2-(1,3-diphenylallylidene)malononitrile (**1**) and PhSH (**a**) in toluene containing 1 mM Et_3N, was determined spectrophotometrically using Benesi-Hildebrand methodology (Figure V.6.8.1). The absorption at 405 nm corresponding to the EDA pair was measured on increasing thiophenol addition to a solution of a fixed concentration of **1** (1 mM) in 1 mM (toluene + Et_3N) solution. Keeping the constant concentration of **1** and increasing the concentration of thiophenol (100 μM, 200 μM, 300μM, …so on), the absorption spectra shifted towards the visible region. A straight line was obtained when the reciprocal of absorbance was plotted against the reciprocal of the concentration of the thiophenol (**a**). The association (binding) constant (K_{EDA}), calculated from the ratio of intercept to the slope was found to be 139.6 mM^{-1}. The calculated magnitude of the association constant for the EDA pair signifies its binding/interaction in toluene. The Benesi–Hildebrand binding constant (K) was determined using the equation: $1/(A - A_0) = 1/(A_{max} - A) +$

$1/K(A_{max} - A)[M]$. Where, A_0 and A are the absorbance of (*E*)-2-(1,3-diphenylallylidene)malononitrile in the presence of thiophenol (**a**), respectively. λ_{max} is the absorbance at saturated concentration and [M] is the concentration of **a**. K was obtained from the ratio of the intercept to the slope in the plot of $1/(A - A_0)$ versus 1/[M] [Figure V.6.8.1 (b)].

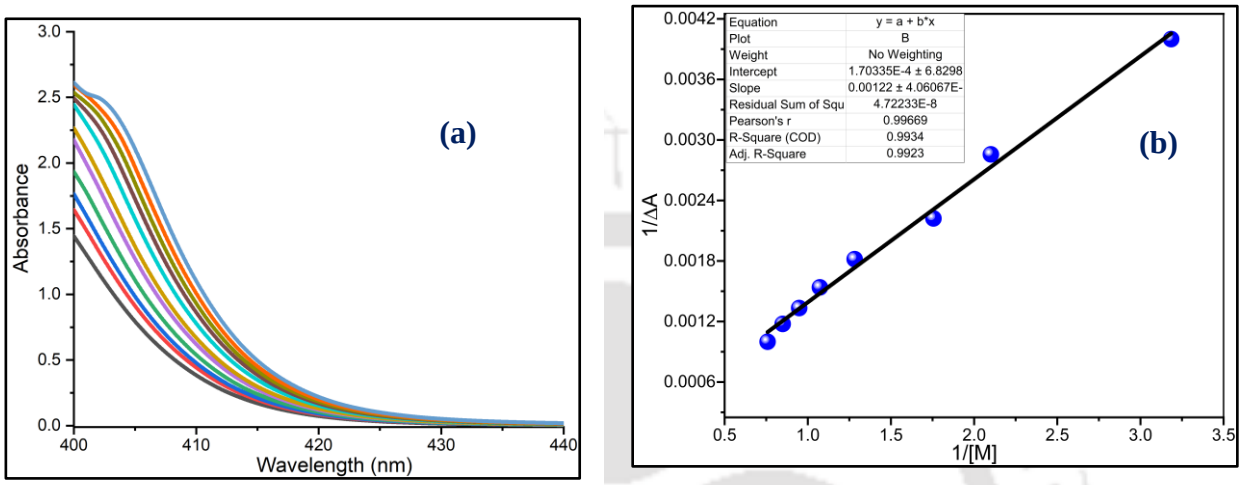

Figure V.6.8.1. *(a) Absorbance of the mixture of (E)-2-(1,3-diphenylallylidene)malononitrile (**1**) and thiophenol (**a**) with an increasing amount of thiophenol in toluene+Et_3N. (b) Benesi-Hildebrand analysis of the titration curve for the complex.*

V.6.9. Crystallographic Information:

V.6.9.1 Crystallographic Information of 2-((4-methoxyphenyl)thio)-4,6-diphenylnicotinonitrile (1d):

(i) Sample Preparation: The single crystal of compound **1d** was prepared by the slow evaporation method for which 10 mg of the compound (**1d**) was dissolved in 1 mL of DCM in a clean and dry 10 mL glass vial. MeOH (0.5 mL) was added to this solution slowly with a dropper. The mouth of the glass vial was covered with a cap having a small hole and kept for slow evaporation at room temperature. Crystals of **1d** were obtained as a transparent white needle-like crystal after around 2–3 days.

(ii) Data Collection: Diffraction data were collected at 298 K with MoKα radiation (λ = 0.71073 Å) using a Bruker Nonius SMART APEX CCD diffractometer equipped with a graphite monochromator and Apex CD camera. The SMART software was used for data collection and for indexing the reflections and determining the unit cell parameters. Data reduction and cell

refinement were performed using SAINT[1,2] software and the space groups of these crystals were determined from systematic absences by XPREP and further justified by the refinement results. The structures were solved by direct methods and refined by full-matrix least-squares calculations using SHELXTL-97[3] software. All the non-H atoms were refined in the anisotropic approximation against F^2 of all reflections.

1. R. H. Blessing, *Acta Crystallogr.*, 1995, **A51**, 33.
2. SMART and SAINT, Siemens Analytical X-ray Instruments Inc., Madison, WI, 1996.
3. G. M. Sheldrick, *Acta Crystallogr.*, 2008, **A64**, 112.

(iii) Crystallographic description of 2-((4-methoxyphenyl)thio)-4,6-diphenylnicotinonitrile (1d):

$C_{25}H_{18}N_2OS$, crystal dimensions 0.25 x 0.21 x 0.15 mm, M_r = 394.47, orthorhombic, space group P b c a, a = 8.3336 (4), b = 18.5187 (9), c = 26.3322 (12) Å, α = 90, β = 90, γ = 90, V = 4063.8 (3) Å^3, Z = 8, ρ_{calcd} = 1.290 g/cm^3, μ = 0.178 mm^{-1}, $F(000)$= 1648.0, reflection collected / unique = 3568 / 2882, refinement method = full-matrix least-squares on F^2, final R indices [I> 2\s(I)]:R_1 = 0.0659, wR_2 = 0.1740, R indices (all data): R_1 = 0.0517, wR_2 = 0.1493, goodness of fit = 1.101. **CCDC-2252567** for **2-((4-methoxyphenyl)thio)-4,6-diphenylnicotinonitrile** (**1d**) contains the supplementary crystallographic data for this paper. These data can be obtained free of charge from The Cambridge Crystallographic Data Centre via www.ccdc.cam.ac.uk/data_request/cif.

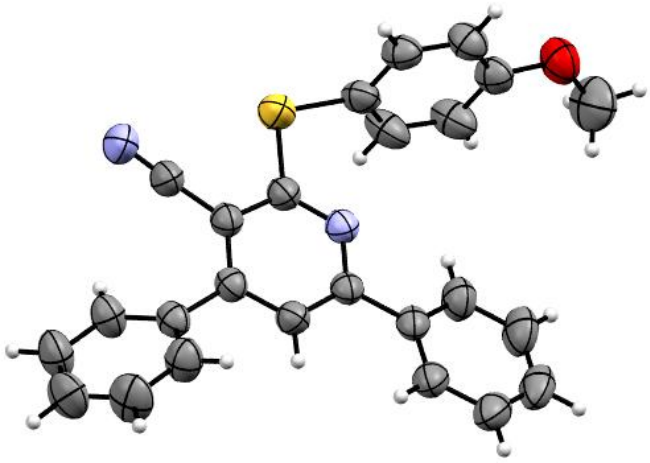

Figure V.6.9.1.1. *ORTEP diagram of 2-((4-methoxyphenyl)thio)-4,6-diphenylnicotinonitrile (**1d**) with 30% ellipsoid probability (CCDC 2252567)*

V.7. Spectral Data:

***4,6-Diphenyl-2-(phenylthio)nicotinonitrile (1a):*[14g]**

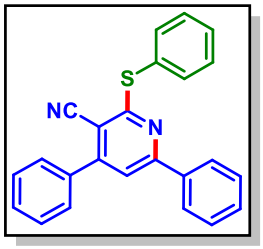

As a white solid (78 mg, 86% yield, mp 170–172 °C); Purification over a column of silica gel (2% EtOAc in hexane); ^{1}H NMR ($CDCl_3$, 500 MHz): δ 7.74 (d, 2H, J = 7.5 Hz), 7.70–7.69 (m, 2H), 7.65–7.63 (m, 2H), 7.56–7.50 (m, 7H), 7.41–7.33 (m, 3H); ^{13}C{^{1}H} NMR ($CDCl_3$, 125 MHz): δ 164.2, 158.4, 154.9, 137.0, 136.4, 136.2, 130.7, 130.2, 129.6, 129.3, 129.2, 128.9, 128.6, 127.3, 116.1, 115.9, 103.3; IR (KBr, cm^{-1}): 2984, 2970, 2205, 1488, 1434, 1278, 915, 750.

***6-Phenyl-2-(phenylthio)-4-(p-tolyl)nicotinonitrile (2a):* [14g]**

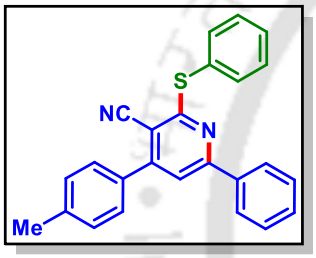

As a white solid (74 mg, 78% yield, mp 178–180 °C); Purification over a column of silica gel (2% EtOAc in hexane); ^{1}H NMR ($CDCl_3$, 400 MHz): δ 7.74–7.72 (m, 2H), 7.70–7.68 (m, 2H), 7.56–7.49 (m, 6H), 7.39–7.32 (m, 5H), 2.45 (s, 3H); ^{13}C{1H} NMR ($CDCl_3$, 100 MHz): δ 164.1, 158.3, 154.9, 140.5, 137.0, 136.2, 133.5, 130.6, 129.9, 129.6, 129.3, 129.0, 128.9, 128.4, 127.3, 116.1, 116.0, 103.2, 21.5; IR (KBr, cm^{-1}): 2959, 2917, 2217, 1730, 1523, 1262, 1023, 817.

***4-(4-Methoxyphenyl)-6-phenyl-2-(phenylthio)nicotinonitrile (3a):*[14g]**

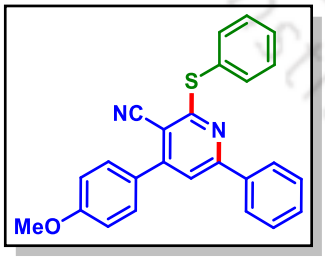

As a white solid (75 mg, 76% yield, mp 175–177 °C); Purification over a column of silica gel (4% EtOAc in hexane); ^{1}H NMR ($CDCl_3$, 500 MHz): δ 7.73 (d, 2H, J = 7.5 Hz), 7.69–7.67 (m, 2H), 7.62 (d, 2H, J = 8.5 Hz), 7.53 (s, 1H), 7.50–7.49 (m, 3H), 7.40–7.32 (m, 3H), 7.06 (d, 2H, J = 8.5 Hz), 3.89 (s, 3H); ^{13}C{^{1}H} NMR ($CDCl_3$, 125 MHz): δ 164.2, 161.3, 158.2, 154.5, 137.1, 136.2, 130.6, 130.1, 129.5, 129.3, 129.0, 128.9, 128.5, 127.3, 116.3, 115.8, 114.7, 102.9, 55.6; IR (KBr, cm^{-1}): 3034, 2823, 2237, 1455, 1265 1034, 749.

4-(4-Fluorophenyl)-6-phenyl-2-(phenylthio)nicotinonitrile (4a): [14g]

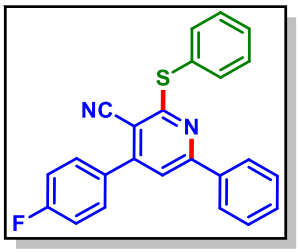

As a white solid (72 mg, 75% yield, mp 214–216 °C); Purification over a column of silica gel (2% EtOAc in hexane); ^{1}H NMR ($CDCl_3$, 500 MHz): δ 7.76 (d, 2H, J = 7.5 Hz), 7.72–7.70 (m, 2H), 7.68–7.65 (m, 2H), 7.55–7.53 (m, 4H), 7.44–7.36 (m, 3H), 7.28 (d, 2H, J = 8.5 Hz); ^{13}C{^{1}H} NMR ($CDCl_3$, 125 MHz): δ 164.4, 164.0 (d, J = 249.5 Hz), 158.5, 153.8, 136.9, 136.2, 132.4 (d, J = 3.3 Hz), 130.8, 130.6 (d, J = 8.5 Hz), 129.7, 129.3, 129.0, 128.8, 127.4, 116.4 (d, J = 21.75 Hz), 115.98, 115.91, 103.2; ^{19}F NMR ($CDCl_3$, 471 MHz): δ –110.2 (s); IR (KBr, cm^{-1}): 2957, 2854, 2215, 1568, 1523, 1260, 1023, 818.

4-(4-Chlorophenyl)-6-phenyl-2-(phenylthio)nicotinonitrile (5a): [14g]

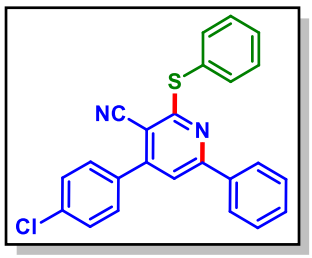

As a white solid (81 mg, 81% yield, mp 219–221 °C); Purification over a column of silica gel (2% EtOAc in hexane); ^{1}H NMR ($CDCl_3$, 500 MHz): δ 7.72 (d, 2H, J = 7.5 Hz), 7.69–7.67 (m, 2H), 7.59–7.57 (m, 2H), 7.53–7.50 (m, 6H), 7.41–7.33 (m, 3H); ^{13}C{^{1}H} NMR ($CDCl_3$, 125 MHz): δ 164.5, 158.6, 153.6, 136.8, 136.7, 136.2, 134.8, 130.8, 129.9, 129.7, 129.5, 129.3, 129.0, 128.7, 127.4, 115.8, 115.7, 103.1; IR (KBr, cm^{-1}): 2962, 2884, 2212, 1595, 1565, 1259, 824.

4-(4-Bromophenyl)-6-phenyl-2-(phenylthio)nicotinonitrile (6a):

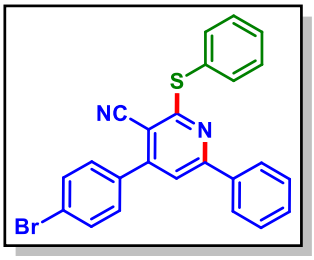

As a white solid (82 mg, 74% yield, mp 210–212 °C); Purification over a column of silica gel (2% EtOAc in hexane); ^{1}H NMR ($CDCl_3$, 500 MHz): δ 7.72 (d, 2H, J = 8.0 Hz), 7.69–7.68 (m, 4H), 7.52–7.50 (m, 6H), 7.41–7.33 (m, 3H); ^{13}C{^{1}H} NMR ($CDCl_3$, 125 MHz): δ 164.5, 158.6, 153.6, 136.8, 136.2, 135.2, 132.5, 130.9, 130.1, 129.7, 129.3, 129.0, 128.7, 127.4, 124.9, 115.7, 103.0; IR (KBr, cm^{-1}): 2919, 2854, 2237, 1520, 1275, 1263, 823; HRMS (ESI/Q-TOF) (m/z) calcd for $C_{24}H_{16}BrN_2S$ $[M + H]^+$ 443.0212; found 443.0216.

4-(2-Bromophenyl)-6-phenyl-2-(phenylthio)nicotinonitrile (7a):

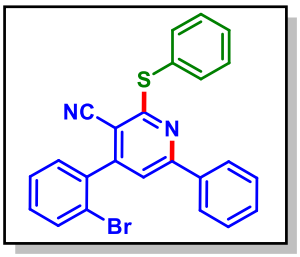

As a white solid (80 mg, 72% yield, mp 206–208 °C); Purification over a column of silica gel (2% EtOAc in hexane); ^{1}H NMR ($CDCl_3$, 500 MHz): δ 7.76–7.71 (m, 5H), 7.53–7.52 (m, 4H), 7.47 (d, 1H, J = 7.5 Hz), 7.76–7.71 (m, 5H); ^{13}C{^{1}H} NMR ($CDCl_3$, 125 MHz): δ 163.5, 158.2, 154.2, 137.3, 136.8, 136.1, 133.6, 131.2, 130.8, 130.5, 129.6, 129.3, 128.9, 128.6, 127.9, 127.4, 122.0, 117.0, 115.0, 104.8; IR (KBr, cm^{-1}): 2917, 2852, 2213, 1569, 1523, 1261, 1022, 742; HRMS (ESI/Q-TOF) (m/z) calcd for $C_{24}H_{16}BrN_2S$ $[M + H]^+$ 443.0212; found 443.0212.

4-Phenyl-2-(phenylthio)-6-(p-tolyl)nicotinonitrile (8a):[14g]

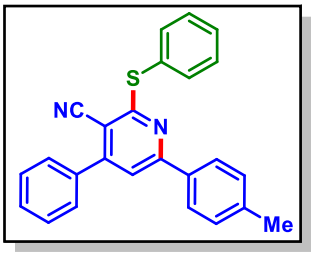

As a white solid (74 mg, 78% yield, mp 199–201 °C); Purification over a column of silica gel (2% EtOAc in hexane); ^{1}H NMR ($CDCl_3$, 500 MHz): δ 7.70–7.68 (m, 2H), 7.63 (d, 4H, J = 8.0 Hz), 7.56–7.49 (m, 7H), 7.15 (d, 2H, J = 8.0 Hz), 2.35 (s, 3H), ^{13}C{^{1}H} NMR ($CDCl_3$, 125 MHz): δ 164.1, 158.4, 154.7, 141.1, 136.5, 136.2, 134.3, 130.1, 129.7, 129.5, 129.3, 129.2, 129.0, 128.6, 127.3, 116.0, 115.7, 102.9, 21.5; IR (KBr, cm^{-1}): 2919, 2852, 2220, 1523, 1260, 1070, 820, 748.

6-(4-Methoxyphenyl)-4-phenyl-2-(phenylthio)nicotinonitrile (9a):[14g]

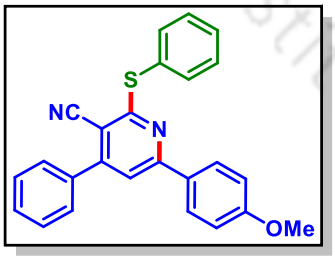

As a white solid (75 mg, 76% yield, mp 170–172 °C); Purification over a column of silica gel (4% EtOAc in hexane); ^{1}H NMR ($CDCl_3$, 500 MHz): δ 7.69 (d, 4H, J = 8.0 Hz), 7.63–7.62 (m, 2H), 7.54–7.50 (m, 6H), 7.46 (s, 1H), 6.85 (d, 2H, J = 8.5 Hz), 3.82 (s, 3H); ^{13}C{^{1}H} NMR ($CDCl_3$, 125 MHz): δ 163.9, 161.8, 158.0, 154.6, 136.5, 136.2, 130.1, 129.54, 129.50, 129.2, 129.1, 129.0, 128.9, 128.5, 116.1, 115.1, 114.3, 102.2, 55.5; IR (KBr, cm^{-1}): 2932, 2859, 2234, 1516, 1265, 749.

6-(4-(tert-Butyl)phenyl)-4-phenyl-2-(phenylthio)nicotinonitrile (10a):

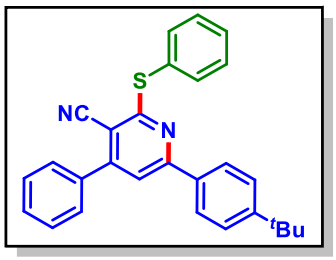

As a white solid (76 mg, 72% yield, mp 144–146 °C); Purification over a column of silica gel (4% EtOAc in hexane); ^{1}H NMR ($CDCl_3$, 500 MHz): δ 7.71–7.70 (m, 4H), 7.66–7.64 (m, 2H), 7.56–7.52 (m, 7H), 7.39 (d, 2H, J = 8.5 Hz), 1.34 (s, 9H); ^{13}C{^{1}H} NMR ($CDCl_3$, 125 MHz): δ 164.0, 158.4, 154.7, 154.2, 136.5, 136.1, 134.2, 130.1, 129.5, 129.2, 129.1, 129.0, 128.5, 127.1, 125.9, 116.0, 115.8, 102.9, 34.9, 31.3; IR (KBr, cm^{-1}): 2954, 2850, 2212, 1611, 1567, 1477, 1262, 1021, 844; HRMS (ESI/Q-TOF) (m/z) calcd for $C_{28}H_{25}N_2S$ [M + H]$^{+}$ 421.1733; found 421.1736.

6-(4-Fluorophenyl)-4-phenyl-2-(phenylthio)nicotinonitrile (11a):[14g]

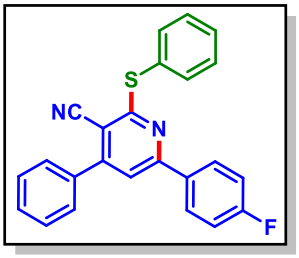

As a white solid (70 mg, 73% yield, mp 215–217 °C); Purification over a column of silica gel (2% EtOAc in hexane); ^{1}H NMR ($CDCl_3$, 500 MHz): δ 7.72 (t, 2H, J = 6.75 Hz), 7.67 (d, 2H, J = 7.0 Hz), 7.63–7.62 (m, 2H), 7.55–7.54 (m, 3H), 7.50 (d, 4H, J = 8.0 Hz), 7.02 (t, 2H, J = 8.5 Hz); ^{13}C{^{1}H} NMR ($CDCl_3$, 125 MHz): δ 164.5 (d, J = 250 Hz), 164.4, 157.3, 155.0, 136.3, 136.2, 133.2 (d, J = 3.1 Hz), 130.3, 129.7, 129.5, 129.4, 129.3, 129.2, 128.9, 128.5, 116.1, 115.9, 115.8, 115.7, 103.3; ^{19}F NMR ($CDCl_3$, 471 MHz): δ –109.9 (s); IR (KBr, cm^{-1}): 2918, 2824, 2215, 1443, 1260, 1024, 748.

6-(4-Chlorophenyl)-4-phenyl-2-(phenylthio)nicotinonitrile (12a):[14g]

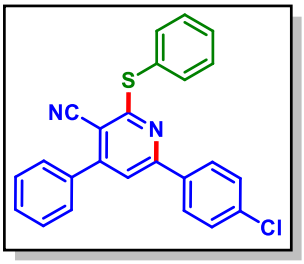

As a white solid (77 mg, 77% yield, mp 223–225 °C); Purification over a column of silica gel (2% EtOAc in hexane); ^{1}H NMR ($CDCl_3$, 500 MHz): δ 7.68–7.62 (m, 6H), 7.55–7.49 (m, 7H), 7.31 (d, 2H, J = 8.5 Hz); ^{13}C{^{1}H} NMR ($CDCl_3$, 125 MHz): δ 164.5, 157.2, 155.1, 137.0, 136.4, 136.3, 135.5, 130.3, 129.7, 129.4, 129.3, 129.2, 128.8, 128.7, 128.6, 115.9, 115.8, 103.6; IR (KBr, cm^{-1}): 2929, 2849, 2217, 1566, 1520, 1260, 1091, 835.

4-(Benzo[d][1,3]dioxol-5-yl)-6-phenyl-2-(phenylthio)nicotinonitrile (13a):

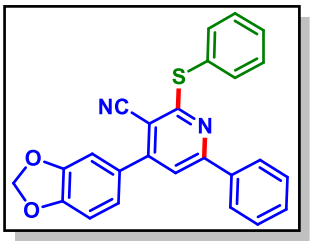

As a white solid (76 mg, 74% yield, mp 199–201 °C); Purification over a column of silica gel (2% EtOAc in hexane); ^{1}H NMR ($CDCl_3$, 500 MHz): δ 7.72 (d, 2H, J = 7.5 Hz), 7.69–7.67 (m, 2H), 7.50–7.49 (m, 4H), 7.38–7.32 (m, 3H), 7.14 (d, 1H, J = 8.0 Hz), 7.10 (s, 1H), 6.96 (d, 1H, J = 8.0 Hz), 6.06 (s, 2H); ^{13}C{^{1}H} NMR ($CDCl_3$, 125 MHz): δ 164.3, 158.3, 154.4, 149.5, 148.5, 137.0, 136.2, 130.6, 130.1, 129.6, 129.3, 129.0, 128.9, 127.3, 123.0, 116.0, 115.9, 109.0, 108.9, 103.1, 101.9; IR (KBr, cm^{-1}): 2959, 2848, 2210, 1525, 1240, 1030, 751; HRMS (ESI/Q-TOF) (m/z) calcd for $C_{25}H_{17}N_2O_2S$ [M + H]$^{+}$ 409.1005; found 409.1007.

6-(4-Fluorophenyl)-2-(phenylthio)-4-(p-tolyl)nicotinonitrile (14a):

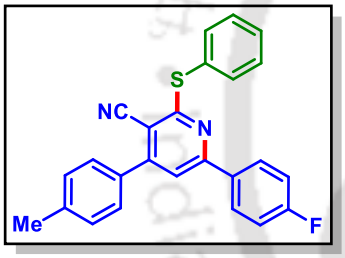

As a white solid (69 mg, 70% yield, mp 201–203 °C); Purification over a column of silica gel (2% EtOAc in hexane); ^{1}H NMR ($CDCl_3$, 500 MHz): δ 7.71 (t, 2H, J = 7.25 Hz), 7.67 (d, 2H, J = 7.5 Hz), 7.54−7.48 (m, 6H), 7.35 (d, 2H, J = 7.5 Hz), 7.01 (t, 2H, J = 8.5 Hz), 2.44 (s, 3H); ^{13}C{^{1}H} NMR ($CDCl_3$, 125 MHz): δ 164.5 (d, J = 250.2 Hz), 164.3, 157.2, 155.0, 140.6, 136.2, 133.4, 133.3 (d, J = 3.0 Hz), 129.9, 129.6, 129.4, 129.3, 129.0, 128.4, 116.0, 115.9, 115.6, 103.2, 21.5; ^{19}F NMR ($CDCl_3$, 471 MHz): δ –110.0 (s); IR (KBr, cm^{-1}): 2921, 2852, 2214, 1598, 1507, 1224, 1153, 815; HRMS (ESI/Q-TOF) (m/z) calcd for $C_{25}H_{18}FN_2S$ [M + H]$^{+}$ 397.1169; found 397.1172.

4-(4-Chlorophenyl)-6-(4-methoxyphenyl)-2-(phenylthio)nicotinonitrile (15a):

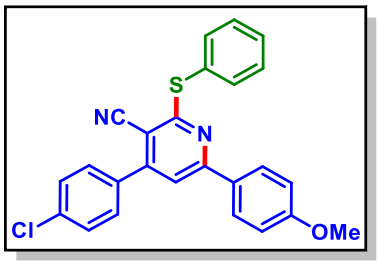

As a white solid (76 mg, 71% yield, mp 229–231 °C); Purification over a column of silica gel (4% EtOAc in hexane); ^{1}H NMR ($CDCl_3$, 500 MHz): δ 7.69–7.66 (m, 4H), 7.57–7.49 (m, 7H), 7.42 (s, 1H), 6.84 (d, 2H, J = 8.5 Hz), 3.82 (s, 3H); ^{13}C{^{1}H} NMR ($CDCl_3$, 125 MHz): δ 164.3, 162.1, 158.3, 153.4, 136.5, 136.2, 135.0, 129.9, 129.6, 129.4, 129.3, 129.1, 129.0, 115.9, 114.9, 114.4, 102.2, 55.6;

IR (KBr, cm^{-1}): 3017, 2923, 2237, 1955, 1468, 1278, 1020, 828, 753; HRMS (ESI/Q-TOF) (m/z) calcd for $C_{25}H_{18}ClN_2OS$ $[M + H]^+$ 429.0823; found 429.0824.

6-(5-Bromothiophen-2-yl)-4-phenyl-2-(phenylthio)nicotinonitrile (16a):

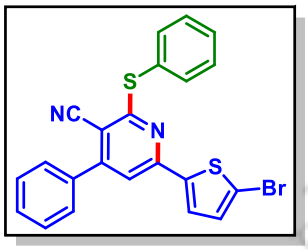

As a white solid (73 mg, 65% yield, mp 180–182 °C); Purification over a column of silica gel (2% EtOAc in hexane); ^1H NMR ($CDCl_3$, 500 MHz): δ 7.65–7.63 (m, 2H), 7.61–7.59 (m, 2H), 7.54–7.51 (m, 6H), 7.27 (s, 1H), 7.22 (d, 1H, J = 4.0 Hz), 6.98 (d, 1H, J = 4.0 Hz); $^{13}C\{^1H\}$ NMR ($CDCl_3$, 125 MHz): δ 164.6, 154.7, 152.9, 144.9, 136.1, 136.0, 131.4, 130.3, 129.8, 129.4, 129.2, 128.4, 128.2, 127.0, 118.7, 115.7, 113.8, 102.7; IR (KBr, cm^{-1}): 3059, 2917, 2215, 1567, 1517, 1264, 1065, 869, 732; HRMS (ESI/Q-TOF) (m/z) calcd for $C_{22}H_{14}BrN_2S_2$ $[M + H]^+$ 448.9776; found 448.9775.

6-(Furan-2-yl)-2-(phenylthio)-4-(p-tolyl)nicotinonitrile (17a):

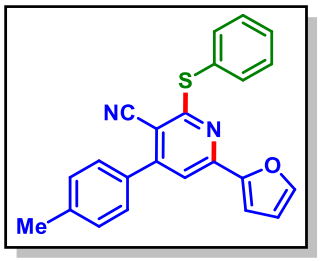

As a yellow solid (51 mg, 55% yield, mp 165–167 °C); Purification over a column of silica gel (2% EtOAc in hexane); ^1H NMR ($CDCl_3$, 500 MHz): δ 7.67–7.65 (m, 2H), 7.54 (d, 2H, J = 7.5 Hz), 7.49–7.48 (m, 4H), 7.44 (s, 1H), 7.33 (d, 2H, J = 8.0 Hz), 6.61 (d, 1H, J = 3.5 Hz), 6.46–6.43 (m, 1H), 2.44 (s, 3H); $^{13}C\{^1H\}$ NMR ($CDCl_3$, 125 MHz): δ 164.2, 154.8, 152.7, 150.2, 144.9, 140.5, 136.0, 133.3, 129.8, 129.5, 129.1, 128.9, 128.4, 116.1, 113.9, 112.7, 112.6, 102.3, 21.5; IR (KBr, cm^{-1}): 2922, 2854, 2215, 1598, 1273, 1008, 745; HRMS (ESI/Q-TOF) (m/z) calcd for $C_{23}H_{17}N_2OS$ $[M + H]^+$ 369.1056; found 369.1052.

2-(Phenylthio)-4,6-di(thiophen-2-yl)nicotinonitrile (18a):

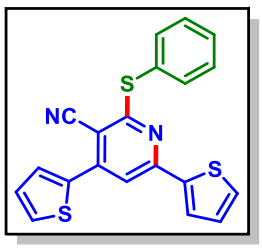

As a white solid (50 mg, 53% yield, mp 136–138 °C); Purification over a column of silica gel (2% EtOAc in hexane); ^1H NMR ($CDCl_3$, 500 MHz): δ 7.89 (d, 1H, J = 3.5 Hz), 7.66–7.64 (m, 2H), 7.55 (d, 1H, J = 5.5 Hz), 7.50–7.49 (m, 4H), 7.43 (s, 1H), 7.38 (d, 1H, J = 5.0 Hz), 7.21 (t, 1H, J = 4.5 Hz), 7.04 (t, 1H, J = 4.25 Hz); $^{13}C\{^1H\}$ NMR

($CDCl_3$, 125 MHz): δ 165.1, 153.9, 146.2, 143.2, 137.3, 136.2, 130.8, 129.7, 129.6, 129.4, 129.3, 128.9, 128.5, 128.4, 127.3, 116.4, 113.2, 100.1; IR (KBr, cm^{-1}): 2962, 2922, 2215, 1569, 1510, 1277, 741, 691; HRMS (ESI/Q-TOF) (m/z) calcd for $C_{20}H_{13}N_2S_3$ $[M + H]^+$ 377.0235; found 377.0235.

***4,6-Di(furan-2-yl)-2-(phenylthio)nicotinonitrile (19a):*[14g]**

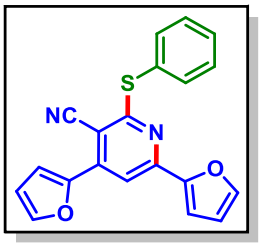

As a black solid (45 mg, 52% yield, mp 150–152 °C); Purification over a column of silica gel (2% EtOAc in hexane); ^1H NMR ($CDCl_3$, 500 MHz): δ 7.80 (s, 1H), 7.64–7.62 (m, 3H), 7.61 (d, 1H, J = 3.5 Hz), 7.50 (s, 1H), 7.47–7.46 (m, 3H), 6.63 (s, 1H), 6.58 (d, 1H, J = 3.5 Hz), 6.44 (s, 1H); $^{13}C\{^1H\}$ NMR ($CDCl_3$, 125 MHz): δ 164.6, 152.7, 150.5, 148.2, 145.1, 145.0, 141.4, 136.1, 129.5, 129.1, 128.8, 116.5, 114.5, 113.0, 112.8, 112.6, 109.1, 97.1; IR (KBr, cm^{-1}): 3068, 2938, 2824, 2215, 1575, 1177, 1065.

***4,6-Diphenyl-2-(p-tolylthio)nicotinonitrile (1b):*[14g]**

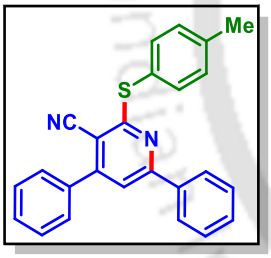

As a white solid (74 mg, 78% yield, mp 187–189 °C); Purification over a column of silica gel (2% EtOAc in hexane); ^1H NMR ($CDCl_3$, 500 MHz): δ 7.77 (d, 2H, J = 7.0 Hz), 7.66–7.64 (m, 2H), 7.59 (d, 2H, J = 8.0 Hz), 7.56–7.54 (m, 4H), 7.42–7.35 (m, 3H), 7.32 (d, 2H, J = 8.0 Hz), 2.48 (s, 3H); $^{13}C\{^1H\}$ NMR ($CDCl_3$, 125 MHz): δ 164.5, 158.3, 154.7, 139.8, 137.0, 136.4, 136.0, 130.6, 130.1, 130.0, 129.1, 128.8, 128.5, 127.3, 125.2, 116.0, 115.9, 103.1, 21.5; IR (KBr, cm^{-1}): 2979, 2850, 2232, 1273, 1051, 753.

***4,6-Diphenyl-2-(o-tolylthio)nicotinonitrile (1c):*[14g]**

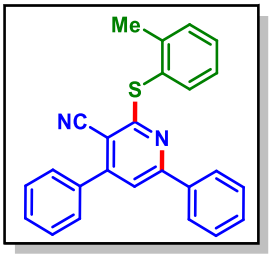

As a white solid (70 mg, 74% yield, mp 118–120 °C); Purification over a column of silica gel (2% EtOAc in hexane); ^1H NMR ($CDCl_3$, 400 MHz): δ 7.69–7.63 (m, 5H), 7.55–7.53 (m, 4H), 7.45–7.43 (m, 2H), 7.38–7.30 (m, 4H), 2.45 (s, 3H); $^{13}C\{^1H\}$ NMR ($CDCl_3$, 100 MHz): δ 164.0, 158.2, 154.8, 143.9, 137.2, 136.9, 136.5, 130.76, 130.7, 130.3, 130.2, 129.2, 128.9, 128.6, 128.4, 127.2, 126.8, 116.1,

115.7, 103.2, 21.1; IR (KBr, cm^{-1}): 2918, 2856, 2218, 1526, 1262, 1080, 820, 750.

2-((4-Methoxyphenyl)thio)-4,6-diphenylnicotinonitrile (1d):[14g]

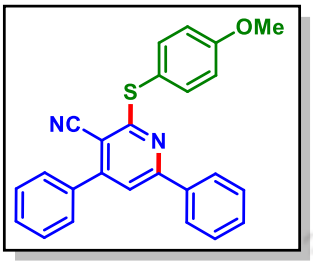

As a white solid (75 mg, 76% yield, mp 202–204 °C); Purification over a column of silica gel (2% EtOAc in hexane); ^{1}H NMR ($CDCl_3$, 500 MHz): δ 7.77 (d, 2H, J = 7.0 Hz), 7.64–7.63 (m, 2H), 7.60 (d, 2H, J = 8.5 Hz), 7.55–7.53 (m, 4H), 7.40–7.34 (m, 3H), 7.03 (d, 2H, J = 8.5 Hz), 3.89 (s, 3H); $^{13}C\{^{1}H\}$ NMR ($CDCl_3$, 125 MHz): δ 164.9, 161.0, 158.4, 154.8, 137.9, 137.1, 136.4, 130.6, 130.2, 129.2, 128.9, 128.5, 127.4, 119.4, 116.0, 114.9, 103.0, 55.6; IR (KBr, cm^{-1}): 3058, 2964, 2827, 2214, 1260, 1062.

2-((3-Methoxyphenyl)thio)-4,6-diphenylnicotinonitrile (1e):[14g]

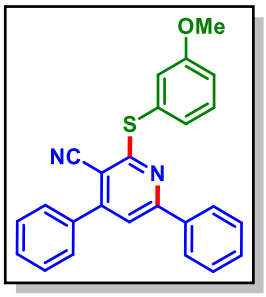

As a white solid (68 mg, 69% yield, mp 166–168 °C); Purification over a column of silica gel (3% EtOAc in hexane); ^{1}H NMR ($CDCl_3$, 500 MHz): δ 7.81 (d, 2H, J = 7.5 Hz), 7.65–7.64 (m, 2H), 7.57–7.54 (m, 4H), 7.42–7.35 (m, 4H), 7.30–7.26 (m, 2H), 7.06 (d, 1H, J = 8.5 Hz), 3.84 (s, 3H); $^{13}C\{^{1}H\}$ NMR ($CDCl_3$, 125 MHz): δ 164.0, 160.1, 158.4, 154.8, 136.9, 136.4, 130.7, 130.2, 129.9, 129.8, 129.2, 128.9, 128.5, 128.2, 127.4, 120.8, 116.2, 116.0, 115.9, 103.4, 55.6; IR (KBr, cm^{-1}): 3059, 2912, 2836, 2212, 1574, 1253, 1175, 1012, 820.

2-((4-Fluorophenyl)thio)-4,6-diphenylnicotinonitrile (1f):[14g]

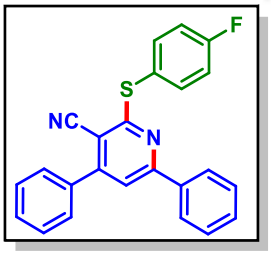

As a white solid (67 mg, 70% yield, mp 194–196 °C); Purification over a column of silica gel (2% EtOAc in hexane); ^{1}H NMR ($CDCl_3$, 500 MHz): δ 7.75 (d, 2H, J = 7.5 Hz), 7.68–7.64 (m, 4H), 7.57–7.54 (m, 4H), 7.43–7.37 (m, 3H), 7.21 (t, 2H, J = 8.25 Hz); $^{13}C\{^{1}H\}$ NMR ($CDCl_3$, 125 MHz): δ 163.9, 163.8 (d, J = 248.7 Hz), 158.4, 154.8, 138.4 (d, J = 8.5 Hz), 136.9, 136.3, 130.8, 130.2, 129.2, 129.0, 128.5, 127.3, 124.0 (d, J = 3.5 Hz), 116.5 (d, J = 22 Hz), 116.2, 115.8, 103.2; ^{19}F NMR ($CDCl_3$, 471 MHz): δ –110.9 (s); IR (KBr, cm^{-1}): 2953, 2856, 2216, 1562, 1262, 1024, 750.

2-((3-Fluorophenyl)thio)-4,6-diphenylnicotinonitrile (1g):

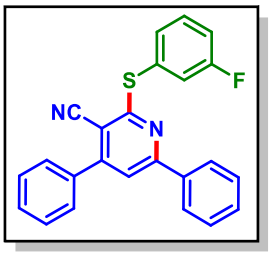

As a white solid (69 mg, 72% yield, mp 182–184 °C); Purification over a column of silica gel (2% EtOAc in hexane); ^{1}H NMR ($CDCl_3$, 500 MHz): δ 7.78 (d, 2H, J = 7.5 Hz), 7.65–7.64 (m, 2H), 7.59 (s, 1H), 7.56–7.55 (m, 3H), 7.47–7.45 (m, 3H), 7.42–7.36 (m, 3H), 7.22 (t, 1H, J = 8.25 Hz); ^{13}C{^{1}H} NMR ($CDCl_3$, 125 MHz): δ 163.3, 162.9 (d, J = 247.5 Hz), 158.6, 155.0, 136.9, 136.3, 131.6 (d, J = 3.1 Hz), 130.8, 130.4 (d, J = 8.1 Hz), 130.3, 129.3, 129.0, 128.6, 127.4, 123.0, 122.8, 116.7 (d, J = 21.25 Hz), 116.5, 115.7, 103.6; ^{19}F NMR ($CDCl_3$, 471 MHz): δ –112.09 (s); IR (KBr, cm^{-1}): 2980, 2854, 2214, 1560, 1274, 1024, 752; HRMS (ESI/Q-TOF) (m/z) calcd for $C_{24}H_{16}FN_2S$ $[M + H]^+$ 383.1013; found 383.1015.

2-((4-Chlorophenyl)thio)-4,6-diphenylnicotinonitrile (1h):[14g]

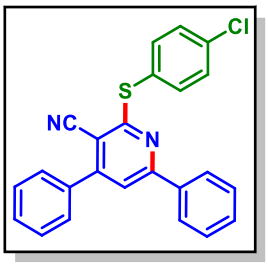

As a white solid (73 mg, 73% yield, mp 207–209 °C); Purification over a column of silica gel (2% EtOAc in hexane); ^{1}H NMR ($CDCl_3$, 500 MHz): δ 7.75 (d, 2H, J = 7.0 Hz), 7.65–7.61 (m, 4H), 7.57 (s, 1H), 7.56–7.54 (m, 3H), 7.48 (d, 2H, J = 8.0 Hz), 7.42–7.37 (m, 3H); ^{13}C{^{1}H} NMR ($CDCl_3$, 125 MHz): δ 163.5, 158.5, 154.9, 137.3, 136.8, 136.2, 136.0, 130.8, 130.3, 129.5, 129.2, 129.0, 128.5, 127.4, 127.3, 116.4, 115.7, 103.4; IR (KBr, cm^{-1}): 2965, 2872, 2210, 1564, 1476, 1258, 1059, 760.

2-((3-Chlorophenyl)thio)-4,6-diphenylnicotinonitrile (1i):[14g]

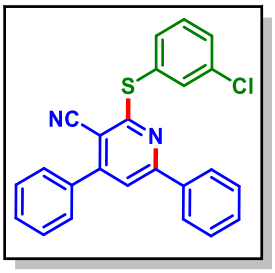

As a white solid (65 mg, 65% yield, mp 190–192 °C); Purification over a column of silica gel (2% EtOAc in hexane); ^{1}H NMR ($CDCl_3$, 500 MHz): δ 7.80 (d, 2H, J = 7.0 Hz), 7.76 (s, 1H), 7.65–7.63 (m, 2H), 7.59 (s, 1H), 7.57–7.54 (m, 4H), 7.49 (d, 1H, J = 8.0 Hz), 7.43–7.37 (m, 4H); ^{13}C{^{1}H} NMR ($CDCl_3$, 125 MHz): δ 163.1, 158.6, 155.0, 136.9, 136.3, 135.9, 134.7, 133.9, 130.9, 130.7, 130.3, 130.2, 129.7, 129.3, 129.1, 128.6, 127.4, 116.6, 115.7, 103.6; IR (KBr, cm^{-1}): 2958, 2860, 2215, 1561, 1471, 1262, 1058, 748.

2-((2-Bromophenyl)thio)-4,6-diphenylnicotinonitrile (1j):[14g]

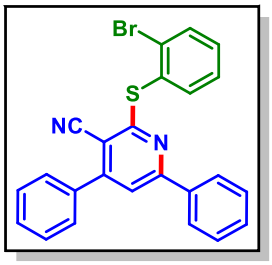

As a white solid (71 mg, 64% yield, mp 160–162 °C); Purification over a column of silica gel (2% EtOAc in hexane); ^{1}H NMR ($CDCl_3$, 500 MHz): δ 7.82 (d, 1H, J = 7.5 Hz), 7.78 (d, 1H, J = 7.5 Hz), 7.72 (d, 2H, J = 7.5 Hz), 7.67–7.65 (m, 2H), 7.57–7.54 (m, 4H), 7.44–7.33 (m, 5H); ^{13}C{^{1}H} NMR ($CDCl_3$, 125 MHz): δ 162.8, 158.5, 154.9, 138.2, 136.9, 136.3, 133.7, 131.5, 131.3, 130.8, 130.7, 130.2, 129.2, 128.9, 128.5, 128.2, 127.3, 116.3, 115.8, 103.4; IR (KBr, cm^{-1}): 2918, 2855, 2214, 1569, 1484, 1264, 1022, 742.

2-(Naphthalen-2-ylthio)-4,6-diphenylnicotinonitrile (1k):[14g]

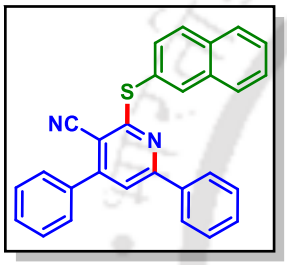

As a white solid (83 mg, 80% yield, mp 172–174 °C); Purification over a column of silica gel (2% EtOAc in hexane); ^{1}H NMR ($CDCl_3$, 500 MHz): δ 8.23 (s, 1H), 7.94 (t, 2H, J = 7.5 Hz), 7.88 (d, 1H, J = 7.5 Hz), 7.72 (d, 1H, J = 8.75 Hz), 7.69 (d, 2H, J = 7.0 Hz), 7.66–7.64 (m, 2H), 7.59–7.54 (m, 6H), 7.32 (t, 1H, J = 7.5 Hz), 7.23 (t, 2H, J = 7.75 Hz); ^{13}C{^{1}H} NMR ($CDCl_3$, 125 MHz): δ 164.1, 158.5, 154.9, 136.9, 136.4, 135.4, 133.9, 133.6, 132.5, 130.6, 130.2, 129.2, 128.9, 128.6, 128.2, 127.9, 127.4, 127.3, 126.7, 126.3, 116.3, 116.0, 103.4; IR (KBr, cm^{-1}): 3002, 2852, 2235, 1574, 1275, 1258, 749.

4,6-Diphenyl-2-(thiophen-2-ylthio)nicotinonitrile (1l):[14g]

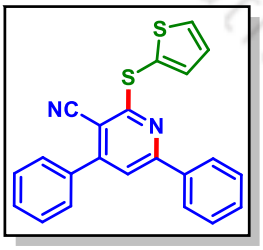

As a white solid (66 mg, 71% yield, mp 164–166 °C); Purification over a column of silica gel (2% EtOAc in hexane); ^{1}H NMR ($CDCl_3$, 500 MHz): δ 7.84 (d, 2H, J = 7.0 Hz), 7.69 (d, 1H, J = 5.5 Hz), 7.64–7.63 (m, 2H), 7.58 (s, 1H), 7.56–7.54 (m, 3H), 7.42–7.38 (m, 4H), 7.21 (t, 1H, J = 4.2 Hz); ^{13}C{^{1}H} NMR ($CDCl_3$, 125 MHz): δ 163.9, 158.8, 154.8, 137.5, 136.8, 136.2, 132.8, 130.8, 130.2, 129.2, 128.9, 128.5, 127.9, 127.4, 125.8, 116.5, 115.7, 102.9; IR (KBr, cm^{-1}): 3024, 2854, 2220, 1523, 1261, 1025, 748.

6-Phenyl-2-(pyridin-4-ylthio)-4-(p-tolyl)nicotinonitrile (2m):

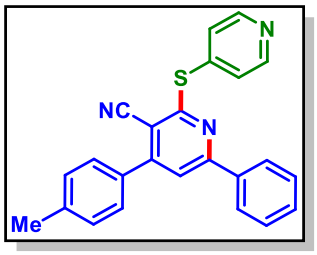

As a yellow solid (30 mg, 32% yield, mp 190–192 °C); Purification over a column of silica gel (15% EtOAc in hexane); ^{1}H NMR ($CDCl_3$, 500 MHz): δ 7.61–7.59 (m, 3H), 7.55–7.53 (m, 4H), 7.52–7.49 (m, 3H), 7.35 (d, 3H, J = 8.0 Hz), 7.24 (s, 1H), 2.44 (s, 3H); ^{13}C{^{1}H} NMR ($CDCl_3$, 125 MHz): δ 181.3, 162.4, 157.3, 142.0, 135.8, 134.7, 131.9, 130.7, 130.5, 130.0, 129.8, 128.3, 127.1, 119.7, 114.8, 106.0, 21.7; IR (KBr, cm^{-1}): 3064, 2924, 2220, 1635, 1486, 1190, 763; HRMS (ESI/Q-TOF) (m/z) calcd for $C_{24}H_{18}N_3S$ $[M + H]^+$ 380.1216; found 380.1214.

2-((4-Chlorobenzyl)thio)-4,6-diphenylnicotinonitrile (1n):

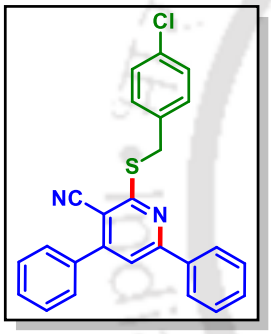

As a white solid (66 mg, 64% yield, mp 175–177 °C); Purification over a column of silica gel (2% EtOAc in hexane); ^{1}H NMR ($CDCl_3$, 500 MHz): δ 8.06–8.04 (m, 2H), 7.62–7.61 (m, 2H), 7.55–7.50 (m, 7H), 7.41 (d, 2H, J = 8.0 Hz), 7.27 (d, 2H, J = 8.5 Hz), 4.63 (s, 2H); ^{13}C{^{1}H} NMR ($CDCl_3$, 125 MHz): δ 163.3, 158.8, 154.8, 137.5, 136.3, 136.0, 133.4, 130.8, 130.5, 130.3, 129.3, 129.2, 128.9, 128.5, 127.6, 116.4, 115.7, 103.8, 34.3; IR (KBr, cm^{-1}): 2962, 2917, 2212, 1570, 1528, 1261, 748; HRMS (ESI/Q-TOF) (m/z) calcd for $C_{25}H_{18}ClN_2S$ $[M + H]^+$ 413.0874; found 413.0876.

2-((4-Chlorobenzyl)thio)-6-phenyl-4-(p-tolyl)nicotinonitrile (2n):

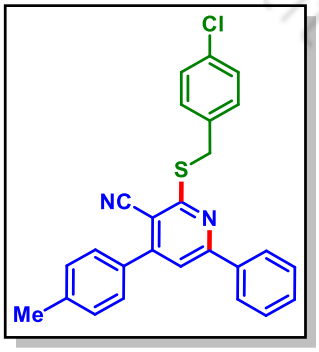

As a white solid (66 mg, 62% yield, mp 178–180 °C); Purification over a column of silica gel (2% EtOAc in hexane); ^{1}H NMR ($CDCl_3$, 500 MHz): δ 8.05–8.03 (m, 2H), 7.54–7.50 (m, 6H), 7.41 (d, 2H, J = 8.5 Hz), 7.33 (d, 2H, J = 8.0 Hz), 7.27 (d, 2H, J = 8.0 Hz), 4.63 (s, 2H), 2.43 (s, 3H); ^{13}C{^{1}H} NMR ($CDCl_3$, 125 MHz): δ 163.2, 158.7, 154.8, 140.6, 137.6, 136.1, 133.44, 133.40, 130.7, 130.5, 129.9, 129.1, 128.9, 128.5, 127.5, 116.3, 116.0, 103.7, 34.3, 21.5; IR (KBr, cm^{-1}): 2959, 2917, 2216, 1525, 1265, 1024, 745; HRMS (ESI/Q-

TOF) (m/z) calcd for $C_{26}H_{20}ClN_2S$ $[M + H]^+$ 427.1030; found 427.1030.

2-(Benzylthio)-4-(4-bromophenyl)-6-phenylnicotinonitrile (6o):

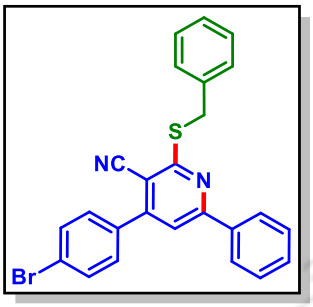

As a white solid (59 mg, 52% yield, mp 215–217 ^oC); Purification over a column of silica gel (2% EtOAc in hexane); ^1H NMR ($CDCl_3$, 500 MHz): δ 8.12 (s, 1H), 7.72 (d, 2H, J = 7.5 Hz), 7.57–7.52 (m, 6H), 7.38–7.31 (m, 6H), 4.73 (s, 2H); $^{13}C\{^1H\}$ NMR ($CDCl_3$, 125 MHz): δ 164.1, 159.0, 153.5, 137.4, 137.1, 135.2, 132.5, 130.9, 130.1, 129.8, 129.5, 129.2, 128.8, 127.6, 124.9, 115.8, 115.6, 103.4, 35.1; IR (KBr, cm^{-1}): 2923, 2850, 2218, 1520, 1263, 824, 748; HRMS (ESI/Q-TOF) (m/z) calcd for $C_{25}H_{18}BrN_2S$ $[M + H]^+$ 457.0369; found 457.0370.

V.8. Representative NMR Spectra:

4,6-Diphenyl-2-(phenylthio)nicotinonitrile (1a): ^{1}H NMR ($CDCl_3$, 500 MHz)

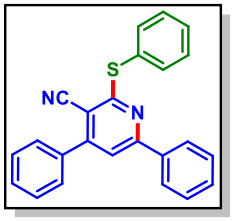

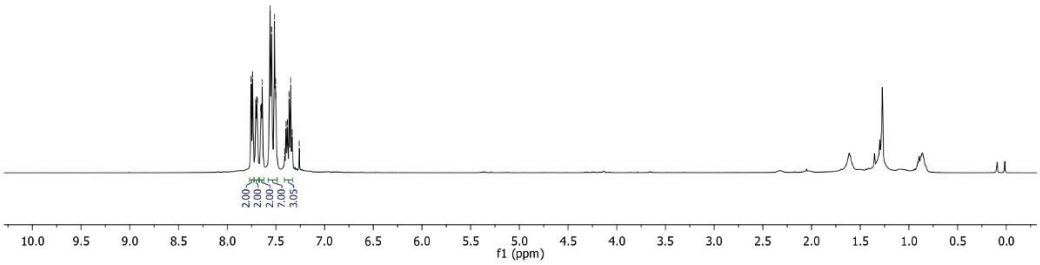

4,6-Diphenyl-2-(phenylthio)nicotinonitrile (1a):$^{13}C\{^{1}H\}$ NMR ($CDCl_3$, 125 MHz)

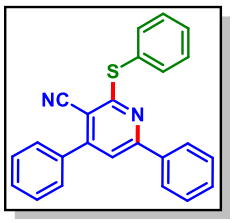

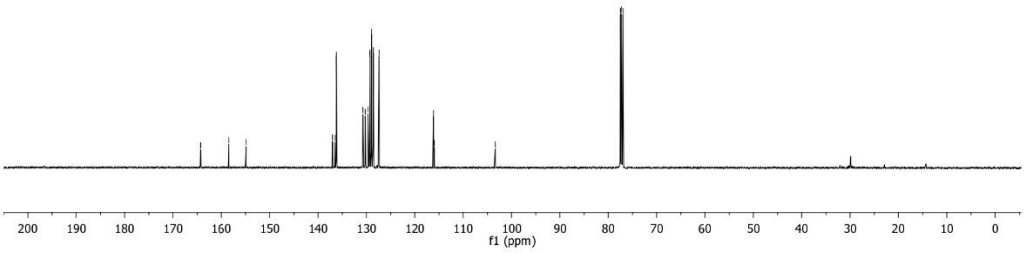

6-Phenyl-2-(phenylthio)-4-(p-tolyl)nicotinonitrile (2a): ^{1}H NMR (CDCl$_3$, 400 MHz)

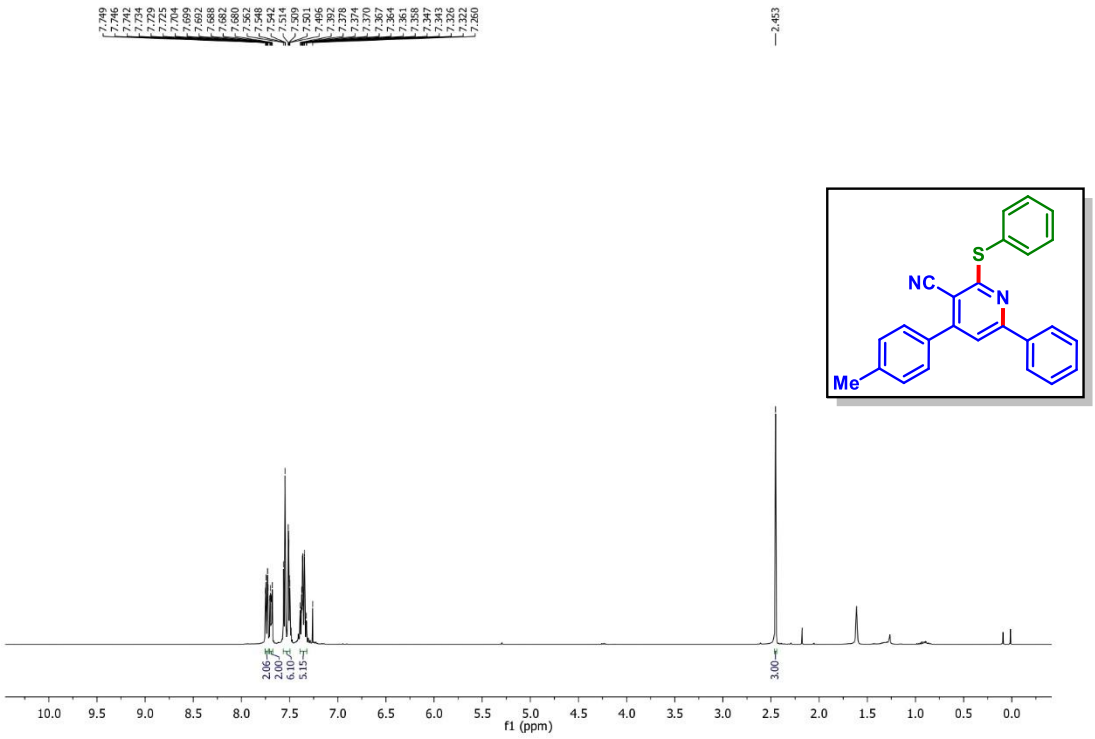

6-Phenyl-2-(phenylthio)-4-(p-tolyl)nicotinonitrile (2a) : ^{13}C{^{1}H} NMR (CDCl$_3$, 100 MHz)

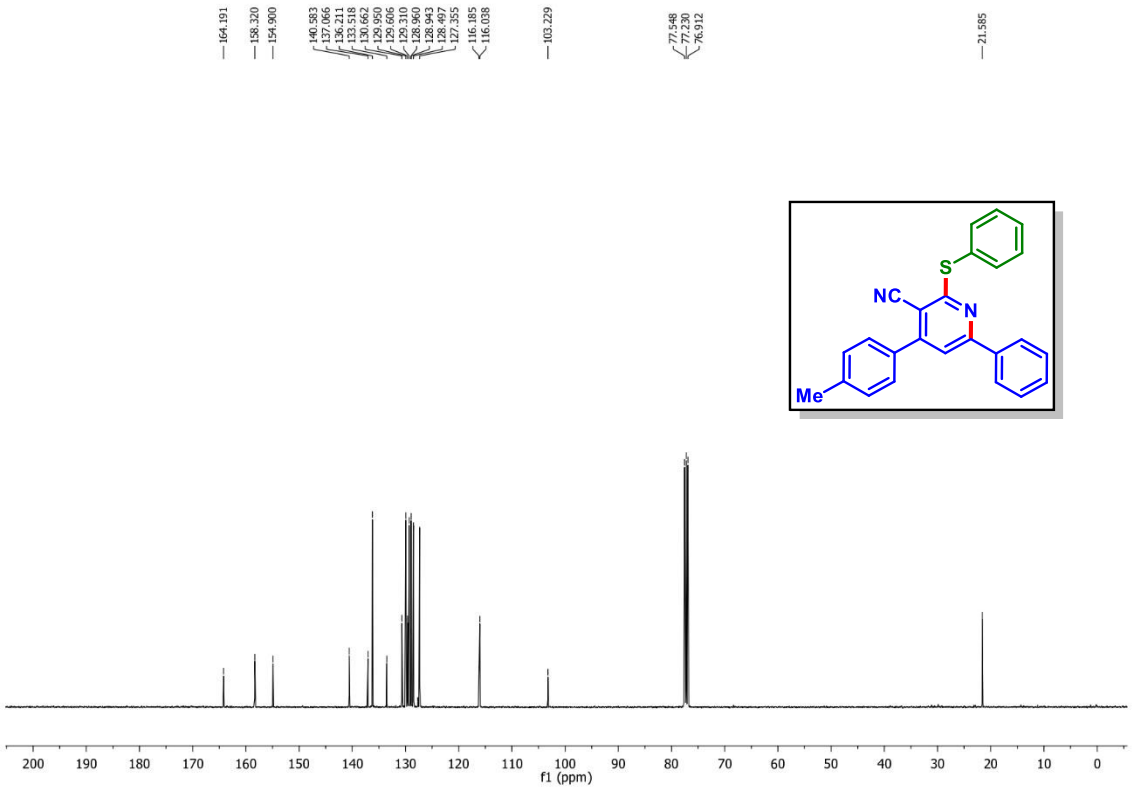

4-(4-Chlorophenyl)-6-phenyl-2-(phenylthio)nicotinonitrile (5a): ^{1}H NMR ($CDCl_3$, 500 MHz)

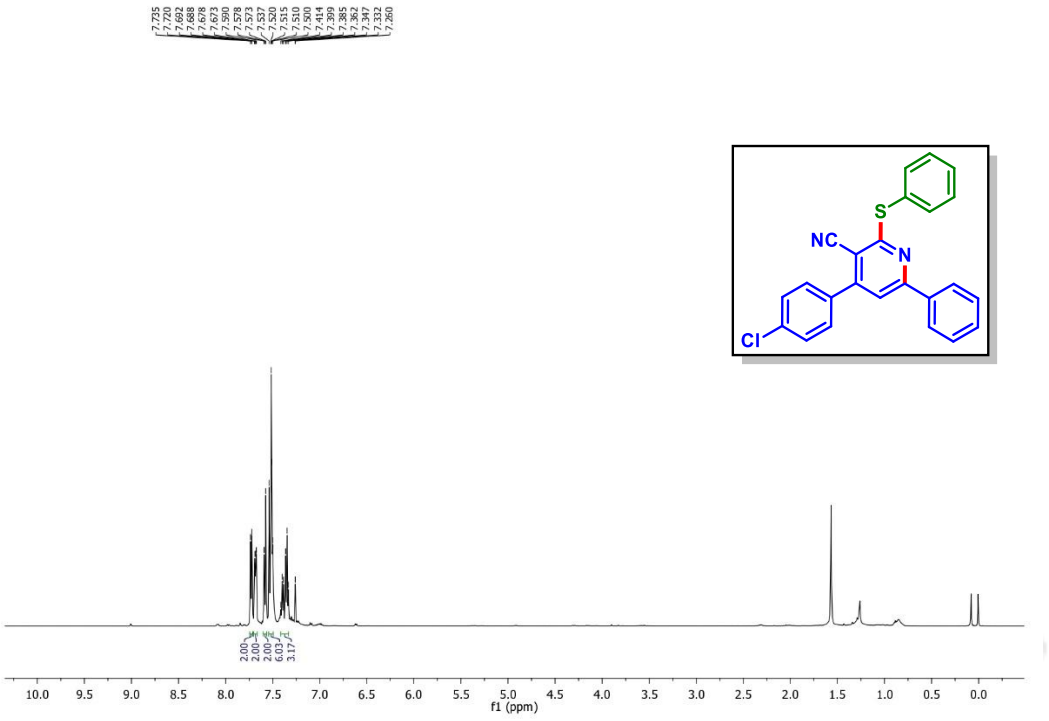

4-(4-Chlorophenyl)-6-phenyl-2-(phenylthio)nicotinonitrile (5a): $^{13}C\{^{1}H\}$ NMR ($CDCl_3$, 125 MHz)

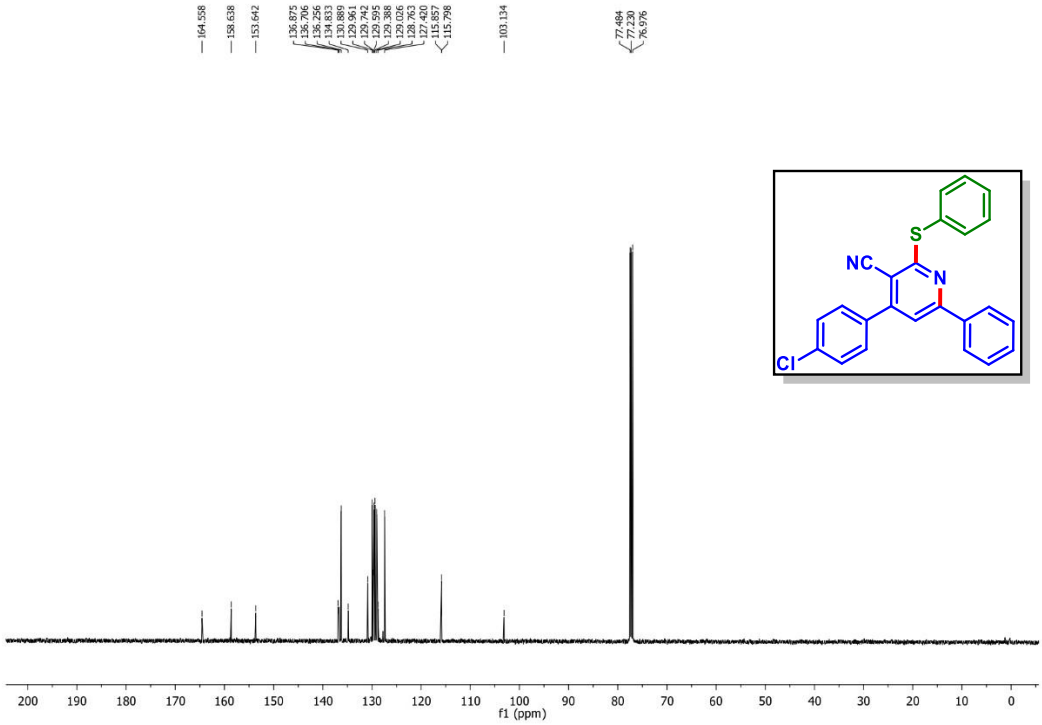

6-(4-Methoxyphenyl)-4-phenyl-2-(phenylthio)nicotinonitrile (9a): ^{1}H NMR ($CDCl_3$, 500 MHz)

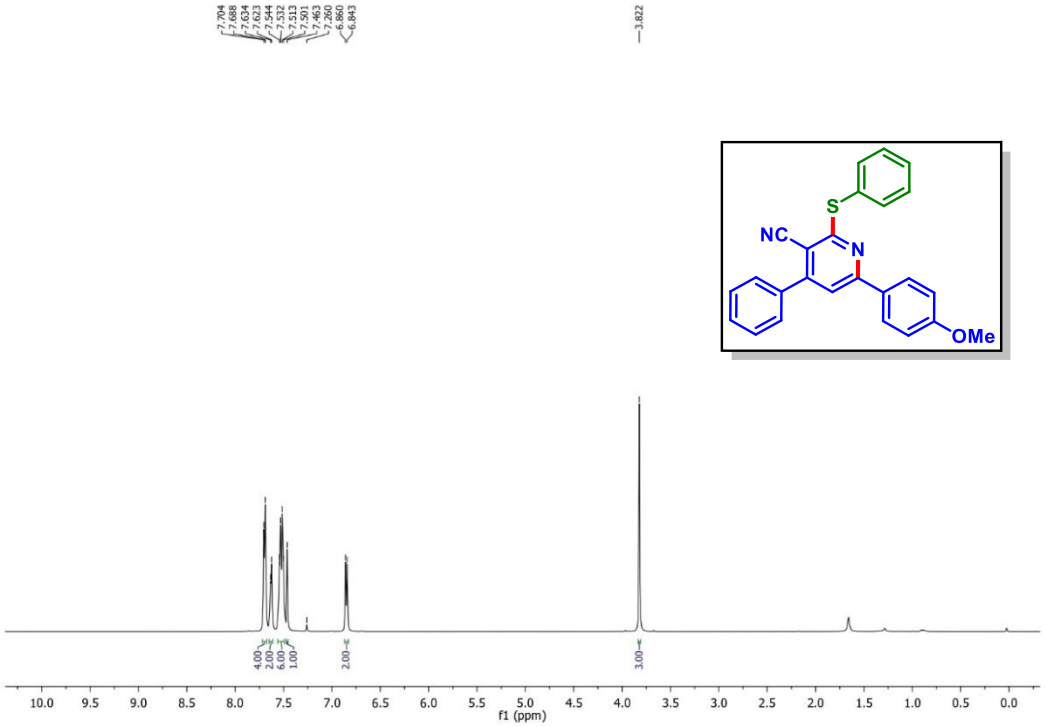

6-(4-Methoxyphenyl)-4-phenyl-2-(phenylthio)nicotinonitrile (9a): $^{13}C\{^{1}H\}$ NMR ($CDCl_3$, 125 MHz)

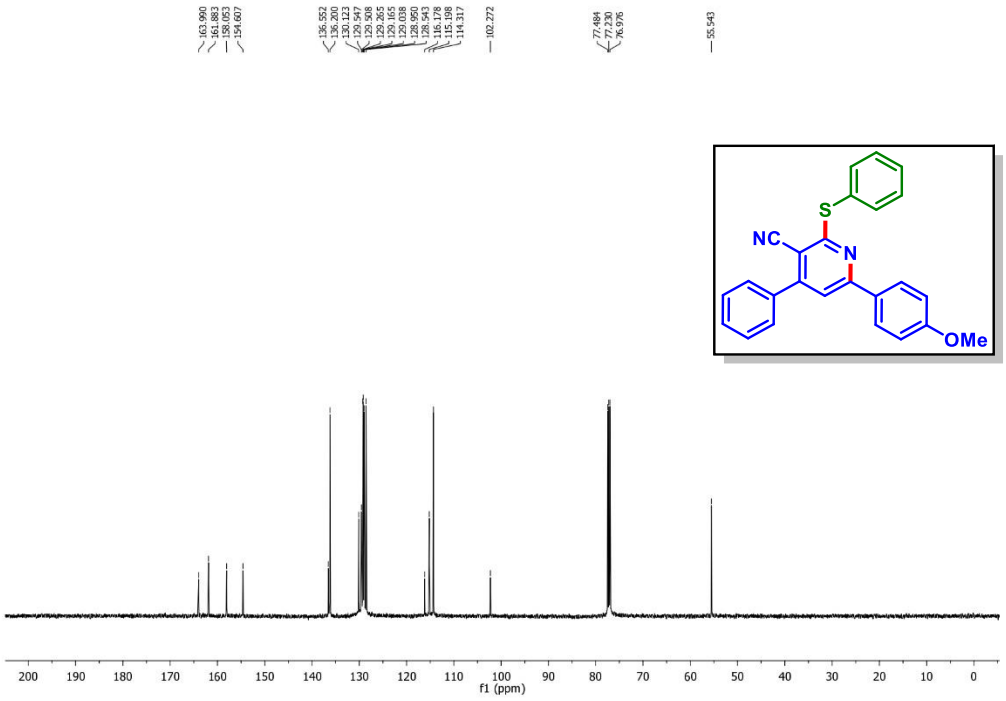

6-(4-Chlorophenyl)-4-phenyl-2-(phenylthio)nicotinonitrile (12a): ^{1}H NMR ($CDCl_3$, 500 MHz)

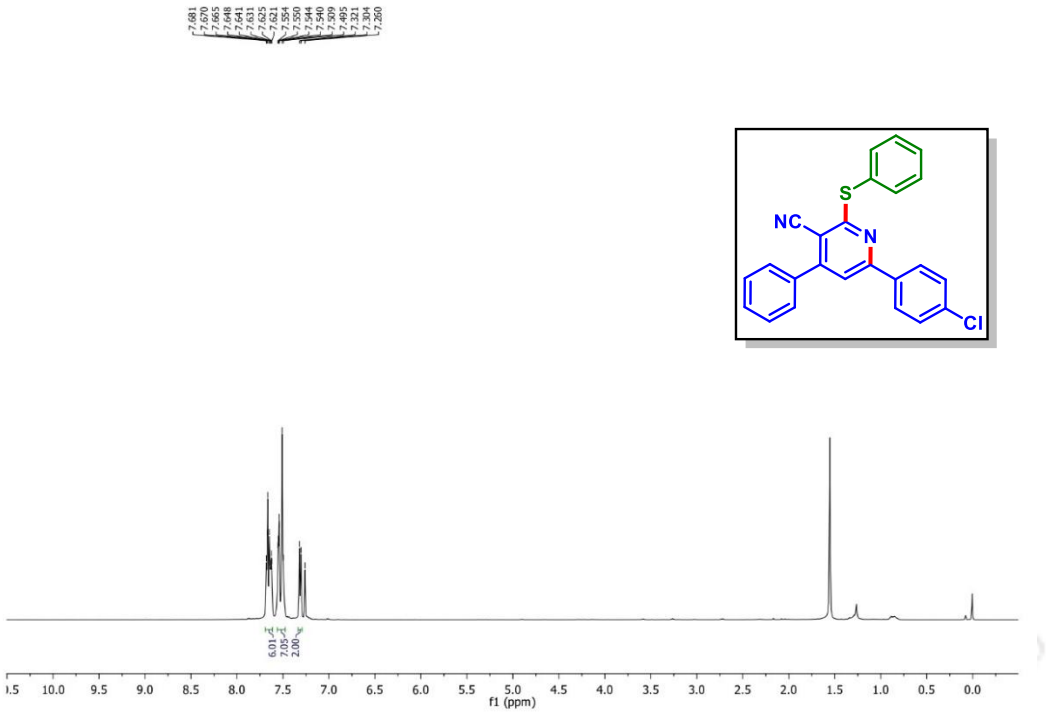

6-(4-Chlorophenyl)-4-phenyl-2-(phenylthio)nicotinonitrile (12a): $^{13}C\{^{1}H\}$ NMR ($CDCl_3$, 125 MHz)

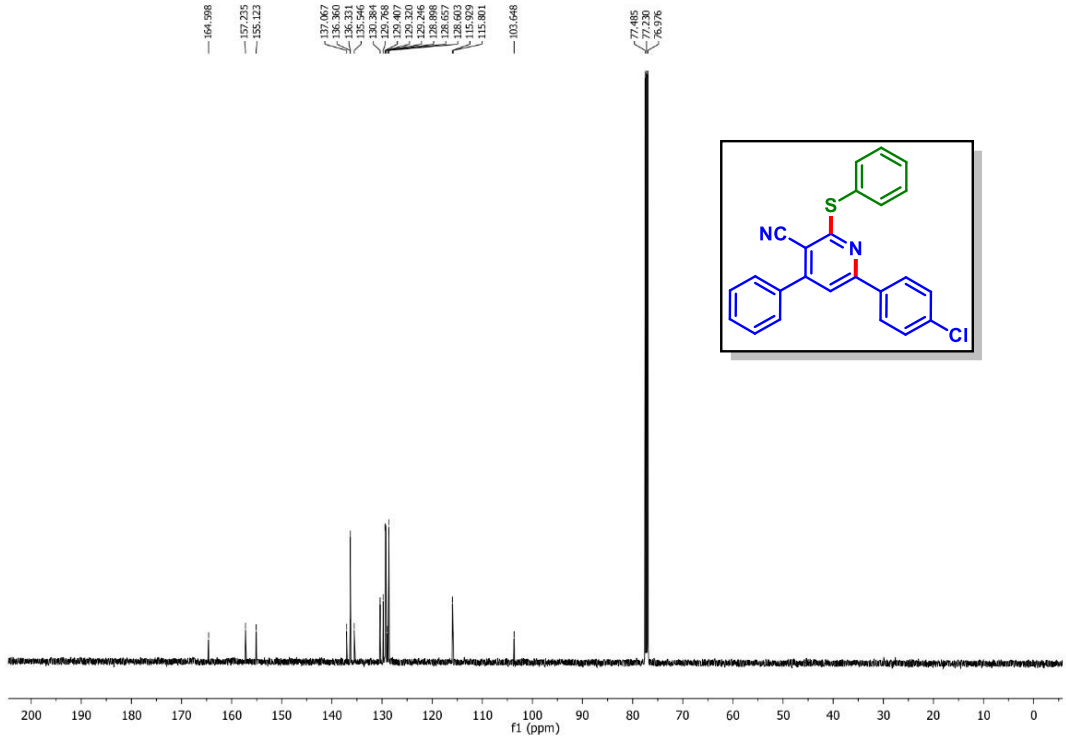

2-(Phenylthio)-4,6-di(thiophen-2-yl)nicotinonitrile (18a): ^{1}H NMR ($CDCl_3$, 500 MHz)

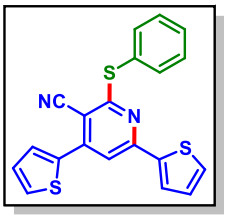

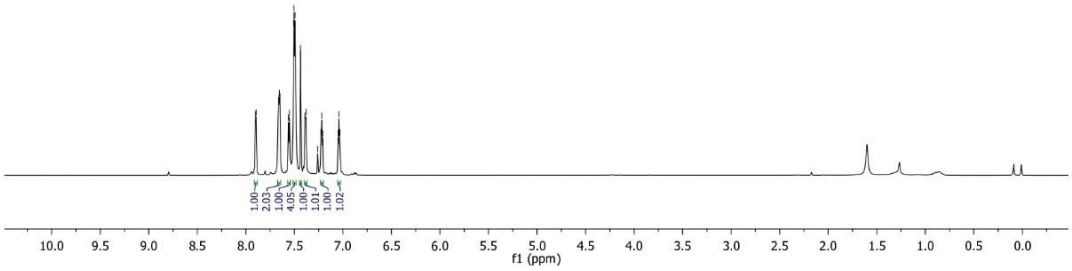

2-(Phenylthio)-4,6-di(thiophen-2-yl)nicotinonitrile (18a): $^{13}C\{^{1}H\}$ NMR ($CDCl_3$, 125 MHz)

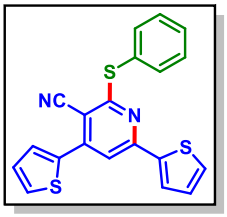

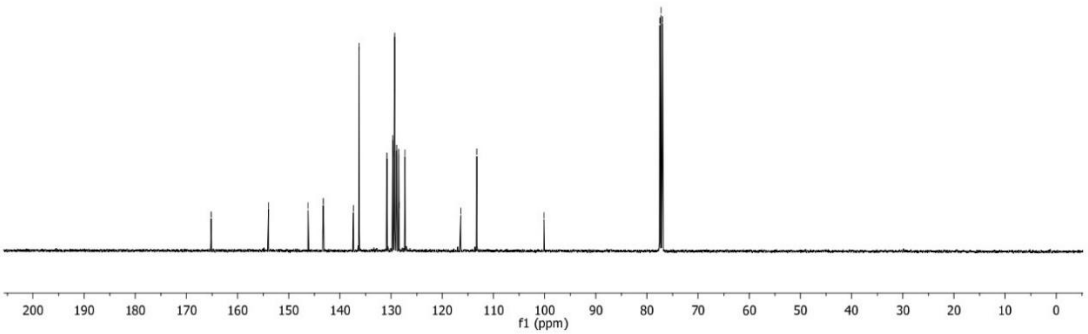

2-((4-Methoxyphenyl)thio)-4,6-diphenylnicotinonitrile (1d): ^{1}H NMR ($CDCl_3$, 500 MHz)

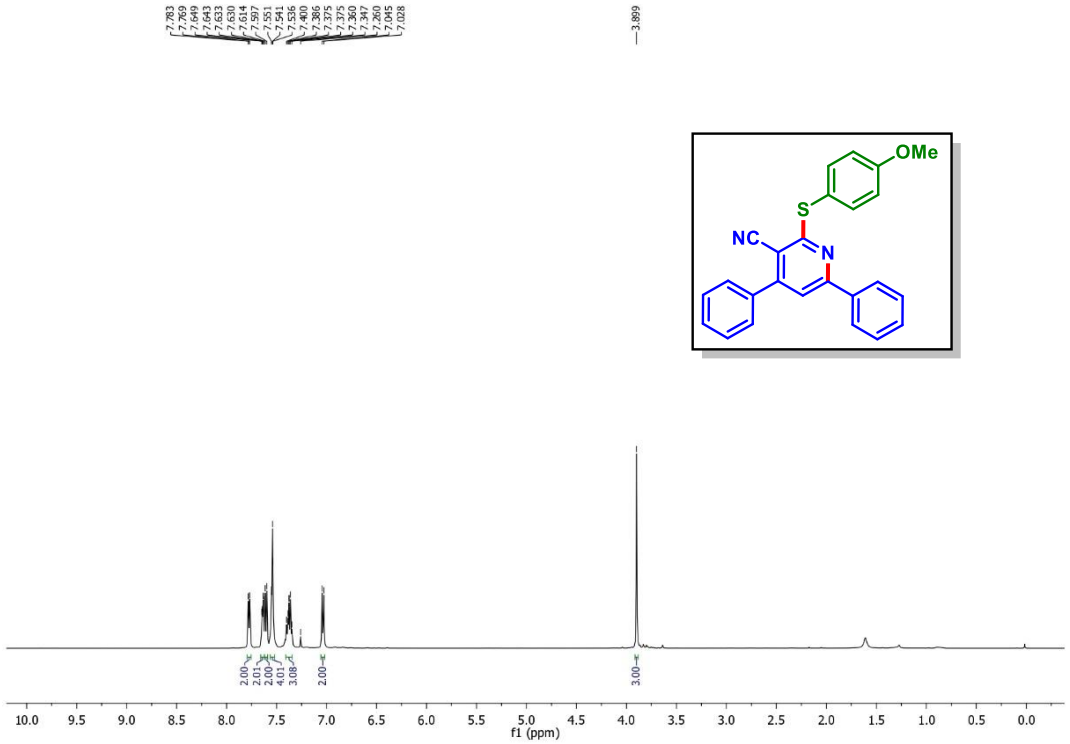

2-((4-Methoxyphenyl)thio)-4,6-diphenylnicotinonitrile (1d): ^{13}C {^{1}H} NMR ($CDCl_3$, 125 MHz)

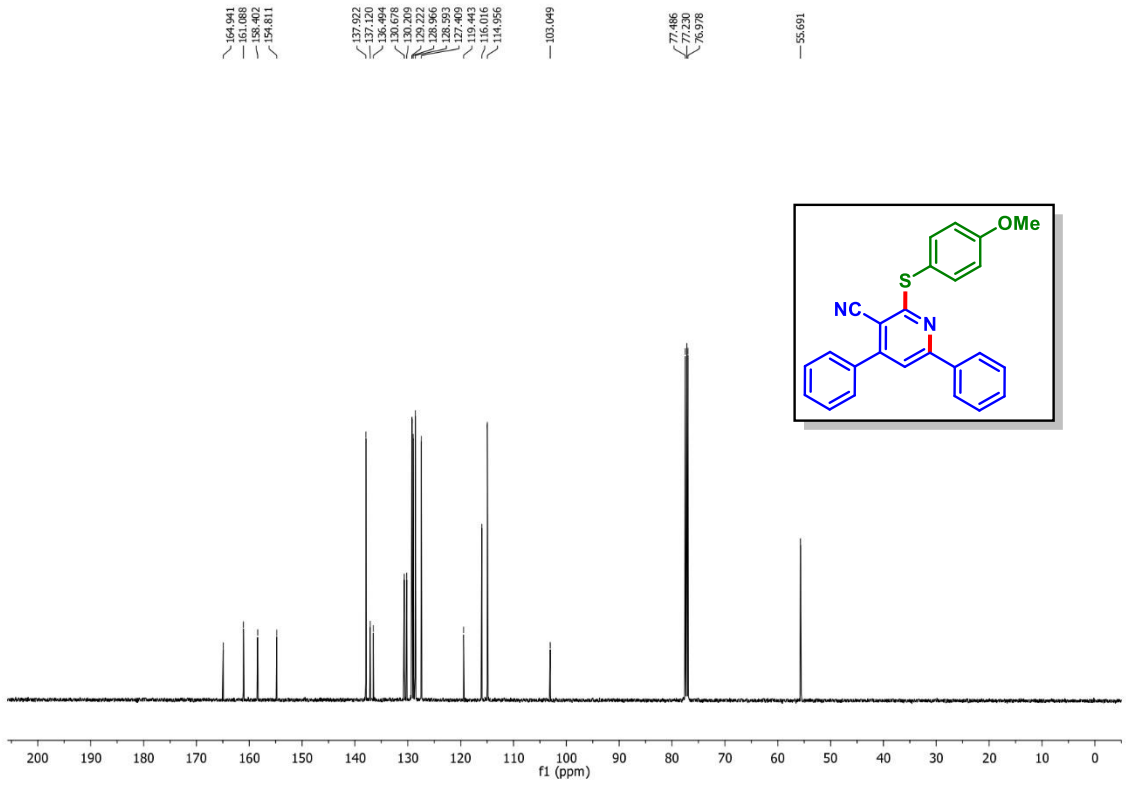

2-((2-Bromophenyl)thio)-4,6-diphenylnicotinonitrile (1j): ^{1}H NMR ($CDCl_3$, 500 MHz)

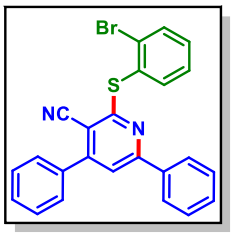

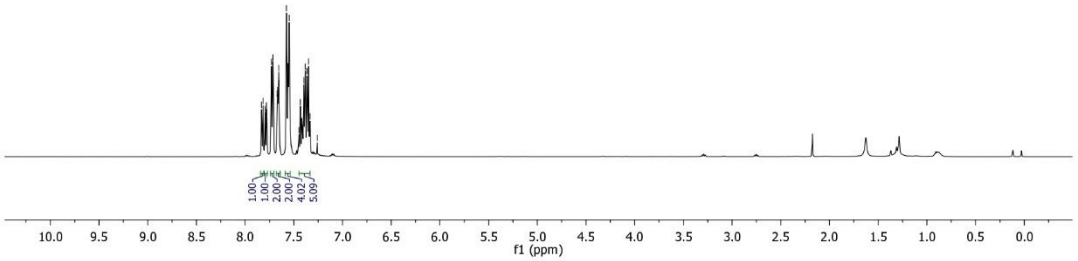

2-((2-Bromophenyl)thio)-4,6-diphenylnicotinonitrile (1j): $^{13}C\{^{1}H\}$ NMR ($CDCl_3$, 125 MHz)

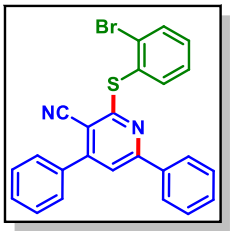

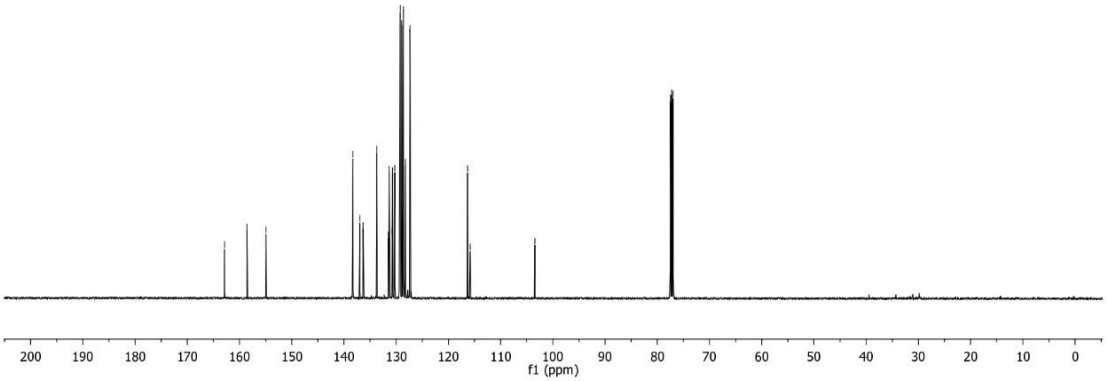

2-(Naphthalen-2-ylthio)-4,6-diphenylnicotinonitrile (1k): ^{1}H NMR (CDCl$_3$, 500 MHz)

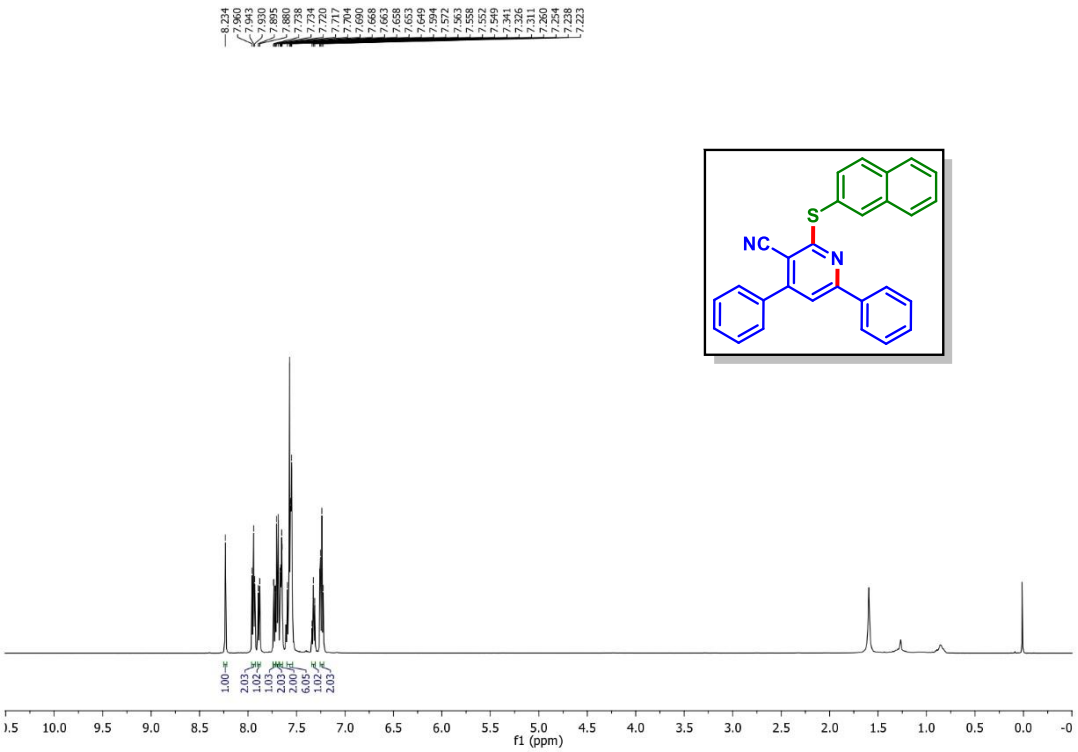

2-(Naphthalen-2-ylthio)-4,6-diphenylnicotinonitrile (1k): ^{13}C{^{1}H} NMR (CDCl$_3$, 125 MHz)

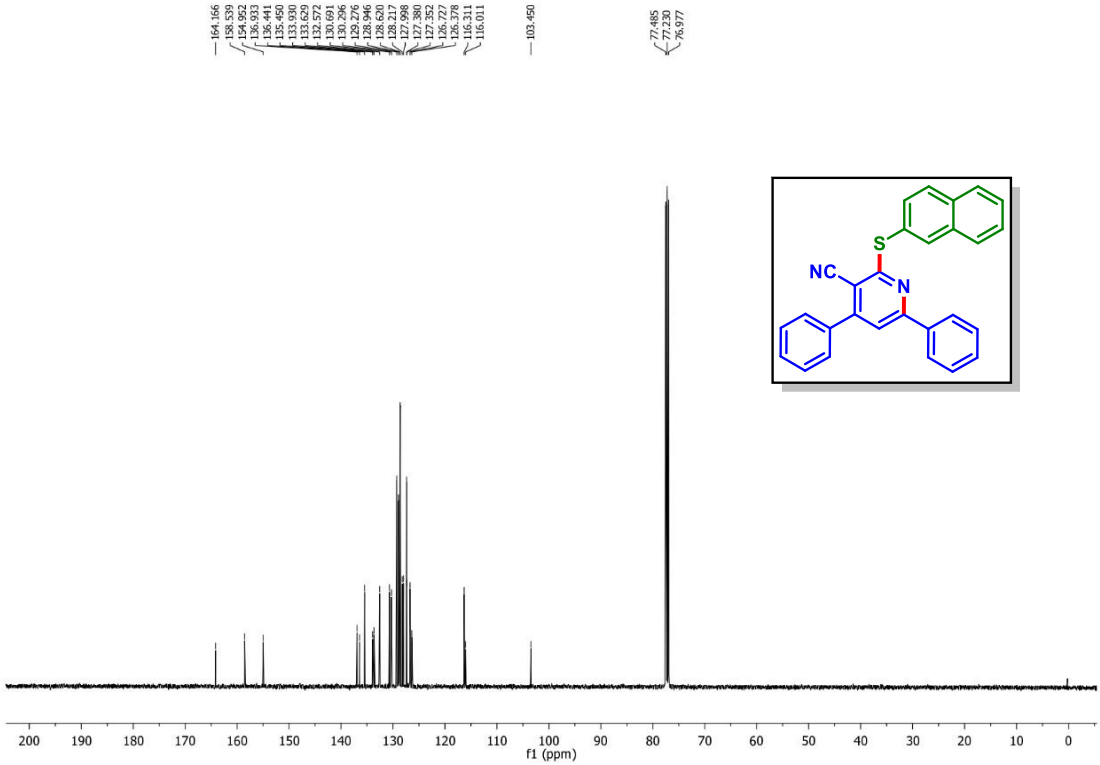

4,6-Diphenyl-2-(thiophen-2-ylthio)nicotinonitrile (1l): ^{1}H NMR ($CDCl_3$, 500 MHz)

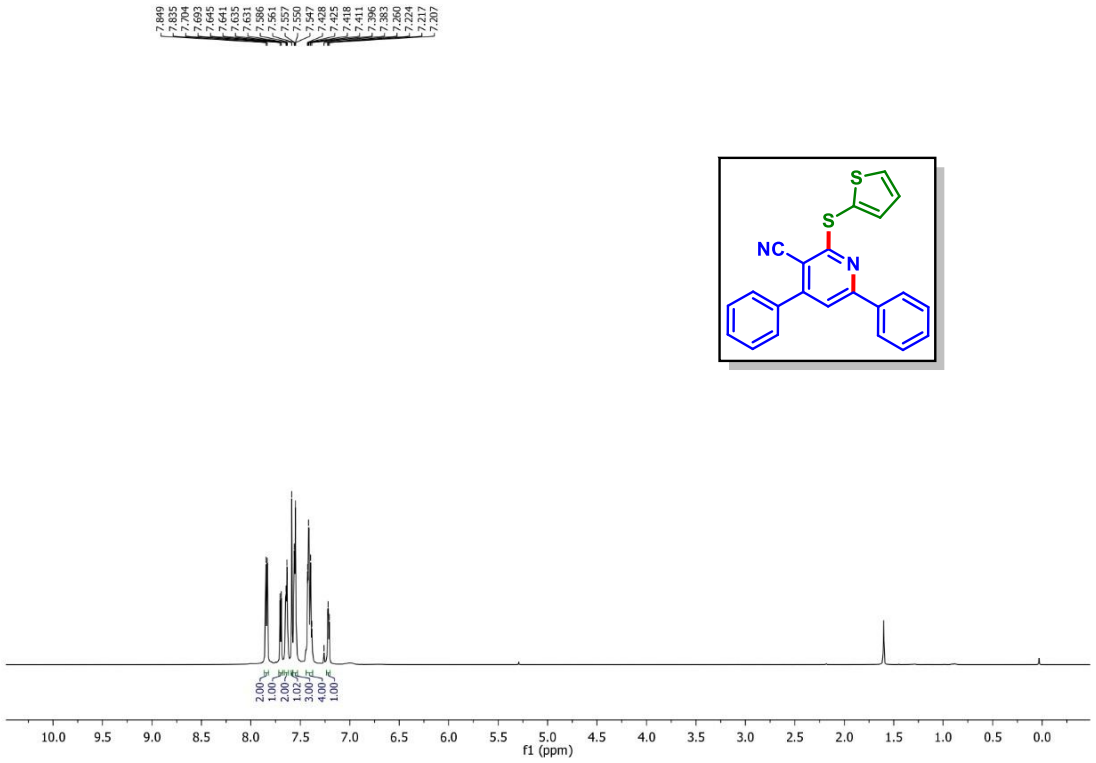

4,6-Diphenyl-2-(thiophen-2-ylthio)nicotinonitrile (1l): $^{13}C\{^{1}H\}$ NMR ($CDCl_3$, 125 MHz)

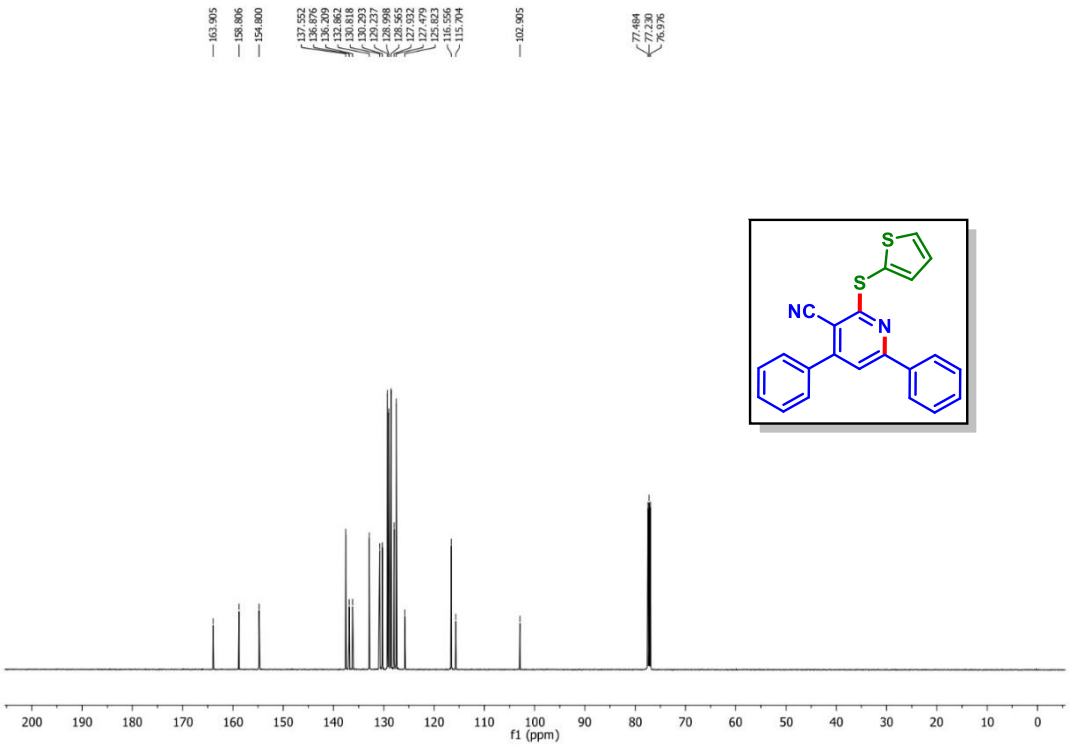

V.9. References:

[1] (a) Sun, K.; Lv, Q.-Y.; Chen, X.-L.; Qua, L.-B.; Yu, B. *Green Chem.* **2021**, *23*, 232–248. (b) Pramanik, M. M. D.; Rastogi, N. *Chem. Commun.* **2016**, *52*, 8557–8560. (c) Dong, J.; Yue, F.; Xu, W.; Song, H.; Liu, Y.; Wang, Q. *Green Chem.* **2020**, *22*, 5599–5604. (d) Crisenza, G. E. M.; Mazzarella, D.; Melchiorre, P. *J. Am. Chem. Soc.* **2020**, *142*, 5461–5476. (e) Zhou, Q.-Q.; Zou, Y.-Q.; Lu, L.-Q.; Xiao, W.-J. *Angew. Chem., Int. Ed.* **2019**, *58*, 1586–1604. (f) McCarver, S. J.; Qiao, J. X.; Carpenter, J.; Borzilleri, R. M.; Poss, M. A.; Eastgate, M. D.; Miller, M. M.; MacMillan, D. W. C. *Angew. Chem., Int. Ed.* **2017**, *56*, 728–732.

[2] (a) Zhu, C.; Yue, H.; Chu, L.; Rueping, M. *Chem. Sci.* **2020**, *11*, 4051–4064. (b) Hari, D. P.; Konig, B. *Chem. Commun.* **2014**, *50*, 6688–6699. (c) Skubi, K. L.; Blum, T. R.; Yoon, T. P. *Chem. Rev.* **2016**, *116*, 10035–10074. (d) Xuan, J.; Hea, X.-K.; Xiao, W.-J. *Chem. Soc. Rev.* **2020**, *49*, 2546–2556. (e) Huang, L.; Kancherla, R.; Rueping, M. *ACS Catal.* **2022**, *12*, 11563–11572. (f) Dai, C.; Zhan, Y.; Liu, P.; Sun, P. *Green Chem.* **2021**, *23*, 314–319.

[3] Cheung, K. P. S.; Sarkar, S.; Gevorgyan, V. *Chem. Rev.* **2022**, *122*, 1543–1625.

[4] (a) Li, T.; Liang, K.; Tang, J.; Ding, Y.; Tong, X.; Xia, C. *Chem. Sci.* **2021**, *12*, 15655–15661. (b) Chen, Z.; Xue, F.; Liu, T.; Wang, B.; Zhang, Y.; Jin, W.; Xia, Y.; Liu, C. *Green Chem.* **2022**, *24*, 3250–3256. (c) Shen, J.; Li, J.; Chen, M.; Chen, Y. *Org. Chem. Front.* **2023**, *10*, 1166–1172. (d) Chen, Z.; Xue, F.; Zhang, Y.; Jin, W.; Wang, B.; Xia, Y.; Xie, M.; Abdukader, A.; Liu, C. *Org. Lett.* **2022**, *24*, 3149–3154. (e) Saux, E. L.; Zanini, M.; Melchiorre, P. *J. Am. Chem. Soc.* **2022**, *144*, 1113–1118. (f) Chen, Z.; Jin, W.; Xia, Y.; Zhang, Y.; Xie, M.; Ma, S.; Liu, C. *Org. Lett.* **2020**, *22*, 8261–8266. (g) Bahamonde, A.; Melchiorre, P. *J. Am. Chem. Soc.* **2016**, *138*, 8019–8030. (h) Ho, H. E.; Pagano, A.; Rossi-Ashton, J. A.; Donald, J. R.; Epton, R. G.; Churchill, J. C.; James, M. J.; O'Brien, P.; Taylor, R. J. K.; Unsworth, W. P. *Chem. Sci.* **2020**, *11*, 1353–1360. (i) Beato, E. P.; Spinnato, D.; Zhou, W.; Melchiorre, P. *J. Am. Chem. Soc.* **2021**, *143*, 12304–12314.

[5] (a) Allais, C.; Grassot, J.-M.; Rodriguez, J.; Constantieux, T. *Chem. Rev.* **2014**, *114*, 10829–10868. (b) Stolar, M.; Baumgartner, T. *Chem. Commun.* **2018**, *54*, 3311–3322. (c) Chelucci, G. *Chem. Soc. Rev.* **2006**, *35*, 1230–1243.

[6] (a) Hantzsch, A. *Ber. Dtsch. Chem. Ges.* **1881**, *14*, 1637–1638. (b) Kröhnke, F. *Synthesis* **1976**, *1*, 1–24. (c) Kelly, T. R.; Lebedev, R. L. *J. Org. Chem.* **2002**, *67*, 2197–2205.

[7] (a) Dhara, H. N.; Rakshit, A.; Alam, T.; Patel, B. K. *Org. Biomol. Chem.* **2022**, *20*, 4243–4277. (b) Rakshit, A.; Dhara, H. N.; Sahoo, A. K.; Patel, B. K. *Chem Asian J.* **2022**, *17*, e202200792. (c) Rakshit, A.; Dhara, H. N.; Alam, T.; Dahiya, A.; Patel, B. K. *J. Org. Chem.* **2021**, *86*, 17504–17510. (d) Cai, B.-G.; Li, Q.; Xuan, J. *Green Synth. Catal.* DOI: 10.1016/j.gresc.2023.01.007.

[8] For metal **Ir**: (a) Onodera, G.; Shimizu, Y.; Kimura, J.; Kobayashi, J.; Ebihara, Y.; Kondo, K.; Sakata, K.; Takeuchi, R. *J. Am. Chem. Soc.* **2012**, *134*, 10515–10531. For **Fe**: (b) Richard, V.; Ipouck, M.; Mérel, D. S.; Gaillard, S.; Whitby, R. J.; Witulski, B.; Renaud, J.-L. *Chem. Commun.* **2014**, *50*, 593–595. For **Co**: (c) Kase, K.; Goswami, A.; Ohtaki, K.; Tanabe, E.; Saino, N.; Okamoto, S. *Org. Lett.* **2007**, *9*, 931–934. For **Ru**: (d) Yamamoto, Y.; Kinpara, K.; Saigoku, T.; Takagishi, H.; Okuda, S.; Nishiyama, H.; Itoh, K. *J. Am. Chem. Soc.* **2005**, *127*, 605–613. For **Ni**: (e) Kumar, P.; Prescher, S.; Louie, J. *Angew. Chem., Int. Ed.* **2011**, *50*, 10694–10698.

[9] (a) Zhen, Q.; Li, R.; Qi, L.; Hu, K.; Yao, X.; Shao, Y.; Chen, J. *Org. Chem. Front.* **2020**, *7*, 286–291. (b) Yao, X.; Qi, L.; Li, R.; Zhen, Q.; Liu, J.; Zhao, Z.; Shao, Y.; Hu, M.; Chen, J. *ACS Comb. Sci.* **2020**, *22*, 114–119. (c) Qi, L.; Li, R.; Yao, X.; Zhen, Q.; Ye, P.; Shao, Y.; Chen, J. *J. Org. Chem.* **2020**, *85*, 1097–1108.

[10] (a) Rakshit, A.; Kumar, P.; Alam, T.; Dhara, H.; Patel, B. K. *J. Org. Chem.* **2020**, *85*, 12482–12504. (b) Dhara, H. N.; Rakshit, A.; Alam, T.; Sahoo, A. K.; Patel, B. K. *Org. Lett.* **2023**, *25*, 471–476.

[11] (a) Sun, K.; Lv, Q.-Y.; Lin, Y.-W.; Yu, B.; He, W.-M. *Org. Chem. Front.* **2021**, *8*, 445–465. (b) Natarajan, P.; Manjeet, M.; Muskan, M.; Brar, N. K.; Kaur, J. J. *Org. Chem. Front.* **2018**, *5*, 1527–1531. (c) Sahoo, A. K.; Rakshit, A.; Dahiya, A.; Pan, A.;

Patel, B. K. *Org. Lett*. **2022**, *24*, 1918–1923. (d) Sahoo, A. K.; Rakshit, A.; Pan, A.; Dhara, H. N.; Patel, B. K. *Org. Biomol. Chem.* **2023**, *21*, 1680–1691.

[12] Guo, W.; Tao, K.; Tan, W.; Zhao, M.; Zheng, L.; Fan, X. *Org. Chem. Front.* **2019**, *6*, 2048–2066.

[13] (a) Rakshit, A.; Dhara, H. N.; Sahoo, A. K.; Alam, T.; Patel, B. K. *Org. Lett.* **2022**, *24*, 3741–3746. (b) Rakshit, A.; Sau, P.; Ghosh, S.; Patel, B. K. *Adv. Synth. Catal*. **2019**, *361*, 3824–3836.

[14] (a) Thimmaiah, M.; Li, P.; Regati, S.; Chen, B.; Zhao, J. C.-G. *Tet. Lett.* **2012**. *53*. 4870–4872. (b) Sobhani, S.; Honarmand, M. *C. R. Chimie* **2013**, *16*, 279–286. (c) Sharma, P.; Sinha, P.; Bansal, R. K. *Beilstein Arch.* **2022**, 202273. doi:10.3762/bxiv.2022.73.v1. (d) Grigor′ev, A. A.; Shtyrlin, N. V.; Gabbasova, R. R.; Zeldi, M. I.; Grishaev, D. Y.; Gnezdilov, O. I.; Balakin, K. V.; Nasakin, O. E.; Shtyrlin, Y. G. *Synth. Commun.* **2018**, *48*, 2288–2304. (e) Chowdhury, H.; Goswami, A. *Org. Biomol. Chem.* **2017**, *15*, 5824–5830. (f) Sahoo, A. K.; Rakshit, A.; Pan, A.; Dhara, H. N.; Patel, B. K. *Org. Biomol. Chem.* **2023**, *21*, 1680–1691. (g) Dashyan, S. Sh.; Babaev, E. V.; Ayvazyan, A. G.; Mamyan, S. S.; Paronikyan, E. G.; Nikoghosyan, T. A.; Hunanyan, L. S.; Paronikyan, R. G. *Bioorg. Chem.* **2024**, *148*, 107435–107447.

[15] Chakraborty, N.; Rajbongshi, K. K.; Dahiya, A.; Das, B.; Vaishnani, A.; Patel, B. K. *Chem. Commun.* **2023**, *59*, 2779–2782.

[16] (a) Li, E.; Huang, Y. *Chem. Commun.* **2014**, *50*, 948–950. (b) Tian, J.; Sun, H.; Zhou, R.; He, Z. *Chin. J. Chem.* **2013**, *31*, 1348–1351. (c) Kang, T.-R.; Chen, L.-M. *Acta Cryst.* **2009**, *65*, o3164.

[17] (a) Chalotra, N.; Shah, I. H.; Raheem, S.; Rizvi, M. A.; Shah, B. A. *J. Org. Chem.* **2021**, *86*, 16770–16784. (b) Runemark, A.; Sunden, H. *J. Org. Chem.* **2023**, *88*, 462–474.

[18] Cai, Y.-P.; Ma, M.-Y.; Xu, X.; Song, Q.-H. *Org. Chem. Front.* **2023**, *10*, 1633–1642.

भारतीय प्रौद्योगिकी संस्थान गुवाहाटी
Indian Institute of Technology Guwahati

List of Publications

Publications for Thesis

1. **Dhara, H. N.**; Manna, S.; Patel, B. K. A Cascade Synthesis of Furo-Pyrrolo-Pyridines via Pd(II)-Catalyzed Dual N−H/C Annulative-Cyclization. *Chem. -Eur. J.* **2024**, e202403470. (DOI: 10.1002/chem.202403470)

2. **Dhara, H. N.**; Das, B.; Barik, D.; Manna, S.; Patel, B. K. Pd(II)-Catalyzed Three-Component Synthesis of Furo[2,3-*d*]pyrimidines from β-Ketodinitriles, Boronic Acids, and Aldehydes. *Org. Lett.* **2023**, *25*, 9070–9075. (DOI: 10.1021/acs.orglett.3c04017)

3. **Dhara, H. N.**; Rakshit, A.; Barik, D.; Ghosh, K.; Patel, B. K. Visible-Light Driven Electron-Donor-Acceptor (EDA) Complex-Initiated Synthesis of Thio-functionalized Pyridines. *Chem. Commun.* **2023**, *59*, 7990–7993. (DOI: 10.1039/d3cc01678a)

4. **Dhara, H. N.**; Rakshit, A.; Alam, T.; Sahoo, A. K.; Patel, B. K. Visible-Light-Mediated Solvent-Switched Photosensitizer-Free Synthesis of Polyfunctionalized Quinolines and Pyridines. *Org. Lett.* **2023**, *25*, 471–476. (DOI: 10.1021/acs.orglett.2c04027)

Publications as Co-author

1. Barik, D.; Chakraborty, N.; Sahoo, A. K.; **Dhara, H. N.**; Patel, B. K. Electron-Donor-Acceptor (EDA) Complex-Driven Regioselective Vicinal and Oxidative Geminal Functionalization of Alkynes. *Chem. Commun.* **2024**, *60*, 12577–12580. (DOI: 10.1039/d4cc04610b)

2. Das, B.; Chakraborty, N.; **Dhara, H. N.**; Bhattacharyya, P.; Patel, B. K. Access to Chromenopyrrole via Tandem [3 + 2] Cycloaddition and Intramolecular C–O Coupling. *J. Org. Chem*. **2024**, *89*, 1331–1335. (DOI: 10.1021/acs.joc.3c02479)

3. Sahoo, A. K.; Rakshit, A.; Pan, A.; **Dhara, H. N.**; Patel, B. K. Visible/Solar-Light-Driven Thiyl-Radical-Triggered Synthesis of Multi-Substituted Pyridines. *Org. Biomol. Chem.* **2023**, *21*, 1680–1691. (DOI: 10.1039/d3ob00009e)

4. Alam, T.; Rakshit, A.; **Dhara, H. N.**; Palai, A.; Patel, B. K. Electrochemical Amidation: Benzoyl Hydrazine/Carbazate and Amine as Coupling Partners. *Org. Lett*. **2022**, *24*, 6619–6624. (DOI: 10.1021/acs.orglett.2c02626)

5. Rakshit, A.; **Dhara, H. N.**; Sahoo, A. K.; Alam, T.; Patel, B. K. Pd(II)-Catalyzed Synthesis of Furo[2,3-*b*]pyridine from β-Ketodinitriles and Alkynes *via* Cyclization and N–H/C Annulation. *Org. Lett*. **2022**, *24*, 3741–3746. (DOI: 10.1021/acs.orglett.2c01472)

6. Rakshit, A.; **Dhara, H. N.**; Alam, T.; Dahiya, A.; Patel, B. K. Cu(II)-Promoted Cascade Synthesis of Fused Imidazo-Pyridine-Carbonitriles. *J. Org. Chem*. **2021**, *86*, 17504–17510. (DOI: 10.1021/acs.joc.1c02198)

7. Rakshit, A.; Kumar, P.; Alam, T.; **Dhara, H.**; Patel, B. K. Visible-Light Accelerated Pd-Catalyzed Cascade Addition/Cyclization of Aryl Boronic Acids to γ- and β-Ketodinitriles for the Construction of 3-Cyanopyridines and 3-Cyanopyrrole Analogues. *J. Org. Chem*. **2020**, *85*, 12482–12504. (DOI: 10.1021/acs.joc.0c01703)

Review Articles

1. **Dhara, H. N.**; Rakshit, A.; Alam, T.; Patel, B. K. Metal-Catalyzed Reactions of Organic Nitriles and Boronic Acids to Access Diverse Functionality. *Org. Biomol. Chem*. **2022**, *20*, 4243–4277. (DOI: 10.1039/d2ob00288d)

2. Rakshit, A.; **Dhara, H. N.**; Sahoo, A. K. Patel, B. K. The Renaissance of Organo Nitriles in Organic Synthesis. *Chem. Asian. J*. **2022**, *17*, e202200792. (DOI: 10.1002/asia.202200792)

Book Chapter

1. Das, B.; **Dhara, H. N.**; Dahiya, A.; Patel, B. K. The Author(s), under exclusive license to Springer Nature Switzerland AG 2022 S. Dave and J. Das (eds.), Trends and Contemporary Technologies for Photocatalytic Degradation of Dyes, Environmental Science and Engineering, https://doi.org/10.1007/978-3-031-08991-6_2.